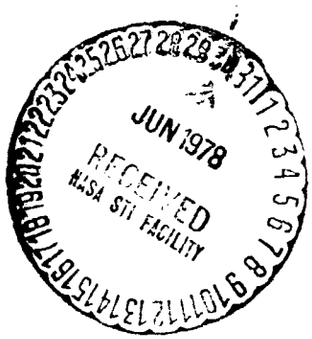

THE UNIVERSITY OF KANSAS CENTER FOR RESEARCH, INC.

2291 Irving Hill Drive—Campus West
Lawrence, Kansas 66045

ERRATA LIST

REPORT: A STUDY OF COMMUTER AIRPLANE DESIGN OPTIMIZATI0N

Page xx: Add: Figure 11.22.1 Flowchart of "CNR"

Page xx: Add: Figure 11.22.2 Listing plus sample ouput "CNR"

Page xxvi: Add: Table 11.22.1 Variables in "CNR"

Page iii: Add: Table D.1 Listing "DYNSTAB"

Add to page 11.16.4 equation 11.16.5:

Power effect may be estimated from:

$$C_{n_{\beta_P}} = X_p \, C_{y'_{\psi_0}} \, (S_p/\text{prop})/S_W \qquad (11.16.5)$$

where: $C_{y'_{\psi_0}}$ follows from section 5.

Add to table 13.1:

"CNR"	2 %	
"CONSURF"	2 %	C_{h_α}
	15 %	C_{h_δ}

Page 2.3: While the report was being printed, the balance per May 31, 1978 was received: $ 44.50 CR.

A STUDY OF COMMUTER AIRPLANE DESIGN OPTIMIZATION

Fourth Status Report
KU-FRL 313-5

This work was performed under
NASA Grant NSG-2145

12 May 1978

Prepared by: Bob van Keppel
Han Eysink
Jim Hammer
Kevin Hawley
Paul Meredith

Principal Investigator: J. Roskam
Ackers Professor of
Engineering

Approved by: J. Roskam, Director
Flight Research Laboratory

TABLE OF CONTENTS

CHAPTERS PAGE

CHAPTERS PAGE

APPENDICES

LIST OF ACRONYMS

Acronym	Definition
FAR	Federal Aviation Regulations
GASP	General Aviation Synthesis Program
KU-FRL	Kansas University - Flight Research Laboratory
NASA	National Aeronautics and Space Administration
SFF	Side Force Factor

LIST OF SYMBOLS

SYMBOL	DEFINITION	DIMENSION
A_i	Aspect ratio defined in Eqn. (5.3)	
a.c.	Aerodynamic Center	
AR, A	Aspect ratio	
b	Span	ft
B	Compressibility correction factor	
b_c	Distance defined in Fig. 5.3.b	ft
b_{i_e}	Distance defined in Fig. 5.3.b (single engine) or Fig. 5.3.c (twin engine)	ft
B_L	Number of propeller blades	
c	Chord	ft
$\bar{c}$	Mean aerodynamic chord	ft
C_D	Drag coefficient	
$C_{D_\alpha} = \frac{\partial C_D}{\partial \alpha}$	Variation of drag coefficient with angle of attack	rad^{-1}
$C_{D_u} = \frac{\partial C_D}{\partial u/U_1}$	Variation of drag coefficient with speed	
$C_{D_{\dot{\alpha}}} = \frac{\partial C_D}{\partial \frac{\dot{\alpha}\bar{c}}{2U_1}}$	Variation of drag coefficient with rate of change of angle of attack	rad^{-1}
$C_{D_q} = \frac{\partial C_D}{\partial \frac{q\bar{c}}{2U_1}}$	Variation of drag coefficient with pitch rate	rad^{-1}
c.g.	Center of Gravity	
$\bar{C}_i$	Distance defined in Fig. 5.3.b (single engine) or in Fig. 5.3.c (twin engine)	ft
C_ℓ	Section lift coefficient	
$C_L = \frac{L}{\bar{q}S}$	Lift coefficient	
$C_{L_\alpha} = \frac{\partial C_L}{\partial \alpha}$	Lift curve slope	rad^{-1}

LIST OF SYMBOLS (Cont'd)

SYMBOL	DEFINITION	DIMENSION
$C_{\ell_\alpha} = \frac{\partial C_\ell}{\partial \alpha}$	Section lift curve slope	rad^{-1}
C_{L_0}	Lift coefficient at zero angle of attack	
$C_{L_{i_H}} = \frac{\partial C_L}{\partial i_H}$	Nondimensional variation of lift coefficient with stabilizer angle of incidence	rad^{-1}
$C_{L_{\delta_E}} = \frac{\partial C_L}{\partial \delta_E}$	Variation of lift coefficient with elevator deflection	rad^{-1}
$C_{L_u} = \frac{\partial C_D}{\partial u/U_1}$	Variation of lift coefficient with speed	
$C_{L_q} = \frac{\partial C_L}{\partial \frac{q\bar{c}}{2U_1}}$	Variation of lift coefficient with pitch rate	rad^{-1}
$C_{L_{\dot{\alpha}}} = \frac{\partial C_D}{\partial \frac{\dot{\alpha}\bar{c}}{2U_1}}$	Variation of lift coefficient with rate of change of angle of attack	rad^{-1}
$C_{L_{\delta_F}} = \frac{\partial C_L}{\partial \delta_F}$	Variation of lift coefficient with flap deflection angle	rad^{-1}
$C_{L_{\delta_E}} = \frac{\partial C_L}{\partial \delta_E}$	Variation of lift coefficient with elevator deflection angle	rad^{-1}
$C_{L_{i_H}} = \frac{\partial C_L}{\partial i_H}$	Variation of lift coefficient with stabilizer incidence angle	rad^{-1}
$C_{\ell_{\delta_A}} = \frac{\partial C_\ell}{\partial \delta_A}$	Variation of rolling moment coefficient with aileron angle	rad^{-1}
$C_{\ell_{\delta_R}} = \frac{\partial C_\ell}{\partial \delta_R}$	Variation of rolling moment coefficient with rudder angle	rad^{-1}

LIST OF SYMBOLS (Cont'd)

SYMBOL	DEFINITION	DIMENSION
$C_{\ell_r} = \frac{\partial C_\ell}{\partial \frac{rb}{2U_1}}$	Variation of rolling moment coefficient with yaw rate	rad^{-1}
$C_{\ell_\beta} = \frac{\partial C_\ell}{\partial \beta}$	Variation of rolling moment coefficient with sideslip angle	rad^{-1}
$C_{\ell_p} = \frac{\partial C_\ell}{\partial \frac{pb}{2U_1}}$	Variation of rolling moment coefficient with roll rate	rad^{-1}
C_m	Pitching moment coefficient	
$C_{m_\alpha} = \frac{\partial C_m}{\partial \alpha}$	Variation of pitching moment coefficient with angle of attack	rad^{-1}
C_{m_o}	Pitching moment coefficient at zero angle of attack	
$C_{m_{\delta_E}} = \frac{\partial C_m}{\partial \delta_E}$	Variation of pitching moment coefficient with elevator deflection	rad^{-1}
$C_{m_q} = \frac{\partial C_m}{\partial \frac{q\bar{c}}{2U_1}}$	Variation of pitching moment coefficient with pitch rate	rad^{-1}
$C_{m_{\dot{\alpha}}} = \frac{\partial C_m}{\partial \frac{\dot{\alpha}\bar{c}}{2U_1}}$	Variations of pitching moment coefficient with rate of change of angle of attack	rad^{-1}
$C_{m_{\delta_F}} = \frac{\partial C_m}{\partial \delta_F}$	Variation of pitching moment coefficient with flap deflection angle	rad^{-1}
$C_{m_{\delta_E}} = \frac{\partial C_m}{\partial \delta_E}$	Variation of pitching moment coefficient with elevator deflection angle	rad^{-1}
$C_{m_{i_H}} = \frac{\partial C_m}{\partial i_H}$	Variation of pitching moment coefficient with stabilizer incidence angle	rad^{-1}

LIST OF SYMBOLS (Cont'd)

SYMBOL	DEFINITION	DIMENSION
C_N	Normal force coefficient	
$C_{n_\beta} = \frac{\partial C_n}{\partial \beta}$	Variation of yawing moment coefficient with sideslip angle	rad^{-1}
$C_{n_p} = \frac{\partial C_n}{\partial \frac{pb}{2U_1}}$	Variation of yawing moment coefficient with roll rate	rad^{-1}
$C_{n_r} = \frac{\partial C_n}{\partial \frac{rb}{2U_1}}$	Variation of yawing moment coefficient with yaw rate	rad^{-1}
$C_{n_{\delta_A}} = \frac{\partial C_n}{\partial \delta_A}$	Variation of yawing moment coefficient with aileron angle	rad^{-1}
$C_{n_{\delta_R}} = \frac{\partial C_n}{\partial \delta_R}$	Variation of yawing moment coefficient with rudder angle	rad^{-1}
$C_{r_{C_L}}$	Root chord at centerline	ft
$(c_{r_i})_e$	Distance defined in Fig. 5.3.b	ft
C_R	Root chord	ft
C_t	Tip chord	ft
C_{t_i}	Distance defined in Fig. 5.3.b	ft
$C_{y'_{\psi_o}}$	Factor obtained from Fig. 5.5	
$C_{y_\beta} = \frac{\partial C_y}{\partial \beta}$	Variation of side force coefficient with sideslip angle	rad^{-1}

LIST OF SYMBOLS (Cont'd)

SYMBOL	DEFINITION	DIMENSION
$C_{y_p} = \frac{\partial C_y}{\partial \frac{pb}{2U_1}}$	Variation of sideforce coefficient with roll rate	rad^{-1}
$C_{y_r} = \frac{\partial C_y}{\partial \frac{rb}{2U_1}}$	Variation of side force coefficient with yaw rate	rad^{-1}
$C_{y_{\delta_A}} = \frac{\partial C_y}{\partial \delta_A}$	Variation of side force coefficient with aileron angle	rad^{-1}
$C_{y_{\delta_R}} = \frac{\partial C_y}{\partial \delta_R}$	Variation of side force coefficient with rudder angle	rad^{-1}
D	Diameter	ft
D	Drag	lbf
d	Fuselage diameter at the wing root chord	ft
e	Oswald's efficiency factor	
f	Propeller in flow factor, see Fig. 5.4	
g	Gravitational acceleration	ft/sec^2
h	Height	ft
h_{ac}	Height of wing aerodynamic center above ground	ft
h_c	Height defined in Fig. 4.4	ft
h_{eff}	Effective height above ground, defined in Fig. 4.2 (no flap deflection) or in Eqn. (4.13) (with flap deflection)	ft
h_f	Height defined in Fig. 4.4	ft
h_H	Height from wing root chord to horizontal tail aerodynamic center	ft
h_{TE}	Height of wing trailing edge above ground	ft

LIST OF SYMBOLS (Cont'd)

SYMBOL	DEFINITION	DIMENSION
i_H	Stabilizer angle of incidence	deg,rad
i_T	Thrust inclination angle	deg,rad
i_w	Wing angle of incidence	deg, rad
K_A	Correction factor for aspect ratio	
K_H	Correction factor for horizontal tail position	
$K_{H_{power}}$	Factor defined in Eqn. (5.36)	
K_{WB}	Empirical factor to correct for body effect on wing lift curve slope	
K_λ	Correction factor for taper ratio	
K 1	Empirical correlation factor in Fig. 5.8	
K 2	Correction factor for maximum lift in Fig. 5.11	
L	Lift	lbf
ℓ_b	Length of fuselage	ft
$\ell_{\bar{c}/4_w}$	Distance defined in Fig. 5.15	ft
ℓ_{cg}	Distance from the nose of the airplane to the center of gravity	ft
ℓ_H	Distance defined in Fig. 5.3.a	ft
ℓ'_H	Distance defined in Fig. 5.3.a	ft
ℓ_n	Distance defined in Fig. 5.16	ft
ℓ_{no}	Distance defined in Fig. 5.18	ft
M	Mach number	
m	Airplane mass	lb
N_p	Propeller normal force	lbf
N	Normal force	lbf
N	Number of engines	
N_{pax}	Number of passengers	

LIST OF SYMBOLS (Cont'd)

SYMBOL	DEFINITION	DIMENSION
q	Pitch rate	rad/sec
$\bar{q}$	Dynamic pressure	lbf/ft^2
R_p	Propeller radius	ft
S	Area	ft^2
S_i	Area defined in Eqn. (5.3b)	ft^2
S_{H_i}	Area defined in Eqn. (5.37) (single engine) or in Eqn. (5.38) (multi-engine)	ft^2
SO	Area defined in section 5	
T	Thrust	lbf
$T_c' = \frac{T}{\bar{q}_\infty S_w}$	Thrust coefficient	
$T_c = \frac{T}{\rho V^2 D^2}$	Thrust coefficient	
V, U_1	Airspeed	ft/sec, knots
V_{mu}	Minimum unstick speed	ft/sec, mph
V_s	Stall speed	ft/sec, mph
V_{ROT}	Rotation speed	ft/sec, mph
W	Weight	lb
w_{aisle}	Width of aisle	ft
w_c	Cabin width	
w_n	Nacelle width	ft
w_{seat}	Width of seat	ft
X	X-axis, positive forward from the center of gravity	
$\bar{X}_{ac}$	Distance from leading edge of the wing to the aerodynamic center in tenths of $\bar{c}$	
$\bar{X}_{cg}$	Distance from the leading edge of the wing m.g.c. to the airplane in tenths of $\bar{c}$	

SYMBOL	DEFINITION	DIMENSION
X_H	Distance from airplane c.g. to the horizontal tail a.c.	ft
X_{pilot}	Distance defined in Fig. 10.12	ft
x'_p	Distance defined in Fig. 5.3.a	ft
x_p	Distance defined in Fig. 5.3.a	ft
X_w	Distance defined in Eqn. (5.49)	ft
$y_{\bar{c}_i}$	Distance defined in Fig. 5.3.b	ft
Z_H	Distance defined in Fig. 5.3.a	ft
$Z_{H_{eff}}$	Distance defined in Fig. 5.3.a	ft
Z_{H_T}	Distance defined in Fig. 5.3.a	ft
Z_s	Distance defined in Fig. 5.3.a	ft
Z_T	Distance defined in Fig. 5.3.a	ft
Z_w	Distance defined in Fig. 5.3.a	ft

GREEK SYMBOLS

$\Lambda_{\bar{c}/4}$	Quarter chord sweep angle	deg, rad
λ	Taper ratio	
Δ	Change of a quantity	
α	Angle of attack	deg, rad
α_o	Angle of attack for zero lift	deg, rad
β	Factor defined in Equation (4.4)	
σ	Factor defined in Equation (4.8)	
α_i	Induced angle of attack	deg,rad

GREEK SYMBOLS (Cont'd)		DIMENSION
$\Lambda_{c/2}$	Half chord sweep angle	deg, rad
δ	Control surface deflection	deg, rad
γ	Flight path angle	deg, rad
$\tau_E = \frac{\partial \alpha_H}{\partial \delta_E}$	Elevator effectiveness	
ϵ	Downwash angle	deg, rad
$\alpha_T = \alpha_b + i_T$	Thrust angle of attack	deg, rad
ϵ_{pow}	Total downwash angle at horizontal tail	deg, rad
λ_{i_e}	Taper ratio of immersed wing (see Fig. 5.3.b)	
α_p	Local angle of attack of the propeller plane	deg, rad
ϵ_u	Upwash angle	deg, rad
$\eta_H = \frac{\bar{q}_H}{\bar{q}_\infty}$	Ratio of dynamic pressures at the horizontal tail	

SUBSCRIPTS	
ac	Aerodynamic center
A	Aileron
b	Body
B	Body axis
cg	Center of gravity
C	Cabin
E	Elevator
e	Elevator
eng	Engine
fus	Fuselage

SUBSCRIPTS (Cont'd)

F	Flaps
f	Flaps
FUS	Fuselage
GE	Ground effect
H	Horizontal tail
L	Landing
LE	Leading edge
LAND	Landing
MIN	Minimum
MAX	Maximum
NAC	Nacelle
p	Power
p	Propeller
prop	Propeller
PROP	Propeller
R	Rudder
R	Root
S	Stability axis
t	tip
TE	Trailing edge
TO	Takeoff
V	Vertical tail
W	Wing
∞	Infinitely far away
1	Steady state

LIST OF FIGURES

LIST OF FIGURES (Cont'd)

LIST OF FIGURES (Cont'd)

LIST OF FIGURES (Cont'd)

LIST OF FIGURES (Cont'd)

LIST OF FIGURES (Cont'd)

LIST OF FIGURES (Cont'd)

LIST OF FIGURES (Cont'd)

LIST OF FIGURES (Cont'd)

LIST OF TABLES

LIST OF TABLES (Cont'd)

LIST OF TABLES (Cont'd)

Chapter 1

INTRODUCTION

This report presents the work performed from August 15, 1977 through May 31, 1978 under the funding of National Aeronautics and Space Administration Grant NSG 2145.

This project is a follow-up of research performed at Kansas University from May 16, 1976 through July 31, 1977. Both projects were aimed at enhancing the usability of the General Aviation Synthesis Program (GASP). The GASP program is an assembly of computerized design methods to aid in the preliminary design phase of, specifically, general aviation airplanes.

The proposal for this project stated the program objectives as follows (Reference 1.1):

1) To determine those stability and control characteristics which are critical to the preliminary design process.
2) To evaluate stability and control analysis methods currently available to determine those methods most appropriate for the preliminary design functions which GASP performs.
3) To determine how the methods of 1) may be used to provide the proper constraints and/or analysis functions for GASP.
4) To develop the appropriate subroutines for the methods of 3) and how they may be appended into GASP.

More specifically, attention will be given to the determination of the following stability and control characteristics in the preliminary design process:

1) Static Longitudinal Stability

1.1 Static Margin dC_M/dC_L

1.2 Static Stability C_{M_α}

1.3 Neutral point for stick free as well as stick fixed case.

2) Static Directional Stability, including propeller effects.

3) Engine-Out Control

Analyze configuration for minimum control speed, V_{MC}, from single degree of freedom as well as three degree of freedom point of view.

4) Rotation Velocity, V_R

5) Dynamic Longitudinal Stability

Determine for stick fixed case:

5.1 Short period damping.

5.2 Short period undamped natural frequency.

5.3 Phugoid damping.

5.4 Phugoid undamped natural frequency.

6) Lateral-Directional Dynamic Stability

Determine characteristics of:

6.1 Spiral mode.

6.2 Dutch roll mode.

7) Trim at Low Speed and forward CG

A trim routine will be incorporated.

The approach taken to comply with above objectives was to develop separate computer subroutines which can be added as a package to GASP. Also these subroutines can be used as a separate subprogram to compute the Dynamic Longitudinal, Lateral-Directional Stability characteristics for a given airplane.

Details of the program as well as of the project organization and financial status are presented in Chapter 2.

REFERENCES:

1.1 Roskam, J. et al., "A Study of Commuter Airplane Design Optimization," Continuation proposal to NASA Ames Research Center, July, 1977.

CHAPTER 2

GENERAL INFORMATION

This chapter will describe briefly the management of the project as well as the financial and research status. Also it will outline some of the peculiarities and limitations of the compute: programs.

2.1 PROJECT MANAGEMENT

Figure 2.1 shows a proposed time schedule. The actual time schedule followed closely the proposed schedule up until February 1978. After that time considerable time was spent on developing subroutines for the computation of stability and control derivatives.

From August 1977 until February 1978 one graduate and one undergraduate research assistant were on the payroll. From February 1978 until May 1978 two more undergraduate research assistants joined in the effort. During the month of May support was received from one additional graduate research assistant.

2.2 RESEARCH STATUS

As of the writing of this report all of the computer subroutines that needed to be developed in order to meet the objectives outlines in Chapter 1 were finished.

In January 1978 word was received of the Computer Center of Kansas University that the transliteration process,started during the previous project at K.U., of the K.U. version of GASP finally was finished. Test runs for two airplanes, one a single engine propeller airplane and the other a twin engine jet airplane, were done and proved satisfactorily.

Use was made of several existing subroutines developed by K.U.-F.R.L.

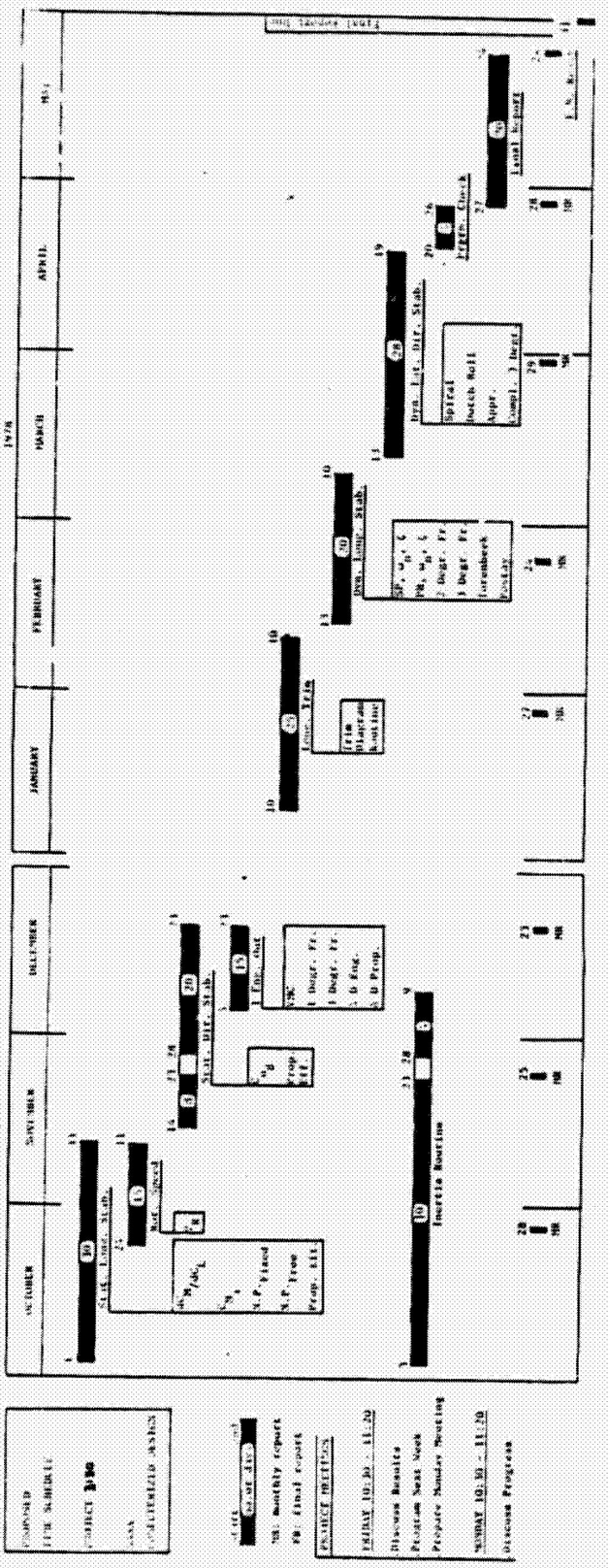

Figure 2.1: Proposed timeschedule

They are documented in References 2.1 and 2.2.

All subroutines have been tested out separately, a test of the complete program has not yet been done. Chapter 13 features a list of all the subroutines developed.

2.3 FINANCIAL STATUS

The budget for project 3130 is presented in Table 2.1. A complete breakdown of expenses through May 31, 1978 was not possible; however, an estimation,at the time of this report, of the balance of funds for NASA Grant NSG 2145 revealed an estimated deficit of $1500.00. This deficit is mainly due to an unforeseen increase in the salary expenditures for the month of May 1978.

2.4 REMARKS CONCERNING COMPUTER ROUTINES

The computer routines are based on a mixture of existing methods. Extensive use was made of empirical data. Care was taken to ensure that the data are applicable to the range of general aviation aircraft considered in this research i.e., ranging from the Cessna 150 type of aircraft to the Learjet type of aircraft. Generally the Mach number range of the methods involved is from M = 0.0 up to M = .99 unless otherwise indicated. Sweep-angles of the wing quarter-chord range from small negative values up to 35^{o} sweep-back. The aspect ratio range goes up to AR = 14 in general, again unless otherwise indicated. If data within these limits were not sufficient then extrapolations or data from other sources were added.

Data for graphs were implemented either one of two ways. Use was made of:

- Curve fitting techniques. An HP-65 calculator with standard routines was used for this.
- A routine "RDP," was developed that interpolates between curves

TABLE 2.1: PROPOSED BUDGET

September 1, 1977 - May 31, 1978

Direct Costs:	NASA	KU	TOTAL
Salaries and Wages			
Principal Investigator (Roskam)			
5% for 8.5 months, Academic	745	744	1,490
100% for 1 month, Summer	1,754	-	1,754
Research Assistants			
1 Graduate			
75% for 8.5 months	6,375	-	6,375
100% for 0.5 month	475	-	475
1 Undergraduate			
50% for 8.5 months	3,188	-	3,188
100% for 0.5 month	350		350
Secretary			
1 month	500	-	500
Total Salaries and Wages	13,387	745	14,132
Fringe Benefits:			
17% Faculty and Staff	510	127	637
7% Sutdent	727	-	727
Other Direct Costs			
Computer Cost	1,500	-	1,500
Travel to NASA and Meetings	800	-	800
Supplies and Reproduction	500	-	500
Telephone	200	-	200
Total Direct Costs	17,624	872	18,496
Indirect Costs:			
54.92% fo Salaries & Wages	7,352	409	7,761
TOTAL PROPOSED COSTS	$24,976	$1,281	$26,257

Salary Schedule:

J. Roskam	$1,754/mo.
Grad. Asst.	950/mo. (750 for 75%)
Undergrad. Asst.	700/mo.
Secretary	500/mo.

and graphs. Points on a curve are input as data in the subroutine whereupon Function "RDP" the correct iteration performs. See Appendix B for a description of "RDP."

The computations for the stability and control derivatives in Chapter 11 are in the airplane stability axis system.

2.5 REFERENCES

2.1 Wyatt, R.D. et al. A Study of Commuter Airplane Design Optimization Third Status Report. KU-FRL 313-4 Aug. 1977.

2.2 Postay, M. A computer Program for Determining Open and Closed Loop Dynamic Stability Characteristics of Airplanes and Control Systems. KU, May 1973.

CHAPTER 3

TRIM

3.1 INTRODUCTION

This subroutine calculates stabilizer angle of incidence, elevator deflection and lift coefficient of the horizontal tail needed for moment equilibrium in cruise. The program distinguishes two cases: one in which there is a fixed stabilizer with an elevator and one in which there is an adjustable stabilizer with an elevator. In the first case the airplane is trimmed with the elevator; in the second case, with the stabilizer while elevator deflection is zero. The resulting stick force is not calculated.

3.2 TRIM EQUATIONS

There are two unknowns to be calculated: angle of attack and either elevator deflection or stabilizer incidence. Therefore, two equations are needed: the lift equation and the pitching moment equation. From Reference 3.1, these are found to be:

$$mg \cos \gamma = (C_{L_0} + C_{L_\alpha} \alpha + C_{L_{i_H}} i_H + C_{L_{\delta_E}} \delta_E) \bar{q} S \qquad (3.1)$$

$$0 = C_{M_0} + C_{M_\alpha} \alpha + C_{M_{i_H}} i_H + C_{M_{\delta_E}} \delta_E \qquad (3.2)$$

Since the airplane is considered to be in level flight, the flight path angle is either zero or very shallow, so $\cos \gamma = 1$. The zero on the left hand side of Equation (3.2) represents the moment equilibrium condition.

All possible power effects are assumed to be included in the above equations. These effects are calculated in the subroutine POWER (see

Chapter 5) and can be added to the stability derivatives as determined by the shape of the airplane.

The above equations can also be written in matrix form. For the case in which the airplane is trimmed with the elevator, they become:

$$\begin{bmatrix} C_{L_\alpha} & C_{L_{\delta_E}} \\ C_{M_\alpha} & C_{M_{\delta_E}} \end{bmatrix} \begin{Bmatrix} \alpha \\ \delta_E \end{Bmatrix} = \begin{Bmatrix} C_{L_1} - C_{L_0} - C_{L_{i_H}} i_H \\ -C_{M_0} - C_{M_{\delta_E}} \delta_E \end{Bmatrix} \tag{3.3}$$

in which:

$$C_{L_1} = \frac{mg}{\bar{q}S} \tag{3.4}$$

The value of i_H is fixed, e.g. at a value which yields minimum trim drag in cruise.

If the airplane is trimmed with i_H, the matrix form of Equations (3.1) and (3.2) becomes:

$$\begin{bmatrix} C_{L_\alpha} & C_{L_{i_H}} \\ C_{M_\alpha} & C_{M_{i_H}} \end{bmatrix} \begin{Bmatrix} \alpha \\ i_H \end{Bmatrix} = \begin{Bmatrix} C_{L_1} - C_{L_0} - C_{L_{\delta_E}} \delta_E \\ -C_{M_0} - C_{M_{\delta_E}} \delta_E \end{Bmatrix} \tag{3.5}$$

The value of δ_E will be taken as zero because it is not necessary to have two deflections at a time for moment trim (for force trim, i.e. zero stick force, it is different). This means that the right hand side of Equation (3.5) is reduced to:

$$\begin{Bmatrix} C_{L_1} - C_{L_0} \\ -C_{M_0} \end{Bmatrix} \tag{3.6}$$

The solution of the matrix equations (3.3) and (3.5) can be written as follows:

$$\{\underline{x}\}=[A]^{-1}\{\underline{b}\} \tag{3.7}$$

If the airplane is elevator trimmed, the solution becomes:

$$\begin{Bmatrix} \alpha \\ \delta_E \end{Bmatrix} = \frac{\begin{bmatrix} C_{M_{\delta_E}} & -C_{L_{\delta_E}} \\ -C_{M_\alpha} & C_{L_\alpha} \end{bmatrix}}{\begin{vmatrix} C_{L_\alpha} & C_{L_{\delta_E}} \\ C_{M_\alpha} & C_{M_{\delta_E}} \end{vmatrix}} \begin{Bmatrix} C_{L_1} & -C_{L_0} & -C_{L_{i_H}} i_H \\ -C_{M_0} & -C_{M_{i_H}} i_H & \end{Bmatrix} \tag{3.8}$$

In the case of trim with stabilizer incidence, the solution becomes, with the reduced right hand side of Equation (3.5):

$$\begin{Bmatrix} \alpha \\ i_H \end{Bmatrix} = \frac{\begin{bmatrix} C_{M_{i_H}} & -C_{L_{i_H}} \\ -C_{M_\alpha} & C_{L_\alpha} \end{bmatrix}}{\begin{vmatrix} C_{L_\alpha} & C_{L_{i_H}} \\ C_{M_\alpha} & C_{M_{i_H}} \end{vmatrix}} \begin{Bmatrix} C_{L_1} & -C_{L_0} \\ -C_{M_0} & \end{Bmatrix} \tag{3.9}$$

Once the airplane is trimmed, the horizontal tail load can be calculated according to:

$$C_{L_H} = C_{L_{\alpha_H}} (\alpha + i_H - \varepsilon + \tau_E \delta_E) \tag{3.10}$$

It is assumed that the horizontal tail is equipped with a symmetrical airfoil. Power effects are assumed to be included in $C_{L_{\alpha_H}}$ and in ε.

Checks will have to be made on limits of control surface deflections and on the maximum lift coefficient of the horizontal tail.

If one or more of the calculated values fall outside the limits, appropriate action must be taken.

3.3 PROGRAM DESCRIPTION

Subroutine TRIM calculates values of i_H, δ_E and C_{L_H} according to the equations described in the previous section. To let the computer know which case it has to consider, there is a control parameter KCONT. For KCONT = 10 the airplane is trimmed with the elevator, and for KCONT = 12 the airplane is trimmed with stabilizer incidence.

To make the program as efficient as possible, the dummy variables PEA, CUE, ARE and ESS are used. Values of these variables depend on the value of KCONT. They are put into a matrix equation; the solution vector of this equation consists of α and another dummy variable, CS. This one is either i_H or δ_E, depending on the value of KCONT. The program flowchart, given in Figure 3.1, shows how this all works out.

The program listing and a sample output are shown in Figure 3.2. The sample output can be compared to the results of the hand calculation in the next section. A list of variables used in the program is given in Table 3.1.

3.4 HAND CALCULATION

A hand calculation has been done for Airplane A, for which data are presented in Appendix C. Since this airplane is trimmed with stabilizer incidence, Equation (3.9) is used to calculate α and i_H while $\delta_E = 0$. The cruise condition for this airplane is a flight at an altitude of 45,000 ft with a cruise Mach number of 0.83. The results of Equation (3.9) are:

α = 1.69 deg

i_H = 0.37 deg

This can be used as input for Equation (3.10), of which the result is:

C_{L_H} = -0.1197.

Compared to the actual horizontal tail load of this airplane in cruise, the result is accurate within 4 percent.

The computer generated a value of:

C_{L_H} = -0.1197.

TABLE 3.1 VARIABLE NAMES AND ORIGINS IN SUBROUTINE TRIM

NAME	ENG. SYMBOL	DIMENSION	ORIGIN	REMARKS
ALPHA	α	rad	---	Dummy
ARE	R	---	---	
CLAH	$C_{L_{\alpha_H}}$	rad^{-1}	Common	
CLALP	C_{L_α}	rad^{-1}	Common	
CLDE	$C_{L_{\delta_E}}$	rad^{-1}	Common	
CLHMAX	$C_{L_{H_{max}}}$	---	Common	
CLHMIN	$C_{L_{H_{min}}}$	---	Common	
CLHT	$C_{L_{H_T}}$	---	---	
CLIH	$C_{L_{I_H}}$	rad^{-1}	Common	

TABLE 3.1 VARIABLE NAMES AND ORIGINS IN SUBROUTINE "TRIM"
(continued)

NAME	ENG. SYMBOL	DIMENSION	ORIGIN	REMARKS
CL0	C_{L_0}	---	Common	
CL1	C_{L_1}	---	Common	
CMALP	C_{M_α}	rad^{-1}	Common	
CMDE	$C_{M_{\delta_E}}$	rad^{-1}	Common	
CMIH	$C_{M_{i_H}}$	rad^{-1}	Common	
CM0	C_{M_0}	---	Common	
CS	---	rad	---	Dummy
CUE	Q	---	---	Dummy
DADDE	$\partial\alpha/\partial\delta_E$	---	Common	
DCLAHP	$\Delta C_{L_{\alpha_{H_P}}}$	rad^{-1}	Common	
DCLALP	$\Delta C_{L_{\alpha_P}}$	rad^{-1}	Common	
DCLDEP	$\Delta C_{L_{\delta_{E_P}}}$	rad^{-1}	Common	
DCLIHP	$\Delta C_{L_{i_{H_P}}}$	rad^{-1}	Common	
DCL0P	$\Delta C_{L_{0_P}}$	---	Common	
DCMALP	$\Delta C_{M_{\alpha_P}}$	rad^{-1}	Common	

TABLE 3.1 VARIABLE NAMES AND ORIGINS IN SUBROUTINE "TRIM"
(continued)

NAME	ENG. SYMBOL	DIMENSION	ORIGIN	REMARKS
DCMDEP	$\Delta C_{M_{\delta_{E_P}}}$	rad^{-1}	Common	
DCMIHP	$\Delta C_{M_{i_{H_P}}}$	rad^{-1}	Common	
DCMOP	$\Delta C_{M_{O_P}}$	---	Common	
DEDEG	δ_E	deg	---	
DELTEL	δ_E	rad	---	
DELTMA	$\delta_{E_{max}}$	rad	Common	
DELTMI	$\delta_{E_{min}}$	rad	Common	
EPS	ϵ	rad	Common	
ESS	S	---	---	Dummy
EYEDEG	i_H	deg	---	
EYEH	i_H	rad	---	
EYEHMA	$i_{H_{max}}$	rad	Common	
EYEHMI	$i_{H_{min}}$	rad	Common	
PEA	P	---	---	Dummy
RAD	---	---	---	Conversion Factor

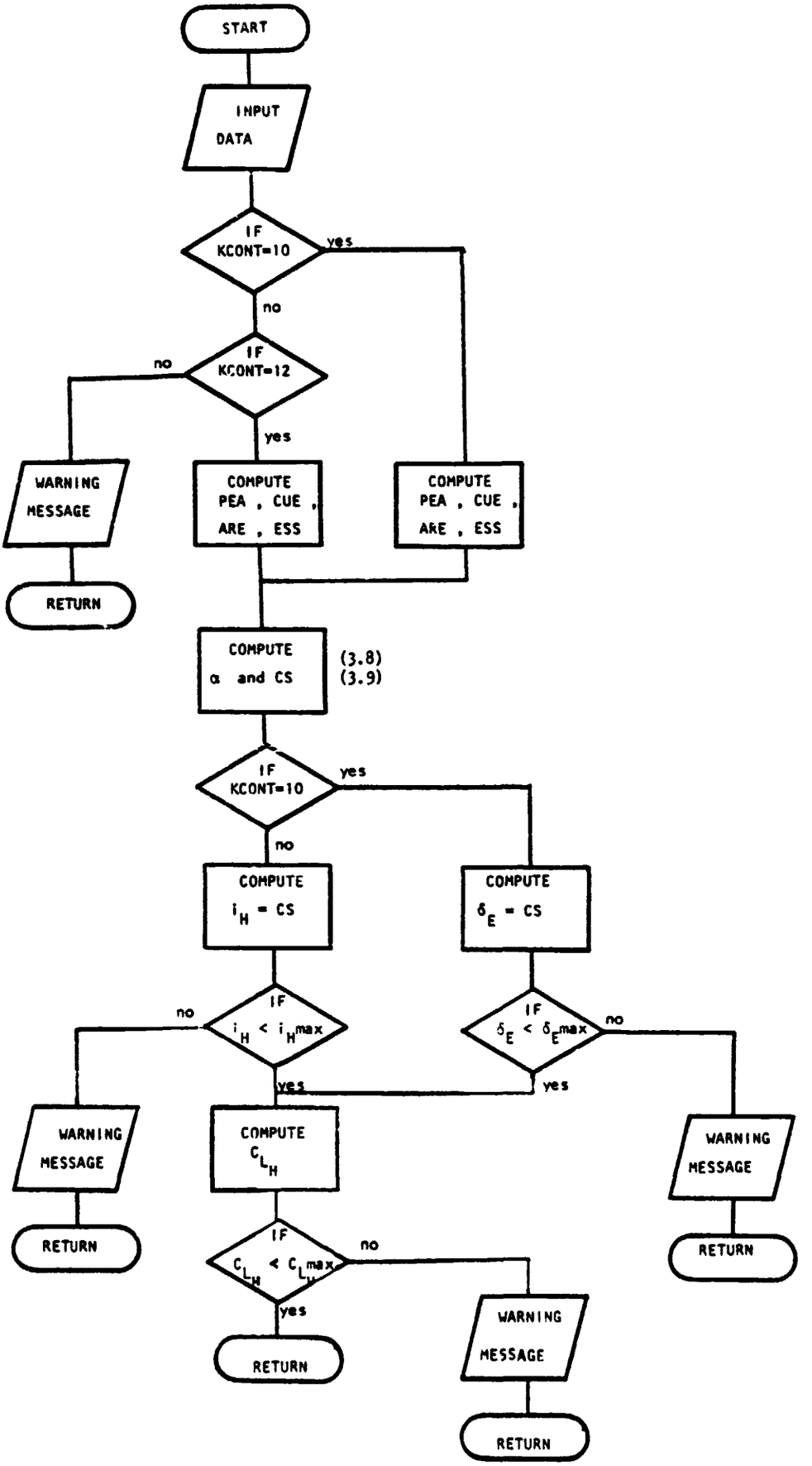

Figure 3.1: Flowchart for subroutine "TRIM"

```
CC15C***** SUBROUTINE TRIM (EYEH,DELTEL,CLHT)                          *****
0020C*****                                                             *****
0030C***** THIS SUBROUTINE CALCULATES TRIM ANGLES AND TAIL LOAD        *****
0040C***** NECESSARY FOR MOMENT EQUILIBRIUM IN CRUISE.                 *****
0050C*****                                                             *****
0051      DATA CL1,CLO,CLALP,CLIH,CLAH/.265,.06,6.76,.848,4.068/
0052      DATA CLDE,CMO,CMALP,CMIH,CMDE/.418,.047,-1.003,-2.693,-1.341/
0053      DATA DCLOP,DCLALP,DCLIHP,DCLAHP,DCLDEP,DCMOP/.0,.0,.0,.0,.0,.0/
0054      DATA DCMALP,DCMIHP,DCMDEP,DADDE,EPS,KCONT/.0,.0,.0,.5,.0654,12/
0055      DATA EYEHMI,EYEHMA,DELTMI,DELTMA/-.1414,.0175,-.2618,.2618/
0056      DATA CLHMIN,CLHMAX/-1.5,1.5/
0060         DIMENSION A(2,2),B(2)
0070         WRITE (6,5)
0080       5 FORMAT (10X,"KU-FRL DEVELOPED SUBROUTINE FOR CALCULATION")
0090         WRITE (6,10)
0100      10 FORMAT (10X,"OF TRIM ANGLES AND TAIL LOAD IN CRUISE")
0102         WRITE (6,11)
0104      11 FORMAT (10X,"TESTRUN LEARJET 26"///)
0110         IF (KCONT.EQ.10) GO TO 15
0120         IF (KCONT.EQ.12) GO TO 20
0130         WRITE (6,12) KCONT
0140      12 FORMAT (10X,"KCONT= ",I2,"   THIS IS AN ILLEGAL VALUE"//)
0150         GO TO 80
0160      15 CONTINUE
0170C*****                                                             *****
0180C***** THIS IS THE CASE IN WHICH THERE IS A FIXED STABILIZER       *****
0190C***** WITH AN ELEVATOR; THERE IS NO TRIM TAB.                     *****
0200C***** THE AIRPLANE IS TRIMMED WITH DELTA E.                       *****
0210C*****                                                             *****
0220         EYEH=.0
0230         PEA=CLDE+DCLDEP
0240         CUE=CMDE+DCMDEP
0250         ARE=(CLIH+DCLIHP)*EYEH
0260         ESS=(CMIH+DCMIHP)*EYEH
0270         GO TO 25
0280      20 CONTINUE
0290C*****                                                       *****
0300C***** THIS IS THE CASE IN WHICH THE AIRPLANE HAS AN ALL-     *****
0310C***** MOVING TAIL WITH AN ELEVATOR; THERE IS NO TRIM TAB.    *****
0320C***** THE AIRPLANE IS TRIMMED WITH IH WHILE DELTA E IS ZERO. *****
0330C*****                                                       *****
0340         DELTEL=.0
0350         PEA=CLIH+DCLIHP
0360         CUE=CMIH+DCMIHP
0370         ARE=.0
0380         ESS=.0
0390      25 CONTINUE
0395C*****                                                 *****
0400C***** COMPUTATION OF THE ELEMENTS OF THE               *****
0410C***** MATRIX EQUATION FOR TRIM WITH DELTA E OR IH      *****
0420C***** AND SOLUTION OF THE EQUATION                     *****
0425C*****                                                 *****
```


Figure 3.2: Listing of subroutine "TRIM"

```
0430        A(1,1)=CLALP+DCLALP
0440        A(1,2)=PEA
0450        A(2,1)=CMALP+DCMALP
0460        A(2,2)=CUE
0470        B(1)=CL1-CLO-DCLOP-ARE
0480        B(2)=-CMC-DCMOP-ESS
0490        DETER=A(1,1)*A(2,2)-A(1,2)*A(2,1)
0500        ALPHA=(B(1)*A(2,2)-B(2)*A(1,2))/DETER
0510        CS=(B(2)*A(1,1)-B(1)*A(2,1))/DETER
0520        RAD=57.29578
0530        IF (KCONT.EQ.10) GO TO 40
0540        EYEH=CS
0550        EYEDEG=EYEH*RAD
0560        DEDEG=DELTEL*RAD
0610C*****                                                    *****
0620C***** CHECK IF IH DOES NOT EXCEED ITS MAXIMUM VALUE *****
0630C*****                                                    *****
0640        IF (EYEH.GE.EYEHMI.AND.EYEH.LE.EYEHMA) GO TO 50
0650        WRITE (6,35) EYEDEG
0660     35 FORMAT (10X,"IH= ",1F10.3," DEG; EXCEEDS MAXIMUM VALUE"//)
0670        GO TO 80
0680     40 CONTINUE
0690        DELTEL=CS
0692        EYEDEG=EYEH*RAD
0694        DEDEG=DELTEL*RAD
0700C*****                                                    *****
0710C***** CHECK IF DELTA E DOES NOT EXCEED ITS MAXIMUM VALUE *****
0720C*****                                                    *****
0730        IF (DELTEL.GE.DELTMI.AND.DELTEL.LE.DELTMA) GO TO 50
0740        WRITE (6,45) DEDEG
0750     45 FORMAT (10X,"DELTA E= ",1F10.3," DEG; EXCEEDS MAXIMUM VALUE"//)
0760        GO TO 80
0770     50 CONTINUE
0780C*****                                                   *****
0790C***** CALCULATION OF HORIZONTAL TAIL LIFT COEFFICIENT   *****
0800C***** AND CHECK IF IT DOES NOT EXCEED ITS MAXIMUM VALUE *****
0810C*****                                                   *****
0820        CLHT=(CLAH+DCLAHP)*(ALPHA+EYEH-EPS+DADDE*DELTEL)
0830        IF (CLHT.GE.CLHMIN.AND.CLHT.LE.CLHMAX) GO TO 60
0840        WRITE (6,55) CLHT
0850     55 FORMAT (10X,"CLH= ",1F10.3,"  EXCEEDS MAXIMUM VALUE"//)
0860        GO TO 80
0870     60 CONTINUE
0880C*****              *****
0890C***** OUTPUT DATA *****
0900C*****              *****
0910        WRITE (6,65) EYEDEG
0920     65 FORMAT (10X,"IH=        ",1F10.5,"  DEG"//)
0930        WRITE (6,70) DEDEG
0940     70 FORMAT (10X,"DELTA E=   ",1F10.5,"  DEG"//)
0950        WRITE (6,75) CLHT
0960     75 FORMAT (10X,"CLH=       ",1F10.5//)
0970     80 WRITE (6,85)
0980     85 FORMAT (10X,"***** END OF SUBROUTINE TRIM *****"///)
0990        STOP
1000        END
```

Figure 3.2: continued

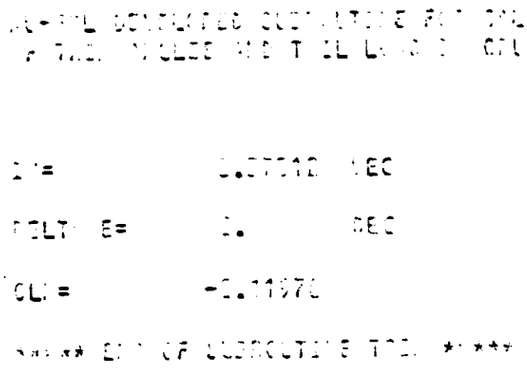

Figure 3.2: continued

3.5. REFERENCES

3.5.1: Roskam, J. — Flight Dynamics of Rigid and Elastic Airplanes, Roskam Aviation and Engineering Corporation, 1972, Lawrence, KS.

CHAPTER 4

GROUND EFFECT

4.1 INTRODUCTION

The method currently used in GASP to compute the ground effect is a simple one from Reference 4.1. This method uses only height above ground and aspect ratio as variables. However, References 4.2 and 4.3 indicate that, among other things, the lift coefficient generated by the wing is of great importance in determining the ground effect. Several methods for calculation of the ground effect were compared, and the method provided by Reference 4.4 was finally chosen for its completeness and relative simplicity.

4.2 DERIVATION OF EQUATIONS

In this chapter the method of Reference 4.4 will be described. Appendix B describes the other methods used in the evaluation. The method used in Reference 4.4 is based on a lifting line theory. In a situation where the ground is within a wingspan distance from the wing, a system of image vortices may be set up to account for the effect of ground proximity on the wing. The image vortex system is set up such that the boundary condition is met: i.e., the normal velocity on the ground plane is zero. Figure 4.1 depicts the situation.

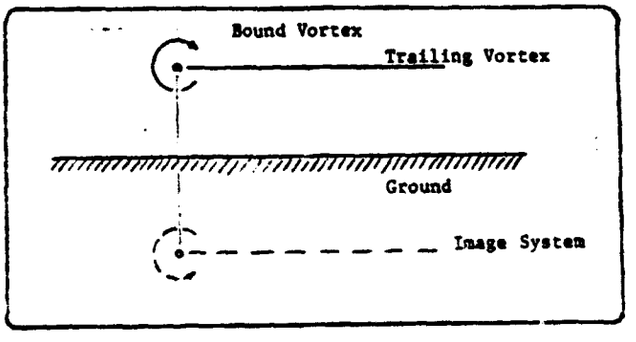

Figure 4.1: Image Vortex System

The effects of the image vortex system may be summarized as follows:

1. The image vortex of the bound vortex induces a velocity distribution in the opposite direction to the free stream velocity, thus reducing the lift. Also the camber and incidence of the wing airfoil are increased, thereby increasing the lift.
2. The image vortices of the trailing vortex system induce upwash at the wing which may be seen as an increase in wing angle of attack.

The effect of the bound image vortex may be found by applying Helmholtz's law which gives the decrease in speed at the airfoil:

$$\frac{\Delta V}{V_\infty} = \frac{C_\ell}{8\pi\ h/c} \tag{4.1}$$

From this the increase in angle of attack to maintain C_ℓ may be found as:

$$\Delta\alpha = \frac{C_\ell^{\,2}}{4\pi\ h/c\ C_{\ell_\alpha}} \tag{4.2}$$

The effective increase in camber is proportional to $\Delta V/V_\infty$ and the chord length inversely proportional to the height. By assuming that the average upwash induced by the image trailing vortex is equal to the upwash at the mid chord point, the decrease in angle of attack to maintain C_ℓ constant may be found as:

$$\Delta\alpha = -.25\ \frac{\Delta V}{V_\infty}\ \frac{c}{2h} = -\ \frac{C_\ell}{64\pi\ (h/c)^2} \tag{4.3}$$

For finite wings the effects described above are less due to the finite length of the vortices. A correction factor β takes this into account. The total effect of the bound image vortex may now be found from:

$$\Delta\alpha_1 = \beta \frac{C_L}{4\pi\ h/c_g} \left(\frac{C_L}{C_{L_\alpha}} - \frac{1}{16\ h/c_g} \right) \tag{4.4}$$

where:

$$\beta = 1 + (2\ h_{eff}/b)^2 - 2\ h_{eff}/b \tag{4.5}$$

The effective height h_{eff} is as defined in Figure 4.2.

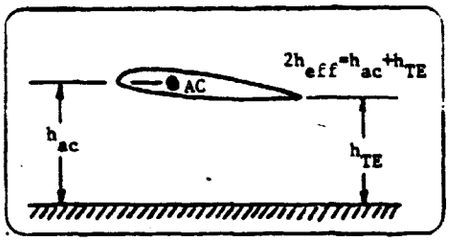

Figure 4.2: Definition of Effective Height

The induced upwash due to the images of the trailing vortex may be seen as a reduction in angle of attack to maintain C_ℓ constant:

$$\Delta_2\alpha = -\sigma\alpha_1 \tag{4.6}$$

$$\text{where:} \quad \alpha_1 = C_L/\pi AR \tag{4.7}$$

$$\sigma = \text{EXP}\left[-2.48\ (2\ h_{eff}/b)^{.768} \right] \tag{4.8}$$

Again, σ is a correction factor which takes the finite length of the vortices into account. A general expression for swept wings of arbitrary aspect ratio is:

$$\Delta_2\alpha = -\sigma C_L \left(1/C_{L_\alpha} - 1/C_{\ell_\alpha} \right) \tag{4.9}$$

The total effect of the ground on the wing lift is as seen in Figure 4.3.

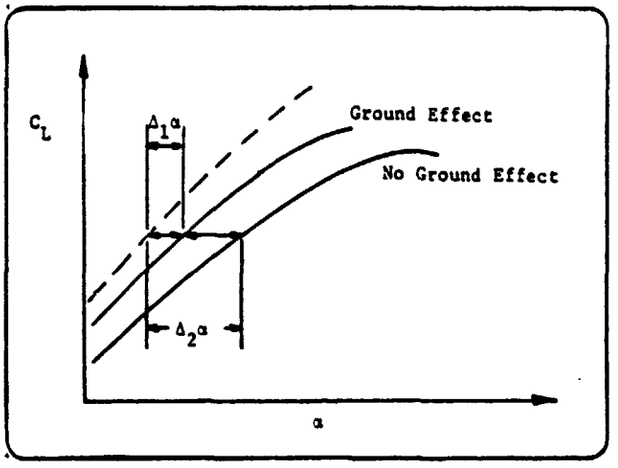

Figure 4.3: Total Effect of Ground-Proximity on Wing Lift

There are several other effects of ground proximity on the lift of the complete aircraft, generally of lesser importance than the effects described above. They are the following:

1. The image vortex system induces an upwash at the horizontal tailplane, thereby changing the lift. Also ground effect causes a shift in the wing center of pressure which causes a moment to be counteracted by elevator deflection. Furthermore, the image vortices of the tailplane itself causes upwash or downwash. All these effects are not easily calculated and of relatively small magnitude and therefore will be disregarded.

2. The pressure distribution around the airfoil changes considerably within ground proximity. The attainable $C_{L_{MAX}}$ usually will be decreased, which can have an important influence on V_{MU}. Again these effects cannot be expressed in a readily usable format.

Summarizing, the total effect of the ground proximity on the airplane lift may be expressed as:

$$\frac{C_L}{C_{L_\infty}} = 1+\sigma-\left[\frac{\sigma \mathcal{R} \cos\Lambda_{1/2}}{2\cos\Lambda_{1/2}+ \mathcal{R}^2 +(2\cos\Lambda_{1/2})^2}\right]-\left[\frac{\beta}{4\pi h/c_g}\left(C_{L_\infty}-\frac{C_{L_\alpha}}{16h/\bar{c}}\right)\right] \quad (4.10)$$

This expression provides the lift increase at constant angle of attack.

To account for the effect of flap deflection on height above the ground, the following expression was derived (see Figure 4.4):

The height of the trailing edge is:

$$h_{TE} \simeq h_{ac} - h_f \quad \text{(disregarding } h_c\text{)} \quad (4.11)$$

$$\text{or: } h_{TE} \simeq h_{ac} - \text{SIN } \delta_f \left(\frac{c_f}{c}\right)(c) \quad (4.12)$$

For the effective height, h_{eff}, it is seen that:

$$h_{eff} \simeq 2\, h_{ac} - \text{SIN } \delta_f \left(\frac{c_f}{c}\right)(c) \quad (4.13)$$

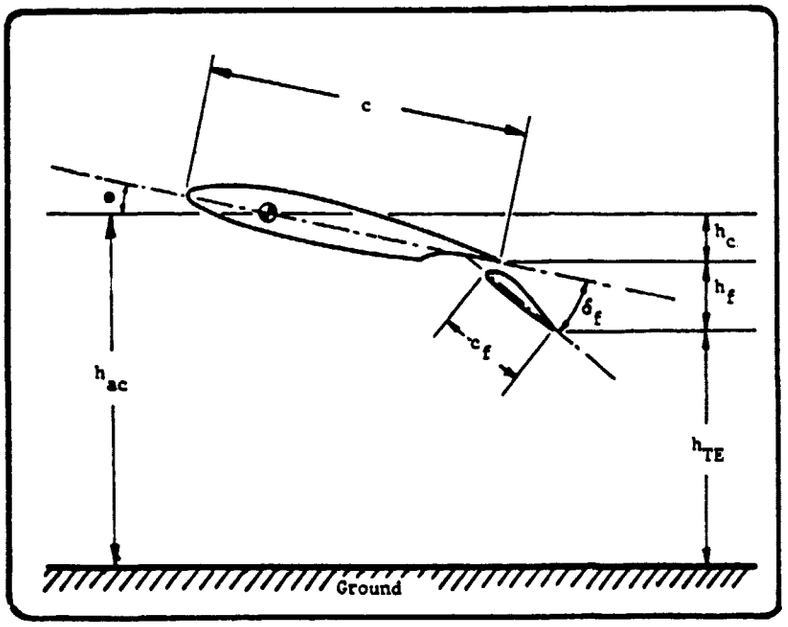

Figure 4.4: Definition of Geometry Parameters

4.3 DESCRIPTION OF PROGRAM

A flowchart for the program is shown in Figure 4.5. The program essentially only calculates the ground effect factor $K_{C_{LGE}}$. Elsewhere, in the calling routine, this factor is used to calculate the increase (or decrease) in lift for a given angle of attack or to calculate the change in angle of attack for a given lift coefficient. Shown in Figure 4.6 is a listing and a sample output of the program.

Table 4.1 shows a listing of the computer parameters. Appendix A shows a comparison with other methods.

4.4 HAND CALCULATION

A hand calculation of subroutine GROUND for Airplane A is given in Appendix A.

TABLE 4.1 VARIABLE NAMES AND ORIGINS IN SUBROUTINE GROUND

NAME	ENG. SYMBOL	DIMENSION	ORIGIN	REMARKS
ALPHA	α	deg	Calling Subroutine	
ALPHLO	α_o	deg	Common	
AR	AR	---	Common	
B	b	ft	Common	
BETAG	β	---	---	Correction Factor
C3	c_3	---	---	Dummy
C4	c_4	---	---	Dummy
CBARW	$\bar{c}_w$	ft	Common	
CFOC	ϵ_f/c	---	Common	

TABLE 4.1 VARIABLE NAMES AND ORIGINS IN SUBROUTINE GROUND (Continued)

NAME	ENG. SYMBOL	DIMENSION	ORIGIN	REMARKS
CLALPH	C_{L_α}	rad^{-1}	Calling Subroutine	
CLOGE	$C_{L_{OGE}}$	---	---	Dummy
DELCL	$\Delta C_{L_{LAND}}$	---	---	Dummy
DELCLL	$\Delta C_{L_{LAND}}$	rad	Common	
DELCLP	$\Delta C_{L_{power}}$			
DELCTO	$\Delta C_{L_{T.O}}$	---	Common	
DELFL	δ_{f_L}	rad	Common	
DELF	δ_f	deg	Common	
DLMC4	$\Lambda_{1/4c}$	deg	Common	
DLMC2	$\Lambda_{1/2c}$	deg	---	Dummy
HAC	h_{ac}	ft	Calling Subroutine	
HEFF	---	---		
KCLGE	$K_{C_{LGE}}$	---	---	
RELF	δ_f	rad	---	Dummy
RLMC4	$\Lambda_{1/4c}$	rad	---	Dummy
RLMC2	$\Lambda_{1/2c}$	rad	---	Dummy
SIGMA	σ	---	---	Dummy
SLM	λ	---	Common	

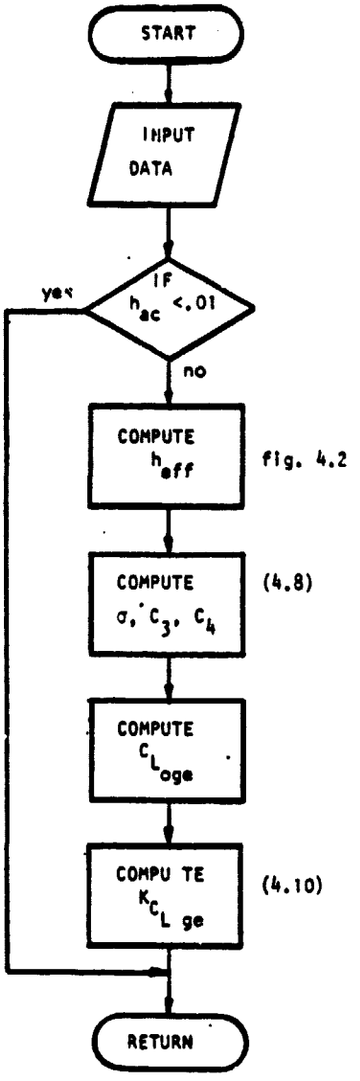

Figure 4.5: Flowchart of subroutine "GROUND"

```
      FUNCTION KCLGE (DELF,CFCC,CLALPH,ALPHA,ALPHLO,
     1DELCL,DELCLP,HAC)
C
C     THIS SUBROUTINE CALCULATES THE GROUND EFFECT
C     FACTOR ACCORDING TO THE TORENBEEK METHOD
C
      COMMON/WING/DLMC4,AR,SLM,B,CRCLW,CBARW,SW,CLAMP
      REAL KCLGE
      IF (ILIFT.EQ.2.OR.ILIFT.EQ.5) GOTO 10
       RELF=.0174533*DELF
      IF (HAC.LE.0.01) GO TO 105
      HEFF=2.*HAC-SIN(RELF)*CFCC*CBARW
      SIGMA=EXP(-2.45*(HEFF/B)**.768)
      BETAG=SQRT(1+(HEFF/B)**2.)-HEFF/B
      RLMC4=.0174533*DLMC4
      RLMC2=ATAN(SIN(RLMC4)/COS(RLMC4)-((1.-SLM)/(1.+SLM)))/AR)
      C3=2.*COS(RLMC2)+SQRT(AR**2.+(2.*COS(RLMC2))**2.)
      C4=BETAG/(12.5664*HAC/CBARW)
      CLCGE=CLALPH*.0174533*(ALPHA-ALPHLO)+DELCL+DELCLP
C
C      NOW THE GROUND EFFECT FACTOR IS CALCULATED
C
      KCLGE=1.+SIGMA-SIGMA*AR*COS(RLMC2)/C3-C4*(CLCGE-CLALPH/
     2(16.*HEFF/CBARW))
  105 CONTINUE
      RETURN
    END
```

HAC	HEFF	KCLGE
45.7560	90.0685	1.0002
43.4682	85.4929	1.0004
41.1804	80.9173	1.0008
38.8926	76.3417	1.0012
36.6048	71.7661	1.0018
34.3170	67.1905	1.0025
32.0292	62.6149	1.0034
29.7414	58.0393	1.0046
27.4536	53.4637	1.0060
25.1658	48.8881	1.0079
22.8780	44.3125	1.0102
20.5902	39.7369	1.0132
18.3024	35.1613	1.0171
16.0146	30.5857	1.0219
13.7268	26.0101	1.0282
11.4390	21.4345	1.0362
9.1512	16.8589	1.0463
6.8634	12.2833	1.0591
4.5756	7.7077	1.0761
2.2878	3.1321	1.1422

Figure 4.6: Listing and sample printout of subroutine "GROUND"

4.5 REFERENCES

4.1	Perkins, C.D. Hage, C.D.	Airplane Performance, Stability and Control, New York, John Wiley & Sons, 1949.
4.2	Corning, G.	Supersonic and Subsonic Airplane Design, Published by the author, 1953.
4.3	Baker, P.A. Schweikhard, W.G.	Flight Evaluation of Ground Effect on Several Low-Aspect-Ratio Airplanes. NASA TN D-6053. 1970.
4.4	Hoak, D.E. Ellisson, D.E.	USAF Stability and Control Datcom. Air Force Flight Dynamics Laboratory, Wright Patterson Air Force Base, Ohio, 44533.

CHAPTER 5

POWER EFFECTS

5.1 INTRODUCTION

This chapter describes the subroutine that calculates the effect of power on lift and moment along the Y-axis. The program uses formulas and empirical data compiled from several references. The current setup only calculates propeller effects. However, the calculation of the effect of jet engines is far more straightforward.

5.2.1 DERIVATION OF EQUATIONS, EFFECTS ON LIFT

The effect of power on the aircraft characteristics may be split up in two parts:

- Direct effect due to propeller forces
- Indirect effect due to propeller slipstream.

The direct effects are the following (see Figure 5.1):

1. The propeller normal force adds to the total lift force.
2. The propeller thrust force adds to the total lift force.

The indirect forces are the following (see Figure 5.2):

3. Due to the slipstream over the wing (increased velocity), there will be an increase in wing normal force.
4. The propeller slipstream will act as a form of boundary layer control, thereby influencing the maximum attainable lift coefficient.
5. Due to the increase in velocity at the tail location, there will be a change in tail-lift.

6. The downwash at the tail will be influenced.

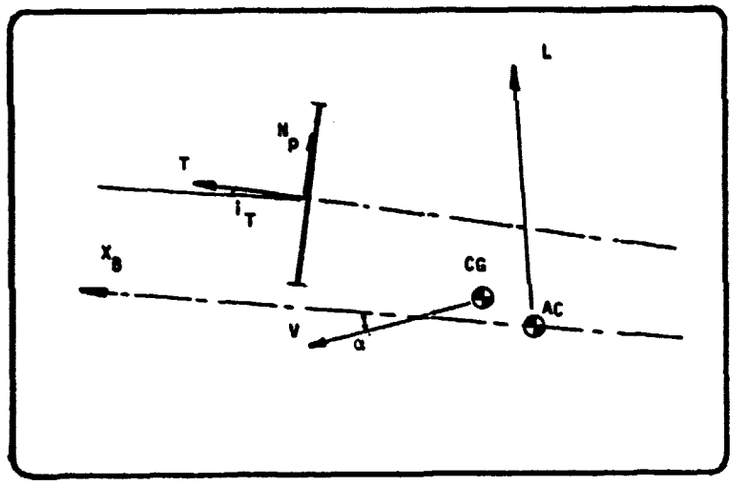

Figure 5.1: Direct effect of power

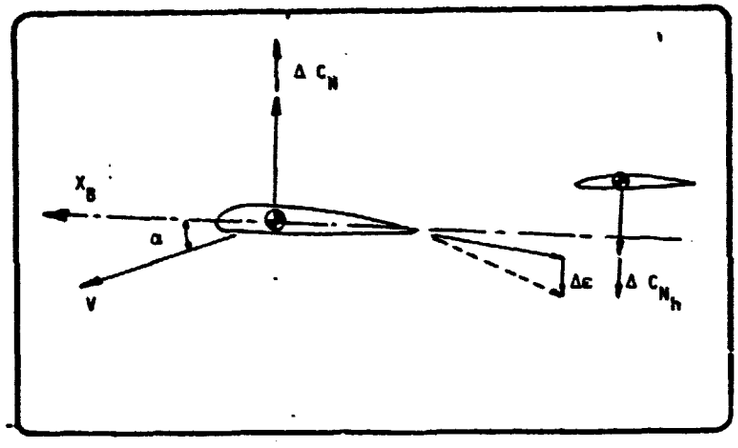

Figure 5.2; Indirect effects of power

The total lift coefficient of the airplane may now be expressed as:

$$C_L = C_{L_{Prop-off}} + (\Delta C_L)_T + (\Delta C_L)_{NP} + (\Delta C_L)_{\Delta \bar{q}_W} + (\Delta C_L)_{\varepsilon_p} + (\Delta C_{L_H})_{\Delta \bar{q}_H} + (\Delta C_{L_H})_{\Delta \varepsilon_H}$$

Wing — Horizontal Tail

Propeller Forces — Propeller Slipstream Effects

(5.1)

5.2.1.1 EFFECT OF PROPELLER FORCES

The definition of the geometric parameters is as given in Figure 5.3.

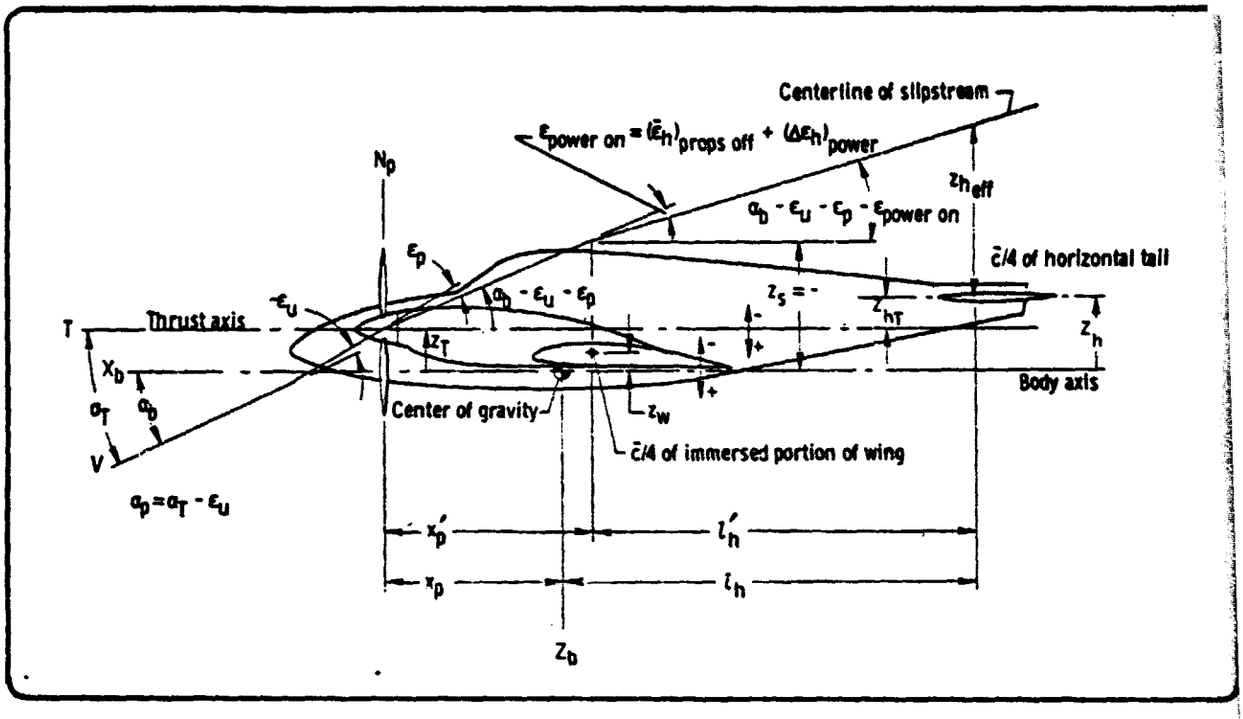

Figure 5.3.a: Definition of geometric parameters

The contribution of the thrust vector to lift is obtained from:

$$(\Delta C_L)_T = N\ (T_c'/prop)\ \sin \alpha_T \qquad (5.2)$$

where:

N is the number of engines

$$T_c'/prop = \frac{Thrust/prop}{\bar{q}_\infty S_W} \qquad (5.2.a)$$

$$\alpha_T = \alpha_b + i_T \qquad (5.2.b)$$

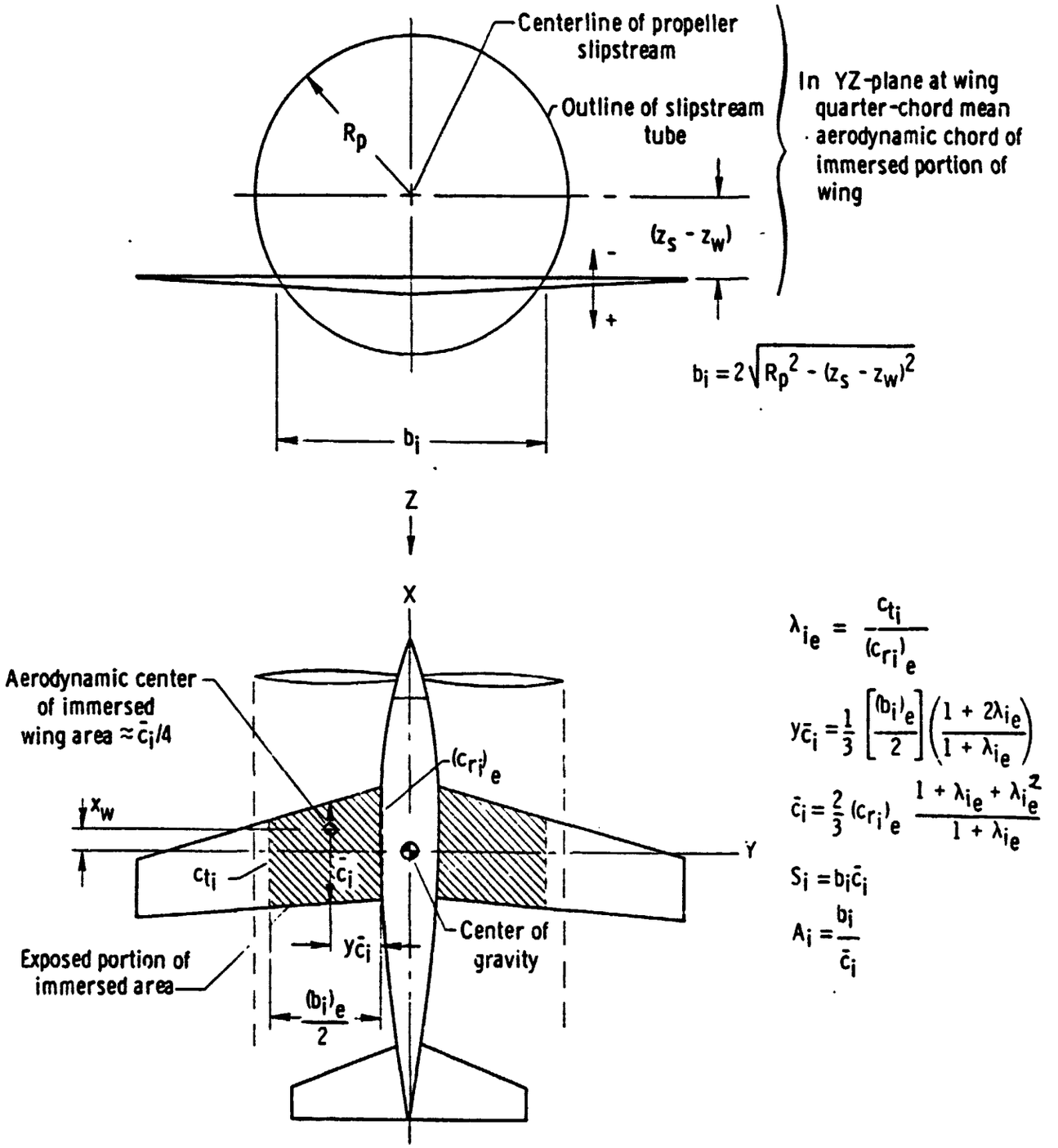

Figure 5.3.b: Definition of geometric parameters, single engine

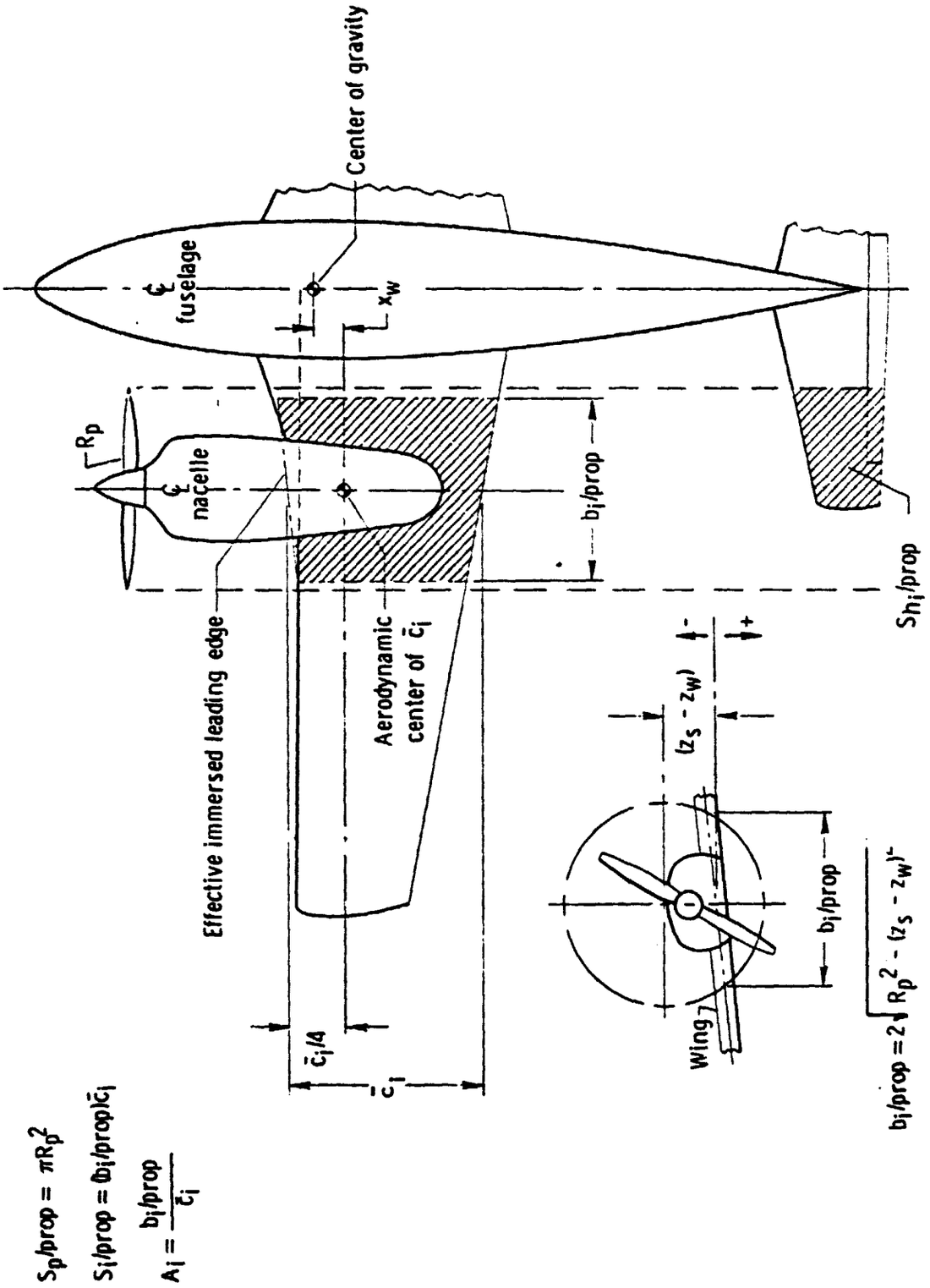

Figure 5.3.c: Definition of geometric parameters, multi engine

The contribution of the propeller normal force to the lift is obtained from the following equation from Reference 5.1:

$$(\Delta C_L)_{N_p} = N\, f\, C_{y,\psi_0}\, \alpha_p \cos\alpha_T \frac{S_p/\text{prop}}{S_W} \qquad (5.3)$$

where:

f is the propeller inflow factor from Figure 5.4 as a function of

$$T_c = (T/\text{prop})/\rho V^2 D^2 \qquad (5.3.a)$$

C_{y,ψ_0} is a function of propeller type and operating condition. The values for a particular propeller family are given in Figure 5.5. Extrapolation to other propellers can be made by means of Figure 5.6 on the basis of the "side-force factor", SFF. This is a geometrical propeller parameter, approximated by Equation (5.4.)

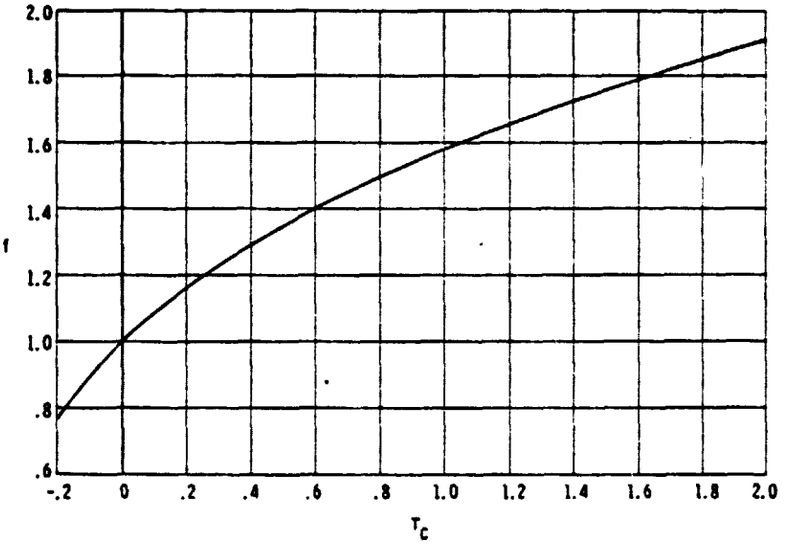

Figure 5.4: Variation of f with T_c (ref 5.1)

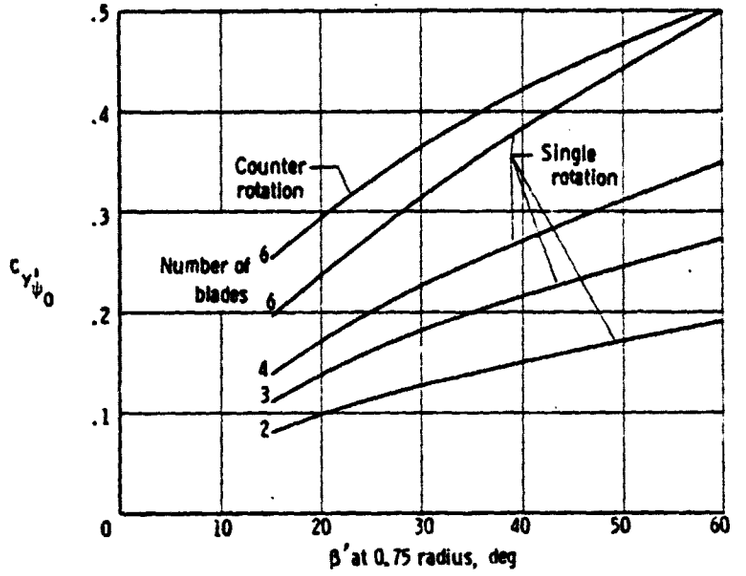

Figure 5.5: Propeller side-force coefficient (ref 5.1)

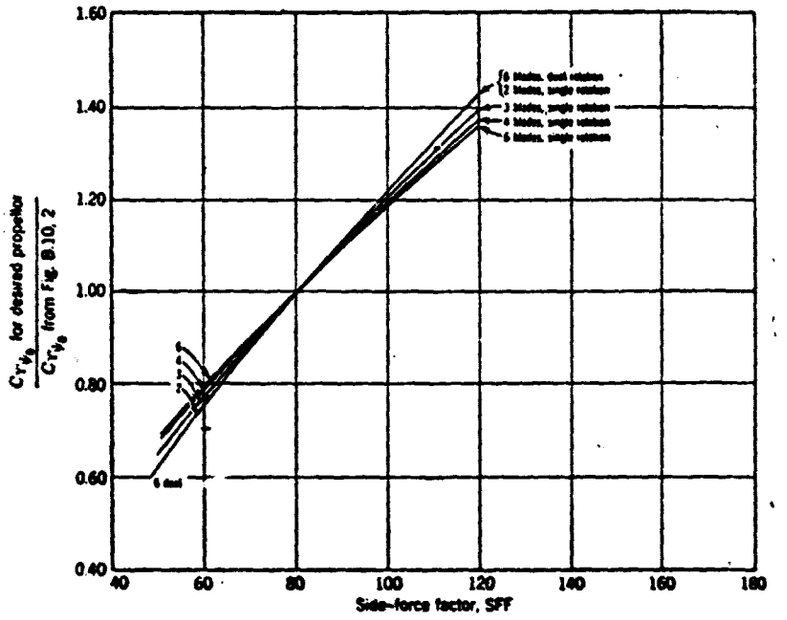

Figure 5.6: Propeller side-force coefficient as function of SFF (ref 5.1)

The propeller side force factor is given by:

$$SFF = 525\ [(b/D)_{0.3} + (b/D)_{0.6}] + 270\ (b/D)_{0.9} \qquad (5.4)$$

where:

b/D is the ratio of blade width to propeller diameter and the subscript is the relative radius at which the ratio is measured.

The local angle of attack of the propeller plane, α_p, may be obtained from:

$$\alpha_p = \alpha_T - \frac{\partial \varepsilon_u}{\partial_\alpha} (\alpha_W - \alpha_0) \qquad (5.5)$$

where:

$-\frac{\partial \varepsilon_u}{\partial_\alpha}$ is the upwash gradient at the propeller, obtained from Figure 5.7.

α_W is the wing angle of attack:

$\alpha_W = \alpha_b + i_W$

α_0 is the zero lift angle of the wing

The total effect of propeller side force on lift may now be calculated as follows:

$$(\Delta C_L)_{N_p} = N\ f\ C_{y'_{\psi_0}} \left[\frac{C_{y'_{\psi_0}} \text{ for desired prop}}{C_{y'_{\psi_0}} \text{ from Figure 5.5}}\right] \left|\alpha_T - \frac{\partial \varepsilon_u}{\partial_\alpha}(\alpha_W - \alpha_0)\right| \left(\frac{(S_p/\text{prop})}{S_W}\right) \qquad (5.6)$$

Using HP 65 curve fitting routines, the following approximations were found:

$$f = 0.652 + 1.183\ LN\ (T_c + 1.3) \qquad (5.7)$$

$$C_{y'_{\psi_0}} = 0.013\beta_{0.75}^{.0657} + \{0.0125 + 0.001125\ \beta_{0.75}\}\ (B_L - 2) \qquad (5.8)$$

where:

$\beta_{0.75}$ is the blade angle at 75% of the propeller radius (in degrees)

$$\frac{C_{y_{\psi_0}}\ \text{actual prop}}{C_{y_{\psi_0}}\ \text{ref prop}} = -2.938 + 0.901\ Ln(SFF) \qquad (5.9)$$

$$\frac{\partial \epsilon_u}{\partial \alpha} = -0.1136\left(\frac{X_p'}{C_i}\right)^{-1.8141} - 0.027\ (AR - 4) \qquad (5.10)$$

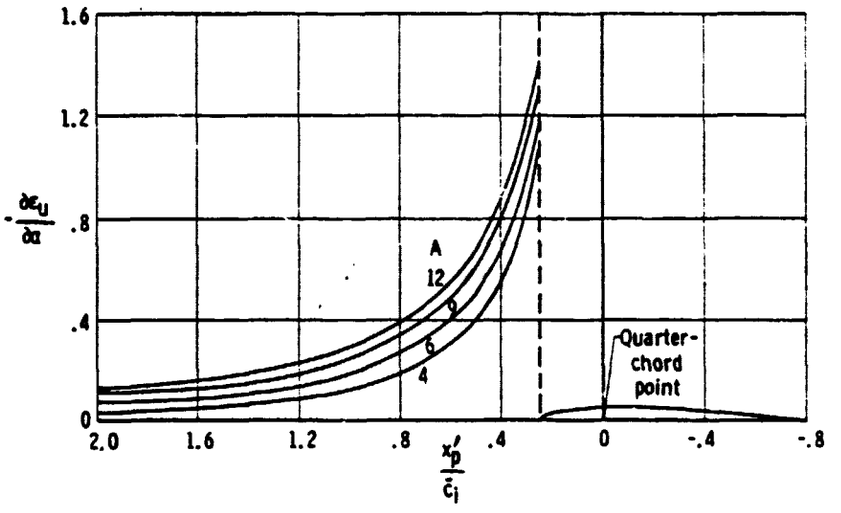

Figure 5.7: Upwash gradient at plane of symmetry for unswept wings (ref 5.2)

5.2.1.2 EFFECT OF PROPELLER SLIPSTREAM, INCREASE IN DYNAMIC PRESSURE

The contribution of power to lift due to change in dynamic pressure on the immersed portion of the wing is obtained from the following equation from Reference 5.2:

$$(\Delta C_L)_{\Delta \bar{q}_W} = N\ K_1 \left(\frac{\Delta \bar{q}_W}{\bar{q}_\infty}\right)\left(C_{L_W}\right)_{\text{prop off}}\left(\frac{(S_i/\text{prop})}{S_W}\right) \qquad (5.11)$$

where:

K_1 is an empirical correlation parameter for additional wing lift due to the power effects. May be obtained from Figure 5.8.

$\frac{\Delta\bar{q}_W}{\bar{q}_\infty}$ is the increase in dynamic pressure due to propeller slipstream on the immersed portion of the wing, as given by Equation 5.12:

$$\frac{\Delta\bar{q}_W}{\bar{q}_\infty} = \frac{S_W\ (T_c'/\text{prop})}{\pi\ R_p^2} \tag{5.12}$$

S_i/prop is the portion of the wing immersed in the propeller slipstream (per propeller), obtained from Figure 5.3 with:

$$S_i/\text{prop} = (b_i/\text{prop})\ C_i \tag{5.13}$$

where:

$$b_i/\text{prop} = 2\sqrt{R_p^2 - (Z_S - Z_W)^2} \tag{5.14}$$

$$Z_S = -X_p'\ (\alpha_b - \varepsilon_u - \varepsilon_p) + Z_T \tag{5.15}$$

The upwash at the propeller plane is obtained from Equation (5.10) and:

$$-\varepsilon_u = -\frac{\partial\varepsilon_u}{\partial\alpha}\ (\alpha_W - \alpha_0) \tag{5.16}$$

The propeller-induced downwash is given by:

$$\varepsilon_p = \frac{\partial\varepsilon_p}{\partial\alpha_p}\ \alpha_p \tag{5.17}$$

The derivative $\partial\varepsilon_p/\partial\alpha_p$ follows from Reference 5.2:

$$\frac{\partial\varepsilon_p}{\partial\alpha_p} = C_1 + C_2\left(C_{y'_{\psi_0}}\right)_p \tag{5.18}$$

where:

C_1 and C_2 follow from Figure 5.9, and

$\left(C_{y'_{\psi_0}} \right)_p$ follows from section 5.2.1.

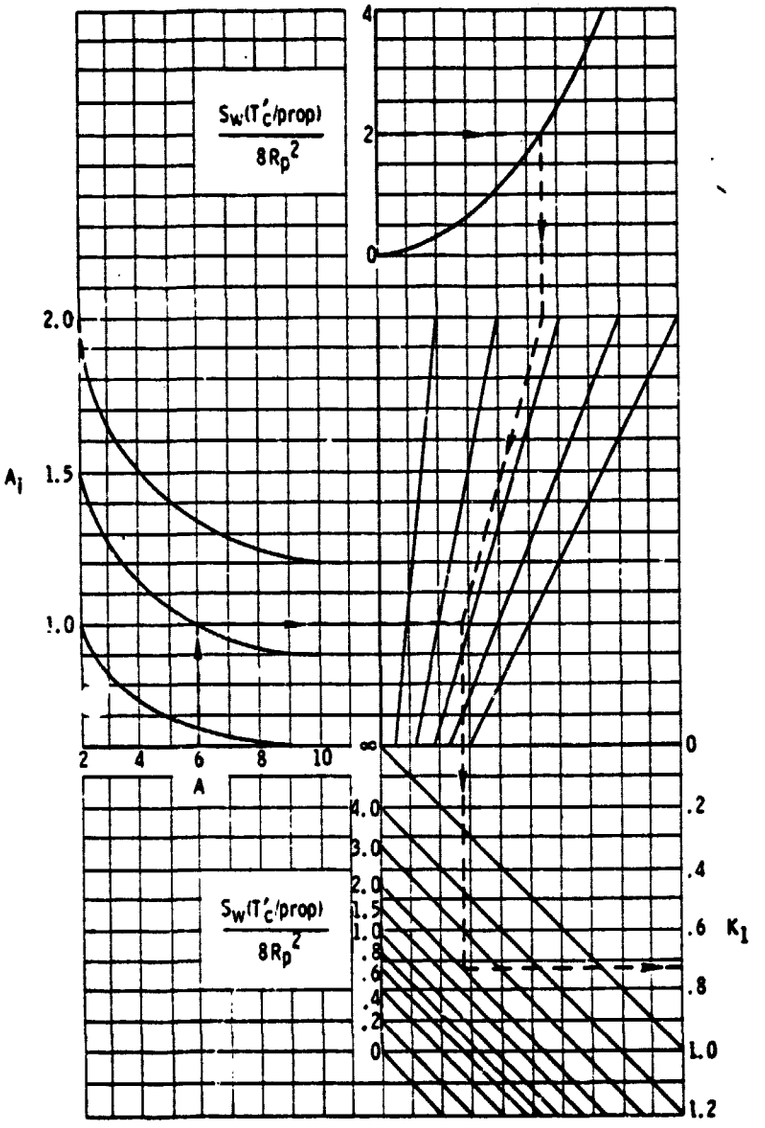

Figure 5.8: Empirical correlation factor for additional lift due to slipstream (ref 5.2)

Propeller angle of attack is given by Equation (5.5). Using HP 65 curve fitting routines, it may be found for Figure 5.8:

$$X_1 = 2.6384\ A_i^{2.0312} + (-3.8116 + 4.2237\ A_i - 1.6186\ A_i^2)\ A + \\ + (0.0418\ A_i^{1.3383})\ A^2 \qquad (5.19)$$

$$X_2 = 1.9938 + 1.2194\ LN\left(\frac{S_W(T_c'/prop)}{8\ R_p^{\ 2}}\right) \qquad (5.20)$$

$$X_3 = \frac{X_2(X_1 + 3)}{10} \qquad (5.21)$$

$$K_1 = + 0.9191\ e^{\left(-0.3663\ \frac{S_W\ (T_c'/prop)}{8\ R_p^{\ 2}}\right)} + \frac{X_3}{5} \qquad (5.22)$$

The equation for the propeller induced downwash was found to be:

$$\frac{\partial \epsilon_p}{\partial \alpha_p} = 0.3732 + 0.1703\ LN\left(\frac{S_W\ (T_c'/prop)}{8\ R_p^{\ 2}}\right) + \\ + \left[0.2155 - 0.0504\left(\frac{S_W(T_c'/prop)}{8\ R_p^{\ 2}}\right)\right]\left(C_{y'_{\psi_0}}\right)_p \qquad (5.23)$$

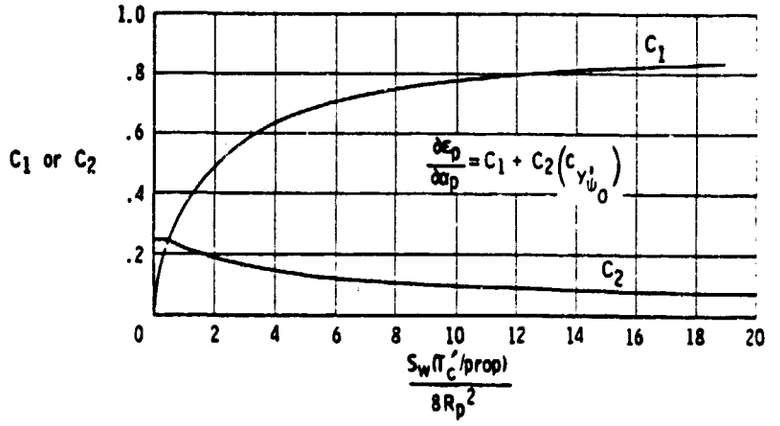

Figure 5.9: Propeller induced downwash (ref 5.2)

5.2.1.3 EFFECT OF PROPELLER SLIPSTREAM, PROPELLER DOWNWASH ϵ_p

The contribution of power to lift due to change in angle of attack as a result of propeller downwash, ϵ_p, may be obtained from:

$$(\Delta C_L)_{\epsilon_p} = N\left(1 + \frac{\Delta \bar{q}_W}{\bar{q}_\infty}\right)\left(C_{L_\alpha}\right)_{\substack{\text{prop} \\ \text{off}}} (\Delta\alpha)_{S_i} \frac{(S_i/\text{prop})}{S_W} \qquad (5.24)$$

(Ref. 5.2)

where:

$\frac{\Delta \bar{q}_W}{\bar{q}_\infty}$ is defined by Equation (5.12)

S_i/prop is defined by Equation (5.13)

and

$$(\Delta\alpha)_{S_i} = -\frac{\epsilon_p}{1 - \frac{\partial \epsilon_u}{\partial \alpha}} \quad \text{is the change in angle of attack} \qquad (5.25)$$

5.2.1.4 EFFECT OF POWER ON MAXIMUM LIFT

So far the effect of power on lift at discrete angles of attack has been calculated. Power also has an effect on maximum attainable lift, since the angle of attack at which stall occurs first will be increased with power. This depends primarily on the ratio of immersed wing area to total wing area. Figure 5.10 illustrates the effect.

The increment in maximum lift due to power may be obtained from the following empirical equation:

$$\Delta C_{L_{MAX}} = K_2 \, (\Delta C_L')_{\text{Power}} \qquad (5.26)$$

where:

$(\Delta C_L')_{\text{Power}}$ is the increment in tail-off lift due to power at power-off maximum lift angle of attack.

K_2 is a correction for immersed wing area, obtained from Figure 5.11.

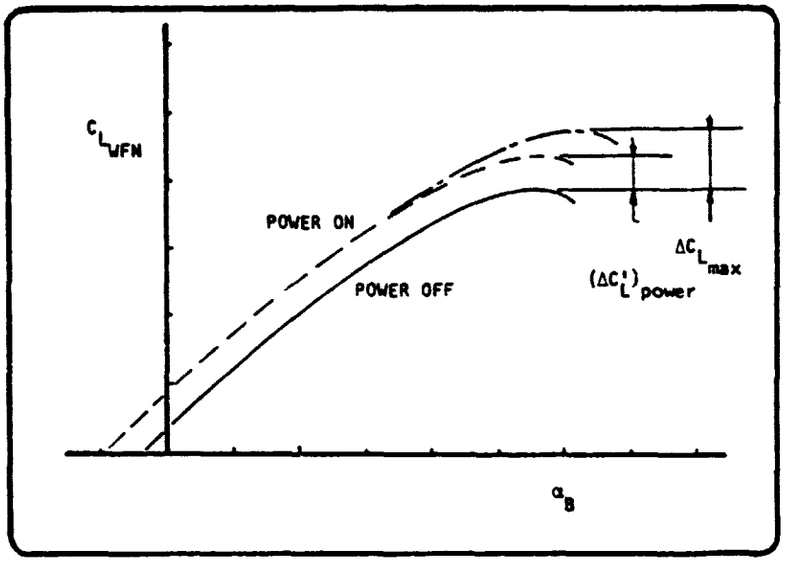

Figure 5.10: Effect of power on maximum lift

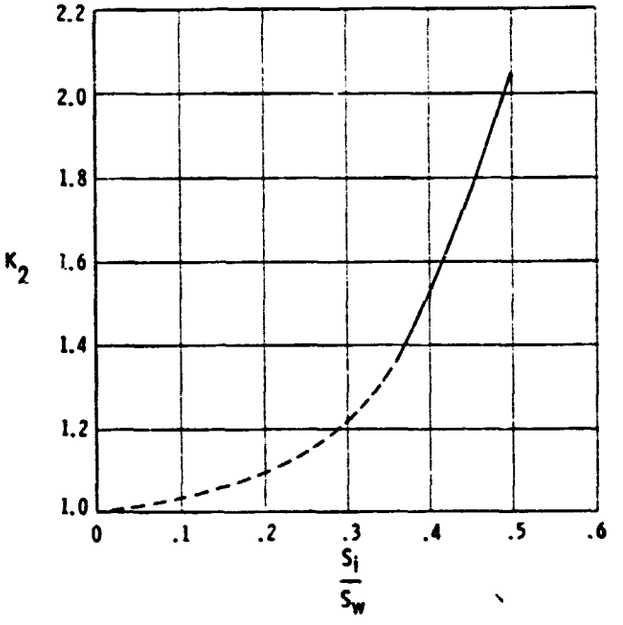

Figure 5.11: Correction factor for maximum lift (ref 5.2)

Using a HP 65 curve-fitting routine, it was found for the Factor K:

$$K_2 = 1.1854 - 2.1129 \frac{S_i}{S_W} + 7.6104 \left(\frac{S_i}{S_W}\right)^2 \qquad (5.27)$$

By using the foregoing procedures, the tail-off lift characteristics of the airplane can be calculated. Now the effect of power on the tail-plane lift will be calculated. The effect of the change in lift of the horizontal tail on the total lift of the airplane is small; however, the effect on pitching moment is significant.

5.2.1.5 EFFECT OF POWER INDUCED DOWNWASH ON HORIZONTAL TAIL-LIFT

The power induced change in downwash at the tail, $(\Delta\varepsilon_H)_{Power}$, may be estimated for single engine airplanes by using Figure 5.12 or for multiengine airplanes by using Figure 5.13. These figures are from Reference 5.2. The variables involved are:

$(\bar{\varepsilon}_H)_{props\ off}$	Propeller-off downwash angle calculated in subroutine DOWNWS.
T'_c/prop	Propeller thrust coefficient.
S_W	Wing area.
R_p	Propeller radius.
Z_{H_T}	Distance from thrust axis to horizontal tail (see Figure 5.3).

By using HP 65 curve-fitting routines, the following approximations may be found from Figures 5.12 and 5.13. The effect of power on downwash for single engine airplanes may be calculated with:

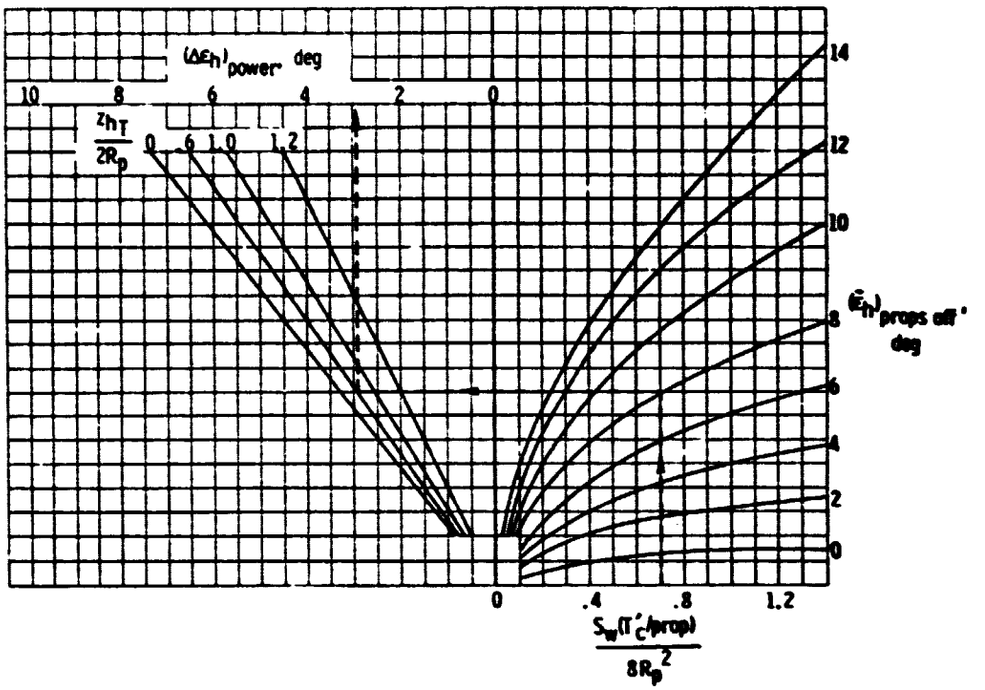

Figure 5.12: Effect of power on downwash for single engine airplanes (ref 5.2)

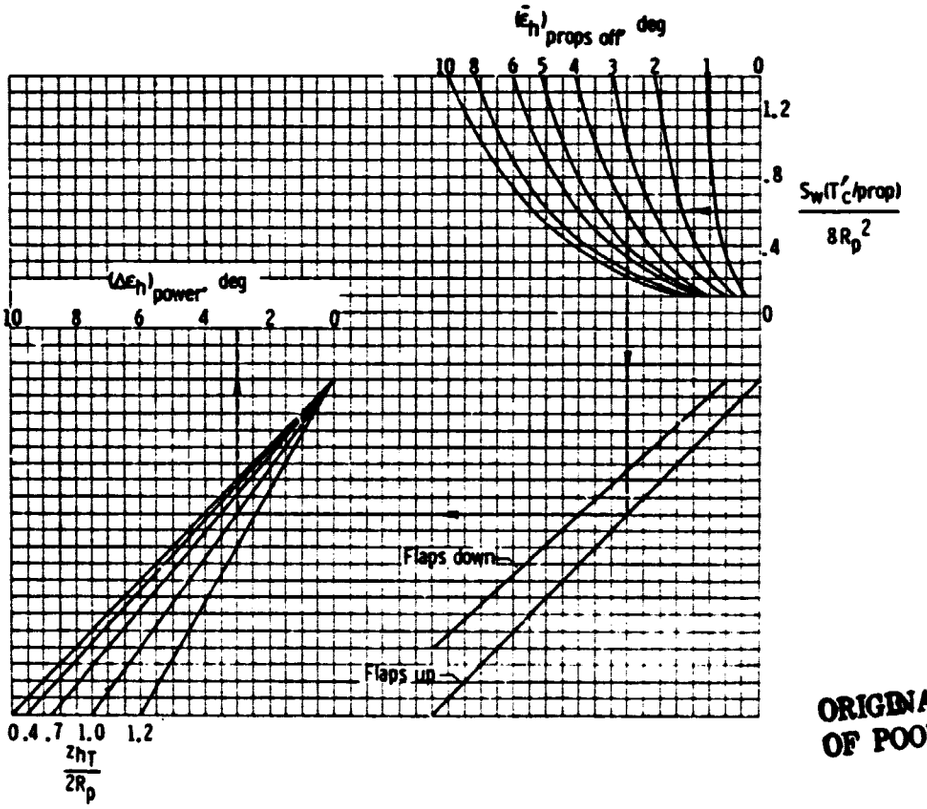

Figure 5.13: Effect of power on downwash for multiengine airplanes (ref 5.2)

$$X_4 = 0.5376e^{0.0688(\bar{\varepsilon}_h)_{\text{props off}}} + 0.4366(\bar{\varepsilon}_h)^{1.2345}_{\text{props off}} \left(\frac{S_W(T_c'/\text{prop})}{8\,R_p^2}\right) -$$

$$0.1091(\bar{\varepsilon}_h)^{1.3152}_{\text{props off}} \left(\frac{S_W(T_c'/\text{prop})}{8\,R_p^2}\right)^2 \qquad (5.28)$$

$$(\Delta\varepsilon_H)_{\text{Power}} = X_4 \left\{ 0.8189 - 0.0185 \frac{Z_{H_T}}{2R_p} - 0.1953 \left(\frac{Z_{H_T}}{2R_p}\right)^2 \right\} \qquad (5.29)$$

For multiengine airplanes the following equations can be used:

$$X_5 = -1.0234 + 0.9775(\bar{\varepsilon}_H)_{\text{prop off}} - 0.1032(\bar{\varepsilon}_H)^2_{\text{prop off}} +$$

$$+ \left\{ 3.5191 - 0.2409(\bar{\varepsilon}_H)_{\text{prop off}} + 0.2025(\bar{\varepsilon}_H)^2_{\text{prop off}} \right\} \left(\frac{S_W(T_c'/\text{prop})}{8\,R_p^2}\right) -$$

$$0.8738e^{0.2253(\bar{\varepsilon}_H)_{\text{prop off}}} \left(\frac{S_W(T_c'/\text{prop})}{8\,R_p^2}\right)^2 \qquad (5.30)$$

$X_6 = X_5$(No Flaps) (5.31.a) OR $X_6 = 0.5 + 0.889\,X_5$ (Flaps) (5.31.b)

where: $(\varepsilon_H)_{\text{power off}}$ in degrees.

$$(\Delta\varepsilon_H)_{\text{power}} = \left\{ 0.9951 + 0.0419 \frac{Z_{H_T}}{2R_p} - 0.3021 \left(\frac{Z_{H_T}}{2R_p}\right)^2 \right\} X_6 \qquad (5.32)$$

where the height of the horizontal tail above the thrust line, Z_{H_T}, is given by the following equation, see Figure 5.3.a,

$$Z_{H_T} = Z_H - Z_T + \left(\tan(i_T)\right)\left(X_p + \ell_H\right) \qquad (5.32.a)$$

To calculate the effect of power on dynamic pressure ratio at the tail, $\frac{\Delta\bar{q}_h}{\bar{q}_\infty}$, use can be made of Figure 5.14 (from Reference 5.2). For low values of T_c' (close to zero), use should be made of the free-flight value for the tail.

$$X_7 = \left\{ 0.34 + \frac{S_W(T_c'/\text{prop})}{8\ R_p^{\ 2}} \right\} 0.865 \left(\frac{S_{h_i}}{S_h} \right) \tag{5.33}$$

$$\frac{\Delta\bar{q}_H}{\bar{q}_\infty} = \left\{ 1.0102 - 0.1438 \frac{Z_{H_{eff}}}{R_p} - 0.3904 \left(\frac{Z_{H_{eff}}}{R_p} \right)^2 \right\} X_7 \tag{5.34}$$

The effective height of the propeller slipstream, $Z_{H_{eff}}$, at the tail, may be calculated as follows (s e Figure 5.3):

$$Z_{H_{eff}} = Z_S - \ell'_H \left\{ \alpha_b - \varepsilon_u - (\varepsilon_H)_{\text{power off}} - (\Delta\varepsilon_H)_{\text{power}} \right\} - Z_H \tag{5.34.a}$$

where:

Z_S is the vertical distance from X - body axis to slipstream centerline at 1/4 c_i:

$$Z_S = -X'_p\ (\alpha_b - \varepsilon_u - \varepsilon_p) + Z_T \tag{5.34.b}$$

The change in lift due to above effects may be obtained from the following relation:

$$C_{L_{H(hf)}} = \left[\left(C_{L_{H(hf)}} \right)_{S_H,\ \bar{q}_H/\bar{q}_\infty = 1} \right] K_{H_{Power}} \quad \text{(Ref. 5.2)} \tag{5.35}$$

where:

$$K_{H_{Power}} = \left(\frac{S_H}{S_W} \right) \left\{ \left(\frac{\bar{q}_H}{\bar{q}_\infty} \right)_{\text{prop off}} + \frac{\Delta\bar{q}_H}{\bar{q}_\infty} \right\} \tag{5.36}$$

$\left(C_{L_{H(hf)}}\right)_{S_H,\ \bar{q}_H/\bar{q}_\infty=1}$ is the lift of the tail, referenced to the tail area and a dynamic pressure of one.

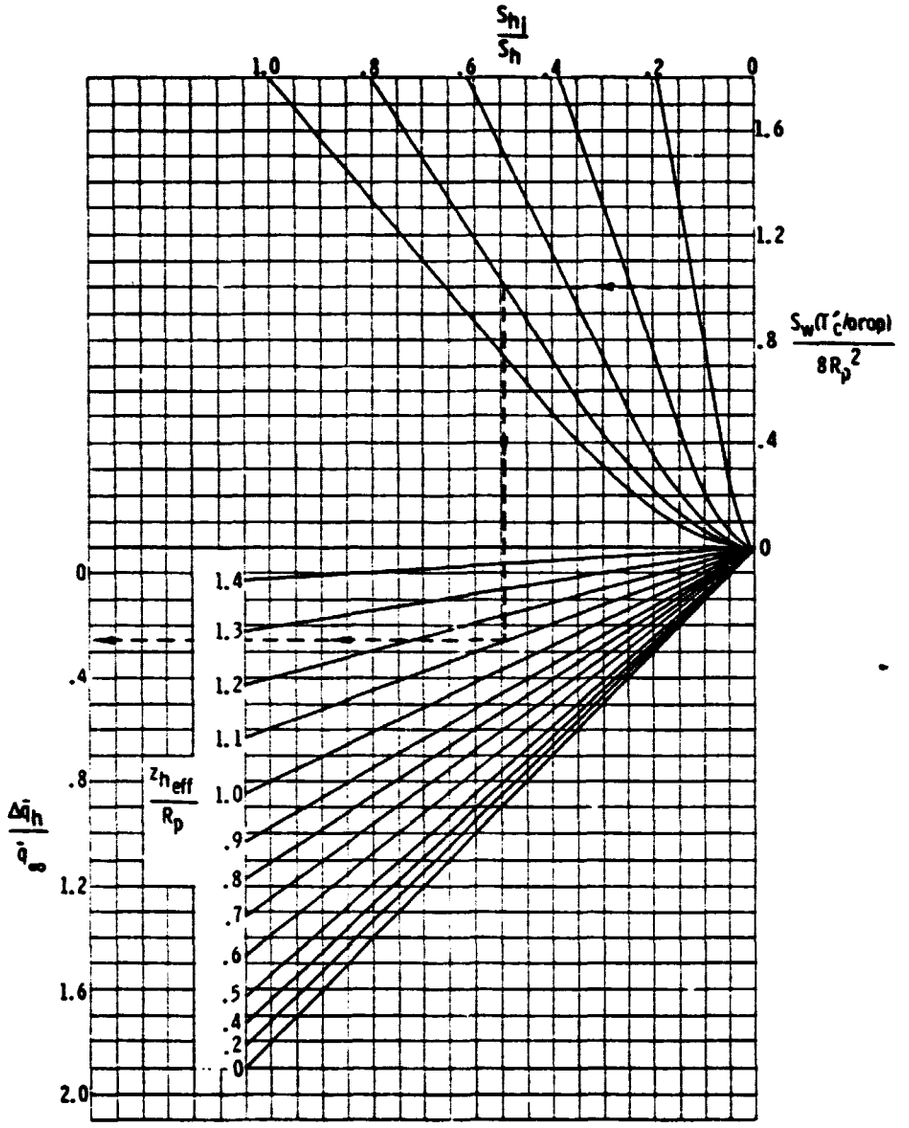

Figure 5.14: Effect of power on the dynamic pressure ratio at the tail (ref 5.2)

The tail lift may be obtained from:

$$C_{L_{H(hf)_{S_H,\ \bar{q}_u/\bar{q}_\infty=1}}} = C_{L_{\alpha_H}} (\alpha_H - \alpha_{0_H}) \tag{5.36.a}$$

where:

$$\alpha_H = \alpha_b - (\varepsilon_H)_{\text{power off}} - \Delta\varepsilon_{H_{\text{power}}} + i_H \tag{5.36.b}$$

The area of the horizontal tail, immersed in the slipstream, may be calculated as follows (see Figure 5.3):

Single-engine airplanes:

$$S_{H_i} = \left(2R_p/b_H\right) S_H \tag{5.37}$$

Multi-engine airplanes:

$$S_{H_i} = \left[\frac{(b_{H_T}/2 - Y_T) + \sqrt{R_p^2 - Z_{H_{eff}}^2}}{b_H/2}\right] S_{H_T} \tag{5.38}$$

The total effect of power on lift may now be calculated as indicated by Equation (5.1.)

Now that the effects of power on the lift force of the airplane are known, the effects on moment about the Y-axis may be calculated.

5.2.2 DERIVATION OF EQUATIONS, EFFECT ON PITCHING MOMENT

The total effect of power on pitching moment may be summarized as in Equation (5.39):

$$C_M = (C_{M_{wfn}})_{\text{Power off}} + (\Delta C_M)_T + (\Delta C_M)_{NP} + (\Delta C_{M_0})_{\Delta\bar{q}_W} + (\Delta C_M)_{WL} + (\Delta C_M)_{np} + \bar{C}_{M_{H(hf)}} \tag{5.39}$$

where:

$(C_{M_{wfn}})_{\text{power off}}$ is the power-off, tail-off pitching moment obtained elsewhere in the program.

$(\Delta C_M)_T$ is the pitching moment due to offset thrust.

$(\Delta C_M)_{N_p}$ is the pitching moment due to offset propeller normal force.

$(\Delta C_{M_O})_{\Delta \bar{q}_W}$ is the effect of propeller slipstream dynamic pressure increment on zero lift pitching moment.

$(\Delta C_M)_{WL}$ is the total effect on pitching moment due to slipstream dynamic pressure and angle of attack changes.

$(\Delta C_M)_{np}$ is the effect of propeller slipstream on nacelle pitching moment.

$(\Delta C_M)_h$ is the effect of dynamic pressure and downwash on pitching moment due to tail-lift.

$(\overline{C_{M_H}})_{hf}$ is the power-on pitching moment of the tail.

5.2.2.1 PITCHING MOMENT DUE TO THRUST OFFSET

The pitching moment due to thrust offset may be obtained from:

$$(\Delta C_M)_T = N\ (T_c'/\text{prop})\left(\frac{Z_T}{Z_W}\right) \tag{5.40}$$

where the geometric parameters are defined in Figure 5.3.

5.2.2.2 PITCHING MOMENT DUE TO PROPELLER NORMAL FORCE

This effect may be calculated with:

$$(\Delta C_M)_{N_p} = (\Delta C_L)_{N_p}\left(\frac{X_p}{\bar{c}_W}\right)\left(\frac{1}{\cos\alpha_T}\right) \tag{5.41}$$

where:

$(\Delta C_L)_{N_p}$ is the propeller normal force, to be obtained from Equation (5.3).

The geometric parameters are defined in Figure 5.3.

5.2.2.3 THE ZERO LIFT PITCHING INCREMENT

Due to the effect of slipstream on the wing and nacelles at zero lift, there will be a change in zero lift pitching moment:

$$(\Delta C_{M_0})_{\Delta\bar{q}_W} = K_{\Delta\bar{q}_W}\,(C_{M_0})_{i_{prop\ off}} \quad \text{(Ref. 5.2)} \tag{5.42}$$

where:

$K_{\Delta\bar{q}_W}$ is the factor that takes the power effect into account, to be calculated from Equation (5.43).

$$K_{\Delta\bar{q}_W} = \left(\frac{\Delta\bar{q}_W}{\bar{q}_\infty}\right)\left(\frac{S_i}{S_W}\right)\left(\frac{\bar{c}_i}{\bar{c}_W}\right) \quad \text{(Ref. 5.2)} \tag{5.43}$$

where:

$\frac{\Delta\bar{q}_W}{\bar{q}_\infty}$ is the increase in dynamic pressure ratio, to be calculated with Equation 5.12.

S_i is the immersed portion of the wing area (see Figure 5.3):

$$S_i = N\,(b_i/prop)\,\bar{c}_i \tag{5.44}$$

The zero lift pitching moment $(C_{M_0})_{i_{prop\ off}}$ may be determined as follows:

For twin-engine airplanes:

$$(C_{M_0})_{i_{prop\ off}} = (C_{M_0})_{wn_{prop\ off}} - (C_{M_0})_{Area\ not\ immersed} \tag{5.45}$$

where:

$(C_{M_0})_{wn_{prop\ off}}$ is the propeller-off C_{M_0} of the wing and nacelles, obtained elsewhere.

and:

$$(C_{M_0})_{Area\ not\ immersed} \simeq (C_{M_0})_{W_{prop\ off}} \left[\frac{S_W - S_i}{S_W}\right]\left[\frac{\bar{c}_{not\ immersed}}{\bar{c}_W}\right] \tag{5.46}$$

where:

$(C_{M_0})_{W_{prop\ off}}$ is obtained elsewhere

$$\bar{c}_{not\ immersed} = \frac{S_W - S_i}{b_W - b_i} \tag{5.47}$$

For a single-engine airplane:

Replace $(C_{M_0})_{wn_{prop\ off}}$ with $(C_{M_0})_{wf_{prop\ off}}$ which is the propeller-off C_{M_0} of the wing and fuselage obtained elsewhere.

5.2.2.4 PITCHING MOMENT INCREMENT DUE TO CHANGE IN WING LIFT

This power effect may simply be obtained from:

$$(\Delta C_M)_{WL} = -\left|(\Delta C_L)_{\Delta\bar{q}_w} + (\Delta C_L)_{\varepsilon_r}\right| \frac{X_W}{\bar{c}_W} \tag{5.48}$$

where:

X_W is the distance between aerodynamic center of the immersed wing and the center of gravity.

$$X_W = \ell_{cg} - \left| \ell_{1/4\bar{c}_W} + (Y_{\bar{c}_i} + b_c/2) \tan \Lambda_{1/4\bar{c}} \right| \qquad (5.49)$$

See Figure 5.15 for geometry definition.

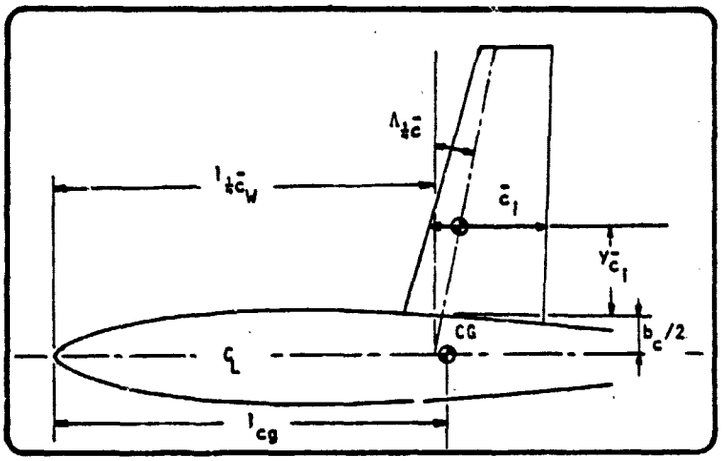

Figure 5.15: Geometry of the wing

The increments in lift due to power, $(\Delta C_L)_{\Delta\bar{q}_w}$ and $(\Delta C_L)_{\varepsilon_p}$, may be found from Equations (5.11) and (5.24), respectively.

5.2.2.5 PITCHING MOMENT DUE TO EFFECT OF SLIPSTREAM ON NACELLE

For multi-engine installations the effect of the propeller slipstream on nacelle pitching moments may be calculated with Equation (5.50)(from Reference 5.2):

$$(\Delta C_M)_{n_p} = -\frac{N}{36.5\, S_W \bar{c}_W} \int_w n^2 (\varepsilon_p + \varepsilon_u) \left(1 + \frac{\Delta\bar{q}_w}{\bar{q}_\infty}\right) dx \qquad (5.50)$$

OR:

$$(\Delta C_M)_{n_p} = \left[-\frac{N(\varepsilon_p + \varepsilon_u)}{36.5\, S_W \bar{c}_W} \left(1 + \frac{\Delta\bar{q}_w}{\bar{q}_\infty}\right) \int_w n^2 dx \right] 57.3 \qquad (5.51)$$

where:

ε_p and ε_u are obtained from Equations (5.16) and (5.17).

$\frac{\Delta \bar{q}_w}{\bar{q}_\infty}$ is obtained from Equation (5.12).

$\int w_n^2 dx$ is a function of the shape of the nacelle (see Figures 5.16 and 5.18).

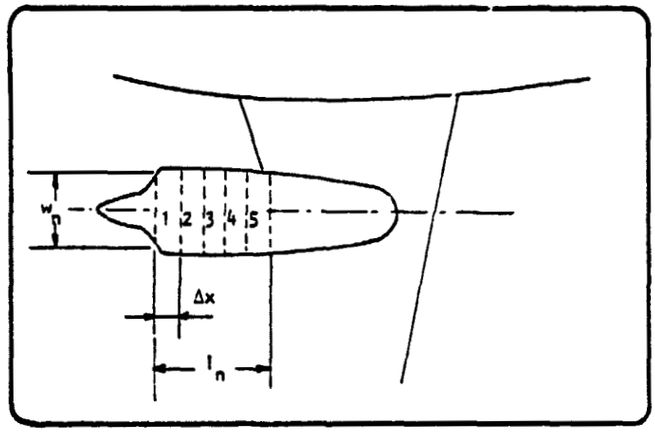

Figure 5.16: Shape of nacelle (twin engine)

To see if there is a general trend in the shape of nacelles, some research was done. Distinction was made between turbine engines and reciprocating engines. The nacelle was divided into five equal parts, as shown in Figure 5.16. Then the parameter $w_n^2 \Delta x$ was determined as a function of nacelle length, ℓ_n. The results are shown in Figures 5.17 and 5.19. Also included in this figure are two straight-line approximations. The equations for the nacelle shape parameter $w_n^2 \Delta x$ thus found for twin engine aircraft are:

Reciprocating engines:

$$w_n^2 \Delta x = -3.07 + 10.51\ \ell_n \tag{5.52}$$

Turbine engines:

$$w_n^2 \Delta x = -6.84 + 6.90\ \ell_n \tag{5.53}$$

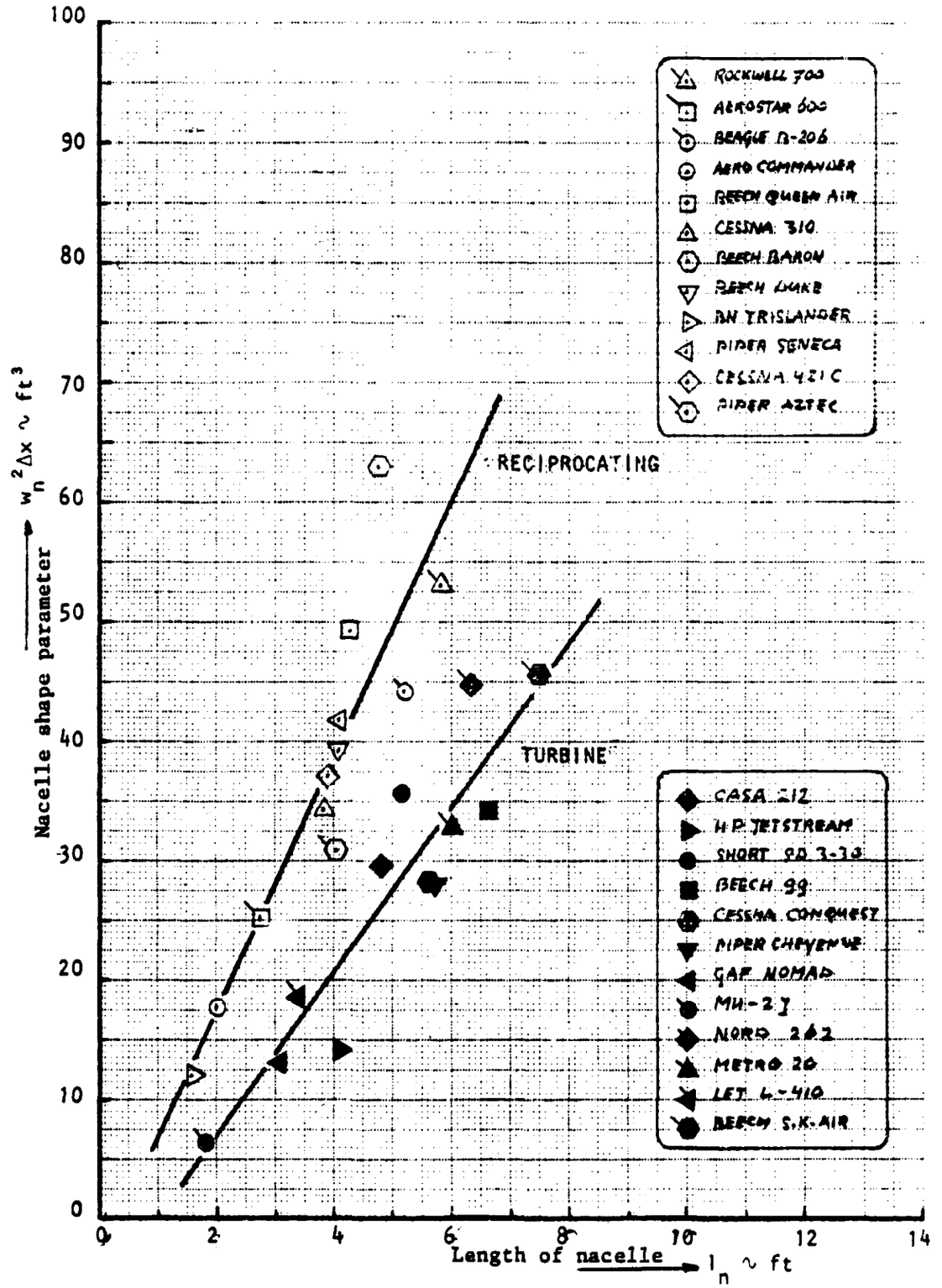

Figure 5.17: Nacelle shape parameter, twin engine airplanes

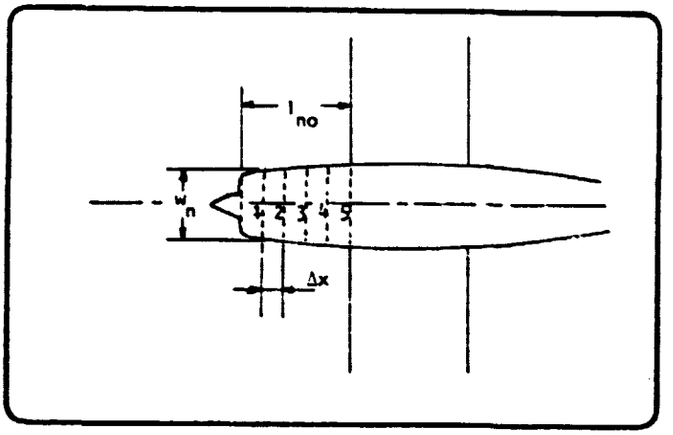

Figure 5.18: Shape of nacelle (single engine)

For single engine aircraft the following approximation was found:

$$w_n^2 \Delta x = -28.06 + 16.59\ \ell_{no} \tag{5.54}$$

5.2.2.6 THE PITCHING MOMENT CONTRIBUTION OF THE HORIZONTAL TAIL

The power-on pitching moment contribution of the horizontal tail may be obtained from:

$$(\bar{C}_{M_H})_{hf} = -\left(\frac{\ell_H}{\bar{c}_W}\right)(\bar{C}_{L_H})_{hf} \tag{5.55}$$

where:

ℓ_H is the distance from c.g. to quarter chord point of tail mac.

$(\bar{C}_{L_H})_{hf}$ is the tail lift based on S_W as a function of:

1) $\alpha_H = \alpha_b - (\bar{\varepsilon}_H)_{\text{prop off}} - (\Delta\varepsilon_H)_{\text{power}} + i_H$ (5.56)

2) and elevator deflection δ_e

3) and $\frac{\bar{q}_H}{\bar{q}_\infty}$, the dynamic pressure ratio.

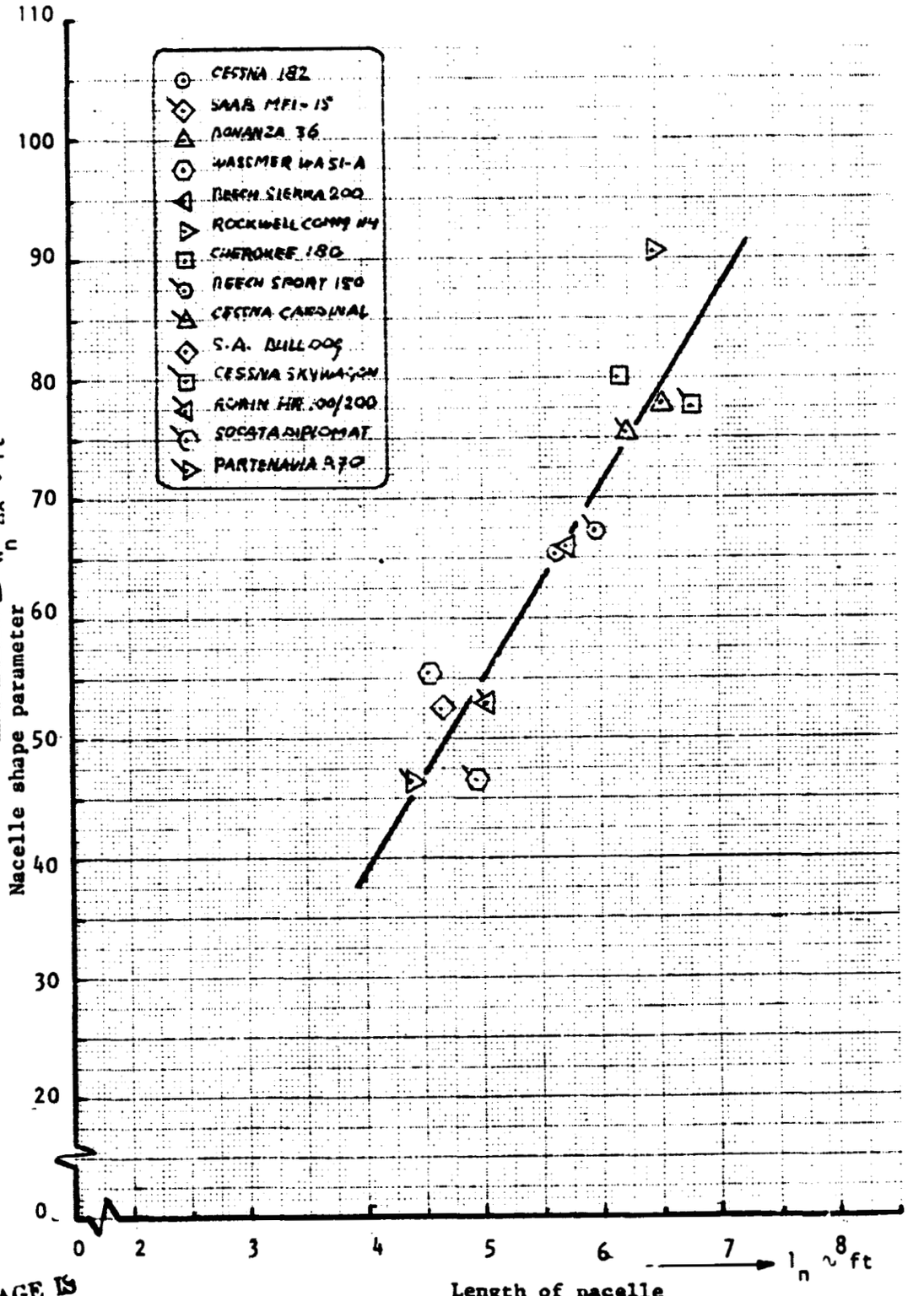

Figure 5.19: Nacelle shape parameter, single engine airplane

The tail-lift coefficient then follows from:

$$(\bar{C}_{L_H})_{hf} = C_{L_{\alpha_H}} (\alpha_H - \alpha_{o_H}) \left(\frac{S_{H_T}}{S_W}\right) \left(1 + \frac{\Delta\bar{q}_h}{\bar{q}_\infty}\right) \qquad (5.57)$$

This concludes the derivation of the equations of the effect of power on the lift and pitching moment characteristics of single or multi-engine propeller aircraft.

5.3 HAND CALCULATION

This is a hand calculation of the power effect subroutine for Airplane C. The data are given in Appendix D.

The computations are for the following flight conditions:

C_L = .797

V = 144 ft/sec

α_b = 0.105 rad

T_{prop} = 965 lbs

The following moment coefficients are from Reference 5.2:

M_{O_W} = -.024

$C_{M_{O_{WN}}}$ = -.024

$C_{M_{O_F}}$ = -.024

$C_{M_{WFN}}$ = -.0143

Following is a step-by-step hand calculation for Airplane C for the above flight conditions:

Eqn. 5.2.b:	α_T	= -.105	rad
Eqn. 5.2.a:	$T_c'/prop$	= 0.22	
Eqn. 5.2:	$(\Delta C_L)_T$	= 0.0461	
Eqn. 5.3.a:	$T_c/prop$	= 0.54	
Eqn. 5.7:	f	= 1.376	
Eqn. 5.8:	$C_{y_{\psi_0}}$	= 0.098	
Eqn. 5.4:	SFF	= 97.847	

Eqn. 5.9:	$\dfrac{C_{y_{\psi_0}}, \text{ actual}}{C_{y_{\psi_0}}, \text{ reference}}$	= 1.192	
Eqn. 5.1.t:	$\bar{c}_i$	= 5.4327	
Eqn. 5.10:	$\partial\epsilon_u/\partial\alpha$	= -0.189	
Eqn. 5.6:	$(\Delta C_L)_{N_p}$	= 0.00705	
Eqn. 5.12:	$\dfrac{\Delta\bar{q}_w}{\bar{q}_\infty}$	= 1.3850	
Eqn. 5.16:	ϵ_u	= -0.0331	rad
Eqn. 5.23:	$\partial\epsilon_p/\partial\alpha$	= 0.2910	
Eqn. 5.5:	α_p	= 0.1381	rad
Eqn. 5.17:	ϵ_p	= 0.0402	rad
Eqn. 5.15:	Z_S	= -1.4564	ft
Eqn. 5.1.m:	b_i/prop	= 5.2677	ft
Eqn. 5.1.n:	S_p/prop	= 28.2743	ft^2
Eqn. 5.1.p:	S_i/prop	= 28.6178	ft^2
Eqn. 5.1.q:	A_i	= 0.9696	
Eqn. 5.19:	X_1	= -3.0406	
Eqn. 5.20:	X_2	= 1.2512	
Eqn. 5.21:	X_3	= -0.0051	
Eqn. 5.22:	K_1	= 0.7521	
Eqn. 5.11:	$(\Delta C_L)_{\Delta\bar{q}_w}$	= 0.2936	

Eqn. 5.25:	$(\Delta\alpha)_{S_i}$	= -0.0321	rad
Eqn. 5.24:	$(\Delta C_L)_{\varepsilon_p}$	= -0.1141	
Eqn. 5.27:	K_2	= 1.3353	
Eqn. 5.26:	$\Delta C_{L_{Max}}$	= 0.3023	
Eqn. 5.30:	X_5	= 0.0769	
Eqn. 5.31.a:	X_6	= 0.0769	
Eqn. 5.32.a:	Z_{H_T}	= -0.801	ft
Eqn. 5.32:	$(\Delta\varepsilon_H)_{power}$	= 0.0765	rad
Eqn. 5.34.b:	Z_S	= -1.4564	ft
Eqn. 5.34.a:	$Z_{H_{EFF}}$	= 1.1373	ft
Eqn. 5.38:	$S_{H_{T_i}}$	= 6.8668	ft^2
Eqn. 5.33:	X_7	= 0.4453	
Eqn. 5.34:	$\Delta\bar{q}_H/\bar{q}_\infty$	= 0.3995	
Eqn. 5.36:	$K_{H_{power}}$	= 0.2555	
Eqn. 5.56:	α_H	= -0.0566	rad
Eqn. 5.57:	$(C_{L_{HF}})_{S_H q/q=1}$	= -0.2324	
Eqn. 5.35:	$(\bar{C}_{L_H})_{hf}$	= -0.0594	
Eqn. 5.40:	$(\Delta C_M)_T$	= -0.0771	
Eqn. 5.41:	$(\Delta C_M)_{NP}$	= 0.0075	

Eqn. 5.43:	$K_{\Delta\bar{q}_w}$	= 0.2424	
Eqn. 5.47:	$\bar{c}_{\text{not imm.}}$	= 4.8442	ft
Eqn. 5.46:	$(C_{M_0})_{\text{not imm.}}$	= -0.0156	
Eqn. 5.45:	$(C_{M_0})_{i_{\text{prop off}}}$	= -0.0084	
Eqn. 5.42:	$(\Delta C_{M_0})_{\Delta\bar{q}_w}$	= -0.0041	
Eqn. 5.49:	X_W	= 0.775	ft
Eqn. 5.48:	$(\Delta C_M)_{WL}$	= -0.0271	
Eqn. 5.52:	$w_n^2 \Delta x$	= 40.757	ft^3
Eqn. 5.51:	$(\Delta C_M)_{np}$	= -0.00273	
Eqn. 5.55:	$(\overline{C_{M_H}})_{hf}$	= 0.1736	

5.4 DESCRIPTION OF PROGRAM

A flowchart of the program is shown in Figure 5.20. The integer variable ENP is used to distinguish between single engine (ENP=1) and twin engine airplanes (ENP=2), since the formulas are not always the same. For the single engine case the dimensions of the immersed area are calculated using an approximation for the height of the propeller slipstream above the body X-axis at the wing quarter chord point (Z_S). After the calculation of Z_S, there is a loop back to recalculate the immersed wing characteristics for the single engine case; this is only done twice. It is possible to calculate only the effects on

lift by setting the integer KLTI equal to 1. It is also possible to include the calculation for $C_{L_{Max}}$; in this case the computer will return to the calling subroutine when the variable KCLM is set to 2. In neither of above cases are the effects on moment calculated. Twice another subroutine is called: subroutine DOWNWS for the calculation of $\partial\varepsilon/\partial\alpha$ and function "SLOPE" for the calculation of wing and tail plane lift-curve slope.

A listing of the program and a sample output for Airplane C are shown in Figure 5.21. A comparison of computed power effects for the fuselage-wing-nacelle combination with wind tunnel test results shown in Figures 5.22, 5.23 and 5.24.

TABLE 5.1 VARIABLES IN SUBROUTINE "POWER"

NAME	ENG. SYMBOL	DIMENSION	ORIGIN	REMARKS/DEFAULT
ALPHA	α_b	rad	Calling Subroutine	
ALPHLO	α_{0_w}	rad	Common	
ALPHT	α_H	rad	Common	
ALPOH	$\alpha_{0_{HT}}$	rad	Common	
ALPPR	α_p	rad	---	
ALPT	α_T	rad	Common	
ALPW	α_W	rad	---	
AR	AR	---	Common	
ARI	AR_i	---	---	
B	b	ft	Common	

TABLE 5.1 VARIABLES IN SUBROUTINE "POWER" (continued)

NAME	ENG. SYMBOL	DIMENSION	ORIGIN	REMARKS/DEFAULT
BD03	$(b/D)0.3$	---	Common	.0693
BD06	$(b/D)0.6$	---	Common	.082
BD09	$(b/D)0.9$	---	Common	.0682
BIMME	b_i	ft	---	
BHT	b_{HT}	ft	Common	
BL	---	---	Common	No. of Blades
BLANG	$\beta_{0.75}$	deg	Common	21.5
CBARI	$\bar{c}_i$	ft	---	
CBARW	$\bar{c}_W$	ft	Common	
CL	C_L	---	Common	
CLHHF	$(\bar{C}_{L_H})_{hf}$	---	---	
CLHSQ	$(C_{L_H})_{S_H q/q}$	---	---	
CLTOT	$C_{L_{TOT}}$	---	---	
CMHHF	$(C_{M_H})_{hf}$	---	---	
CMODQW	$\Delta(C_{M_0})_{\Delta\bar{q}_w}$	---	---	
CMOIP	$(C_{M_0})_{i_{prop\ off}}$	---	---	
CMONI	$(C_{M_0})_{\text{area not immersed}}$	---	---	

TABLE 5.1 VARIABLES IN SUBROUTINE "POWER" (continued)

NAME	ENG. SYMBOL	DIMENSION	ORIGIN	REMARKS/DEFAULT
CM0W	$(C_{M_0})_{w_{prop\ off}}$	---	Common	
CM0WF	$(C_{M_0})_{wf_{prop\ off}}$	---	Common	
CM0WN	$(C_{M_0})_{wn_{prop\ off}}$	---	Common	
CMTOT	$(C_M)_{TOT}$	---	---	
CMWFN	$(C_M)_{wfn}$	---	---	
CN0TJ	$\bar{c}_{not\ immersed}$	---	---	
CRCLW	$(C_R)_{C_L}$	ft	Common	
CR0OTW	C_R	ft	Common	
CTIPI	C_{t_i}	ft	---	
CTIPW	C_t	ft	Common	
CYPSA	$C_{y'_{\psi_0}}$ actual	---	---	
CYPSR	$C_{y'_{\psi_0}}$ reference	---	---	
DALPSI	$(\Delta\alpha)_{S_i}$	rad	---	
DCLDQW	$(\Delta C_L)_{\Delta\bar{q}_w}$	---	---	
DCLEP	$(\Delta C_L)_{\epsilon_p}$	---	---	

TABLE 5.1 VARIABLES IN SUBROUTINE "POWER" (continued)

NAME	ENG. SYMBOL	DIMENSION	ORIGIN	REMARKS/DEFAULT
DCLNP	$(\Delta C_L)_{NP}$	---	---	
DCLMAX	$(\Delta C_L)_{Max}$	---	---	
DCLT	$(\Delta C_L)_{T}$	---	---	
DCLWF	$(\Delta C_L)_{WF}$	---	---	
DCMNAC	$(\Delta C_M)_{np}$	---	---	
DCMNP	$(\Delta C_M)_{NP}$	---	---	
DCMT	$(\Delta C_M)_{T}$	---	---	
DCMTOT	$(\Delta C_M)_{TOT}$	---	---	
DCMWL	$(\Delta C_M)_{WL}$	---	---	
DEHP	$(\Delta\epsilon_H)_{power}$	rad	---	
DEPDA	$\partial\epsilon/\partial\alpha$	---	---	
DEUDA	$\partial\epsilon_u/\partial\alpha$	---	---	
DPROP	D	ft	Common	
DQHQI	$\frac{\Delta\bar{q}_H}{\bar{q}_\infty}$	---	---	
DQWQI	$\frac{\Delta\bar{q}_w}{\bar{q}_\infty}$	---	---	
ELCG	ℓ_{cg}	ft	Common	

TABLE 5.1 VARIABLES IN SUBROUTINE "POWER" (continued)

NAME	ENG. SYMBOL	DIMENSION	ORIGIN	REMARKS/DEFAULT
ELC4W	$\ell_{1/4\bar{c}_W}$	ft	Common	
ELHT	ℓ'_H	ft	Common	
ELTH	ℓ_H	ft	Common	
ENP	N	---	Common	No. of Engines
EPS	(ϵ_H)	rad	Common	
EPSP	ϵ_p	rad	---	
EPSU	ϵ_u	rad	---	
EYET	i_T	rad	Common	
EYEW	i_w	rad	Common	
FN	T	lb	Common	
FPR	f	---	---	
FWOB	b_c	ft	Common	
K1	K_1	---	---	
K2	K_2	---	---	
K3	K_3	---	---	
KCLM	---	---	---	
KDWQ	$K_{\Delta\bar{q}_w}$	---	---	
KNPOW	---	---	---	
LN	ℓ_n	ft	Common	
LNO	ℓ_{nose}	ft	Common	

TABLE 5.1 VARIABLES IN SUBROUTINE "POWER" (continued)

NAME	ENG. SYMBOL	DIMENSION	ORIGIN	REMARKS/DEFAULT
NTYE	---	---	---	
QINF	q_∞	lb/ft^2	Common	
QHQI	$\bar{q}_H/\bar{q}_\infty$	---	---	
RATCYP	$\frac{C_{y,\ \text{actual}}}{C_{y,\ \text{reference}}}$	---	---	
RHO	ρ	$lb\ sec^2/ft^4$	Common	
RPROP	R_p	ft	Common	
SFF	SFF	---	---	
SHT	S_H	ft^2	Common	
SHTI	S_{H_i}	ft^2	---	
SLMI	λ_i	---	---	
SLOPE	C_{L_α}	rad^{-1}	Common	
SLOPEH	$C_{L_{\alpha_H}}$	rad^{-1}	Common	
SPROP	S_{prop}	ft^2	---	
SW	S	ft^2	Common	
SWI	S_i	ft^2	---	
SWPQC	$\Lambda_{1/4\bar{c}}$	rad	Common	
SWTRP	$\frac{S_W(T'_c/prop}{8\ R_p^2}$	---	---	

TABLE 5.1 VARIABLES IN SUBROUTINE "POWER" (continued)

NAME	ENG. SYMBOL	DIMENSION	ORIGIN	REMARKS/DEFAULT
TCPRIM	$\frac{\text{Thrust/prop}}{\bar{q}_\infty S_W}$	---	---	
TCPROP	$\frac{\text{Thrust/prop}}{\rho \cdot V^2 D_{prop}^2}$	---	---	
V	V	ft/sec	Common	
WNDX	$w_n^2 \Delta x$	ft^3	---	
X1 thru X7	X_1 thru X_7	---	---	
XP	X_p	ft	Common	
XPP	X'_p	ft	Common	
XW	X_W	ft	---	
YCI	Y_{c_i}	ft	---	
YT	Y_T	ft	Common	
ZS	Z_S	ft	---	
ZW	Z_W	ft	Common	
ZT	Z_T	ft	Common	
ZHT	Z_H	ft	Common	
ZHHT	Z_{H_T}	ft	---	
ZHEFF	$Z_{H_{eff}}$	ft	---	

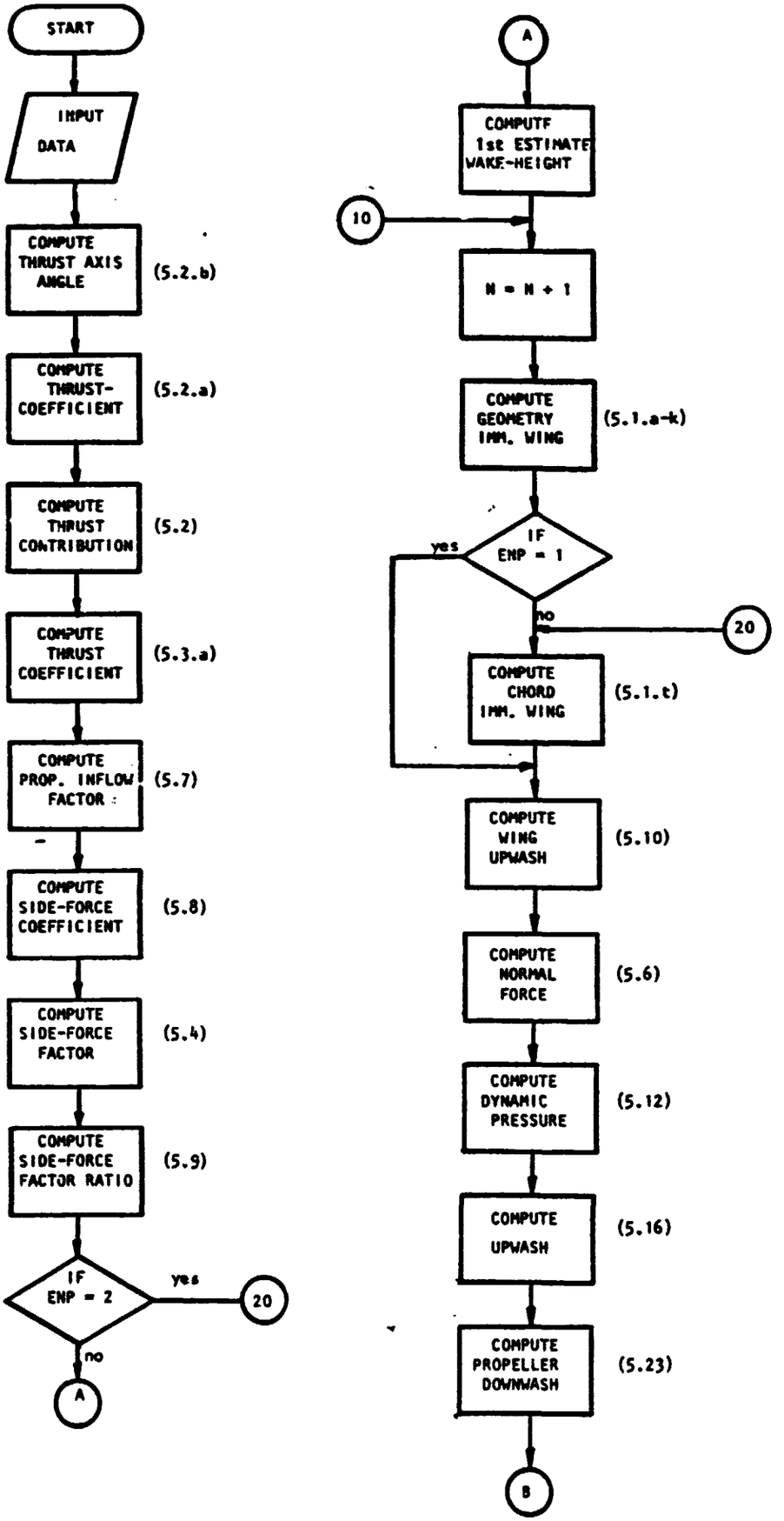

Figure 5.20: Flowchart of subroutine "POWER"

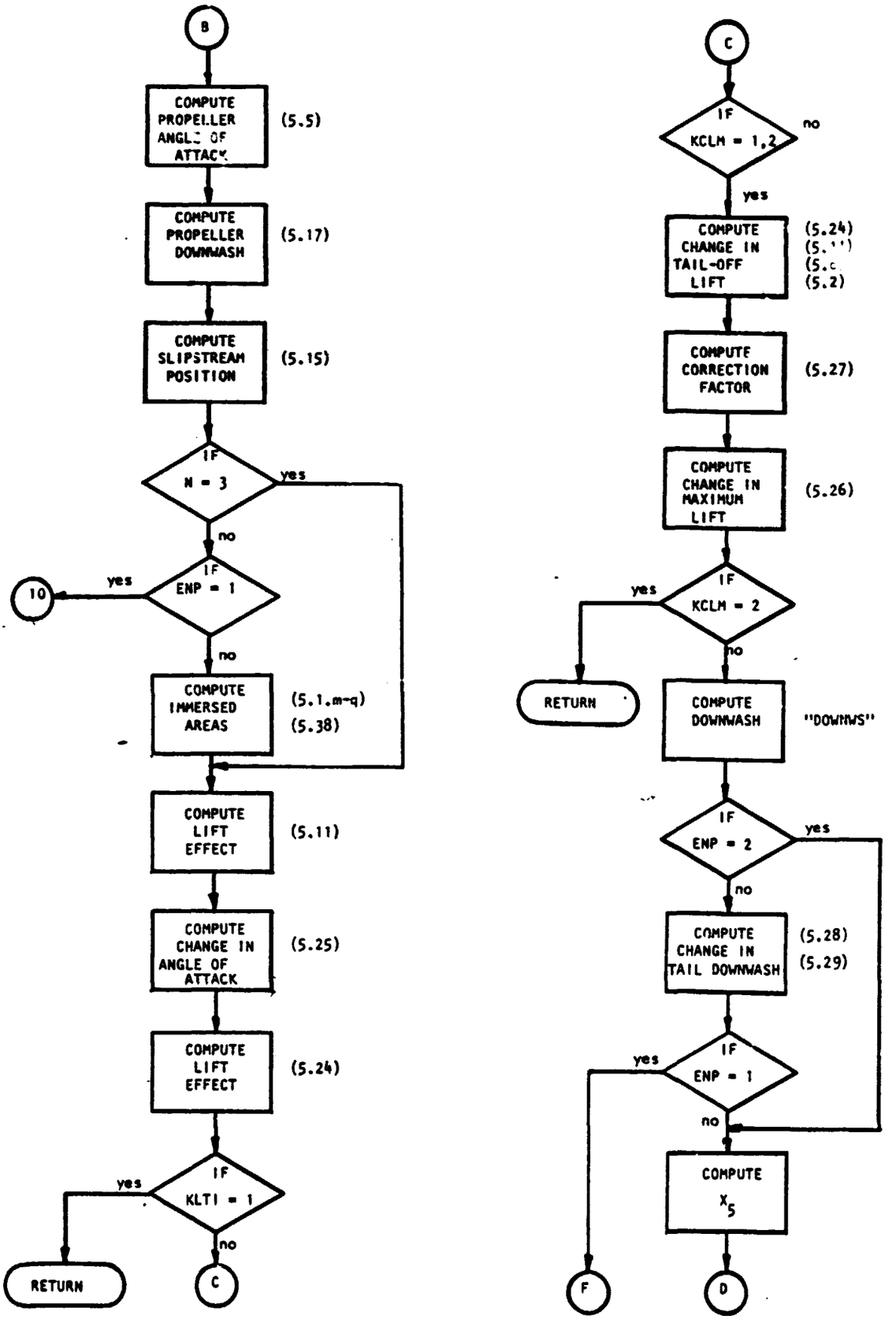

Figure 5.20: Continued

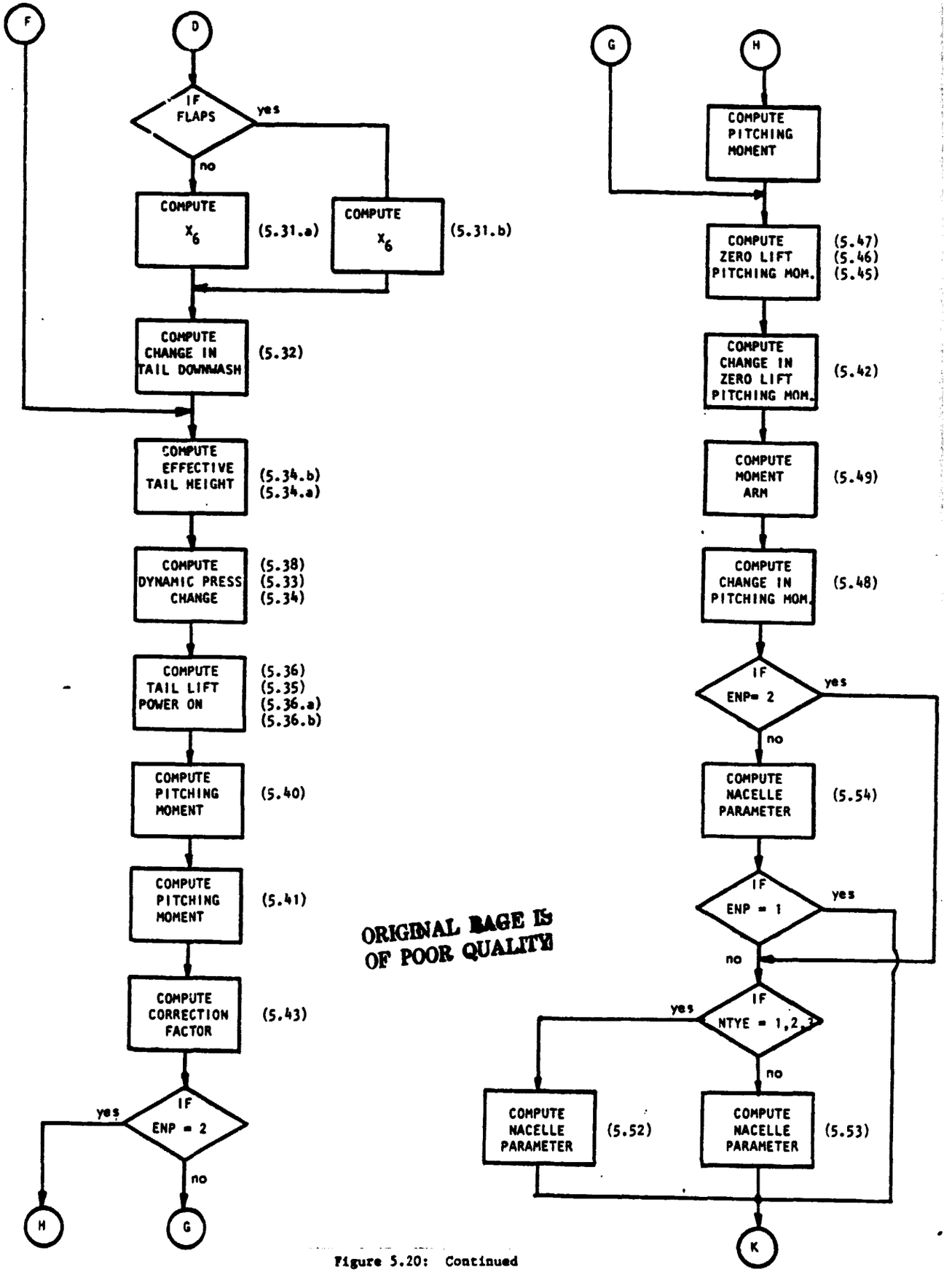

Figure 5.20: Continued

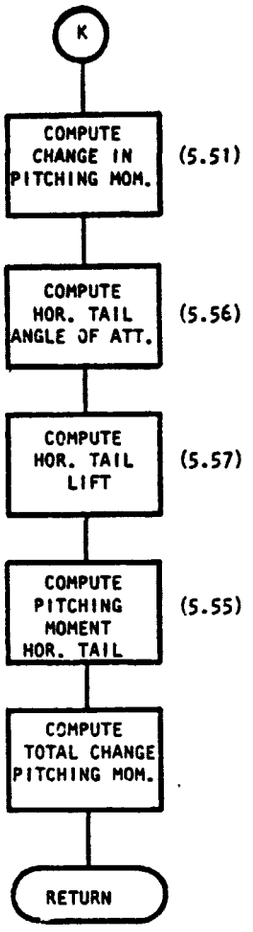

Figure 5.20: Continued

```
10          SUBROUTINE POWER (CLTOT,DCMTOT,DEHD,DQHQI,DQWQI,EPS,EPSP)
20          REAL K1,K2,K3,KHPOW,LN,LNO
30          INTEGER ENP,NTYE,TEST1
40          COMMON/WING/DLMC4,AR,SLM,B,CRCLW,CBARW,SW,CLAWP
50          COMMON/HORZ/DLMC4H,ARH,SLMH,BHT,CBARHT,SHT,CLAHP,CRCLHT
60          COMMON/FLITE/ALPHA,EM,CL
70          COMMON/GEOM/DIHD,ZW,SAH,XHMAC,ELINC
80          COMMON/FUS/ELF,DFUS,HC,WC,LN,ELTH,HH,SO,R2I,LV,ZV
90          COMMON/WING2/CROOTW,CTIPW,EYEW
100         COMMON/PRPLSN/ENP,NTYE,EYET,YT,ZT,FN
110         COMMON/PROP/BLANG,BD03,BD06,BD09,BL,DPROP,XPP,XP
120         COMMON/SHAPE/MY1,NY1,MC,NC,ELC4W,DELTLC,ELODT
130         COMMON/TEST/ILIFT,TEST1,KCLM,KLTI
140         COMMON/FUS2/ZHHT,FWOB,ELHT,LNO
150         COMMON/WEIGHT/ELCG,WEIGHT
160         COMMON/TRIM/EYEH,CLHT,DELTEL
170         COMMON/AERO/RHO,TAS
180         COMMON/HORT2/ALPHLO,ALPOH
190         ALPT=ALPHA+EYET
200         QINF=.5*RHO*(V**2.)

210         TCPRIM=FN/(QINF*SW)
220         DCLT=ENP*TCPRIM*SIN(ALPT)
230         ALPOUT=ALPHA*57.3
240         WRITE (6,1011) ALPOUT
250         WRITE (6,1012) TCPRIM
260         WRITE (6,1015) DCLT
270        TCPROP=FN/(RHO*(V**2.)*(DPROP**2.))
280        FPR=.652+1.183*ALOG(TCPROP+1.3)
290        CYPSR=.013*(BLANG**.657)+(.0125+.00125*BLANG)*(BL-2.)
300        SFF=525.*(BD03+BD06)+270.*BD09
310        RATCYP=-2.938+.901*ALOG(SFF)
320        IF (ENP.EQ.2) GOTO 20
330        ZS=ZT-ATAN(ALPHA)*XPP
340 10   CONTINUE
350        N=N+1
360        BIMME=2.*SQRT(ABS(RPROP**2-(ZS-ZW)**2))
370        SLMI=CTIPI/CROOTW
380        YCI=.333*(BIMME/2.)*((1.+2.*SLMI)/(1.+SLMI))
390        CBARI=.6667*CROOTW*((1.+SLMI+SLMI**2.)/(1.+SLMI))
400        SWI=BIMME*CBARI
410        ARI=BIMME/CBARI
420        IF (ENP.EQ.1) GOTO 30
430    20  CONTINUE
440        CBARI=CTIPW+((((CRCLW-CTIPW)*(B/2.-YT))/(B/2.))
450    30  CONTINUE
460        DEUDA=-.1136*((XPP/CBARI)**(-1 8141))-.027*(AR-4.)
470        ALPW=ALPHA+EYEW
480        DCLNP=ENP*FPR*CYPSR*RATCYP*(ALPT-DEUDA*(ALPW-ALPHLO))*
490       &((3.1416*RPROP**2.)/SW)
```

Figure 5.21: Listing of Subroutine "POWER"

```
500         WRITE (6,1020) DCLNP
510         DQWQI=(SW*TCPRIM)/(3.1416*(RPROP**2.))
520         EPSU=DEUDA*(ALPW-ALPHLO)
530         SWTRP=(SW*TCPRIM)/(8.*(RPROP**2.))
540         CYPSA=CYPSR*RATCYP
550         DEPDA=.3732+.1703*ALOG(SWTRP)+(.2115-.0504*SWTRP)*CYPSA
560         ALPPR=ALPT-DEUDA*(ALPW-ALPHLO)
570         EPSP=DEPDA*ALPPR
580         IF (ENP.EQ.1) GOTO 33
590         BIMME=2.*SQRT(RPROP**2.-(ZS-ZW)**2)
600         SWI=BIMME*CBARI
610         ARI=BIMME/CBARI
620         YCI=YT
630   33    CONTINUE
640         X1=2.6384*(ARI**2.0312)+(-3.8116+4.2237*ARI-1.6186*(ARI**2.))*AR
650        &+(.0418*(ARI**1.3383))*(AR**2.)
660         X2=1.9938+1.2194*ALOG(SWTRP)
670         X3=(X2*(X1+3.))/10.
680         K1=.9191*EXP(-.3663*SWTRP)+X3/5
690         DCLDQW=ENP*K1*DQWQI*CL*(SWI/SW)
700         WRITE (6,1025) DCLDQW
710         DALPSI=-(EPSP/(1.-DEUDA))
720         DCLEP=ENP*(1.+DQWQI)*SLOPE*DALPSI*(SWI/SW)
730         WRITE (6,1030) DCLEP
740         IF (KLTI.EQ.1) GOTO 140
750         IF (KCLM.EQ.1.OR.KCLM.EQ.2) GOTO 35
760         GOTO 40
770   35    CONTINUE
780         DCLWF=DCLEP+DCLDQW+DCLNP+DCLT
790         K2=1.1854-2.1129*(SWI/SW)+7.604*((SWI/SW)**2.)
800         DCLMAX=K2*DCLWF
810         WRITE (6,1032) K2
820   40    CONTINUE
830         IF (KCLM.EQ.2) GOTO 140
840C        CALL SUBROUTINE DOWNWS (DEPDAL)
850         EPS=DEPDAL*(ALPW-ALPHLO)
860         IF (ENP.EQ.2) GOTO50
870         X4=(.5376*EXP(3.9419*EPS)+.4366*((EPS*57.3)**1.2345)*SWTRP-
880        &(.1091*((EPS*57.3)**1.3152))*(SWTRP**2))/57.3
890         ZHT=ZHHT-ZT+ATAN(EYET)*(XP+ELTH)
900         DEHP=.6*X4*(.8189-.0185*(ABS(ZHT)/(2.*RPROP))-
910        &.1953*((ABS(ZHT)/(2.*RPROP))**2))
920         IF (ENP.EQ.1) GOTO 90
930   50    CONTINUE
940         ZHT=ZHHT-ZT+ATAN(EYET)*(XP+ELTH)
950         X5=(-1.0234+56.01*EPS-.1032*((EPS*57.3)**2)+
960         &(3.5191-13.8*EPS+.2025*((EPS*57.3)**2))*SWTRP-
970        &(.8738*EXP(12.909*EPS))*(SWTRP**2))/57.3
980         IF (ILIFT.EQ.2.OR.ILIFT.EQ.3.OR.ILIFT.EQ.5.OR.ILIFT.EQ.6) GOTO 60
990         X6=X5
1000         GOTO 80
1010  60     X6=.5+.889*X5
1020  80     CONTINUE
```

Figure 5.21: Continued

```
1030       DEHP=.6*(.9951+.0419*(ZHT/(2.*RPROP))-.3021*((ZHT/(2.*RPROP))
1040      &**2))*X6
1050  90   CONTINUE
1060       ZS=-XPP*(ALPHA-EPSU-EPSP)+ZT
1070       IF (N.EQ.3) GOTO 95
1080       IF (ENP.EQ.1) GOTO 10
1090  95   CONTINUE
1100       ZHEFF=ZS-ELHT*(ALPHA-EPSU-EPSP-EPS-DEHP)-ZHT
1110       SHTI=(((BHT/2.-YT)+SQRT(ABS(RPROP**2-ZHEFF**2)))
1120      &/(BHT/2.))*SHT
1130       X7=(.34+SWTRP)*(.865*(SHTI/SHT))
1140        DQHQI=(1.01-.1438*(ZHEFF/RPROP)-.3904*((ZHEFF/RPROP)**2))*X7
1150       KHPOW=(SHT/SW)*(QHQI+DQHQI)
1160       ALPHT=ALPHA-EPS-DEHP+EYEH
1170       CLHSQ=SLOPEH*(ALPHT-ALPOH)
1180       CLHF=CLHSQ*KHPOW
1190       WRITE (6,1035) CLHF
1200       DCMT=ENP*TCPRIM*(ZT/CBARW)
1210       WRITE (6,1037)
1220       WRITE (6,1040) DCMT
1230       DCMNP=DCLNP*(XP/CBARW)/COS(ALPT)
1240       WRITE (6,1045) DCMNP
1250       KDQW=DQWQI*(SWI/SW)*(CBARI/CBARW)
1260       IF (ENP.EQ.2) GOTO 100
1270       CMOWN=CMOWF
1280  100   CONTINUE
1290       CNOTI=(SW-SWI)/(B-BIMME)
1300       CMONI=CMOW*((SW-SWI)/SW)*(CNOTI/CBARW)
1310      CMOIP=CMOWN-CMONI
1320      CMODQW=KDQW*CMOIP
1330      WRITE (6,1050) CMODQW
1340      XW=ELCG-(ELC4W+(YCI+FWOB/2.)*ATAN(SWPQC))
1350      DCMWL=-(DCLDQW+DCLEP)*(XW/CBARW)
1360      WRITE (6,1055) DCMWL
1370      IF (ENP.EQ.2) GOTO 110
1380      WNDX=-28.06+16.59*LNO
1390      IF (ENP.EQ.1) GOTO 130
1400  110  CONTINUE
1410      IF (NTYE.EQ.1.OR.NTYE.EQ.2.OR.NTYE.EQ.3) GOTO 120
1420      WNDX=-6.84+6.9*LN
1430      GOTO 130
1440  120 WNDX=-3.07+10.51*LN
1450  130 CONTINUE
1460      DCMNAC=-ENP*((EPSP+EPSU)/(36.5*SW*CBARW))*(1.+DQWQI)*WNDX*57.29
1470      WRITE (6,1060) DCMNAC
1480      ALPHTP=ALPHA-EPS-DEHP
1490       CMHHF=-(ELTH/CBARW)*CLHF
1500      WRITE (6,1065) CMHHF
```

Figure 5.21: Continued

```
1510       DCMTOT=DCMT+DCMNP+CMODQW+DCMWL+DCMNAC
1520      CLTOT=CL+DCLWF+CLHF
1530      WRITE (6,1067)
1540      WRITE (6,1068) CLTOT
1550      WRITE (6,1070) DCMTOT
1560      CMTOT=CMWFN+DCMTOT+CMHHF
1570      WRITE (6,1075) CMTOT
1580      WRITE (6,1080)
1590  140 CONTINUE
1600 100C FORMAT (10X,"*** KU-FRL DEVELOPED SUBROUTINE: POWER EFFECTS***"///)
1610 1005 FORMAT (10X,"---TESTRUN FOR AIRPLANE C---"///)
1620 1010 FORMAT (10X,"... EFFECTS ON LIFT ..."//)
1630 1011 FORMAT(10X,"* BODY ANGLE OF ATTACK=   ",1F5.1," DEG"//)
1640 1012 FORMAT(10X,"* THRUST COEFFICIENT=    ",1F4.2//)
1650 1015 FORMAT (10X,"DCLT=    ",1F10.4/)
1660 1020 FORMAT (10X,"DCLNP=   ",1F10.4/)
1670 1025 FORMAT (10X,"DCLDQW=  ",1F10.4/)
1680 1030 FORMAT (10X,"DCLEP=   " ,1F10.4/)
1690 1032 FORMAT (10X,"K2=      ",1F10.4/)
1700 1035 FORMAT (10X,"CLHF=    ",1F10.4///)
1710 1037 FORMAT (10X,"... EFFECTS ON PITCHING MOMENTS ..."//)
1720 1040 FORMAT (10X,"DCMT=    ",1F10.5/)
1730 1045 FORMAT (10X,"DCMNP=   ",1F10.5/)
1740 1050 FORMAT (10X,"CMODQW=  ",1F10.5/)
1750 1055 FORMAT (10X,"DCMWL=   ",1F10.5/)
1760 1060 FORMAT (10X,"DCMNAC=  ",1F10.5/)
1770 1065 FORMAT (10X,"CMHHF=   ",1F10.5///)
1780 1067 FORMAT (10X,"... TOTAL EFFECTS OF POWER ..."//)
1790 1068 FORMAT (10X,"CLTOT=   ",1F10.4//)
1800 1070 FORMAT (10X,"DCMTOT=  ",1F10.5//)
1810 1075 FORMAT (10X,"CMTOT=   ",1F10.5///)
1820 1080 FORMAT (10X,"*** END OF SUBROUTINE POWER ***"///)
1830C     RETURN
1840      STOP
1850      END
```

Figure 5.21: Continued

```
*** KU-FRL DEVELOPED SUBROUTINE: POWER EFFECTS***

---TESTRUN FOR AIRPLANE C---

... EFFECTS ON LIFT ...

* BODY ANGLE OF ATTACK=    11.7 DEG

* THRUST COEFFICIENT=    0.22

DCLT=         0.0895
DCLNP=        0.0131
DCLDQW=       0.4881
DCLEP=       -0.2232
K2=           1.0495
CLHF=         0.0019

... EFFECTS ON PITCHING MOMENTS ...

DCMT=      -0.07708
DCMNP=      0.01415
CMODQW=    -0.00125
DCMWL=     -0.05738
DCMNAC=    -0.00784
CMHHF=     -0.00567

... TOTAL EFFECTS OF POWER ...

CLTOT=        1.6944

DCMTOT=    -0.12941

CMTOT=     -0.14308

*** END OF SUBROUTINE POWER ***
```

Figure 5.21: Continued

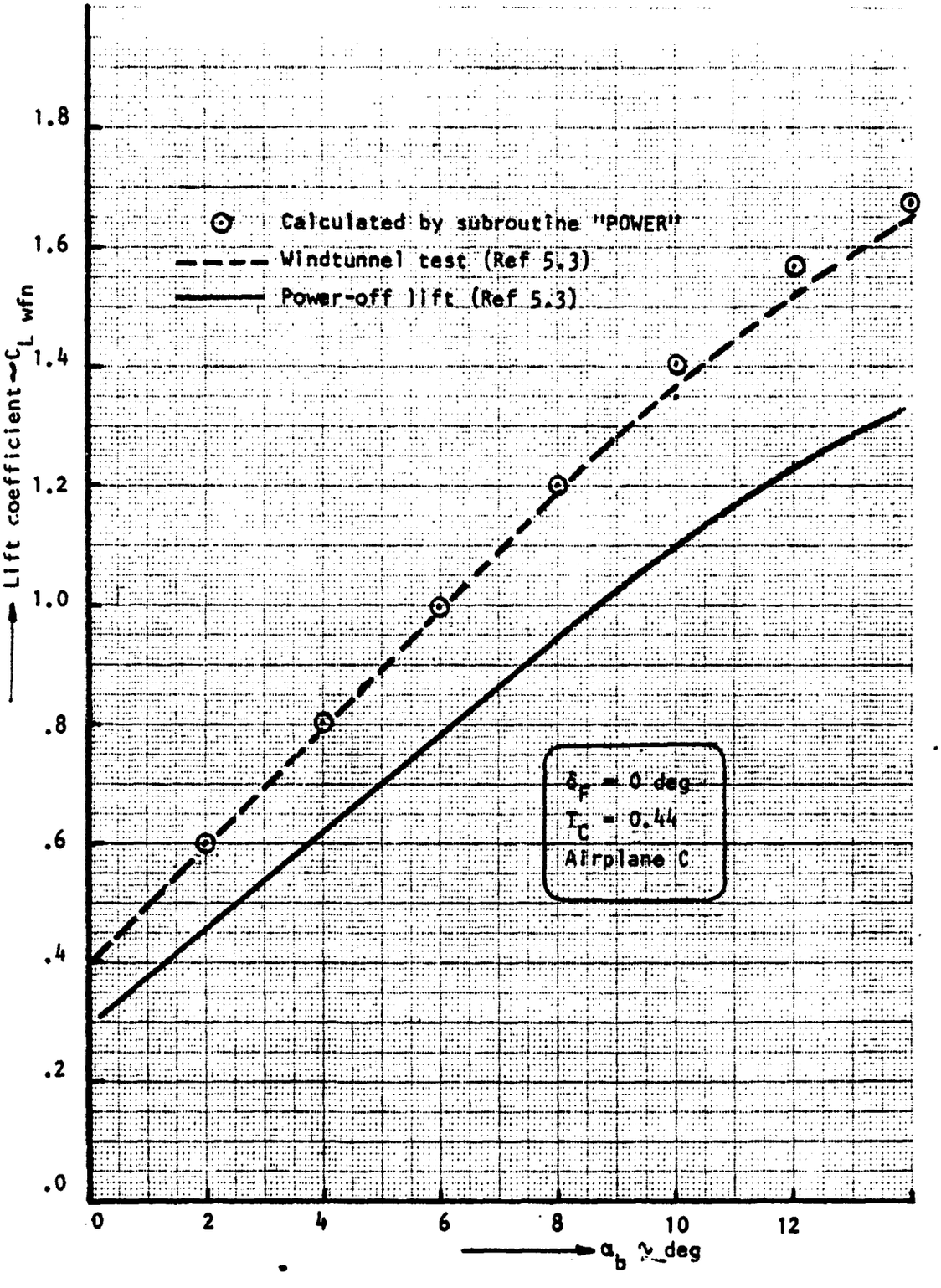

Figure 5.22: Comparison of power effects

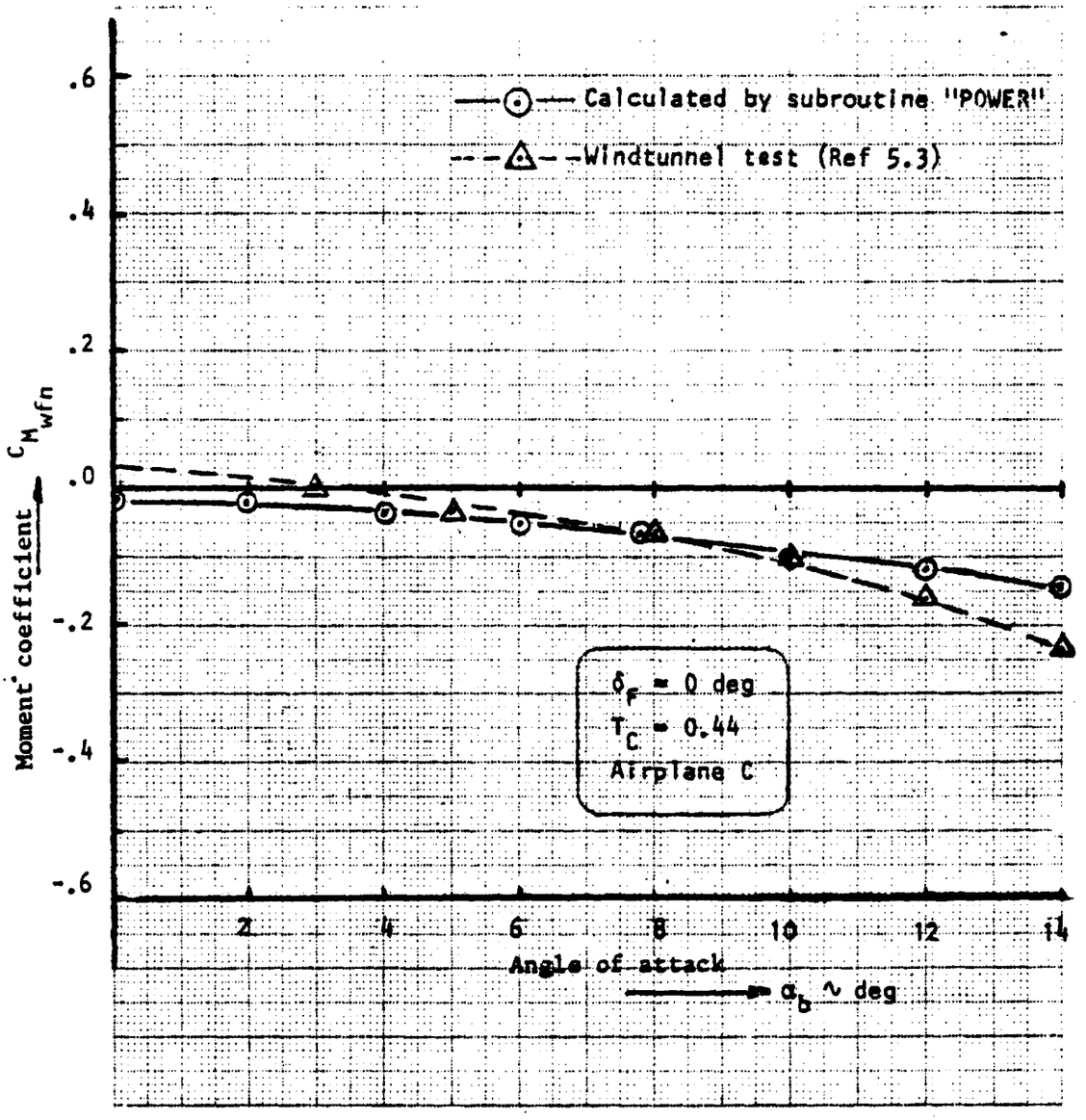

Figure 5.23: Comparison of power effects

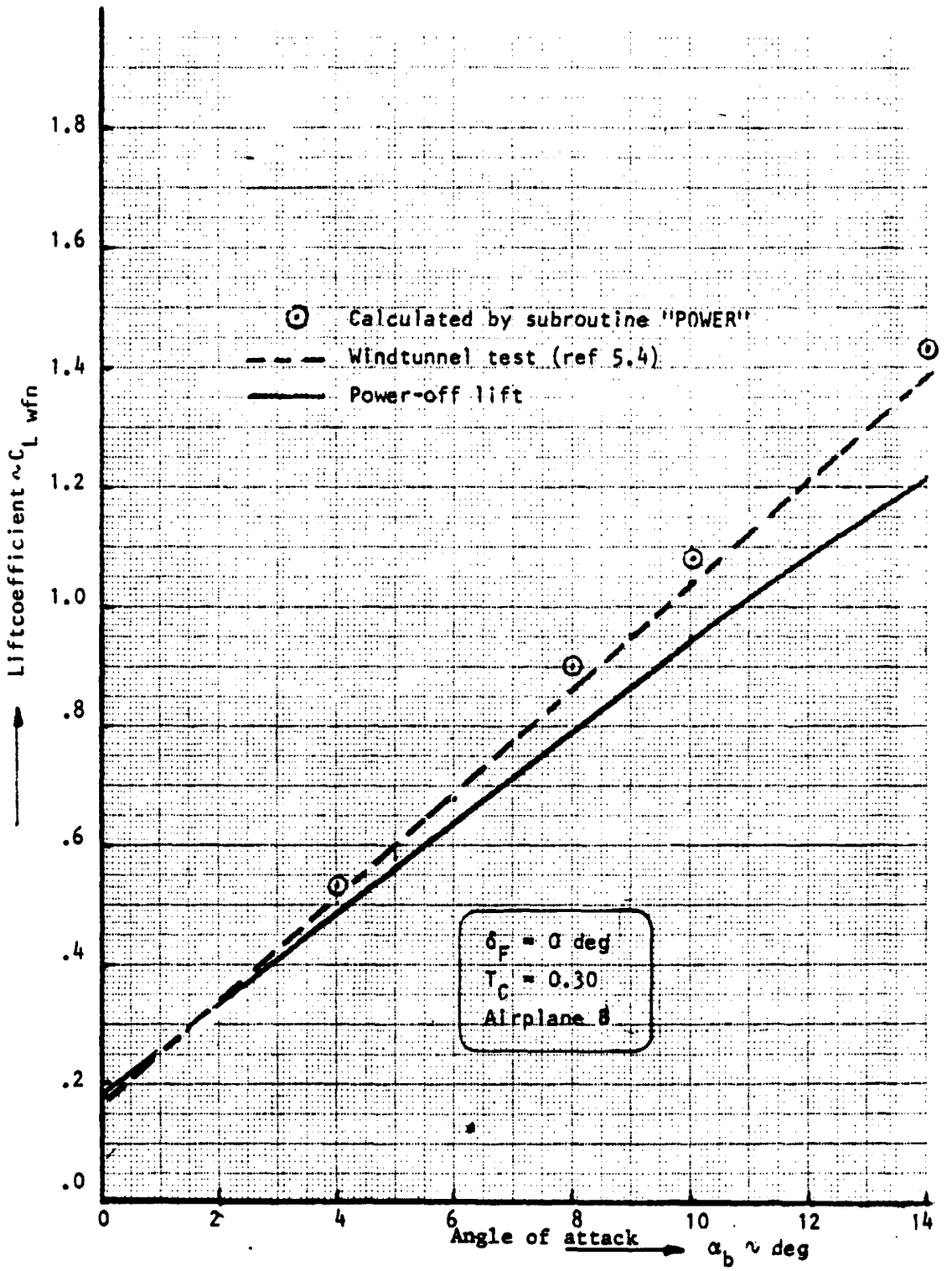

Figure 5.24: Comparison of power effects

5.5 CONCLUSIONS

A comparison of computer generated data with the handcalculation showed that the program worked properly. Figures 5.22 through 5.24 show that the computer program predicts the power-on characteristics fairly well. No run for the effect on pitching moment for airplane B was done, however figure 5.23 indicates that this effect also is fairly well predicted.

The program also computes the propeller side force derivative, which is used in the computation of C_{n_β}. Comparison with data in Reference 5.2 shows that this variable is predicted within 5 % accuracy.

5.6 REFERENCES

5.6.1	Hoak, D.E. & Ellison, D.E.	USAF Stability and Control DATCOM; Air Force Flight Dynamics Lab., Wright-Patterson Air Force Base, Ohio
5.6.2	Wolowicz, C.H. & Yancey, R.B.	Longitudinal Aerodynamic Characteristics of Light, Twin-engine Propeller Driven Airplanes. NASA TN D-6800
5.6.3	Fink, M.P. & Freeman, D.C.	Full-scale Wind-tunnel Investigation of Static Longitudinal and Lateral Characteristics of a Light Twin-engine Airplane. NASA TN D-4983
5.6.4	Greer, H.D. & Shivers, J.P. & Fink, M.P.	Wind-tunnel Investigation of Static Longitudinal and Lateral Characteristics of a Full-scale Mockup of a Light Single-engine High-wing Airplane. NASA TN D-7149

CHAPTER 6

STATIC LONGITUDINAL STABILITY

6.1 INTRODUCTION

This chapter describes the computation of static stability, C_{M_α}, static margin, dC_M/dC_L, and neutral point, for both stick fixed and stick free cases. Power effects are accounted for by referring to subroutine POWER (Chapter 5). The method is based on Reference 6.1. The center of gravity location is assumed to be known.

6.2 DERIVATION OF EQUATIONS

The static stability parameter, C_{M_α}, may be computed from:

$$C_{M_\alpha} = \left(\frac{dC_M}{dC_L}\right) \cdot C_{L_\alpha} \qquad (rad^{-1}) \tag{6.1}$$

where: C_{L_α} is the lift-curve slope of the complete airplane, as computed in subroutine LCSLOPE.

$\frac{dC_M}{dC_L}$ is the static margin which may be found from:

$$\frac{dC_M}{dC_L} = \bar{X}_{cg} - \bar{X}_{ac} \tag{6.2}$$

The airplane aerodynamic center location, $\bar{X}_{ac}$, may be obtained from:

$$\bar{X}_{ac_{Fixed}} = \frac{\bar{X}_{ac_{WB}} + \frac{C_{L_{\alpha_H}}}{C_{L_{\alpha_{WB}}}} \eta_H \left(\frac{S_H}{S}\right) \bar{X}_{ac_H} \left(1 - \frac{d\epsilon}{d\alpha}\right)}{1 + \frac{C_{L_{\alpha_H}}}{C_{L_{\alpha_{WB}}}} \eta_H \left(\frac{S_H}{S}\right) \left(1 - \frac{d\epsilon}{d\alpha}\right)} \tag{6.3}$$

Equation (6.3) is for the stick fixed case. For the stick free case the following equation should be used:

$$\bar{X}_{ac_{Free}} = \frac{\bar{X}_{ac_{WB}} + \frac{C_{L_{\alpha_H}}}{C_{L_{\alpha_{WB}}}} \eta_H \left(\frac{S_H}{S}\right) \bar{X}_{ac_H} \left(1 - \frac{d\epsilon}{d\alpha}\right) \left(1 - \frac{C_{h_\alpha} \tau_E}{C_{h_{\delta_e}}}\right)}{1 + \frac{C_{L_{\alpha_H}}}{C_{L_{\alpha_{WB}}}} \eta_H \left(\frac{S_H}{S}\right) \left(1 - \frac{d\epsilon}{d\alpha}\right) \left(1 - \frac{C_{h_\alpha} \tau_E}{C_{h_{\delta_e}}}\right)} \tag{6.4}$$

The various variables in Equations (6.3) and (6.4) are calculated as follows:

The lift-curve slope of the horizontal tail angle of the wing body combination, $C_{L_{\alpha_H}}$ and $C_{L_{\alpha_{WB}}}$, respectively, are computed in subroutine "LIFCRV".

The downwash $d\epsilon/d\alpha$ is calculated in subroutine "DOWNWS".

The control-surface parameters C_{h_α}, τ_E and $C_{h_{\delta_e}}$ are computed in subroutine "CONSURF". Section 11.26.

The aerodynamic center of the horizontal tail plane and of the wing, $\bar{X}_{ac_H}$ and $\bar{X}_{ac_W}$, respectively, are defined in Figure 6.1. They may be computed with reference to Figure 6.2.

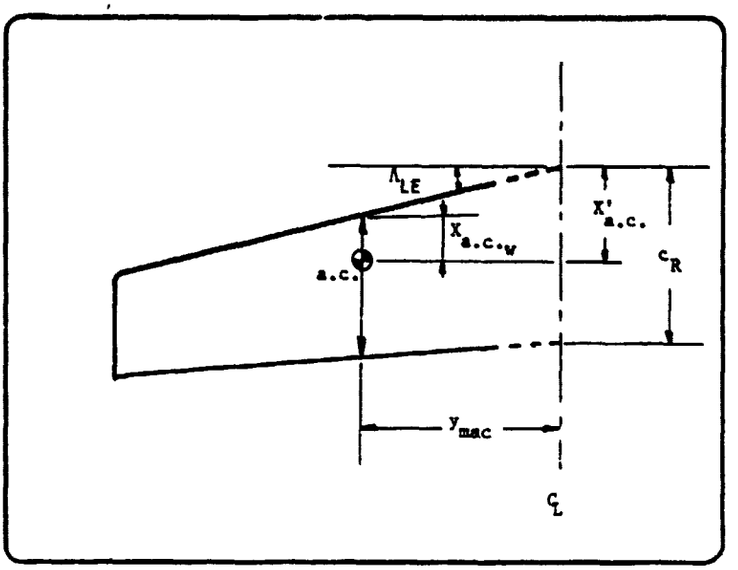

Figure 6.1: Definition of dimensional and non-dimensional aerodynamic center locations

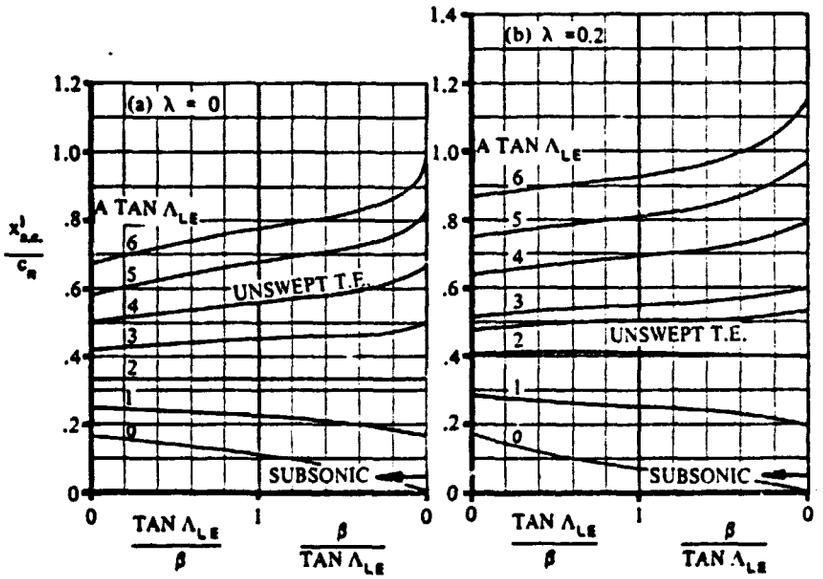

Figure 6.2: Aerodynamic center locations of lifting surfaces

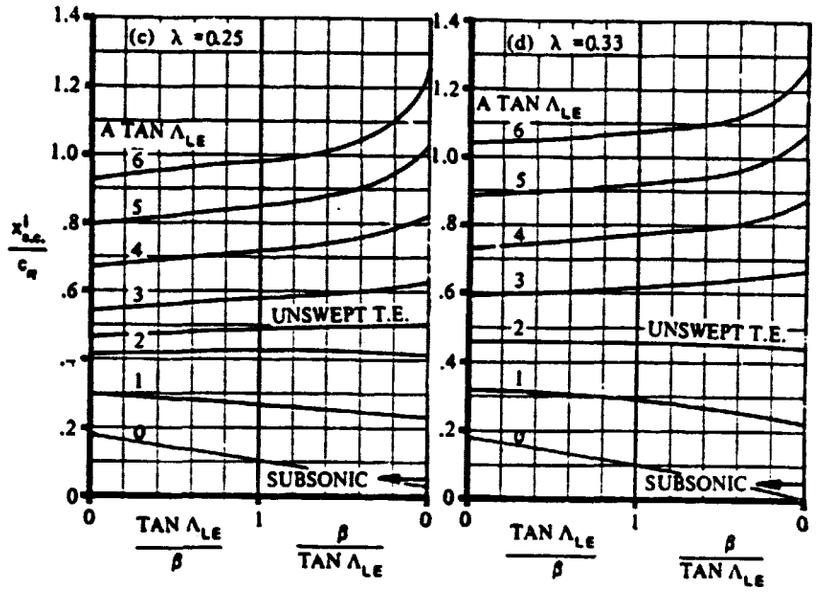

Figure 6.2: Continued

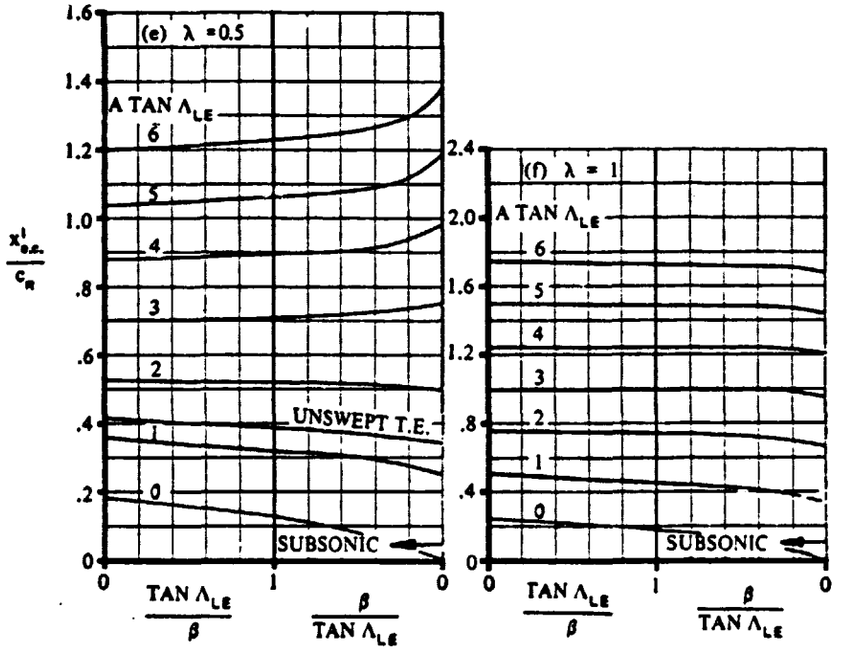

Figure 6.2: continued

To convert the value of X'_{ac}/C_R, from Figure 6.2, to the nondimensional value $\bar{X}_{ac}$, use is made of Equation (6.5):

$$\bar{X}_{ac} = K_1 \left(X'_{ac}/C_R - K_2\right) \tag{6.5}$$

where K_1 and K_2 are given as:

$$K_1 = 1.5 - .1475\,\lambda - .625\,\lambda^2 \tag{6.6}$$

$$K_2 = (.09396 + .16246\,\lambda + .02113\,\lambda^2)\,AR\,\Lambda_{LE} \tag{6.7}$$

where Λ_{LE} in rad.

Note: The Equations (6.6) and (6.7) were obtained from Figures 3.10 and 3.11 of Reference 6.1 by curve fitting techniques.

The wing-body aerodynamic center may be computed from:

$$\bar{X}_{ac_{WB}} = \bar{X}_{ac_W} + \Delta\,\bar{X}_{ac_B} \tag{6.6}$$

The body-induced aerodynamic center shift $\Delta\bar{X}_{ac_B}$ in Equation (6.6) follows from:

$$\Delta\,\bar{X}_{ac_B} = \frac{-dM/d\alpha\ \text{(Body and/or Nacelles, Tailboom)}}{\bar{q}S\bar{c}C_{L_{\alpha_W}}} \tag{6.7}$$

where:

$$\frac{dM}{d\alpha} = \frac{\bar{q}}{36.5}\sum_{i=1}^{i=h} W_f^{\,2}\,(X_i)\,\frac{d\epsilon}{d\alpha}\Big|_i\,\Delta X_i \tag{6.8}$$

The geometric variables in Equation (6.8) are defined in Figure 6.3.

The downwash ahead of the wing may be found from Figure 6.4. Note the different curves for different parts of the body forward of the wing.

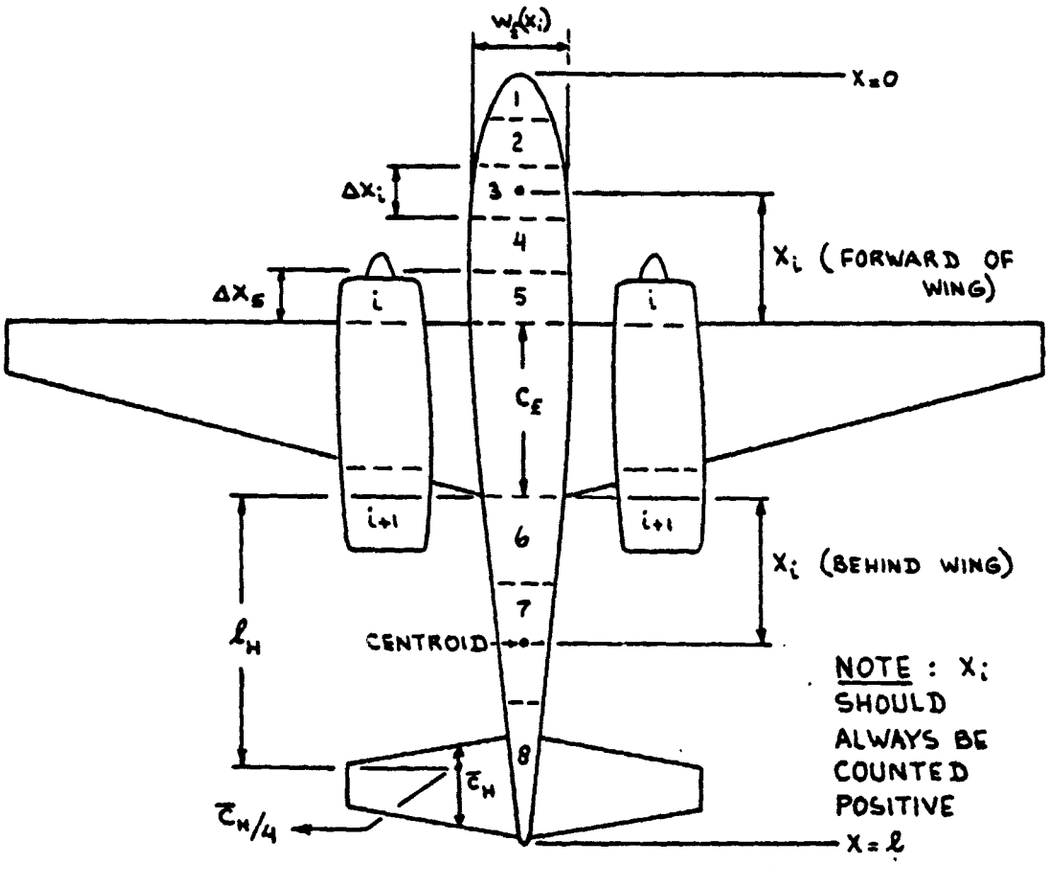

Figure 6.3: Geometric parameters for the computation of the effect of body or nacelles on a.c. location

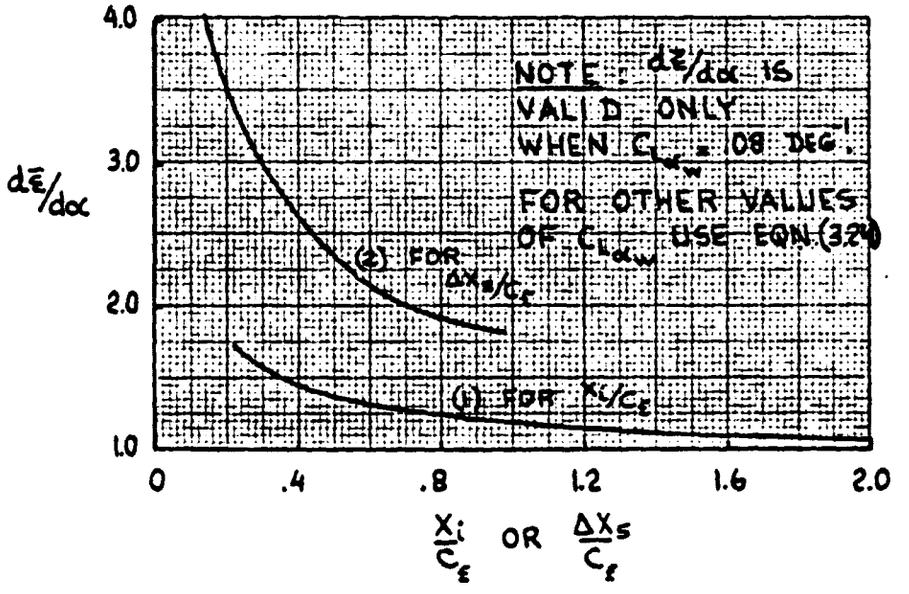

Figure 6.4: Upwash ahead of the wing

The downwash behind the wing may be found from:

$$\left.\frac{d\epsilon}{d\alpha}\right|_{X_i} = \left(1 - \frac{d\epsilon}{d\alpha}\right) \frac{X_i}{\ell_H} \tag{6.9}$$

where $\frac{d\epsilon}{d\alpha}$ is found from Section 11.3, Equation (11.3.1).

If $C_{L_{\alpha_W}} \neq .08 \text{ deg}^{-1}$, then a correction has to be applied to Equation (6.9):

$$\left.\frac{d\bar{\epsilon}}{d\alpha}\right|_{C_{L_{\alpha_W}}} = \left(\left.\frac{d\bar{\epsilon}}{d\alpha}\right|_{C_{L_{\alpha_W}}=.08}\right) \left(\frac{C_{L_{\alpha_W}}}{.08}\right) \tag{6.10}$$

This concludes the derivation of equations for the Static Longitudinal Stability.

6.3 HAND CALCULATION

Following is a hand calculation for Airplane C. Data for this airplane are provided in Appendix C.

A separate checkout for Function "ACEM" was done to make sure that this program works properly. Tests were done for three different wings; data are given in Table 6.1.

TABLE 6.1 WING GEOMETRY (Test Wings for "ACEM")

	#1	#2	#3
Span (ft)	34.0	30.0	30.0
Surface (ft^2)	204.0	165.0	180.0
Aspect Ratio	5.667	5.45	5.00
Root Chord (ft)	6.0	7.0	10.0
Tip Chord (ft)	6.0	4.0	2.0

TABLE 6.1 WING GEOMETRY (Test Wings for "ACEM") (continued)

WING	#1	#2	#3
MAC (ft)	6.0	5.65	7.0
Taper Ratio	1.0	.571	.20
L.E. Sweep (deg)	0.0	6.843	43.13
Lat. Pos. AC.	8.5	6.75	5.8

Calculations were done for different Mach numbers for each wing. The results of these calculations are given in Table 6.2.

TABLE 6.2 RESULTS OF CALCULATIONS FOR "ACEM"

WING	#1		#2		#3	
MACH	.0	.5	.0	.95	.0	.85
β	1.0	.866	1.0	.312	1.0	.527
AR $\tan\Lambda_{LE}$	0.0	0.0	.654	.654	4.685	4.685
$\tan\Lambda_{LE}/\beta$	0.0	0.0	.12	.384	.937	1.779
X'_{ac}/C_R	.24	.24	.31	.297	.738	.804
$\bar{X}_{ac_W}$	.24	.24	.241	.225	.278	.373

A comparison with the values as computed by the computer program is given in Table 6.3.

TABLE 6.3 COMPARISON OF CALCULATIONS FOR "ACEM"

WING	#1		#2		#3	
MACH	.0	.5	.0	.95	.0	.85
$\bar{X}ac_W$ (Hand calc.)	.24	.24	.241	.225	.278	.373
$\bar{X}_{ac_W}$ (Computer)	.267	.267	.244	.226	---	.373
% error	11.3	11.3	1.2	.44	---	1.1

From these results it appears that Function "ACEM" works properly.

The hand check for Airplane C was done for the following flight conditions:

$$\alpha_b = 2.0 \quad (\text{deg})$$

$$C_L = 0.461$$

$$M = 0.175$$

Function "SLOPE" gives:

$$C_{L_{\alpha_H}} = 4.495 \quad (\text{rad}^{-1})$$

$$C_{L_{\alpha_W}} = 4.653 \quad (\text{rad}^{-1})$$

Subroutine "LIFCRV" then computes:

$$C_{L_{\alpha_{WB}}} = 4.651 \quad (\text{rad}^{-1})$$

The downwash is computed in subroutine "DOWNSW" as:

$$d\varepsilon/d\alpha = 0.627$$

Function "ACEM" computes the aerodynamic center positions as:

$$\bar{X}_{ac_H} = 0.219$$

$$\bar{X}_{ac_W} = 0.352$$

Subroutine "MULTOP" computes the aerodynamic center shift due to body as:

$$\Delta \bar{X}_{ac_B} = -0.038$$

Assuming a dynamic pressure ratio at the horizontal tail of

$$\eta_H = 1.0$$

Equation (6.3) then gives:

$$\bar{X}_{ac_{Fixed}} = 0.305$$

Equation (6.4) gives the aerodynamic center position for the stick-free case as:

$$\bar{X}_{ac_{Free}} = 0.304$$

In this case the hing-moment data were obtained from Reference 6.2 as:

$$C_{h_\alpha} = .115 \ (rad^{-1})$$

$$C_{h_\delta} = -.74 \ \ (rad^{-1})$$

$$\tau_E = .674$$

The static margin now can be computed according to Equation (6.2) as:

$$dC_M/dC_L = -0.205 \quad \text{(stick fixed)}$$

$$dC_M/dC_L = -0.204 \quad \text{(stick free)}$$

The lift-curve slope of the complete airplane is computed in subroutine "LIFCRV" as:

$$C_{L_{\alpha}}{}_{WBM} = 5.183 \quad (rad^{-1})$$

Finally, Equation (6.1) computes the static longitudinal stability as:

$$C_{M_{\alpha}} = -1.061 \quad (rad^{-1}) \text{ for the stick-fixed case;}$$

$$\text{or: } C_{M_{\alpha}} = -1.057 \quad (rad^{-1}) \text{ for the stick-free case.}$$

6.4 PROGRAM DESCRIPTION

The computation of the Static Longitudinal Stability parameters is split into several parts.

1) Function "ACEM" computes the aerodynamic center position for a given lifting surface.
2) Subroutine "MULTOP" computes the aerodynamic center shift due to body presence.
3) A mainline that performs the computations and calls the respective subroutines as functions.

Function "ACEM" will be described hereafter. The curves of Figure 6.2 are input as straight lines. The curved sections of the curves may be ignored, since these parts apply only for high Mach numbers and high sweep angle combinations. To avoid the problem of the dual nature of the X-axis, the following conversion can be made:

$$\frac{\text{Tan}\Lambda_{LE}}{\beta} = 2. - \frac{\beta}{\text{Tan}\Lambda_{LE}} \qquad (6.11)$$

All the curves of Figure 6.2 are put in an array DD. An interpolation routine is internal in Function "ACEM" to compute the aero-

dynamic center position for given planform parameters.

Subroutine "MULTOP" is an existing routine that is documented in Reference 6.3. It performs an iteration according to Equation (6.7). Two variables in the subroutine "MULTOP" need special mention: the shape parameters N_{Y_1} and M_{Y_1}. They define the shape of the nose as seen from above and, therefore, the width of the fuselage at a certain station. They are defined and computed in Reference 6.3.

TABLE 6.4 VARIABLES IN SUBROUTINE "CMALPHA"

NAME	ENG. SYMBOL	DIMENSION	ORIGIN	REMARKS
ALPHA	α	rad	Common	
AR	AR	---	Common	
ARC	---	---	---	
ARH	AR_H	---	Common	
B	B	ft	Common	
CBARH	$\bar{c}_H$	ft	---	
CBARW	$\bar{c}_W$	ft	---	
CHA	C_{h_α}	rad^{-1}	"CONSURF"	
CHD	C_{h_δ}	rad^{-1}	"CONSURF"	
CL	C_L	---	Common	
CLAH	$C_{L_{\alpha_H}}$	rad^{-1}	"SLOPE"	
CLAHP	$C_{\ell_{\alpha_H}}$	rad^{-1}	Common	

TABLE 6.4 VARIABLES IN SUBROUTINE "CMALPHA" (continued)

NAME	ENG. SYMBOL	DIMENSION	ORIGIN	REMARKS
CLALPA	C_{L_α}	rad^{-1}	"LIFCRV"	
CLAW	$C_{L_{\alpha_W}}$	rad^{-1}	"SLOPE"	
CLAWB	$C_{L_{\alpha_{WB}}}$	rad^{-1}	---	
CLAWP	$C_{\ell_{\alpha_W}}$	rad^{-1}	Common	
CMAFIX	$C_{M_{\alpha_{fix}}}$	rad^{-1}	---	
CMAFR	$C_{M_{\alpha_{free}}}$	rad^{-1}	---	
CMAFRE	$C_{M_{\alpha_{free}}}$	rad^{-1}	---	
CMCLFI	$dC_M/dC_{L_{fix}}$	rad^{-1}	---	
CMCLFR	$dC_M/dC_{L_{free}}$	rad^{-1}	---	
CMFI	---	rad^{-1}	---	
CMFIX	---	rad^{-1}	---	
CMFR	---	rad^{-1}	---	
CMFREE	---	rad^{-1}	---	
CRCLW	$C_{R_{C_{L_W}}}$	ft	Common	
CRCLWC	---	ft	---	
DCMTOT	$\Delta C_{M_{tot}}$	rad^{-1}	"POWER"	
DEHP	$\Delta\varepsilon_p$	rad	"POWER"	

TABLE 6.4 VARIABLES IN SUBROUTINE "CMALPHA" (continued)

NAME	ENG. SYMBOL	DIMENSION	ORIGIN	REMARKS
DEHPA	$d\epsilon/d\alpha\|_p$	---	---	
DELTC	---	---	---	
DERDAL	$d\epsilon/d\alpha$	---	"DOWNWS"	
DFUS	D_{fus}	ft	Common	
DLMC4	$\Lambda_{1/4\bar{c}}$	deg	Common	
DLMC4C	---	deg	---	
DLMC4H	$\Lambda_{1/4\bar{c}_H}$	deg	Common	
DQHQI	$\Delta\eta_H$	---	"POWER"	
DXACB	$\Delta\bar{X}_{ac_B}$	ft	"MULTOP"	
ELC4W	$\ell_{1/4\bar{c}_W}$	ft	Common	
ELF	ℓ_{fus}	ft	Common	
ELODT	ℓ_{fus}/D_{fus}	---	Common	
ELTH	ℓ_H	ft	Common	
EM	M	---	Common	
EMC	---	---	---	
FACT	---	---	---	
HC	h_c	ft	Common	
HH	h_H	ft	Common	
KSURF	---	---	---	
LN	ℓ_{nose}	ft	Common	

TABLE 6.4 VARIABLES IN SUBROUTINE "CMALPHA" (continued)

NAME	ENG. SYMBOL	DIMENSION	ORIGIN	REMARKS
MY1	M_{Y_1}	---	Common	
MC	M_C	---	Common	
NY1	N_{Y_1}	---	Common	
NC	N_C	--	Common	
SHT	S_H	ft^2	Common	
SLM	λ	---	Common	
SLMH	λ_H	---	Common	
SLMC	---	---	Common	
SW	S_W	ft^2	Common	
TE	τ_E	---	"CONSURF"	
QHQI	η_H	---	---	
QHWIP	$\eta_H\|_p$	---	"POWER"	
XBARCG	$\bar{X}_{cg}$	ft	Common	
XBARFI	$\bar{X}_{ac_{fixed}}$	ft	---	
XBARFR	$\bar{X}_{ac_{free}}$	ft	---	
XBARH	$\bar{X}_{ac_H}$	ft	---	
XBARW	$\bar{X}_{ac_W}$	ft	---	
XBARWB	$\bar{X}_{ac_{WB}}$	ft	---	
XNAC	X_{nac}	ft	Common	

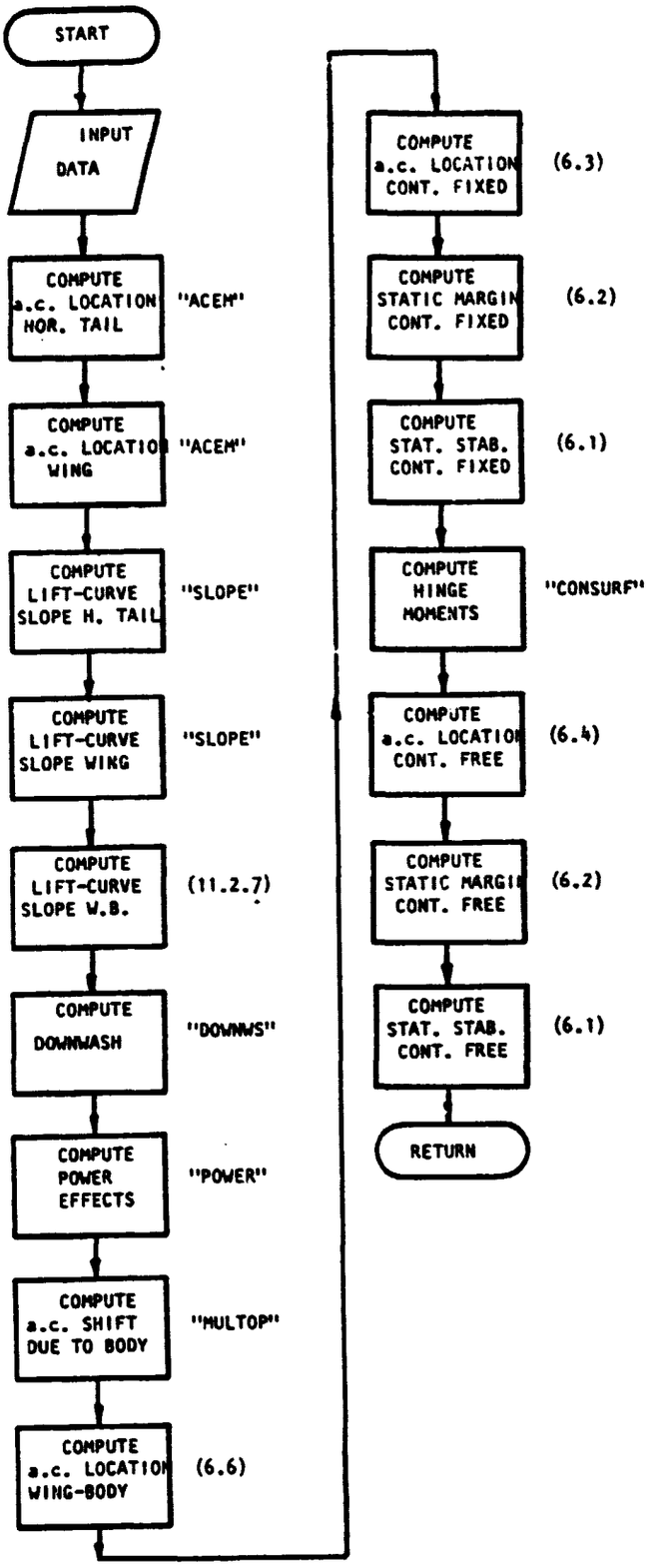

Figure 6.5: Flowchart for subroutine "CHALPHA"

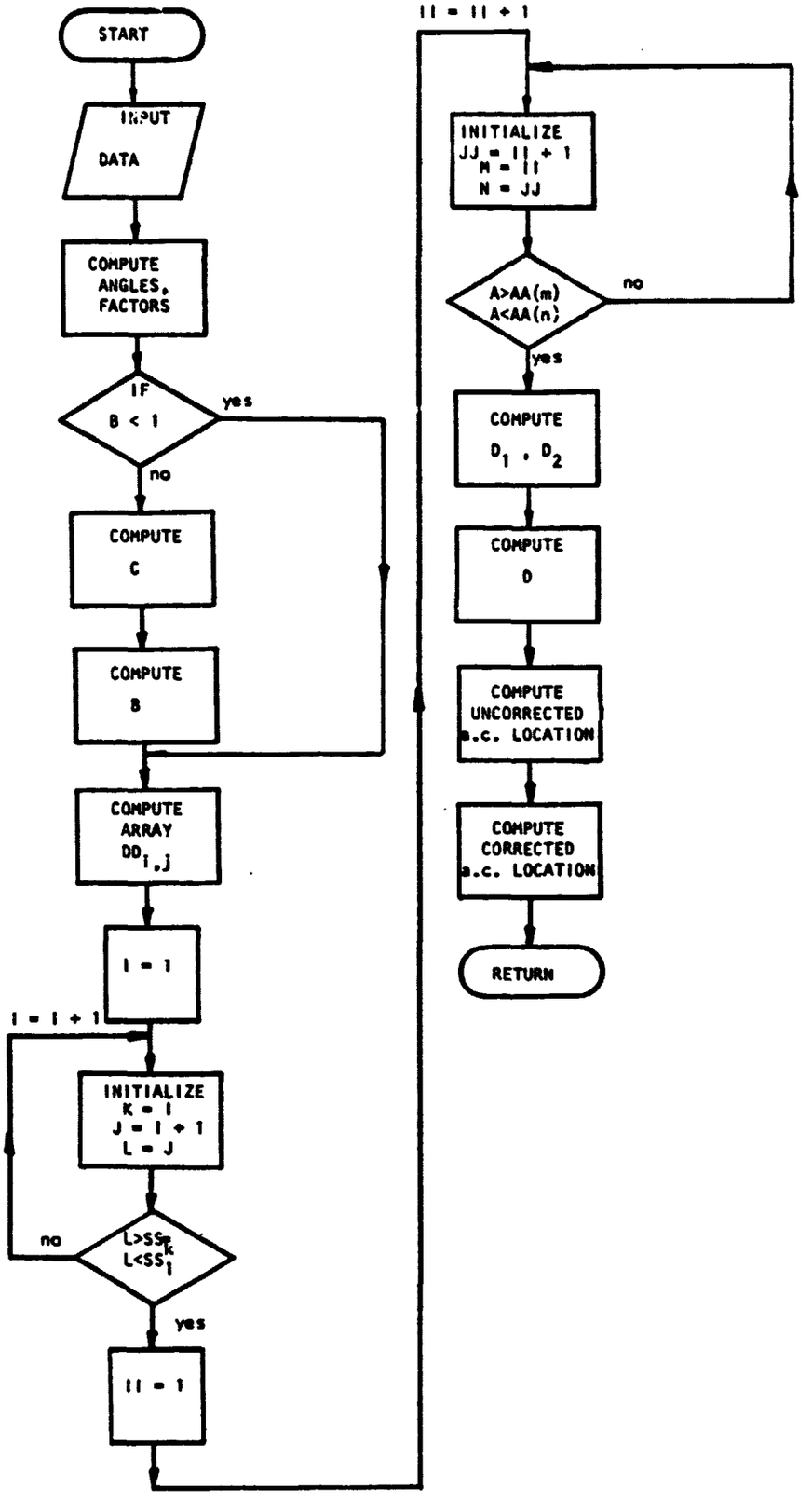

Figure 6.5: Continued

```
      SUBROUTINE CMALPHA (CMCLFI,CMAFIX,XBARFI,XBARFR,CMCLFR,
     &CMAFRE)
      WRITE (6,1000)
      REAL LN,MY1,NY1,MC,NC
      COMMON/WING/DLMC4,AR,SLM,B,CRCLW,CBARW,SW,CLAWP
      COMMON/HORTAIL/DLMC4H,ARH,SLMH,CBARH,SHT,CLAHP
      COMMON/FUS/ELF,DFUS,HC,WC,LN,ELTH,HH
      COMMON/WEIGHT/XBARCG,WEIGHT
      COMMON/NAC/XNAC
       COMMON/SHAPE/MY1,NY1,MC,NC,ELC4W,DELTC,ELODT
      COMMON/FLITE/ALPHA,EM,CL
      XBARH=ACEM (EM,ARH,SLMH,DLMC4H,CRCLH)
      XBARW=ACEM (EM,AR,SLM,DLMC4,CRCLW)
      CLAH=SLOPE (DLMC4H,SLMH,ARH,EM,CLAHP)
      CLAW=SLOPE (DLMC4,SLM,AR,EM,CLAWP)
       CLAWB=CLAW*(1.-.25*(DFUS/B)**2.+.025*DFUS/B)
       CALL DOWNWS (DEPDAL)
      CALL POWER (DEHP,DQHQI)
      DEHPA=DEHP/ALPHA
      DEPDAL=(1.-(DEPDAL+DEHPA))
      QHQIP=QHQI+DQHQI
      CALL MULTOP (ELF,DXACB)
      XBARWB=XBARW+DXACB
      FACT=(CLAH/CLAWB)*QHQIP*(SHT/SW)*DEPDAL
      XBARFI=(XBARWB+FACT*XBARH)/(1.+FACT)
      CMCLFI=XBARCG-XBARFI
      CLALPA=CLAWB+CLAH*QHQIP*(SHT/SW)*DEPDAL
      CMAFI=CMCLFI*CLALPA
      CMFI=CMAFI*ALPHA
      CMFIX=CMFI+DCMTOT
      CMAFIX=CMFIX/ALPHA
      IF (KSURF.EQ.1) GOTO 50
      CALL CONSURF (CHATE,CHDE)
 50   XBARFR=(XBARWB+FACT*XBARH*(1.-CHA*TE/CHD))/
     &(1.+FACT*(1.-CHA*TE/CHD))
      CMCLFR=XBARCG-XBARFR
      CMAFR=CMCLFR*CLALPA
      CMFR=CMAFR*ALPHA
      CMFREE=CMFR+DCMTOT
      CMAFRE=CMFREE/ALPHA
      WRITE (6,1050) XBARFI
1050  FORMAT (10X,"XBARFI   =            ",1F10.5)
      WRITE (6,1060) CMCLFI
1060  FORMAT (10X,"CMCLFI   =            ",1F10.5)
      WRITE (6,1070) CMAFIX
1070  FORMAT (10X,"CMAFIX   =            ",1F10.5)
      WRITE (6,1080) XBARFR
1080  FORMAT (10X,"XBARFR   =            ",1F10.5)
      WRITE (6,1090) CMCLFR
1090  FORMAT (10X,"CMCLFR   =            ",1F10.5)
      WRITE (6,1100) CMAFRE
1100  FORMAT (10X,"CMAFRE   =            ",1F10.5)
333   CONTINUE
      RETURN
      END
```


Figure 6.5: Listing of subroutine "CMALPHA"

```
10     FUNCTION ACEM (EMC,ARC,SLMC,DLMC4C,CRCLWC)
20     REAL K1,K2
30     RLMC4C=DLMC4C*.01745
40     SWPLE=ATAN(SIN(RLMC4C)/COS(RLMC4C)+(1./ARC)*((1.-SLMC)/(1.+SLMC)))
50     SWPLL=SWPLE
60     DIMENSION DD(6,7),AA(7),SS(6)
70     DATA  AA(1),AA(2),AA(3),AA(4),AA(5),AA(6),AA(7)
80    &/0.,1.,2.,3.,4.,5.,6./,SS(1),SS(2),SS(3),SS(4),
90    &SS(5),SS(6)/0.,.2,.25,.33,.5,1.0/
100    BETAM=SQRT(1.-EMC**2.)
110    TSWPLE=(SIN(SWPLL))/(COS(SWPLL))
120    A=ARC*TSWPLE
130    B=TSWPLE/BETAM
140    IF(B.LE.1.)GO TO 1
150    C=BETAM/TSWPLE
160    B=2.0-C
170   1 DD(1,1)=.1736-.0645*B
180    DD(1,2)=.253-.0311*B
190    DD(1,3)=.335
200    DD(1,4)=.4217+.0274*B
210    DD(1,5)=.5042+.0594*B
220    DD(1,6)=.5858+.0889*B
230    DD(1,7)=.6814+.0929*B
240    DD(2,1)=.1586-.08*B
250    DD(2,2)=.2862-.035*B
260    DD(2,3)=.407
270    DD(2,4)=.518+.0313*B
280    DD(2,5)=.639+.055*B
290    DD(2,6)=.745+.0718*B
300    DD(2,7)=.8634+.0735*B
310    DD(3,1)=.1784-.0752*B
320    DD(3,2)=.299-.0325*B
330    DD(3,3)=.4159+.008*B
340    DD(3,4)=.5409+.0368*B
350    DD(3,5)=.6683+.054*B
360    DD(3,6)=.7938+.065*B
370    DD(3,7)=.9313+.0625*B
380    DD(4,1)=.1823-.0844*B
390    DD(4,2)=.325-.0406*B
400    DD(4,3)=.4603-.0061*B
410    DD(4,4)=.5904-.029*B
420    DD(4,5)=.7287+.0464*B
430    DD(4,6)=.8821+.0441*B
440    DD(4,7)=1.0344+.0479*B
450    DD(5,1)=.1939-.0757*B
460    DD(5,2)=.358-.0364*B
470    DD(5,3)=.5275-.0094*B
480    DD(5,4)=.6944+.0183*B
490    DD(5,5)=.8772+.0214*B
500    DD(5,6)=1.0346+.032*B
510    DD(5,7)=1.1856+.0483*B
520    DD(6,1)=.2675-.1001*B
```

Figure 6.6: continued

```
      DD(6,2)=.5118-.0648*B
      DD(6,3)=.7609-.0238*B
      DD(6,4)=1.0
      DD(6,5)=1.2456-.0028*B
      DD(6,6)=1.4989-.011*B
      DD(6,7)=1.7449-.0195*B
      DO 2 I=1,5
      K=I
      J=I+1
      L=J
      IF(SLMC.GE.SS(K).AND.SLMC.LE.SS(L))GO TO 3
    2 CONTINUE
    3 DO 4 II=1,6
      JJ=II+1
      M=II
      N=JJ
      IF(A.GE.AA(M).AND.A.LE.AA(N))GO TO 5
    4 CONTINUE
    5 D1=DD(K,N)-(AA(N)-A)*(DD(K,N)-DD(K,M))
      D2=DD(L,N)-(AA(N)-A)*(DD(L,N)-DD(L,M))
      D=D2-(SS(L)-SLMC)*(D2-D1)/(SS(L)-SS(K))
      XPACW=D*CRCLWC
      IF (SLMC.GE..3) K1=-.571*(SLMC-2.751)
      K1=1.5-.1475*SLMC-.625*SLMC**2
      K2=(.09396+.16246*SLMC+.02113*SLMC**2)*ARC*SWPLE
      ACEM=K1*(D-K2)
      RETURN
      END
```

```
      SUBROUTINE MULTOP (LHNEW,DXACB)
      COMMON/WING/DLMC4,AR,SLM,B,CRCLW,CBARW,SW,CLAWP
      COMMON/AERO/EM,RHO,TAS
      COMMON/FUS/ELF,DFUS,HC,WC,LN,ELTH,HH
      COMMON/NAC/XNAC
      COMMON/SHAPE/MY1,NY1,MC,NC,ELC4W,DELTLC,ELODT
      POLY(X,C,C1,C2,C3,C4)=C+C1*X+C2*X**2.+C3*X**3.+C4*X**4.
      REAL LN,NY1,MY1,LT,ELF,LCOLD,LCNEW,NC,MC,LH,LHNEW
      DATA C0,C1,C2,C3,C4 /1.90,-1.6958,1.5759,-0.7292,0.1302/
      DATA D0,D1,D2,D3,D4/6.2503,-23.0908,60.3553,-78.4540,38.2895/
      CLAWM=SLOPE (DLMC4,SLM,AR,EM,CLAWP)
      QBAR=.5*RHO*TAS**2
      XLE = ELC4W - (CRCLW/4.)
      CRF = WC*CRCLW*(SLM-1.)/B +CRCLW
      DXI = XLE/5.
      SUM = 0.
      DO 100 I=1,5
      XI = XLE - (DXI*0.5)- DXI*(I-1)
      IF(XI.LE.(XLE-LN)) GO TO 10
      WFI = WC*((1.-(((LN+XI-XLE)/LN)**NY1))**(1./MY1))
      GO TO 20
   10 WFI = WC
      IF(I.LT.5)GO TO 20
      WFI = WC+XNAC
   20 XCF = XI/CRF
      DEDA = POLY(XCF,C0,C1,C2,C3,C4)
```

Figure 6.6: continued

```
270       IF(I.GT.4) DEDA = POLY(XCF,D0,D1,D2,D3,D4)
280       DEDAI = DEDA*CLAWM/0.08
290   100 SUM = SUM + (DXI*WFI*WFI*DEDAI)
300       LT = ELF + DELTLC - XLE - CRF
310       DXI = LT/5
320       LCNEW = ELODT * HC
330       DO 200 I=1,5
340       XI = DXI*(I-1)+(0.5*DXI)
350       IF(XI.LE.(LT-LCNEW)) GO TO 30
360       WFI = WC*((1.-(((LCNEW+XI-LT)/LCNEW)**NC))**(1./MC))
370       GO TO 40
380    30 WFI = WC
390    40 LH = LHNEW-CRF+.25*CBARW+((B/6.)*(1.+2.*SLM)/(1.+SLM)-WC/2.)
400       RLMC4=DLMC4*.01745
410       SWPLE=ATAN(SIN(RLMC4)/COS(RLMC4)+(1./AR)*((1.-SLM)/(1.+SLM)))
420      **SIN(SWPLE)/COS(SWPLE)
430       CALL DOWNWS (DEPDAL)
440       DEDAI = (1.-DEPDAL)*XI/LH
450   200 SUM = SUM + (DXI*WFI*WFI*DEDAI)
460       DMDA = (QBAR/36.5)*SUM
470       DXACB = -1.*DMDA/(QBAR*CBARW*SW*CLAWM)
480       RETURN
490       END
```

Figure 6.6: Continued

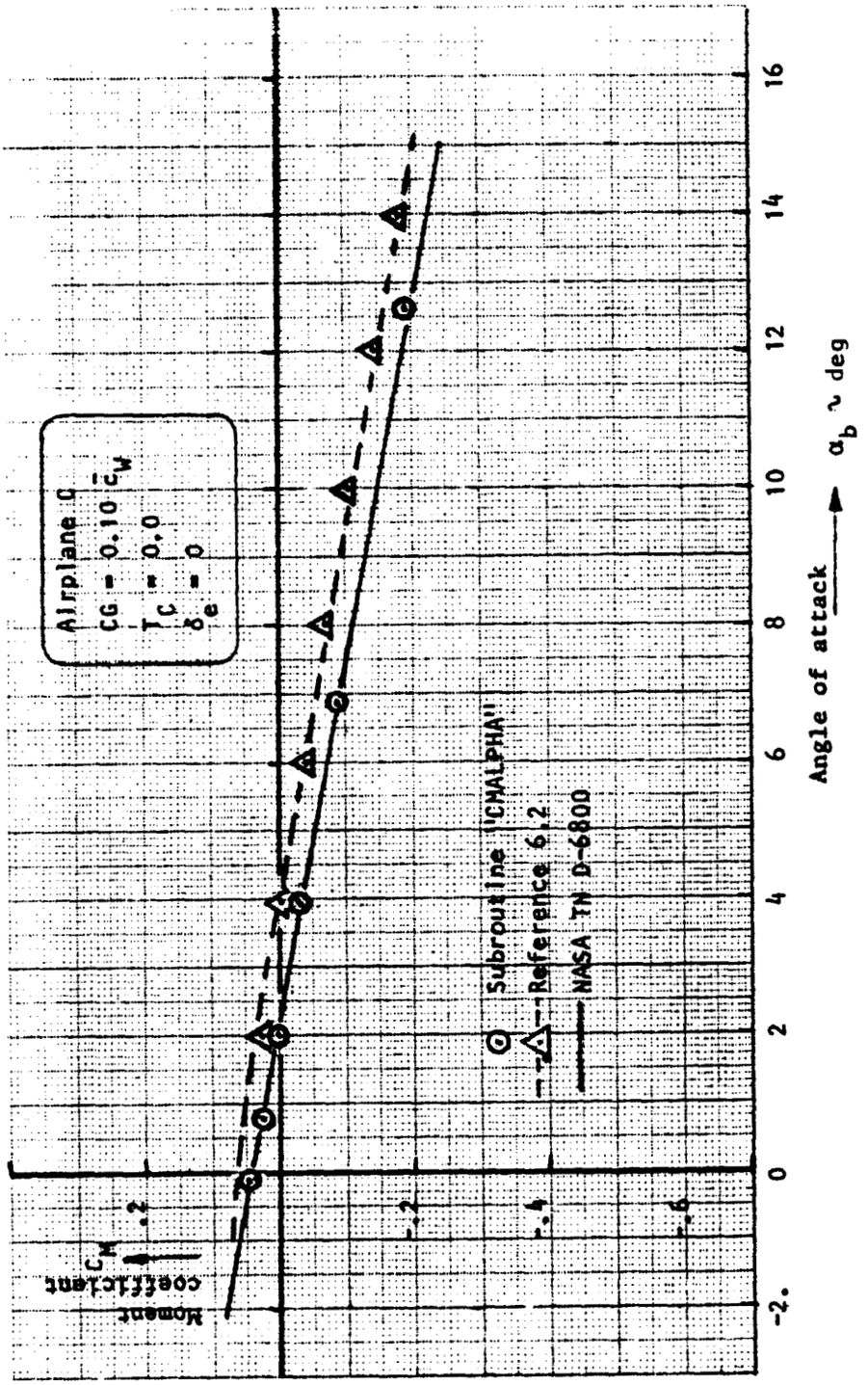

Figure 6.7: Comparison of predicted airplane pitching moments with literature

A flowchart of the program is given in Figure 6.5*. A listing and a sample output are given in Figure 6.6.

To check the validity of the program, a comparison was made with test data of Reference 6.2. The results are reproduced in Figure 6.7 for the stick-fixed case. To compute the moment about $X_{CG} = .10\bar{c}$, use was made of the following equation:

$$C_M = C_{M_0} + C_{M_\alpha}\,\alpha$$

where C_{M_0} was found from Reference 6.2 as $C_{M_0} = .04$.

As may be seen from Figure 6.7, the program works quite well.

6.5 REFERENCES

6.1 Roskam, J. Methods for Estimating Stability and Control Derivatives of Conventional Subsonic Aircraft (Roskam Aviation and Engineering Corp., Lawrence, Ks.)

6.2 Fink, M. P. & Freeman, D. C. Full Scale Windtunnel Investigation of Static Longitudinal and Lateral Characteristics of Light Twin Engine Airplanes (NASA TN D-4983)

6.3 Wyatt, R. D., Griswold, D. A., & Hammer, J. L. A Study of Commuter Airplane Design Optimization (KU-FRL 313-4/1977)

---

* Note: A flowchart of Subroutine "MULTOP" may be found in Reference 6.3.

CHAPTER 7

DIRECTIONAL STABILITY

7.1 INTRODUCTION

Generally it is quite difficult to calculate the lateral-directional aerodynamic characteristics. The vertical tail plane is the dominant factor and this surface is situated in a complex asymmetrical flow field behind the wing/fuselage combination. This chapter will describe some of the criteria important for the preliminary design phase. Also it will describe some of the methods available for computation.

7.2 DISCUSSION OF DESIGN CRITERIA

The primary preliminary design criteria for the vertical tail are the following:

1) The aircraft must possess positive directional static stability and the short-period later/directional oscillation must be well damped.
2) After failure of the critical engine, the aircraft must remain controllable, in the case of multi-engine aircraft.

To assure compliance with criterium 1), an adequate value for C_{n_β}, the static directional stability parameter has to be provided. For single-engine subsonic airplanes the value for C_{n_β} is often found to lie between .04 and .10 (Ref. 7.1). A method for the estimation of the parameter C_{n_β} is discussed in section 11.16.

To comply with criterium 2), the vertical tail has to be able to produce a certain minimum sideforce C_{y_V} to counteract the disturbing yawing moment of a stopped engine. In this case also the control-surface (i.e. rudder) parameters are important. A discussion of a method to compute these parameters is given in section 11.25 as well as in 11.14. A method to derive the minimum control speed, V_{MC}, is given in section 8.

7.3 REFERENCES

7.1 Torenbeek, E. Synthesis of Subsonic Airplane Design, Delft University Press, Delft, The Netherlands. 1976.

CHAPTER 8

VMC ROUTINE

8.1 INTRODUCTION

V_{MC} will be defined in this chapter as the minimum speed at which level or slightly climbing flight is maintained with one engine out and the remaining engine at maximum thrust, in a steady state flight condition.

The GASP program in its original form does not check for V_{MC}. Three methods for determining V_{MC} were evaluated for inclusion into GASP: the method of Torenbeek (Ref. 8.2), and single-degree-of-freedom and three-degree-of-freedom methods from Ref. 8.1.

The method of Torenbeek was found to be similar to the first method from Ref. 8.1. Hand calculations and computer solutions for the methods of Ref. 8.1 are presented in the following sections.

8.2 SINGLE-DEGREE-OF-FREEDOM APPROXIMATION

From Ref. 8.1, p. 5.37, the moment equation about the aircraft Z axis is given by:

$$C_{n_\beta}\,\beta + C_{n_{\delta_R}}\,\delta_R + \frac{N_T}{\bar{q}Sb} = 0 \tag{8.1}$$

$$\delta_R = \frac{-C_{n_\beta}\,\beta\,\dfrac{-N_T}{\bar{q}Sb}}{C_{n_{\delta_R}}} \tag{8.2}$$

To check the roll axis, the maximum sideslip angle reached if the pilot does nothing is given by:

$$\beta_{max} = \frac{-N_T}{C_{n_\beta}\,\bar{q}Sb} \tag{8.3}$$

and the aileron deflection required for this condition is given by:

$$\delta_A = \frac{-C_{\ell_\beta}\,\beta_{max}}{C_{\ell_{\delta_A}}} \tag{8.4}$$

A HP-25 routine was written to allow a fast check calculation. A list of this routine is included as Table 8.1. The routine finds rudder deflection as a function of flight speed V; V is incremented by 0.5 mph after each iteration. The airplane used for a check case was a Piper Aztec. Input values and results are listed below. Input values are taken from Ref. 8.3. Runs were made for two values of sideslip angle, 0 deg. and 5 deg. (in a helpful direction). Bank angle is not taken into account by this method.

Results by this method appear to be quite high. Maximum rudder deflection for the Aztec is 22 degrees, yielding a V_{MC} of about 103 mph at $\beta = 5°$. This is 1.5 (V_{Stall}), much higher than the 1.2 V_{Stall} requirement. From Ref. 8.4, V_{MC} for the Aztec E, a later 250 hp version, is 80.6 mph. This large a prediction error is unacceptable for preliminary design, leading to the use of the three-degree-of-freedom method.

8.3 THREE-DEGREE-OF-FREEDOM METHOD

From Ref. 8.1, p. 5.38, if a fixed bank angle is assumed, the three remaining variables are β, δ_A, and δ_R; these may be found by the following equations: 8.5, 8.6 and 8.7.

Examining these equations, it is seen that in addition to the stability derivatives of the delta matrix, the necessary input variables are: weight, flight path angle γ, bank angle ϕ_1, wing span and area, dynamic pressure $\bar{q}$, rolling moment due to thrust L_{T_1}, and yawing moment due to thrust N_{T_1}.

Bank angle ϕ is the independent variable. Yawing moment due to thrust, N_{T_1}, is found by adding the thrust of the remaining engine to the drag of the feathered propeller and multiplying by the engine moment arm, which is the lateral distance from the c.g. Rolling moment due to thrust is a function of

$$\beta_1 = \frac{\begin{vmatrix} -\dfrac{\left[mg \sin \phi, \cos \gamma, + F_{T_{Y_1}}\right]}{\bar{q}_1 S} & C_{Y_{\delta_A}} & C_{Y_{\delta_R}} \\ -L_{T_{1/\bar{q}_1 Sb}} & C_{\ell_{\delta_A}} & C_{\ell_{\delta_R}} \\ -N_{T_{1/\bar{q}_1 Sb}} & C_{n_{\delta_A}} & C_{n_{\delta_R}} \end{vmatrix}}{\begin{vmatrix} C_{Y_\beta} & C_{Y_{\delta_A}} & C_{Y_{\delta_R}} \\ C_{\ell_\beta} & C_{\ell_{\delta_A}} & C_{\ell_{\delta_R}} \\ C_{n_\beta} & C_{n_{\delta_A}} & C_{n_{\delta_R}} \end{vmatrix}} \qquad (8.5)$$

$$\delta_{A_1} = \frac{\begin{vmatrix} C_{Y_\beta} & -\dfrac{\left[mg \sin \phi, \cos \gamma, + F_{T_{Y_1}}\right]}{\bar{q}_1 S} & C_{Y_{\delta_R}} \\ C_{\ell_\beta} & -L_{T_{1/\bar{q}_1 Sb}} & C_{\ell_{\delta_R}} \\ C_{n_\beta} & -N_{T_{1/\bar{q}_1 Sb}} & C_{n_{\delta_R}} \end{vmatrix}}{[\Delta]} \qquad (8.6)$$

$$\delta_{R_1} = \frac{\begin{vmatrix} C_{Y_\beta} & C_{Y_{\delta_A}} & -\dfrac{\left[mg \sin \phi, \cos \gamma, + F_{T_{Y_1}}\right]}{\bar{q}_1 S} \\ C_{\ell_\beta} & C_{\ell_{\delta_A}} & -L_{T_{1/\bar{q}_1 Sb}} \\ C_{n_\beta} & C_{n_{\delta_A}} & -N_{T_{1/\bar{q}_1 Sb}} \end{vmatrix}}{[\Delta]} \qquad (8.7)$$

the thrust inclination angle and the aircraft angle of attack; at the angles of attack typical of low speed flight, the components of asymmetrical thrust and drag in the Z direction produce an appreciable rolling moment, in a direction which requires more aileron deflection and increases V_{MC}. An additional rolling moment is produced by lift due to the slipstream for propeller aircraft. Flight path angle is found from the engine-out maximum rate of climb from GASP at an assumed forward speed of 1.2 V_{Stall}; this approximation should be reasonable for most aircraft.

8.4 COMPUTER ROUTINE

Fig. 8.1 illustrates the variable definitions for V_{MC}.

Fig. 8.2 is a flowchart of the subroutine in the checkout state. Variables listed under "Input" are input interactively for checkout purposes.

Referring to Fig. 8.2, the delta matrix and flight path angle are computed first because they are used in the computational loop which follows. Asymmetrical drag due to the failed engine is calculated for a propeller, turbojet, or turbofan. Thrust and drag are used to find the yawing moment. In the propeller case the POWER subroutine is called and returns a value for the additional lift due to the slipstream of the operating engine. The thrust rolling moment is then computed. Rudder deflection is computed and compared with the maximum; if the deflection is too great, the routine returns to Step 10 and increases forward speed by 0.2 fps. After the rudder deflection is brought down to the maximum, aileron deflection is checked in a similar manner.

The routine assumes a symmetrical aircraft; i.e., no critical engine. Inclusion of engine rotation direction and P-factor was considered unnecessarily complex for this program; in addition, the difference in V_{MC} due to torque and P-factor would usually be within the error due to other factors. A listing of the subroutine is included as Fig. 8.3. A variable list is included in Table 8.2.

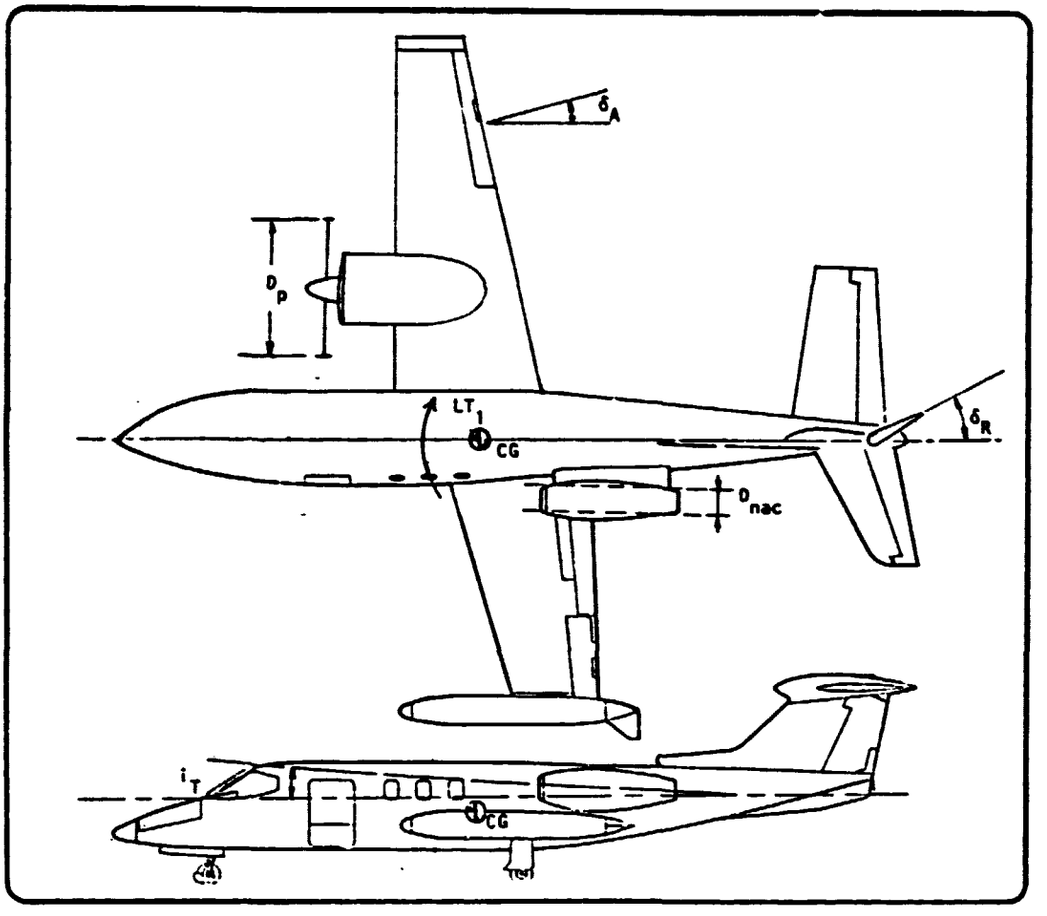

Figure 8.1 V_{mc} Variable Geometric Definitions

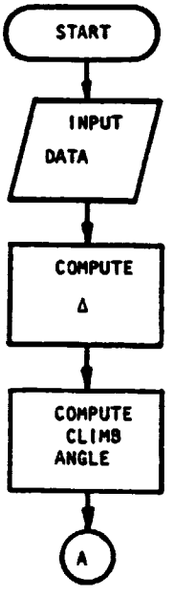

Figure 8.2: Flowchart for subroutine "VMC"

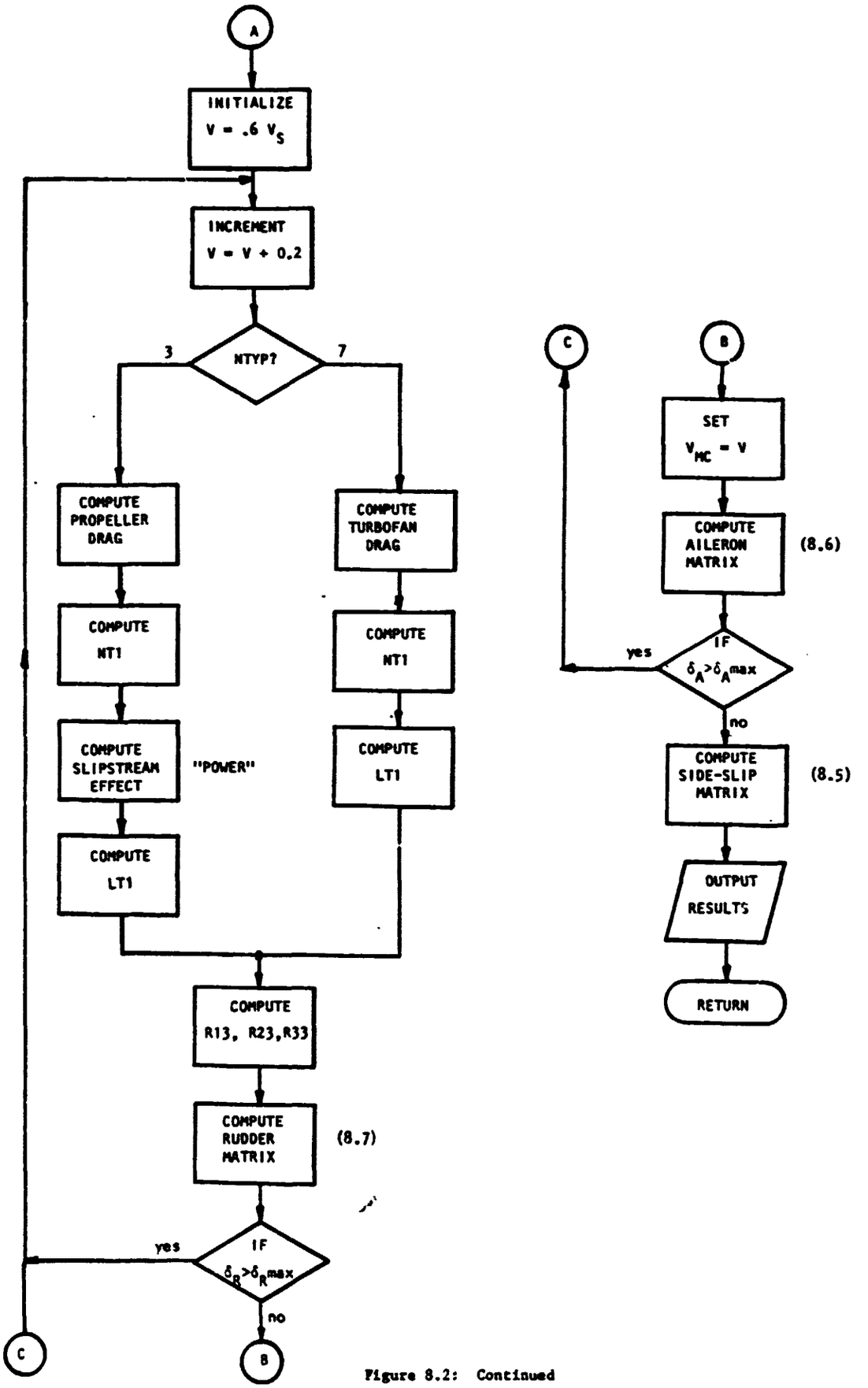

Figure 8.2: Continued

```
10      REAL NP,MAXAIL
20      PRINT:"CYB,CLB,CNB"
30      READ: CYB,CLB,CNB
40      PRINT:"CYDA,CLDA,CNDA"
50      READ: CYDA,CLDA,CNDA
60      PRINT:"CYDR,CLDR,CNDR"
70      READ:CYDR,CLDR,CNDR
80      PRINT:"VSTALL IN FPS.,CLALPHA IN RAD-1"
90      READ: VSTALL,CLALPH
100      PRINT:"WING AREA, WING SOPAN,ENG.SPAN/WING SPAN"
110      READ: SW,BW,BENGOB
120      PRINT:"PROP. EFF., MAX. HP. ONE ENG.,MAX. THRUST"
130      READ: NP,HPMSLS,THIN
140      PRINT:"MAX. RUDDER DEFL., MAX.AIL. DEFL. IN DEG."
150      READ: RUDDRM,MAXAIL
160      PRINT: "GROSS WEIGHT, ONE ENGINE CLIMB RATE"
170      READ:WG,RC3
180      PRINT: "BANK ANGLE DEG."
190      READ: BANK
200      PRINT:"PROP. DIAM. IN FT, NUMBER OF BLADES,THRUST INCL. ANGLE IN DEG"
210      READ: DPROP,BL,THRANG
215      PRINT:"IF JET ENGINE,ENTER 7,OTHERWISE ENTER 3"
216      READ:NTYP
217      PRINT:"AVERAGE NACELLE DIA."
218      READ:DBARN
220      DENSIT = 0.0023769
230      FTY=0.0
240      RUDDRM=RUDDRM/57.3
250      MAXAIL=MAXAIL/57.3
260      BANK = BANK/57.3
265      THRANG=THRANG/57.3
270      DELTA =CYB*CLDA*CNDR+CYDA*CLDR*CNB+CYDR*CLB*CNDA
280     &-CNB*CLDA*CYDR-CNDA*CLDR*CYB-CNDR*CLB*CYDA
285      ARG=(RC3*0.167)/(1.76*VSTALL)
286      GAMMA=ATAN(ARG)
290      V = 0.6*VSTALL
320  10  V = V + 0.2
330      QBAR=0.5*DENSIT*V**2
331      ALPHA=WG/(QBAR*SW*CLALPH)
332      IF(NTYP.LT.5)GO TO 13
334  12  FANDR=0.3722*DBARN**2*QBAR
335      NT1=(BENGOB*BW*0.5)*(THIN+FANDR)
336      LT1=SIN(THRANG+ALPHA)*NT1
337      GO TO 14
340  13  PROPDR = QBAR*0.00125*BL*DPROP**2
350      NT1 = (BENGOB*BW*0.5)*(HPMSLS*NP*550.0/V + PROPDR)
351C     CALL POWER(SLIFT)
360      LT1= NT1*SIN(ALPHA+THRANG)+SLIFT*BENGOB*BW*0.5
370  14  R13=-(WG*SIN(BANK)*COS(GAMMA) + FTY)/(QBAR*SW)
380      R23 = -LT1/(QBAR*SW*BW)
390      R33 = -(NT1)/(QBAR*SW*BW)
400      DRUDDR=(CYB*CLDA*R33+CYDA*R23*CNB+R13*CLB*CNDA
410     &-CNB*CLDA*R13-CNDA*R23*CYB-R33*CLB*CYDA)/DELTA
420      R=DRUDDR*DELTA
```

Figure 8.3: Listing of subroutine "VMC"

```
440   15  FORMAT(7(F10.4,5X))
450       IF(ABS(DRUDDF).GT.RUDDRM)GO TO 10
460       VMC=V
470       DAILER = (CYB*R23*CNDR+R13*CLDR*CNB+CYDR*CLB*R33
480      &-CNB*R23*CYDR-R33*CLDR*CYB-CNDR*CLB*R13)/DELTA
490       IF(ABS(DAILER).GT.MAXAIL)GO TO 10
500       BETA =(R13*CLDA*CNDR+CYDA*CLDR*R33-R33*CLDA*CYDR
510      &-CNDA*CLDR*R13-CNDR*R23*CYDA)/DELTA
520       VMC = VMC*0.6818
530       DAILER=DAILER*57.3
540       BETA =BETA*57.3
550       WRITE(6,20)VMC,DAILER,BETA
560   20  FORMAT(/,'VMC = ',F8.2,2X,'MPH',//,'AILERON DEFLECTION = ',F8.2,
570      &2X,'DEG',//,'BETA = ',F8.2,2X,'DEG.')
575       STOP
580       END
```

```
VMC =     95.18  MPH

AILERON DEFLECTION =   -13.67  DEG

BETA =     -7.44  DEG.
```

Figure 8.3: Continued

TABLE 8.1 HP-25 ROUTINE FOR SINGLE DEGREE OF FREEDOM V_{MC}

1	R/S	25	RCL1
2	STO1	26	+
3	R/S	27	CHS
4	STO2	28	RCL2
5	R/S	29	CHS
6	STO3	30	+
7	R/S	31	RCL3
8	+	32	+
9	R/S	33	STO6
10	x	34	f PAUSE
11	1	35	RCL0
12	;	36	.
13	0	37	6
14	0	38	8
15	x	39	2
16	R/S	40	x
17	+	41	f PAUSE
18	STO5	42	f PAUSE
19	RCL5	43	.
20	RCL0	44	7
21	+	45	3
22	3	46	3
23	f y^x	47	STO+0
24	+	48	GTO19

Table 8.2 VMC Variable List

VMC Variable	Symbol	Description	Units	Type, Origin
ALPHA	α	Angle of Attack	rad	Internal
BANK	ϕ	Bank Angle	deg.	Input
BENGOB	$\frac{2y_e}{b_w}$	Engine Span over Wing Span	-	Input, Common
BETA	β	Sideslip Angle	rad, deg.	Output
BL	-	Number of propeller blades	-	Input, Common
BW	b_w	Wing span	ft.	Input, Common
CLALPH	C_{L_α}	Lift-Curve Slope	rad^{-1}	Input
CLB	C_{ℓ_β}	Rolling Moment due to Sideslip	rad^{-1}	Input
CLDA	$C_{\ell_{\delta_A}}$	Rolling Moment due to Aileron Deflection	rad^{-1}	Input
CLDR	$C_{\ell_{\delta_R}}$	Rolling Moment due to Rudder Deflection	rad^{-1}	Input
CNB	C_{n_β}	Yawing Moment due to Sideslip	rad^{-1}	Input
CNDA	$C_{n_{\delta_A}}$	Yawing Moment due to Aileron	rad^{-1}	Input
CNDR	$C_{n_{\delta_R}}$	Yawing Moment due to Rudder	rad^{-1}	Input
CYB	C_{Y_β}	Side Force Coefficient due to Sideslip	rad^{-1}	Input
CYDA	$C_{Y_{\delta_A}}$	Side Force Coefficient due to Aileron	rad^{-1}	Input
CYDR	$C_{Y_{\delta_R}}$	Side Force Coefficient due to Rudder	rad^{-1}	Input
DAILER	δ_A	Aileron Deflection	rad, deg.	Output

Table 8.2 VMC Variable List (continued)

VMC Variable	Symbol	Description	Units	Type, Origin
DBARN	$\bar{D}_{NAC}$	Mean Nacelle Diameter	ft	Input, Common
DELTA	Δ	Determinant of Delta matrix	-	Internal
DENSIT	ρ	Air density	slugs/ft^3	Internal
DPROP	D_p	Propeller Diameter	ft	Input, Common
DRUDDR	δ_R	Rudder Deflection	rad, deg.	Internal
FANDR	-	Drag of Windmilling turbofan	lb	Internal
GAMMA	γ	Flight Path Angle	rad	Internal
HPMSLS	HP_{max}	Maximum sea-level horsepower	hp	Input, Common
LT1	L_{T_1}	Thrust Rolling Moment	ft lb	Internal
MAXAIL	$\delta_{A_{max}}$	Maximum Aileron Deflection	deg	Input
NP	η_p	Propeller Efficiency	-	Input
NT1	N_{T_1}	Yawing Moment due to Thrust	ft lb	Internal
NTYE	-	GASP Engine type indicator	-	Common
NTYP	-	GASP Propulsor type indicator	-	Common
PROPDR	-	Drag of feathered propeller	lb	Internal
R13,R23,R33	-	Matrix elements	-	Internal
RC3	-	Engine-Out Rate of Climb	ft /min	Input, Common
SW	S_W	Wing Area	ft^2	Input, Common
THRANG	-	Thrust inclination angle		Common

Table 8.2 VMC Variable List (continued)

VMC Variable	Symbol	Description	Units	Type, Origin
V	V	Velocity	ft/sec	Internal
VMC	V_{MC}	Minimum engine-out control speed	ft/sec, mph	Output
VSTALL	V_s	Stall speed	ft/sec	Input
WG	W_G	Gross Weight	lbs.	Input, Common

8.5 HAND CALCULATION

With the aid of an HP 25 calculator a handcalculation was done for airplane C. See Appendix C for a threeview and data. Table 8.3 shows the results of the calculation. Comparison with the computer-run indicated perfect agreement.

TABLE 8.3 RESULTS HANDCALCULATION

$\beta = 0^\circ$	δ_R deg	41.3	37.7	35.8	33.5	29.0	26.7	22.1
	V_{MC} mph	89.1	91.8	93.6	95.7	100.4	103.1	110.0
$\beta = 5^\circ$	δ_R deg	38.0	36.6	32.0	29.2	26.7	22.3	21.5
	V_{MC} mph	88.0	89.0	92.5	95.0	97.5	102.5	103.5

8.6 RESULTS

Check-runs were made for airplanes A, C and H for various bankangles. The results are shown in Table 8.4. Also a comparison was made with available testdata, again see Table 8.4. Figure 8.4 shows the dependency of V_{MC} on bankangle, the data used were for airplane H. It may be concluded that V_{MC} is computed with reasonable accuracy.

TABLE 8.4 RESULTS COMPUTER-RUNS

	Airplane	A	C	H
V_{MC}, mph	Subr. "VMC"	103.5	83.9	94.2
	Testdata	---	80.6	97.8

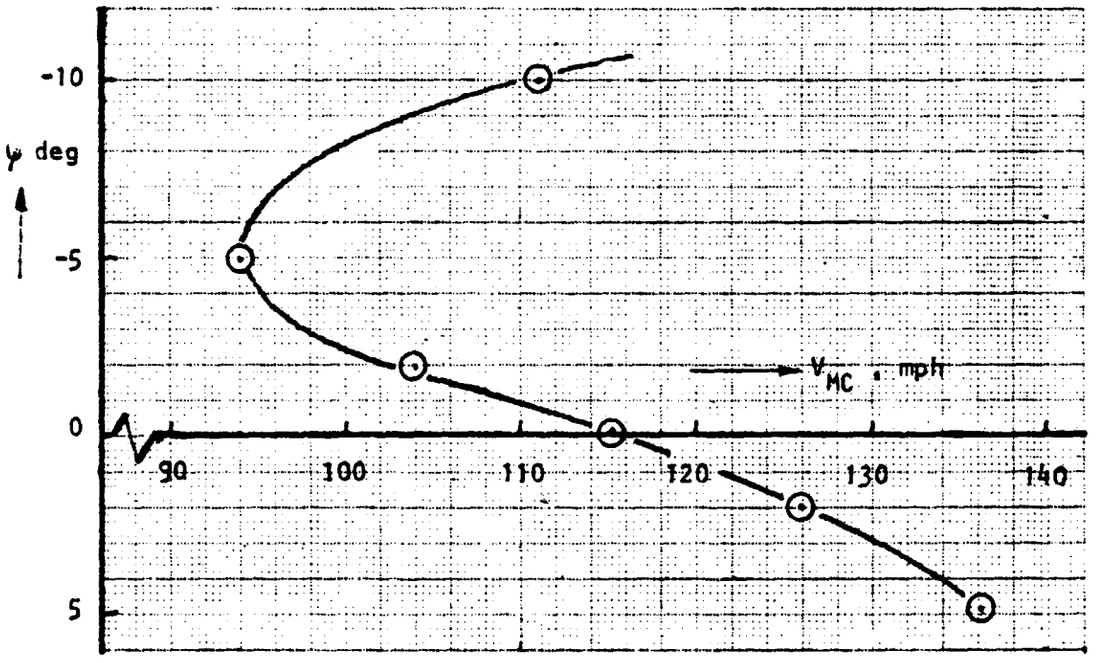

Figure 8.4: Minimum Speed V_{MC} as a Function of Bank Angle Takeoff Parameters

8.7 REFERENCES

8.1: Roskam, J. Flight Dynamics of Rigid and Elastic Airplanes. Roskam Aviation & Engineering Corp. Lawrence, Kansas. 1972

8.2: Torenbeek, E. Synthesis of Subsonic Airplane Design, Delft University Press, Delft, The Netherlands, 1976.

8.3: Wolowicz, C.H.& Yancey, R.B. Longitudinal Aerodynamic Characteristics of Light, Twin-engine, Propeller-driven Airplanes. NASA TN D-6800

CHAPTER 9

ROTATION SPEED

9.1 INTRODUCTION

The speed at which the aircraft rotates at takeoff, V_R, is calculated using a method from Reference 9.1. This method was originally developed by Perry (Ref. 9.2) and is based on a constant rate of pitch-up after lift-off. The advantage of the method is that it is representative of piloting techniques used in civil aviation since pitch angle can be directly observed, contrary to lift coefficient. The equations of motion are linearized by assuming V = constant and (T - 0) = constant.

9.2 DERIVATION OF EQUATIONS

There are certain criteria concerning the speed during the takeoff (Ref. 9.3). The most important are the following:

- V_R — The rotation speed is the speed at which the pilot raises the nose wheel.
- $V_R \geq V_1$ — Where V_1 is the decision speed.
- $V_R \geq 1.05V_{MCG}$ — Where V_{MCG} is the minimum speed for control during engine out cases.
- V_R — Should be chosen such that V_2 is reached at 35 ft, taking into account the speed increment, ΔV, between V_R and V_1.
- $V_2 = 1.2V_S$ — V_S is the 1-g stall speed.
- V_{LOF} — Is the speed at which the landing gear leaves the ground.

$V_{LOF} \leq 1.1 V_{MU}$ All engines or:

$V_{LOF} \leq 1.05 V_{MU}$ For engine out conditions, where V_{MU} is the minimum unstick speed, or the minimum speed at which the aircraft is still controllable when it leaves the ground.

For low T/W ratios, V_R and V_{LOF} may be increased to ensure positive climb gradient.

Figure 9.1 shows a schematic diagram of the takeoff.

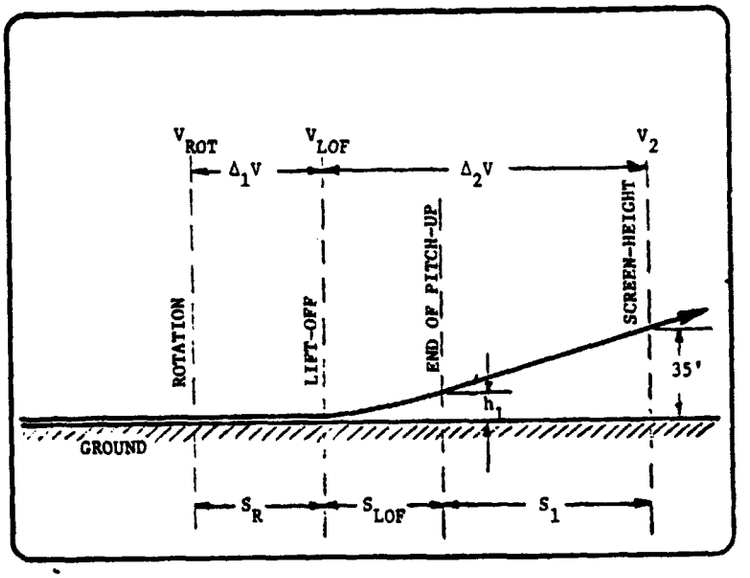

Figure 9.1: Take-off parameters.

9.2.1 ROTATION PHASE

Assuming that the acceleration along the X-axis during the rotation phase is equal to the value at lift-off and assuming a mean rate of rotation about the Y-axis $(d\theta/dt)_R$, it may be found

for the rotation distance:

$$S_R = 1/2\ (V_R + V_{LOF}) \cdot \frac{\alpha_{LOF} - \alpha_g}{(d\theta/dt)_R} \tag{9.1}$$

where: α_{LOF}: The angle of attack at which lift-off occurs; this follows from the $C_L - \alpha$ curve in ground effect.

The speed at lift-off may be calculated as follows:

$$V_{LOF} = V_R + \Delta_1 V = V_R + g\{\frac{T-D}{W}\}_{LOF} \frac{\alpha_{LOF} - \alpha_g}{(d\theta/dt)_R} \tag{9.2}$$

The rotation rate $(d\theta/dt)_R$ depends mainly on elevator power and moment of inertia about the Y-axis. As an average value 4.6 deg/sec may be taken (Ref. 9.1).

9.2.2 AIRBORNE PHASE

The speed increment from lift-off speed to the speed at 35' may be obtained from the energy equation:

$$\Delta_2 V = \frac{g(S_{LOF} + S_1)}{V_{LOF}} \{\frac{T-D}{W} - \frac{35}{S_{LOF} + S_1}\} \tag{9.3}$$

The airborne distance is composed of two phases:

- A flare-up, the flight path angle increases from zero during the ground run to γ_2 at V_2.
- A phase with constant climb angle γ_2.

The calculations for this part of the takeoff are based on Perry's method (Ref. 9.2). Perry based his method on numerous observations of takeoffs concerning light as well as heavy aircraft. From these observations functions were derived that describe the path of the aircraft after lift-off. Using these functions, it is possible to

calculate the gain in height and the flight path angle during flare-up.

The gain in height after lift-off is given by:

$$h = \frac{V_{LOF}^2}{g} \frac{T - D}{W} F(\dot{\theta}) \; F(h) \tag{9.4}$$

where:

$$F(\dot{\theta}) = 1 + \frac{V_{LOF}}{2g} \frac{W}{T - D} \eta_\alpha \left(\frac{d\theta}{dt}\right)_A \tag{9.5}$$

$$\eta_\alpha = \frac{dC_{L/d\alpha}}{C_{L_{LOF}}} \tag{9.6}$$

$F(h)$ is a non-dimensional function of height; may be determined from Figure 9.2.

The rotation rate during flare-up may be approximated by using a value of $(d\theta/dt)_A$ of 2-3°/sec for the engine failure case and 5°/sec for the all-engine case.

The climb-angle during flare-up is given by:

$$\gamma = \frac{dh}{ds} = \frac{T - D}{W} F(\dot{\theta}) \; F(\gamma) \tag{9.7}$$

where: $F(\gamma)$ is a non-dimensional flight-path angle function depicted in Figure 9.2.

The end of the flare-up is reached when $\gamma = \gamma_2$ (for the engine out case) or $\gamma = \gamma_3$ (for the all-engine case).

It should be noted that γ_2 can only be calculated when V_2 is known. Also, the functions $F(h)$ and $F(\gamma)$ are a function of the distance traveled after lift-off. The calculations are therefore iterative.

By using Hp 65 curve fitting routines, the following set of formulas was found to fit the curves in Figure 9.2:

$$F(h) = (-.01867 - .02682\ X_f + .21233\ X_f^2) + \\ + \{(3 - n_\alpha)\ (.0023 + .0543[X_f - .5])\} \qquad (9.8)$$

$$F(\gamma) = (-.09813 + .56022\ X_f - .06661\ X_f^2) + \\ + \{(3 - n_\alpha)\ (.009 + .0468\ [X_f - .4])\} \qquad (9.9)$$

where: $$X_f = \frac{g \cdot s}{V_{LOF}^2} \qquad (9.10)$$

and s is the total distance from lift-off.

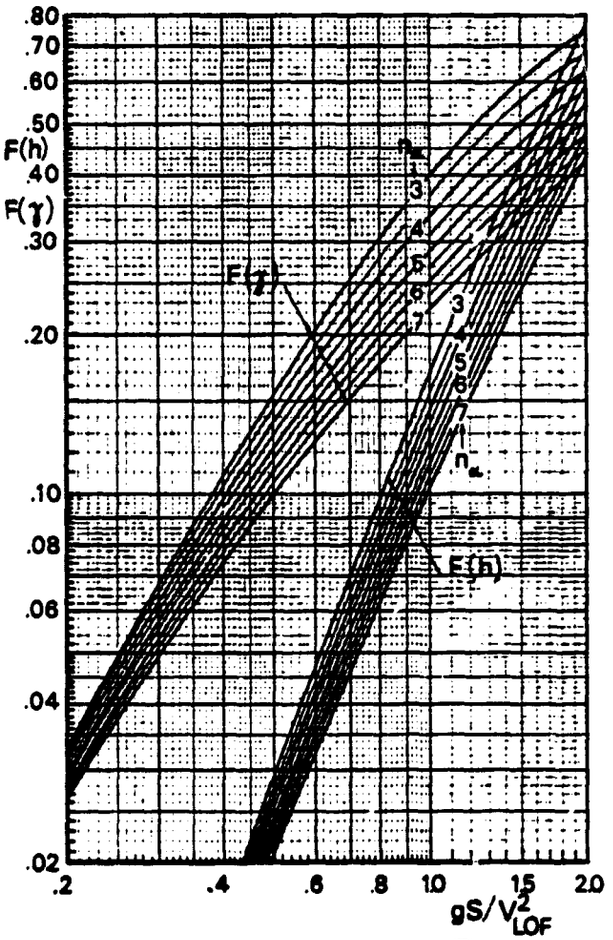

Figure 9.2: The functions F(h) and F(γ) used in Perry's method for the analysis of the airborne path (Derived from ref. 9.2)

9.3 PROGRAM DESCRIPTION

A flowchart of the program is shown in Figure 9.3. Figure 9.4 depicts the listing of the program. Included is a sample output for the airplane A. Table 9.1 defines the variables.

The lift-off speed is set slightly below the stall speed. The rotation rates $(d\theta/dt)_R$ and $(d\theta/dt)_A$ have default values .08 rad/sec and .04 rad/sec, respectively. Since these parameters are of prime importance for the rest of the calculations, they can be set at any other value that suits more closely the configuration considered. (A routine that calculates these parameters as a function of inertia along the Y-axis and elevator control power may be useful.) The lift-off speed is incremented by 2.5 ft/sec. The lift-coefficient at this value of lift-off speed is calculated, using an increment in normal acceleration of .05 ft/sec^2. If this value of the lift coefficient is greater than the maximum lift coefficient (without ground-effect), the lift-off speed is incremented. The angle of attack in ground effect is calculated by subroutine "GROUND". For the calculated value of the lift-off speed, the value of (T-D)/W is calculated, using data obtained via "COMMON". Now the rotation speed is calculated. A check is made to see if the rotation speed exceeds the speed for minimum control on the ground; if so, the lift-off speed is incremented and above procedure repeated. In the current setup, the $V_{MC_{GROUND}}$ is defaulted at .95 V_S. Now the rotation distance is calculated. The total distance traveled so far is incremented for the next loop in the program: the airborne phase. Via subroutine "GROUND" the value for the lift curve slope is calculated. At this stage the functions $F(\gamma)$ and $F(h)$ are calculated,

from the height and the climb angle. The lift-off distance S_{LOF} is incremented till the climb angle equals the climb angle for the speed V_2. ($V_2 = 1.2\ V_S$.) The distance needed to climb to 35' is calculated. Then a check is made for the speed at 35'; if this is lower than V_2, then the lift-off speed is incremented again and the complete procedure repeated till $V_{35'} = 1.2\ V_S$.

9.4 TEST-RUN

The data for the testruns were found in Reference 9.4. The testrun was done for airplane A, see Appendix C for data.

WEIGHT DEPENDENT DATA:

W	= 9000 lb	W	= 11400 lb
V_S	= 152 fps	V_S	= 175 fps
$(T-D)/W_{LIFTOFF}$	= .13	$(T-D)/W_{LIFTOFF}$	= .071
$(T-D)/W_{35'}$	= .13	$(T-D)/W_{35'}$	= .071
C_D	= .079	C_D	= .0854
C_L	= .97	C_L	= 1.163

Figure 9.4 shows the computer output for both runs.

TABLE 9.1: VARIABLES IN SUBROUTINE ROTSPEED

NAME	ENG. SYMBOL	DIMENSION	ORIGIN	REMARKS/DEFAULT
A1	---	rad^{-1}	---	Dummy
ALPHA	α	rad	Common	
ALPGR	α_g	rad	---	
ALPLØF	α_{LOF}	rad	---	

TABLE 9.1: VARIABLES IN SUBROUTINE ROTSPEED (continued)

NAME	ENG. SYMBOL	DIMENSION	ORIGIN	REMARKS/DEFAULT
BØDANG	α_{bGR}	rad	---	
CD	C_D	---	Common	
CL	C_L	---	Common	
CLLØF	$C_{L_{LOF}}$	---	---	
DCLDAG	$\Delta C_{L_{\alpha_{GR}}}$	---		
DELTS1	ΔS_1	ft	---	10
DELTV1	ΔV_1	ft/sec	---	2.5
DTDTA	$(d\theta/dt)_A$	rad/sec	---	0.087
DTDTR	$(d\theta/dt)_R$	rad/sec	---	0.087
EYEW	i_w	rad	Common	
FG1	---	---	---	Dummy
FGAM	$F(\gamma)$	---	---	
FH	F(h)	---	---	
FH1	---	---	---	Dummy
FTHDØT	$F(\dot{\theta})$	---	---	
G	g	ft/sec^2	---	32.1741
GAMMA	γ	rad	---	
GAMMA2	γ_2	rad	---	
HAC	H_{AC}	ft	---	
HEIGHT	H_g	ft	Common	

TABLE 9.1: VARIABLES IN SUBROUTINE ROTSPEED (continued)

NAME	ENG. SYMBOL	DIMENSION	ORIGIN	REMARKS/DEFAULT
H1	h_1	ft	---	
L_1-L_3	---	---	---	Dummy
NALP	n_α	rad^{-1}	---	
RHØ	ρ	lb sec^2/ft^4	Common	
S1	S_1	ft	---	
SAIR	S_{AIR}	ft	---	
SLØF	S_{LOF}	ft	---	
SN	n	ft/sec^2	---	
SRØT	S_{ROT}	ft	---	
STØT	S_{TOT}	ft	---	
SW	S_W	ft^2	Common	
T	T	lb	Common	
TDØW	$\frac{T-D}{W}$	---	---	
TDOWLØ	$(\frac{T-D}{W})_{LIFTOFF}$	---	---	
V2	V_2	ft/sec	---	
V12	---	---	---	Dummy
VLØF	V_{LOF}	ft/sec	---	
VMCG	V_{MCG}	ft/sec	---	.95 V_S
VRØT	V_{ROT}	ft/sec	---	
VSTALL	V_S	ft/sec	Common	
W	W	lb	Common	
XF	X_f	---	---	Dummy

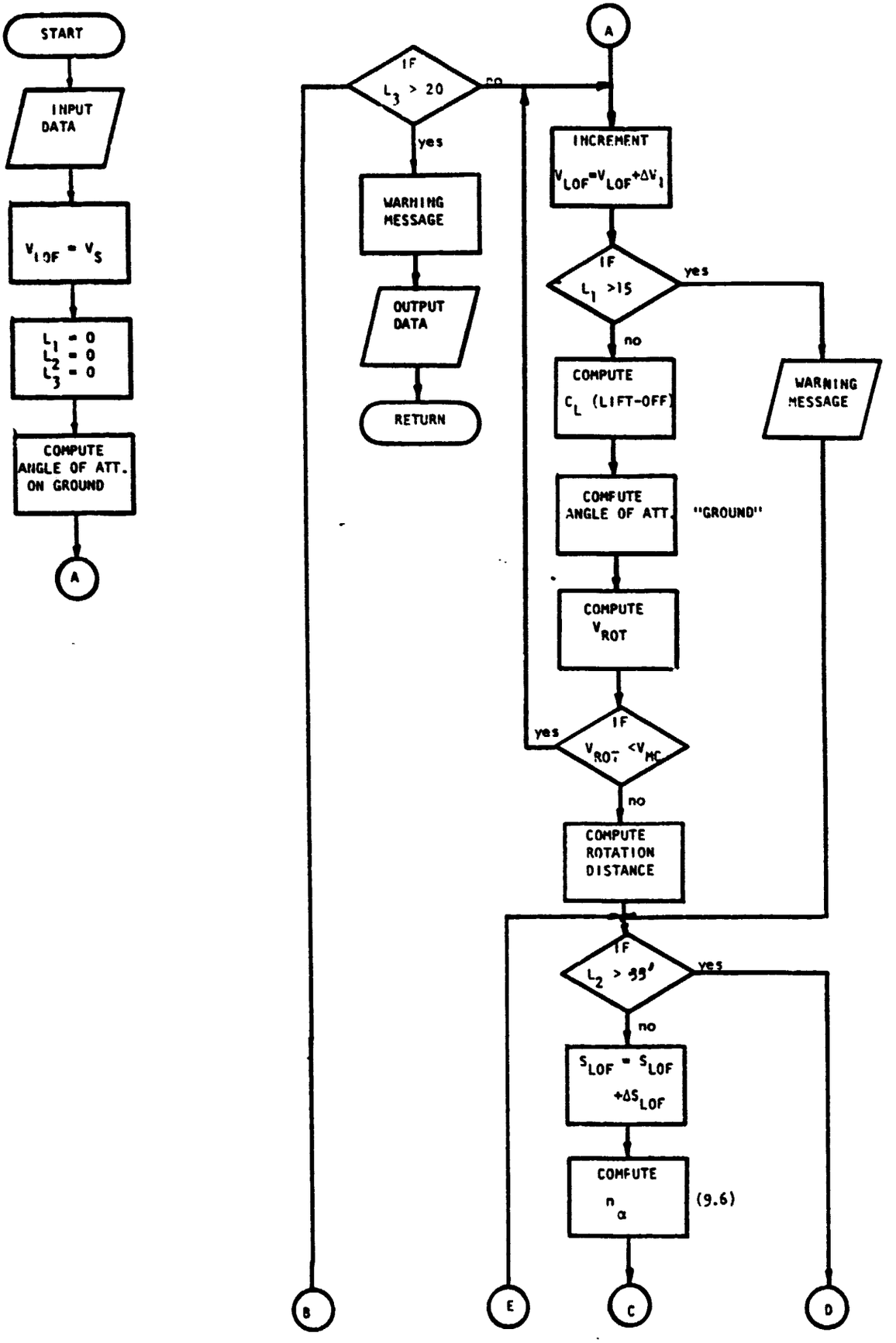

Figure 9.3: Flowchart for subroutine "ROTSPD"

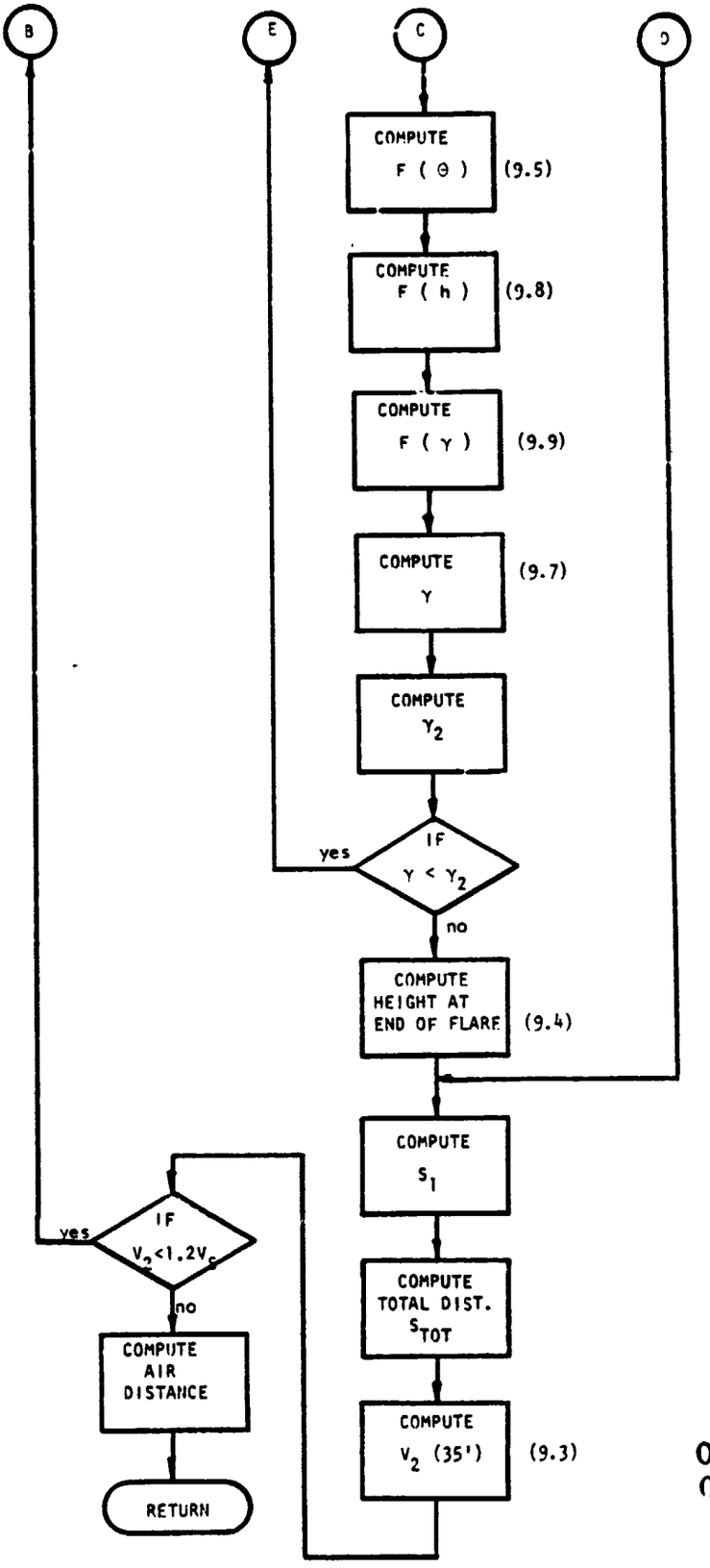

ORIGINAL PAGE IS
OF POOR QUALITY

Figure 9.3: continued

```
1     DATA VSTALL,EYEW,BODANG/168.9,.044,.0/
2     DATA SN,W,RHO,SW/0.,11400.,.0023769,231.77/
3     DATA HEIGHT,ALPHA,TDOWLO/2.7,.124,.122/
4     DATA A1,TDOW,T,CD,CL/5.114,.096,2000.,.0834,1.163/
5     DATA VMCG,CLMAX/0.,1.32/
6     DATA DTDTR,DTDTA/.09,.04/
10C        SUBROUTINE ROTSPD (VROT)
20C
30C        THIS SUBROUTINE CALCULATES THE ROTATION
40C        SPEED, ACCORDING TO THE METHOD OF TORENBEEK.
50C
60         WRITE (6,5)
70     5   FORMAT (10X,"KU-FRL DEVELOPED SUBROUTINE FOR CALCULATION")
80         WRITE (6,6)
90     6   FORMAT (10X,"OF THE ROTATION AND THE LIFT-OFF SPEED")
95         WRITE (6,4)
96      4  FORMAT (10X,"TESTRUN FOR LEARJET MODEL 26"///)
100        REAL NALP
105
110        VLOF=VSTALL-2.5
115        L1=0
116        L2=0
117        L3=0
130        G=32.1741
140        IF (DTDTR.EQ.0.) DTDTR=0.08
145        CONTINUE
150        IF (DTDTA.EQ.0.) DTDTA=0.04
155        ALPGR=EYEW+BODANG
159        GO TO 20
160     2  CONTINUE
161        L3=L3+1
162        IF (L3.GT.20) GO TO 3
170    20  CONTINUE
180        VLOF=VLOF+2.5
181        L1=L1+1
182        IF (L1.GT.15) GO TO 12
185        IF (SN.EQ.0.) SN=1.05
190        CLLOF=2.*SN*W/(RHO*SW*(VLOF**2.))
195        IF (CLLOF.GT.CLMAX) GOTO 20
200        HAC=HEIGHT
210C       CALL GROUND
220        ALPLOF=ALPHA
223C
224C       COMPUTATION OF ROTATION SPEED AND DISTANCE
225C
228C       TDOWLO=(T-D)/W
230        VROT=VLOF-G*TDOWLO*((ALPLOF-ALPGR)/DTDTR)
235        IF (VMCG.EQ.0.) VMCG=.95*VSTALL
240        IF (VROT.LT.VMCG) GO TO 20
250        SROT=.5*((VROT+VLOF)*((ALPLOF-ALPGR)/DTDTR))
258    41  CONTINUE
260        SLOF=0.
```

Figure 9.4: Listing of subroutine "ROTSPD"

```
270    30 CONTINUE
271       L2=L2+1
272       IF (L2.GT.50) GOTO 74
280       SLOF=SLOF+10.
285       HAC=H1
290C      CALL CLIFT
300       DCLDAG=A1
310       NALP=DCLDAG/CLLOF
313C
314C      THE FOLLOWING FORMULAS ARE HP-65 CURVE
315C      FITTINGS FOR FIG. 9.2 (REF 9.1), USED
316C      FOR COMPUTATION OF HEIGHT AND CLIMB-
317C      ANGLE DURING PITCH-UP
318C
320       FTHDOT=1.+(VLOF/(2.*G))*(1./TDOW)*NALP*DTDTA
330       XF=G*SLOF/(VLOF**2.)
340       FH1=(-.01367-.02682*XF+.21233*XF**2.)
341       FH=FH1+((3.-NALP)*(.0023+.0543*(XF-.5)))
350       FG1=(-.09813+.56022*XF-.06661*XF**2.)
351       FGAM=FG1+((3.-NALP)*(.009+.0468*(XF-.4)))
360       GAMMA=TDOW*FTHDOT*FGAM
370       GAMMA2=(T/W-CD/CL)
380       IF (GAMMA.LT.GAMMA2) GOTO 30
390       H1=(VLOF**2./G)*TDOW*FTHDOT*FH
408    50 CONTINUE
409       L2=0
410       S1=(35.-H1)/GAMMA2
420       STOT=SROT+SLOF+S1
424C
425C      CHECK FOR V2 AT 35 FEET
426C
430       V2=VLOF+((G*(SLOF+S1)/VLOF)*(TDOW-35./(SLOF+S1)))
440       V12=1.2*VSTALL
445       L1=0
446       SAIR=STOT-SROT
450       IF (V2.LE.V12) GO TO 2
451
461       GO TO 100
464C
465C      WARNING MESSAGES
466C
470    90 FORMAT (10X,"MORE THAN 15 ITERATIONS IN GROUNDROTATION"///)
475    74 WRITE (6,81)
476    81 FORMAT (10X,"MORE THAN 20 ITERATIONS IN LIFT-OFF PHASE"///)
477       GO TO 50
480    3  WRITE (6,86)
481    86 FORMAT (10X,"ITERATION FOR V2 EXCEEDS LIMITS"///)
482       GO TO 100
486    12 WRITE (6,90)
489       GO TO 41
498C      RETURN
499   100 CONTINUE
```


Figure 9.4: continued

```
504C
505C      OUTPUT DATA
506C
507         WRITE (6,109) W
508   109   FORMAT (10X,"WEIGHT=                ",1F10.2,"   LB"//)
510         WRITE (6,101) VROT
511   101   FORMAT (10X,"ROTATION SPEED=        ",1F10.2,"   FPS"//)
512         WRITE (6,102) VLOF
513   102   FORMAT (10X,"LIFT-OFF SPEED=        ",1F10.2,"   FPS"//)
514         WRITE (6,103) V2
515   103   FORMAT (10X,"SPEED AT 35 FT=        ",1F10.2,"   FPS"//)
516         WRITE (6,104) SROT
517   104   FORMAT (10X,"ROTATION DISTANCE=     ",1F10.2,"   FT"//)
518         WRITE (6,105) SLOF
519   105   FORMAT (10X,"LIFT-OFF DISTANCE=     ",1F10.2,"   FT"//)
520         WRITE (6,106) S1
521   106   FORMAT (10X,"CLIMB-OUT DISTANCE=    ",1F10.2,"   FT"//)
522         WRITE (6,107)STOT
523   107   FORMAT (10X,"TOTAL DISTANCE=        ",1F10.2,"   FT"//)
524         WRITE (6,108) SAIR
525   108   FORMAT (10X,"AIR-DISTANCE=          ",1F10.2,"   FT"//)
530         WRITE (6,87)
531    87   FORMAT (10X,"***END OF SUBROUTINE ROTSPD***"///)
540         STOP
550         END
```

```
KU-FRL DEVELOPED SUBROUTINE FOR CALCULATION
OF THE ROTATION AND THE LIFT-OFF SPEED
TESTRUN FOR LEARJET MODEL 36

WEIGHT=                  11400.00   LB

ROTATION SPEED=            205.47   FPS

LIFT-OFF SPEED=            207.50   FPS

SPEED AT 35 FT=            211.10   FPS

ROTATION DISTANCE=         183.54   FT

LIFT-OFF DISTANCE=         690.00   FT

CLIMB-OUT DISTANCE=        129.77   FT

TOTAL DISTANCE=           1003.31   FT

AIR-DISTANCE=              919.77   FT.
```

Figure 9.4: continued

9.5 RESULTS AND DISCUSSION

Figure 9.5 shows a comparison of calculated take-off speeds with flight manual data (Ref. 9.4). The data used in the calculations were found in Reference 9.5. As stated earlier, the parameters $(d\theta/dt)_R$ and $(d\theta/dt)_A$ have a great influence on the results of the calculations. An increase in $(d\theta/dt)_A$ decreases the air distance, while an increase in $(d\theta/dt)_R$ increases the rotation speed. No data on actual pitch-up rates were available, but the ones used for the computation seem to be reasonable. The GASP run shows a lower V_R and V_2, mainly because of a low pitch-up rate during take-off. The air distances are all higher than actual values, but within 10%. Figure 9.6 shows the air distances.

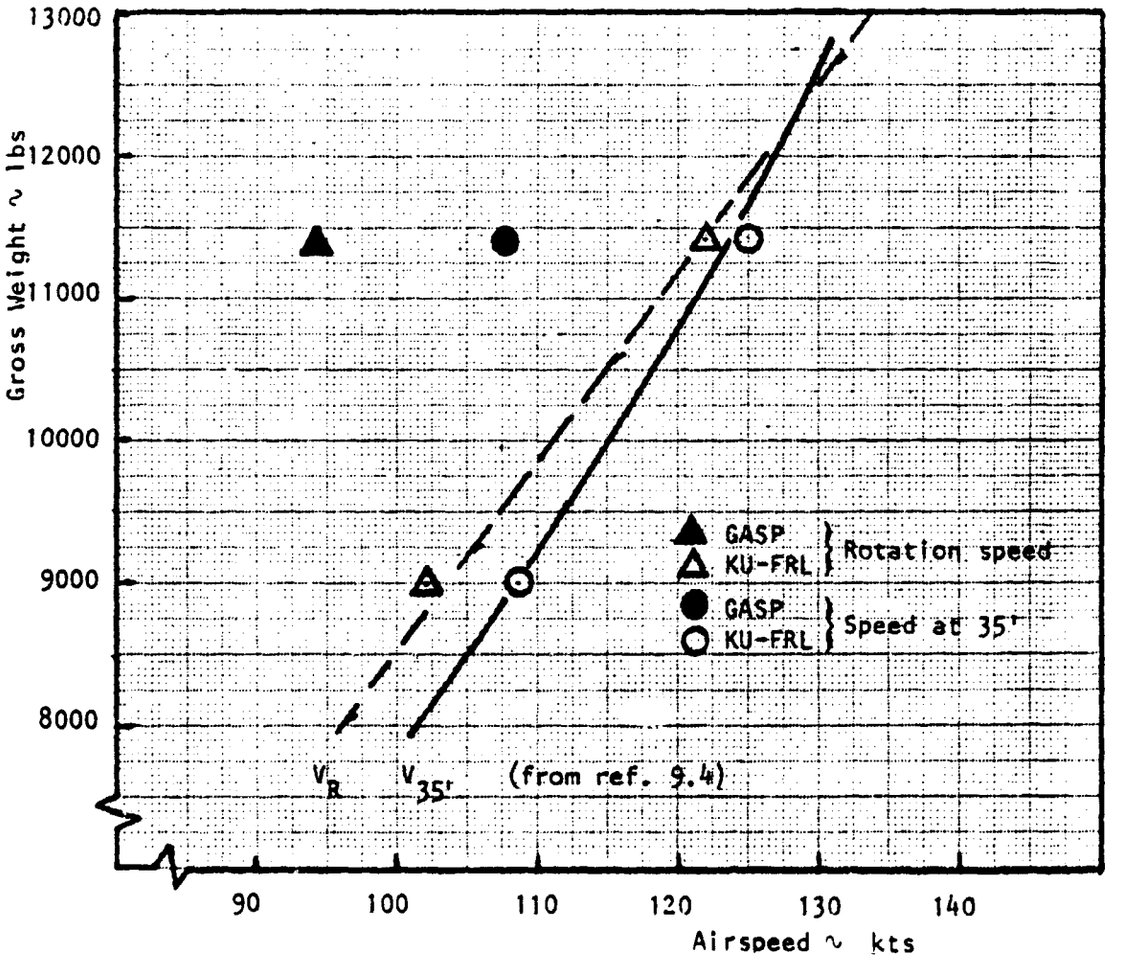

Figure 9.5: Comparison of take-off speeds

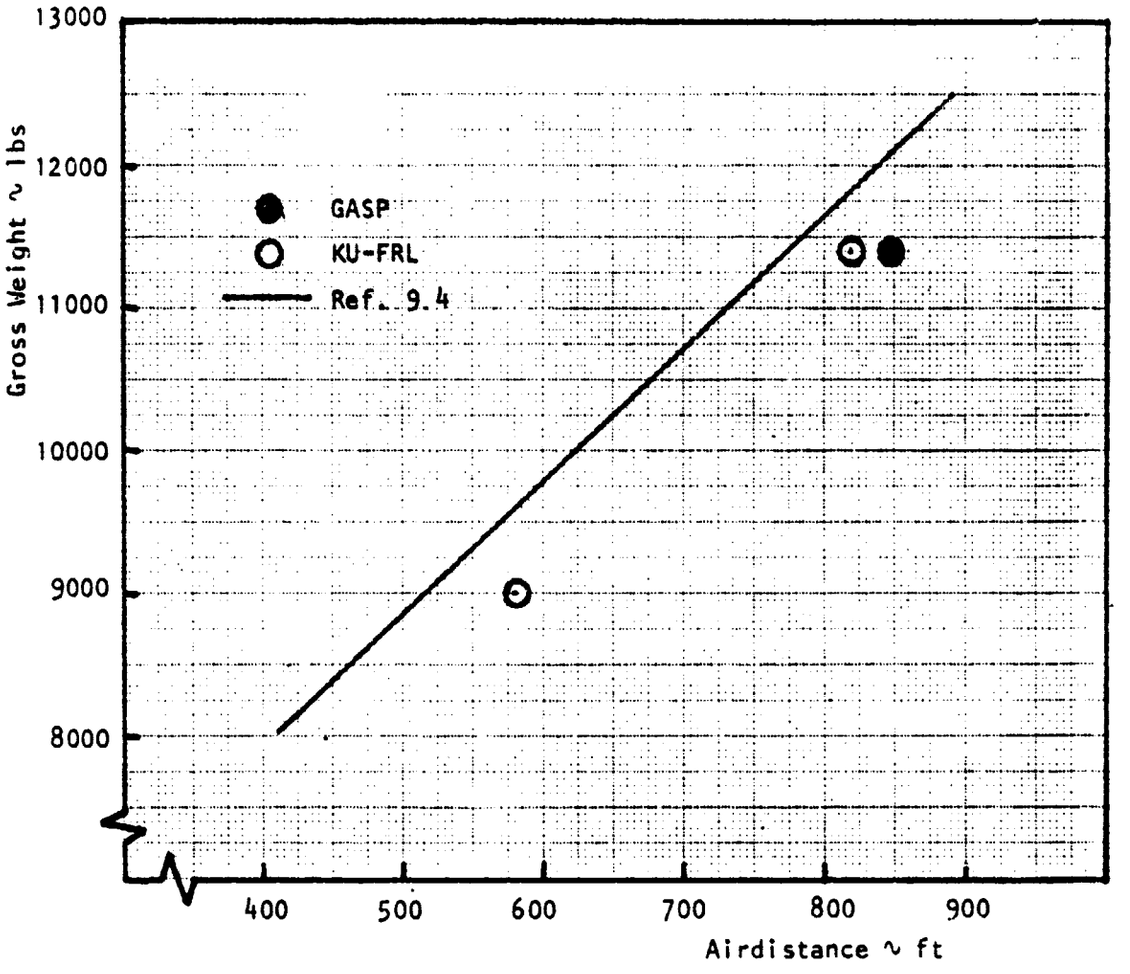

Figure 9.6: Comparison of air-distances

9.6 REFERENCES

9.1	Torenbeek, E.	Synthesis of Subsonic Airplane Design, Delft University Press, Delft, The Netherlands, 1976.
9.2	Perry, D.H.	The Airborne Path During Take-off for Constant Rate of Pitch Maneuvres, ARC CP # 1042, 1969.
9.3	Anon	Federal Aviation Regulations, FAR Part 25.
9.4	Anon	Confidential Report.
9.5	Anon	Confidential Report.

CHAPTER 10

INERTIA ROUTINE

10.1 INTRODUCTION

Moments of inertia are used in the determination of the dynamic stability characteristics of an aircraft. The specific values needed for input into the dynamic stability routine are I_{XX}, I_{YY}, I_{ZZ}, and I_{XZ}, representing moments of inertia in roll, pitch, and yaw, respectively, and the XZ cross product.

In its original form GASP does not compute inertias. Several ideas were cons: .ered for producing an inertia routine. It was determined that the ideal routine should use mainly GASP variables and compute inertias within $\pm$ 10%.

Inertia data were solicited from a number of airframe manufacturers to provide baseline data. Data for 18 aircraft were graphed and examined for trends, in the hope that a modified statistical method could be derived. These are presented as Figure 10.1-3. This method did not produce the desired results.

A trial run was made with a method from Reference 10.1. This method is re_atively simple and provides the required accuracy; it was, therefore, chosen for inclusion into GASP. A description of the method and results follows.

10.2 DISCUSSION OF METHOD

The moment of inertia of a body about its own axis of rotation is given by:

$$I = \int r^2 \rho_A \, dV \tag{10.1}$$

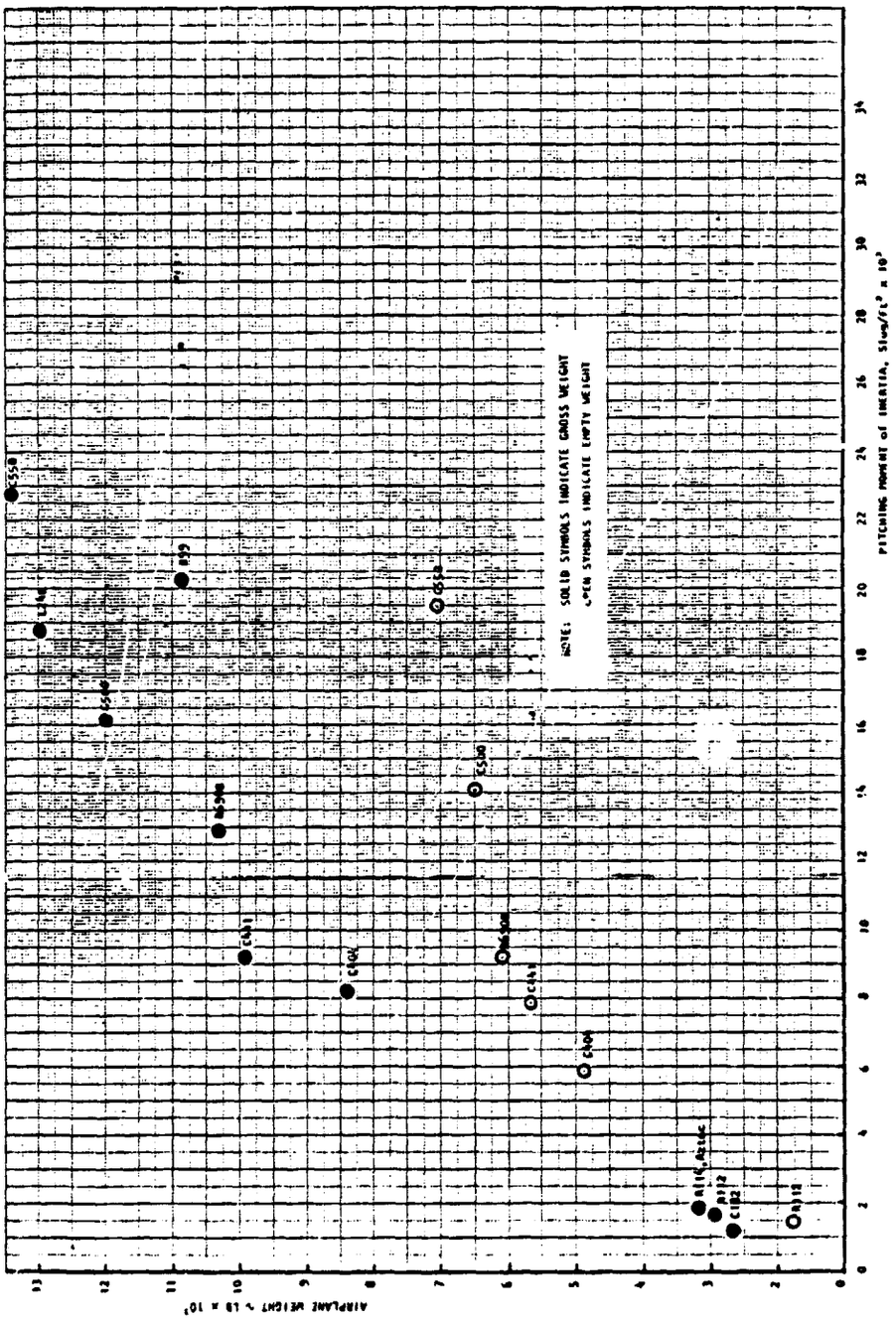

Figure 10.1: Statistical data for pitching moment of inertia

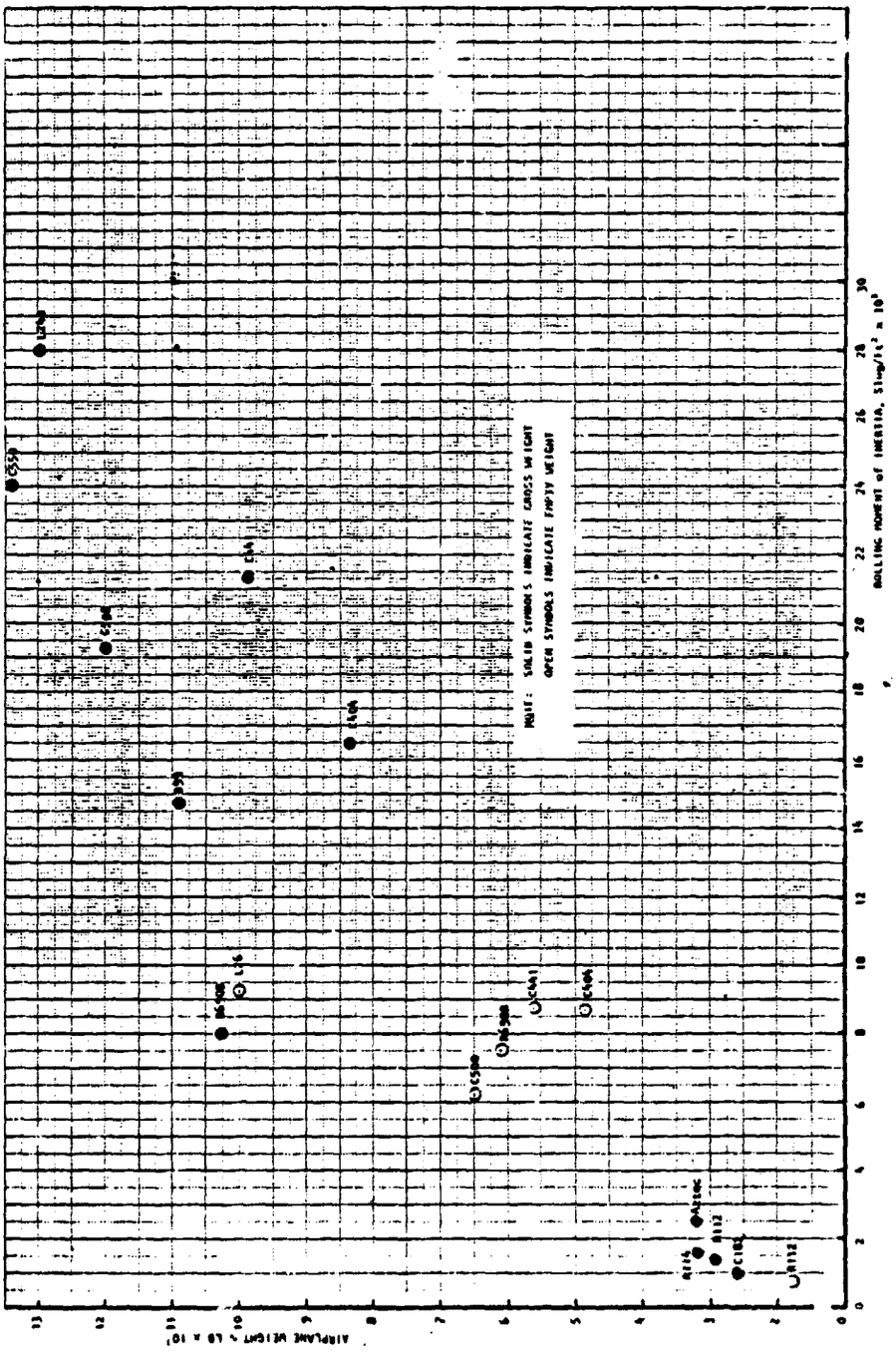

Figure 10.2: Statistical data for rolling moment of inertia

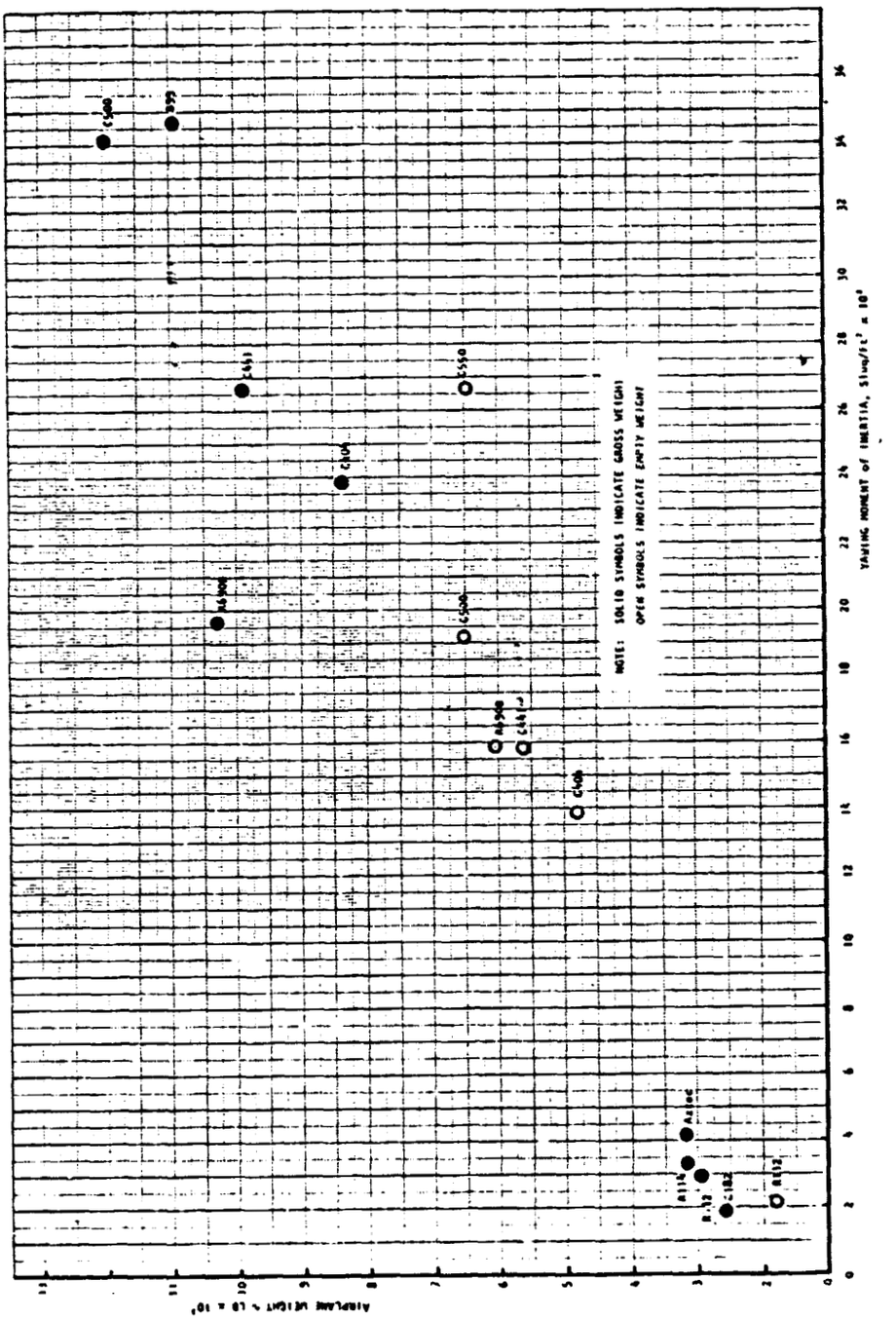

Figure 10.3: Statistical data for yawing moment of inertia

where: r is the distance to a point from the rotation axis, and

$\int \rho_A dV$ is the mass.

The inertia thus obtained will be refered to as I_0, for a body about its own axis. This inertia may be transformed to a remote axis by the parallel axis theorem:

$$I = I_0 + mr_2^2 \tag{10.2}$$

where: r^2 is the radius to the remote axis.

In the detail design phase the aircraft may be broken up into several hundred sections to determine inertias. This is not practical in preliminary design. From the graphs of inertia data (Figures 10.1 through 10.3) it is apparent that a purely statistical approach would be difficult. The method of Reference 10.1 combines some aspects of weight breakdown and statistical methods to produce relatively rapid results.

The method of Reference 10.1 divides the empty aircraft into five major sections:

1) Wing
2) Fuselage
3) Horizontal Stabilizer
4) Vertical Stabilizer
5) Power Plant (Engine and Nacelle)

Mass and distance from the rotation axis are determined for each section, resulting in the mr^2 term of Equation (10.2); I_0's for each section are given by statistically based equations.

The inertias thus obtained are for the empty aircraft, gear up. Variable item inertias are estimated with formulas for standard geometric shapes.

Formulas for the various I_0's are presented below. Figure 10.4 illustrates geometric variables.

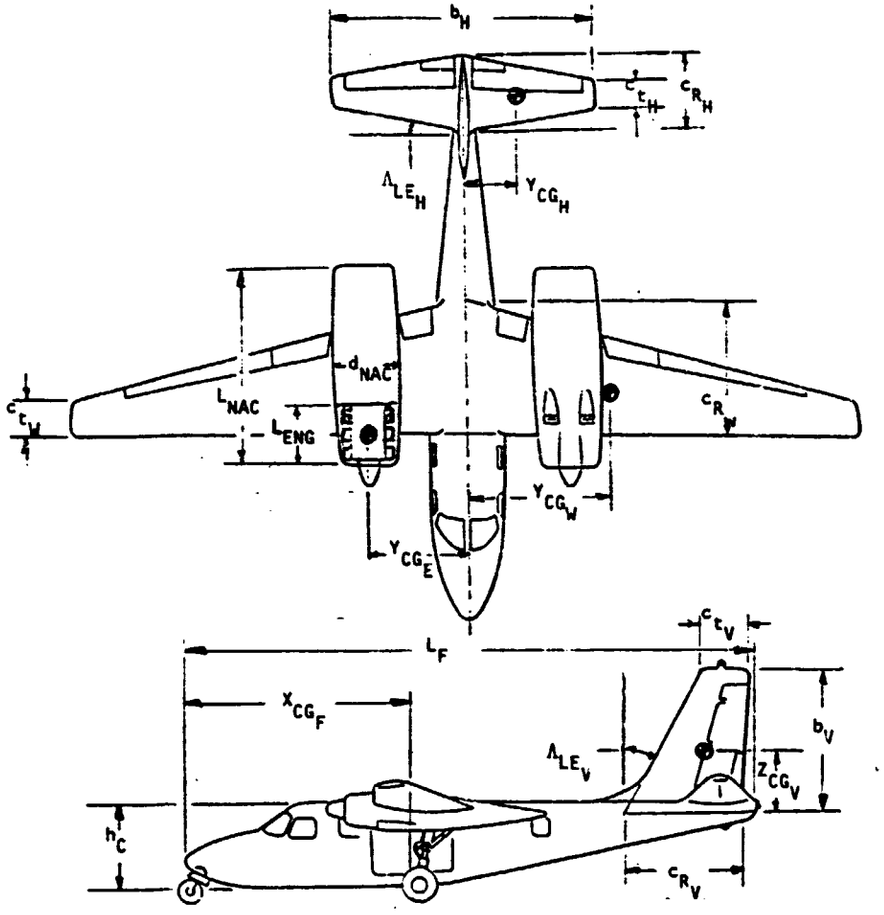

Figure 10.4: Airplane geometry

a. Wing Pitching Moment of Inertia, I_{0Y}

$$\text{if:} \quad (1) = \frac{\rho}{6}\left(-C_a^{\,2} + C_b^{\,2} + C_c\, C_b + C_c^{\,2}\right)$$

$$\text{and:} \quad (2) = \frac{\rho}{12}\left(-C_a^{\,3} + C_b^{\,3} + C_c^{\,2}\, C_b + C_c\, C_b^{\,2} + C_c^{\,3}\right) \qquad (10.3)$$

then: $(3) = (2) - \frac{(1)^2}{M_W}$

where:

$$\rho = \frac{M_W}{.5\ (-C_a + C_b + C_c)} \tag{10.4}$$

C_a is the smallest of the following values:

$$c_{R_W};\ \frac{b_W \tan\Lambda_{LE_W}}{2};\ c_{t_W} + \frac{b_W \tan\Lambda_{LE_W}}{2} \tag{10.5}$$

C_b is the intermediate value

C_c is the largest of these values

then:

$$I_{OY} = .703\ (3) \tag{10.6}$$

b. Wing Rolling Moment of Inertia, I_{OX}

$$I_{OX} = \frac{M_W b_W^2 K_1}{24}\left(\frac{c_{R_W} + 3c_{t_W}}{c_{R_W} + c_{t_W}}\right) \tag{10.7}$$

(For value of K_1, see Figure 10.5.)

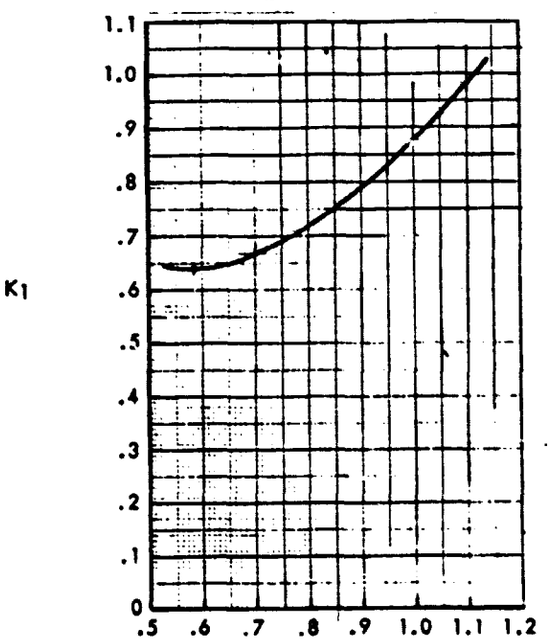

Note: X-axis parameter: $\frac{Y_{CG_W}}{\frac{b_W}{6}\left(\frac{c_{R_W} + 2\,c_{t_W}}{c_{R_W} + c_{t_W}}\right)}$

Figure 10.5: Parameter for Wing Rolling Moment of Inertia, I_{O_X}

c. Wing Yawing Moment of Inertia, I_{0Z}

$$I_{0Z} = I_{0X} + I_{0Y} \tag{10.8}$$

d. Fuselage Pitching Moment of Inertia, I_{0Y}

$$I_{0Y} = \frac{M_{fus} S K_2}{37.68} \left(\frac{3h_C}{2L_{fus}} + \frac{L_{fus}}{h_C} \right) \tag{10.9}$$

(For value of K_2, see Figure 10.6.)

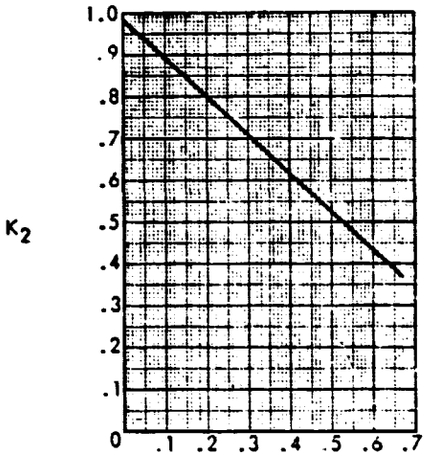

Note: X-axis parameter: $\frac{L_F/2 - X_{CG_F}}{L_F/2}$

Figure 10.6:
Parameter for Fuselage Pitching Moment of Inertia, I_{o_Y}

e. Fuselage Rolling Moment of Inertia, I_{0X}

$$I_{0X} = \frac{M_f K_3}{4} \left(\frac{S_{fus}}{\pi L_{fus}} \right)^2 \tag{10.10}$$

(For value of K_3, see Figure 10.7.)

f. Fuselage Yawing Moment of Inertia, I_{0Z}

$$I_{0Z} = I_{0Y} \tag{10.11}$$

g. Horizontal Stabilizer Pitching Moment of Inertia, I_{0Y}

if:

$$(1) = \frac{\rho}{6} (-C_a^2 + C_b^2 + C_c C_b + C_c^2)$$

$$(2) = \frac{\rho}{12} (-C_a^3 + C_b^3 + C_c^2 C_b + C_c C_b^2 + C_c^3) \tag{10.12}$$

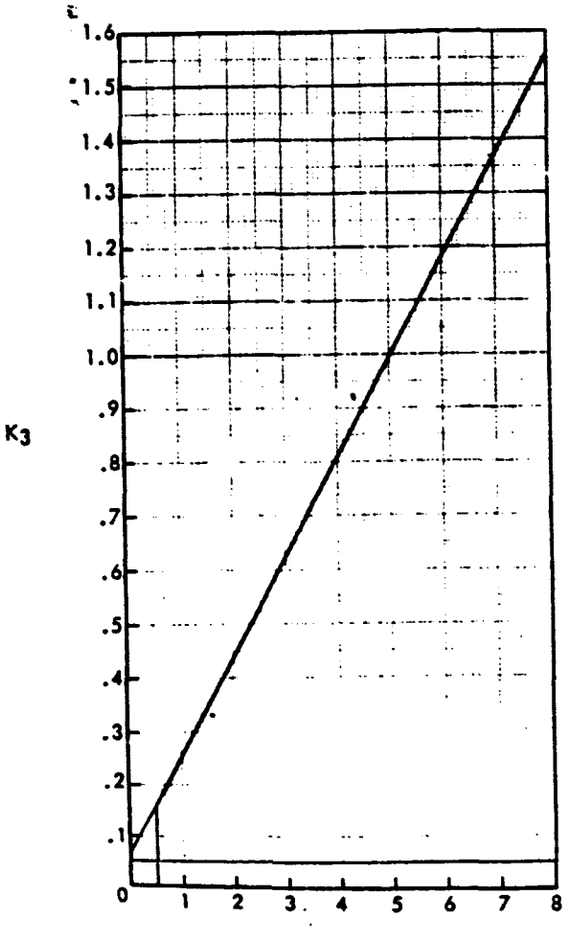

Figure 10.7: Parameter for Fuselage Rolling Moment of Inertia, I_{o_X}

$$(3) = (2) - \frac{(1)^2}{M_H} \tag{10.13}$$

where:

$$\rho = \frac{M_H}{.5\ (-C_a + C_b + C_c)} \tag{10.14}$$

C_a is the smallest of the following values:

$$c_{R_H};\ \frac{b_H \tan\Lambda_{LE_H}}{2};\ c_{t_H} + \frac{b_H \tan\Lambda_{LE_H}}{2} \tag{10.15}$$

C_b is the intermediate value

C_c is the largest of these values

then:

$$I_{OY} = .771 \quad (3) \tag{10.16}$$

h. Horizontal Stabilizer Rolling Moment of Inertia, I_{OY}

$$I_{OX} = \frac{M_H \, b_H^{\,2} \, K_4}{24} \left(\frac{c_{R_H} + 3c_{t_H}}{c_{R_H} + c_{t_H}} \right) \tag{10.17}$$

(For value of K_4, see Figure 10.8.)

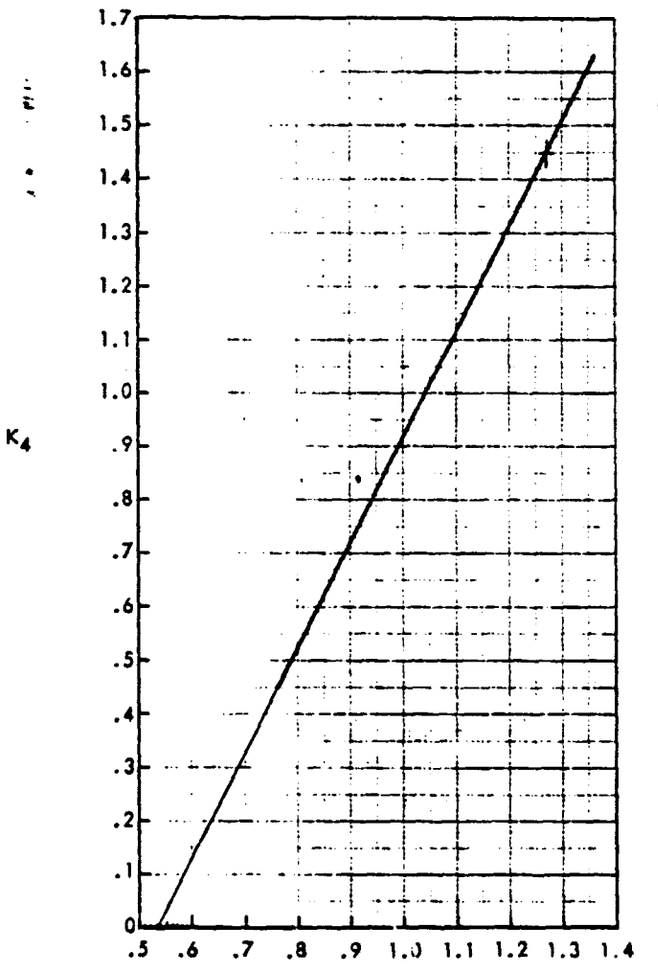

Figure 10.8: Parameter for Horizontal Tail Rolling Moment of Inertia, I_{O_X}

i. Horizontal Stabilizer Yawing Moment of Inertia, I_{0Z}

$$I_{0Z} = I_{0Y} + I_{0X} \tag{10.18}$$

j. Vertical Stabilizer Pitching Moment of Inertia, I_{0Y}

$$I_{0Y} = I_{0X} + I_{0Z} \tag{10.19}$$

k. Vertical Stabilizer Rolling Moment of Inertia, I_{0X}

$$I_{0X} = \frac{M_V \, b_V^{\,2} \, K_5}{18} \left[1 + \frac{2 c_{R_V} c_{t_V}}{(c_{R_V} + c_{t_V})^2} \right] \tag{10.20}$$

(For value of K_5, see Figure 10.9.)

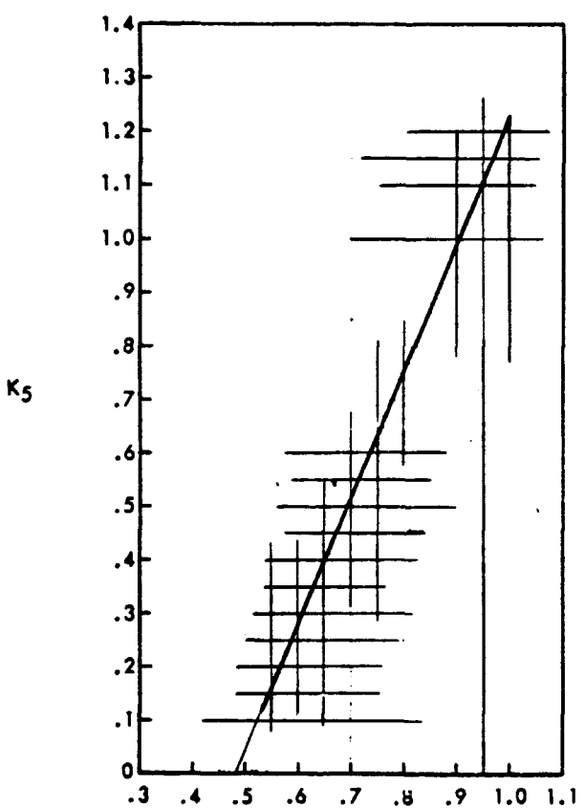

Note: X-axis parameter: $\dfrac{2 c G_V}{\frac{b_V}{3}\left(\frac{c_{R_V} + 2 c_{t_V}}{c_{R_V} + c_{t_V}}\right)}$

Figure 10.9: Parameter for Vertical Tail Rolling Moment of Inertia, I_{0_X}

l. Vertical Stabilizer Yawing Moment of Inertia, I_{0Z}

if: $$(1) = \frac{\rho}{6}\left(-C_a^{\,2} + C_b^{\,2} + C_c\,C_b + C_c^{\,2}\right) \tag{10.21}$$

$$(2) = \frac{\rho}{12}\left(-C_a^{\,3} + C_b^{\,3} + C_c^{\,2}\,C_b + C_c\,C_b^{\,2} + C_c^{\,3}\right) \tag{10.22}$$

$$(3) = (2) - \frac{(1)^2}{M_V} \tag{10.23}$$

where:

$$\rho = \frac{M_V}{.5\left(-C_a + C_b + C_c\right)} \tag{10.24}$$

C_a is the smallest of the following values:

$$c_{R_V};\quad b_V \tan\Lambda_{LE_V};\quad c_{t_V} + b_V \tan\Lambda_{LE_V} \tag{10.25}$$

C_b is the largest of these values

then:

$$I_{0Z} = .771\ \ (3) \tag{10.26}$$

m. Power Plant Pitching Moment of Inertia, I_{0Y}

$$I_{0Y} = .061\left[\frac{3}{4} M_p d_{Nac}^{\,2} + M_e L_{Eng}^{\,2} + (M_p - M_e)\, L_{Nac}^{\,2}\right] \tag{10.27}$$

n. Power Plant Rolling Moment of Inertia, I_{0X}

$$I_{0X} = .083\, M_p d_{Nac}^{\,2} \tag{10.28}$$

o. Power Plant Yawing Moment of Inertia, I_{0Z}

$$I_{0Z} = I_{0Y} \tag{10.29}$$

K values are statistically based and presented in graphic form as Figures 10.5 - 10.9, reproduced from Reference 10.1. An equation was fitted to the K1 line with a power curve fit. K2 - K5 are linear

equations of the form y = mx + b.

$$K1 = 1.2454\ (X1 - .585)^{1.8438} + .64 \tag{10.30}$$

where:

$$X1 = Y_{cg_v}/\{B \cdot 0.1667 \cdot (c_{R_{C_L}} + 2 \cdot c_t)/(c_R + c_t)\} \tag{10.30a}$$

$$K2 = .98 - .915\{(.5\ell_f - X_{cg_{fus}})/(.5\ell_f)\} \tag{10.31}$$

$$K3 = .07 + .186\sqrt{H_C}\ (W_{f_s}/W_f) \tag{10.32}$$

$$K4 = 1.97 \cdot X2 - 1.055 \tag{10.33}$$

where:

$$X2 = Y_{cg_{HT}}/\{b_{HT} \cdot 0.1667(c_{R_{HT}} + 2c_{t_{HT}})/(c_{R_{HT}} + c_{t_{HT}})\} \tag{10.33a}$$

$$K5 = 2.362 \cdot X3 - 1.134 \tag{10.34}$$

where:

$$X3 = Z_{cg_{VT}}/\{b_{VT} \cdot 0.3333(c_{R_{VT}} + 2c_{t_{VT}})/(c_{R_{VT}} + c_{t_{VT}})\} \tag{10.34a}$$

Fuel and passenger inertias are not accounted for by the method of Reference 10.1.

Assuming that all fuel is carried in the wing and tip tanks, fuel inertias may be approximated as follows:

Referring to Figure 10.11, the fuel tank is assumed to start at the fuselage and continue a distance, $b_{fuel}/2$, to a station, R. The fraction of the wing chord filled with fuel is given by C_{fuel}.

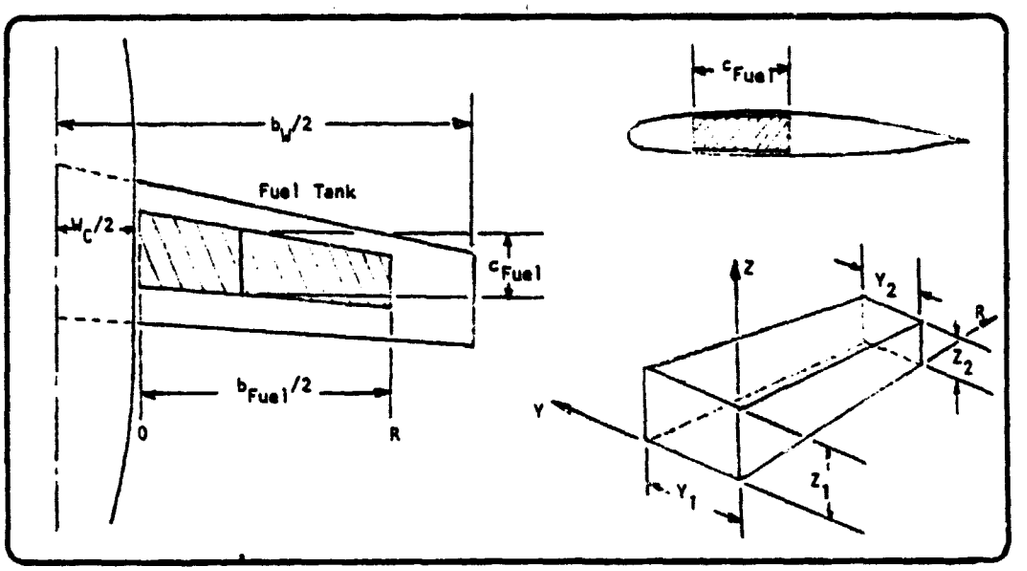

Figure 10.10: Fuel tank geometry

Fuel volume is assumed trapezoidal. Integrating over the trapezoidal volume with z, y, and r coordinates as shown, the inertia about the r = 0 plane is given by:

$$I_{0XX} = 2X \int_0^R r^2 \rho dM dr$$

$$= 2X \int_0^R r^2 \rho (Z_1 - Z_1 r + Z_2 r)(Y_1 - Y_1 r + Y_2 r) dr \qquad (10.35)$$

Z_1, Z_2, Y_1, Y_2, and ρ are constants, allowing integration of the equation to yield:

$$I_{0XX} = R^3(0.0333\rho X_1 Y_1 + 0.05\rho X_2 Y_1 + 0.05\rho X_1 Y_2 + 0.2\rho X_2 Y_2) \qquad (10.36)$$

The variables Z_1, Z_2, Y_1, and Y_2 are functions of known variables:

$$Z_1 = (t/c_r - t/c_t)(1 - W_C/b_W) + t/c_t C_1 \qquad (10.37)$$

where:

$$C_1 = (c_{R_{C_L}} - c_t)(1 - W_C/b_W) + c_t$$

$$Z_2 = (t/c_r - t/c_t)(1 - b_{fuel}/b_W) + t/c_t C_2 \qquad (10.38)$$

where:

$$C_2 = (c_{R_{C_L}} - c_t)(1 - b_{fuel}/b_W) + c_t$$

$$Y_1 = c_{fuel} \times C_1$$

$$Y_2 = c_{fuel} \times C_2 \qquad (10.39)$$

ρ = fuel density in $\frac{lb/ft^3}{32.174}$

GASP approximates tip tanks as prolate spheroids. Tip tank variables are illustrated in Figure 10.11.

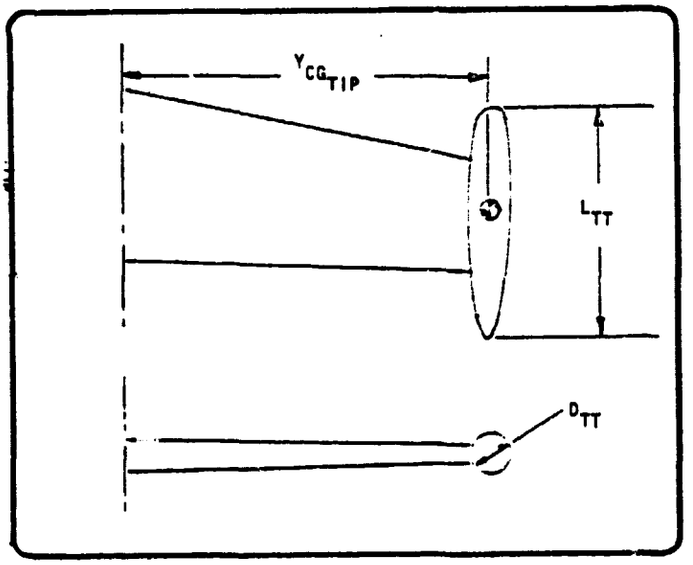

Figure 10.11: Tip tank geometry

The tip tank lateral location variable has a default value of $b_w/2$; using other values drop tanks or nacelle fuel may be simulated.

I_0 inertias are calculated for tip tanks about the pitch and yaw axes by:

$$I_0 = \frac{M_{tip}}{5}\left\{\left(\frac{Axis}{2}\right)^2 + \left(\frac{Bxis}{2}\right)^2\right\} \qquad (10.40)$$

using the inertia formula for an elliptical body of revolution. I_0 for the roll axis is considered negligible.

Passenger inertia variables are illustrated in Figure 10.12.

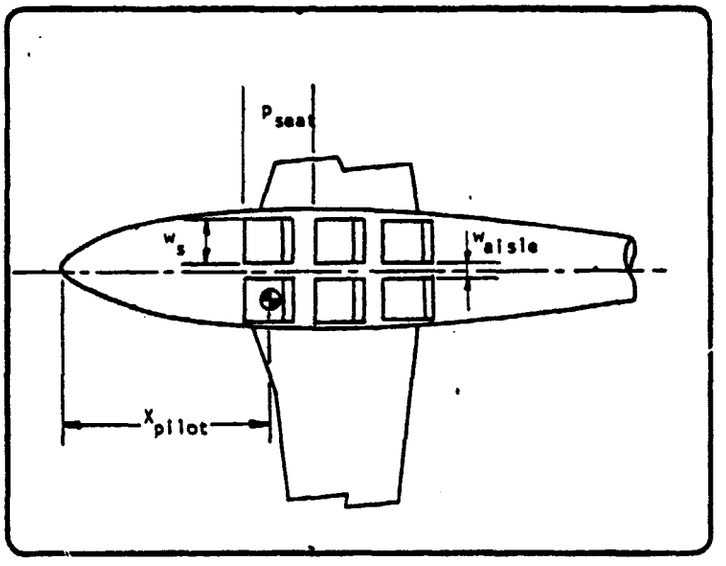

Figure 10.12: Passenger compartment.

Passenger I_0's about the roll axis are found by assuming the passenger's mass to be uniformly distributed over a 4.3 by 1.5 ft. rectangle. I_0's in the pitch and yaw axes are considered negligible.

I_{XZ}'s required for the dynamic stability derivatives are approximated by considering the I_{XZ}'s of the tail, and the wing where applicable.

10.3 CHECK CALCULATIONS

The sample aircraft of Reference 10.1 was used for a check calculation. See Appendix D for data.

a. Wing Pitching Moment of Inertia I_{OY}

$C_a = 8.75$

$C_b = 17.08$

$C_c = 25$

$\rho = 27.98$

(1) = 5908.3

(2) = 88370.4

(3) = 13492.6

$I_{OY} = 9485.3$ slug ft^2

b. Wing Rolling Moment of Inertia I_{OX}

$I_{OX} = 135546$ slug ft^2

c. Wing Yawing Moment of Inertia I_{OZ}

$I_{OZ} = I_{OX} + I_{OY} = 145031$ slug ft^2

d. Fuselage Pitching Moment of Inertia I_{OY}

$I_{OY} = 311319$ slug ft^2

e. Fuselage Rolling Moment of Inertia I_{OX}

K3 = .98

$I_{OX} = 11899.9$ slug ft^2

f. Fuselage Yawing Moment of Inertia I_{OZ}

$I_{OZ} = I_{OY} = 311319$ slug ft^2

g. Horizontal Stabilizer Pitching Moment of Inertia, I_{OY}

$C_a = 3.539$

$C_b = 7.709$

$C_c = 8.33$

$\rho = 4.97$

(1) = 149.61

(2) = 837.4

(3) = 117.2

$I_{OY} = 90.38$

h. Horizontal Stabilizer Rolling Moment of Inertia, I_{OX}

K4 = .72

$I_{OX} = 1723.8$

i. Horizontal Stabilizer Yawing Moment of Inertia, I_{OZ}

$I_{OZ} = I_{OY} + I_{OX} = 1814.2$

j. Vertical Stabilizer Rolling Moment of Inertia, I_{OX}

K5 = .93

$I_{OX} = 188.6$

k. Vertical Stabilizer Yawing Moment of Inertia, I_{OZ}

$C_a = 12.56$

$C_b = 20.8$

$C_c = 20.89$

$\rho = 0.64$

(1) = 122.2

(2) = 1815.17

(3) = 213.6

$I_{OZ} = 164.7$

l. Vertical Stabilizer Pitching Moment of Inertia, I_{OY}

$$I_{OY} = I_{OX} + I_{OZ} = 353.3 \text{ slug ft}^2$$

m. Power Plant Pitching Moment of Inertia, I_{OY}

$$I_{OY} = 2748.8$$

n. Power Plant Rolling Moment of Inertia, I_{OX}

$$I_{OX} = 448.6 \text{ slug ft}^2$$

o. Power Plant Yawing Moment of Inertia, I_{OZ}

$$I_{OZ} = I_{OY} = 2748.8 \text{ slug ft}^2$$

p. Aircraft Cross Product Inertia, I_{XZ}

$$I_{XZ_V} = -Z_{CG_V} (X_{CG_V}) M_V$$

$$I_{XZ_V} = 2892.1$$

$$I_{XZ_V} = Z_{CG_{Wing}} (X_{CG_{Wing}}) M_W$$

$$I_{XZ_W} = 0$$

A comparison of these results with the results of Reference 10.1, as well as with the computer testrun output, will be done in Section 10.4.

10.4 PROGRAM DESCRIPTION

The method described in Section 10.2 was transformed into a FORTRAN computer routine. Table 10.1 shows the computer variables as used in the program. Figure 10.13 shows a flow chart of the program. A listing of the program as well as a sample output is shown in Figure 10.14. A description and three-view of the aircraft used in the tests are given in Appendix D.

TABLE 10.1 VARIABLE NAMES IN SUBROUTINE "INERTA"

NAME	ENG. SYMBOL	DIMENSION	ORIGIN	REMARKS
AXIS	s	ft	Common	Major axis of tip tank
BENGOB	b_{eng}/b_W	---	Common	
BFUEL	b_{fuel}	ft	Common	
BHT	b_{HT}	ft	Common	
BVT	b_{VT}	ft	Common	
BW	b_W	ft	Common	
BXIS	b	ft	Common	Minor axis of tip tank
CA	C_a	---	---	
CB	C_b	---	---	
CC	C_c	---	---	
CGLG	CG_{LG}	ft	Common	Radial distance from fuselage center line
CFUEL	C_{fuel}	ft	---	

TABLE 10.1 VARIABLE NAMES IN SUBROUTINE "INERTA" (continued)

NAME	ENG. SYMBOL	DIMENSION	ORIGIN	REMARKS
CHORD1	---	---	---	Dummy
CHORD2	---	---	---	Dummy
CON	---	---	---	Dummy
CONST1	---	---	---	Dummy
CONST2	---	---	---	Dummy
CONST3	---	---	---	Dummy
CRCLHT	$C_{R_{HT}}$	ft	Common	
CRCLVT	$C_{R_{VT}}$	ft	Common	
CRCLW	$C_{R_{G_W}}$	ft	Common	
CTHT	$C_{t_{HT}}$	ft	Common	
CTVT	$C_{t_{VT}}$	ft	Common	
CTW	C_{t_W}	ft	Common	
DBARN	$\bar{d}_{nac}$	ft	Common	
ELCG	X_{CG}	ft	Common	
ELCGH	$X_{CG_{HT}}$	ft	Common	
ELCGV	$X_{CG_{VT}}$	ft	Common	
ELF	ℓ_{fus}	ft	Common	
ELN	ℓ_{nac}	ft	Common	

TABLE 10.1 VARIABLE NAMES IN SUBROUTINE "INERTA" (continued)

NAME	ENG. SYMBOL	DIMENSION	ORIGIN	REMARKS
ELTIP	$X_{CG_{Tip}}$	ft	Common	
ELWING	X_{CG_W}	ft	Common	
ENGIOX	$I_{OX_{eng}}$	slug ft^2	---	
ENGIOY	$I_{OY_{eng}}$	slug ft^2	---	
ENGIX	$I_{XX_{eng}}$	slug ft^2	---	
ENGIY	$I_{YY_{eng}}$	slug ft^2	---	
ENGIZ	$I_{ZZ_{eng}}$	slug ft^2	---	
FUELD	ρ_{fuel}	lb/gal	Common	
FUSIOX	$I_{OX_{fus}}$	slug ft^2	---	
FUSIOY	$I_{OY_{fus}}$	slug ft^2	---	
FUSIX	$I_{XX_{fus}}$	slug ft^2	---	
FUSIY	$I_{YY_{fus}}$	slug ft^2	---	
FUSIZ	$I_{ZZ_{fus}}$	slug ft^2	---	
GEARIX	$I_{XX_{LG}}$	slug ft^2	---	
GEARIY	$I_{YY_{LG}}$	slug ft^2	---	
GEARIZ	$I_{ZZ_{LG}}$	slug ft^2	---	

TABLE 10.1 VARIABLE NAMES IN SUBROUTINE "INERTA" (continued)

NAME	ENG. SYMBOL	DIMENSION	ORIGIN	REMARKS
HC	h_c	ft	Common	
HORIOX	$I_{OX_{HT}}$	slug ft^2	---	
HORIOY	$I_{OY_{HT}}$	slug ft^2	---	
HORIX	$I_{XX_{HT}}$	slug ft^2	---	
HORIY	$I_{YY_{HT}}$	slug ft^2	---	
HORIZ	$I_{ZZ_{HT}}$	slug ft^2	---	
INERTX	I_{XX}	slug ft^2	---	
INERTY	I_{YY}	slug ft^2	---	
INERTZ	I_{ZZ}	slug ft^2	---	
IOY	---	---	---	Dummy
IROW	---	---	---	Dummy
IROW2	---	---	---	Dummy
IXXP	$I_{XX_{pax}}$	slug ft^2	---	
IXZ	I_{XZ}	slug ft^2	---	
IXZH	$I_{XZ_{HT}}$	slug ft^2	---	
IXZV	$I_{XZ_{VT}}$	slug ft^2	---	
IXZW	$I_{XZ_{W}}$	slug ft^2	---	
IYYP	$I_{YY_{pax}}$	slug ft^2	---	

TABLE 10.1 VARIABLE NAMES IN SUBROUTINE "INERTA" (continued)

NAME	ENG. SYMBOL	DIMENSION	ORIGIN	REMARKS
IZZP	$I_{ZZ_{pax}}$	slug ft^2	---	
K1	K1	---	---	
K2	K2	---	---	
K3	K3	---	---	
K4	K4	---	---	
K5	K5	---	---	
LENG	ℓ_{eng}	ft	Common	
M	M	lb	---	Dummy
MB	W	lb	Common	
MBT	W_B	slugs	---	
MEP	W_{pe}	slugs	---	
MFTP	$W_{fuel_{tip}}$	slugs	---	
MFW	W_{fuel_W}	slugs	---	
MHT	W_{HT}	slugs	---	
MLG	W_{LG}	slugs	---	
MP	W_p	slugs	---	
MPASS	W_{pax}	slugs	---	
MPLMAX	$W_{pax_{max}}$	slugs	---	
MTIP	W_{tip}	slugs	---	

TABLE 10.1 VARIABLE NAMES IN SUBROUTINE "INERTA" (continued)

NAME	ENG. SYMBOL	DIMENSION	ORIGIN	REMARKS
MVT	W_{VT}	slugs	---	
MW	W_W	slugs	---	
PAX	N_{pax}	---	Common	Excluding pilot
PS	P_{seat}	ft	Common	
R	---	---	---	Dummy
R1	---	---	---	Dummy
RELP	$X_{CG_{eng}}/\ell_{fus}$	---	---	
RELR	$X_{CG_{fus}}/\ell_{fus}$	---	---	.33
RHO	ρ	lb sec^2/ft^4	---	
SAB	---	---	Common	
SAH	---	---	Common	
SF	S_{fus}	ft^2	Common	
SWPLE	Λ_{LE_W}	rad	Common	
SWPLEH	$\Lambda_{LE_{HT}}$	rad	Common	
SWPLEV	$\Lambda_{LE_{VT}}$	rad	Common	
TCR	$t/c\|_R$	---	Common	
TCT	$t/c\|_t$	---	Common	
TIPIOY	$I_{OY_{tip}}$	slug ft^2	---	
HWPAX	W_{pax}	lb	Common	

TABLE 10.1 VARIABLE NAMES IN SUBROUTINE "INERTA" (continued)

NAME	ENG. SYMBOL	DIMENSION	ORIGIN	REMARKS
VERIOX	$I_{OX_{VT}}$	slug ft^2	---	
VERIOY	$I_{OY_{VT}}$	slug ft^2	---	
VERIOZ	$I_{OZ_{VT}}$	slug ft^2	---	
VERIX	$I_{XX_{VT}}$	slug ft^2	---	
VERIY	$I_{YY_{VT}}$	slug ft^2	---	
VERIZ	$I_{ZZ_{VT}}$	slug ft^2	---	
WAS	W_{aisle}	ft	Common	
WB	W_{B_S}	lb	Common	Fuselage section weight
WBT	W_B	lb	Common	Fuselage weight
WC	W_C	ft	Common	
WEIGHT	W	lb	---	
WEP	W_{pe}	lb	Common	
WFIOX	$I_{OX_{fuel}}$	slug ft^2	---	
WFIX	$I_{XX_{fuel}}$	slug ft^2	---	
WFIY	$I_{YY_{fuel}}$	slug ft^2	---	
WFTP	$W_{fuel_{tip}}$	lb	Common	
WFW	W_{fuel_W}	lb	Common	

TABLE 10.1 VARIABLE NAMES IN SUBROUTINE "INERTA" (continued)

NAME	ENG. SYMBOL	DIMENSION	ORIGIN	REMARKS
WHT	W_{HT}	lb	Common	
WLG	W_{LG}	lb	Common	
WNGIOX	I_{OX_W}	slug ft^2	---	
WNGIOY	I_{OY_W}	slug ft^2	---	
WNGIOZ	I_{OZ_W}	slug ft^2	---	
WNGIX	I_{XX_W}	slug ft^2	---	
WNGIY	I_{YY_W}	slug ft^2	---	
WNGIZ	I_{ZZ_W}	slug ft^2	---	
WP	W_p	lb	Common	
WPLMAX	$W_{pax_{max}}$	lb	Common	
WS	W_{seat}	ft	Common	
WTIP	W_{tip}	lb	Common	
WVT	W_{VT}	lb	Common	
WW	W_w	lb	Common	
XPILOT	X_{pilot}	ft	Common	
Y1	---	---	---	Dummy
Y2	---	---	---	Dummy
YCGENG	$\bar{Y}_{CG_{eng}}$	ft	Common	

TABLE 10.1 VARIABLE NAMES IN SUBROUTINE "INERTA" (continued)

NAME	ENG. SYMBOL	DIMENSION	ORIGIN	REMARKS
YCGHOR	$\bar{Y}_{CG_{HT}}$	ft	Common	.2 b_{HT}
YCGTIP	$\bar{Y}_{CG_{tip}}$	ft	Common	
YCGWNG	$\bar{Y}_{CG_{wing}}$	ft	Common	.18 b_W
Z1	---	---	---	Dummy
Z2	---	---	---	Dummy
ZCGHOR	$\bar{Z}_{CG_{HT}}$	ft	Common	
ZCGVER	$\bar{Z}_{CG_{VT}}$	ft	Common	.6 b_{VT}
ZCGWNG	$\bar{Z}_{CG_W}$	ft	Common	

Table 10.2 illustrates the comparison between the results of the hand calculation, the data of Reference 10.1, and the computer output for the test airplane K (see Appendix D for details).

TABLE 10.2 COMPARISON OF INERTIA COMPUTATIONS

	KU-FRL "INERTA" Hand Calculation	Ref. 10.1	KU-FRL "INERTA" Computer
I_{OY_W}	9,485.3	9,493.2	9,443.9
I_{OX_W}	135,546.0	135,591.5	135,861.6
I_{OZ_W}	145,031.0	145,084.7	143,305.5

TABLE 10.2 COMPARISON OF INERTIA COMPUTATIONS (continued)

	KU-FRL "INERTA" Hand Calculation	Ref. 10.1	KU-FRL "INERTA" Computer
$I_{OY_{fus}}$	311,319.0	311,473.4	311,994.9
$I_{OX_{fus}}$	11,899.9	11,798.5	11,191.9
$I_{OZ_{fus}}$	311,319.0	311,473.4	311,994.9
$I_{OY_{Hoz}}$	90.4	95.7	90.3
$I_{OX_{Hoz}}$	1,723.8	1,774.9	1,724.4
$I_{OZ_{Hoz}}$	1,814.2	1,870.6	1,814.7
$I_{OY_{Vert}}$	353.3	305.2	339.3
$I_{OX_{Vert}}$	188.6	188.4	189.2
$I_{OZ_{Vert}}$	164.7	116.7	150.1
$I_{OY_{eng}}$	2,748.8	2,748.8	2,761.8
$I_{OX_{eng}}$	448.6	447.9	448.6
$I_{OZ_{eng}}$	2,748.8	2,748.8	1,966.8

NOTE: All inertias in slug ft^2.

Table 10.3 gives the results of computer runs to determine the mass properties for several general aviation aircraft. Also given are manufacturers' data.

TABLE 10.3 INERTIA CALCULATIONS, COMPARISON

AIRPLANE TYPE	WEIGHT	SOURCE	I_{XX} slug ft^2	% ERR.	I_{YY} slug ft^2	% ERR.	I_{ZZ} slug ft^2	% ERR.	I_{XZ}
E	MWE	INERTA	650.6	2.9	644.4	2.7	1231.9	6.0	-25.96
		MANF.	631.7		661.5		1157.9		
E	MTOW	INERTA	697.8		645.9		1254.9		
		MANF.	---		---		---		
F	MWE	INERTA	829.6	4.3	1860.2	15.5	2993.7	24.7	-1891.7
		MANF.	794.2		1571.3		2252.4		
F	MTOW	INERTA	1215.2	27.7	1879.8	.1	3334.7	1.0	
		MANF.	1551.4		1878.3		3301.0		
H	MWE	INERTA	9467.5	6.6	13930.9	2.8	22076.5	1.1	-267.5
		MANF.	8846.0		14318.0		21830.0		
H	MTOW	INERTA	17512.7	15.0	21554.0	6.0	37267.6	9.2	
		MANF.	14884.0		20270.0		33836.0		
A	MWE	INERTA	6793.2	11.0	17260.9	13.4	22919.0	14.6	-1320.4
		MANF.	6045.0		14948.0		19572.8		
A	MTOW	INERTA	34319.6		22561.9		52960.9		-
		MANF.	---		---		---		

The average error in the computations is as follows:

I_{XX}	I_{YY}	I_{ZZ}
11.3%	6.8%	5.7%

It may be concluded that the subroutine INERTA performs well within the accuracy required for preliminary design work. No data were available for comparison with the I_{XZ} computations.

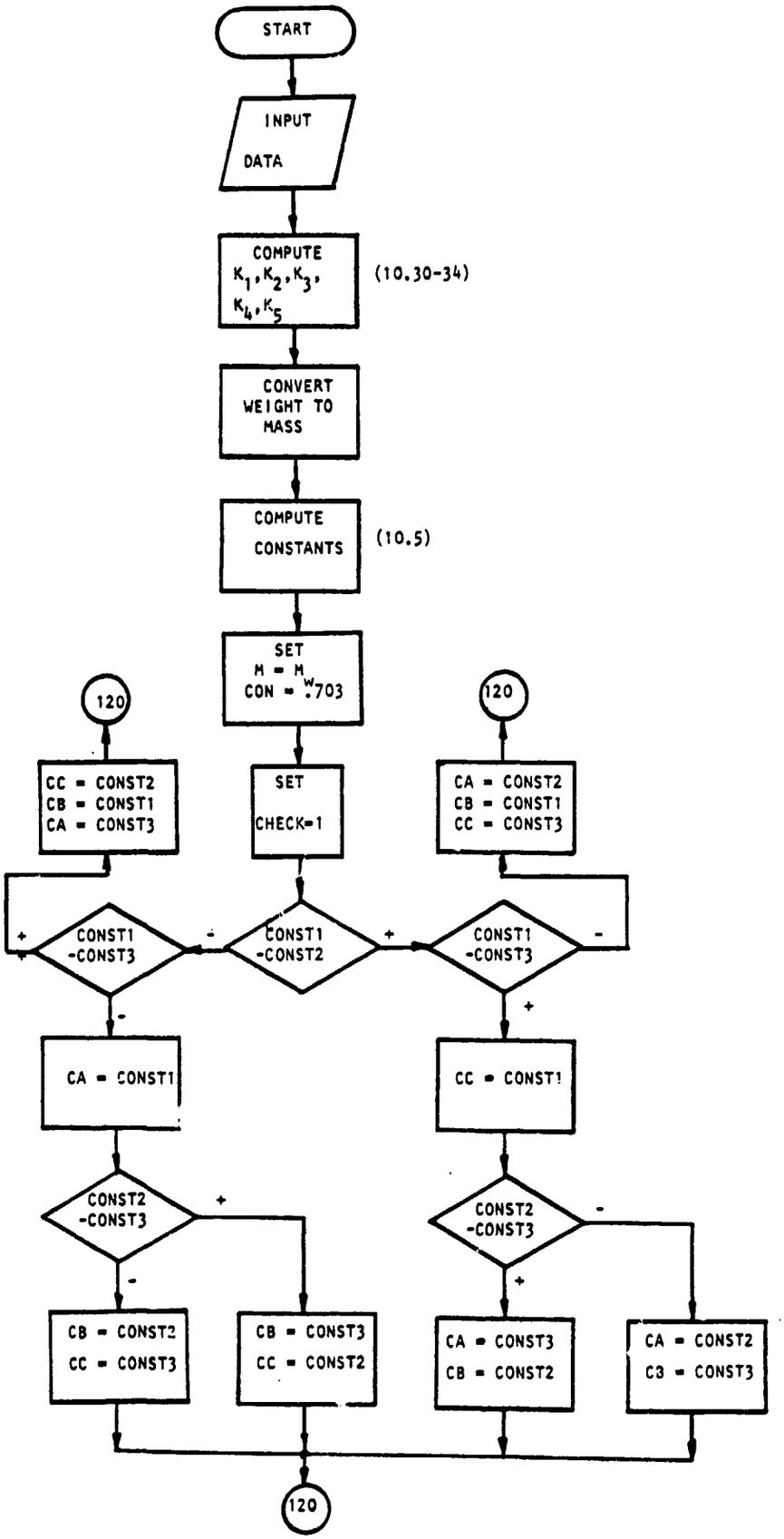

Figure 10.13: Flowchart of subroutine "INERTA"

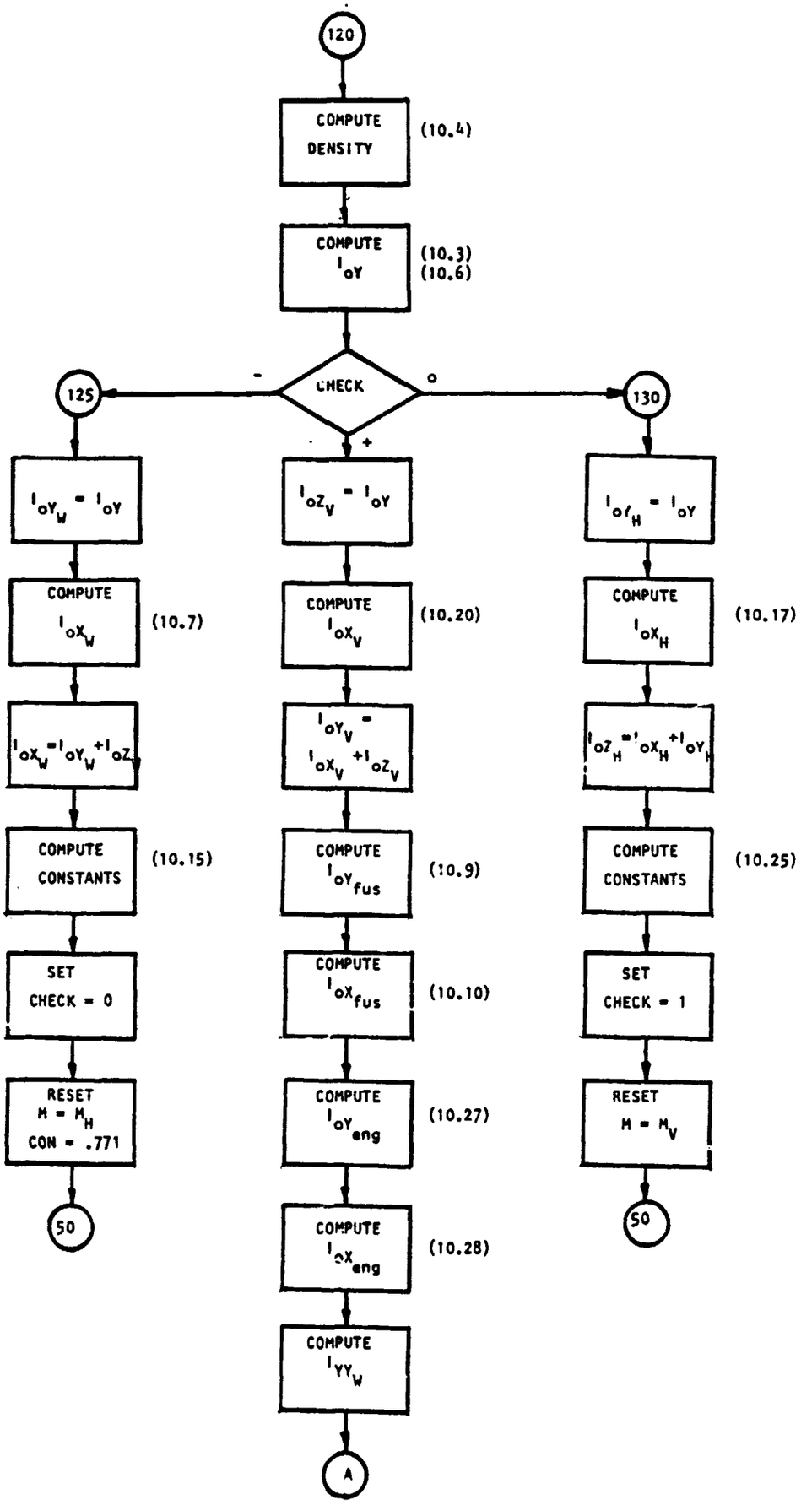

Figure 10.13: continued

C-3

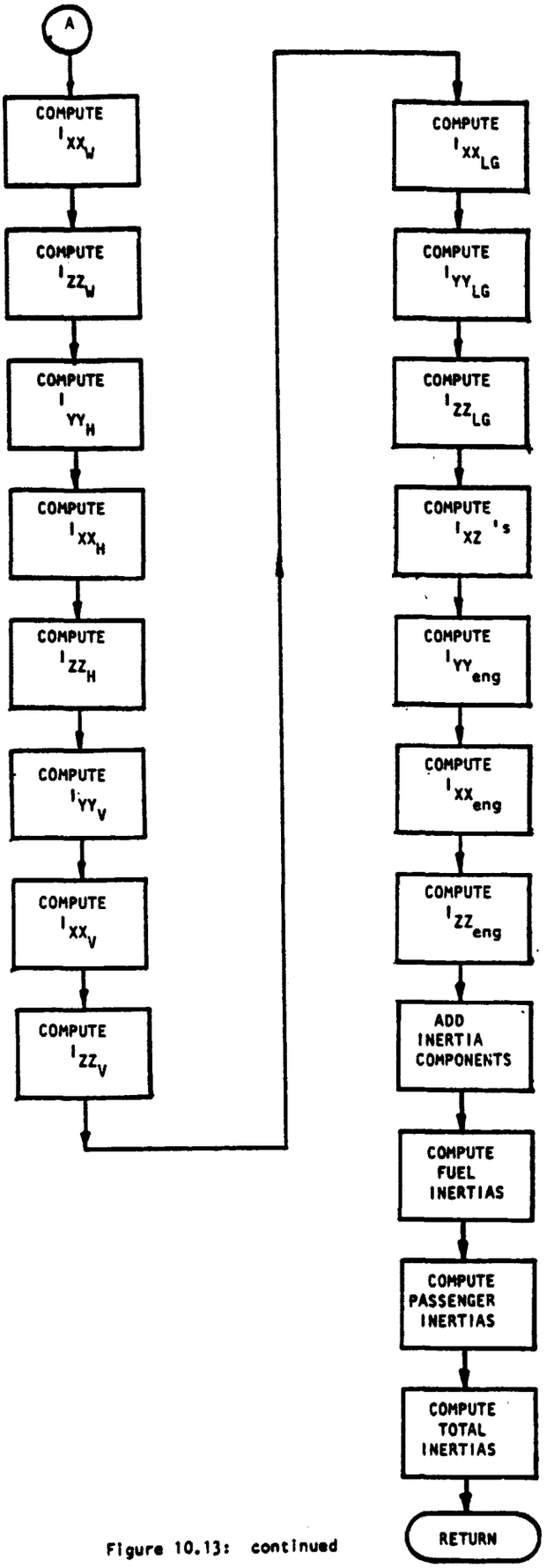

Figure 10.13: continued

```
C              SUBROUTINE INERTA
      REAL K1,K2,K3,K4,K5,K6,WWT,WVT,WW,WP,WE,WLG,
     &WFLMAX,WFW,WFTP,WTIP,WREM,WPEI,LENG,INERTY,
     &IXY,INERTY,INERTZ,IXZ,IYZW,IXZV,IXZH,LPILOT,IXYP,IYYP,IZZP,NPASS
      PRINT:"              KU FRL INERTIA ROUTINE"
      PRINT:""
      PRINT:"AIRCRAFT NAME, TAIL TYPE: 1=T TAIL"
      READ:NAME,SAH
      PRINT:"WHT,WVT,WW,WP,WEP,WB,WBT,WLG,WTIP,WFW,WFTP"
       READ:WHT,WVT,WW,WP,WEP,WB,WBT,WLG,WTIP,WFW,WFTP
       PRINT:"WING SPAN,HOR. SPAN,VERT SPAN,ENG.SPAN/WING SPAN"
       READ:BW,BHT,BVT,PENCOD
       PRINT:"CRCLW,CTW,CRCLHT,CTHT,CRCLVT,CTVT"
       READ:CRCLW,CTW,CRCLHT,CTHT,CRCLVT,CTVT
       PRINT:"FUS. LENGTH, FUS. WETTED AREA,AV. DIAM."
       READ:ELF,SF,HC
       PRINT:"ELCG,ELWING,ELCGH,ELCGV"
       READ:ELCG,ELWING,ELCGH,ELCGV
       PRINT:"YCGWNG,YCGHOR,YCGENG"
       READ:YCGWNG,YCGHOR,YCGENG
       PRINT:"SWPLE,SWPLEV,SWPLEH"
       READ:SWPLE,SWPLEV,SWPLEH
       PRINT:"ENGINE DIAM.,ENGINE LENGTH,NACELLE LENGTH"
       READ:DRARM,LENG,ELN
       PRINT:"RELP,RELR,ZCGVER"
       READ:RELP,RELR,ZCGVER
       PRINT:"CGLG,ZCGWING,FUEL DENSITY,WT.PER PASS."
       READ:CGLG,ZCGWNG,FUELD,WPAX
       PRINT:"FUEL TANK SPAN,,TCR,TCT,WC"
       READ:BFUEL,TCR,TCT,WC
       PRINT:"TIP T. LGTH.,DIAM."
       READ:AXIS,EXIS
       ZCGHOR=0.0
       PRINT:"YCGTIP,PAX,WAS,WS,PS,XPILOT,ELTIP,SAE"
       READ:YCGTIP,PAX,WAS,WS,PS,XPILOT,ELTIP,SAB
       IF(WBT.EQ.0)WBT=WB+WCC+WCFW+WSAS+WFE
       IF(SAH.EQ.1)ZCGHOR= -BVT
       IF(YCGWNG.EQ.0)YCGWNG=0.18*BW
       IF(YCGHOR.EQ.0)YCGHOR=0.2*BHT
       IF(ZCGVER.EQ.0)ZCGVER=0.6*BVT
       IF(RELR.EQ.0)RELR=0.33
       X1=YCGWNG/(BW*0.1667*(CRCLW+2.0*CTW)/
      &(CRCLW+CTW))
       K1=(X1-0.535)**1.8438*1.2454+0.64
       K2=0.98-0.915*(ABS(0.5*ELF-RELR*ELF)/(0.5*ELF))
       K3=0.07+0.186*(HC*12)**0.5*WB/WBT
       K4=1.97*YCGHOR/(BHT*0.1667*(CRCLHT+2*CTHT)
      &/(CRCLHT+CTHT))-1.055
       K5=2.762*ZCGVER/(BVT*0.3333*(CRCLVT+2*CTVT)
      &/(CRCLVT+CTVT))-1.134
```

Figure 10.14: Listing of subroutine "INERTA"

```
      WT=WT/32.174
      WLG=WLC/32.174
      WVT=WVT/32.174
      WW=WW/32.174
      WP=WP/32.174
      WEP=WEP/32.174
      WPLMAX=WPLMAX/32.174
      WFW=WFW/32.174
      WFTP=WFTP/32.174
      WTIP=WTIP/32.174
      WET=WET/32.174
      PRINT:"K1      K2      K3      K4      K5"
      WRITE(6,51)K1,K2,K3,K4,K5
51    FORMAT(5(F7.3,1X))
      CONST1=CROLL
      CONST2=EN*(SIN(SWPLE)/COS(SWPLE))*0.5
      CONST3=CTN+CONST2
      CON=0.703
      M=MN
      CHECK=-1
10    IF(CONST1.LE.CONST2)GO TO 90
      IF(CONST1.LE.CONST3)GO TO 70
      CC=CONST1
      IF(CONST2.LE.CONST3)GO TO 60
      CA=CONST3
      CB=CONST2
      GO TO 120
60    CA = CONST2
      CB=CONST3
      GO TO 120
70    CA = CONST2
      CB=CONST1
      CC=CONST3
      GO TO 120
90    IF(CONST1.LT.CONST3)GO TO 100
      CA=CONST3
      CB=CONST1
      CC=CONST2
      GO TO 120
100   CA=CONST1
      IF(CONST2.LT.CONST3)GO TO 110
      CB=CONST3
      CC=CONST2
      GO TO 120
110   CB=CONST2
      CC=CONST3
120   CONTINUE
      RHO=M/(0.5*(-CA+CB+CC))
      IOY=CON*(RHO*0.0833*(-CA**3+CB**3+CC**2*CB+CC*CB**2
     3+CC**3)-((RHO*0.1667*(-CA**2+CB**2+CC*CB+CC**2))**2/M))
```

ORIGINAL PAGE IS
OF POOR QUALITY

Figure 10.14: continued

```
1110       IF(CHECK)125,130,140
1120  125 WNGICY=ICY
1130       WNGICX=MW*GW**2*K3*0.0417*((CRCLW+3*CTW)/(CRCLW+CTW))
1140       WNGICZ=WNGICY+WNGICX
1150       CONST1=CRCLHT
1160       CONST2=BHT*(SIN(SWPLEH)/COS(SWPLEH))*0.5
1170       CONST3=CTHT+CONST2
1180       CHECK=0
1190       M=MHT
1200       CON=0.771
1210       GO TO 50
1220  130  HORICY=ICY
1230       HORICX=MHT*BHT**2*K4*0.0417*((CRCLHT+3*CTHT)/
1240      1((CRCLHT+CTHT))
1250       HORICZ=HORICX+HORICY
1260       CONST1=CRCLVT
1270       CONST2=BVT*(SIN(SWPLEV)/COS(SWPLEV))*0.5
1280       CONST3=CTVT+CONST2
1290       CHECK=1
1300       M=MVT
1310       GO TO 50
1320  140  VERICZ=ICY
1330       VERICX=MVT*BVT**2*K5*0.0556*(1+(2*CRCLVT*CTVT)
1340      1/((CRCLVT+CTVT)**2))
1350       VERICY=VERICX+VERICZ
1360       FUSICY=MBT*SF*K2*0.0265*(3*HC/(2*ELF)+ELF/HC)
1370       FUSICX=MBT*K3*0.25*((SF/(3.142*ELF))**2)
1380       ENGICY=0.061*(0.75*MP*DBARN**2+MEP*LENG**2+
1390      1(MP-MEP)*ELN**2)
1400       ENCICX=0.023*MP*DBARN**2
1410       WAGIY=WNGICY+MW*(ELCG-ELWING)**2
1420       WNGIX=WNGICX+MW*YCGWNG**2+MTIP*YCGTIP**2
1430       WNGIZ=MW*YCGWNG**2+WNGICZ+MTIP*YCGTIP**2
1440       HORIY=HORICY+MHT*(ELCGH-ELCG)**2
1450       HORIX=HORICX+MHT*YCGHCR**2
1460       HORIZ=HORICZ+MHT*(ELCGH-ELCG)**2
1470       VERIY=VERICY+MVT*(ELCGV-ELCG)**2
1480       VERIX=VERICX+MVT*ZCGVER**2
1490       VERIZ=VERICZ+MVT*(ELCGV-ELCG)**2
1500       FUSIY=FUSICY+(ELF*RELR-ELCG)**2*MBT
1510       FUSIX=FUSICX
1520       FUSIZ=FUSIY
1530       GEARIX=MLG*CGLG**2
1540       GEARIY=GEARIX
1550       GEARIZ=GEARIX
1560       IXZW=(ELWING-ELCG)*ZCGWNG*MW
1570       IXZH=(ELCGH-ELCG)*ZCGHCR*MHT
1580       IXZV=(ELCGV-ELCG)*(-ZCGVER)*MVT
1590       IXZ=IXZW+IXZH+IXZV
1600       ENGIY=ENGICY+MP*(ELF*RELP-ELCG)**2
```

Figure 10.14: continued

```
      ENGIX=ENGIX+MF*(FENGCG+EW*0.5)**2
      ENGIZ=ENGIZ(Y+MF*(YCGENG**2+(ELF*RELF-ELCG)**2)
      INERTX=WNGIX+FUSIX+HORIX+VERIX+ENGIX+GEARIX
      INERTY=WNGIY+FUSIY+HORIY+VERIY+ENGIY+GEARIY
      INERTZ=WNGIZ+FUSIZ+HORIZ+VERIZ+ENGIZ+GEARIZ
      WEIGHT=(MW+MHT+MVT+MET+MF+MTIP+MLG)*32.174
      WRITE (6,166) WEIGHT
  166 FORMAT(10X,"INERTIAS AT EMPTY WEIGHT OF: ",1F10.2," LB"//)
      WRITE (6,167)
  167 FORMAT(10X,"       IXX              IYY              IZZ              IXZ"/)
      WRITE (6,168) INERTX,INERTY,INERTZ,IXZ
  168 FORMAT(10X,1F10.2,"   ",1F11.2,"   ",1F11.2,"   ",1F11.2//)
      WEIGHT=WEIGHT+WFTP+WFW+UWPAX*(PAX+1)
      TIPIOY=0.2*(MFTP+MTIP)*((AXIS/2)**2+(BXIS/2)**2)
      R1=WC/BW
      CHORD1=(CRCLW-CTW)*(1-R1)+CTW
      CHORD2=(CRCLW-CTW)*(1-EFUEL)+CTW
      Z1=((TCR-TCT)*(1-R1)+TCT)*CHORD1
      Z2=((TCR-TCT)*(1-EFUEL)+TCT)*CHORD2
      RHO=FUELD*0.0025
      R=(EFUEL*BW-WC)/2
      CFUEL=(MFW/RHO)/(CHORD1*.0666*RHO*Z1*R+CHORD1*0.1*Z2*R
     3+CHORD2*0.4*RHO*Z2*R+CHORD2*0.1*RHO*Z1*R)
      Y1=CFUEL*CHORD1
      Y2=CFUEL*CHORD2
      WFIOX=(0.0666*RHO*Z1*Y1+0.1*RHO*Z1*Y2+0.1*RHO*Z2*Y1+
     30.4*RHO*Z2*Y2)*R**3
      WFIY=(ELWING-ELCG)**2*MFW
      WFIX=WFIOX+MFW*(WC/2)**2
      MPASS=UWPAX/32.174
      IXXP=(WAS/24+WS/24)**2*(PAX+1)*MPASS+UWPAX*.0544*(PAX+1)
      IROW=(PAX+1)/SAB
      IF((IROW*SAB).LT.(PAX+1))IROW=IROW+1
      IROW2=IROW + 1
      DO 250 I=1,IROW2
      IF(((I-1)*SAB).GT.(PAX+1))SAB=SAB-(IROW*SAB)+PAX+1
      IYYP=IYYP+(ELCG-XPILOT-((I-1)*PS/12))**2*SAB*MPASS
  250 CONTINUE
      INERTX=INERTX+WFIX+(MFTP)*YCGTIP**2+IXXP
      INERTY=INERTY+WFIY+TIPIOY+(MFTP)*(ELTIP-ELCG)**2+IYYP
      INERTZ=INERTZ+WFIX+(MFTP)*YCGTIP**2+IYYP
      WRITE (6,270) WEIGHT
  270 FORMAT(10X,"INERTIAS AT MAX WEIGHT OF: ",1F10.2," LB"//)
      WRITE (6,167)
      WRITE(6,271) INERTX,INERTY,INERTZ
  271 FORMAT(10X,1F10.2,"   ",1F11.2,"   ",1F11.2//)
      STOP
      END
```

Figure 10.14: continued

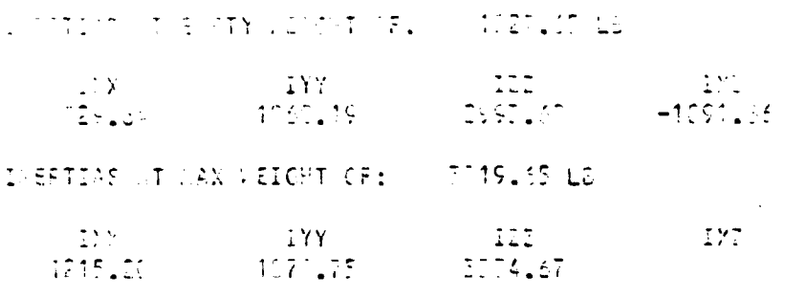

Figure 10.14: Sample printout for subroutine "INERTA"

10.5 REFERENCES

10.1 Marsh, D. Mass Moment of Inertia Estimation Methods, Manned Aircraft, SAWE Technical Paper # 313, 1962

11.1 VARIATION OF DRAG COEFFICIENT WITH ANGLE OF ATTACK, C_{D_α}

11.1.1 INTRODUCTION

This derivative is of importance only for slow speed flight. The computation is according to the method as described in Reference 11.1.1.

11.1.2 DERIVATION OF EQUATIONS

This derivative may be estimated, using the parabolic approximation of the drag polar:

$$C_D = C_{D_0} + \frac{C_L^2}{AR\pi e} \qquad (11.1.1)$$

By differentiation, the derivative C_{D_α} may be found:

$$C_{D_\alpha} = \frac{\partial C_{D_0}}{\partial \alpha} + \frac{2C_L C_{L_\alpha}}{\pi AR\, e} \qquad (11.1.2)$$

The first term in the right hand of the equation is often very small; it is also difficult to calculate. Therefore, it will be disregarded.

The lift curve slope, C_{L_α}, may be computed according to Section 11.2.

If the Oswald Efficiency Factor, e, is not explicitly given, it may be computed using Figure 11.1.1.

11.1.3 HAND CALCULATION

A hand calculation for Airplane A, using data presented in Appendix C, provides the following results:

From Section 11.2 follows:

$$C_{L_\alpha} = 5.25 \ (rad^{-1})$$

The Oswald efficiency factor follows from figure 11.1.1:

$$e = .87$$

For a lift coefficient of $C_L = .3$, equation 11.1.2 then gives:

$$C_{D_\alpha} = .1939 \ (rad^{-1})$$

This compares with a computer generated value of:

$$C_{D_\alpha} = .1952 \ (rad^{-1})$$

Reference 11.1.2 gives:

$$C_{D_\alpha} = .225 \ (rad^{-1})$$

This is a difference of 13.2 % compared to the computer generated value.

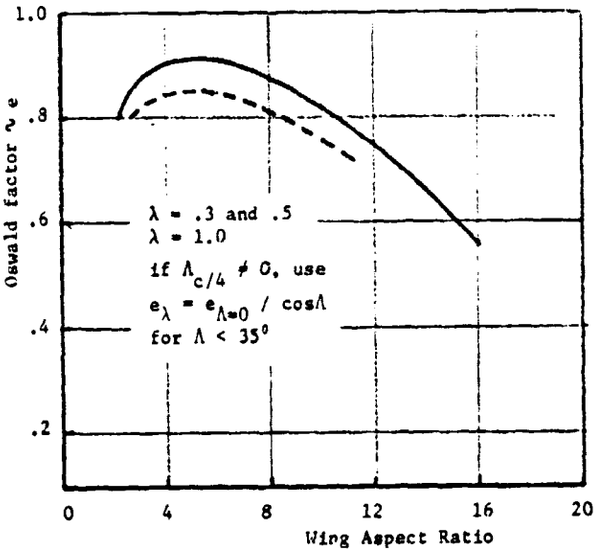

Figure 11.1.1: Method for estimating the Oswald efficiency factor

11.1.4 DESCRIPTION OF PROGRAM

Table 11.1.1 provides a listing of the variables used in the program, Figure 11.1.2 shows a flowchart, while a listing and a sample

printout are given in Figure 11.1.3. The Oswald Efficiency Factor, e, may be input; if not, it will be calculated according to Figure 11.1.1.

TABLE 11.1.1 VARIABLE NAMES IN SUBROUTINE "CDALPHA"

NAME	ENG. SYMBOL	DIMENSION	ORIGIN	REMARKS
AR	AR	---	Common	
CDA	C_{D_α}	rad^{-1}	---	
CL	C_L	---	Common	
CLALPH	C_{L_α}	rad^{-1}	"LIFTCURV"	
E	e	---	---	Default

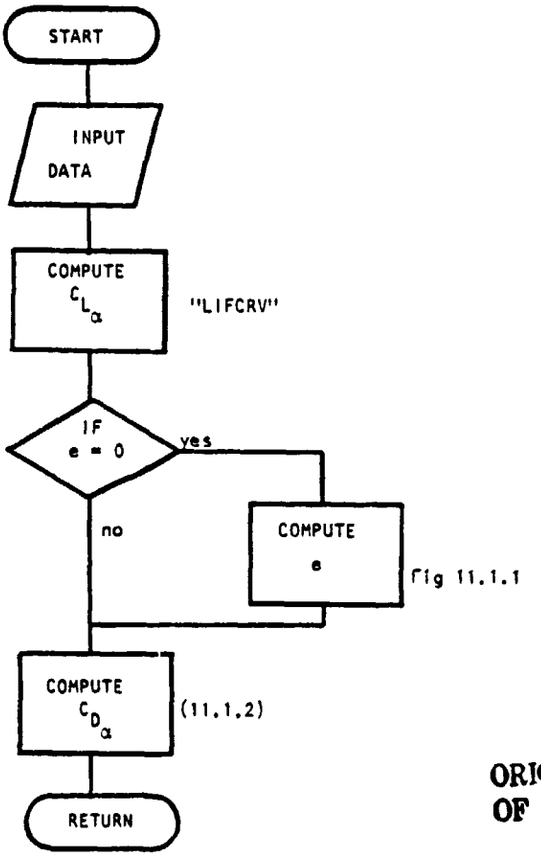

Figure 11.1.2: Flowchart of "CDALPH"

```
      SUBROUTINE E CD ALPH (CDA)
      COMMON/WING/DL,C4,AR,SLM,B,CDCL,CDCM,SA,CLALP
      COMMON/FLITE/ALPH,CL
      CALL LIFCRV (CLALPH)
      RL=C4=DL*C4*.0174S
      IF (E.NE.0.) GOTO 10
      DIMENSION DD(2,3),VV(3),DDD(4),WW(8),UU(1)
      DATA VV/.3,1./
      DATA UU/1./
       DATA WW/2.,4.,6.,8.,10.,12.,14.,16./
       DATA DD/.8,.9,.9025,.97,.91,.74,.65,.55,
     1.7?,.94,.94,.8,.75,.7,.64,.55/
      E=SDP(1.,CL*,AR,1,3,3,2,UU,VV,WW,DD)
      IF (RL?C4.NE.0.) E=E/COS(RL*C4)
   10 CONTINUE
      CDA=2.*CL*CLALPH/(3.141?*AR*E)
    WRITE (6,1000)
    1000 FORMAT (10X,"KU-FRL SUBROUTINE FOR CDALPHA"///)
    WRITE(6,1010) CDA
    1010 FORMAT(10X,"CDA  =   ",1F10.5," RAD-1 "///)
      RETURN
      END
```

KU-FRL SUBROUTINE FOR CDALPHA

CDA = 0.19518 RAD-1

Figure 11.1.3: Listing and sample printout for subroutine "CDALPHA"

REFERENCES

11.1.1 Roskam, J. Methods for Estimating Stability and Control Derivatives for Conventional Subsonic Airplanes. Roskam Aviation and Engineering Corporation, Lawrence, KS. 1977.

11.2 LIFT-CURVE SLOPE

11.2.1 INTRODUCTION

The method currently used in GASP to calculate the lift-curve slope of the airplane is one derived from Reference 11.2.1. The accuracy of this method is less than desired for the calculation of a variable that is of prime importance in design work. Therefore, a subroutine was developed that uses a refined method for the calculation of the lift-curve slope.

11.2.2 DERIVATION OF EQUATIONS

The lift-curve slope of a surface may be computed using the Polhamus Formula (Reference 2):

$$C_{L_\alpha} = \frac{2\pi AR}{2 + \sqrt{\frac{AR^2\beta^2}{\kappa^2}\left(1 + \frac{TAN^2\Lambda_{1/2\bar{c}}}{\beta^2}\right) + 4}} \qquad (11.2.1)$$

This formula calculates the lift-curve slope of the surface without body. Using a lifting surface method (Ref. 11.2.3), calculations were made for the lift-curve slope of a wing without body and tail, as a function of aspect ratio and leading-edge sweep angle. These results were compared with the results obtained with the Polhamus Formula. From this comparison an error-function was found. The error thus found is added to the value for the lift-curve slope found with the Polhamus Formula to yield a corrected value for the lift-curve slope. The derivation of the error function is given in Appendix A. The error function is given by:

$AR \leq 4$: $K_{POL} = 1+(1.87-.000223 \cdot \Lambda_{LE}) \cdot AR/100$ (11.2.2 a)

$AR > 4$: $K_{POL} = 1+([8.2-2.30 \cdot \Lambda_{LE}]-[.22-.153 \cdot \Lambda_{LE}] \cdot AR)/100$ (11.2.2 b)

where: Λ_{LE} in rad.

The corrected lift-curve slope is now given by:

$$C_{L_{\alpha_{CORR}}} = K_{POL} \cdot C_{L_{\alpha}} \quad (11.2.3)$$

To convert sweep angles of one chord position to another, use is made of the following formulas (Ref. 11.2.2):

$$TAN\Lambda_{c/2} = TAN\Lambda_{c/4} - \frac{1}{AR}\left(\frac{1-\lambda}{1+\lambda}\right) \quad (11.2.4)$$

$$TAN\Lambda_{LE} = TAN\Lambda_{c/2} + \frac{2}{AR}\left(\frac{1-\lambda}{1+\lambda}\right) \quad (11.2.5)$$

For a ratio of wing span to fuselage diameter, b/d>2, the following approximation may be made:

$$C_{L_{\alpha_{WB}}} = K_{WB}\, C_{L_{\alpha_W}} \quad (11.2.7)$$

where:

$$K_{WB} = 1 - .25\left(\frac{d}{b}\right)^2 + .025\frac{d}{b} \quad (11.2.8)$$

The lift-curve slopes for wing and horizontal tail may be found using Equations (11.2.1) through (11.2.5). The downwash ratio $d\varepsilon/d\alpha$ may be found using Section 11.3.

11.2.3 HAND CALCULATION

Following is a hand calculation for Airplane A for which data are presented in Appendix C.

For a Mach number of M = .2, the lift-curve slope of the wing is:

(11.2.1) $C_{L_{\alpha_W}} = 4.401 \ (rad^{-1})$

(11.2.2b) $K_{POL} = 1.066$

(11.2.3) $C_{L_{\alpha_W}} = 4.690 \ (rad^{-1})$

The lift-curve slope of the horizontal tail is:

(11.2.1) $C_{L_{\alpha_H}} = 3.795 \ (rad^{-1})$

(11.2.2a) $K_{POL} = 1.075$

(11.2.3) $C_{L_{\alpha_H}} = 4.079 \ (rad^{-1})$

The body correction factor is:

(11.2.8) $K_{WB} = .999$

The downwash follows from Section 11.3 as:

$$d\varepsilon/d\alpha = 0.338$$

The total airplane lift-curve slope then is:

(11.2.6) $C_{L_\alpha} = 5.260 \ (rad^{-1})$

The computer program generated a value of:

$$C_{L_\alpha} = 5.254 \quad (rad^{-1})$$

Reference 11.2.2 provided a value of:

$$C_{L_\alpha} = 4.956 \ (rad^{-1})$$

This is a difference of 5.7% compared to the computer value.

11.2.4 PROGRAM DESCRIPTION

Table 11.2.1 provides a listing of the variables used in subroutine "LIFTCURV." Figure 11.2.1 shows a flowchart and Figure 11.2.2 shows a

listing and a sample printout. The computation of the lift-curve slope of a lifting surface is done in function "SLOPE" to provide more versatility to the program.

TABLE 11.2.1 VARIABLE NAMES IN SUBROUTINE "LIFTCURV"

NAME	ENG. SYMBOL	DIMENSION	ORIGIN	REMARKS
AR	AR	---	Common	
ARH	AR_H	---	Common	
BATA	β	---	---	
B	b	ft	Common	
C1	C_1	---	---	
C2	C_2	---	---	
CLAHT	$C_{L_{\alpha_H}}$	rad^{-1}	---	
CLALP1	---	rad^{-1}	---	
CLAPH	$C_{\ell_{\alpha_H}}$	rad^{-1}	Common	
CLAW	$C_{L_{\alpha_W}}$	rad^{-1}	---	
DEPDAL	$d\epsilon/d\alpha$	---	"DOWNWS"	
DFUS	D_{fus}	ft	Common	
DLMC4	$\Lambda_{c/4}$	deg	Common	
DLMC4H	$\Lambda_{c/4H}$	deg	Common	
EM	M	---	Common	
ETAHT	η_H	---	Common	

TABLE 11.2.1 VARIABLE NAMES IN SUBROUTINE "LIFTCURV" (continued)

NAME	ENG. SYMBOL	DIMENSION	ORIGIN	REMARKS
KAPPA	κ	---	---	
KPOL	K_{POL}	---	---	
KWB	K_{WB}	---	---	
RLMC2P	$\Lambda_{c/2}$	rad	---	Dummy
RLMC4P	$\Lambda_{c/4}$	rad	---	Dummy
RLMLEP	Λ_{LE}	rad	---	Dummy
SHT	S_H	ft^2	Common	
SLM	λ	---	Common	
SLMH	λ_H	---	Common	
SLOPE	C_{L_α}	rad^{-1}	---	
SW	S	ft^2	Common	

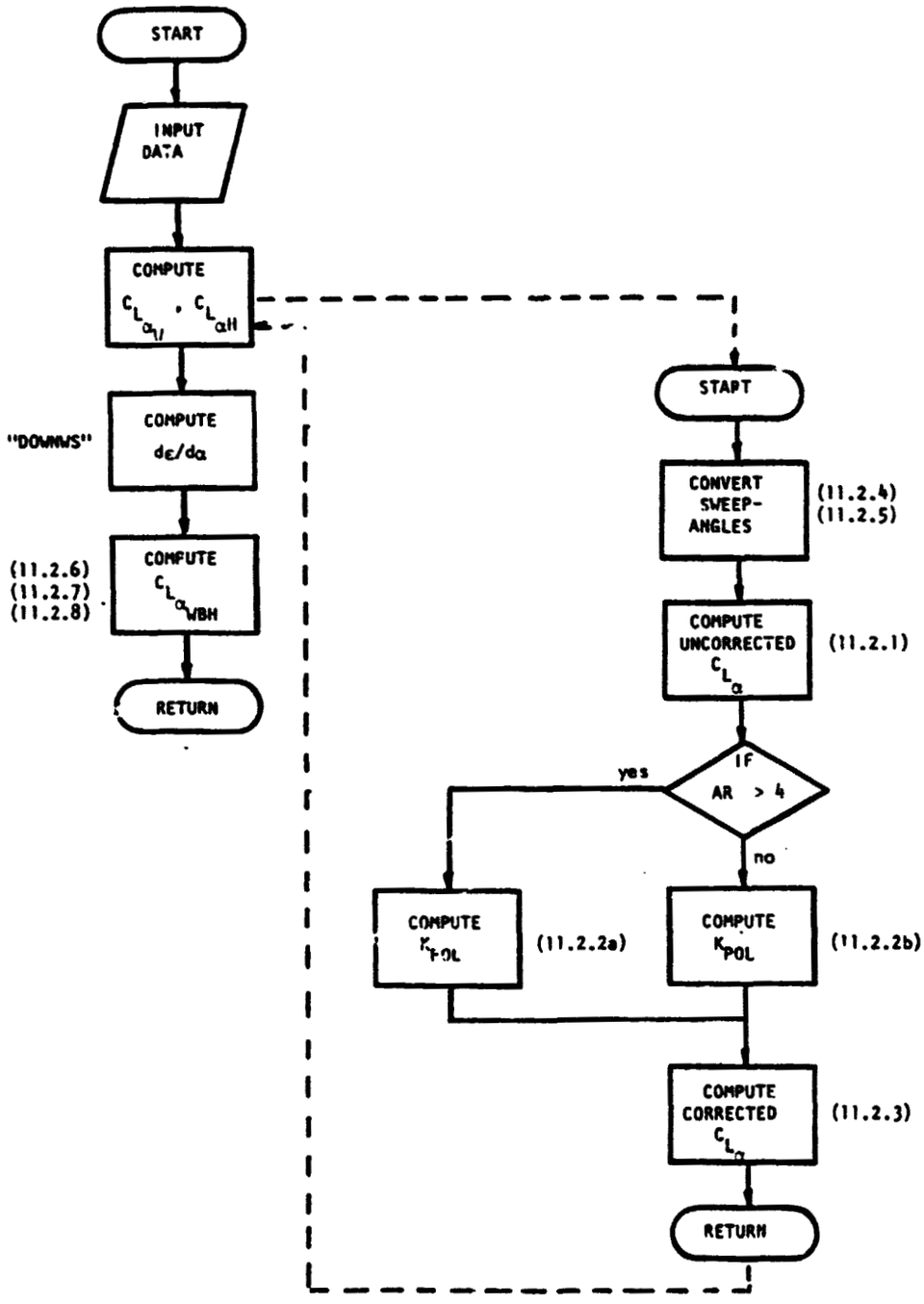

Figure 11.2.1: Flowchart for subroutine "LIFCRV"

```
10        SUBROUTINE LIFCRV (CLALPH)
15        REAL KWB
20        COMMON/WING/DLMC4,AR,SLM,B,CRCLW,CBARW,SW,CLAWP
30        COMMON/HORZ/DLMC4H,ARH,SLMH,BHT,CBARHT,SHT,CLAHP,CRCLHT
35        COMMON/FUS/ELF,DFUS,HC,WC,LN,ELTH,HH,SO,R2I,LV,ZV
40        COMMON/AERO/EM,RHO
50     DATA EM,RHO,ETAHT/.2,.0,.99/
60        CLAW=SLOPE(DLMC4,SLM,AR,EM,CLAWP)
70        CLAHT=SLOPE(DLMC4H,SLMH,ARH,EM,CLAHP)
80        CALL DOWNWS (DEPDAL)
90        KWB=1.-.25*(DFUS/B)**2+.025*(DFUS/B)
100       CLALPH=CLAW*KWB+CLAHT*ETAHT*(SHT/SW)*(1.-DEPDAL)
103     WRITE (6,1000)
104  1000 FORMAT (10X,"KU-FRL SUBROUTINE FOR LIFTCURVE ALOPE"///)
105     WRITE (6,1010) CLALPH
106  1010 FORMAT(10X,"CLALPH  =   ",1F10.5," RAD-1 "//)
110       RETURN
120       END

10        FUNCTION SLOPE (DLMC4P,SLMP,ARP,EMP,CLALPP)
20        REAL KPOL,KAPPA
30        RLMC4P=DLMC4P*.0174533
40        RLMC2P=ATAN(SIN(RLMC4P)/COS(RLMC4P)-(((1.-SLMP)/(1.+SLMP))/ARP))
50        BATA=SQRT(1.-EMP**2.)
60        KAPPA=CLALPP/6.28319
70       C1=(1.+((SIN(RLMC2P)/COS(RLMC2P))/BATA)**2)
80        C2=(ARP*BATA/KAPPA)**2.
90        CLALP1=6.28319*ARP/(2.+SQRT(C1*C2+4.))
100       RLMLEP=ATAN(SIN(RLMC2P)/COS(RLMC2P)+(2.*((1.-SLMP)/(1.+SLMP))/ARP))
110       IF (ARP.GT.4.) GO TO 10
120       KPOL=1.+(1.87-.000223*RLMLEP)*ARP/100.
130       GO TO 20
140    10 KPOL=1.+((8.2-2.3*RLMLEP)-(.22-.153*RLMLEP)*ARP)/100.
150    20 CONTINUE
160       SLOPE=CLALP1*KPOL
170       RETURN
180       END
```

CLALPH = 5.254 PER RADIAN

Figure 11.2.2: Listing and sample printout for subroutine "LIFCRV"

11.2.5 REFERENCES

11.2.1:	C.D. Perkins & R.E. Hage	Airplane Performance, Stability and Control. New York John Wiley & Sons, Inc. 1949.
11.2.2:	Dr. Jan Roskam	Methods for Estimating Stability and Control Derivatives of Conventional Subsonic Airplanes. Roskam Aviation & Engineering Corporation, Lawrence, KS. 1977
11.2.3:	Dr. E. Lan	Lifting Surface Computer Program, University of Kansas, Aerospace Department.

11.3 DOWNWASH BEHIND THE WING

11.3.1 INTRODUCTION

The downwash behind the wing is frequently needed for the calculation of other variables. Therefore, it is useful to have a subroutine for the calculation of the downwash.

11.3.2 DERIVATION OF EQUATIONS

Reference 11.3.1 provides the formulas for this subroutine. The downwash may be found from:

$$\left.\frac{d\varepsilon}{d\alpha}\right|_M = \left.\frac{d\varepsilon}{d\alpha}\right|_{M=0} \left(\frac{C_{L_{\alpha_W}}|_M}{C_{L_{\alpha_W}}|_{M=0}} \right) \tag{11.3.1}$$

For the downwash gradient at low speeds, the following formula is applicable:

$$\left.\frac{d\varepsilon}{d\alpha}\right|_{M=0} = 4.44 \left(K_A K_\lambda K_H \sqrt{\cos\Lambda_{c/4}} \right)^{1.19} \tag{11.3.2}$$

where:

$$K_A = 1/AR - \frac{1}{1 + AR^{1.7}} \qquad \text{(Correction factor for aspect ratio)} \tag{11.3.3}$$

$$K_\lambda = \frac{10 - 3\lambda}{7} \qquad \text{(Correction factor for taper ratio)} \tag{11.3.4}$$

$$K_H = \frac{1 - h_{H/b}}{\sqrt[3]{2\ell_{H/b}}} \qquad \text{(Correction factor for geometry)} \tag{11.3.5}$$

The parameters ℓ_H and h_H are defined in Figure 11.3.1.

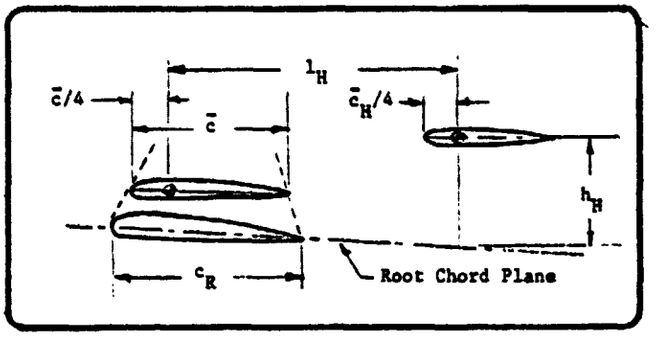

Figure 11.3.1: Geometric parameters for horizontal tail location

11.3.3 DESCRIPTION OF SUBROUTINE

A flowchart of the subroutine is shown in Figure 11.3.2. The calculation of the variables is quite straightforward. When the variable DOWN1 is set at 0, the subroutine skips the calculations for low mach numbers, returning directly to the calling routine. A listing and a sample output of the program are given in Figure 11.3.2-3.

11.3.4 HAND CALCULATION

This is a hand calculation of the subroutine for Airplane H.

The following data are avilable:

$\Lambda_{c/4}$ = 0 deg

AR = 7.54

λ = 0.41

h_H = 3.35 ft

b = 45.88 ft

ℓ_H = 21.75 ft

M = .066

$C_{L_\alpha}|_M$ = 5.021 rad^{-1}

$C_{L_\alpha}|_{M=0}$ = 5.015 rad^{-1}

With these data the following variables can be calculated:

$\Lambda_{1/4c}$ = 0 rad

K_{AR} = 0.1014

K_λ = 1.2529

K_H = 0.9436

FACT = 0.3557

$d\varepsilon/d\alpha|_M$ = 0.3561

Which compares to a computer calculated value of:

$d\varepsilon/d\alpha|_M$ = 0.3561

According to flight test data the downwash without power is:

$d\varepsilon/d\alpha|_M$ = 0.333

11.3.5 DESCRIPTION OF PROGRAM

The variables used in the computer program are listed in Table 11.3.1. A flowchart is shown in Figure 11.3.2, while Figure 11.3.3 shows a listing as well as a sample output of the program.

Note: Calculations in Chapter 6 show a computed downwash for airplane C of $d\varepsilon/d\alpha$ = 0.627, this compares to a wind tunnel value of $d\varepsilon/d\alpha$ = 0.633 (Ref. 6.2).

TABLE 11.3.1 VARIABLE NAMES AND ORIGINS IN SUBROUTINE DOWNWS

NAME	ENG. SYMBOL	DIMENSION	ORIGIN	REMARKS
AR	AR	___	common	
B	b	ft	common	
CLAWM	$C_{L_{\alpha_W}}\|_M$	rad^{-1}	"SLOPE"	
CLAWO	$C_{L_{\alpha_W}}\|_{M=0}$	rad^{-1}	"SLOPE"	
DEPDAL	$d\epsilon/d\alpha\|_M$	---	"DOWNWS"	
DLMC4	$\Lambda_{1/4\bar{c}}$	deg	common	
DOWN1	---	---	common	Switch to avoid loops
ELTH	ℓ_H	ft	common	
EM	M	---	common	
EMP	M	---	---	Dummy variable
FACT	---	---	---	Dummy variable
HH	H_h	---	common	
KAR	K_{AR}	---	---	
KTAPR	K_λ	---	---	
KH	K_H	---	---	
RLMC4	$\Lambda_{1/4\bar{c}}$	rad	---	
SLM	λ	---	common	
SLOPE	$C_{L_\alpha}\|_M$	rad^{-1}	---	
SLOPE0	$C_{L_\alpha}\|_{M=0}$	rad^{-1}	---	

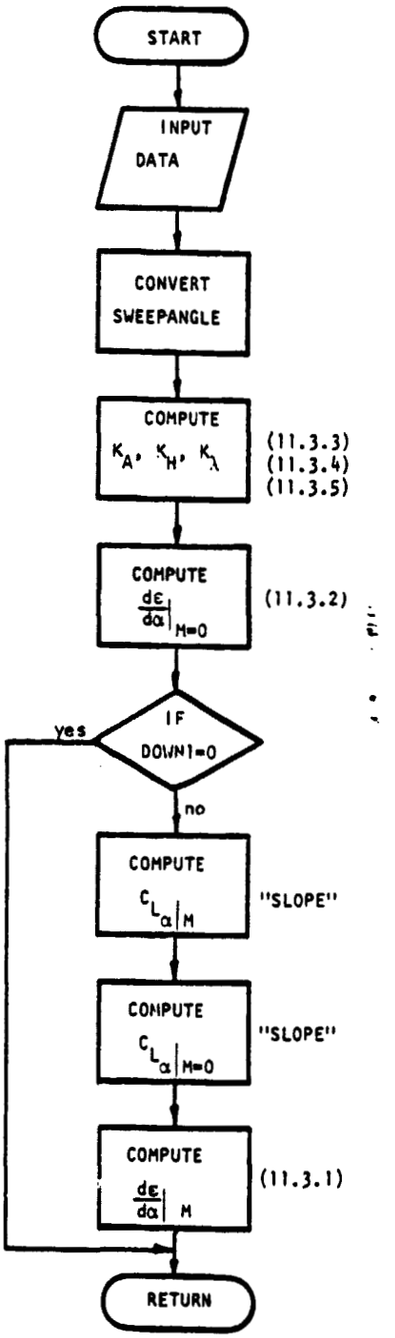

Figure 11.3.2: Flowchart for subroutine "DOWNWS"

```
      SUBROUTINE DOWNWS (CL-ALPHA,CL)
C
C
C     THIS SUBROUTINE CALCULATES THE DOWNWASH CONSTANT AND THE LIFT
C
      INTEGER DCAFT
      REAL KAP,KTMPR,MH
      COMMON/AIRC/DLRC4,AR,SLM,E,CFCLM,CRRM,SM,CLAMP
      COMMON/GRC/EM,RMC
      COMMON/FLG/ELF,CFLG,MC,LC,LM,ELTM,IP
      BLMC4=DLMC4*.0174533
      KAP=1./AR-1./(1.+AR**1.7)
      KTMPR=(1.-(.*CLAM))/.
      KM=(1.-KAP/2)/(((2.*ELTM)/2)**.5555)
      FACT=4.44*((MH*KTMPR*BLMC4))**1.19)
      IP=0
      CLAMP=SLOPE (CLMC4,SLM,AR,EM,CLAMP)
      EM=.001
      CLAMP=SLOPE (CLMC4,SLM,MC,EM,CLAMP)
      DEPSDL=(CLAMP/CLAMW)*FACT
      RETURN
      END
```

DOWNWASH = 0.356

Figure 11.3.3: Listing and sample printout for subroutine "DOWNWS"

11.3.6 REFERENCES

11.3.1 Roskam, J. Methods for Estimating Stability and Control Derivatives for Conventional Subsonic Airplanes. Roskam Aviation & Engineering Corporation, Lawrence, KS., 1977.

11.4 VARIATION OF PITCHING MOMENT WITH ANGLE OF ATTACK, C_{M_α}

The computation of this derivative has been discussed in chapter 6, Longitudinal Stability.

11.5 VARIATION OF DRAG COEFFICIENT WITH FORWARD SPEED, C_{D_U}

This derivative is usually negligible in the subsonic Mach range. It may be computed from the drag-polars at higher Mach numbers according to equation 11.5.1:

$$C_{D_U} = \frac{\partial C_D}{\partial M} M \qquad (11.5.1)$$

Where: M is the Mach number in steady state flight, for the condition considered.

$\frac{\partial C_D}{\partial M}$ is the slope of the curve of drag coefficient versus Mach number at the Mach number considered.

Since the drag polars at high Mach numbers are not available in the GASP program, this derivative is not computed.

11.6 C_{L_u}, VARIATION OF LIFT COEFFICIENT WITH SPEED PERTURBATIONS

11.6.1 DERIVATION OF EQUATIONS

According to Reference 11.6.1, C_{L_u} can be estimated from:

$$C_{L_u} = \left[\frac{M^2}{1 - M^2}\right] C_L \qquad (11.6.1)$$

where: M is the Mach number and C_L is the lift coefficient.

11.6.2 HAND CALCULATION

Test #1 was done for the Airplane A at M=.7 and C_L= .410. Equation 11.6.1 yields: C_{L_u} = .394. Flight test data gives C_{L_u} = .400, so the approximation (Equation 11.6.1) is very good in this instance.

11.6.3 DESCRIPTION OF THE PROGRAM

The C_{L_u} subroutine is a very simple program. It requires M and C_L as input and then calculates C_{L_u} according to Equation 11.6.1 above. Table 11.6.1 gives the variables used in the program.

TABLE 11.6.1 VARIABLE LIST

NAME	ENG. SYMBOL	DIMENSION	ORIGIN	REMARKS
CL	C_L	---	Common	
EM	M	---	Common	
CLU	C_{L_u}	---	Output	

A flowchart is given in Figure 11.6.1, while Figure 11.6.2 shows a listing as well as a sample printout.

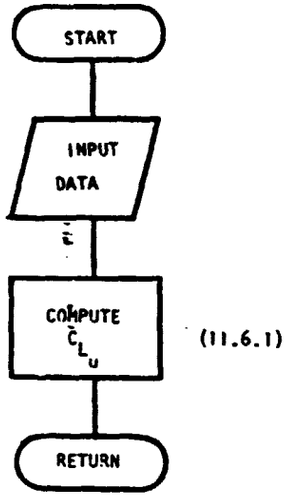

Figure 11.6.1: Flowchart for subroutine "CLUU"

```
      SUBROUTINE CLUU (CLU)
C******                                                        ******
C******  THIS SUBROUTINE COMPUTES THE VARIATION                ******
C******  OF LIFT COEFFICIENT WITH FORWARD SPEED                ******
C******                                                        ******
      COMMON/FLITE/ALPHA,EM,CL
      CLU=((EM**2)/(1-EM**2))*CL
      WRITE(6,10) CLU
   10 FORMAT (10X,"CLU = ",F10.3//)
      RETURN
      END
```

CLU = 0.394

Figure 11.6.2: Listing and sample printout for subroutine "CLUU"

11.6.4 REFERENCES

11.6.1 Roskam, J. Methods for Estimating Stability and Control Derivatives of Conventional Subsonic Airplanes. Roskam Aviation & Engineering Corporation, Lawrence, KS., 1977.

11.7 C_{m_u} ; VARIATION OF PITCHING MOMENT COEFFICIENT DUE TO SPEED PERTURBATIONS, C_{m_u}

11.7 1 DERIVATION OF EQUATIONS

Reference 11.7.1, pp. 4.1, eq. 4.3 gives C_{m_u} as:

$$C_{m_u} = -C_L \frac{\partial \bar{X}_{ac_W}}{\partial M} \qquad (11.7.1)$$

where: C_L is the lift coefficient

$\bar{X}_{ac_W}$ is the non-dimensional aerodynamic center of the wing

M is the Mach number

Because $\partial \bar{X}_{ac_W} / \partial M$ is very hard, if not impossible to determine analytically, reference 11.7.1 suggests plotting $\bar{X}_{ac_W}$ v.s. M for Mach numbers adjacent to the cruise Mach number and drawing a line through the points. The slope of the line is $\partial \bar{X}_{ac_W} / \partial M$.

Figure 3.9, page 3.12 in reference 1 presents families of curves for the parameters:

$\frac{\bar{X}_{ac}}{C_R}$ X'_{ac} is the wing a.c. location measured positive aft along the root chord. C_R is the root chord.

L is the wing taper ratio.

A $\tan\Lambda_{LE}$ A is the wing aspect ratio, Λ_{LE} is the leading edge sweep angle

$\frac{\tan \Lambda_{LE}}{\beta}$ $\beta = \sqrt{1 - M^2}$

$\frac{\beta}{\tan \Lambda_{LE}}$ $\beta = \sqrt{1 - M^2}$

The pertinent wing geometry is given below in Figure 11.7.1:

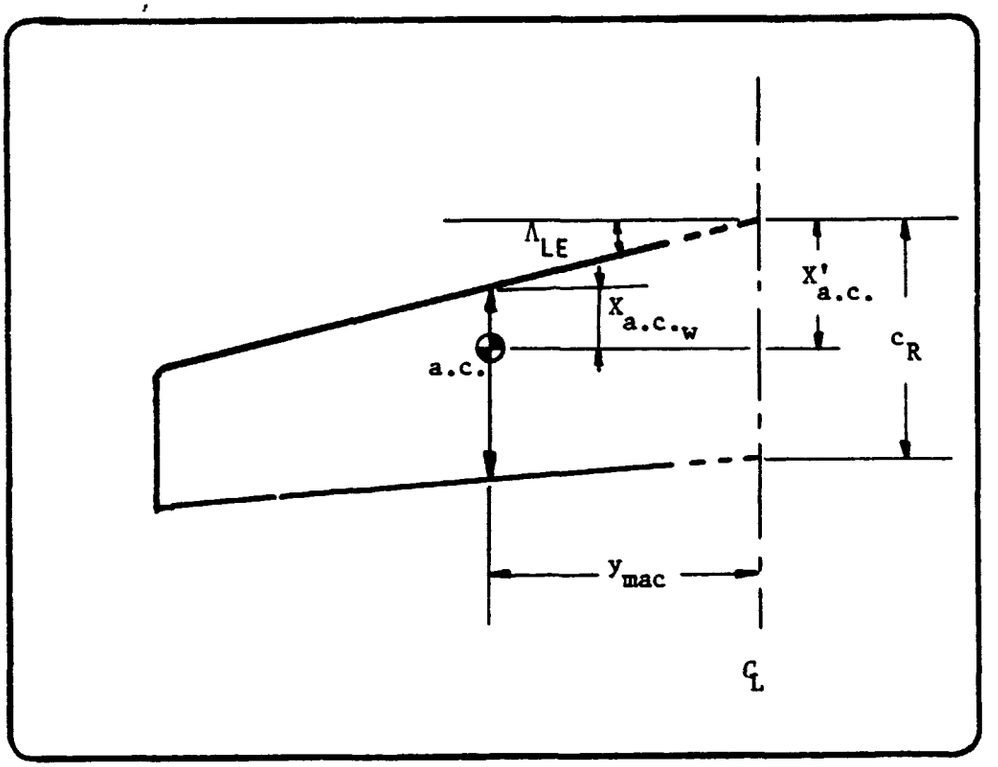

Figure 11.7.1: Wing geometry

From Figure 11.7.1, it is possible to find $\bar{X}_{ac_w}$ in terms of X'ac, Ymac, Λ_{LE}, and $\bar{c}$:

$$X_{ac_w} = X'_{ac} - Y_{mac} \tan\Lambda_{LE}$$

or:

$$\bar{X}_{ac_w} = \frac{X'_{ac} - Y_{mac} \tan\Lambda_{LE}}{\bar{c}} \qquad (11.7.2)$$

The computation of X'_{ac} is done with function "ACEM" and is described in detail in Chapter 6.

11.7.2 HAND CALCULATION

Three cases where computed:

1) Wing alone at M = .8, .85, .9

2) Wing alone at M = .75, .8, .85, .9, .95

3) Airplane A, Cruise Mach = .83

The data for the wing are:

$b = 30$ ft $\qquad \bar{c} = 7.0$ ft

$S = 180$ ft^2 $\qquad \lambda = .2$ ft

$A = 5.0$ $\qquad \Lambda_{LE} = 43.13$ deg

$C_R = 10.0$ ft $\qquad Y_{MAC} = 5.8$ ft

$C_t = 2.0$ ft

The data for airplane A are given in Appendix D. The computations for case 1) are given in table 11.7.1.

Table 11.7.1 Hand Calculation for Wing 1)

M	β	$\frac{\beta}{\tan\Lambda_{LE}}$	$A \tan\Lambda_{LE}$	$\bar{X}ac_w$
.8	.60	.640	4.685	.362
.85	.527	.562	4.685	.373
.9	.436	.465	4.685	.390

By linear regression a line is constructed through the points defined by M and $\bar{X}_{ac_W}$ to find:

$$\frac{\partial \bar{X}_{ac_W}}{\partial M} = .280$$

For a lift coefficient of $C_L = .15$ it then follows with eqn. 11.7.1:

$$C_{m_u} = -.042$$

Table 11.7.2 shows the results for case 2):

Table 11.7.2: Hand Calculation for Wing 2)

M	β	$\frac{\beta}{\tan\Lambda_{LE}}$	A $\tan\Lambda_{LE}$	$\bar{X}ac_w$
.75	.661	.706	4.685	.354
.80	.60	.640	4.685	.362
.85	.527	.562	4.685	.373
.90	.436	.465	4.685	.390
.95	.312	.333	4.685	.419

By linear regression it was found that:

$$\frac{\partial \bar{X}_{ac_w}}{\partial M} = .316$$

Again, for a lift coefficient of $C_L = .15$, equation 11.7.1 then gives:

$$C_{m_u} = -.047$$

In exactly the same manner as for the wing above, the computations for airplane A produced for a cruise Mach number of .83:

$$C_{m_u} = -.036$$

11.7.3 DESCRIPTION OF PROGRAM

The computation of C_{m_u} is split in two parts. The aerodynamic center of the wing $\bar{X}_{ac_W}$. is computed in Function "ACEM." This program is described in Chapter 6. The mainline of subroutine "CMUU" computes the derivative C_{m_u}. It calls Function "ACEM" three times for consecutive Mach numbers to compute the slope $\partial\bar{X}_{ac_W}/\partial M$. Table 11.7.3 explains the variables used in the program. Figure 11.7.2 shows a flowchart, while Figure 11.7.3 shows a listing of the program, including a sample output.

Table 11.7.3: Variable List

Name	Eng. Symbol	Dimension	Origin	Remarks
AM	---	---	---	
AR		---	Common	
CBARW	$\bar{c}_w$	ft	Common	
CL	C_L	---	Common	
CMU	C_{m_u}	rad^{-1}	---	
CRCLW	$C_{R_{C_L}}$	ft	Common	
SX	---	---	---	
SY	---	---	---	
SXSQ	---	---	---	
SUMXY	---	---	---	
XBARW	$\bar{X}_{ac_W}$	ft	Common	

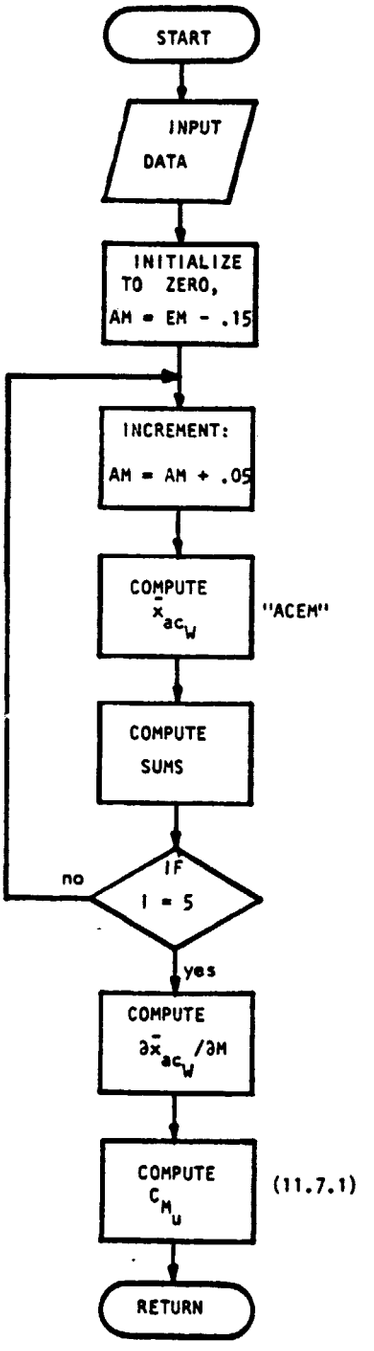

Figure 11.7.2: Flowchart for subroutine "CMUU"

```
10          SUBROUTINE CMUU (CMU)
20         COMMON/WING/DLMC4,AR,SLM,B,CRCLW,CBARW,SW,CLAWP
30         COMMON/FLITE/ALPHA,EM,CL
40          SUMXY=0.
50          SX=0.
60          SY=0.
70          SXSQ=0.
80          AM=EM-.15
90          DO 1 I=1,5
100         AM=AM+.05
110         XBARW=ACEM (AM,AR,SLM,DLMC4,CRCLW)
120         SUMXY=SUMXY+XBARW*AM
130         SX=SX+AM
140         SY=SY+XBARW
150         SXSQ=SXSQ+AM**2
160   1     CONTINUE
170         PXBPEM=(SUMXY-SX*SY/5.)/(SXSQ-(SX**2)/5.)
180         CMU=-CL*PXBPEM
190         WRITE (6,2) CMU
200     2   FORMAT(10X,"CMU    =    ",1F10.4)
210    STOP
220         END
```

Figure 11.7.3: Listing and sample printout for subroutine "CMUU"

11.7.4 PROGRAM RESULTS

Table 11.7.4 summarizes the results of calculations for C_{m_u}.

Table 11.7.4 CMU Subroutine test results

Test #	Description	$\partial\bar{X}_{ac}/\partial M$ by hand	$\partial\bar{X}_{ac}/\partial M$ by computer	C_{m_u} (hand)	C_{m_u} (computer)	% Error
1	wing $.8 \leq M \leq .9$ $\Delta M = .05$	.280	.166	-.042	-.025	40.48% (too small)
2	wing $.75 \leq M \leq .95$ $\Delta M = .05$	.316	.175	-.047	-.026	44.68% (too small)
3	Airplane A $.73 \leq M \leq .93$ $\Delta M = .05$	---	-.078	-.036	+.0117	Wrong Sign

Notes: C_{m_u} from eq. 11.4.1 with $C_L = .15$.

% error as in section 11.4.5.2.

Table 11.7.5 - CMU Test #1

Wing #3, $.8 \leq M \leq .9$, $\Delta M = .05$, Cruise M = .85

M	$\bar{X}_{ac_W}$ (hand)	$\bar{X}_{ac_W}$ (computer)	% Error
.80	.362	.369	1.93% (too big)
.85	.373	.377	1.07% (too big)
.90	.390	.386	1.03% (too small)

These errors combine in a way which makes the slope of the least squares line (and therefore the value of C_{m_u}) much too small, about 40% too small as shown in Table 11.7.4. The way the small errors in $\bar{X}_{ac_W}$ change the slope is illustrated in Figure 11.7.4.

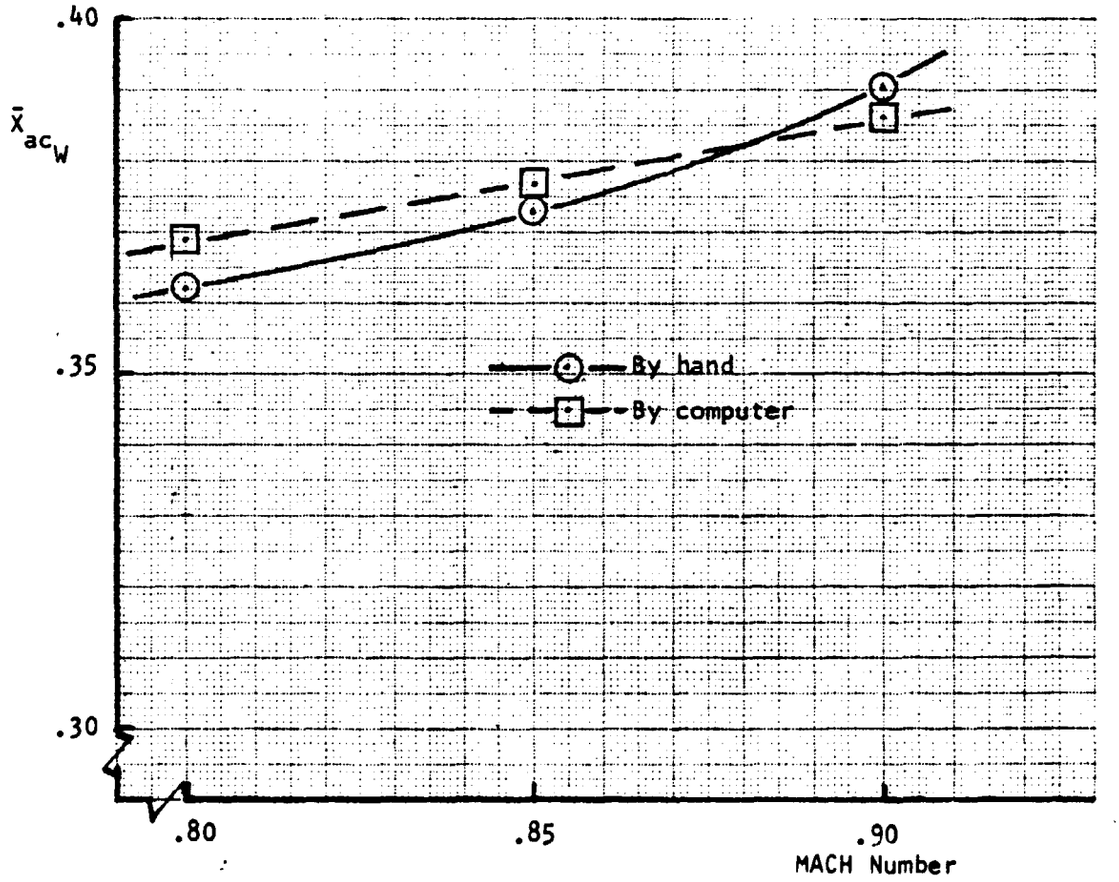

Figure 11.7.4: Comparing $\bar{X}_{ac_W}$'s

A similar situation happens in Test #2. The $\bar{X}_{ac_W}$'s at the low end of the Mach range are a little too big while the $\bar{X}_{ac_W}$'s at the high end of the Mach range are a little too small. Table 11.7.6 illustrates this.

Table 11.7.6 - CMU Test #2

Wing #3, $.75 \leq M \leq .95, \Delta M = .05$, Cruise M = .85

M	$\bar{X}_{ac_W}$ (hand)	$\bar{X}_{ac_W}$ (computer)	% Error
.75	.354	.363	2.54% (too big)
.80	.362	.369	1.93% (too big)
.85	.373	.377	1.07% (too big)
.90	.390	.386	1.03% (too small)
.95	.419	.399	4.77% (too small)

Consideration was given to the possibility of using a correction factor since in Tests 1 and 2 C_{m_u} was about 40% too small. However, the idea was dropped because the direction of the errors in the $\bar{X}_{ac_W}$'s (too big for low M or high M) is what determines whether the computer predicted C_{m_u} is too big or too small. Imagine the errors going the other way in Figure 11.7.4 and it becomes obvious that the slope of the line will be too big instead of too small.

The subroutine was subsequently tested for airplane A. Another error in the basic method became apparent. The CMU program predicted a positive C_{m_u} while the airplane data gives C_{m_u} as negative. A check was done to see if the computer was generating an error or if Figure 6.5 actually predicted a forward movement of the aerodynamic center with increasing Mach number. Table 11.7.7 gives the results.

Table 11.7.7 - CMU Test #3

Airplane A, $.73 \leq M \leq .93$, $\Delta M = .05$, Cruise M = .83

M	$\bar{X}_{ac_W}$ (hand)	$\bar{X}_{ac_W}$ (computer)
.73	.284	.285
.78	---	.284
.83	---	.282
.88	.279	.280
.93	---	.275

The hand-check shows that Figure 6.5 indeed predicts a negative $\partial\bar{X}_{ac_W}/\partial M$ for the wing of airplane A.

In light of this difficulty, work on the CMU subroutine was stopped. There may be other ways to predict C_{m_u} but they have not been investigated at this time. In any case, the ACEM subroutine gives reasonable predictions of $\bar{X}ac_w$ to the extent that Figure 6.5 is accurate.

11.7.5 REFERENCES

11.7.1 Roskam, J. Methods for Estimating Stability and Control Derivatives for Conventional Subsonic Airplanes. Roskam Aviation & Engineering Corporation, Lawrence, KS., 1977.

11.8 C_{D_q}, VARIATION OF DRAG COEFFICIENT WITH PITCH RATE

This derivative is usually negligible in the subsonic Mach range.

11.9 C_{L_q}, VARIATION OF LIFT COEFFICIENT WITH PITCH RATE

11.9.1 DERIVATION OF EQUATIONS

Reference 1 presents the method used for calculating C_{L_q}.

C_{L_q} may be considered to be the sum of a wing and tail contribution, the fuselage effect being usually small.

$$C_{L_q} = C_{L_{q_W}} + C_{L_{q_H}} \tag{11.9.1}$$

For the wing contribution:

$$C_{L_{q_{W|M}}} = \left(\frac{A + 2 \cos \Lambda_{c/4}}{AB + 2 \cos \Lambda_{c/4}} \right) C_{L_{q_{W|M=0}}} \quad (\text{rad}^{-1}) \tag{11.9.2}$$

where:

$$C_{L_{q_{W|M=0}}} = \left(\frac{1}{2} + \frac{2X_W}{\bar{c}} \right) C_{L_{\alpha_{W|M=0}}} \quad (\text{rad}^{-1}) \tag{11.9.3}$$

A is the aspect ratio

B is the compressibility factor

$$= \sqrt{1 - M^2 \cos^2 \Lambda_{c/4}} \tag{11.9.4}$$

$\Lambda_{c/4}$ is the quarter chord sweep of the wing

X_W is the distance (positive rearward) from the airplane center of gravity to the aerodynamic center

$\bar{c}$ is the wing mean geometric chord

$C_{L_{\alpha_W}}$ is the lift-curve slope of the wing

M is the Mach number

For the horizontal tail contribution:

$$C_{L_{q_{H|M}}} = 2\, C_{L_{\alpha_{H|M}}}\, \eta_H\, \bar{V}_H \quad (\text{rad}^{-1})$$

where:

$C_{L_{\alpha_{H|M}}}$ is the lift-curve slope of the horizontal tail

η_H is the ratio of dynamic pressure at the horizontal tail to the free stream dynamic pressure

$\bar{V}_H$ is the horizontal tail volume coefficient

11.9.2 HAND CALCULATION

The hand calculation check utilizes data from Reference 2. The data is for Airplane C; data are given in Appendix C. These data are for a center of gravity condition of $\bar{X}_{c.g.} = 12$ and a Mach number of M = .083.

First, B must be calculated.

$$B = \sqrt{1 - (.083)^2 \ (\cos^2 \ -.044 \text{ rad})}$$

$$= \sqrt{1 - (.077) \quad (.998)}$$

$$= .997$$

C_{L_q} may be calculated now.

$$C_{L_{q_{W|M=0}}} = \left[\frac{1}{2} + \frac{2(.645 \text{ ft})}{4.958 \text{ ft}}\right] 4.35/\text{rad}$$

$$= 3.301/\text{rad}$$

$$C_{L_{q_{W|M}}} = \left[\frac{7.5 + 2 \cos \ -.044 \text{ rad}}{(7.5) \ (.997) + 2 \cos \ -.044 \text{ rad}}\right] 3.301/\text{rad}$$

$$= 3.315/\text{rad}$$

$$C_{L_{q_{H|M}}} = (2)(4.08/\text{rad})\ (1.0)\ (.547)$$

$$= 4.464/\text{rad}$$

$$C_{L_q} = 3.315/\text{rad} + 4.464/\text{rad}$$

$$C_{L_q} = 7.779/\text{rad}$$

Subroutine C_{L_q} is a simple, straightforward program. The equations of 11.9.1 were programmed directly into the computer. The program calls various subroutines for needed data, and calls on the common block for the remaining data.

One variable, X_W, appearing in 11.9.1, must be calculated. X_W is not drawn from the common block but can be derived from subroutine products. Subroutine "SIZE" produces the required variables for calculation of X_W.

11.9.3 DESCRIPTION OF PROGRAM

Table 11.9.1 presents the variables used within the C_{L_q} subroutine.

TABLE 11.9.1 VARIABLE NAMES AND ORIGINS IN SUBROUTINE C_{L_q}

NAME	ENG. SYMBOL	DIMENSION	ORIGIN	REMARKS
ARW	A	---	Common	
B	B	---	---	Compressibility Correction Factor
CBARW	$\bar{c}$	ft.	Common	
CLQ	C_{L_q}	rad^{-1}	---	

TABLE 11.9.1 VARIABLE NAMES AND ORIGINS IN SUBROUTINE C_{L_q} (continued)

NAME	ENG. SYMBOL	DIMENSION	ORIGIN	REMARKS
CLQWM	$C_{L_{q_{W\|M}}}$	rad^{-1}	---	Dummy
CLQWMO	$C_{L_{q_{W\|M=0}}}$	rad^{-1}	---	Dummy
CLQHM	$C_{L_{q_{H\|M}}}$	rad^{-1}	---	Dummy
DLMC4	$\Lambda_{c/4}$	rad	Common	
ELCG		ft.	Calling Subroutine	
ELWING		ft.	Calling Subroutine	
EM	M	---	Common	
SLOPE	$C_{L_{\alpha_W}}$	rad^{-1}	Calling Subroutine	
SLOPEH	$C_{L_{\alpha_H}}$	rad^{-1}	Calling Subroutine	
QHQI	η_H	---	Calling Subroutine	
VBARHX	$\bar{V}_H$	---	Common	
XW	X_W	ft	---	Dummy

A flowchart of the program is given in figure 11.9.1 , a listing and sample output is shown in figure 11.9.2.

Reference 11.9.2 presents a value of C_{L_q} =8.579 rad^{-1} for the same flight condition. This is a difference of 8.5% as compared to the computer generated value. However, the method of reference 11.9.1

as used for this subroutine only accounts for the effect of wing and horizontal tail. Subtracting the body effects from the C_{L_q} value as given in reference 11.9.2 produces a value of:

$$C_{L_q} = 8.579 - .9087 \text{ rad}^{-1}$$

$$= 7.67 \text{ rad}^{-1}$$

This produces an error of 1.4% as compared to the computer value.

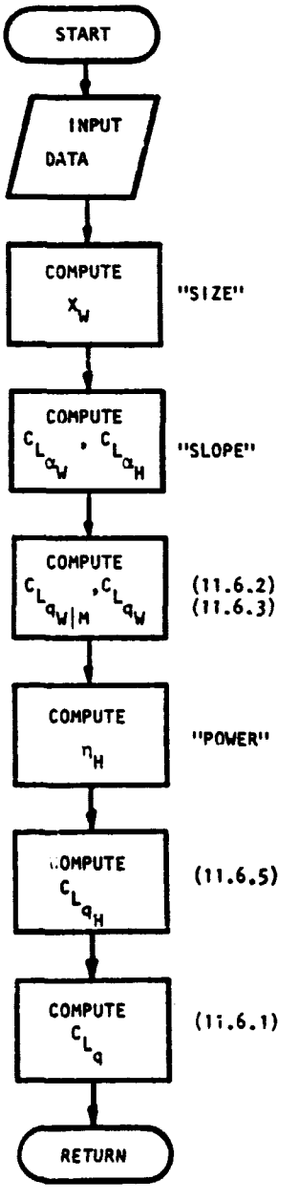

Figure 11.9.1: Flowchart of "CLQUE"

```
      SUBROUTINE CLQUE (CLQ)
C******                                                        ******
C****** THIS SUBROUTINE COMPUTES CLQ, VARIATION                ******
C****** OF LIFT COEFFICIENT WITH PITCH RATE                    ******
C******                                                        ******
      COMMON/WING/DLMC4,AR,SLM,TR,CRCLW,CBARW,SW,CLAWP
      COMMON/FLITE/ALPHA,EM,CL
      COMMON/HORZ/DLMC4H,ARH,SLMH,TRH,CBARHT,SHT,CLAHP,CRCLHT
      COMMON/FUS/ELF,DFUS,HC,WC,LM,ELTH,HH,SO,RZI,LV,ZV
       RLMC4=DLMC4*.0174533
       B=SQRT(1.-(EM*COS(RLMC4))**2)
      CALL SIZE (ELWING,ELCG)
      XW=ELWING-ELCG
      SLOPEW=SLOPE(DLMC4,SLM,AR,EM,CLAWP)
      SLOPEH=SLOPE(DLMC4H,SLMH,ARH,EM,CLAHP)
      CLQWC=(.5+2.*XW/CBARW)*SLOPEW
      CLQWF=((AR+2.*COS(RLMC4))/(AR*B+2.*COS(RLMC4)))*CLQWC
      CALL POWER (CHQI)
      VBARHY=(SHT/SW)*(ELTH/CBARW)
      CLQHW=2.*SLOPEH*CHQI*VBARHY
      CLQ=CLQHW+CLQWF
      WRITE(6,2) CLQ
    2 FORMAT(1OX,"CLQ = ",F5.3," PER RADIAN")
      RETURN
      END
```

```
CLQ = 7.779 PER RADIAN
```

Figure 11,9.2: Listing and sample output for subroutine "CLQUE"

11.9.4 REFERENCES

11.9.1: Roskam, J. — Methods for Estimating Stability and Control Derivatives of Conventional Subsonic Aircplanes. Roskam Aviation & Engineering Corporation, Lawrence, KS. 1977

11.9.2: Wolowicz, C.H. & Yancey, R.B. — Longitudinal Aerodynamic Characteristics of Light, Twin-Engine, Propeller-Driven Airplanes. NASA TN D-6800, June 1972.

11.10 C_{m_q}, VARIATION OF PITCHING MOMENT COEFFICIENT WITH PITCH RATE

11.10.1 DERIVATION OF EQUATIONS

Reference presents the method used for the calculation of the C_{m_q} derivative.

C_{m_q} may be considered to be the sum of a wing and a tail contribution, the contribution of the fuselage usually being small.

$$C_{m_q} = C_{m_{q_W}} + C_{m_{q_H}} \tag{11.10.1}$$

For the wing contribution:

$$C_{m_{q_W}}\Big|_M = \left[\frac{\frac{A^3\tan^2\Lambda_{c/4}}{AB + 6\cos\Lambda_{c/4}} + \frac{3}{B}}{\frac{A^3\tan^2\Lambda_{c/4}}{A + 6\cos\Lambda_{c/4}} + 3}\right] \quad (\text{rad}^{-1}) \tag{11.10.2}$$

where:

$$C_{m_{q_W}}\Big|_{M=0} = -KC_{\ell_{\alpha_W}}\left(\cos\Lambda_{c/4}\right)\left[\frac{A\left[2\left(\frac{Xw}{\bar{c}}\right)^2 + \frac{1}{2}\left(\frac{Xw}{\bar{c}}\right)\right]}{A + 2\cos\Lambda_{c/4}} + \left(\frac{1}{24}\right)\frac{A^3\tan^2\Lambda_{c/4}}{A + 6\cos\Lambda_{c/4}} + \frac{1}{8}\right] \quad (\text{rad}^{-1}) \tag{11.10.3}$$

A is the aspect ratio

B is the compressibility correction factor

$$= \sqrt{1 - M^2\cos^2\Lambda_{c/4}} \tag{11.10.4}$$

$\Lambda_{c/4}$ is the quarter-chord sweep angle of the wing

$\bar{c}$ is the mean geometric chord

X_w is the distance from the aircraft center of gravity to the wing aerodynamic center (positive rearward)

$C_{\ell_{\alpha_W}}$ is the spanwise average value of wing section lift-curve slope

K is the correction constant for the wing (Figure 11.10.1)

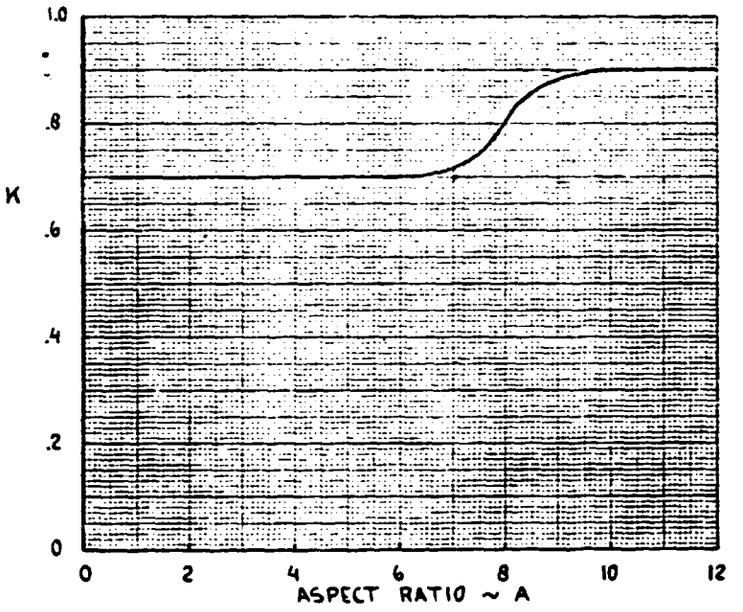

Figure 11.10.1: Correction constant K for wing contribution

For the horizontal tail contribution:

$$C_{m_{q_H}} = -2\, C_{L_{\alpha_H}}\, \eta_H\, \bar{V}_H\, \frac{X_H}{\bar{c}} \quad (\text{rad}^{-1}) \qquad (11.10.5)$$

where:

$C_{L_{\alpha_H}}$ is the horizontal tail lift-curve slope

η_H is the ratio of dynamic pressure at the horizontal tail to free stream dynamic pressure

$\bar{V}_H$ is the horizontal tail volume coefficient

X_H is the distance from the aircraft center of gravity to the aerodynamic center of the horizontal tail

$\bar{c}$ is the mean geometric chord of the wing

11.10.2 HAND CALCULATION

The hand calculation utilizes data from Appendix C, for Airplane C.

A = 7.5

$\bar{c}$ = 4.958 ft

$C_{L_{\alpha_W}}$ = 5.44/rad

$\Lambda_{c/4}$ = -.044 rad (-2.5°)

ELCG = distance from nose to aircraft c.g.
= .595 ft

ELWING = distance from nose to a.c. (wing)
= 1.240 ft

M = .083

$C_{L_{\alpha_H}}$ = 4.08/rad

H_X = 14.396 ft

$\bar{V}_H$ = .547

$0\eta_H$ = 1.0

Note: For ELCG and ELWING, the distances from the leading edge of $\bar{c}$ to the c.g. and a.c. were used. The values will yield the same results as the distances from the nose.

First, B and K must be determined:

$$B = \sqrt{1 - (.083)^2(\cos^2 -.044 \text{ rad})}$$

$$= .997$$

From Figure 11.10.1, for A = 7.5,

$$K = .745$$

Next, X_w must be calculated. This is accomplished by equating the difference between ELCG and ELWING.

$$X_w = \text{ELWING} - \text{ELCG}$$

$$= 1.240 \text{ ft} - .595 \text{ ft}$$

$$= .645 \text{ ft}$$

$$C_{m_{q_w}}\Big|_{M=0} = -(.745)(5.44/\text{rad})\cos -.044 \text{ rad}$$

$$\left[\left(\frac{7.5\ 2\left(\frac{.645}{4.958}\right)^2 + \frac{1}{2}\left(\frac{.645}{4.958}\right)}{7.5 + 2\cos -.044 \text{ rad}}\right) + \left(\frac{1}{24}\right)\right.$$

$$\left.\left(\frac{7.5^3\ [\tan^2 -.044 \text{ rad}]}{7.5 + 6\cos -.044 \text{ rad}}\right) + \frac{1}{8}\right] (\text{rad}^{-1}) \qquad (11.10.3)$$

$$= -4.049\ (.078 + .227)\ (\text{rad}^{-1})$$

$$= -1.235\ (\text{rad}^{-1})$$

$$C_{m_{q_w}}\Big|_M = -1.235 \left[\frac{\frac{7.5^3\ (\tan^2 .044 \text{ rad})}{(7.5)(.997) + 6\cos -.044 \text{ rad}} + \frac{3}{.997}}{\frac{7.5^3\ (\tan^2 -.044 \text{ rad})}{7.5 + 6\cos -.044 \text{ rad}} + 3}\right] (\text{rad}^{-1})$$

(11.10.2)

$$C_{m_{q_w}} = -1.235\ (\text{rad}^{-1})\ (1.003)$$

$$C_{m_{q_{w_m}}} = -1.239\ (\text{rad}^{-1})$$

$$C_{m_{q_H}}\Big|_M = -2(4.08/\text{rad})(1.0)(.547)(14.396\ \text{ft})/(4.958\ \text{ft})(\text{rad}^{-1}) \tag{11.10.5}$$

$$C_{m_{q_H}}\Big|_M = -12.960\ (\text{rad}^{-1})$$

$$C_{m_q} = -1.239\ (\text{rad}^{-1}) + (-12.960)(\text{rad}^{-1}) \tag{11.10.1}$$

$$C_{m_q} = 14.199/\text{rad}$$

As a second test, the data for airplane A was used. This test also incorporates a variation of Mach number.

Because of Mach number variation, the lift-curve slope of the horizontal tail must be individually calculated for each Mach number.

Reference 1, Chapter 3, presents the method for calculating this lift-curve slope: the Polhamus formula.

$$C_{L_{\alpha_H}} = \frac{2\pi A_H}{2 + \sqrt{\frac{A_H^2 \beta^2}{K^2}\left(1 + \frac{\tan^2 \Lambda_{c/2}}{\beta^2}\right) + 4}}$$

where:

A_H is the aspect ratio of the horizontal tail

β is the compressibility correction factor $= \sqrt{1 - M^2}$ (M = Mach number)

K is the ratio for actual section lift-curve slope to 2π

For airplane A, Reference 11.10.3 presents the following values:

$\bar{V}_H$	= .630	$QH \cdot \eta_H$	= 1.0
A_W	= 5.70	$\Lambda_{c/4_W}$	= .227 rad
$\bar{c}$	= 6.896 ft.	$C_{\ell_{\alpha_W}}$	= 6.446/rad
H_x	= 20.393 ft		
A_H	= 4.0	ELCG	= 1.0
		ELWING	= 1.0
$C_{\ell_{\alpha_H}}$	= 6.02/rad	$\Lambda_{c/4}$	= 25.0 deg

(Note: The value of 1.0 is used for ELCG and ELWING because $\bar{X}_{cg}$ for the test of Reference 3 is .25. X_W becomes equal to 0.)

Furthermore, Chapter 11.2 indicates that a correction factor for lift-curve slope must be included. For A = 4.0, the correction factor is an increase of $C_{L_{\alpha_H}}$ of 6.5%, so:

$$C_{L_{\alpha_H}}{}_{Actual} = \left(C_{L_{\alpha_H}}{}_{(Polhamus)}\right)\left(1.065\right)$$

For the hand check, a HP 29C calculator was used. The Polhamus formula and the correction factor were programmed into the calculator. The results of this test, for M = 0 to M = .9, appear in Table 11.10.1.

TABLE 11.10.1 $C_{L_{\alpha_H}}$ VS. MACH NO.

Mach No.	$C_{L_{\alpha_H}}$ (rad^{-1})
.0	3.886
.1	3.986

TABLE 11.10.1 $C_{L_{\alpha_H}}$ VS. MACH NO. (continued)

Mach No.	$C_{L_{\alpha_H}}$
.3	3.980
.4	4.059
.5	4.169
.6	4.319
.7	4.523
.8	4.806
.9	5.221

Next, the equations for $C_{m_{q_{W|M=0}}}$, $C_{m_{q|M}}$, and $C_{m_{q_H}}$ were programmed into the HP-29C. These values, for different Mach numbers, appear in Table 11.10.2.

TABLE 11.10.2 $C_{m_{q_{W|M}}}$, $C_{m_{q_H}}$, and C_{m_q} vs. M

Mach No.	$C_{m_{q_{W\|M}}}$	$C_{m_{q_H}}$	C_{m_q}
.0	- .706	-14.480	-15.186
.1	- .708	-14.517	15.225
.2	- .714	-14.632	-15.346
.3	- .725	-14.830	-15.555
.4	- .740	-15.124	-15.864
.5	- .762	-15.534	-16.296
.6	- .793	-16.093	-16.886
.7	- .838	-16.853	-17.691

TABLE 11.10.2 $C_{m_{q_{W|M}}}$, $C_{m_{q_H}}$, and C_{m_q} vs. M (continued)

Mach No.	$C_{m_{q_{W\|M}}}$	$C_{m_{q_H}}$	C_{m_q}
.8	- .907	-17.908	-18.815
.9	-1.032	-19.454	-20.486

Note: All values in (rad^{-1})

11.10.3 DESCRIPTION OF PROGRAM

Table 11.10.3 presents the variables contained within the program.

TABLE 11.10.3 VARIABLE NAMES AND ORIGINS IN SUBROUTINE C_{m_q}

NAME	ENG. SYMBOL	DIMENSION	ORIGIN	REMARKS
ARW	A	---	Common	
B	B	---	---	Compressibility Correction Factor
CBAR	$\bar{c}$	ft	Common	
CLAPP	$C_{\ell_{\alpha_H}}$	rad^{-1}	Common	
CMQ	C_{m_q}	rad^{-1}	---	
CMQ	$C_{m_{q_{W\|M}}}$	rad^{-1}	---	Dummy
CMQWM0	$C_{m_{q_{W\|M=0}}}$	rad^{-1}	---	Dummy
CMQHM	$C_{m_{q_H}}$	rad^{-1}	---	Dummy
DLMC4	$\Lambda_{c/4}$	rad	Common	

TABLE 11.10.3 VARIABLE NAMES AND ORIGINS IN SUBROUTINE C_{m_q} (continued)

NAME	ENG. SYMBOL	DIMENSION	ORIGIN	REMARKS
ELCG	---	ft	Call Subroutine	
ELWING	---	ft	Call Subroutine	Dummy
EM	M	---	Common	
HX	ℓ_n	ft	Common	
SLOPEH	$C_{L_{\alpha_H}}$	rad^{-1}	Common	
QHQI	η_H	---	Common	
VBARHX	$\bar{V}_H$	---	Common	
XW	X_W	ft	---	Dummy

Figure 11.10.2 shows a flowchart of the program, a listing and sample output is shown in figure 11.10.3.

The difference between the computer generated value of C_{m_q} and the value from the handcalculation is 3% for airplane C. Reference 11.10.2 presents a test value of

$$C_{m_q} = -13.76 \quad rad^{-1}$$

Since the subroutine does not compute the body effect, this should be subtracted from above test value to yield:

$$C_{m_q} = -13.76 + .136$$
$$= -13.624 \quad rad^{-1}$$

This indicates an error of 1.4% as compared to the subroutine generated value.

For airplane A the handcalculation and the computer results are off by .8%. Reference 11.10.3 provides test data. These data and the computer results are

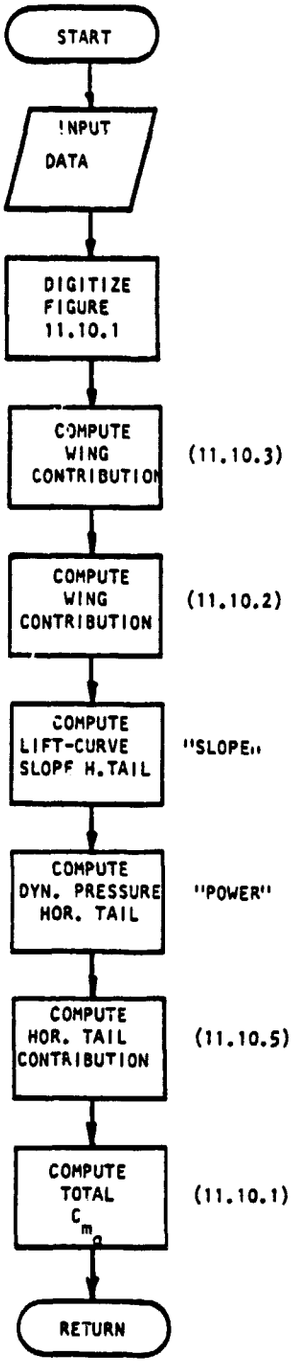

Figure 11.10.2: Flowchart for subroutine "CMQUE"

```
C     SUBROUTINE CMQUE
C*****                                                        ******
C*****  THIS SUBROUTINE COMPUTES CMQ , VARIATION OF          ******
C*****  PITCH DAMPING COEFFICIENT WITH PITCH RATE            ******
C*****                                                        ******
      REAL K
      COMMON/WING/DLMC4,AR,SLM,T,CRCLW,CBARW,SW,CLAWP
      COMMON/HORIZ/DLMC4H,ARH,SLMH,EMT,CBARHT,SHT,CLAHP,CRCLHT
      COMMON/FLITE/ALPHA,EM,CL
      COMMON/FUS/ELF,DFUS,WC,WC,LF,ELTH,HH,SC,RDI,LV,ZV
      RLMC4=DLMC4*.0174533
      IF(AR.LT.6.) K=.7
      IF(AR.GE.10.) K=.9
      IF(AR.GE.6..AND.AR.LT.6.4) K=.0037*AR+.6502
      IF(AR.GE.6.4.AND.AR.LT.7.2) K=.033*AR+.405
      IF(AR.GE.7.2.AND.AR.LT.7.7) K=.06*AR+.141
      IF(AR.GE.7.7.AND.AR.LT.8.2) K=.106*AR-.272
      IF(AR.GE.8.2.AND.AR.LT.9.0) K=.07*AR+.259
      IF(AR.GE.9.0.AND.AR.LT.9.4) K=.0317*AR+.505
      IF(AR.GE.9.4.AND.AR.LT.10.) K=.051*AR+.5
      TAN=SIN(RLMC4)/COS(RLMC4)
      CALL SIZE (ELWING,ELCG)
      XW=ELWING-ELCG
      CMQWNG=(((AR*(2.*(XW/CBARW)**2+.5*(XW/CBARW)))/(AR+2.*COS
     1(RLMC4)))+(1./24.)*(AR**3*TAN**2)/(AR+6.*COS(RLMC4
     2))+.125)*COS(RLMC4)*CLAWF*(-K)
      B=SQRT(1.-(EM*COS(RLMC4))**2)
      CMQWH=((((AR**3*TAN**2)/(AR*B+6.*COS(RLMC4)))+3./B)/
     1(((AR**3*TAN**2)/(AR+6.*COS(RLMC4)))+3.))*CMQWNG
      SLOPEH=SLOPE(DLMC4H,SLMH,ARH,EM,CLAHP)
      CALL POWER
      VBARHX=(SHT/SW)*(ELTH/CBARW)
      CMQH=-(2.*SLOPEH*GHOI*VBARHX*HX/CBARW)
      CMQ=CMQWN+CMQH
      WRITE(6,2) CMQ
    2 FORMAT(10X,"CMQ = ",F7.3," PER RADIAN"//)
      RETURN
      END
```

```
 M = 0.          CMQ = -15.210 PER RADIAN
 M = 0.10        CMQ = -15.352 PER RADIAN
 M = 0.20        CMQ = -15.482 PER RADIAN
 M = 0.30        CMQ = -15.604 PER RADIAN
 M = 0.40        CMQ = -16.002 PER RADIAN
 M = 0.50        CMQ = -16.447 PER RADIAN
 M = 0.60        CMQ = -17.046 PER RADIAN
 M = 0.70        CMQ = -17.963 PER RADIAN
 M = 0.80        CMQ = -19.013 PER RADIAN
 M = 0.90        CMQ = -20.733 PER RADIAN
```

Figure 11.10.3: Listing and sample printout for subroutine "CMQUE"

reproduced in Figure 11.10.4. The trend is correct, but the results are off by 29.9% on the average. As of this time, the reason for this error is not yet known.

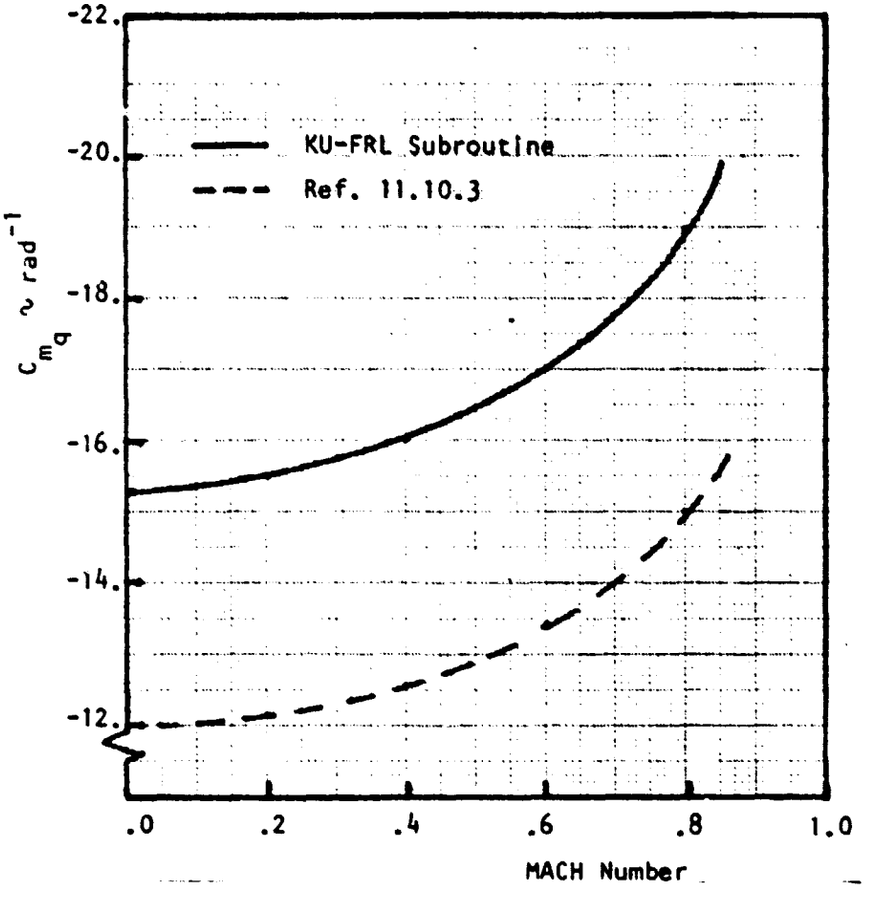

Figure 11.10.4: Results of subroutine "CMQUE"

11.10.4 REFERENCES

11.10.1 Roskam, J. Methods for Estimating Stability and Control Derivatives of Conventional and Subsonic Airplanes. Lawrence, Ks., 1977.

11.10.2 Wolowicz, C.H. & Yancey, R.B. Longitudinal Aerodynamic Characteristics of Light, Twin Engine, Propeller Driven Airplanes. NASA TN D-6800. 1972

11.10.3 Anon. Confidential Report.

11.11 $C_{D_{\dot{\alpha}}}$, VARIATION OF DRAGCOEFFICIENT WITH ANGLE OF ATTACK RATE

This derivative is usually negligible in the subsonic Machnumber range.

11.12 $C_{L_{\dot{\alpha}}}$, VARIATION OF LIFT COEFFICIENT WITH ANGLE OF ATTACK RATE

11.12.1 DERIVATION OF EQUATIONS

Reference 11.12.1 suggests that the following relation be used to estimate $C_{L_{\dot{\alpha}}}$:

$$C_{L_{\dot{\alpha}}} = C_{L_{\dot{\alpha}_W}} + C_{L_{\dot{\alpha}_H}} \quad (\text{rad}^{-1}) \tag{11.12.1}$$

where:

$$C_{L_{\dot{\alpha}_W}} = \left[1.5\left(\frac{X_{ac_W}}{C_R}\right) C_{L_{\alpha_W}} + 3\, C_L(g)\right] \quad (\text{rad}^{-1}) \tag{11.12.2}$$

$$C_{L_{\dot{\alpha}_H}} = 2\, C_{L_{\alpha_H}}\, \eta_H\, \bar{V}_H\left(\frac{d\epsilon}{d\alpha}\right) \quad (\text{rad}^{-1}) \tag{11.12.3}$$

Because the major contribution to $C_{L_{\dot{\alpha}}}$ is the $C_{L_{\dot{\alpha}_H}}$ component and because the above expression for $C_{L_{\dot{\alpha}_W}}$ is very hard to program, it is suggested to use

$$C_{L_{\dot{\alpha}}} = (1.2)\, C_{L_{\dot{\alpha}_H}} \tag{11.12.4}$$

or:

$$C_{L_{\dot{\alpha}}} = (2.4)\, C_{L_{\alpha_H}}\, \eta_H\, \bar{V}_H\left(\frac{d\epsilon}{d\alpha}\right) \quad (\text{rad}^{-1}) \tag{11.12.5}$$

11.12.2 HAND CALCULATIONS

Two tests were run, for Airplane A, at Mach = .53 and Mach = .83. Table 11.12.1 presents the required data and the $C_{L_{\dot{\alpha}}}$'s for the airplane (from References 10.12.2 and 10.12.3).

Table 11.12.1 Airplane A $C_{L_{\dot{\alpha}}}$ Tests

Test #	M	$C_{L_{\alpha_H}}$	η_H	$\bar{V}_H$	$d\varepsilon/d\alpha$	$C_{L_{\dot{\alpha}}}$
1	.53	3.512/rad	1.0	.63	.415	1.83/rad
2	.83	4.091/rad	1.0	.63	.514	2.68/rad

11.12.3 DESCRIPTION OF THE PROGRAM

The $C_{L_{\dot{\alpha}}}$ program is very straight forward, it uses eq. 11.12.1 along with the appropriate input data to compute $C_{L_{\dot{\alpha}}}$. Table 11.12.2 below is a variable list.

Table 11.12.2 - Variable List

Name	Eng. Symbol	Dimension	Origin	Remarks
CLAD	$C_{L_{\dot{\alpha}}}$	rad^{-1}	output	
SLOPEH	$C_{L_{\alpha_H}}$	rad^{-1}	common	Lift curve slope of the horiz. tail
QHQI	η_H	———	common	
VBARHX	$\bar{V}_H$	———	common	Horizontal tail volume coefficient
DEDA	$\frac{d\varepsilon}{d\alpha}$	———	common	

The $C_{L_{\dot{\alpha}}}$ subroutine flowchart is given in figure 11.12.1.

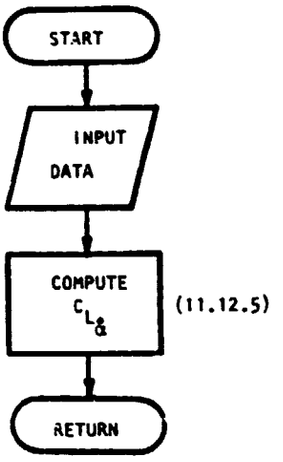

Figure 11.12.1: Flowchart for "CLAD"

A list of subroutine C_{L_α} (CLAD) is given in Figure 11.12.2, a sample printout is included.

```
1C        SUBROUTINE CLADOT (CLAD)
2CC******                                                    ******
3CC****** THIS SUBROUTINE COMPUTES CLAD, VARIATION           ******
4CC******OF LIFT COEFFICIENT WITH ANGLE OF ATTACK RATE       ******
5CC******                                                    ******
6C        COMMON/HCPZ/DLPC4H,ARH,SLPH,EHT,CEARHT,SHT,CLAHP,CRCLHT
7C        COMMON/FUS/ELF,DFUS,HC,WC,LF,ELTH,FH
8C        COMMON/WING/DLPC4,AR,SLP,E,CRCLW,CEARW,SW,CLAWP
9C        COMMON/FLITE/ALPHA,EM,CL
1CC       CALL DOWNWS (DEPDAL)
11C       SLOPEH=SLOPE(DLPC4H,SLPH,ARH,EM,CLAHP)
12CC      CALL POWER (GHGI)
13C       VBARHX=(SHT/SW)*(ELTH/CEARW)
14C       CLAD=2.4*SLOPEH*GHGI*VBARHX*DEPDAL
15C       WRITE(6,1C) CLAD
16C 1C    FORMAT(1CX,"CLAD = ",F1C.4," PER RADIAN"//)
17C       RETURN
18C       END
```

CLAD = 2.2057 PER RADIAN

Figure 11.12.2: Listing and sample printout for subroutine "CLADOT"

Two tests were run using the data given in Table 11.12.1. The results and comparisons are given below in Table 11.12.3.

Table 11.12.3- $C_{L_{\dot{\alpha}}}$ Test Results

Test #	M	$C_{L_{\dot{\alpha}}}$ (data)	$C_{L_{\dot{\alpha}}}$ (computer)	% Error
1	.53	1.83/rad	2.20/rad	20% (too big)
2	.83	2.68/rad	3.18/rad	19% (too big)

It is interesting to note that very good predictions (in these cases) could have been obtained by taking $C_{L_{\dot{\alpha}}}$ to be just the tail contribution, $C_{L_{\alpha_H}}$ instead of adding the 20%. However, two checks do not provide enough information to warrant such correction. At this time, the necessary data for more tests is not available.

11.12.4 REFERENCES

11.12.1 Roskam, J. Methods for estimating stability and control derivatives of conventional subsonic airplanes. Roskam Aviation & Engineering Corporation, Lawrence, Kansas , 1977.

11.12.2 Anon Confidential report.

11.12.3 Anon Confidential report.

11.13 $C_{m_{\dot{\alpha}}}$, VARIATION OF PITCHING MOMENT COEFFICIENT WITH ANGLE OF ATTACK RATES.

11.13.1 DERIVATION OF EQUATIONS

Reference 11.13.1 gives $C_{m_{\dot{\alpha}}}$ as:

$$C_{m_{\dot{\alpha}}} = C_{m_{\dot{\alpha}_w}} + C_{m_{\dot{\alpha}_H}} \quad (\text{rad}^{-1}) \tag{11.13.1}$$

Except for triangular wings, no explicit methods are available to estimate $C_{m_{\dot{\alpha}_w}}$. Because $C_{m_{\dot{\alpha}_w}}$ is small, it will not be used. Instead, reference 11.13.2 suggests using the tail contribution plus 20%:

$$C_{m_{\dot{\alpha}}} = (1.2)C_{m_{\dot{\alpha}_H}} \quad (\text{rad}^{-1}) \tag{11.13.2}$$

where:

$$C_{m_{\dot{\alpha}_H}} = -2C_{L_{\alpha_H}} \eta_H \bar{V}_H \frac{X_H}{\bar{c}} \left(\frac{d\epsilon}{d\alpha}\right) \quad (\text{rad}^{-1})$$

$$C_{m_{\dot{\alpha}}} = -2.4C_{L_{\alpha_H}} \eta_H \bar{V}_H \frac{X_H}{\bar{c}} \left(\frac{d\epsilon}{d\alpha}\right) \quad (\text{rad}^{-1}) \tag{11.13.3}$$

11.13.2 HAND CALCULATION

Two tests were run; for Airplane A at M = .53 and M = .83. Table 11.13.1 gives the required data and the $C_{m_{\dot{\alpha}}}$'s as listed in references 11.13.3 and 11.13.4.

Table 11.13.1 - Airplane A $C_{m_{\dot{\alpha}}}$ Data

Test #	M	$C_{L_{\alpha_H}}$	η_H	$\bar{V}_H$	$X_H/\bar{c}$	$d\epsilon/d\alpha$	$C_{m_{\dot{\alpha}}}$
1	.53	3.512/rad	1.0	.63	$\frac{20.4Ft}{6.896Ft}$	.415	-5.5/rad.
2	.83	4.091/rad	1.0	.63	2.958	.514	-6.8/rad.

11.13.3 DESCRIPTION OF THE PROGRAM

The $C_{m_{\dot{\alpha}}}$ subroutine is very basic. It computes $C_{m_{\dot{\alpha}}}$ directly from eq. 11.13.1, using the required input data. Table 11.13.2 gives the variable names. Figure 11.13.1 shows a flowchart, Figure 11.13.2 shows the listing including a sample printout.

Table 11.13.2 - Variable List

Name	Eng. Symbol	Dimension	Origin	Remarks
CMAD	$C_{m_{\dot{\alpha}}}$	rad^{-1}	---	
SLOPEH	$C_{L_{\alpha_H}}$	rad^{-1}	"LIFCRU"	
QHQI	η_H	---	Common	$\bar{q}$ wing/ $\bar{q}$ tail
VBARHX	$\bar{V}_H$	---	Common	horizontal tail volume coefficient
ELTH	l_H	Ft	common	distance from c.g. to horz. tail a.c.
CBAW	$\bar{c}_w$	Ft	Common	
DEPDAL	$d\epsilon/d\alpha$	---	"DOWNWS"	

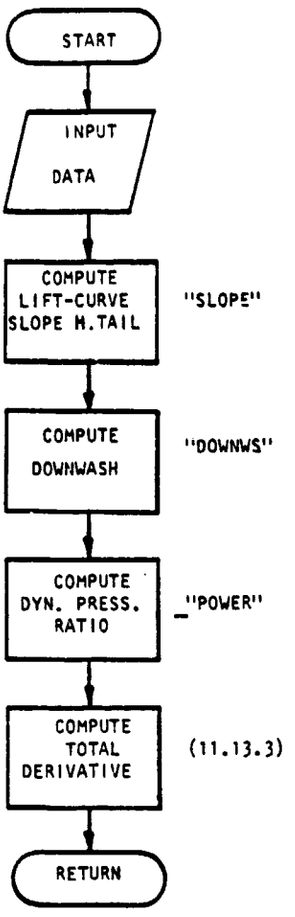

Figure 11.13.1: Flowchart for subroutine "CMADOT"

```
10          SUBROUTINE CMADOT (CMAD)
20C******                                                    ******
30C****** THIS SUBROUTINE COMPUTES VARIATION OF PITCHING ******
40C****** MOMENT WITCH ANGLE OF ATTACK RATE               ******
50C******                                                    ******
60          COMMON/WING/DLMC4,AR,SLM,B,CRCLW,CBARW,SW,CLAWP
70          COMMON/HORZ/DLMC4H,ARH,SLMH,BHT,CBARHT,SHT,CLAHP,CRCLHT
80          COMMON/FUS/ELF,DFUS,HC,WC,LN,ELTH,HH,SO,R2I,LV,ZV
90          COMMON/FLITE/ALPHA,EM,CL
100          SLOPEH=SLOPE(DLMC4H,SLMH,ARH,EM,CLAHP)
110          VBARHX=(SHT/SW)*(ELTH/CBARW)
120          CALL DOWNWS (DEPDAL)
130          CALL POWER (QHQI)
140          CMAD=-2.4*SLOPEH*QHQI*VBARHX*ELTH*DEPDAL/CBARW
150       WRITE (6,1000) CMAD
160  1000 FORMAT (10X,"CMAD = ",F10.4," PER RADIAN"//)
170         RETURN
180         END
```

```
CMAD =      -5.542 PER RADIAN
```


Figure 11.13.2: Listing and sample printout for subroutine "CMADOT"

Table 11.13.3 gives a comparison of $C_{m_{\dot{\alpha}}}$ from the computer and then using section 11.13.2.

$$\%\text{Error} = \left[\frac{C_{m_{\dot{\alpha}}}|_{\text{data}} - C_{m_{\dot{\alpha}}}|_{\text{computer}}}{C_{m_{\dot{\alpha}}}|_{\text{data}}} \right] \cdot 100$$

Table 11.13.3 - $C_{m_{\dot{\alpha}}}$ Test Results

Test #	M	$C_{m_{\dot{\alpha}}}$ (data)	$C_{m_{\dot{\alpha}}}$ (computer)	%Error
1	.53	-5.5/rad	-6.503/rad	18% (too big)
2	.83	-6.8/rad	-9.405/rad	38% (too big)

These % errors are too big, it seems that the 20% correction is not justified in this case. However, more tests should be run to find the cause of this error.

11.13.4 REFERENCES

11.13.1: Roskam, J. Methods for Estimating Stability and Control Derivatives for Conventional Subsonic Airplanes. Roskam Aviation & Engineering Corporation. Lawrence, KS. 1977

11.13.2: Roskam, J. Personal Correspondence. April 1978

11.13.3: Anon. Confidential Report.

11.13.4: Anon. Confidential Report.

11.14 VARIATION OF SIDE FORCE COEFFICIENT WITH SIDESLIP ANGLE, C_{Y_β}

11.14.1 DERIVATION OF EQUATION

This derivative can be estimated from:

$$C_{Y_\beta} = C_{Y_{\beta_W}} + C_{Y_{\beta_B}} + C_{Y_{\beta_V}} + C_{Y_{\beta_p}} \qquad (11.14.1)$$

The contribution of the wing, $C_{Y_{\beta_W}}$, is only significant in the case of nonzero dihedral angle. For modest values of wing sweep angle (up to 30 deg) the contribution due to wing sweep is negligible (according to Reference 11.14.1). Reference 11.14.2 suggests the following formula for the calculation of the wing effect:

$$C_{Y_{\beta_W}} = -.0001\ |\Gamma|\ 57.3\ (\text{rad}^{-1}) \qquad (11.14.2)$$

where: Γ is the geometric dihedral angle of the wing (in deg)

The fuselage contribution, $C_{Y_{\beta_B}}$, may be estimated from:

$$C_{Y_{\beta_B}} = -2\ K_i \left(\frac{S_0}{S}\right) \quad (\text{rad}^{-1}) \qquad (11.14.3)$$

where K_i is a wing-body interference factor, a function of wing position (high-low), maximum body height at wing body intersection, d. This parameter may be obtained from Figure 11.14.1.

S_0 is the cross-sectional area of the fuselage at the point X_0 where the flow

ceases to be potential. The distance X_0 is a function of X_1, the distance from the nose where dS_X/d_X first reaches its maximum negative value. The distance X_0 may be calculated from X_1 as follows:

$$X_0 = \ell_B \left[0.378 + 0.427 \left(\frac{X_1}{\ell_B} \right) \right] \qquad (11.14.4)$$

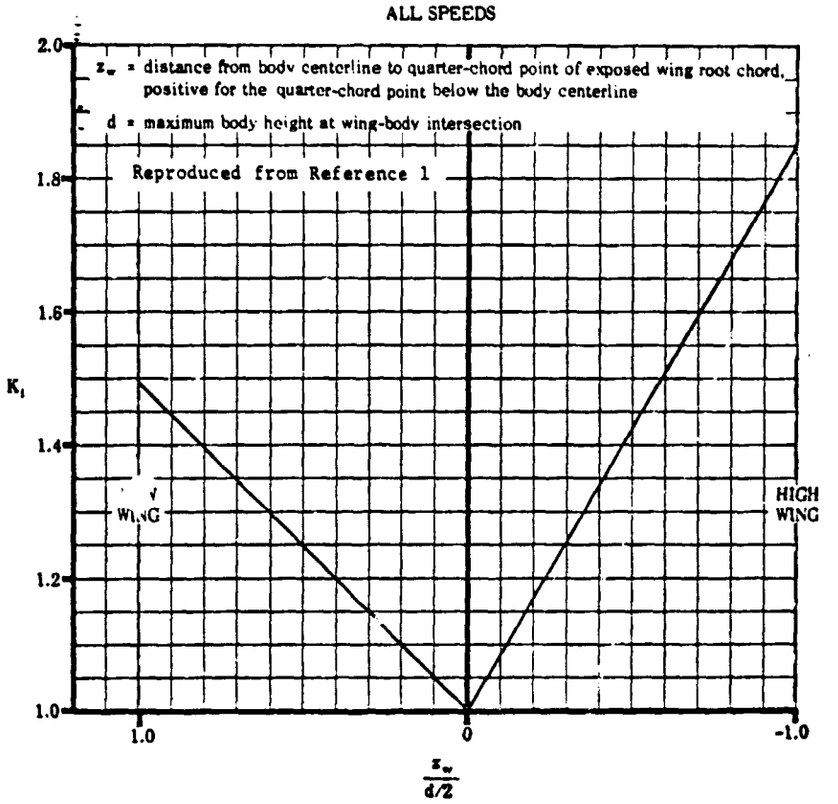

Figure 11.14.1: Wing-body interference factor for wing-body sideslip derivative C_{y_β}

In Reference 11.14.2 a program, developed by the KU-FRL, is documented that simulates the shape of an aircraft fuselage. Both the nose and the tail of the fuselage are represented by ellipses.

It is very convenient to use this program for the calculation of fuselage parameters, since it is based on mathematical methods. However, due to the nature of an ellipse, the point X_1 at which dS_X/d_X reaches its first maximum negative value will always be at the extreme end of the tail, so $X_1 = \ell_B$. In this case the value for X_D, according to Formula (11.14.4), will be:

$$X_D = 0.905\ \ell_B \tag{11.14.5}$$

This value may then be used for the computation of the cross-sectional area S_0, which can be done again by referring to the FUSE program.

The contribution for the vertical tail ($C_{Y_{\beta_V}}$), in the case of the vertical tail in the plane of symmetry, may be obtained from (Ref. 1):

$$C_{Y_{\beta_V}} = -k\ C_{L_{\alpha_V}} \left(1 + \frac{d\sigma}{d\beta}\right) \eta_V \frac{S_V}{S} \quad (\text{rad}^{-1}) \tag{11.14.6}$$

where: k is an empirical factor that takes the body influence into account, defined in Figure 11.14.2.

$\left(1 + \frac{d\sigma}{d\beta}\right)$ takes the sidewash at the vertical tail into account. This term may be obtained from (Ref. 11.14.1).

$$\left(1 + \frac{d\sigma}{d\beta}\right) = .724 + 3.06 \frac{\left(S_V/S\right)}{1 + \cos\Lambda_{c/4}} + .4 \frac{Z_W}{d} + .009\, AR_{V_{EFF}} \tag{11.14.7}$$

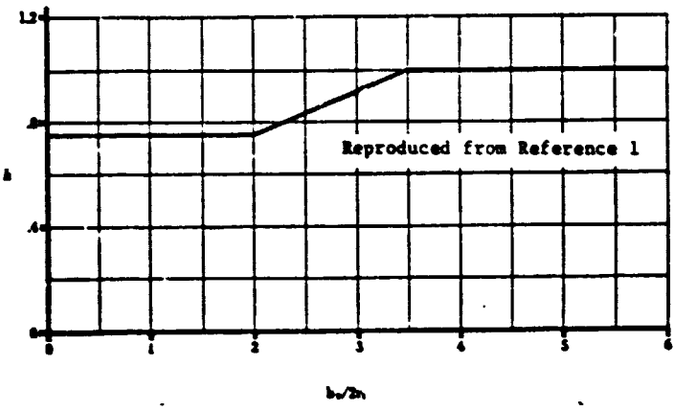

Figure 11.14.2: Empirical factor for estimating sideslip derivative for single vertical tails

is the vertical tail lift-curve slope. This variable may be obtained from the Polhamus equation (see Chapter 11.2), using the effective aspect ratio $AR_{V_{EFF}}$ i.s.o. AR_V. This effective aspect ratio may be obtained from:

$$AR_{V_{EFF}} = \frac{AR_{V(B)}}{AR_V} \; AR_V \left[1 + K_H \left(\frac{AR_{V(HB)}}{AR_V(B)} - 1 \right) \right] \qquad (11.14.8)$$

where: $AR_V = b_V^2 / S_V$ (11.14.9)

$\frac{AR_{V(B)}}{AR_V}$ is the ratio of the aspect-ratio of the vertical panel in the presence of a body to that of the isolated panel; may be found from Figure 11.14.3.

*Note: Defined in Figure 11.14.3.

$\frac{AR_{V(HB)}}{AR_{V(B)}}$ is the ratio of the vertical tail aspect ratio in the presence of the horizontal tail plus body to that of the tail in the presence of the body alone. This ratio is given in Figure 11.14.4.

K_H is a factor that takes the relative sizes of the horizontal and the vertical tail into account; given in Figure 11.14.5.

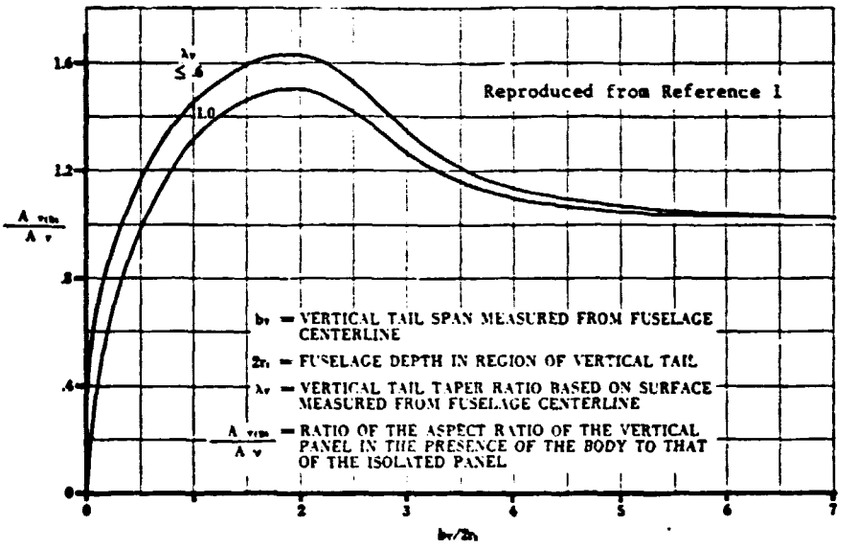

Figure 11.14.3: Effect of body interference on aspect ratio, used for estimating sideslip derivative for single vertical tails

* Note: Use the position of the vertical tail quarter chord line.

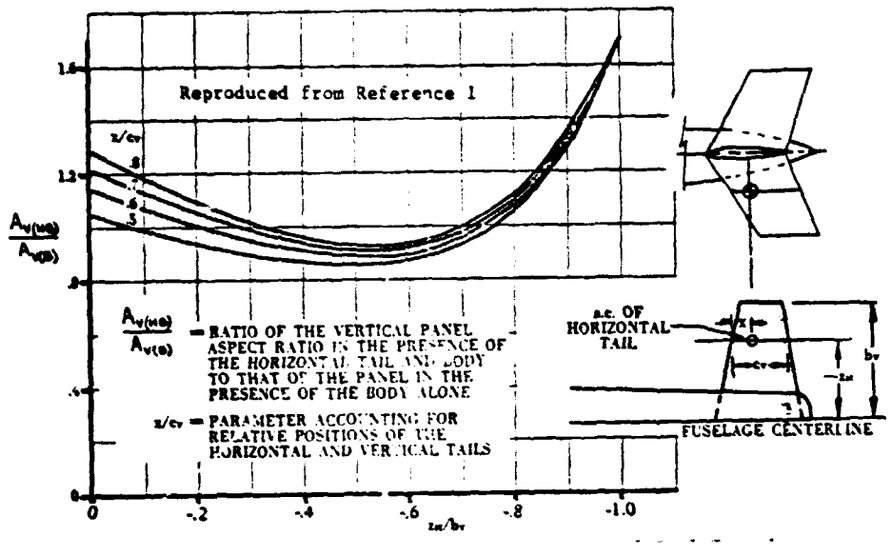

Figure 11.14.4: Effect of horizontal tail interference on aspect ratio, used for estimating the sideslip derivative for single vertical tails

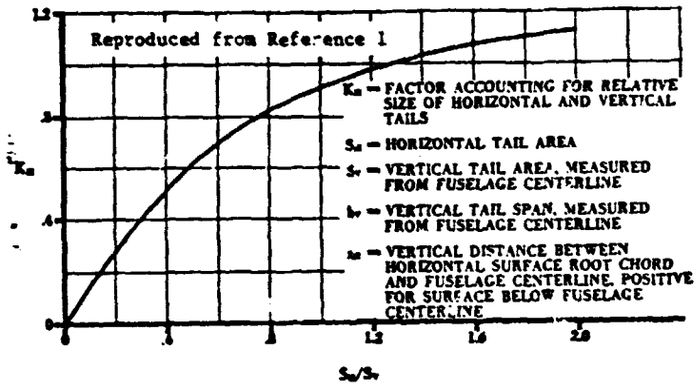

Figure 11.14.5: Factor accouting for relative size of horizontal and vertical tail

The contribution of the propeller, $C_{Y_{\beta_p}}$, may be obtained in a similar way as in Chapter 5 for the normal force of the propeller angle of attack, α_p. Reference is made to this chapter for the

derivation of the propeller normal force coefficient. The propeller angle of sideslip, β_p, is assumed to be equal to the sideslip angle β. For tractor propellers this seems to be reasonable. For pusher propellers, however, the exact angle of attack in the X-Y plane is not easy to estimate. It is conservative to assume that $C_{Y_{\beta_p}}$ is zero in this case.

During checkout of this subroutine, it was found that using Formula 11.14.5 for the calculation of the cross-sectional area at the point where the flow ceases to be potential did not produce satisfactory results. Using the cross-sectional area at the point where the cross-section decreases most rapidly produced better results. This point usually is located near the end of the cabin section. Also from an aerodynamic point of view, using this location seems more reasonable, since flow separation is likely to occur closer to this point instead of further aft. It is suggested to use a (default) value of $X_0 = .75\ \ell_B$, since this position generally fulfills above requirements. To implement the graphs used for the calculations in the computer porgram, an HP 65 calculator was used to produce the following curve fittings:

For the correction factor for wing body interference (Figure 11.14.1):

$$K_i = 1 - .85\left(\frac{Z_W}{d/2}\right) \quad \text{for } \frac{Z_W}{d/2} < 0 \tag{11.14.10}$$

$$\text{or} \quad K_i = 1 + .495\left(\frac{Z_W}{d/2}\right) \quad \text{for } \frac{Z_W}{d/2} > 0 \tag{11.14.11}$$

For the influence of body interference on aspect ratio (Figure 11.14.3):*

$$\frac{AR_{V(B)}}{AR_V} = .712 + .9031\left(\frac{b_V}{2r_i}\right) - .2371\left(\frac{b_V}{2r_i}\right)^2 \qquad (11.14.12)$$

$$\text{for} \quad \frac{b_V}{2r_i} < 3$$

or

$$\frac{AR_{V(B)}}{AR_V} = 2.0491 - .344\left(\frac{b_V}{2r_i}\right) + .0287\left(\frac{b_V}{2r_i}\right)^2 \qquad (11.14.13)$$

For the empirical factor of Figure 11.14.2:

$$\kappa = .76 \qquad \text{for } b_V/2r_i < 2 \qquad (11.14.14)$$

$$\kappa = .76 + \left(\frac{b_V}{2r_i} - 2\right).16 \qquad \text{for } 2 < b_V/2r_i < 3.5 \qquad (11.14.15)$$

$$\kappa = 1. \qquad \text{for } b_V/2r_i > 3.5 \qquad (11.14.16)$$

For the horizontal tail interference factor (Figure 11.14.4):

$$\frac{AR_{V(HB)}}{AR_{V(B)}} = \left[1.0429 + .6085\frac{Z_H}{b_V} + .4285\left(\frac{Z_H}{b_V}\right)^2\right] \left[\left(\frac{X}{c_v} - .5\right)(.73)\left(1 + \frac{Z_H}{b_V}\right)\right] \qquad (11.14.17)$$

$$\text{for} \quad \frac{Z_H}{b_V} < -.5$$

or

$$\frac{AR_{V(HB)}}{AR_{V(B)}} = \left[2.4029 + 5.4036\frac{Z_H}{b_V} + 4.6786\left(\frac{Z_H}{b_V}\right)^2\right] \left[\left(\frac{X}{c_v} - .5\right)(.73)\left(1. + \frac{Z_H}{b_V}\right)\right] \qquad (11.14.18)$$

$$\text{for} \quad \frac{Z_H}{b_V} > -.5$$

* Note: An average value of $\lambda_V = .8$ was used.

For the effect of relative size of vertical and horizontal tail:

$$K_H = .0385 + 1.2244 \frac{S_{HT}}{S_{VT}} - .3488 \left(\frac{S_{HT}}{S_{VT}}\right)^2 \qquad (11.14.19)$$

11.14.2 HAND CALCULATION

Following is a hand calculation for airplane A, data for this airplane are given in Appendix C.

From Equation (11.14.2) for the wing contribution:

$$C_{Y_{\beta_W}} = -0.01433 \ (rad^{-1})$$

From Figure 11.14.1 for $\frac{Z_W}{d/2} = 0.63$:

$$K_i = 1.32$$

From Equation (11.14.3) for the fuselage contribution:

$$C_{Y_{\beta_B}} = -0.1998 \ (rad^{-1})$$

From Figure 11.14.2 for $b_V/2r_i = 2.08$:

$$\kappa = .77$$

From Figure 11.14.3 for $b_V/2r_i = 2.08$:

$$\frac{AR_{V(B)}}{AR_V} = 1.55$$

From Figure 11.14.4 for $ZH/b_V = -1.0$:

$$\frac{AR_{V(HB)}}{AR_{V(B)}} = 1.7$$

From Figure 11.14.5 for $S_{HT}/S_{VT} = 1.41$:

$$K_H = 1.04$$

From Equation (11.14.8) now follows the effective aspect ratio:

$$AR_{V_{EFF}} = 2.10$$

For the sidewash factor Equation (11.14.7) yields:

$$\left(1 + \frac{d\sigma}{d\beta}\right) = 1.10383$$

The lift-curve slope of the vertical tail may be obtained from the (corrected) Polhamus Equation (see Chapter 11.2), using $AR_{V_{EFF}}$ instead of AR_V:

$$C_{L_{\alpha_V}} = 2.934 \ (rad^{-1})$$

From Equation (11.14.6) now follows the vertical tail contribution:

$$C_{Y_{\beta_V}} = 0.37756$$

Disregarding the effect of the engines, the total side force derivative is:

$$C_{Y_\beta} = -.5917 \ (rad^{-1})$$

This compares to a test value of:

$$C_{Y_\beta} = -.6010 \ (rad^{-1})$$

The computer calculated a value of:

$$C_{Y_\beta} = -0.5920 \ (rad^{-1})$$

The difference between the hand calculation and the computer calculation has to be attributed to errors in the curve-fitting routines.

11.14.3 PROGRAM DESCRIPTION

The computer variables as used in the program are given in table 11.14.1. A flowchart of the subroutine is given in figure 11.14.6 , a listing and a sample output are given in figure 11.14.7.

TABLE 11.14.1: VARIABLE NAMES IN SUBROUTINE "CYB"

NAME	ENG. SYMBOL	DIMENSION	ORIGIN	REMARKS
ARBOV	$\frac{AR_{V(B)}}{AR_V}$	---	---	
ARHBAV	$\frac{AR_{V(HB)}}{AR_{V(B)}}$	---	---	
ARVEFF	$AR_{V_{EFF}}$	---	---	
BVORI	$B_V/2r_i$	---	---	
BVT	b_V	ft	Common	
CBARHT	$\bar{c}_{HT}$	ft	Common	
CLALPV	$C_{L_{\alpha_V}}$	rad^{-1}	Slope Subroutine	
CRCLVT	C_{R_V}	ft	Common	
CYB	C_{Y_β}	rad^{-1}	---	
CYBB	$C_{Y_{\beta_B}}$	rad^{-1}	---	
CYBP	$C_{Y_{\beta_p}}$	rad^{-1}	Power Subroutine	
CYBV	$C_{Y_{\beta_V}}$	rad^{-1}		
CYBW	$C_{Y_{\beta_W}}$	rad^{-1}	---	

TABLE 11.14.1: VARIABLE NAMES IN SUBROUTINE "CYB" (continued)

NAME	ENG. SYMBOL	DIMENSION	ORIGIN	REMARKS
DIHD	Γ	deg	Common	
ELF	ℓ_B	ft	Common	
EL2RI	X_{2r_i}	ft	Fuse Subroutine	
ELINC	---	ft	Common	
ETAHVT	η_V	---	Power Subroutine	
FACT	---	---	---	
HC	H_C or D	ft	Common	
KBODY	κ	---	---	
KH	K_H	---	---	
KI	K_i	---	---	
R2I	r_{2_i}	ft	Fuse Subroutine	
SAH	---	---	Common	
SHT	S_H	ft^2	Common	
SIGOBE	$(1 + \frac{d\sigma}{d\beta})$	---	---	
S0	S_0	ft^2	Fuse Subroutine	
SVT	S_V	ft^2	Common	
SW	S	ft^2	Common	
SWPQC	$\Lambda_{1/4\bar{c}}$	rad	Common	
X	X	ft	---	
X0	X_0	ft	---	$.75 \cdot \ell_B$

TABLE 11.14.1: VARIABLE NAMES IN SUBROUTINE "CYB" (continued)

NAME	ENG. SYMBOL	DIMENSION	ORIGIN	REMARKS
XHMAC	---	ft	Common	
ZW	Z_W	ft	Common	
ZWOD2	$\frac{Z_W}{d/2}$	---	---	

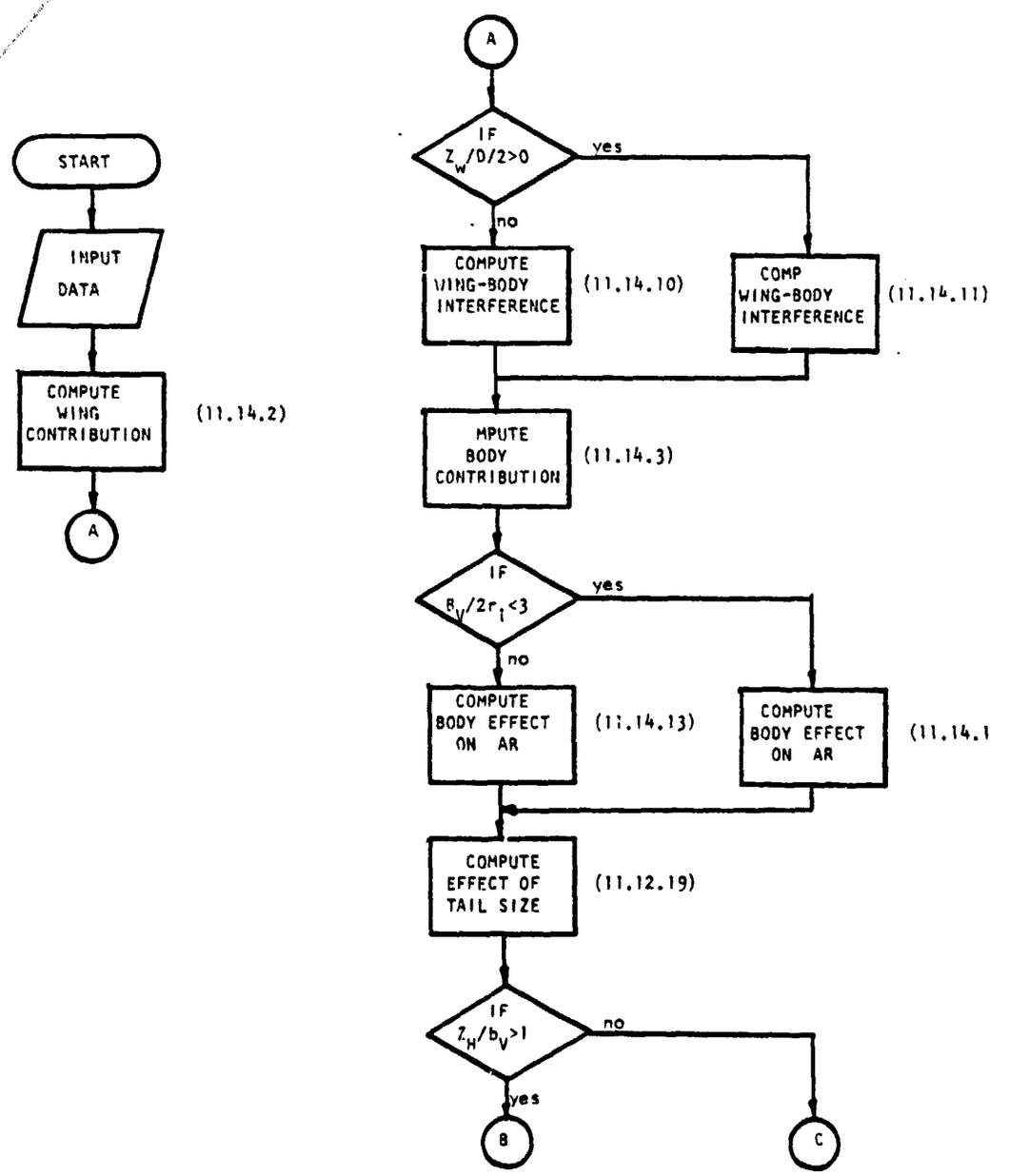

Figure 11.14.6: Flowchart for subroutine "CYBETA"

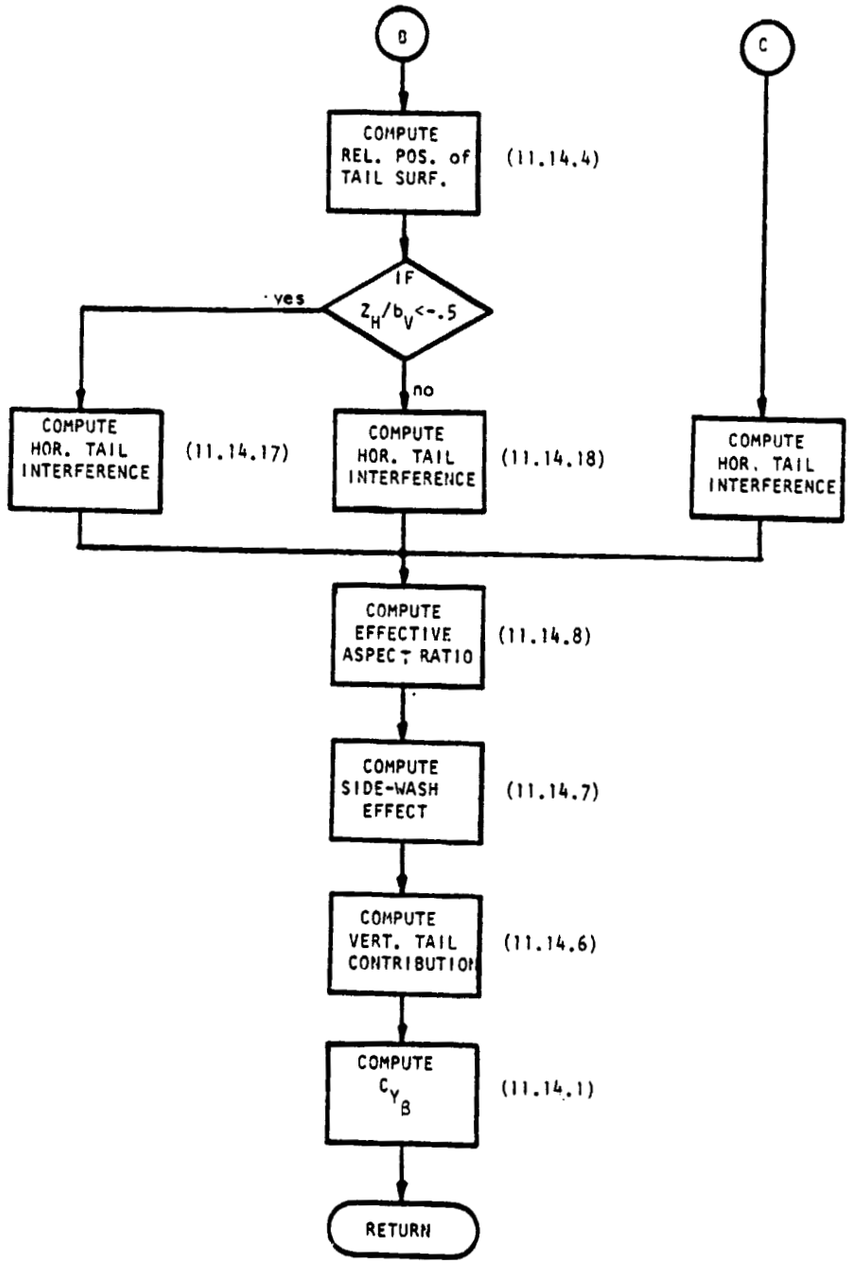

Figure 11.14.6: continued

```
      SUBROUTINE CYBETA (CYB,CYBV,ARVEFF)
      COMMON/WING/DLMC4,ARW,SLMW,EW,CLAWF,CRCLWT
      COMMON/HORZ/DLMC4H,ARH,SLMH,EHT,CLAHF,CRCLHT
      COMMON/FLITE/ALPHA,CL
      COMMON/AERO/EM,FMC,TAS
      COMMON/VERT/DLMC4V,ARV,SLMV,EVT,CLAVF,CRCLVT
      COMMON/GEOM/DIHD,ZW,SAH,XHAC,ELINC
      COMMON/FUS/FLF,DFUS,HC,WC,LF,ELTH,HF,SC,RZI,LV,ZV
      COMMON/POWER/ETAHVT,CYBP
      DATA ETAHVT,CYBP/1.,0./
       REAL K1,KBODY,KH,LB,LV
       CYBV=-.0873*ABS(DIHD)
       ZWOC=ZW/(WC/2.)
       IF (ZWOC.GE.1.) GOTO 10
       K1=1.-.5*ZWOC
       GOTO 20
   10   K1=1.+.495*ZWOC
   20   CONTINUE
       IF (XC.EQ.0.) XC=.75*ELF
       CYBB=-2.*K1*(SC/SW)
       ELBR1=ELF-.75*CRCLVT
       EVORI=EVT/RZI
       IF (EVORI.LE.0.) GOTO 30
       AREQV=2.0491-.344*(EVORI)+.0207*(EVORI**2.)
       GOTO 40
   30  AREQV=.712+.9001*EVORI-.2771*(EVORI**2.)
   40  CONTINUE
       KH=.0005+1.2044*(SHT/SVT)-.3486*(SHT/SVT)**2
       IF (SAH.LT.1.) GOTO 45
       ARHEAV=1.7
       GOTO 60
   45  X=XHAC+.25*CBARHT+ELINC
       FACT=((X/CRCLVT-.5)*.75)*(1.+SAH)
       IF (SAH.LE.-.5) GOTO 50
       ARHEAV=(2.4029+5.4036*SAH+4.6706*SAH**2.)*FACT
       GOTO 60
   50  ARHEAV=(1.0429+.6005*SAH+.4285*SAH**2.)*FACT
   60  CONTINUE
       ARVEFF=AREQV*(EVT**2./SVT)*(1.+KH*(ARHEAV-1.))
       CLALPV=SLOPE (DLMC4V,SLMV,ARV,EM,CLAVP)
       RLMC4=ATAN(SIN(DLMC4V)/COS(DLMC4V)+(1./ARV)*((1-SLMV)/(1.+SLMV)))
       SIGBEE=.724+3.06*((SVT/SW)/(1.+COS(RLMC4)))+.4*ZW/HC+
      3.009*ARVEFF
       IF (EVORI.LE.2.) KBODY=.76
       IF (EVORI.GT.2..AND.EVORI.LT.3.5) KBODY=.76+(EVORI-2.)*.16
       IF (EVORI.GE.3.5) KBODY=1.
       CYBV=-KBODY*CLALPV*SIGBEE*(SVT/SW)*ETAHVT
       CYB=CYBV+CYBB+CYBV+CYBP
         WRITE (6,1000)
       WRITE (6,1010) ARVEFF
          WRITE (6,1110)CYBV
```


Figure 11.14.7: Listing of subroutine "CYBETA"

```
C
      WRITE(2,1100)
1000  FORMAT (10X,"***KU-FRL DEVELOPED SUBROUTINE: CYB***"///)
1010  FORMAT (10X,"CYBW    =     ",1PE10.3/)
1020  FORMAT(10X,"ARVEFF  =     ",1PE10.3/)
1030  FORMAT (10X,"CYB     =     ",1PE10.3/)
1100  FORMAT (10X,"***END OF SUBROUTINE***"///)
      RETURN
      END
```

```
***KU-FRL DEVELOPED SUBROUTINE: CYB***

---TESTRUN FOR LEARJET MODEL 26---

CYBW    =      -0.014325
CYBB    =      -0.198978
ARVEFF  =       2.144245
CYBV    =      -0.378734
CYB     =      -0.592037
***END OF SUBROUTINE***
```

Figure 11.14.7: continued

11.14.4 REFERENCES

11.14.1 Roskam, J. — Methods for estimating Stability and Control Characteristics of Conventional Subsonic Airplanes, Roskam Aviation & Engineering Corporation, Lawrence,KS, 1977.

11.14.2 Hoak, D.E. & Ellison, D.E. — USAF Stability and Control DATCOM; Flight Control Division; Air Force Flight Dynamics Laboratory, Wright Patterson Air Force Base, Ohio, 45433.

11.15 C_{ℓ_β}, VARIATION OF ROLLING MOMENT COEFFICIENT WITH SIDESLIP ANGLE

11.15.1 DERIVATION OF EQUATIONS

Reference 1 presents the method used for calculating C_{ℓ_β}. C_{ℓ_β} may be estimated from three contributions: the wing, the horizontal tail, and the vertical tail contributions.

$$C_{\ell_\beta} = C_{\ell_{\beta_{WB}}} + C_{\ell_{\beta_H}} + C_{\ell_{\beta_V}} \tag{11.15.1}$$

The wing body contribution is found from:

$$C_{\ell_{\beta_{WB}}} = 57.3 \left[C_{L_{WB}} \left(\frac{C_{\ell_\beta}}{C_L} \right)_{\Lambda_{c/2}} K_{M_\Lambda} K_F + \left(\frac{C_{\ell_\beta}}{C_L} \right)_A + \Gamma \left(\frac{C_{\ell_\beta}}{\Gamma} K_{M_\Gamma} + \frac{\Delta C_{\ell_\beta}}{\Gamma} \right) + (C_\ell)_{ZW} + \Theta \tan \Lambda_{c/4} \left(\frac{\Delta C_{\ell_\beta}}{\Theta \tan \Lambda_{c/4}} \right) \right] \quad (\text{rad}^{-1}) \tag{11.15.2}$$

where:

$C_{L_{WB}} \approx C_L$ is the steady state lift coefficient.

$\left(\frac{C_{\ell_\beta}}{C_L} \right)_{\Lambda_{c/2}}$ is the wing sweep contribution obtained from Figure 11.15.1.

K_{M_Λ} is the compressibility (Mach number) correction to sweep obtained from Figure 11.15.2)

K_F is a fuselage correction factor obtained from Figure 11.15.3

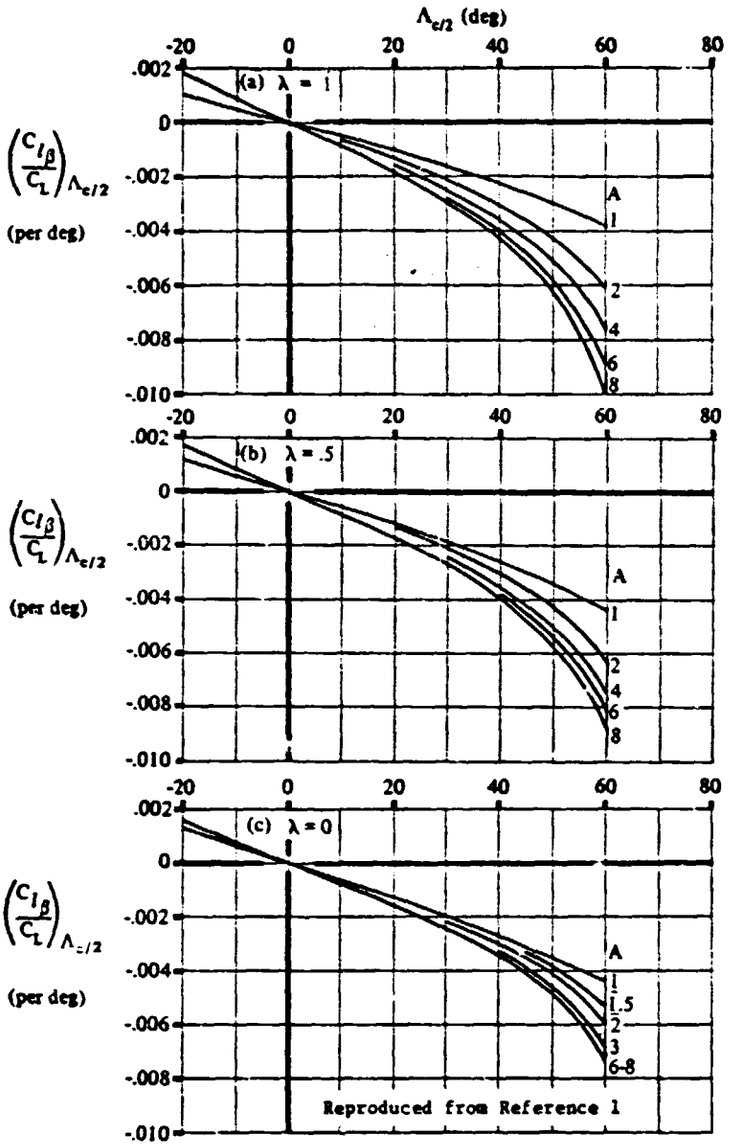

Figure 11.15.1: Wing Sweep Contribution to C_{l_β}

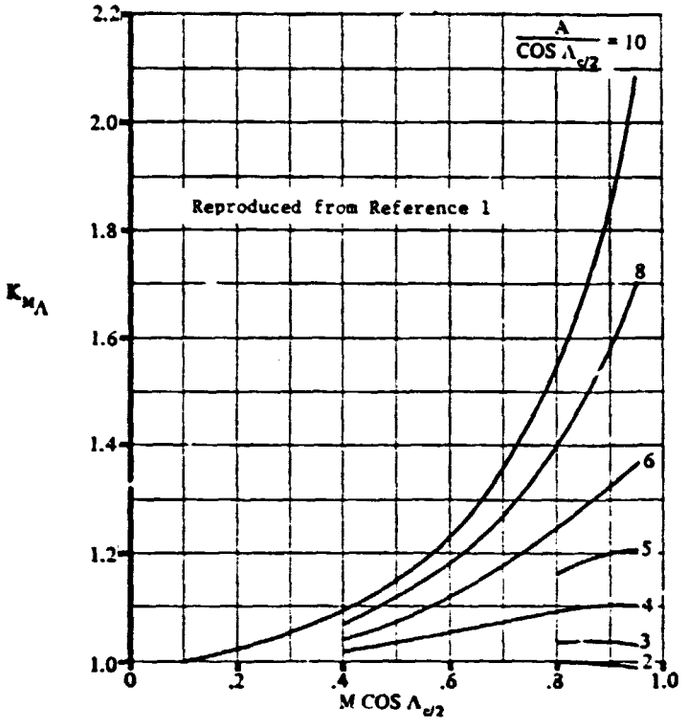

Figure 11.15.2: Compressibility Correction Factor to Sweep Contribution to Wing C_{L_β}

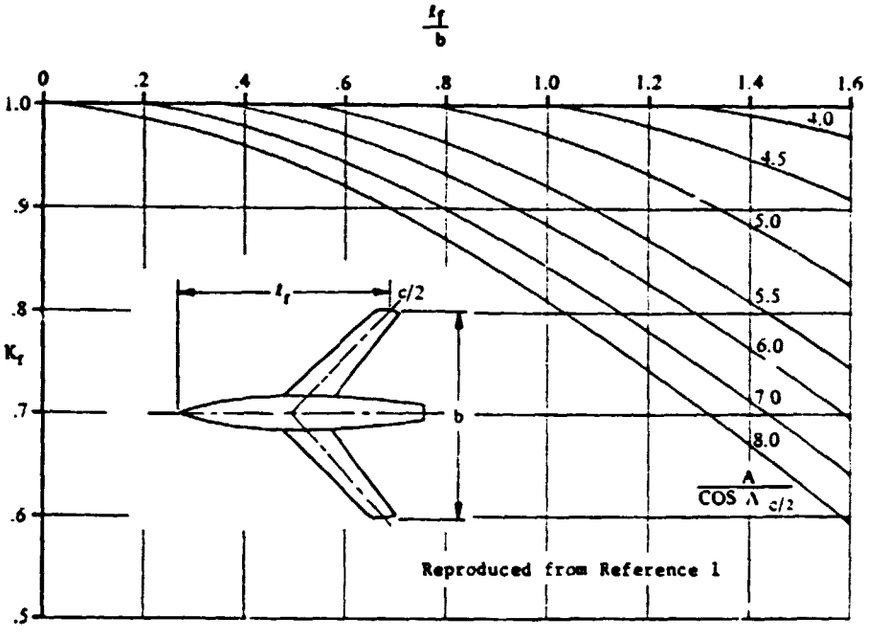

Figure 11.15.3: Fuselage Correction Factor

$\frac{C_{\ell_\beta}}{C_L}_A$ is the aspect ratio contribution obtained from Figure 11.15.4.

Γ is the wing dihedral angle, positive up

$\frac{C_{\ell_\beta}}{\Gamma}$ is the wing dihedral effect obtained from Figure 11.15.5.

K_{M_Γ} is the compressibility correction to dihedral obtained from Figure 11.15.6.

$\frac{\Delta C_{\ell_\beta}}{\Gamma}$ is the body-induced effect on the wing height and is given by:

$$\frac{\Delta C_{\ell_\beta}}{\Gamma} = -.005\ \sqrt{A}\left(\frac{d}{b}\right)^2 \ (\text{deg}^{-2}) \qquad (11.15.3)$$

where: b is the wing span, and

d is given by:

$$d = \sqrt{\frac{\text{average fuselage cross sectional area}}{.7854}} \qquad (11.15.4)$$

$\left(\Delta C_{\ell_\beta}\right)_{ZW}$ is another body induced effect on the wing height given by:

$$\left(\Delta C_{\ell_\beta}\right)_{ZW} = -\frac{1.2\sqrt{A}}{57.3}\left(\frac{Z_W}{b}\right)\frac{2d}{b}\ (\text{deg}^{-1}) \qquad (11.15.5)$$

where: Z_W is the vertical distance from the wing root quarter chord point to the fuselage centerline, positive downward.

d is the same as in equation (11.15.4)

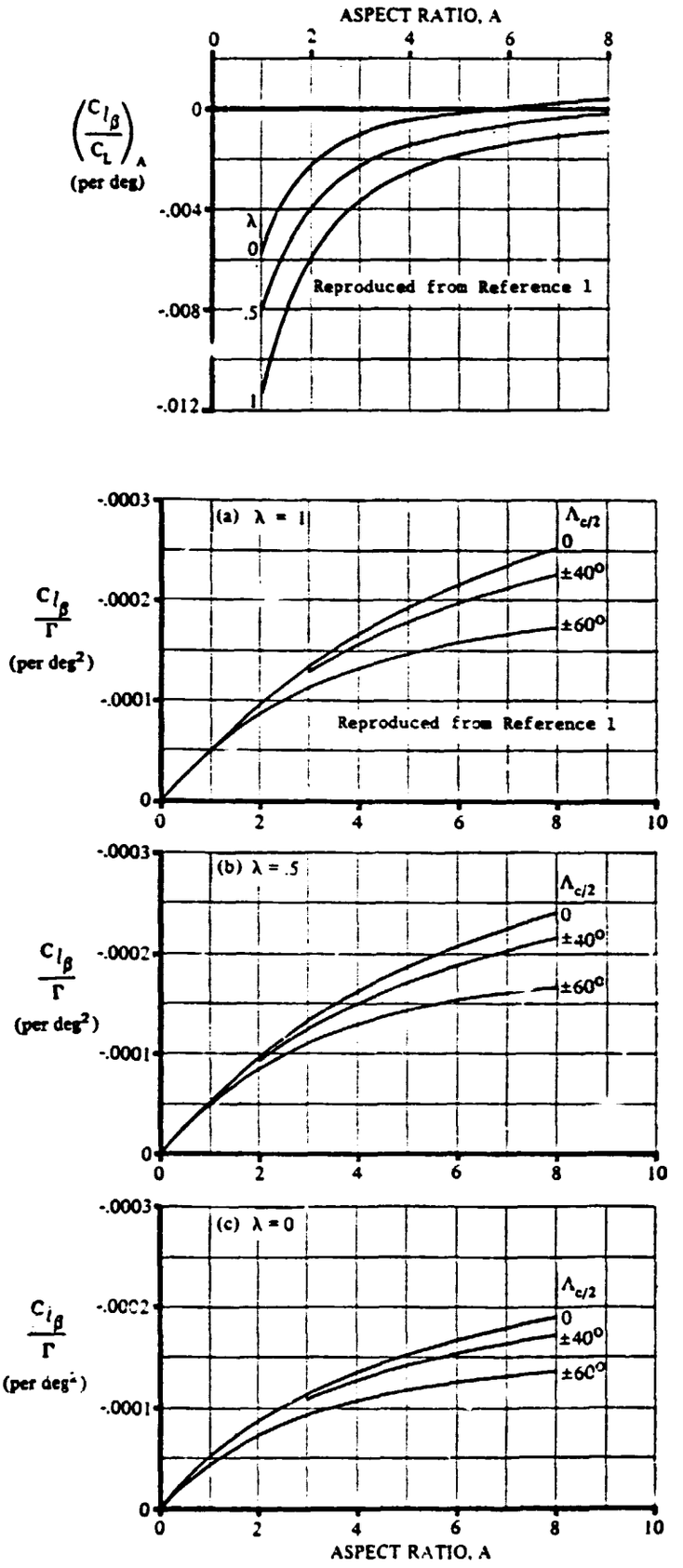

Figure 11.15.5 Effect of Uniform Geometric Dihedral on Wing C_{l_β}

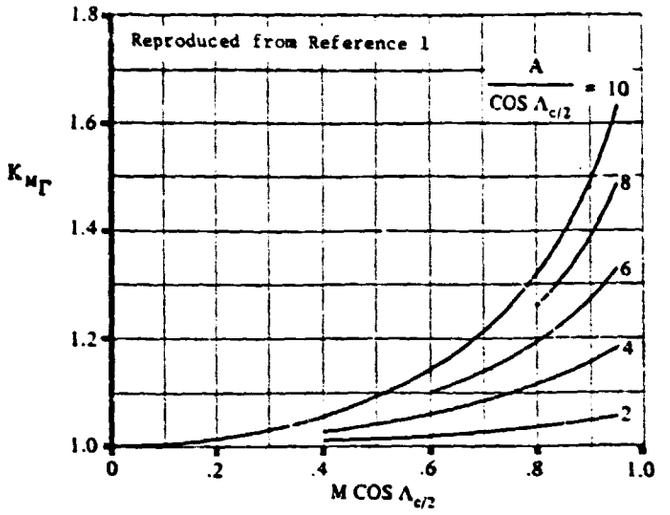

Figure 11.15.6 Compressibility Correction to Dihedral Effect on Wing C_{ℓ_β}

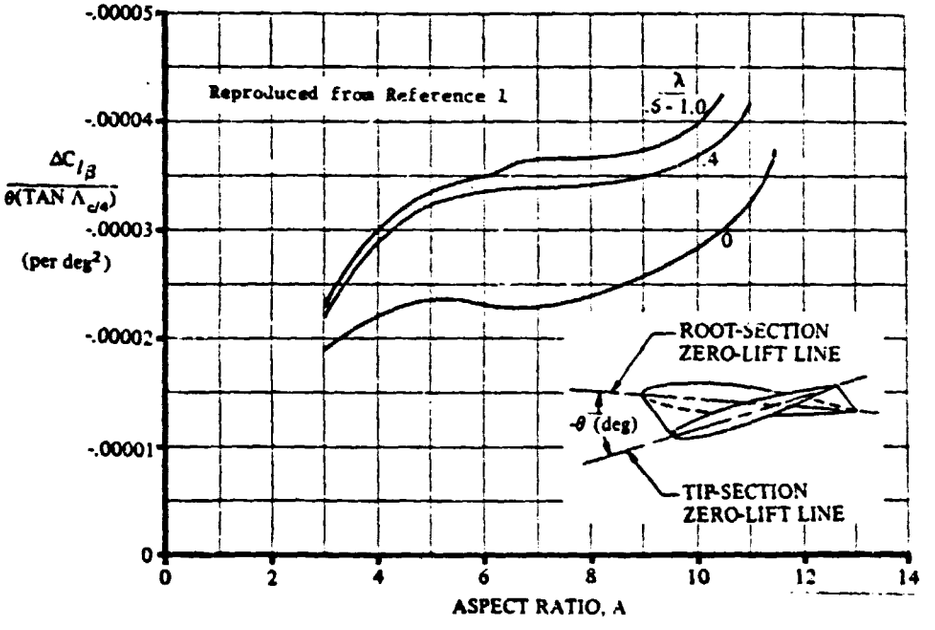

Figure 11.15.7 Effect of Wing Twist on Wing C_{ℓ_β}

$\frac{\Delta C_{\ell_\beta}}{\Theta \tan \Lambda_{c/4}}$ is a wing twist correction factor obtained from Figure 11.15.7.

Θ is the wing twist between root and tip sections, negative for washout.

The contribution of the horizontal tail, $C_{\ell_{\beta_H}}$, can be approximated by:

$$C_{\ell_{\beta_H}} = C_{\ell_{\beta_{HB}}} \frac{S_H \, b_H}{S \, b} \tag{11.15.6}$$

where:

$C_{\ell_{\beta_{HB}}}$ is found from Equation (11.15.2), treating the fuselage horizontal tail the same way (and using $C_{L_{WB}}$ = the C_L of the horizontal tail).

The contribution of the vertical tail, $C_{\ell_{\beta_V}}$, can be estimated from:

$$C_{\ell_{\beta_V}} = C_{y_{\beta_V}} \frac{(Z_V \cos\alpha - \ell_V \sin\alpha)}{b} \text{ rad}^{-1} \tag{11.15.7}$$

where:

Z_V and ℓ_V are defined in Figure 11.19.2a, and

$C_{y_{\beta_V}}$ is calculated from the methods of Section 11.14.

11.15.2 HAND CALCULATION

For the hand calculation, data for Airplane A are used. Appendix C details the geometric data.

Flight Conditions

$M = .42$

$\alpha = 10.9°$

$C_L = 1.4$

Applying these data to the previous figures, the following values are obtained:

	For the Wing:	For the Horizontal Tail:
$\frac{C_{\ell_\beta}}{C_L}_{\Lambda_{c/2}}$	$= -.00075$	$-.0015$
K_{M_Λ}	$= 1.04$	1.0025
K_F	$= .95$	$.7$ (by extrapolation)
$\frac{C_{\ell_\beta}}{C_L}_A$	$= .0077$	$-.0013$
$\frac{C_{\ell_\beta}}{\Gamma}$	$= -.00021$	$-.0016$
K_{M_Γ}	$= 1.03$	1.03
$\frac{\Delta C_{\ell_\beta}}{\theta \tan \Lambda_{c/4}}$	$= .0000345$	$-.00003$

By Equation (11.15.4), for the wing

$d = 5.25$ ft.

Then, by Equation (11.15.3):

$$\frac{\Delta C_{\ell_\beta}}{\Gamma} = -.00002 \text{ deg}^{-2}$$

$$\left(\Delta C_{\ell_\beta}\right)_{ZW} = -.00058$$

Therefore, the wing-body contribution becomes:

$$C_{\ell_{\beta_{WB}}} = -.157 \text{ rad}^{-1}$$

For the horizontal tail:

again, d = 5.25 ft

$$\frac{\Delta C_{\ell_\beta}}{\Gamma} = -.00013$$

For the horizontal tail on the airplane, $\left(\Delta C_{\ell_\beta}\right)_{ZW}$ is not calculated (= 0) because the tail is detached from the fuselage and not affected by body influences.

C_{L_H}, from Reference 2, for the given flight condition is:

$$C_{L_H} = .192$$

$$C_{L_{H_B}} = -.0259$$

Therefore:

$$C_{\ell_{\beta_H}} = -.00213 \text{ (rad}^{-1})$$

For the vertical tail, from Section11.14, under the same flight conditions,

$$C_{y_{\beta_V}} = -.168 \text{ (rad}^{-1})$$

$$C_{\ell_{\beta_V}} = -.00879 \text{ (rad}^{-1})$$

The total airplane derivative, C_{ℓ_β}, is:

$$C_{\ell_\beta} = -.1679 \text{ (rad}^{-1})$$

11.15.3 DESCRIPTION OF PROGRAM

The CLBETA subroutine comprises several functions that calculate (curve fit) the values displayed in the graphs presented earlier. The function scheme is preferred because it allows the multiple usage of each curve fit, required by $C_{\ell_{\beta_{WB}}}$ and $C_{\ell_{\beta_H}}$.

Most of the curve fits use the function RDP for determining the values, with assorted linear and nonlinear interpolations intermixed to derive the proper values. The reader is referred to the following flow chart section, and the listing of the program for calculation details (Section 11.15.5).

TABLE 11.15.1 VARIABLE LIST FOR SUBROUTINE CLBETA

NAME	ENG. SYMBOL	DIMENSION	ORIGIN	REMARKS
AFSA	---	ft^2	Common	Average Fuselage Area
ALPHA	α	deg	Common	
ALF1	ℓ_{f_W}	ft	Calculated	
ALF2	ℓ_{f_H}	ft	Calculated	
AR	A	---	Common	
ARH	A_H	---	Common	
B	b	ft	Common	
BHT	b_H	ft	Common	
CL	C_L	---	Common	
CLH	C_{L_H}	---	Common	

TABLE 11.15.1 VARIABLE LIST FOR SUBROUTINE CLBETA (continued)

NAME	ENG. SYMBOL	DIMENSION	ORIGIN	REMARKS
CLB	C_{ℓ_β}	rad^{-1}	Calculated	Output
CLBH	$C_{\ell_{\beta_H}}$	rad^{-1}	Calculated	Dummy Variable
CLBV	$C_{\ell_{\beta_V}}$	rad^{-1}	Calculated	Dummy Variable
CLBWB	$C_{\ell_{\beta_{WB}}}$	rad^{-1}	Calculated	Dummy Variable
CRCLH	C_{R_H}	ft	Common	
CRCLW	C_{R_W}	ft	Common	
CYBV	$C_{y_{\beta_V}}$	rad^{-1}	Subroutine CYB	
DIHD	Γ	deg	Common	
DIHDH	Γ_H	deg	Common	
DLMC4	$\Lambda_{c/4}$	deg	Common	
DLMC4H	$\Lambda_{c/4_H}$	deg	Common	
ELC4W	---	ft	Common	Distance from nose to L.E. C_{R_W}
ELC4H	---	ft	Common	Distance from nose to L.E. C_{R_H}
EM	M	---	Common	
LV	ℓ_V	ft	Common	

TABLE 11.15.1 VARIABLE LIST FOR SUBROUTINE CLBETA (continued)

NAME	ENG. SYMBOL	DIMENSION	ORIGIN	REMARKS
SHT	S_H	ft^2	Common	
SLM	λ	---	Common	
SLMH	λ_H	---	Common	
SW	S_W	ft^2	Common	
THETA	Θ	deg	Common	
THETAH	Θ_H	deg	Common	
ZV	Z_V	ft	Common	
ZW	Z_W	ft	Common	

Figure 11.15.8 shows a flowchart of the program, figure 11.15.9 shows a listing and a sample output of the program.

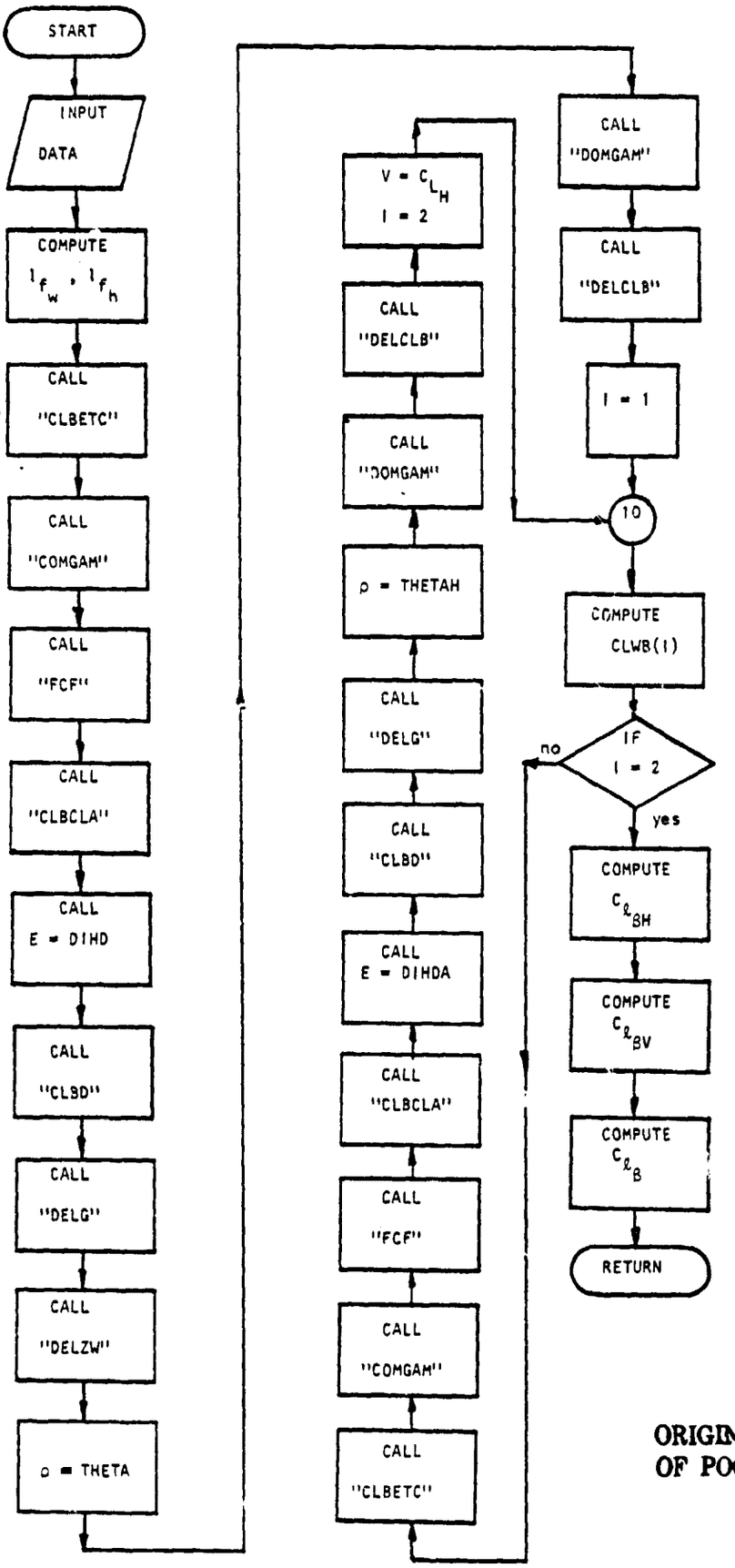

Figure 11.15.9 Flowchart for Subroutine "CLBETA"

```
10C       SUBROUTINE CLBETA(CLB)
20        COMMON /WING/ DLMC4,AR,SLM,B,CRCLW,CBARW,SW,CLAWP
30        COMMON /HORZ/ DLMC4H,ARH,SLMH,BHT,CBARHT,SHT,
40       &CLAHP,CRCLHT
50        COMMON /VERT/ DLMC4V,ARV,SLMV,BVT,CBARVT,SVT,
60       &CLAVP,CRCLVT
70        COMMON /GEOM/ DIHD,ZW,SAH,XHMAC,ELINC
80        COMMON /FUS/ ELF,DFUS,HC,WC,LN,ELTH,HH,SO,R2I,LV,ZV
90       COMMON /FLITE/ ALPHA,EM,CL
100       REAL LV,LN
110       DIMENSION CLBWB(2)
120       AFSA=21.65
130       THETA=0.
140       THETAH=0.
150       DIHDH=0.
160       ELC4W=22.85
170       ELC4H=43.59
180       CRCLH=5.
190       CLH=.178847
200       RADD4W=.017453*DLMC4
210       RADD4H=.017453*DLMC4H
220       RADD2W=ATAN(SIN(RADD4W)/COS(RADD4W)-(((1.-SLM)
230      &/(1.+SLM))/AR))
240       RADD2H=ATAN(SIN(RADD4H)/COS(RADD4H)-(((1.-SLMH)
250      &/(1.+SLMH))/ARH))
260       ALF1=(B/2.)*SIN(RADD2W)/COS(RADD2W)+CRCLW/4.+ELC4W
270       ALF2=(BHT/2.)*SIN(RADD2H)/COS(RADD2H)+CRCLH/4.+ELC4H
280       A=CLBETC(AR,RADD2W,SLM)
290       BB=COMGAM(AR,RADD2W,EM)
300       C=FCF(AR,RADD2W,ALF1,B)
310       D=CLBCLA(AR,SLM)
320       E=DIHD
330       F=CLBD(AR,RADD2W,SLM)
340       G=DELG(AR,B,AFSA)
350       H=DELZW(AR,B,ZW,AFSA)
360       P=THETA
370       R=DOMGAM(AR,EM,RADD2W)
380       Q=DELCLB(AR,SLM)
390       S=SIN(RADD4W)/COS(RADD4W)
400       V=CL
410       I=1
420       GO TO 2
430     1 A=CLBETC(ARH,RADD2H,SLMH)
440       BB=COMGAM(ARH,RADD2H,EM)
450       C=FCF(ARH,RADD2H,ALF2,BHT)
460       D=CLBCLA(ARH,SLMH)
470       E=DIHDH
480       F=CLBD(ARH,RADD2H,SLMH)
490       G=DELG(ARH,BHT,AFSA)
500       H=0.
```

Figure 11.15.9: Listing for Subroutine "CLBETA"

```
      P=THETAH
      R=DOMGAM(ARH,EM,RADD2H)
      Q=DELCLB(ARH,SLMH)
      S=SIN(RADD4H)/COS(RADD4H)
      V=CLH
      I=2
    2 CLBWB(I)=57.3*(V*(A*BB*C+D)+E*(F*R+G)+H+P*S*Q)
      IF(I.EQ.2) GO TO 3
      GO TO 1
    3 CLBH=(CLBWB(2)*SHT*BHT)/(SW*B)
      CALL CYBETA(CYB,CYBV)
      ALPHAR=ALPHA*.017453
      CLBV=CYBV*(ZV*COS(ALPHAR)-LV*SIN(ALPHAR))/B
      CLB=CLBWB(1)+CLBH+CLBV
      WRITE(6,4) CLB
    4 FORMAT(//,10X,'***KU-FRL DEVELOPED SUBROUTINE: CLBETA***',
     &//,10X,'  CLBETA  =  ',F10.5,//,10X,'***
     &**END OF SUBROUTINE*****')
      STOP
      END
C     KU FRL SUBROUTINE CLBETA
      FUNCTION CLBETC(ARW,DLMC2,TAPER)
C     CLB/CL CURVE FIT
      DIMENSION CO(3),Y(6),B(3),CLB(3)
      DLM=DLMC2*57.3
      CO(1)=(.05624+2.8456*ALOG(ARW))/6.2
      CO(2)=(.2+1.9997*ALOG(ARW))/4.35
      CO(3)=(.3671+1.3888*ALOG(ARW))/2.95
      IF(DLMC2.GT.0.0) GO TO 10
      Y(1)=-(5.25E-05*DLM)
      Y(2)=-(9.25E-05*DLM)
      Y(3)=-(6.E-05*DLM)
      Y(4)=-(9.E-05*DLM)
      Y(5)=-(6.5E-05*DLM)
      Y(6)=-(8.E-05*DLM)
      GO TO 20
   10 Y(1)=-(6.E-05+3.989E-05*DLM+3.75E-07*DLM**2)
      Y(2)=-(6.964E-05+6.403E-05*DLM+1.116E-06*DLM**2)
      Y(3)=-(6.25E-06+4.967E-05*DLM+3.795E-07*DLM**2)
      Y(4)=-(5.089E-05+5.737E-05*DLM+1.103E-06*DLM**2)
      Y(5)=-(2.669E-04+4.339E-05*DLM+4.268E-07*DLM**2)
      Y(6)=-(6.786E-05+5.746E-05*DLM+7.679E-07*DLM**2)
   20 DO 1 I=1,3
      B(I)=Y(I*2)-Y(I*2-1)
      CLB(I)=CO(I)*B(I)+Y(I*2-1)
    1 CONTINUE
      IF(TAPER.LE.1.0.AND.TAPER.GE..5)GO TO 30
      GO  TO 40
   30 CLBETC=GRAB(1.0,.5,CLB(1),CLB(2),TAPER)
      GO TO 50
```

Figure 11.15.9: Continued

```
1010    40 CLBETC=GRAB(.5,0.0,CLB(2),CLB(3),TAPER)
1020    50 RETURN
1030       END
1040       FUNCTION DOMGAM(ARW,EM,DLMC2)
1050C      KMGAMMA CURVE FIT
1060       DIMENSION XF(10),YF(5),CD(10,5)
1070       DATA YF/2.,4.,6.,8.,10./
1080       DATA CD/1.001,1.0025,1.006,1.01,1.015,1.02,1.025,1.035,
1090      &1.05,1.0575,1.002,1.005,1.012,1.025,1.0425,1.060,1.085,
1100      &1.175,1.16,1.185,1.003,1.0075,1.018,1.040,1.065,1.1,
1110      &1.145,1.195,1.275,1.33,1.004,1.01,1.024,1.045,1.08,1.1225,
1120      &1.18,1.235,1.39,1.49,1.005,1.0125,1.03,1.0505,1.095,1.145,
1130      &1.215,1.32,1.5,1.635/
1140       F=ARW/COS(DLMC2)
1150       G=EM*COS(DLMC2)
1160       DC=1.0
1170       CB=.0
1180       DO 1 I=1,9
1190       CB=CB+.1
1200       XF(I)=CB
1210     1 CONTINUE
1220       XF(10)=.95
1230       IF(F.GT.10.0) F=10.
1240       DOMGAM=RDP(1.0,F,G,1,5,10,10,DC,YF,XF,CD)
1250       RETURN
1260       END
1270       FUNCTION DELCLB(ARW,TAPER)
1280C      WASHOUT EFFECT CURVE FIT
1290       DIMENSION BC(9,4),XFT(9),YFT(4)
1300       DATA XFT/3.,4.,5.,6.,7.,8.,9.,10.,11./
1310       DATA YFT/0.,.4,.6,1.0/
1320       DATA BC/-.000019,-.000022,-.0000235,-.000023,-.000023,-.000024,-.00002575,
1330      &-.000022,-.000029,-.00003225,-.0000335,-.000034,-.00003425,-.000035,
1340      &-.000023,-.000030,-.0000335,-.000035,-.0000365,-.00003675,-.000036875,
1350      &-.000023,-.000030,-.0000335,-.000035,-.0000365,-.00003675,-.000036875,
1360       DW=1.0
1370       DELCLB=RDP(1.0,TAPER,ARW,1,4,9,9,DW,YFT,XFT,BC)      -.00002825,-.00003275,
1380       RETURN                                            -.000037,-.0000415,
1390       END                                                 -.00003975,-.000048,
1400       FUNCTION CLBCLA(ARW,TAPER)                          -.00003975,-.000048/
1410C      CLBETA/CLA CURVE FIT
1420       DIMENSION AF(8),TF(3),CC(8,3),P(1),PD2(3),CCEPT(3)
1430       DATA CCEPT/-.0011,-.00175,-.0025/
1440       DATA CC/-.0056,-.00225,-.00105,-.0004,-.00015,0.,.0003,.00053,
1450      &-.008,-.004,-.00225,-.0014,-.00095,-.0006,-.00035,-.00015,
1460      &-.0112,-.006,-.0036,-.0025,-.00175,-.0014,-.0011,-.0009/
1470       D=1.0
1480       IF(ARW.GE.8.0) GO TO 3
1490       B=0.
1500       DO 1 I=1,8
```

C.4

Figure 11.15.9: Continued

```
      B=B+1.0
      AF(I)=B
    1 CONTINUE
      B8=-.5
      DO 2 II=1,3
      B8=B8+.5
      TF(II)=B8
    2 CONTINUE
      CLBCLA=RDP(1.0,TAPER,ARW,1,3,8,8,P,TF,AF,CC)
      GO TO 7
    3 DO 4 J=1,3
      PD2(J)=.0002*ARW+CCEPT(J)
    4 CONTINUE
      IF(TAPER.GE..5.AND.TAPER.LE.1.0) GO TO 6
      CLBCLA=GUESS(TAPER,.5,.0,PD2(2),PD2(1))
      GO TO 7
    6 CLBCLA=GUESS(TAPER,1.0,.5,PD2(3),PD2(2))
    7 RETURN
      END
      FUNCTION COMGAM(ARW,DLMC2,EM)
C       KMLAMDA CURVE FIT
      DIMENSION C(18,7),ACF(7),BCF(18)
      DATA ACF/2.,3.,4.,5.,6.,8.,10./
      DATA C/1.0,1.0,1.0,1.0,1.0,1.0,1.0,1.0,1.0,
     &1.0,1.0,1.0,1.0,1.0,1.0,.995,.992,.988,
     &1.0,1.001,1.003,1.005,1.007,1.010,1.012,1.014,1.016,
     &1.018,1.025,1.03,1.033,1.034,1.035,1.035,1.035,1.03,
     &1.0,1.002,1.005,1.007,1.01,1.017,1.02,1.025,1.032,
     &1.042,1.053,1.063,1.072,1.08,1.09,1.1,1.105,1.104,
     &1.0,1.003,1.01,1.015,1.017,1.027,1.034,1.037,1.052,
     &1.067,1.085,1.1,1.125,1.135,1.16,1.182,1.2,1.207,
     &1.0,1.004,1.015,1.022,1.03,1.0375,1.042,1.052,1.073,
     &1.092,1.117,1.142,1.172,1.207,1.247,1.282,1.325,1.362,
     &1.0,1.007,1.02,1.025,1.042,1.055,1.0655,1.09,1.117,
     &1.1375,1.18,1.217,1.265,1.32,1.4,1.475,1.58,1.69,
     &1.0,1.01,1.025,1.035,1.05,1.07,1.095,1.115,1.147,
     &1.18,1.23,1.277,1.355,1.43,1.52,1.65,1.85,2.06/
      F=ARW/COS(DLMC2)
      G=EM*COS(DLMC2)
      D=1.0
      B=.05
      DO 1 I=1,18
      B=B+.05
      BCF(I)=B
    1 CONTINUE
      IF(F.GT.10.) F=10.
      COMGAM=RDP(1.0,F,G,1,7,18,18,D,ACF,BCF,C)
      RETURN
      END
      FUNCTION FCF(ARW,DLMC2,ALF,B)
```

Figure 11.15.9: Continued

```
2010C      FUSELAGE CORRECTION FACTOR
2020       DIMENSION BBB(9,7),XFB(9),YFB(7)
2030       DATA XFB/0.,.2,.4,.6,.8,1.0,1.2,1.4,1.6/
2040       DATA YFB/4.0,4.5,5.0,5.5,6.0,7.0,8.0/
2050       DATA BBB/1.0,1.0,1.0,1.0,1.0,1.0,1.0,.9902,.9696,
2060      &1.0,1.0,1.0,1.0,1.0,1.0,.9804,.9478,.9109,
2070      &1.0,1.0,1.0,1.0,.9967,.9717,.9228,.8478,.8489,
2080      &1.0,1.0,1.0,.9924,.963,.9217,.8706,.8098,.7456,
2090      &1.0,1.0,.9967,.9696,.9326,.8848,.8185,.76196,.6946,
2100      &1.0,1.0,.9783,.9435,.8989,.8446,.7804,.71196,.6402,
2110      &1.0,.986,.959,.9196,.8696,.8109,.7435,.6696,.5913/
2120       DA=1.0
2130       FUS=ALF/B
2140       F=ARW/COS(DLMC2)
2150       IF(FUS.GT.1.5) GO TO 4
2160       IF(F.GT.8.0) GO TO 1
2170       FCF=RDP(1.0,F,FUS,1,7,9,9,DA,YFB,XFB,BBB)
2180       GO TO 2
2190     1 FCFE=RDP(1.0,8.0,FUS,1,7,9,9,DA,YFB,XFB,BBB)
2200       DE=F-3.
2210       CPD=(-7.0804+112.954*ALOG(DE))/171.
2220       CF=.9696-(CPD*.3783)
2230       DF=.5913-CF
2240       FCF=FCFE-(((3.857+10.7*FUS)/21.)*DF)
2250       GO TO 2
2260     4 EX1=1.233-.4*FUS
2270       EX2=1.13-.1*FUS
2280       DED=F-3.
2290       EEX=EX2-EX1
2300       FCF=EX2-(((-7.084+112.954*ALOG(DED))/171.)*EEX)
2310     2 RETURN
2320       END
2330       FUNCTION CLBD(ARW,DLMC2,TAPER)
2340C      DIHEDRAL EFFECT
2350       DIMENSION AAA(11,2),ABA(11,2),ACA(11,2),ADF(11),D(1),PX(6),XDF(2),PT(3)
2360       DATA XDF/1.,2./
2370       DATA ADF/0.,1.,2.,3.,4.,5.,6.,7.,8.,9.,10./
2380       DATA AAA/0.,-.00005,-.000095,-.00135,-.0001675,-.0001925,
2385      &-.00215,-.0002375,-.0002523,-.00027,-.0002875,
2390      &0.,-.00005,-.000075,-.000125,-.0001352,-.0001475,-.0001875,
2395      &-.0001675,-.0001752,-.0001775-.0001825/
2400       DATA ABA/0.,-.0000525,-.0000975,-.0001325,-.0001625,-.0001875,
2405      &-.0002075,-.0002275,-.00024,-.000255,-.00027,
2410      &0.,-.00005,-.000085,-.00011,-.00013,-.0001425,-.0001525,-.00016,
2415      & -.000165,-.00017,-.0001725/
2420       DATA ACA/0.,-.0000525,-.0000875,-.000115,-.000135,
2425      &-.0001525,-.0001675,-.00018,-.00019,-.0002,-.00021,
2430      &0.,-.0000425,-.0000725,-.000095,-.0001075,-.0001175,
2435      &-.000125,-.0001325,-.0001375,-.00014,-.000145/
```

Figure 11.15.9: Continued

```
2440      DNM=DLMC2*57.3
2450      DNM=ABS(DNM)
2460      PX(1)=RDP(1.0,1.0,ARW,1,2,11,11,D,XDF,ADF,AAA)
2470      PX(2)=RDP(1.0,2.0,ARW,1,2,11,11,D,XDF,ADF,AAA)
2480      PX(3)=RDP(1.0,1.0,ARW,1,2,11,11,D,XDF,ADF,ABA)
2490      PX(4)=RDP(1.0,2.0,ARW,1,2,11,11,D,XDF,ADF,ABA)
2500      PX(5)=RDP(1.0,1.0,ARW,1,2,11,11,D,XDF,ADF,ACA)
2510      PX(6)=RDP(1.0,2.0,ARW,1,2,11,11,D,XDF,ADF,ACA)
2520      DO 3 K=1,3
2530      PT(K)=PX(K*2)-PX(K*2-1)
2540    3 CONTINUE
2550      PT(1)=((.00045*DNM**2.774)/38.5)*PT(1)+PX(1)
2560      PT(2)=((.00055*DNM**2.7095)/36.)*PT(2)+PX(3)
2570      PT(3)=((.00018*DNM**2.9069)/26.)*PT(3)+PX(5)
2580      IF(TAPER.LE..5.AND.TAPER.GE.0.) GO TO 5
2590      CLBD=GUESS(TAPER,1.0,.5,PT(1),PT(2))
2600      GO TO 6
2610    5 CLBD=GUESS(TAPER,.5,0.,PT(2),PT(3))
2620    6 RETURN
2630      END
2640      FUNCTION GRAB(A,B,C,D,X)
2650      GRAB=C-((A-X)*(C-D)/(A-B))
2660      RETURN
2670      END
2680      FUNCTION GUESS(X,Y,Z,W,U)
2690      GUESS=((X-Z)*(W-U)/(Y-Z))+U
2700      RETURN
2710      END
2720      FUNCTION DELG(ARW,B,AFSA)
2730C      DELTA CLB/GAMMA
2740      D=SQRT(AFSA/.7854)
2750      DELG=-(.0005*SQRT(ARW)*(D/B)**2)
2760      RETURN
2770      END
2780      FUNCTION DELZW(ARW,B,ZW,AFSA)
2790C      DELTA CLB/ZW
2800      D=SQRT(AFSA/.7854)
2810      DELZW=-((1.2*SQRT(ARW)/57.3)*(ZW/B)*(2.*D/B))
2820      RETURN
2830      END
```

```
***KU-FRL DEVELOPED SUBROUTINE: CLBETA***

  CLBETA  =     -0.11700

*****END OF SUBROUTINE*****
```

Figure 11.15.9: Continued

Comparison of the computer generated values with the hand calculation shows that the functions, and the total subroutine, calculate with good accuracy:

$$C_{\ell_\beta}\ \text{Hand check} = -.1679\ (\text{rad}^{-1})$$

$$C_{\ell_\beta}\ \text{Subroutine} = -.16844\ (\text{rad}^{-1})$$

The subroutine was tested for 3 flight conditions on airplane A, see Appendix C. The following table illustrates these conditions.

Table 11.15.2 Flight Conditions

Flight Condition	α (deg)	M	C_L	C_{ℓ_β} (rad^{-1})
1	11.3	.152	1.04	-.188
2	1.74	.83	.265	-.130
3	10.9	.42	.192	-.192

These flight conditions were applied to subroutine CLBETA with the following results (sample outputs).

FC	C_{ℓ_β} (rad^{-1})
1	-.16517
2	-.1170
3	-.16844

Comparison of these results with the C_{ℓ_β} values of Reference 11.15.2 (Table 11.15.2) indicate that subroutine CLBETA underpredicts by about 10% - 12%. This value is acceptable, for preliminary design purposes.

11.15.4 REFERENCES

11.15.1 Roskam, J. Methods for Estimating STability and Control Derivatives for Conventional Subsonic Airplanes. Roskam Aviation & Engineering Corporation, Lawrence, KS.1977.

11.15.2 Anon. Confidential Report.

11.16 VARIATION OF YAWING MOMENT COEFFICIENT WITH SIDESLIP ANGLE C_{n_β}

11.16.1 DERIVATION OF EQUATIONS

Reference[11.16.1] provides the following method for the calculation of this variable.

For a tail-aft configuration this derivative may be broken up in the following dontributions:

$$C_{n_\beta} = C_{n_{\beta_W}} + C_{n_{\beta_B}} + C_{n_{\beta_V}} + C_{n_{\beta_p}} \tag{11.16.1}$$

Usually, the wing contribution $C_{n_{\beta_W}}$ is small, except at high angles of attack. In that case it may be calculated using a formula from Reference 11.16.2.

Wing yawing moment derivative at low speeds:

$$\left.\frac{C_{n_{\beta_{c.r}}}}{C_L^2}\right|_{M=0} = \left[\frac{1}{4\pi AR} - \frac{\tan\Lambda_{c/4}}{\pi AR(AR + 4\cos\Lambda_{c/4})}\left(\cos\Lambda_{c/4} - \frac{AR}{2} - \frac{AR^2}{8\cos\Lambda_{c/4}} + 6\frac{\bar{X}}{\bar{c}}\frac{\sin\Lambda_{c/4}}{AR}\right)\right] \quad (\text{rad}^{-1}) \tag{11.16.2a}$$

where: $\bar{X}$ is the longitudinal distance from the center of gravity to the wing aerodynamic center, positive rearward.

At high sweep angles the above formula is no longer correct. In that case, the Prandtl-Glauert Rule may be applied to yield a correction for the first order three-dimensional effects of compressibility. The resulting expression is:

$$\left.\frac{C_{n_\beta}}{C_L^2}\right|_M = \left(\frac{AR + 4\cos\Lambda_{1/4\bar{c}}}{AR\,B + 4\cos\Lambda_{1/4\bar{c}}}\right)\left(\frac{AR^2B^2 + 4AR\,B\cos\Lambda_{1/4\bar{c}} - 8\cos^2\Lambda_{1/4\bar{c}}}{}\right)\left.\frac{C_{n_\beta}}{C_L^2}\right|_{M=0} \qquad (11.16.2b)$$

where:

$$B = \sqrt{1 - M^2\cos^2\Lambda_{c/4}} \qquad (11.16.2c)$$

The body contribution, $C_{n_{\beta_B}}$, including the interference effect of the wing on the body, may be found using:

$$C_{n_{\beta_B}} = -57.3\left[K_N\, K_{R_\ell}\left(\frac{S_{B_S}}{S}\right)\frac{\ell_B}{b}\right](\text{rad}^{-1}) \qquad (11.16.3)$$

where: K_N is an empirical factor for body and body and wing effect, found from Figure 11.16.2.

K_{R_ℓ} is a Reynolds Number correction factor for the fuselage, found from Figure 11.16.3.

S_{B_S} & ℓ_B are geometric parameters, defined in Figure 11.16.1.

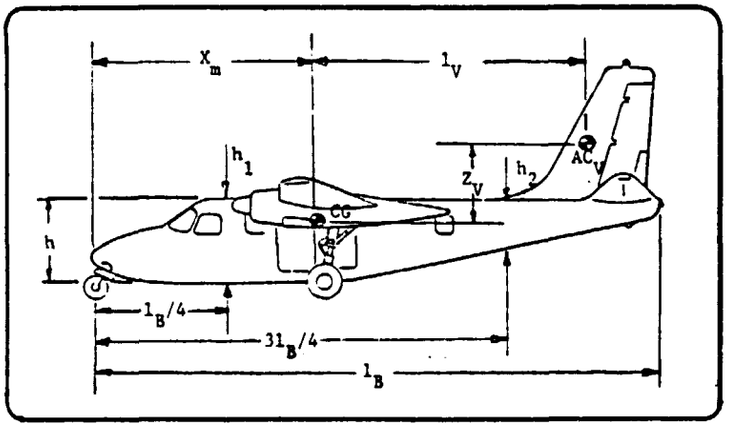

Figure 11.16.1: Definition of geometric parameters.

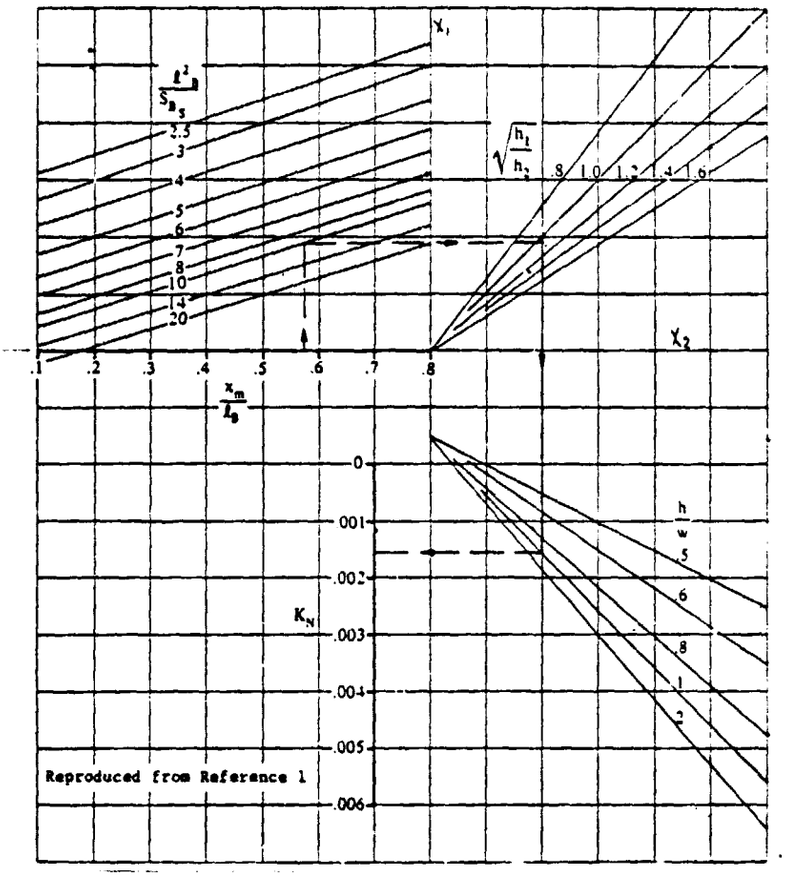

Figure 11.16.2: Empirical Factor for Wing + Wing-Body Interference

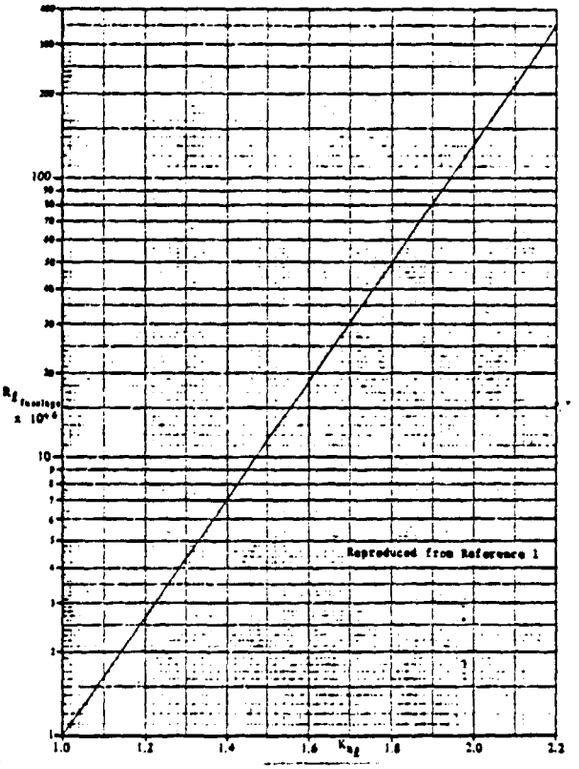

Figure 11.16.3: Effect of Fuselage Reynolds Number on Wing-Body Combinations

The vertical tail contribution, $C_{n_{\beta_V}}$, may be obtained from:

$$C_{n_{\beta_V}} = -C_{Y_{\beta_V}} \left(\frac{\ell_V \cos\alpha + Z_V \sin\alpha}{b} \right) \ (\text{rad}^{-1}) \qquad (11.16.4)$$

where:

ℓ_V and Z_V are defined in Figure 11.16.1.

The side-force derivative $C_{Y_{\beta_V}}$ may be obtained from Section 11.14.

The fuselage length, ℓ_B, is readily available in GASP. However, other fuselage parameters, like H_1, H_2 and S_{B_S} are not. The representation of the fuselage as it is in the current setup is not very realistic, and therefore the above parameters should not be derived using the GASP method. Reference 11.16.3 documents a program, developed by the K.U. Flight Research Laboratory, that provides a very realistic representation of the fuselage. This program will therefore be used to calculate the fuselage parameters.

By using HP 65 curve fitting routines, the following approximations were found for Figures 11.16.2 and 11.16.3:

$$K_N = \left[-1.0147 + 4.4649\left(\frac{H_C}{W_C}\right) - 3.3626\left(\frac{H_C}{W_C}\right)^2 + \right.$$

$$\left. + 1.0794\left(\frac{H_C}{W_C}\right)^3 - .1217\left(\frac{H_C}{W_C}\right)^4 \right] \frac{Y}{M_1} - .0005 \qquad (11.16.6)$$

where:

$$M_1 = 3.6497 - 3.5796\sqrt{\frac{H_1}{H_2}} - .39\left(\frac{H_1}{H_2}\right) +$$

$$+ 2.0149\left(\frac{H_1}{H_2}\right)^3 - .6946\left(\frac{H_1}{H_2}\right)^4 \qquad (11.16.7)$$

$$Y = 2.8333 \frac{X_{cg}}{\ell_b} - .41667 + X_1 \qquad (11.16.8)$$

$$\frac{\ell_b^2}{S_{B_S}} < 8: \qquad X_1 = 6.0942 - 1.3516 \frac{\ell_b^2}{S_{B_S}} + .13525\left(\frac{\ell_b^2}{S_{B_S}}\right)^2 - .0062\left(\frac{\ell_b^2}{S_{B_S}}\right)^3 + .001\left(\frac{\ell_b}{S_{B_S}}\right)^4 \qquad (11.16.9)$$

$$8 < \frac{\ell_b^2}{S_{B_S}} < 12: \quad X_1 = -.12 \frac{\ell_b^2}{S_{B_S}} + 1.91 \qquad (11.16.10)$$

$$\frac{\ell_b^2}{S_{B_S}} > 12: \quad X_1 = -.05875 \frac{\ell_b^2}{S_{B_S}} + 1.175 \qquad (11.16.11)$$

$$K_{R_L} = -1.830754 + .20494 \cdot LN(R_\ell) \qquad (11.16.9)$$

where: R_ℓ is the Reynolds number of the fuselage $\left(= \frac{\rho V \ell_b}{\mu}\right)$

11.16.2 HAND CALCULATION

Following is a hand calculation for Airplane *A*, using the graphs as provided in this chapter. The input data are given in Appendix C.

The wing contribution at low Mach numbers follows from Equation (11.16.20):

$$\left.\frac{C_{n_{\beta_W}}}{C_L^2}\right|_{M=0} = 0.0219 \quad (rad^{-1})$$

The compressibility correction yields:

$$C_{n_{\beta_W}}\Big|_M = 0.00732 \quad (rad^{-1})$$

From Figure 11.16.2 follows the factor K_N, using the following variables:

$$\ell^2_B/S_{B_S} = 13.3$$

$$X_m/\ell_B = 0.538$$

$$\sqrt{h_1/h_2} = 1.22$$

$$h/w = 1$$

This yields:

$$K_N = 0.00155$$

For a fuselage Reynolds number of:

$$R_{FUS} = 69.9 \times 10^6$$

It follows for the correction factor in Figure 11.16.3:

$$K_{R_L} = 1.87$$

The body contribution now follows from Equation (11.16.3):

$$C_{n_{\beta_B}} = -0.1271 \quad (rad^{-1})$$

The vertical tail contribution follows from Equation (11.16.4): (The vertical tail sideforce derivative is calculated in Chapter 11.14.)

$$C_{n_{\beta_V}} = 0.190 \ (rad^{-1})$$

Assuming that the power effect is negligible, the result is:

$$C_{n_\beta} = 0.07024 \quad (rad^{-1})$$

The computer generated a value of:

$$C_{n_\beta} = 0.06296 \quad (rad^{-1})$$

The difference is mainly attributable to an accumulation of errors in curve fittings for Figure 11.16.2. This compares to a test value of:

$$C_{n_\beta} = 0.08594 \quad (rad^{-1})$$

One of the reasons for this higher value could be the effect of the extension of the vertical tail below the fuselage. This could account for an increase of 8% in $C_{Y_{\beta_V}}$ or an increase of 21% in C_{n_β}. This would produce a value of $C_{n_\beta} = 0.0854$ (rad^{-1}) for the hand calculation. Table 11.16.1 lists the variable names in the routine.

TABLE 11.16.1: VARIABLE NAMES IN SUBROUTINE "CNB"

NAME	ENG. SYMBOL	DIMENSION	ORIGIN	REMARKS
ALPHA	α	rad	Common	
AR	AR	---	Common	
B	b	ft	Common	
BATA	β	---	---	Compressibility Correction
CBARW	$\bar{c}$	---	Common	
CL	C_L	---	Common	
CNB	C_{n_β}	rad^{-1}	---	
CNBB	$C_{n_{\beta_B}}$	rad^{-1}	---	
CNBV	$C_{n_{\beta_V}}$	rad^{-1}	---	

TABLE 11.16.1: VARIABLE NAMES IN SUBROUTINE "CNB" (continued)

NAME	ENG. SYMBOL	DIMENSION	ORIGIN	REMARKS
CNBW	$C_{n_{\beta_W}}\|_M$	rad^{-1}	---	
CNBWL	$C_{n_{\beta_W}}\|_{M=0}$	rad^{-1}	---	
CYBV	$C_{Y_{\beta_V}}$	rad^{-1}	---	
DENSIT	ρ	$lb\ sec^2/ft^4$	Common	
EKCG	X_{cg}	ft	Common	
ELF	ℓ_B	ft	Common	
ELTV	ℓ_V	ft	Common	
ELWING	X_{ac}	ft	Common	
EM	M	---	Common	
FACT1	---	---	---	
FACT2	---	---	---	
FACT3	---	---	---	
HC	H_C	ft	Common	
H1	H_1	ft	Subroutine Fuse	
H2	H_2	ft	Subroutine Fuse	
KN	K_N	---	---	
KRL	K_{RL}	---	---	
RENUMF	$R_{C_{FUS}}$	---	---	

TABLE 11.16.1: VARIABLE NAMES IN SUBROUTINE "CNB" (continued)

NAME	ENG. SYMBOL	DIMENSION	ORIGIN	REMARKS
SBS	S_{B_S}	ft^2	Subroutine Fuse	
SW	S_W	ft^2	Common	
SWPQC	$\Lambda_{1/4\bar{c}}$	rad	Common	
V	V	ft/sec	Common	
VISCOS	ν	ft^2/sec		
WC	W_C	ft	Common	
X1	X_1	---	---	
X2	X_2	---	---	
ZVT	Z_V	ft	Common	

Figure 11.16.4 shows a flowchart of the routine, figure 11.16.5 shows a listing as well as a sample printout.

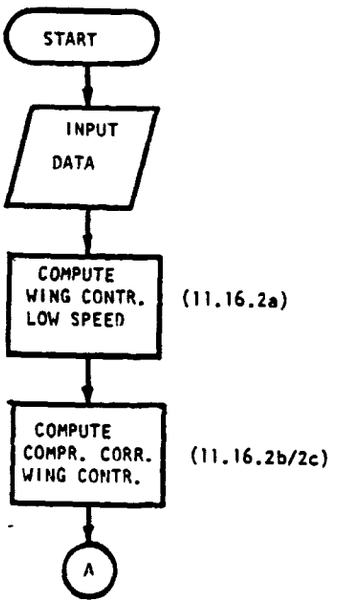

Figure 11.16.4: Flowchart of Subroutine "CNBETA"

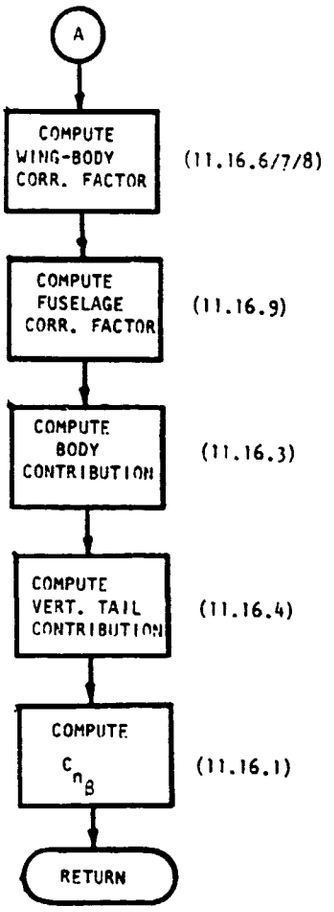

Figure 11.16.4: Continued

```
10          WRITE (6,1001)
20    1001 FORMAT (10X,"KU-FRL DEVELOPED SUBROUTINE FOR THE COMPUTATION
30         & OF CNB"///)
40C        SUBROUTINE CNB (CNB)
50         REAL KN,KRL,KA,KV,KC,KW,H1,H2,LN,LT,M1,M2
60         COMMON/WING/DLMC4,AR,SLM,B,CRCLW,CBARW,SW,CLAWP
70         COMMON/FUS/ELF,DFUS,HC,WC,LN,ELTH,HH,SO,R2I,LV,ZV
80        COMMON/FLITE/ALPHA,EM,CL
90        COMMON/SHAPE2/H1,H2,LT,PHIC1,PHIN1
100        COMMON/WEIGHT/ELCG,WEIGHT
110         CNBWL=(1./(12.566*AR)-((ATAN(SWPQC))/(3.142*
120        &AR*(AR+4.*COS(SWPQC))))*(COS(SWPQC)-.5*AR-AR**2./(8.*COS
130        &(SWPQC))+6.*((ELWING-ELCG)/CBARW)*((SIN(SWPQC))/AR)))
140         BATA=SQRT(1.-(EM**2.)*(COS(SWPQC)**2.))
150         FACT1=(AR+4.*COS(SWPQC))/(AR*BATA+4.*COS(SWPQC))
160         FACT2=((AR**2.)*(BATA**2.)+4.*AR*BATA*COS(SWPQC)-8.*(COS(SWPQC)**2.))
170         FACT3=(AR**2.+4.*AR*COS(SWPQC)-8.*(COS(SWPQC)**2.))
180         CNBW=CNBWL*(CL**2.)*FACT1*(FACT2/FACT3)
190         CALL CONPAR (PHIC1,KA,KV,KC,KW)
200         SBSU=HC*(ELF-LN-LT)
```

Figure 11.16.5: Listing and Sample Printout for Subroutine "CNBETA"

```
      IF (SBSRAT.EQ.0.) SBSRAT=.75
       SBSEC2=KA*LT*DFUS
       CALL CONPAR(PHIN1,KA,KV,KC,KW)
      SBSN=KA*LN*DFUS
      SBS=SBSRAT*SBSN+SBSU+SBSEC2
      LB2SBS=ELF**2./SBS
      IF (LB2SBS.GE.8.) GOTO 30
      SHIFT1=6.0942-1.3516*LB2SBS+.13525*LB2SBS**2.-.0062*LB2SBS**3.+
     &.0001*LB2SBS**4.
      GOTO 50
30    IF (LB2SBS.GE.12.) GOTO 40
      SHIFT1=-.12*LB2SBS+1.91
      GOTO 50
40    SHIFT1=-.05875*LB2SBS+1.175
50    CONTINUE
      YVALUE=2.8333*ELCG/ELF-.41667+SHIFT1
      H1H2=SQRT(H1/H2)
      M1=3.6497-3.5796*H1H2-.39*H1H2**2.+2.0149*H1H2**3.-.6946*H1H2**4.
      ZVALUE=YVALUE/M1
      HWRAT=HC/WC
      M2=(-1.0147+4.4649*HWRAT-3.3626*HWRAT**2.+1.0794*HWRAT**3.-.1217*
     &HWRAT**4.)*.001
      KN=M2*ZVALUE-.0005
      RENUMF=RENUM(DENSIT,VISCOS,V,ELF)
      KRL=-1.830754+.20494*ALOG(RENUMF)
      CNBB=-57.3*KN*KRL*(SBS/SW)*(ELF/B)
      CALL CYBETA (CYB,CYBV)
      CNBV=-CYBV*((ELTV*COS(ALPHA)+ZVT*SIN(ALPHA))/B)
      CNB=CNBW+CNBB+CNBV
      WRITE (6,1007) CNBV
1007  FORMAT (10X,"VERT. TAIL CONTR.=            ",1F10.5,"   /RAD"/)
      WRITE (6,1008) CNB
1008  FORMAT (10X,"TOTAL CNB        =            ",1F10.5,"   /RAD"//)
      WRITE (6,1009)
1009  FORMAT (10X,"***END OF SUBROUTINE***"///)
C     RETURN
      STOP
      END
       FUNCTION RENUM (DENSIT,VISCOS,TAS,ALNGTH)
C
C      THIS FUNCTION COMPUTES THE REYNOLDS NUMBER OF A BODY
C
       RENUM=(TAS*ALNGTH)/VISCOS
       RETURN
       END
```

Figure 11.16.5: Continued

```
660         SUBROUTINE CONPAR (PHI,KA,KV,KC,KW)
670         REAL KA,KV,KC,KW
680C
690C        THIS SUBROUTINE COMPUTES THE AREA CORRECTION FACTORS
700C        KA,KV,KC AND KW WHEN THE SHAPE PARAMETER PHI IS INPUT
710C        THIS SUBROUTINE WAS DERIVED FROM TORENBEEK PG.447
720C
730         DATA AK,AK1,AK2,AK3,AK4/-.59,3.8109,-5.721,6.4168,-2.9167/
740         DATA VK,VK1,VK2,VK3,VK4/-.9095,5.803,-13.0927,16.5927,-7.4074/
750        DATA CK,CK1,CK2,CK3,CK4/2.96,-12.0488,22.8752,-18.3335,5.5556/
760        DATA WK,WK1,WK2,WK3,WK4/-172.721,1008.8388,-2162.25,2023.9877,-69
770       &7.9097/
780         POLY(X,C,C1,C2,C3,C4)=C+C1*X+C2*X**2.+C3*X**3.+C4*X**4.
790         KA=POLY(PHI,AK,AK1,AK2,AK3,AK4)
800         KV=POLY(PHI,VK,VK1,VK2,VK3,VK4)
810         KC=POLY(PHI,CK,CK1,CK2,CK3,CK4)
820         KW=POLY(PHI,WK,WK1,WK2,WK3,WK4)
830         CONTINUE
840         RETURN
850         END
```

-FRL DEVELOPED SUBROUTINE FOR THE COMPUTATION OF CMP

TESTRUN FOR LEARJET MODEL 25

SPS	=	174.14199	SQFT
KA	=	0.00151	
KVL	=	1.07139	
SPEED	=	208.00000	FPS
WING CONTRIBUTION	=	0.00733	/RAD
BODY CONTRIBUTION	=	-0.13441	/RAD
VERT. TAIL CONTR.	=	0.19003	/RAD
TOTAL CMB	=	0.06296	/RAD

Figure 11.16.5: Continued

11.16.4 REFERENCES

11.16.1	Roskam, J.	Methods for Estimating Stability and Control Derivatives of Conventional Subsonic Airplanes, Roskam Aviation & Engineering Corporation, Lawrence, KS, 1977.
11.16.2	Hoak, D.E. & Ellison, D.E.	USAF Stability and Control Datcom; Air Force Flight Dynamics Laboratory, Wright Patterson Air Force Base, Ohio, 45433.
11.16.3	Wyatt, R.D. et al	A Study of Commuter Airplane Design Optimization, Kansas University, Flight Research Laboratory, 1977.

11.17 C_{y_p}, VARIATION OF SIDE FORCE DUE TO ROLL RATE PERTURBATIONS

11.17.1 DERIVATION OF EQUATIONS

Reference 11.7.1, page 8.1 gives C_{y_p} as:

$$C_{y_p} \simeq C_{y_{p_v}} \simeq 2\left(\frac{Z_v \cos\alpha - \ell_v \sin\alpha}{b}\right) C_{y_{\beta_v}} \quad (\text{rad}^{-1}), \tag{11.17.1}$$

$C_{y_{\beta_v}}$ is obtained from the C_{y_β} subroutine, section 11.14.

11.17.2 HAND CALCULATIONS

Three tests were set-up using Airplane A data at three angles of attack. The data are from references 11.17.2 and 11.17.3. Table 11.17.1 shows these test results.

Table 11.17.1 - C_{y_p} Tests

Test #	α	C_{y_p}
1	0	-.084/rad
2	5	-.058/rad
3	10	-.030/rad

Note: $\bar{X}_{c.g.} = .25$. Table 11.17.1 is all data, C_{y_p} was not computed from eq. 11.17.1.

11.17.3 DESCRIPTION OF THE PROGRAM

The C_{y_p} subroutine computes C_{y_p} directly from eq. 11.17.1. Except for $C_{y_{\beta_v}}$, which is obtained by calling the C_{y_β} subroutine, the data is obtained

from a common block. Table 11.17.2 is a variable list for the C_{y_p} subroutine.

Table 11.17.2 - Variable List

Name	Eng. Symbol	Dimension	Origin	Remarks
ZV	Z_v	Ft	Common	Vertical distance from c.g. to vert. tail a.c.
ZLV	L_v	Ft	Common	Horizontal distance from c.g. to vert. tail a.c.
B	b	Ft	Common	
CYBV	$C_{y_{\beta_v}}$	rad^{-1}	C_{y_β} Subroutine	Variation of Side Force due to sideslip due to vertical tail
CYP	C_{y_p}	rad^{-1}	---	

Figure 11.17.1 shows a flowchart, Figure 11.17.2 shows a listing as well as a sample output. Table 11.17.3 shows the results of several tests.

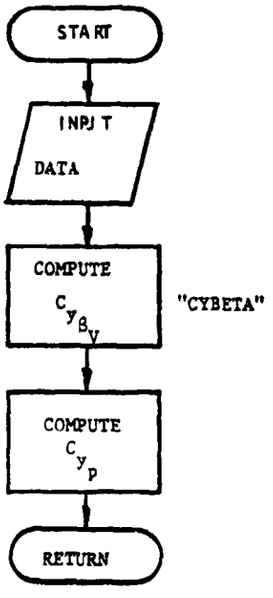

Figure 11.17.1: Flowchart for Subroutine "CYPE"

```
10          SUBROUTINE CYPE (CYP)
20          COMMON/FLITE/ALPHA,EM,CL
30          COMMON/FUS/ELF,DFUS,HC,WC,LN,ELTH,HH,SO,R2I,LV,ZV
40          CALL CYBETA (CYB,CYBV)
50          CYP=(2*CYBV/B)*(ZV*COS(ALPHA)-LV*SIN(ALPHA))
60          WRITE (6,1000) CYP
70    1000  FORMAT (10X,"CYP  = ",F10.4," PER RADIAN"//)
80          RETURN
90          END
```

```
CYP     = -0.103 PER RADIAN
```

Figure 11.17.2: Listing and Sample Printout for Subroutine "CYPE"

Table 11.17.3 C_{y_p} Tests, Airplane A

Test #	C_{y_p} (Data)	C_{y_p} (Computer)	% Error *
1	-.084/rad	-.103/rad	22.62% (too big)
2	-.058/rad	-.075/rad	29.31% (too big)
3	-.030/rad	-.045/rad	50.00% (too big)

$$* \% \text{ Error} = \left[\frac{C_{y_p}|_{data} - C_{y_p}|_{computer}}{C_{y_p}|_{data}} \right] (100)$$

The C_{y_p} subroutine method is on the right track, but more tests and refinement of the program is needed to make it more accurate.

11.17.4 REFERENCES

11.17.1 Roskam, J. Methods for Estimating Stability and Control Derivatives for Conventional Subsonic Airplanes, Roskam Aviation & Engineering Corp. Lawrence, KS, 1977.

11.17.2 Anon Confidential Report

11.17.3 Anon Confidential Report

11.18 C_{ℓ_p}, VARIATION OF ROLLING MOMENT COEFFICIENT WITH ROLL RATE PERTURBATIONS

11.18.1 DERIVATION OF EQUATIONS

According to Reference 11.8.1, C_{ℓ_p} can be estimated as follows:

$$C_{\ell_p} = C_{\ell_{p_{WB}}} + C_{\ell_{p_H}} + C_{\ell_{p_V}} \tag{11.18.1}$$

and:

$$C_{\ell_{p_{WB}}} \simeq C_{\ell_{p_W}} = \left(\frac{\beta C_{\ell_p}}{K}\right)\frac{K}{\beta} \tag{11.18.2}$$

where:

$\left(\frac{\beta C_{\ell_p}}{K}\right)$ is the roll damping parameter

$$K = \frac{C_{\ell_{\alpha_W}}\big|_{avg.}}{2\pi} \tag{11.18.2a}$$

$$\beta = \sqrt{1 - M^2} \tag{11.18.2b}$$

$\left(\frac{\beta C_{\ell_p}}{K}\right)$ is found from Reference 1, Figure 8.1. Figure 8.1 is given on the following pages as Figure 11.18.1. Use of Figure 11.18.1 is explained in Section 11.18.3.

$$C_{\ell_{p_H}} = 1/2\left(C_{\ell_p}\right)_H \frac{SH}{S}\left(\frac{bH}{b}\right)^2 \tag{11.18.3}$$

where:

$$\left(C_{\ell_p}\right)_H = \left(\frac{\beta C_{\ell_p}}{K}\right)\frac{K}{\beta} \tag{11.18.3a}$$

$\left(\frac{\beta C_{\ell_p}}{K}\right)$ is found from Figure 11.18.1 using the horizontal tail geometry.

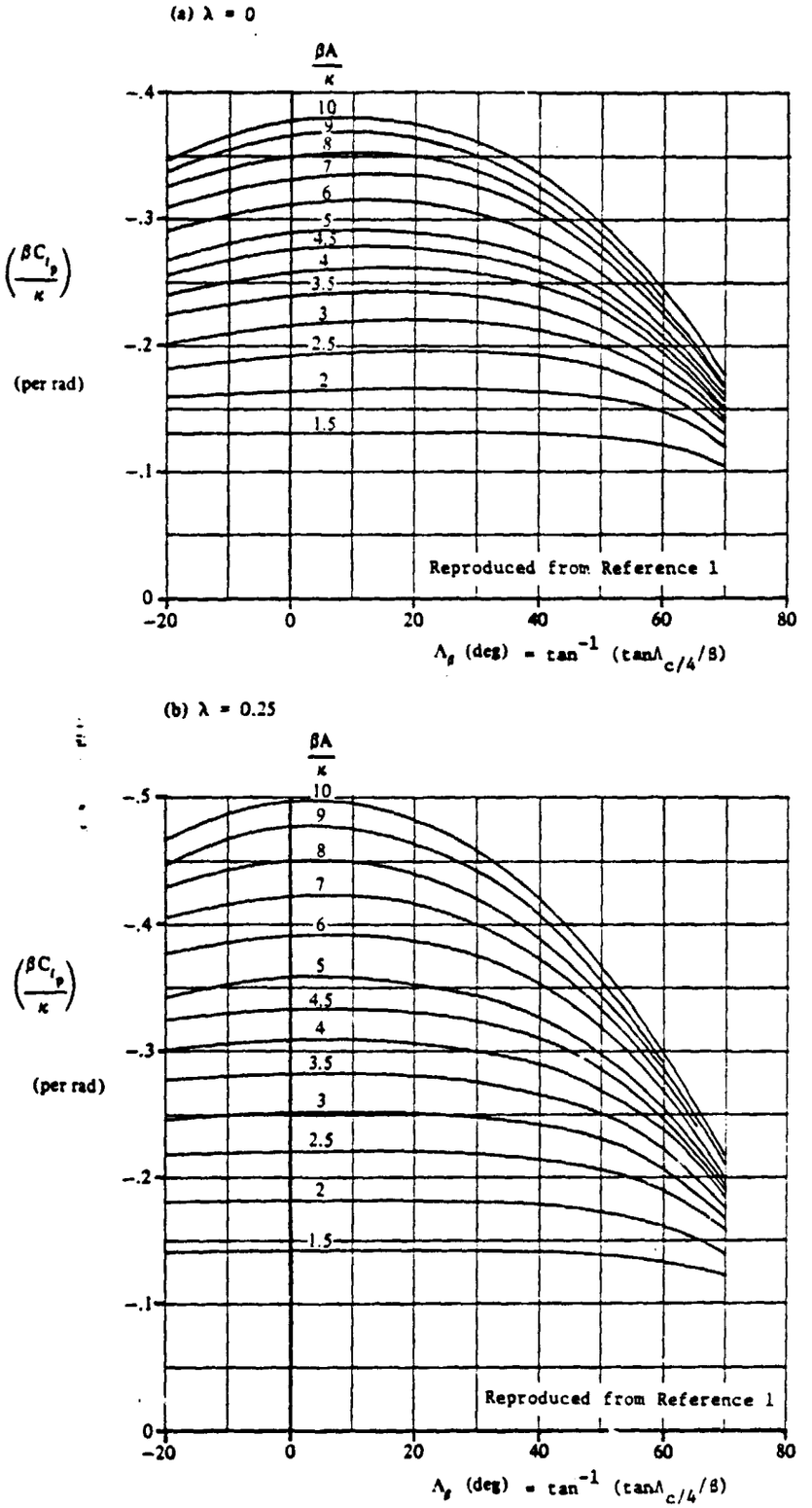

Figure 11.18.1: Roll damping parameter, used for computation of C_{ℓ_p}

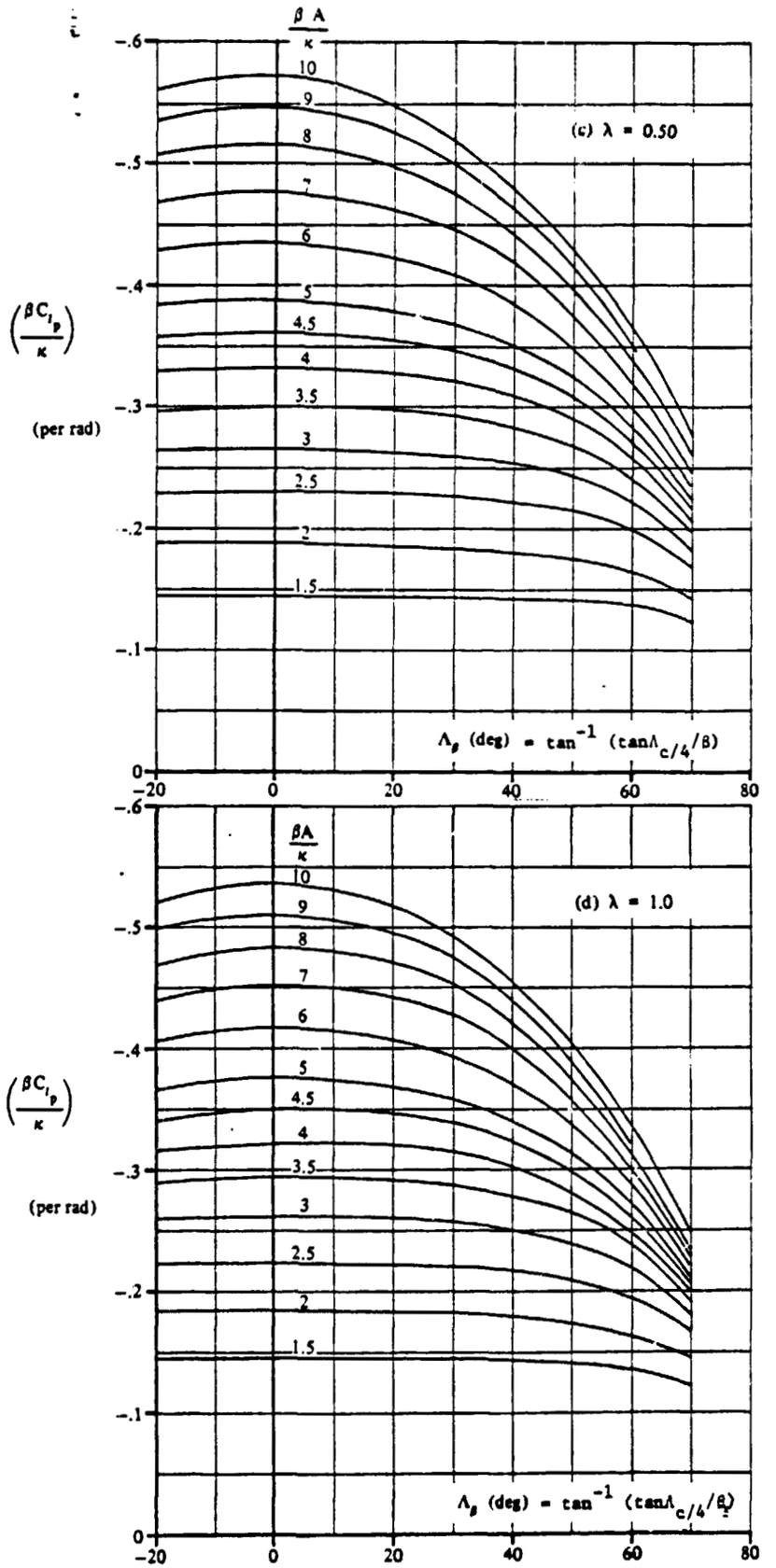

Figure 11.18.1: continued

$$C_{\ell_{p_V}} = 2\left(\frac{Z_V}{b}\right)^2 C_{Y_{\beta_V}} \qquad (11.18.4)$$

where: Z_V is the vertical distance from the body X-axis to the vertical tail aerodynamic center:

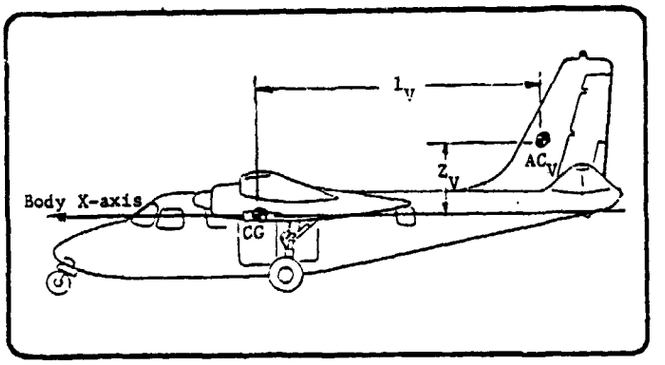

Figure 11.18.2: Geometry for determining distance vertical tail A.C. to body X-axis

11.18.2 HAND CALCULATION

In view of the simplicity of Equations 11.18.1 through 11.18.4, an entire hand calculation was not carried out. Instead, the use of Figure 8.1, Reference 11.18.1 was checked.

In the C_{ℓ_p} subroutine, interpolations of Figure 8.1 are done in Function RDP. The input data from Figure 8.1 is discussed in Section 11.18.3. Table 11.18.1 gives hand calculated interpolations versus RDP generated interpolations for Figure 8.1.

TABLE 11.18.1 HAND CHECK OF FIGURE 8.1, REFERENCE 11.18.1.

TEST #	η	BA/κ	Λ_B	$(B\,C_{\ell_p}/\kappa)_{hand}$	$(B\,C_{\ell_p}/\kappa)_{computer}$
1	.25	2.5	40	-.2140	-.2140
2	1.0	10.0	70	-.2778	-.2778
3	.33	4.2	22	-.3186	-.3193
4	.72	6.6	56	-.3269	-.3255

Table 11.18.1 shows that Function RDP interpolates Figure 11.18.1 very accurately.

A second source of error is $C_{Y_{B_V}}$. The C_{ℓ_p} subroutine calls the C_{Y_B} subroutine to find $C_{Y_{B_V}}$. To see how the C_{Y_B} subroutine compares to a hand calculation, see Section 11.14.2.

The entire C_{ℓ_p} subroutine was checked against Airplane A (Reference 11.18.2) and Airplane D (Reference 11.18.3) data. Table 11.18.2 gives relevant data and C_{ℓ_p} for the two aircraft.

TABLE 11.18.2 C_{ℓ_p} TEST CASES

TEST #	AIRPLANE	MACH #	α (deg.)	C_{ℓ_p} (rad^{-1})
1	Airplane A	.83	1.74°	-.535
2	"	.83	.95°	-.550
3	"	.53	1.07°	-.440
4	"	.152	11.30°	-.370
5	Airplane D	.11	14.50°	-.330
6	"	.60	3.00°	-.361

11.18.3 DESCRIPTION OF THE PROGRAM

The C_{ℓ_p} subroutine is straight forward. The most complex part is the interpolation of Figure 11.18.1, which is done by Function RDP.

The limitations of the subroutine are as follows:

1) $.25 \leq \eta \leq 1.0$

2) $0° \leq \Lambda_\beta \; 70°$

where: $\Lambda_\beta = \tan^{-1} (\tan\Lambda_{c/4}/\beta)$

$\beta = \sqrt{1 - M^2}$

3) $1.5 \leq \frac{\beta A}{\kappa} \leq 10$

where: $\beta = \sqrt{1 - M^2}$ $\qquad$ $\kappa = \frac{C_{\ell_{\alpha_W}}|_{avg}}{2\pi}$

A = Aspect Ratio

4) Any limitations in the C_{Y_β} subroutine also apply because the C_{ℓ_p} subroutine obtains $C_{Y_{\beta_V}}$ from the former.

5) $M < 1.0$

Table 11.18.3 gives variable names and origins.

TABLE 11.18.3 VARIABLE LIST

NAME	ENG. SYMBOL	DIMENSION	ORIGIN	REMARKS
CLP	C_{ℓ_p}	rad^{-1}	Output	
CLPWB	$C_{\ell_{p_{WB}}}$	rad^{-1}	Internal	Wing-body contribution to C_{ℓ_p}
CLPV	$C_{\ell_{p_V}}$	rad^{-1}	Internal	Vertical tail contribution to C_{ℓ_p}
CLPH	$C_{\ell_{p_H}}$	rad^{-1}	Internal	Horizontal tail contribution to C_{ℓ_p}
EM	M	---	Common	Mach number
CLAWP	$C_{\ell_{\alpha_W}}$	rad^{-1}	Common	Wing section lift-curve slope
CLAHP	$C_{\ell_{\alpha_H}}$	rad^{-1}	Common	Horizontal tail section lift-curve slope
KAPPA	κ_W	---	Internal	$C_{\ell_{\alpha_W}}/2\pi$
KAPPAH	κ_H	---	Internal	$C_{\ell_{\alpha_H}}/2\pi$
SW	S, S_W	ft^2	Common	Wing area

TABLE 11.18.3 VARIABLE LIST (continued)

NAME	ENG. SYMBOL	DIMENSION	ORIGIN	REMARKS
SHT	S_H	ft^2	Common	Horiz. tail area
B	b, b_W	ft	Common	Wing span
BHT	b_H	ft	Common	Horiz. tail span
ZV	Z_V	ft	Common	Vertical distance from body X-axis to vert. tail a.c.
CYBV	$C_{Y_{B_V}}$	rad^{-1}	Subroutine C_{Y_B}	Vertical tail contribution to C_{Y_B}
D2	$B\ C_\ell/\kappa$	rad^{-1}	Internal	Roll damping parameter
AR	A, AR	---	Common	Wing aspect ratio
ARH	A_H	---	Common	Horiz. tail aspect ratio
DLMC4	$\Lambda_{c/4}$	deg.	Common	1/4 C_W wing sweep angle
DLMC4H	$\Lambda_{c/4_H}$	deg.	Common	1/4 C_H Horiz. tail sweep angle
SLM	λ, λ_W	---	Common	Wing taper ratio
SLMH	λ_H	---	Common	Horiz. tail taper ratio
SWPBW	Λ_{β_W}	deg.	Internal	$\mathrm{Tan}^{-1}\frac{\tan\Lambda_{c/4_W}}{\beta}$
SWPBH	Λ_{β_H}	deg.	Internal	$\mathrm{Tan}^{-1}\frac{\tan\Lambda_{c/4_H}}{\beta}$

TABLE 11.18.3 VARIABLE LIST (continued)

NAME	ENG. SYMBOL	DIMENSION	ORIGIN	REMARKS
AW	BA/κ	---	Internal	
AH	BA_H/κ_H	---	Internal	

Figure 11.18.3 shows a flowchart of the program, figure 11.18.4 shows a listing as well as a sample printout.

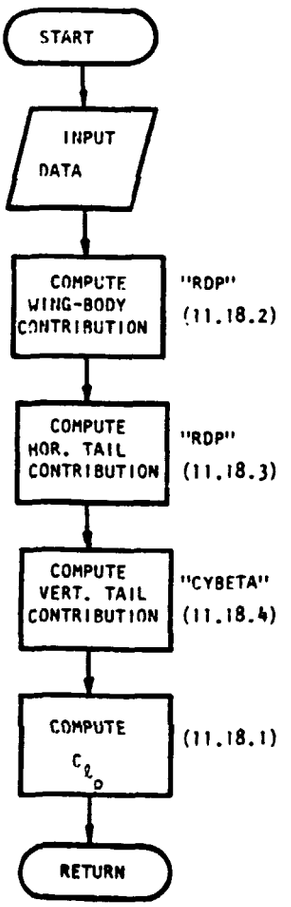

Figure 11.18.3: Flowchart of Subroutine "CLPE"

```
10      SUBROUTINE CLPP(CLP,CLPWB)
20       REAL KAPPA,KAPPAH,LN,LV
30       DIMENSION DD(24,9),VV(9),UU(3),DDD(4),WW(8)
40       COMMON /WING/DLMC4,AR,SLM,B,CRCLW,CBARW,SW,CLAWP
50       COMMON /HORZ/DLMC4H,ARH,SLMH,BHT,CBARHT,SHT,CLAHP,CRCLHT
60       COMMON /FLITE/ALPHA,EM,CL
65       COMMON /FUS/ELF,DFUS,HC,WC,LN,ELTH,HH,SO,R2I,LV,ZV
70      DATA VV/1.5,2.,2.5,3.5,4.5,5.,7.,9.,10./
80      DATA UU/.25,.5,1./
90      DATA WW/0.,10.,20.,30.,40.,50.,60.,70./
100      DATA DD/4*.1418,.1412,.1385,.1321,.1218,3*.1449,
110     &.144,.143,.1406,.1347,.121,.1445,.1444,.144,.1432,
120     &.1423,.1415,.1374,.1229,.1805,.1809,.1811,.1802,.1786,
130     &.1726,.1605,.1383,.1851,.1841,.1831,.1822,.179,.1737,.1621,
140     &.1447,.1877,.187,.1858,.1834,.1802,.1749,.1636,.1427,
150     &.2202,.2206,.2204,.2183,.214,.2058,.1893,.1574,.2233,
160     &.2226,.2214,.2199,.2168,.2083,.1935,.1653,.2303,.2301,
170     &.2293,.2267,.2216,.2151,.1982,.1682,.2819,.2821,.28,.2753,
180     &.2654,.2498,.222,.1749,.2937,.2942,.2915,.2876,.2778,
190     &.2645,.2378,.1906,.3,.2997,.298,.2925,.2828,.2686,.241,
200     &.1977,2*.3331,.3309,.3235,.3097,.2858,.2447,.1893,.3501,
210     &.3496,.346,.339,.3232,.2983,.2591,.2054,.3614,.359,.3552,
220     &.3467,.3234,.3085,.2702,.2165,2*.358,.3521,.3436,.3261,
230     &.2973,.2531,.1934,.3762,.374,.3682,.358,.3399,.3136,.271,
240     &.2097,.3873,.3847,.3789,.3678,.3503,.3251,.2828,.2233,
250     &.4218,.4226,.4167,.3996,.3728,.3323,.2772,.2049,.4526,.4502,
260     &.4425,.4275,.3994,.3583,.2991,.2267,.4774,.4718,.4618,
270     &.4461,.4191,.3753,.3187,.2455,.4772,.4747,.4638,.442,.407,
280     &.356,.2912,.214,.5097,.5059,.495,.4747,.4398,.39,.3196,.2403,
290     &.546,.5403,.5265,.5008,.4628,.4159,.3503,.2702,.4965,.4955,
300     &.4821,.4588,.4198,.3669,.2984,.216,.5364,.5306,.5178,.4923,
310     &.4543,.4045,.3358,.2475,.572,.5659,.5472,.519,.4795,.4295,
320     &.3656,.2778/
323       RLMC4=DLMC4*3.14159/180.
326       RLMC4H=DLMC4H*3.14159/180.
330        KAPPA=CLAWP/6.28319
340        KAPPAH=CLAHP/6.28319
350        BATA=SQRT(1.-EM**2)
360        AW=BATA*AR/KAPPA
370        AH=BATA*ARH/KAPPAH
380        SWFBW=ATAN((SIN(RLMC4)/COS(RLMC4))/BATA)
390       SWPBH=ATAN((SIN(RLMC4H)/COS(RLMC4H))/BATA)
400        D=RDP(SLM,AW,SWPBW,3,9,8,24,UU,VV,WW,DD)
430       CLPWB=-D*KAPPA/BATA
440       D2= RDP(SLMH,AH,SWPBH,3,9,8,24,UU,VV,WW,DD)
470       CLPHH=-D2*KAPPAH/BATA
480       CLPH=.5*CLPHH*(SHT/SW)*((BHT/B)**2)
490       CALL CYBETA(CYB,CYBV)
500       CLPV=2.*((ZV/B)**2)*CYBV
510       CLP=CLPWB+CLPH+CLPV
```


Figure 11.18.4: Listing and Sample Printout of Subroutine "CLPP"

```
      WRITE(6,1)EM,CLPWB,CLPH,CLPV,CLP
    1 FORMAT(10X,'CRUISE MACH =',F5.3,/,15X,'CLPWB =',
     &F8.3,/,15X,'CLPH =',F8.3,/,15X,'CLPV =',F8.3,/,
     &9X,'CLP =',F8.3,2X,'PER RADIAN')
      RETURN
      END
```

CLP = -0.501 PER RADIAN

Figure 11.18.4: Continued

Table 11.18.4 below compares the computer generated C_{ℓ_p}'s with those from References 11.18.2 and 11.18.3 for the tests outlined previously in section 11.18.2.

Table 11.18.4 - C_{ℓ_p} Output

Test #	Airplane	C_{ℓ_p} (data)	C_{ℓ_p} (computer)	% Error
1	A	-.535/rad	-.501/rad	6.4%
2	"	-.550/rad	-.501/rad	8.9%
3	"	-.440/rad	-.446/rad	5.9%
4	"	-.370/rad	-.416/rad	12.4%
5	D	-.330/rad	-.418/rad	26.7%
6	"	-.361/rad	-.446/rad	23.6%

It is important to note that the C_{ℓ_p}'s for airplane A are themselves predictions while the C_{ℓ_p}'s for airplane D are predictions for the full scale airplane based on model wind tunnel tests.

11.18.4 REFERENCES

11.18.1 Roskam, J. Methods for Estimating Stability and Control Derivatives of Conventional Subsonic Airplanes. Printed by the author. 519 Boulder, Lawrence, Ks., 1971.

11.18.2 Anon. Confidential Report.

11.18.3 Anon. Confidential Report.

11.19 C_{n_p}; VARIATION OF YAWING MOMENT COEFFICIENT WITH ROLL RATE PERTURBATION

11.19.1 DERIVATION OF EQUATIONS

C_{n_p} is estimated in the conventional manner, as the sum of the wing contribution and the vertical tail contribution:

$$C_{n_p} = C_{n_{p_w}} + C_{n_{p_v}} \tag{11.19.1}$$

The following equations used to determine $C_{n_{p_w}}$ and $C_{n_{p_v}}$ are equations (8.7) through (8.11), pages 8.2 to 8.3 from reference 11.19.1

The wing contribution can be expressed as:

$$C_{n_{p_w}} = - C_{\ell_{p_w}} \text{Tan } \alpha - \left[- C_{\ell_p} \text{Tan } \alpha - \left(\frac{C_{n_p}}{C_L} \right)_{\substack{C_L = 0 \\ m}} C_L \right] + \frac{\Delta C_{n_p}}{\theta} \theta + \frac{\Delta C_{n_p}}{\alpha_{\delta_F} \delta_F} \alpha_{\delta_F} \delta_F \tag{11.19.2}$$

where:

$C_{\ell_{p_w}}$ is the wing contribution to C_{ℓ_p}

α is the wing angle of attack ($\alpha_\omega = \alpha_{A/C}$)

C_L is the wing lift coefficient ($C_{L_W} = C_{L_{A/C}}$)

$\left(\frac{C_{n_p}}{C_L}\right)_{\substack{C_L = 0 \\ m}}$ is the slope of the yawing moment due to rolling at zero lift given by:

$$\left(\frac{C_{n_p}}{C_L}\right)_{\substack{C_L = 0 \\ m}} = \left[\frac{A + 4 \cos \Lambda_{c/4}}{AB + 4 \cos \Lambda_{c/4}}\right]\left[\frac{AB + \frac{1}{2}(AB + \cos \Lambda_{c/4}) \tan^2 \Lambda_{c/4}}{A + \frac{1}{2}(A + \cos \Lambda_{c/4}) \tan^2 \Lambda_{c/4}}\right]\left(\frac{C_{n_p}}{C_L}\right)_{\substack{C_L = 0 \\ m = 0}} \tag{11.19.3}$$

where: $B = \sqrt{1 - m^2\cos^2\Lambda_{c/4}}$

$\left(\frac{C_{n_p}}{C_L}\right)_{\substack{C_L = 0 \\ m = 0}}$ is the slope of the low-speed yawing moment due to rolling at zero lift given by:

$$\left(\frac{C_{n_p}}{C_L}\right)_{\substack{C_L = 0 \\ m = 0}} = -\frac{1}{6}\left[\frac{A + 6(A + \cos\Lambda_{c/4})\left(\frac{\bar{x}}{\bar{c}}\frac{\tan\Lambda_{c/4}}{A} + \frac{\tan^2\Lambda_{c/4}}{12}\right)}{A + 4\cos\Lambda_{c/4}}\right] \qquad (11.19.4)$$

where: $\bar{x}$ is the distance from the center of gravity to the aerodynamic center of the wing, positive when the a.c. is aft of the c.g.

$\bar{c}$ is the wing mean aerodynamic chord.

Referring to eq. 11.19.2 again:

where: $\frac{\Delta C_{n_p}}{\theta}$ is the effect of linear wing twist obtained from Figure 11.19.1

θ is the wing twist in degrees, negative for washout

$\frac{\Delta C_{n_p}}{\alpha_\delta \delta_F}_F$ is the effect of symmetric flap deflection obtained from Figure 11.19.2

δ_F is the streamwise flap deflection in degrees.

α_{δ_F} is the two-dimensional lift-effectiveness parameter, obtained from Figure 11.23. Reproduced here as Figure 11.19.3.

The vertical tail contribution to C_{n_p} can be estimated from:

$$C_{n_{p_v}} = -\frac{2}{b}[\ell_v\cos\alpha + Z_v\sin\alpha]\left[\frac{Z_v\cos\alpha - \ell_v\sin\alpha}{b}\right]C_{y_{\beta_v}} \qquad (11.19.5)$$

where: ℓ_v and Z_v are defined in Figure 11.

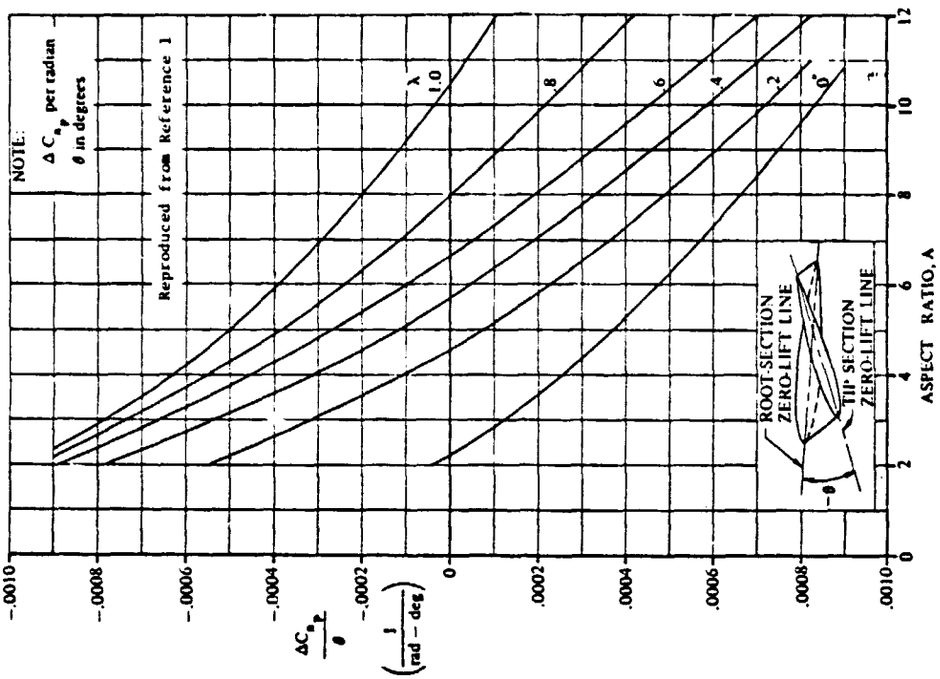

Figure 11.19.1: Effect of wing twist on wing rolling derivative C_{n_p}

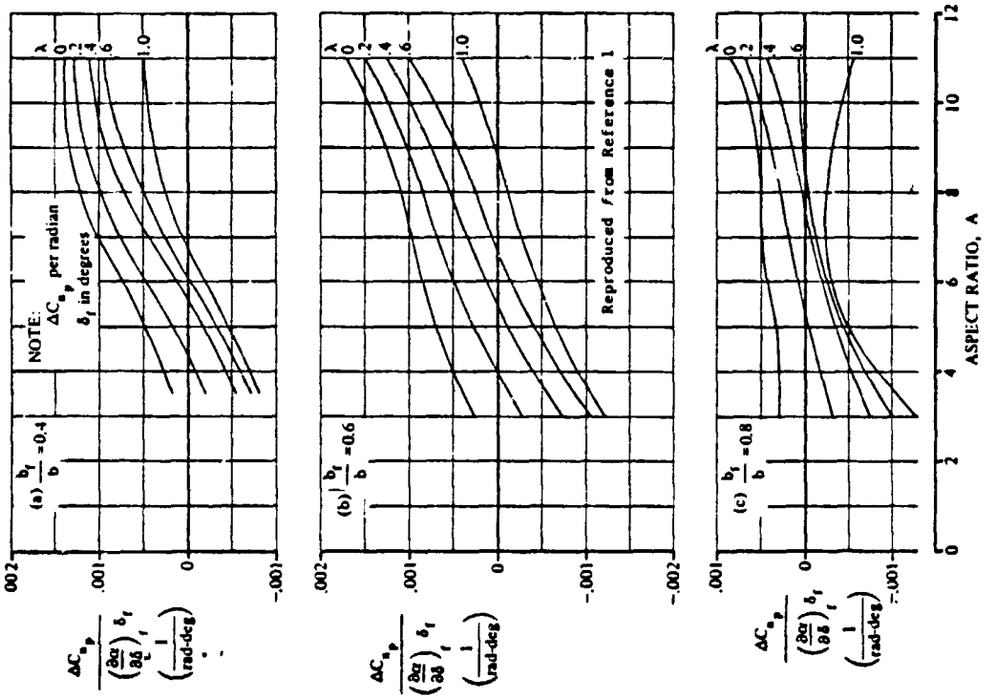

Figure 11.19.2: Effect of flap deflection on wing rolling derivative C_{n_p}

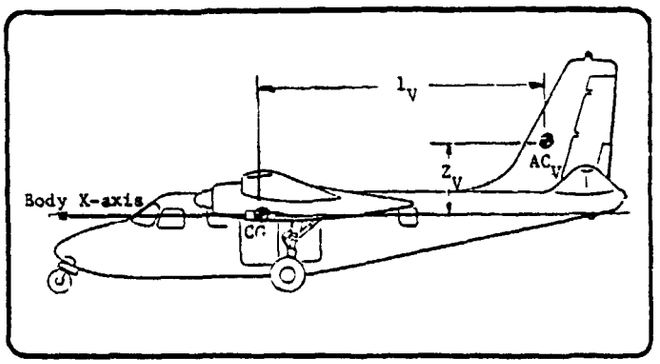

Figure 11.19.2a: efinition of geometric parameters

$C_{y_{\beta_V}}$ is the vertical tail contribution to C_{y_β}.

11.19.2 HAND CALCULATION

Six test cases and two hand checks were done to test the C_{n_p} subroutine. The hand checks are explained first.

The first hand check was done to determine if function RDP interpolated the graphs (Figs. 11.19.1-.2) correctly. As Table 11.19.1 shows, RDP works well for interpolating Figures 11.19.1 and 11.19.2. For a full account of function RDP, see Appendix B.1.

Figure 11.19.3 (the upper-right hand graph only) is expressed in C_{n_p} as an equation derived in section 11.23:

$$(\alpha_\delta)_{C_\ell} = -.2747 - 1.4584(c_F/c_w) + .7406(c_F/c_w)^2 \qquad (11.19.6)$$

Table 11.19.1 - Test of Function RDP for Figures 11.19.1 and 11.19.2

Test #	AR	λ	$\Delta C_{n_p}/\theta$ (hand)	$\Delta C_{n_p}/\theta$ (RDP)	%Error
1	5.74	.564	-.000116	-.000115	.86%

Test #	AR	λ	bF/b	$\frac{\Delta C_{n_p}}{(\partial\alpha/\partial\delta)_F \delta_F}$ (hand)	$\frac{\Delta C_{n_p}}{(\partial\alpha/\partial\delta)_F \delta_F}$ (RDP)	%Error
1	5.74	.564	.482	-.000117	-.000111	5.13%

Test case #1, C_{n_p} hand check

α = 11.3°; angle of attack; ref.2

C_L = 1.04; lift coefficient; ref.2

m = .152; mach number; ref.2

X_{cg} = 2.174';

δ_F = 0°; flap deflection; ref. 2

C_{ℓ_p} = -.416/rad; C_{ℓ_p} subroutine

$C_{\ell_{p_w}}$ = -.404/rad; C_{ℓ_p} subroutine

$C_{y_{\beta_v}}$ = -.168/rad; C_y subroutine

$\bar{X}_{ac} = .25 \rightarrow X_{ac} = 1.724$

Find $C_{n_{p_w}}$:

Starting with eq. 11.19.4: $\bar{x} = 1.724 - 2.174 = -.450$

gives: $\left(\frac{C_{n_p}}{C_L}\right)_{\substack{C_L = 0 \\ m = 0}} = -.101$

substituting into eq. 11.19.3: $B = \sqrt{1 - (.152)^2 \cos^2 13^\circ} = .99$

$$\left(\frac{C_{n_p}}{C_L}\right)_{\substack{C_L = 0 \\ m}} = -.101$$

From Fig. 11.19.1: $\frac{\Delta C_{n_p}}{\theta} = -.000116$

From Fig. 11.19.2: $\frac{\Delta C_{n_p}}{\alpha_{\delta_F} \delta_F} = -.000117$

From Fig. 11.19.3: $\alpha_{\delta_F} = -.625$

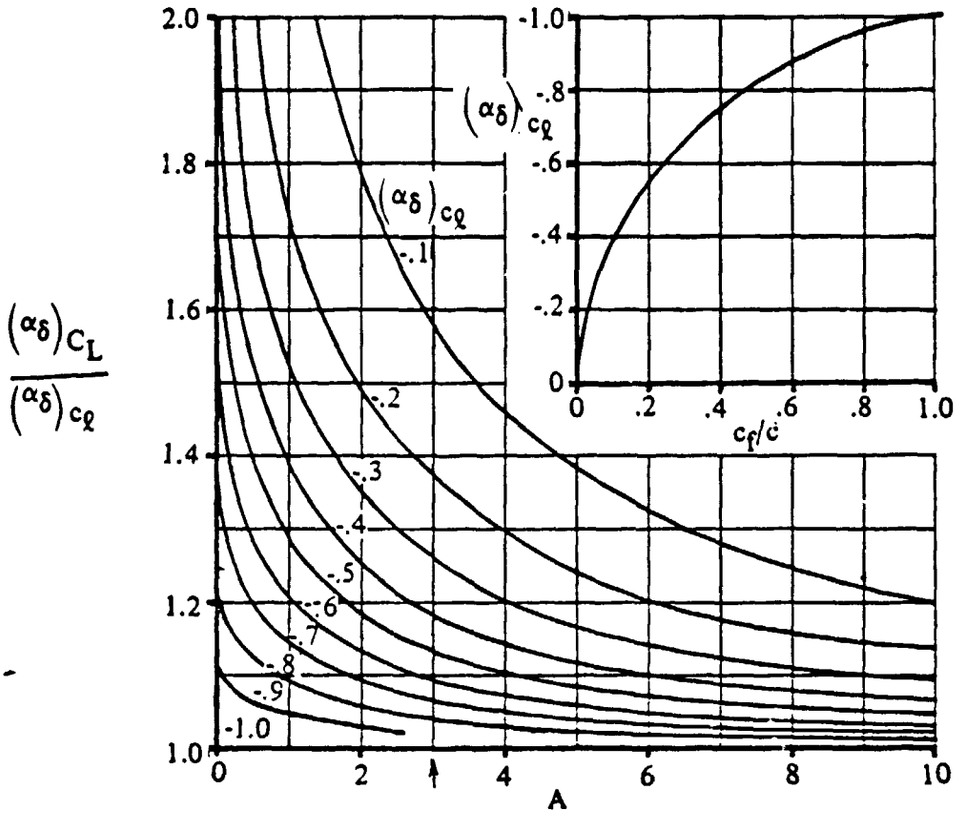

Figure 11.19.3: Influence of flap chord on flap effectiveness

The second hand check is a calculation of C_{n_p} by equations 11.19.1 through 11.19.4 for the conditions of test case #1 (described later). Because C_{n_p} calls $C_{y_{\beta_v}}$, $C_{\ell_{p_w}}$, and C_{ℓ_p} from subroutines C_{y_β} and C_{ℓ_p}, the values of these for use in the hand check are also obtained from subroutines C_{y_β} and C_{ℓ_p}. In this way, errors in the C_{n_p} program can be spotted and corrected. Test case #1 is for aircraft A, for which data are given in Appendix D.

Substituting into eq. 11.19.2:

$$C_{n_{p_w}} = -.107/\text{rad}$$

Using eq. 11.19.5:

$$C_{n_{p_v}} = +.007/\text{rad}$$

$$C_{n_p} = C_{n_{p_w}} + C_{n_{p_v}} \qquad (11.19.1)$$

$$C_{n_p} = -.107 + .007 \qquad C_{n_p} = -.100/\text{rad}$$

The subroutine found (for Test case #1)

$$C_{n_p} = -.098/\text{rad}$$

$$\%\text{error} = \frac{-.100 + .098}{-.100} \times 100 \qquad \%\text{error} = 2\%$$

This error is negligible.

Thus it appears that the C_{n_p} subroutine follows the method of reference 11.19.1 quite well.

The six test cases for C_{n_p} are now discussed. The first four cases involve checking C_{n_p} against the data of reference 11.19.2 for aircraft A. The last two cases are checks with aircraft D of reference 11.19.4. Table 11.19.2 gives the data for the six test cases.

Table 11.19.2 - C_{n_p} Test Cases

Test #	Airplane	m	C_L	α(deg)	C_{n_p} (rad^{-1})
1	Airplane A	.152	1.04	11.3	-.035
2	"	.83	.265	1.74	+.027
3	"	.83	.172	.95	+.034
4	"	.42	1.04	10.9	-.035
5	Airplane D	.11	1.42	14.5	-.090
6	"	.60	.149	3.0	+.070

11.19.3 DESCRIPTION OF THE PROGRAM

The program operates as follows. Equations 11.19.1 through 11.19.5 are contained in the program. Most of the data is input via common statements, but Figures 11.19.1 and 11.19.2 are input in data statements for use by function RDP (see Appendix B.1 for a description of RDP). Figure 11.19.3 is expressed in the form of an equation, see eq. 11.19.6, page 11.19.4. $C_{\ell_{p_w}}$, C_{ℓ_p}, and $C_{y_{\beta_v}}$ are obtained from their respective subroutines. Using this data and information, the program computes C_{n_p}. A variable list is given as Table 11.19.3 below.

Table 11.19.3 - Variable List

Name	Eng. Symbol	Dimension	Origin	Remarks
CNP	C_{n_p}	rad^{-1}	output	--------
CNPV	$C_{n_{p_v}}$	rad^{-1}	internal	vertical tail contribution to C_{n_p}
CNPW	$C_{n_{p_w}}$	rad^{-1}	internal	wing contribution to C_{n_p}
CLP	C_{ℓ_p}	rad^{-1}	Sub. C_{ℓ_p}	---------
CLPW	$C_{\ell_{p_w}}$	rad^{-1}	Sub. C_{ℓ_p}	wing contribution to C_{ℓ_p}
CYBV	$C_{y_{\beta_v}}$	rad^{-1}	Sub. C_{y_β}	vertical tail contribution to C_{y_β}
ALPHA	α	deg	common	angle of attack
ALCLOMO	$(C_{n_p}/C_L)_{\substack{C_L=0 \\ M=0}}$	rad^{-1}	internal	----------
DLMC4	$\Lambda_{c/4}$	deg	common	1/4 chord wing sweep angle
AR	AR	----	common	Aspect ratio
CFOC	c_F/c_w	----	common	flap chord/wing chord
BFOB	b_F/b_w	----	common	flap span/wing span
ACLOM	$(C_{n_p}/C_L)_{\substack{C_L=0 \\ M}}$	rad^{-1}	internal	----------

Table 11.19.3 - Variable List (continued)

Name	Eng. Symbol	Dimension	Origin	Remarks
EM	M	----	common	cruise mach number
CBARW	$\bar{c}_w$	ft.	common	wing MAC length
THETW	ϑ	deg.	common	wing twist (washout negative)
CTHETW	$\Delta C_{n_p}/\theta$	$rad^{-1}deg^{-1}$	internal	------
CNPDEF	$\frac{\Delta C_{n_p}}{\alpha_{\delta_F}\delta_F}$	$rad^{-1}deg^{-1}$	internal	------
DFLAP	δ_F	deg.	common	flap deflection
ADCL	α_{δ_F}	----	internal	---------
LV	ℓ_v	ft.	common	A.C.$_v$ to c.g.(horizontally)
ZV	Z_v	ft.	common	A.C.$_v$ to c.g.(vertically)
B	b	ft.	common	wing span
CL	C_L	---	common	lift coefficient
SLM	λ	---	common	wing taper ratio

Figure 11.19.4 shows a flowchart of the program, figure 11.19.5 gives a listing as well as a sample printout of the program.

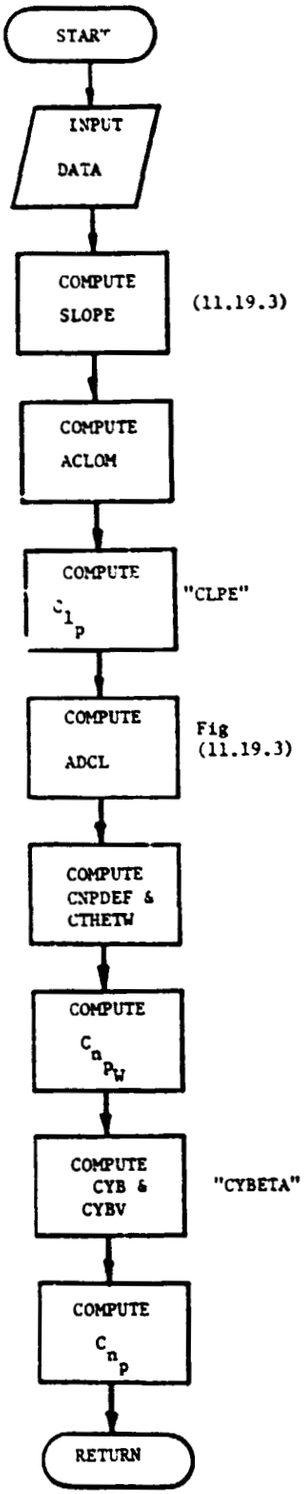

Figure 11.19.4: Flowchart of Subroutine "CNPE"

```
10C      SUBROUTINE CNPP(CNP)
20       DIMENSION UU(1),VV(5),WW(4),DD(4,5),BFB(3),SLMI(4),
30      &ASRRI(5),DED(15,4)
40       COMMON /WING/DLMC4,AR,SLM,B,CRCLW,CBARW,SW,CLAWP
50       COMMON /FUS/ELF,DFUS,HC,WC,LN,ELTH,HH,SO,R2I,LV,ZV
55       REAL LN,LV
60       COMMON /FLITE/ALPHA,EM,CL
70       DATA THETW,CFOC,BFOB,DFLAP,XCG/-3.5,1.,1.,0.,1.35/
80       DATA UU,VV,WW/1.,.2,.4,.6,.8,1.,3.,6.,9.,12./
90       DATA DD/-.00032,.00022,.00061,.00092,-.00054,
100     &.00005,.00046,.00082,-.00066,-.0001,.00033,.0007,
110     &-.00074,-.00024,.00011,.00042,-.00078,-.00039,-.00011
120     &,.0001/
130      DATA BFB,SLMI,ASRRI/.4,.6,.8,.2,.4,.6,1.,
140     &3.,5.,7.,9.,11./
150      DATA DED/-.00028,.00015,.00077,.00115,.00129,-.00028,
160     &.00028,.00069,.00103,.0015,-.00031,-.00004,.0002,.00039,
170     &.00067,-.00066,-.00015,.00043,.00092,.00111,-.00074,-.00012,
180     &.00034,.00075,.00127,-.00074,-.00034,-.00007,.00014,.00043,
190     &-.00082,-.00032,.00025,.00071,.00095,-.00106,-.00041,
200     &.00007,.00046,.001,-.00099,-.00043,-.00013,.00002,.00007,
210     &-.00089,-.00045,.00007,.00037,.0005,-.00121,-.00065,-.00026,
220     &.00002,.0004,-.00126,-.00049,-.00023,-.00031,-.00054/
230      ALPHAR=ALPHA*3.14159/180.
240      RLMC4=DLMC4*3.14159/180.
250      XBARW=ACEM(EM,AR,SLM,DLMC4,CRCLW)
255      XBAR=XBARW-(XCG/CBARW)
260      COSC4=COS(RLMC4)
270      TANC4=SIN(RLMC4)/COSC4
280      TANSQ4=TANC4**2
290      ZEB=(XBAR*TANC4)/(AR)+(TANSQ4/12.)
300      ZAB=6.*(AR+COSC4)
310      ZIB=AR+4.*COSC4
320      ACLOMO=-((AR+ZAB*ZEB)/ZIB)/6.
330      BB=SQRT(1.-(EM**2)*(COSC4**2))
340      XAB=(AR+4.*COSC4)/(AR*BB+4.*COSC4)
350      XEB=AR*BB+.5*(AR*BB+COSC4)*TANSQ4
360      XIB=AR+.5*(AR+COSC4)*TANSQ4
370      ACLOM=XAB*XEB*ACLOMO/XIB
380      CALL CLPP(CLP,CLPWB)
390      ADCL=-.2747-1.4584*CFOC+.7406*CFOC**2
400      XI=BFOB
410      CNPDEF=RDP(XI,SLM,AR,3,4,5,15,BFB,SLMI,ASRRI,DED)
420      CTHETW=RDP(1.,SLM,AR,1,5,4,4,UU,VV,WW,DD)
430      TANALF=SIN(ALPHAR)/COS(ALPHAR)
440      CNPW=-CLPWB*TANALF+CLP*TANALF+ACLOM*CL
450     &+CTHETW*THETW+CNPDEF*ADCL*DFLAP
460      CALL CYBETA(CYB,CYBV)
470      COALFA=COS(ALPHAR)
480      SIALFA=SIN(ALPHAR)
490      CNPV=(-2./(B**2))*CYBV*(LV*COALFA+ZV*SIALFA)
500     &*(ZV*COALFA-LV*SIALFA)
```

Figure 11.19.5: Listing and Sample Printout of Subroutine "CNPE"

```
510      CNP=CNPW+CNPV
520      WRITE(6,1)CNPW,CNPV,CNP
530    1 FORMAT(2X,"CNPW =",F7.3,/,2X,"CNPV =",F7.3,
540     &/,2X,"CNP =",F7.3,3X,"PER RADIAN")
550C     RETURN
560      STOP
570      END
```

CNP = -0.098 PER RADIAN

Figure 11.19.5: Continued

11.19.4 RESULTS

The CNP subroutine was checked out for the six test cases outlined in section 11.17.2. As will be seen, the CNP subroutine does not match the CNP data very well. Table 11.19.4 gives a comparison.

Table 11.19.4 - C_{n_p} Test Case Comparisons

Test #	Airplane	C_{n_p} (rad^{-1}) From Table 11.17.2	C_{n_p} (rad^{-1}) as computed by sub. CNP	% Error	
1	A	-.035	-.098	180%	Too Negative
2	"	+.027	-.002	93%	Too Negative
3	"	+.034	+.006	82%	Too Small
4	"	-.035	-.094	169%	Too Negative
5	D	-.090	-.129	43%	Too Negative
6	"	+.070	+.030	57%	Too Small

Table 11.19.4 shows that subroutine CNP always predicts too negatively. It is interesting to see that the computer predictions for C_{y_p} are also too negative by a fair amount, again it may be the asymmetric flow around the tail that compounds the errors.

11.19.5 REFERENCES

11.19.1 Roskam, J. Methods for Estimating Stability and Control Derivatives of Conventional Subsonic Airplanes. Dr. Jan Roskam, Published by the author, 519 Boulder, Lawrence, KS, 66044, 1971.

11.19.2 Anon. Confidential Report.

11.19.3 Anon. Confidential Report.

11.19.4 Anon. Confidential Report.

11.20 VARIATION OF SIDE FORCE COEFFICIENT WITH YAW RATE, C_{y_r}

11.20.1 DERIVATION OF EQUATIONS

Usually this derivative is of minor importance. It can be easily calculated however. Reference 11.20.1 suggests the following formula:

$$C_{y_r} = C_{y_{r_V}} = -\frac{2}{b}(\ell_V \cos\alpha + Z_V \sin\alpha) C_{y_{\beta_V}} \qquad (11.20.1)$$

where ℓ_V and Z_V are defined in Figure 11.16.1

$C_{y_{\beta_V}}$ is computed in section 11.14.

11.20.2 HAND CALCULATION

A hand calculation was done for airplane A, see Appendix D for data.

Section 11.14 gives:

$$C_{y_{\beta_V}} = -0.37756 \ (\text{rad}^{-1})$$

For an angle of attack of 11.3 deg equation 11.20.1 then gives:

$$C_{y_r} = 0.313 \ (\text{rad}^{-1})$$

Reference 11.21.2 gives:

$$C_{y_r} = 0.295 \ (\text{rad}^{-1})$$

this constitutes a difference of 5.6% with the computer value.

11.20.3 PROGRAM DESCRIPTION

The variables used in the program are listed in Table 11.20.1 Figure 11.20.1 shows a flowchart, Figure 11.20.2 shows a listing plus a sample printout.

Table 11.20.1 Variables in Subroutine "CYARE"

NAME	ENG. SYMBOL	DIMENSION	ORIGIN	REMARKS
ALPHA	α	rad	Common	
B	b	ft	Common	
CYR	C_{y_r}	rad^{-1}	---	
CYBV	C_{y_β}	rad^{-1}	"CYBETA"	
ELTV	ℓ_V	ft	Common	V
ZV	Z_V	ft	Common	

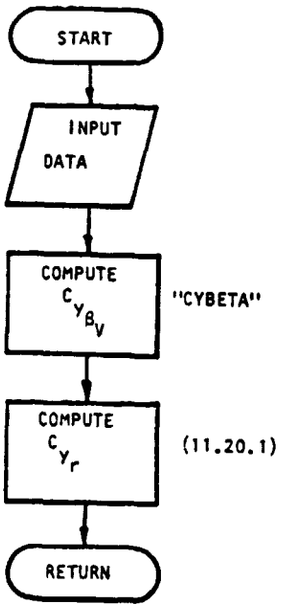

Figure 11.20.1: Flowchart of Subroutine "CYARE"

```
10      SUBROUTINE CYARE (CYR)
20      COMMON /WING/ DLMC4,AR,SLM,B,CRCLW,CBARW,SW,CLAWP
30      COMMON /FUS/ ELF,DFUS,HC,WC,LN,ELTH,HH,SO,R2I,LV,ZV
40      COMMON /FLITE/ ALPHA,EM,CL
50      REAL LV
60      CALL CYBETA(CYB,CYBV)
70      CYR=-((2./B)*CYBV*(LV*COS(ALPHA)+ZV*SIN(ALPHA)))
80      WRITE(6,1) CYR
90    1 FORMAT(//,10X,'***KU-FRL DEVELOPED SUBROUTINE CYR***',
100     &//,10X,'CYR   =   ',F8.6,//,10X,'***END OF SUBROUTINE***')
110      STOP
120      END
```

```
CYR =    0.31499 PER RAD
```

Figure 11.20.2: Listing and Sample Printout Subroutine "CYARE"

11.20.4 REFERENCES

11.20.1 Roskam, J. Methods for Estimating Stability and Control Derivatives for Conventional Subsonic Airplanes. Roskam Aviation & Engineering Corporation. Lawrence, Ks.1977.

11.20.2 Anon. Confidential Report.

11.21 SUBROUTINE "CLARE" (CLR), VARIATION OF ROLLING MOMENT WITH YAW RATE

11.21.1 DERIVATION OF EQUATIONS

Reference 1 indicates that C_{ℓ_r} may be estimated from:

$$C_{\ell_r} = C_{\ell_{r_W}} + C_{\ell_{r_V}} \tag{11.21.1}$$

The variation of the wing yawing derivative with lift coefficient is given by:

$$C_{\ell_{r_W}} = C_L\left(\frac{C_{\ell_r}}{C_L}\right)_{\substack{C_L=0\\M}} + \left(\frac{\Delta C_{\ell_r}}{\Gamma}\right)\Gamma + \left(\frac{\Delta C_{\ell_r}}{\Theta}\right)\Theta + \left(\frac{\Delta C_{\ell_r}}{\alpha_{\delta_F}\delta_F}\right)\alpha_{\delta_F}\delta_F \ (\text{rad}^{-1}) \tag{11.21.2}$$

where:

$\left(\frac{C_{\ell_r}}{C_L}\right)_{\substack{C_L=0\\M}}$ is the slope of the rolling moment due to yawing at zero lift given by:

$$\left(\frac{C_{\ell_r}}{C_L}\right)_{\substack{C_L=0\\M}} = \frac{1 + \frac{A(1-B^2)}{2B(AB+2\cos\Lambda_{c/4})} + \frac{AB+2\cos\Lambda_{c/4}}{AB+4\cos\Lambda_{c/4}}\left(\frac{\tan^2\Lambda_{c/4}}{8}\right)}{1 + \frac{A+2\cos\Lambda_{c/4}}{A+4\cos\Lambda_{c/4}}\left(\frac{\tan^2\Lambda_{c/4}}{8}\right)}\left(\frac{C_{\ell_r}}{C_L}\right)_{\substack{C_L=0\\M}} \tag{11.21.3}$$

where:

$$B = \sqrt{1 - M^2\cos^2\Lambda_{c/4}} \tag{11.21.4}$$

$\left(\frac{C_{\ell_r}}{C_L}\right)_{\substack{C_L=0\\M=0}}$ is the slope of the low-speed rolling moment due to yawing at zero lift, obtained from Figure 11.21.1 as a function of aspect ratio, quarter chord sweep, and taper ratio.

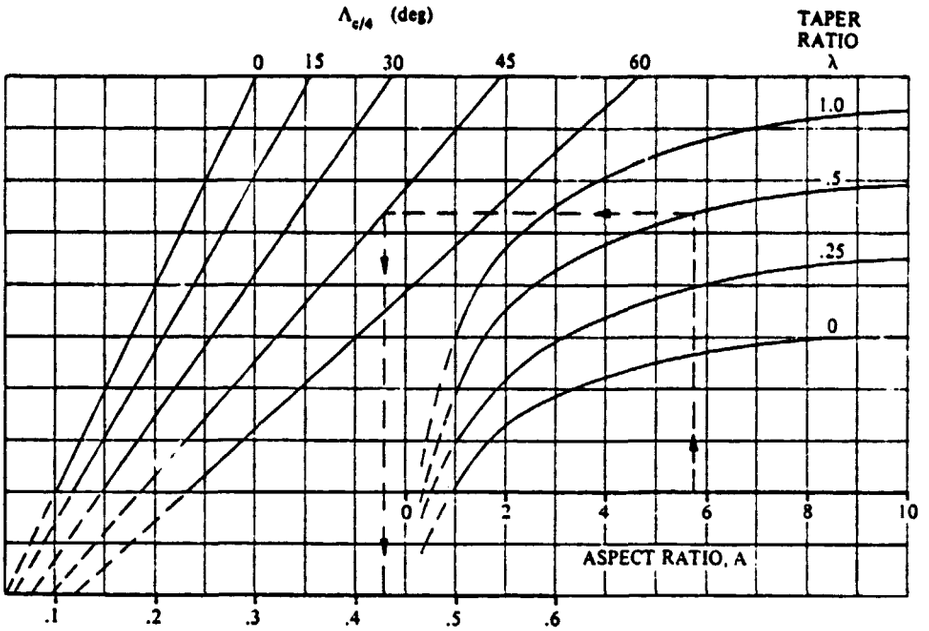

Figure 11.21.1: Wing Yawing Derivative, C_{l_r}

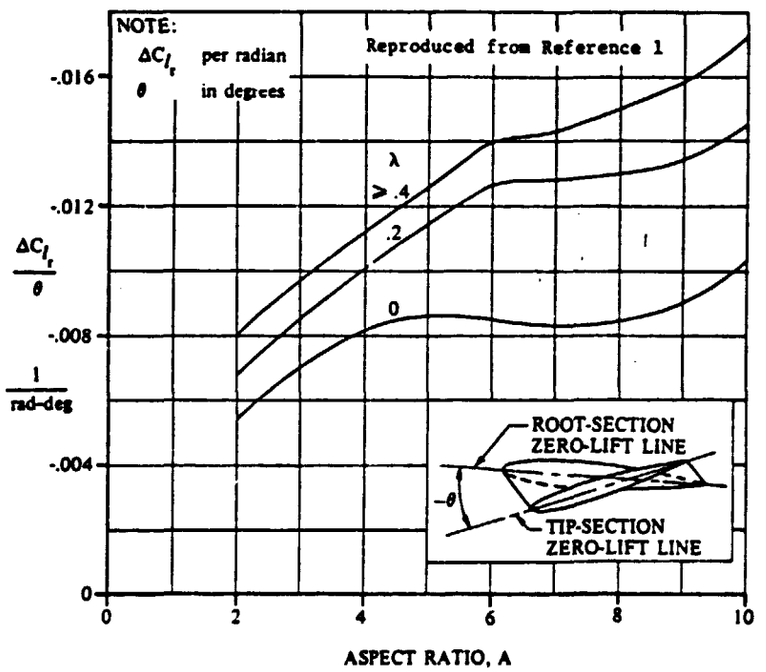

Figure 11.21.2: Effect of Wing Twist on C_{l_r}

C_L is the wing lift coefficient

$\frac{\Delta C_{\ell_r}}{\Gamma}$ is the increment in C_{ℓ_r} due to dihedral, given by:

$$\frac{\Delta C_{\ell_r}}{\Gamma} = \frac{1}{12} \frac{\pi A \sin \Lambda_{c/4}}{A + \cos \Lambda_{c/4}} \text{ (rad}^{-2}\text{)} \qquad (11.21.5)$$

Γ is the geometric dihedral angle, here in radians, positive for the wing tip above the plane of the root chord.

$\frac{\Delta C_{\ell_r}}{\Theta}$ is the increment due to wing twist obtained from Figure 11.21.2.

Θ is the wing twist, negative for washout

$\frac{\Delta C_{\ell_r}}{\alpha_{\delta_F} \delta_F}$ is the effect of symmetric flap deflection obtained from Figure 11.21.3.

δ_F is the streamwise flap deflection in degrees.

$\alpha_{\delta_F} \delta_F$ is the two dimensional lift-effectiveness parameter α_δ obtained from Section 11.23.

The vertical tail contribution is found from

$$C_{\ell_{r_V}} = \frac{2}{b^2} (\ell_V \cos\alpha + Z_V \sin \alpha)(Z_V \cos \alpha - \ell_V \sin \alpha) C_{y_{\beta_V}}$$

where:

ℓ_V and Z_V are defined in Figure 11.16.1 and

$C_{y_{\beta_V}}$ is determined in Section 11.14.

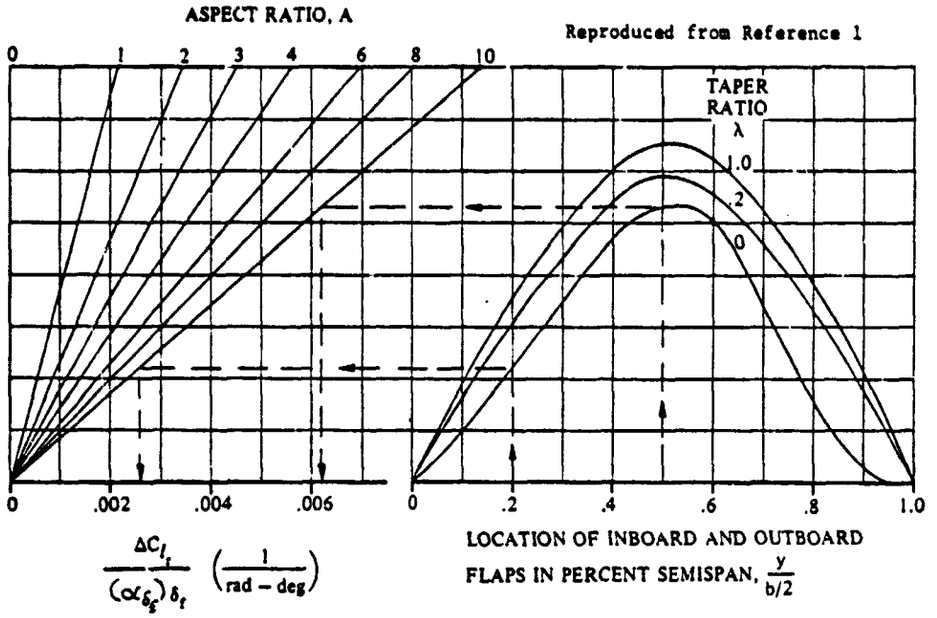

NOTE: ΔC_{l_t} per radian, δ_f in degrees

NOTE: $\frac{\Delta C_{l_t}}{(\alpha_{\delta_\epsilon})\delta_f} = \left[\frac{\Delta C_{l_t}}{(\alpha_{\delta_\epsilon})\delta_f}\right]_{\text{outboard}} - \left[\frac{\Delta C_{l_t}}{(\alpha_{\delta_\epsilon})\delta_f}\right]_{\text{inboard}}$

Figure 11.21.3: Effect of Flaps on C_{l_r}

11.21.2 HAND CALCULATION

Airplane A is used for the test aircraft in this section (Reference 2). Appendix D presents the data for this aircraft.

Flight conditions:

$M = .152$

$\alpha = 11.3°$

$C_L = 1.04$

$\delta_F = 0$

First, β must be calculated:

$$\beta = \sqrt{1 - (.152)^2(\cos 13°)^2}$$

$$\beta = .989$$

From Figure 11.21.1, $\left(\frac{C_{\ell_r}}{C_L}\right)_{\substack{C_L=0 \\ M=0}}$

$$\left(\frac{C_{\ell_r}}{C_L}\right)_{\substack{C_L=0 \\ M=0}} = .26 \ (\text{rad}^{-1})$$

Then

$$\cos \Lambda_{c/4} = \cos(13°) = .9744$$

$$\left(\frac{C_{\ell_r}}{C_L}\right)_{\substack{C_L=0 \\ M}} = .262$$

$$\frac{\Delta C_{\ell_r}}{\Gamma} = .0351$$

From Figure 11.21.2:

$$\frac{\Delta C_{\ell_r}}{\theta} = -.0137 \ (\text{rad}^{-1} - \text{deg}^{-1})$$

From Figure 11.21.3 and Section

$$\frac{\Delta C_{\ell_r}}{\alpha_{\delta_F} \delta_F} = .604 \qquad \alpha_{\delta_F} = .66$$

Therefore, for the wing:

$$C_{\ell_{r_W}} = .273 \ \text{rad}^{-1}$$

From Section

$$C_{y_{\beta_V}} = -.1675 \ (\text{rad}^{-1})$$

Therefore:

$$C_{\ell_{r_V}} = -.00743 \quad \text{rad}^{-1}$$

$$C_{\ell_r} = .273 + .00743$$

$$C_{\ell_r} = .28043 \quad \text{rad}^{-1}$$

11.21.3 DESCRIPTION OF PROGRAM

Subroutine CLARE utilizes functions as the primary calculators for the required curve fits. RDP is used throughout the program, not only for interpolating along given curves, but also for proper interpolation between curves.

The characteristics of some of the figures (curves) required for C_{ℓ_r} posed some problems. RDP could easily determine the proper values along a curve. Interpolating between the curves was difficult, though. Many of the curves, as in Figure 11.21.2, did not present a constant separation or trend between curves. To solve the problem, RDP was used to interpolate between curves.

The reader is referred to the flowchart, and the listing following this section.

TABLE 11.21.1 VARIABLE LIST

NAME	ENG. SYMBOL	DIMENSION	ORIGIN	REMARKS
ALPHA	α	deg	Common	
AR	A	---	Common	
B	b	ft	Common	
CFOC	c_f/c	---		

TABLE 11.21.1 VARIABLE LIST (continued)

NAME	ENG. SYMBOL	DIMENSION	ORIGIN	REMARKS
CL	C_L	---	Common	
CYB	C_{y_β}	rad^{-1}	Subroutine CYBETA	
CLR	C_{ℓ_r}	rad^{-1}	Calculated	
DELTD	δ_F	deg	Common	Positive for deflection downward
DIHD	Γ	deg		Degrees
DLMC4	$\Lambda_{c/4}$	deg	Common	
EM	M	---	Common	
FIN	---	ft	Common	Distance from fus. centerline to inboard flap station
FOUT	---	ft	Common	Distance from fus. centerline to outboard flap station
LV	ℓ_V	ft	Common	
SLM	λ	---	Common	
THETA	Θ	deg	Common	
ZV	Z_V	ft	Common	

Figure 11.21.4 shows a flowchart of the program, figure 11.21.5 shows a listing.

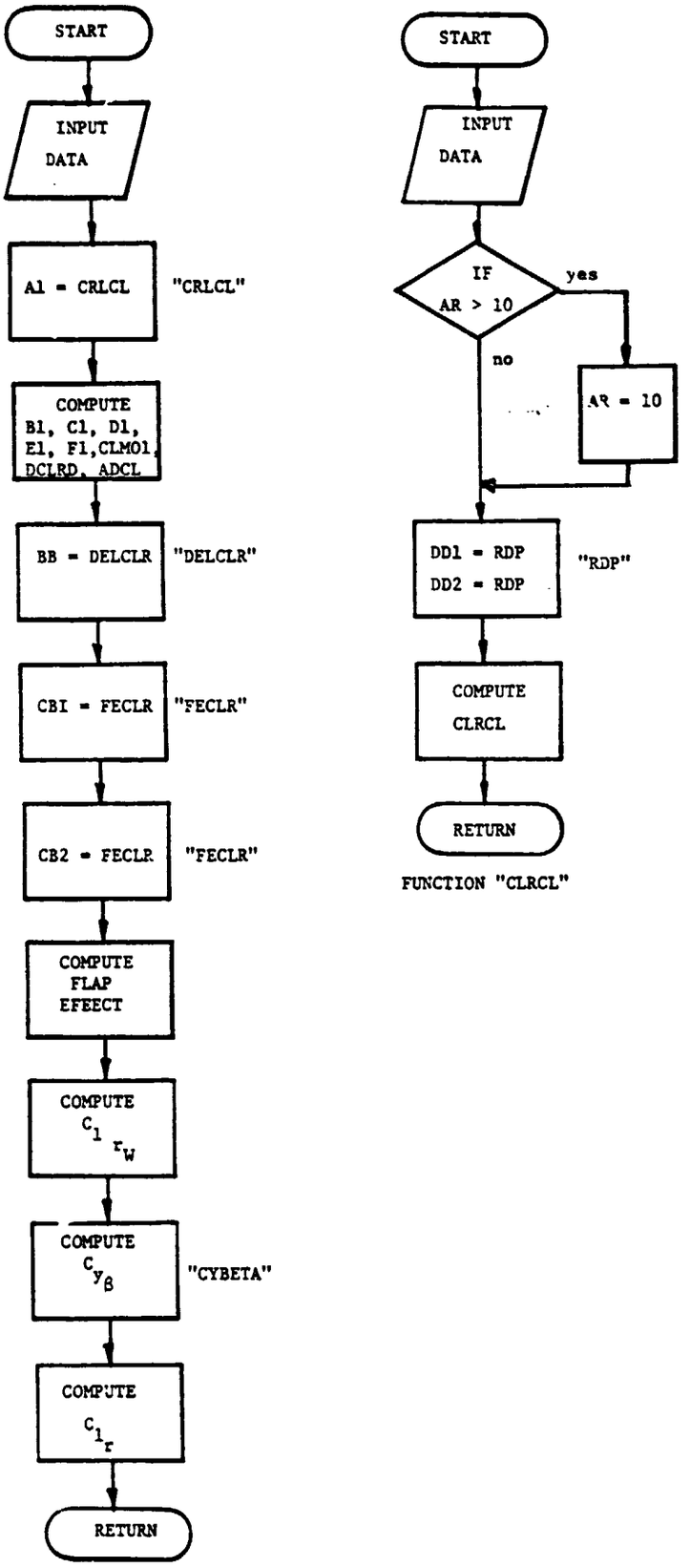

Figure 11.21.4: Flowchart of Subroutine "CLARE"

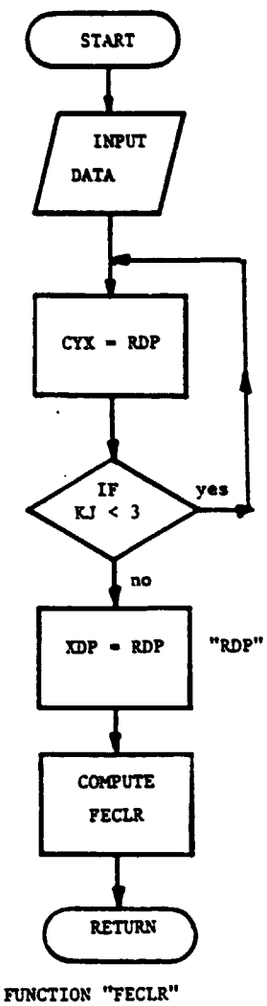

FUNCTION "FECLR"

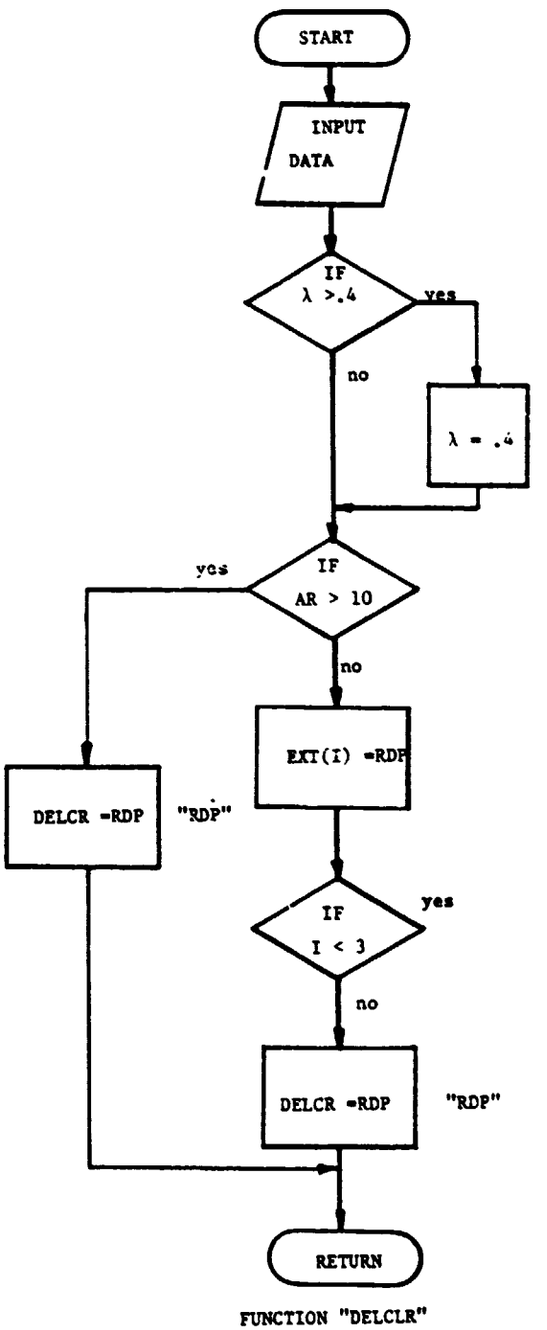

FUNCTION "DELCLR"

Figure 11.21.4: Continued

```
10C       SUBROUTINE CLARE(CLR)
20C       VARIATION OF ROLLING MOMENT
30C       COEFFICIENT WITH YAW
40        REAL LN,LV
50        COMMON /WING/ DLMC4,AR,SLM,B,CRCLW,CBARW,SW,CLAWP
60        COMMON /GEOM/ DIHD,ZW,SAH,XHMAC,ELINC
70        COMMON /FUS/ ELF,DFUS,HC,WC,LN,ELTH,HH,SO,R2I,LV,ZV
80        COMMON /FLITE/ ALPHA,EM,CL
90        THETA=0.
100       CFOC=.3
110       FIN=1.09
120       FOUT=11.2
130       DELFD=0.
140       RADD4=DLMC4/57.3
150       BM=SQRT(1.-(EM*COS(RADD4))**2)
160       A1=CLRCL(AR,DLMC4,SLM)
170       B1=(AR*BM)+2.*COS(RADD4)
180       C1=(SIN(RADD4)/COS(RADD4))**2/8.
190       D1=((1.-BM**2)*AR)/(2.*BM*B1)
200       E1=B1/(AR*BM+4.*COS(RADD4))
210       F1=(AR+2.*COS(RADD4))/(AR+4.*COS(RADD4))
220       CLM01=((1.+D1+E1*C1)/(1.+F1*C1))*A1
230       DCLRD=((3.1416*AR*SIN(RADD4))/(AR+4.*COS(RADD4)))/12.
240       ADCL=+.2747+1.4584*CFOC-.7406*CFOC**2
250       BB=DELCLR(AR,SLM)
260       CB1=FECLR(FOUT,B,SLM,AR)
270       CB2=FECLR(FIN,B,SLM,AR)
280       CB=CB1-CB2
290       CLRW=(CL*CLM01)+(DCLRD*DIHD/57.3)+(BB*THETA)
300      &+(CB*ADCL*DELFD)
310       ALPHAR=ALPHA/57.3
320       CALL CYBETA(CYB,CYBV)
330       CLRV=-(2./B**2)*(LV*COS(ALPHAR)+ZV*SIN(ALPHAR))
340      &*(ZV*COS(ALPHAR)-LV*SIN(ALPHAR))*CYBV
350       CLR=CLRW+CLRV
360       WRITE(6,1) CLR
370      1 FORMAT(//,10X,'***KU-FRL DEVELOPED SUBROUTINE: CLR
380      &***',//,10X,'CLR  =  ',F10.6,//,10X,'****
390      &END OF SUBROUTINE****')
400       STOP
410       END
420       FUNCTION CLRCL(A,SWP,TAPER)
430C       CLRCL CURVE FIT
440       DIMENSION AXF(10),GO(10,2),YF(2)
450       DATA AXF/1.,2.,3.,4.,5.,6.,7.,8.,9.,10./
460       DATA GO/2.,3.25,3.83,4.23,4.5,4.7,4.85,4.93,5.,5.,
470      &5.,6.7,7.5,8.05,8.45,8.75,9.0,9.17,9.28,9.35/
480       DATA YF/1.,2./
490       EE=1.0
500       IF(A.GT.10.) A=10.
```

Figure 11.21.5: Listing and Sample Printout of Subroutine "CLARE"

```
      DD1=RDP(1.0,1.0,A,1,2,10,10,EE,YF,AXF,GO)
      DD2=RDP(1.0,2.,A,1,2,10,10,EE,YF,AXF,GO)
      XEF=(TAPER**.764)*(DD2-DD1)+DD1
      DD3=.03*XEF
      DD4=.12+.0562*XEF
      CLRCL=(((.243+.9909*SWP+.02365*SWP**2)/144.837)*(DD4-
     &DD3))+DD3
      RETURN
      END
      FUNCTION DELCLR(A,TAPER)
C      DELTA CLR/THETA CURVE FIT
      DIMENSION AAXF(9),CLT(9,3),EXT(3),EEX(3)
      DATA AAXF/2.,3.,4.,5.,6.,7.,8.,9.,10./
      DATA CLT/-.0054,-.007,-.0082,-.0086,-.0085,-.00835,-.0085,-.009,-.00104,
     &-.0068,-.00855,-.01015,-.0114,-.0127,-.0128,-.013,-.0134,-.0145,
     &-.006,-.0097,-.0112,-.0126,-.014,-.0143,-.015,-.0158,-.0172/
      DATA EEX/0.,.2,.4/
      ET=1.
      IF(TAPER.GT..4) TAPER=.4
      IF(A.GT.10.) GO TO 2
      DO 1 KI=1,3
      EXT(KI)=RDP(1.0,EEX(KI),A,1,3,9,9,ET,EEX,AAXF,CLT)
    1 CONTINUE
      DELCLR=RDP(1.0,1.0,TAPER,1,1,3,3,ET,1.0,EEX,EXT)
      GO TO 3
    2 XX1=.0056-.0016*A
      XX2=-.0012-.0016*A
      DELCLR=((1.9646*TAPER**.737)*(XX2-XX1))+XX1
    3 RETURN
      END
      FUNCTION FECLR(FY,B,TAPER,A)
C      FLAP EFFECT CURVE FIT
      DIMENSION FXX(11,3),EXC(11),CYO(3),CYX(3)
      DATA EXC/0.,.1,.2,.3,.4,.5,.6,.7,.8,.9,1.0/
      DATA CYO/0.,.2,1.0/
      DATA FXX/0.,1.,2.2,3.5,4.7,5.3,5.,3.4,1.5,.3,0.,
     &0.,1.6,3.075,4.3,5.4,5.9,5.55,4.6,3.3,1.8,0.,
     &0.,1.9,3.5,4.7,6.,6.5,6.2,5.2,3.8,2.1,0./
      FF=1.
      Z=FY/(B/2.)
      DO 1 KJ=1,3
      CYX(KJ)=RDP(1.0,CYO(KJ),Z,1,3,11,11,FF,CYO,EXC,FXX)
    1 CONTINUE
      XDP=RDP(1.0,1.0,TAPER,1,1,3,3,FF,1.0,CYO,CYX)
      FECLR=(.001169*XDP)*(.23638*A**.63)
      RETURN
      END
```


Figure 11.21.5: Continued

11.21.4 RESULTS

To test the subroutine three flight conditions for Airplane A were used, see Table 11.21.2.

Table 11.21.1 Test Data (Ref. 11.21.2)

Flight Condition	M	α (deg)	C_L	C_{ℓ_r} (rad^{-1})
1 flaps up	.152	11.3	1.04	.260
2 flaps down 40^o	.150	5.9	1.04	.130
3 flaps up	.83	1.74	.265	.453

Comparison of the values given in Table 11.21.2 (from Reference 11.21.2) and those generated by the subroutine indicate the following. The subroutine is accurate for flap up conditions, with error reaching only 6%. With flaps down, however, the error becomes 15%. This value is acceptable, but it is not known exactly what causes it. One possibility is that the subroutine utilizes just a plain flap as a model. The type of flap on the aircraft could be the cause of error.

11.21.5 REFERENCES

11.21.1 Roskam, J. Methods for Estimating Stability and Control Derivatives of Conventional Subsonic Airplanes. Roskam Aviation & Engineering Corporation. Lawrence, KS.

11.21.2 Anon. Confidential Report.

11.22 VARIATION OF YAWING MOMENT COEFFICIENT WITH YAW RATE, C_{n_r}

11.22.1 DERIVATION OF EQUATIONS

Reference 11.22.1 indicates that this derivative can be estimated from:

$$C_{n_r} = C_{n_{r_W}} + C_{n_{r_V}} \tag{11.22.1}$$

The contribution of the vertical tail follows from:

$$C_{n_{r_V}} = \frac{2}{B^2} (\ell_V \text{ COS } \alpha + Z_V \text{ SIN } \alpha)^2 \, C_{y_{\beta_V}} \tag{11.22.2}$$

where: ℓ_V and Z_V are defined in figure 11.16.1,

$C_{y_{\beta_V}}$ follows from section 11.14.

The wing contribution may be estimated from a series of graphs in reference 11.22.1, based on experimental data, as a function of wing sweep, taper ratio, aspect ratio, lift-coefficient and zero-lift drag. A close examination of these graphs revealed that, for the class of airplanes considered in this report, the average contribution of the wing is 7.5 % in the negative sense. Since this is a relative small amount that does not vary very much for different wing planforms, this value was used to adjust the contribution of the vertical tail. The result is:

$$C_{n_r} = 1.075 \frac{2}{B^2} (\ell_V \text{ COS } \alpha + Z_V \text{ SIN } \alpha)^2 C_{y_{\beta_V}} \tag{11.22.3}$$

11.22.2 HANDCALCULATION

A handcalculation for Airplane A (for data see Appendix C) pro-

duced:

Section 11.14: $C_{y_{\beta_V}} = -0.137679 \ \text{rad}^{-1}$

For an angle of attack of $\alpha = 5$ deg then follows:

Eqn. 11.22.3: $C_{n_r} = -0.1403 \ \text{rad}^{-1}$

11.22.3 PROGRAM DESCRIPTION

Table 11.22.1 gives the variables used in the program, a flowchart is shown in figure 11.22.1, a listing plus a sample output is shown in figure 11.22.2.

TABLE 11.22.1: VARIABLES IN SUBROUTINE "CNR"

NAME	ENG. SYMBOL	DIMENSION	ORIGIN	REMARKS
ALPHA	α	rad	common	
B	b	ft	common	
CNR	C_{n_r}	rad^{-1}	---	
CYBV	$C_{y_{\beta_V}}$	rad^{-1}	"CYBETA"	
LV	ℓ_V	ft	common	
ZV	Z_V	ft	common	

For the flowchart and listing, see next page.

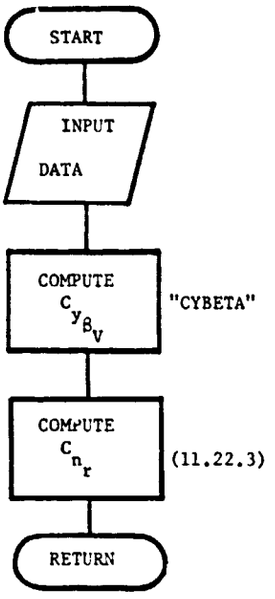

Figure 11.22.1 Flowchart of "CNR"

```
10          SUBROUTINE CNARE (CNR)
20          REAL LV
30          COMMON/WING/DLMC4,AR,SLM,B,CRCLW,CBARW,SW,CLAWP
40          COMMON/FLITE/ALPHA,EM,CL
50          COMMON/FUS/ELF,DFUS,HC,WC,LN,ELTH,HH,SO,R2I,LV,ZV
60          CALL CYBETA (CYBV,CYB,ARVEFF)
70          CNR=1.07*(2/(B**2))*((LV*COS(ALPHA)+ZV*SIN(ALPHA))**2)*CYBV
80          WRITE (6,1000) CNR
90    1000  FORMAT (10X,"CNR = ",F10.4," PER RADIAN"//)
100         RETURN
110         END
```

```
CNR =    -0.1403 PER RADIAN
```

Figure 11.22.2 Listing and sample ouput "CNR"

11.22.4 RESULTS

Reference 11.22.2 gives a test value of:

$$C_{n_r} = -0.143 \text{ rad}^{-1}$$

The computer program computed a value of:

$$C_{n_r} = -0.1403 \text{ rad}^{-1}$$

This is within 2 % accuracy, so it may be concluded that the program gives a correct estimation of this derivative.

11.22.5 REFERENCES

11.22.1	Roskam, J.	Methods for Estimating Stability and Control Derivatives of Conventional Subsonic Airplanes, Roskam Aviation & Engineering Corporation, Lawrence, KS, 1977.
11.22.2	Anon	Confidential Report.

11.23 LONGITUDINAL CONTROL DERIVATIVES

11.23.1 INTRODUCTION

This chapter describes the computation of the longitudinal control derivatives. The method that calculates lift increment with flap deflection is valid only for the so-called plain flap type. See Figure 11.23.1. It should be pointed out that this method is equally well suited for the computation of variation of lift coefficient for control surface deflection; therefore, it is written in a generalized form.

11.23.2 DERIVATION OF EQUATIONS

11.23.2.1 VARIATION OF LIFT COEFFICIENT WITH FLAP DEFLECTION

The derivation of this derivative is based on Reference 11.23.1, unless otherwise indicated. The layout of the lifting surface and the control surface is as indicated in Figure 11.23.1.

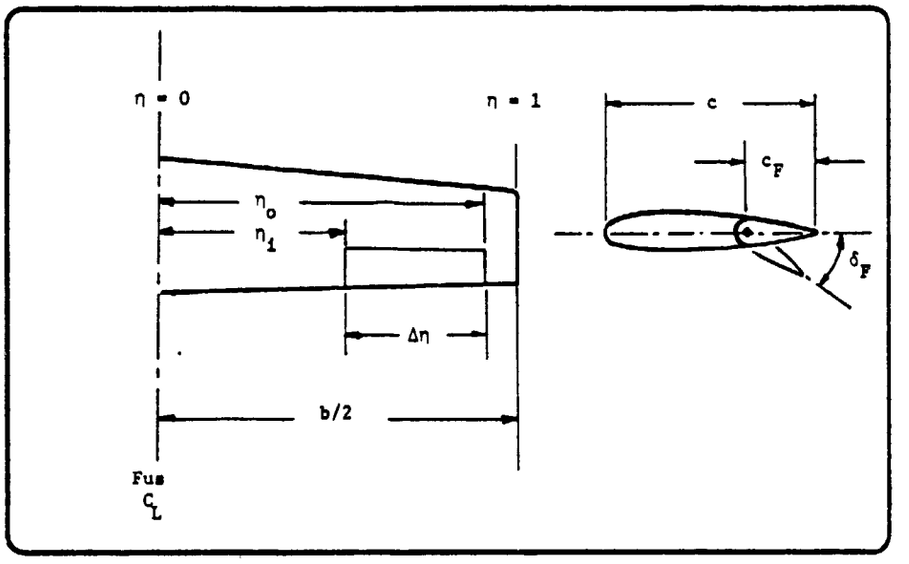

Figure 11.23.1: Geometric Parameters for Control Surface Flap

The derivative $C_{L_{\delta_F}}$ may be estimated from:

$$C_{L_{\delta_F}} = C_{\ell_{\delta_F}} \frac{C_{L_\alpha}|_M}{C_{\ell_\alpha}|_M} \frac{(\alpha_\delta)_{C_L}}{(\alpha_\delta)_{C_\ell}} K_b \qquad (11.23.1)$$

where:

$C_{L_\alpha}|_M$ is the lift-curve slope of the surface without flap deflection, obtained from Section 11.2.

$C_{\ell_\alpha}|_M$ is the section lift-curve slope, corrected for Mach number:

$$C_{\ell_\alpha}|_M = C_{\ell_\alpha} / \sqrt{1 - M^2} \qquad (11.23.2)$$

$\frac{(\alpha_\delta)_{C_L}}{(\alpha_\delta)_{C_\ell}}$ is the factor that takes three dimensional effects into account. It is given in Figure 11.23.2 as a function of aspect ratio, A_h, and the value of $(\alpha_\delta)_{C_L} = \frac{C_{\ell_{\delta_{flap}}}}{(C_{\ell_\alpha})_{surface}}$, based on experiments. If these data are not available, it may be obtained from the inset of Figure 11.23.3. Average values for c_F/c_w may be used.

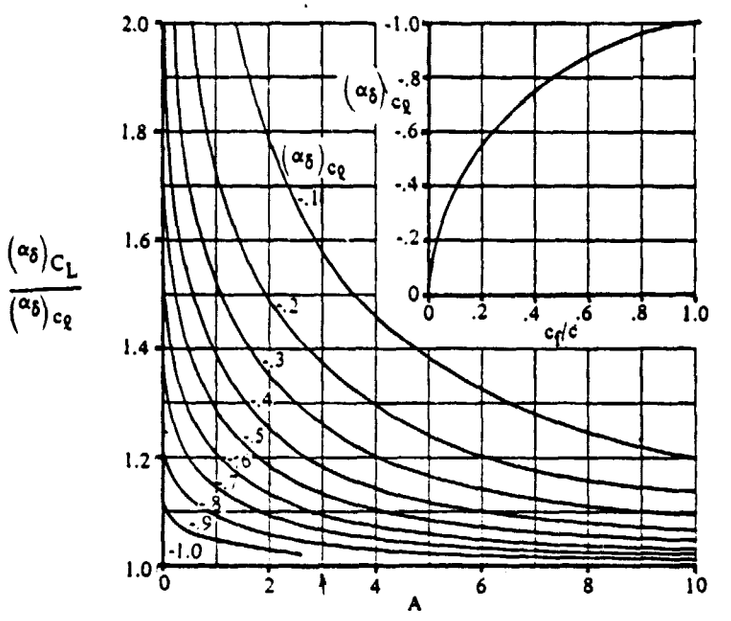

Figure 11.23 2: Influence of flap chord on flap effectiveness

K_b is a factor that takes the spanwise position of the flap into account. It can be obtained from Figure 11.23.3 as a function of taper ratio λ_h and span ratio $\eta = \frac{Y}{b/2}$.

$C_{\ell_{\delta_F}}$ is the section lift effectiveness of the flap; may be obtained from the following equation:

$$C_{\ell_{\delta_F}} = \frac{1}{\sqrt{1 - M^2}} \left[\frac{C_{\ell_{\delta_F}}}{\left(C_{\ell_{\delta_F}}\right)_{Theory}} \right] \left(C_{\ell_{\delta_F}}\right)_{Theory} \left(K'\right) \qquad (11.23.3)$$

where: $\left(C_{\ell_{\delta_F}}\right)_{Theory}$ is the theoretical lift effectiveness of the flap, obtained from Figure 11.23.4 as a function of c_F/c_w and thickness ratio.

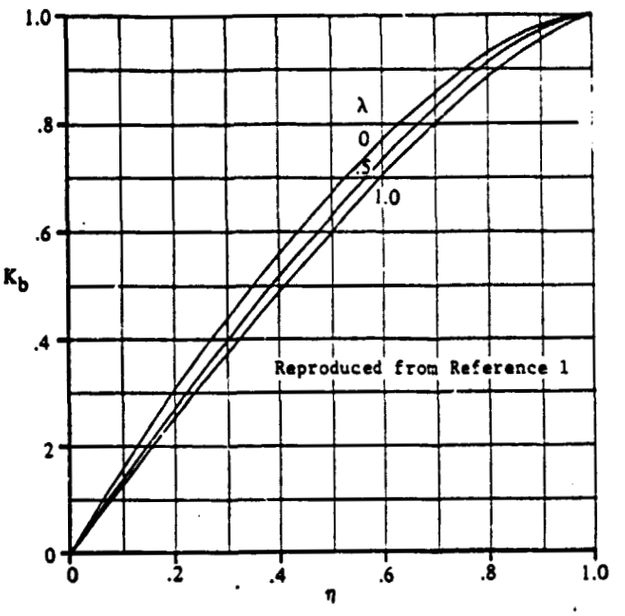

Figure 11.23.3: Span factor for inboard flaps

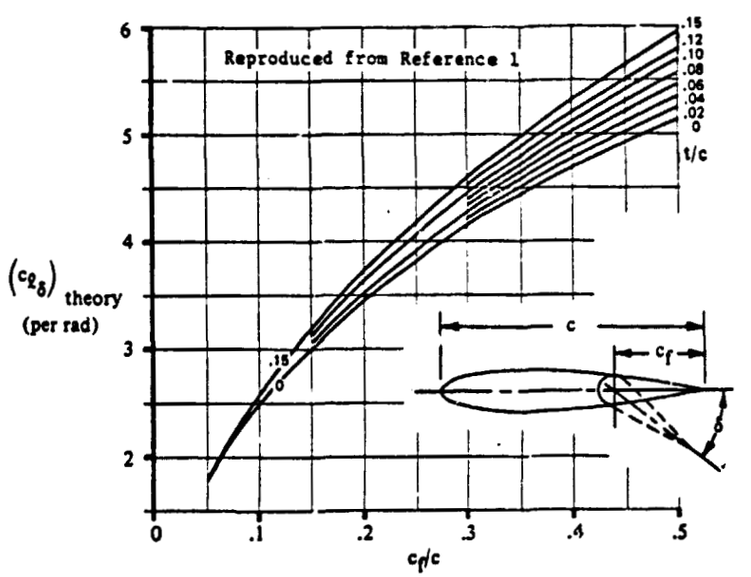

Figure 11.23.4: Theoretical lift effectiveness of plain trailing edge control flap

$\frac{C_{\ell_{\delta_F}}}{C_{\ell_{\delta_F}}}$ is an empirical correction factor based on experimental data; may be obtained from Figure 11.23.5 as a function of c_F/c_w and $(C_{\ell_\alpha})/(C_{\ell_\alpha})_{\text{Theory}}$.

The theoretical section lift curve, $(C_{\ell_\alpha})_{\text{Theory}}$ may be obtained from:

$$(C_{\ell_\alpha})_{\text{Theory}} = 6.28 + 4.7\ t/c\ (1 + .00375\phi_{TE}) \qquad (11.23.4)$$

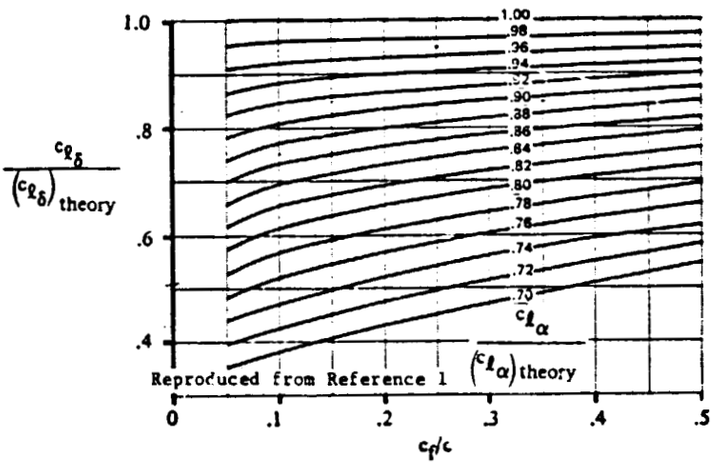

Figure 11.23.5: Empirical correction for lift effectiveness of plain trailing edge control flaps

K' is an empirical correction factor to the lift effectiveness at large deflections of the flap. May be obtained from Figure 11.23.6.

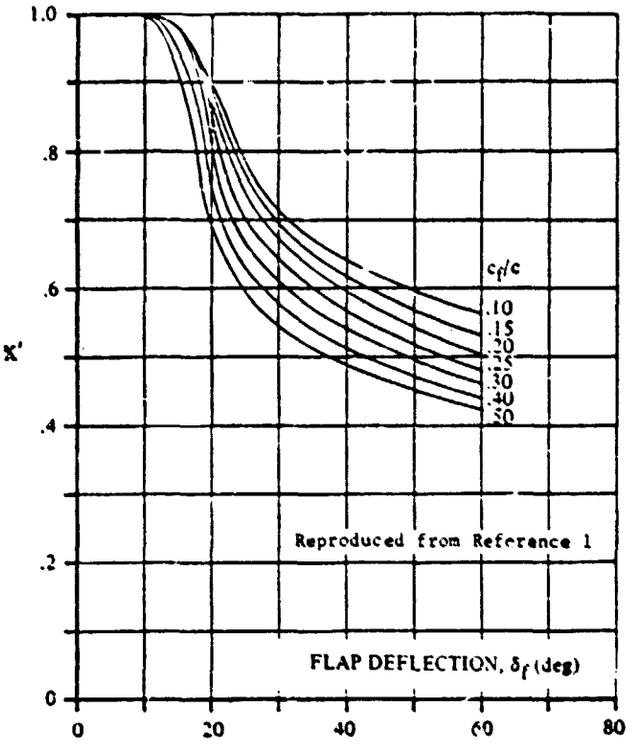

Figure 11.23.6: Empirical correction for lift effectiveness of plain trailing edge control flaps at high control deflections

To implement above method in a computer program, the following curve fittings were derived from the figures, using a HP 65 calculator.

For the inset of Graph 11.23.2:

$$(\alpha_\delta)_{C_\ell} = -.2747 - 1.4584 \times \left(\frac{c_F}{c_w}\right) + .7406 \times \left(\frac{c_F}{c_w}\right)^2 \qquad (11.23.5)$$

For Graph 11.23.3:

$$K_b = -.0091 + 1.5447 \times \eta - .5175 \times \eta^2 \qquad (11.23.6)$$

It should be noted that Equation (11.23.5) is accurate for $\lambda = .5$. However, due to the way K_b is calculated, the result will be accurate also for other values of the taper ratio.

For graph 11.23.4:

$$(C_{\ell_{\delta_{flap}}})_{theory} = 1.2572 + 12.8356\ c_f/c - 10.3788\ (c_f/c)^2 + A \qquad (11.23.7)$$

where: $A = 12.14\ t/c\ (c_f/c - .05)$ (11.23.8)

For graph 11.23.6:

$\delta_f < 10^0$: $K' = 1$ (11.23.9a)

$10^0 < \delta_f < 20^0$: $K' = .8014 + .01441\ \delta_f - .00246\ \delta_f^2 +$

$+ (-2.5\ c_f/c + 1.25).(.1672 - .0352\ \delta_f + .0019\ \delta_f^2)$ (11.23.9b)

$\delta_f > 20^0$: $K' = 1.0356 - .0217\ \delta_f + .000194\ \delta_f -$

$2.5\ (c_f/c - .5).(-.00154\ \delta_f + .231)$ (11.23.9c)

11.23.2.2 VARIATION OF PITCHING MOMENT COEFFICIENT WITH FLAP DEFEECTION.

This derivative will not be discussed, because of its minor importance in preliminary design work.

11.23.2.3 VARIATION OF LIFT COEFFICIENT WITH STABILIZER INCIDENCE

The derivative $C_{L_{i_H}}$ may be computed from:

$$C_{L_{i_H}} = C_{L_{\alpha_H}}\ S_H/S \qquad (11.23.10)$$

where: $C_{L_{\alpha_H}}$ is computed in section 11.2.

11.23.2.4. VARIATION OF PITCHING MOMENT WITH STABILIZER DEFLECTION

The derivative $C_{M_{i_H}}$ may be computed from:

$$C_{M_{i_H}} = - C_{L_{\alpha_H}} \bar{V}_H \qquad (11.23.11)$$

where: $C_{L_{\alpha_H}}$ is obtained from section 11.2.

11.23.2.5. VARIATION OF LIFT COEFFICIENT WITH ELEVATOR DEFLECTION

The derivative $C_{L_{\delta_E}}$ may be computed from:

$$C_{L_{\delta_E}} = C_{L_{\delta_F}} S_H/S \qquad (11.23.12)$$

where: $C_{L_{\delta_F}}$ is found from section 11.23.2.1

11.23.2.6. VARIATION OF PITCHING MOMENT WITH ELEVATOR DEFLECTION

The derivative $C_{M_{\delta_E}}$ may be found from:

$$C_{M_{\delta_E}} = - C_{L_{\delta_F}} \bar{V}_H \qquad (11.23.13)$$

11.23.3. HAND CALCULATION

In this section a handcalculation for the elevator of airplane B is presented. For data see Appendix C.

From section 11.2 follows the lift-curve slope:

$$C_{L_{\alpha_H}}\Big|_M = 3.959 \quad (\text{rad}^{-1})$$

The inset of figure 11.23.2 provides:

$$(\alpha_\delta)_{c_\ell} = -.75$$

Figure 11.23.2 then gives:

$$\frac{(\alpha_\delta)_{C_L}}{(\alpha_\delta)_{c_\ell}} = 1.02$$

The span correction factor follows from figure 11.23.3:

$$K_b = 0.88$$

The theoretical lift-curve slope follows from figure 11.23.3:

$$(c_{\ell_\alpha})_{th} = 6.713 \quad (rad^{-1})$$

The theoretical lift effectiveness follows from figure 11.23.4:

$$(c_{\ell_{\delta_f}})_{th} = 5.2 \quad (rad^{-1})$$

The correction factor in figure 11.23.5. is:

$$\frac{(c_{\ell_{\delta_f}})}{(c_{\ell_{\delta_f}})_{th}} = .89$$

The correction factor for flap deflection follows from figure 11.23.6:

$$K' = .88$$

Now the lift increment due to flap deflection may be computed according to equations 11.23.1 and 11.23.2:

$$C_{L_{\delta_F}} = 2.313 \quad (rad^{-1})$$

From equation 11.23.10 follows:

$$C_{L_{i_H}} = 0 \qquad (rad^{-1})$$

From equation 11.23.11 follows:

$$C_{M_{i_H}} = 0 \qquad (rad^{-1})$$

From equation 11.23.12 follows:

$$C_{L_{\delta_E}} = 0.612 \qquad (rad^{-1})$$

From equation 11.23.15 follows:

$$C_{M_{\delta_E}} = 1.797 \qquad (rad^{-1})$$

11.23.4 DESCRIPTION OF ROUTINE

Table 11.23.1 gives the variables as they are used in the computer routine. A flowchart of the routine is given in figure 11.23.7. A listing and a sample printout are given in figure 11.23.8.

TABLE 11.23.1: VARIABLE NAMES IN FUNCTION "FCLDF"

NAME	ENG, SYMBOL	DIMENSION	ORIGIN	REMARKS
ADCL	$(\alpha_\delta)_{c_\ell}$	---	---	
ADADCL	$\frac{(\alpha_\delta)_{C_L}}{(\alpha_\delta)_{c_\ell}}$	---	---	
CCLAM	$C_{L_{\alpha_M}}$	rad^{-1}	SLOPE	
CFOCS	c_F/c	---	common	

TABLE 11.23.1 Continued.

NAME	ENG. SYMBOL	DIMENSION	ORIGIN	REMARKS
CLATH	$(C_{\ell_\alpha})_{th}$	rad^{-1}	---	
CLCLAT	$\frac{(C_{\ell_\alpha})}{(C_{\ell_\alpha})_{th}}$	---	---	
CLCLDT	$\frac{C_{\ell_{\delta_f}}}{(C_{\ell_{\delta_f}})_{th}}$	---	---	
CLDFT	$(C_{\ell_{\delta_f}})_{th}$	rad^{-1}	---	
CPLAM	C_{ℓ_α}	rad^{-1}	---	
DFCON	δ_F	deg	common	
EM	M	---	common	
ETA1	η_i	---	common	
ETA0	η_o	---	common	
FAR	AR	---	common	dummy
FB	b	ft	common	dummy
FCLAP	C_{ℓ_α}	rad^{-1}	common	
FCLDF	$C_{L_{\delta_F}}$	rad_{-1}	---	
FDLMC4	$\Lambda_{\frac{1}{4}c}$	deg	common	dummy
FPHTE	ϕ_{TE}	deg	common	dummy
FSLM	λ	---	common	dummy
FTOC	t/c	---	common	dummy

TABLE 11.23.1 Continued

NAME	ENG. SYMBOL	DIMENSION	ORIGIN	REMARKS
KB	K_b	---	---	
KB1	K_{b_1}	---	---	
KB0	K_{b_0}	---	---	
KPRIM	K'	---	---	

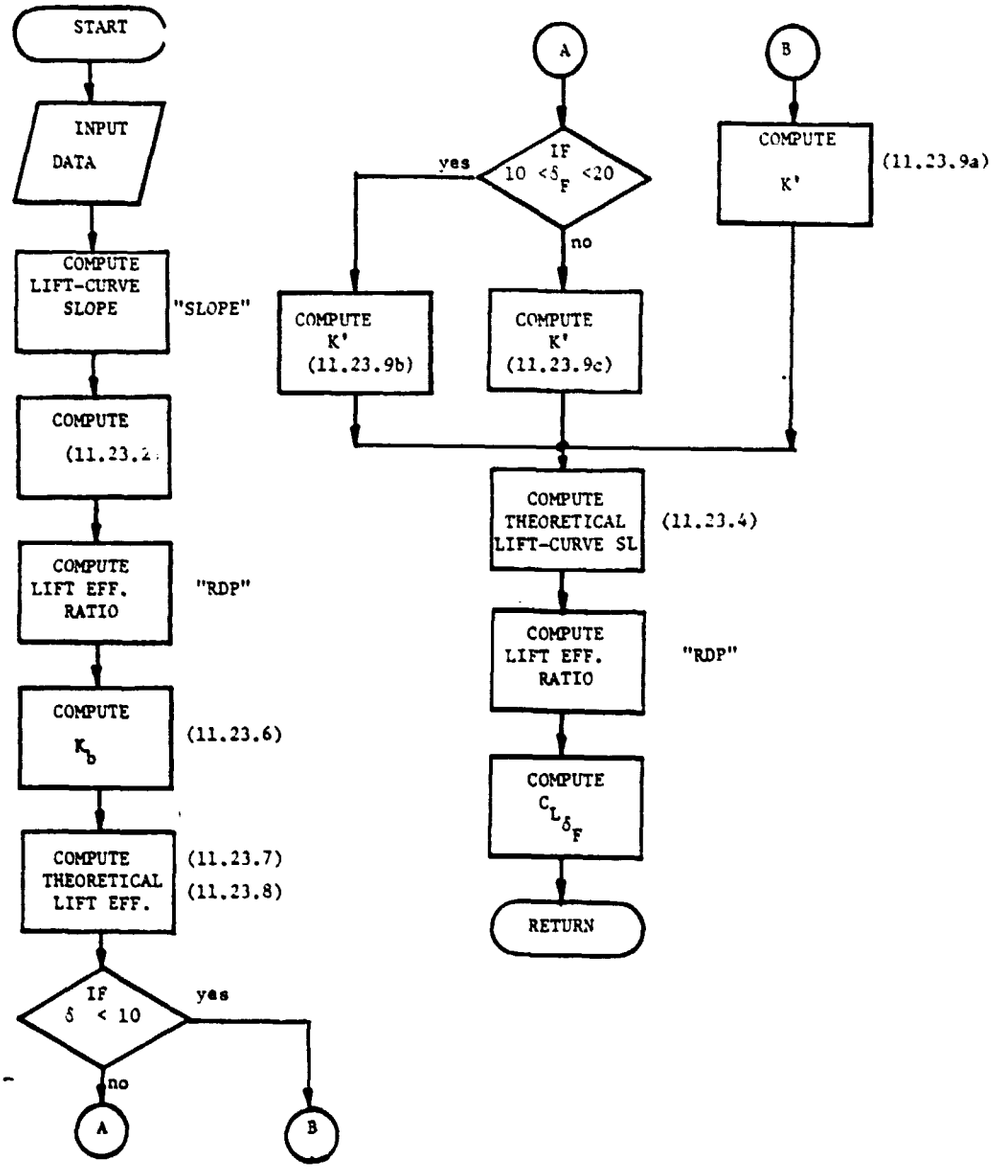

Figure 11.23.7: Flowchart of Subroutine "FCLDF"

```
10        FUNCTION FCLDF(CFOCS,ETA1,ETA0,DFCON,FAR,FSLM,FTOC,FPHTE,FCLAP,
20       &FDLMC4,FB)
30        COMMON/CONEFF/CLCLDT,CLDFT,KB,KPRIM,ADADCL,ADCL
60        REAL KB0,KB1,KB,KPRIM
80        COMMON/AERO/EM,RHO,TAS
90        COMMON/FUS/ELF,DFUS,HC,WC,LN,ELTH,HH,SO,R2I,LV,ZV
130     DATA ADCL/1./
140         CCLAM=SLOPE(FDLMC4,FSLM,FAR,EM,FCLAP)
150         CPLAM=FCLAP/(SQRT(1.-EM**2))
160C***** FIGURE 11.21.2 ***************************************************
170         IF (ADCL.EQ.1.) ADCL=-.2747-1.4584*CFOCS+.7406*CFOCS**2
180         DFCON=ABS(DFCON)
190       DIMENSION DD(8,11),VV(8),DDD(4),WW(11),UU(1)
200       DATA VV/-.1,-.2,-.3,-.4,-.5,-.6,-.8,-1./
210       DATA UU/1./
220       DATA WW/0.,1.,2.,3.,4.,5.,6.,7.,8.,9.,10./
230       DATA DD/2.,2.24,1.79,1.58,1.46,1.38,1.33,1.27,1.24,1.22,1.2,
240      &2.,1.73,1.495,1.37,1.3,1.24,1.2,1.17,1.16,1.15,1.14,
250      &2.,1.52,1.35,1.26,1.2,1.165,1.14,1.125,1.11,1.1,1.095,
260      &1.8,1.39,1.25,1.18,1.14,1.12,1.1,1.09,1.08,1.075,1.07,
270      &1.6,1.29,1.18,1.13,1.1,1.08,1.07,1.065,1.06,1.055,1.05,
280      &1.4,1.21,1.13,1.09,1.07,1.06,1.05,1.045,1.04,1.033,1.03,
290      &1.15,1.09,1.05,1.04,3*1.03,3*1.02,1.01,
300      &1.05,10*1./
310       ADADCL=RDP (1.,ADCL,FAR,1,8,10,8,UU,VV,WW,DD)
320C***** FIGURE 11.21.3 ***************************************************
330       KB0=-.0091+1.5447*ETA0-.5175*ETA0**2
340       KB1=-.0091+1.5447*ETA1-.5175*ETA1**2
350       KB=KB0-KB1
360       CLDFT=1.2572+12.8356*CFOCS-10.3788*CFOCS**2
370       CLDFT=CLDFT+12.14*FTOC*(CFOCS-.05)
380C***** FIGURE 11.21.6 ***************************************************
390       IF (DFCON.LE.10.) KPRIM=1.
400       IF (DFCON.GT.10..AND.DFCON.LE.20.) KPRIM=.8014+.0441*DFCON
410      &-.00246*DFCON**2+(-2.5*CFOCS+1.25)*(.1672-.0352*DFCON+
420      &.00186*DFCON**2)
430       IF (DFCON.GT.20.) KPRIM=1.0356-.0217*DFCON+.000194*DFCON**2-2.5*
440      &(CFOCS-.5)*(-.00154*DFCON+.231)
450C***** FIGURE 11.21.5 ***************************************************
460       DIMENSION DD1(8,10),VV1(8),DDD1(4),WW1(10),UU1(1)
470       DATA UU1/1./
480       DATA VV1/.72,.76,.8,.84,.88,.92,.96,1./
490       DATA WW1/.05,.1,.15,.2,.25,.3,.35,.4,.45,.5/
500       DATA DD1/.4,.425,.45,.475,.5,.52,.535,.55,.565,.575,
510      &.48,.525,.55,.565,.58,.61,.62,.63,.64,.65,
520      &.57,.62,.635,.65,.675,.685,.695,.715,.725,.735,
530      &.652,.69,.72,.73,.742,.752,.765,.775,.785,.795,
540      &.735,.77,.783,.8,.815,.825,.83,.835,.84,.85,
550      &.825,.845,.86,.87,.875,.88,.882,.885,.89,.9,
560      &.91,.92,.925,.927,.93,2*.935,.94,2*.95,
570      &10*1./
```


Figure 11.23.8: Listing and Sample Printout of Subroutine "FCLDF"

```
      CLATH=6.28+4.7*FTOC*(1.+.00375*FPHTE)
      CLCLAT=FCLAP/CLATH
      CLCLDT=RDP (1.,CLCLAT,CFOCS,1,8,10,8,UU1,VV1,WW1,DD1)
      FCLDF=CLCLDT*CLDFT*KPRIM*(CCLAM/CPLAM)*ADADCL*KB*(1./SQRT(1.-EM**2))
      WRITE (6,1020) FCLDF
 1020 FORMAT (10X,"LIFT DUE TO CONTROL DEFLECTION =   ",1F10.5,
     &"PER RADIAN"///)
      RETURN
      END
```

Figure 11.23.8: Continued

11.23.5 RESULTS

The lift and pitching moment variation with angle of incidence of the horizontal tail is not valid in this case. The variation with elevator deflection compares as follows with data from reference 11.23.2:

	"FCLDF"	Ref. 11.23.2	Error %
$C_{L_{\delta_E}}$	0.612	0.686	10
$C_{M_{\delta_E}}$	1.797	1.833	2

It may be concluded that the program works properly.

11.23.6 REFERENCES

11.23.1 Roskam, J. — Methods for Estimating Stability and Control Derivatives of Conventional Subsonic Airplanes, Roskam Aviation& Engineering Corp., Lawrence, KS, 1977

11.23.2 Greer, D. et al — Wind-tunnel Investigation of Static Longitudinal and Lateral Characteristics of a Full-scale Mockup of a Light Single-engine High-wing Airplane, NASA TN D-7149, May 1973.

11.24 AILERON STABILITY DERIVATIVES $C_{\ell_{\delta_A}}$, $C_{n_{\delta_A}}$, $C_{y_{\delta_A}}$

11.24.1 INTRODUCTION

$C_{\ell_{\delta_A}}$ is the most important of the aileron stability derivatives and it is calculated with a combination of the methods used in References 11.24.1 and 11.24.2. The program is valid for any wing aspect ratio between 4 and 16. Compressibility effects are taken into account, but the influence of wing taper ratio is neglected.

$C_{n_{\delta_A}}$ is much smaller than $C_{\ell_{\delta_A}}$; preferably it should be positive because this means that there are no adverse yaw effects in making turns. It is calculated with the method used in Reference 11.24.1; this part of the program is valid for any wing aspect ratio between 4 and 12. The wing taper ratio is an important variable in the determination of $C_{n_{\delta_A}}$, so it is not neglected here.

The value of $C_{y_{\delta_A}}$ is usually so small that it can be ignored; the program does not calculate this derivative.

11.24.2 CALCULATION OF $C_{\ell_{\delta_A}}$

A shortcoming of the method of Reference 11.24.1 is that only moderate wing aspect ratios are allowed in cases with β and κ close to one. With the method of Reference 11.24.2, which basically works the same way, wing aspect ratios from 6 to 16 can be taken. This method, however, does not take the effect of wing sweep angle into account or the effect of wing taper ratio. This latter influence is a minor one: for taper ratios normally used, the aileron rolling moment parameter is hardly dependent on taper ratio. The effect of sweep angle can be greater; therefore a mixture of both methods has been used to produce Fig. 11.24.1. According to Reference 11.24.2, it is valid

for aileron deflections up to 20 degrees.

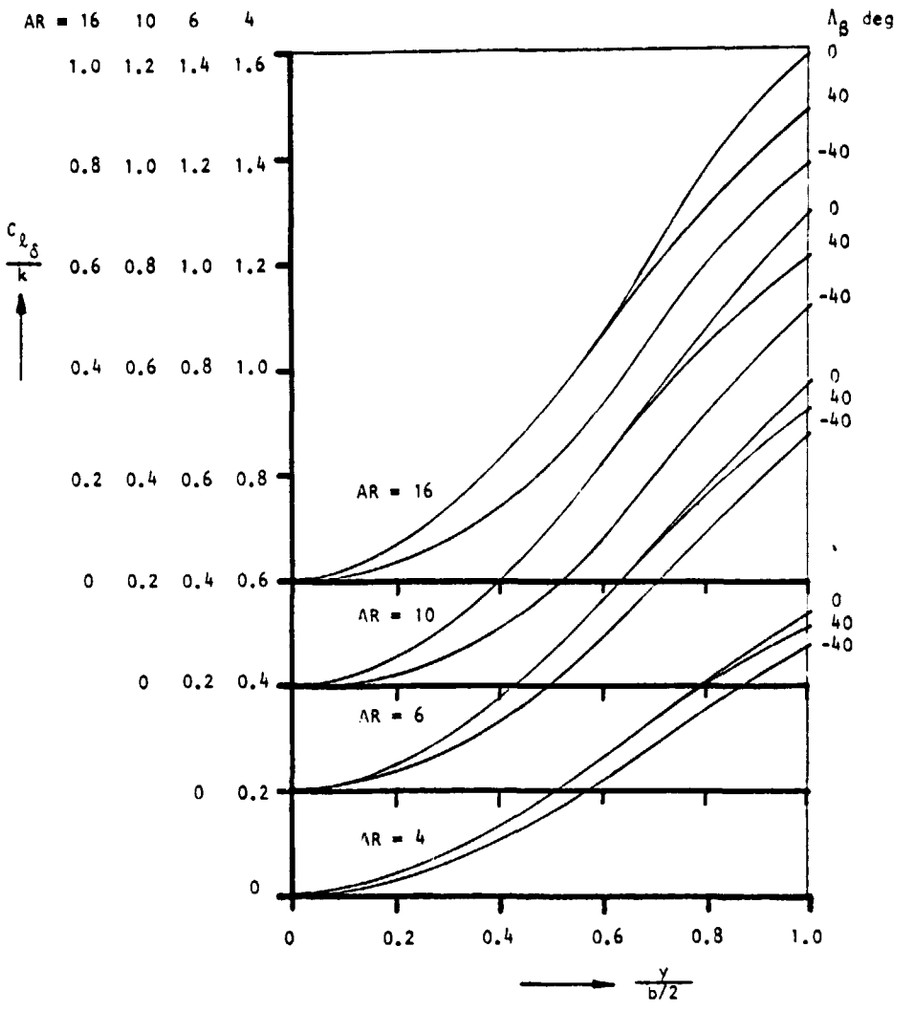

Figure 11.24.1: Determination of C_{ℓ_δ}/k

Fig. 11.24.1 is meant for full-chord controls; for partial-chord controls there is a correction factor, taken from Reference 11.24.2 and presented in Fig. 11.24.2. The variable Λ_β in Fig. 11.24.1 is computed as follows:

$$\Lambda_\beta = \arctan\left(\frac{\tan\Lambda_{\bar{c}/4}}{\beta}\right) \qquad (11.24.1)$$

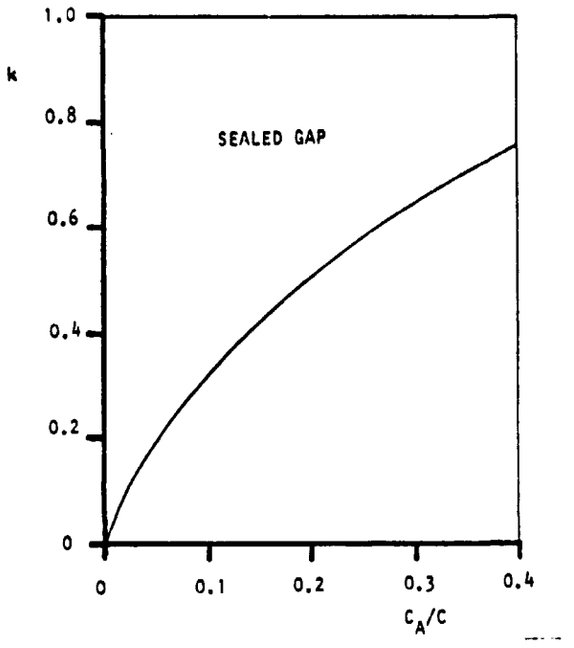

Figure 11.24.2: Correction for Flap-Span Effect

The effect of partial-span controls is taken into account by using Fig. 11.24.1 two times, one time for the inboard lateral coordinate of the aileron and another for the outboard lateral coordinate. The difference in the results is then the actual aileron rolling moment parameter.

It is assumed that the effectiveness of the right aileron is equal to that of the left aileron, so Fig. 11.24.1 gives the total aileron rolling moment parameter. The aileron deflection associated with it is defined as:

$$\delta_A = \tfrac{1}{2}(\delta_L - \delta_R) \qquad (11.24.2)$$

in which a positive control deflection is trailing edge down. $C_{\ell_{\delta_A}}$ is found as the product of $\frac{C_{\ell_\delta}}{k}$ (from Fig. 11.24.1) and k (from Fig. 11.24.2)

11.24.3 CALCULATION OF $C_{n_{\delta_A}}$

This derivative is calculated with the metho. in Reference 11.24.1, according to:

$$C_{n_{\delta_A}} = K\, C_L\, C_{\ell_{\delta_A}} \qquad (11.24.3)$$

The factor K is a correlation constant which depends on wing aspect ratio, taper ratio and inboard location of the aileron; it is given in Fig. 11.24.3. The lines for A = 12 are the result of extrapolating Fig. 11.3 in Reference 11.24.1.

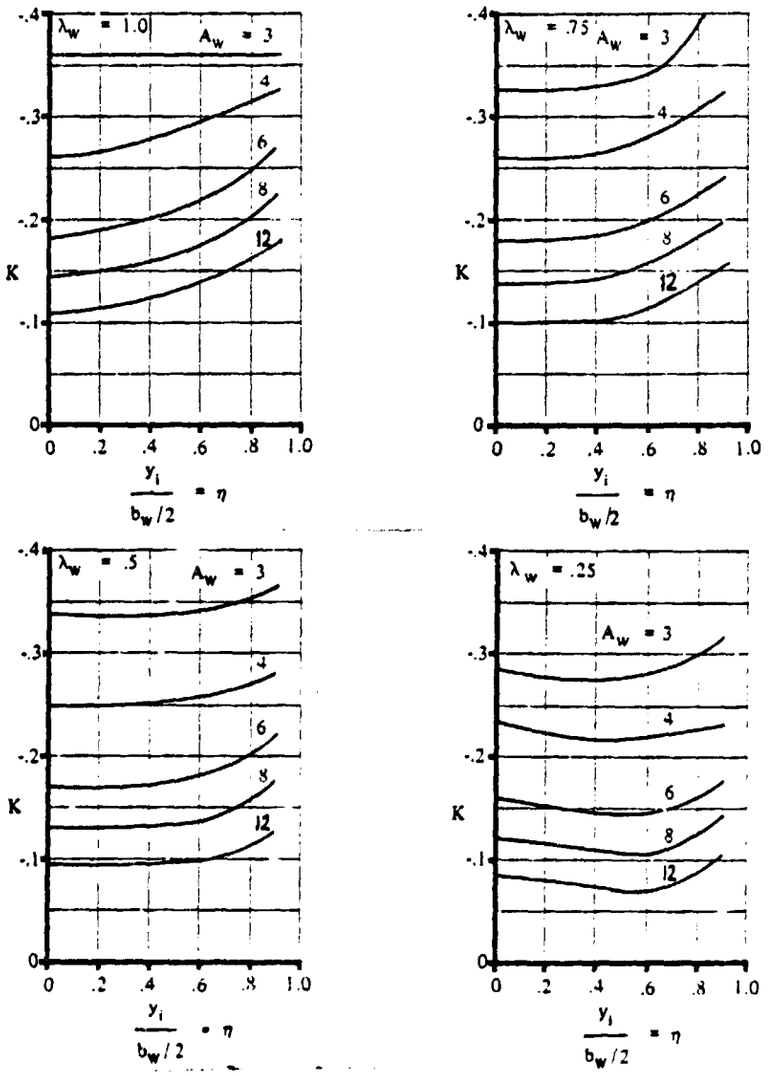

Figure 11.24.3: Correlation Consta... for $C_{n_{\delta_A}}$

This figure is only valid for ailerons which extend to the wingtip. To calculate $C_{n_{\delta_A}}$ for ailerons which do not extend to the wingtip, Eqn. (11.24.1) must be used two times: one time for an imaginary aileron which extends from the inboard location of the actual aileron to the tip and one time for another imaginary aileron which extends from the outboard location of the actual aileron to the tip. Subtracting the $C_{n_{\delta_A}}$ of the second imaginary aileron from that of the first one gives $C_{n_{\delta_A}}$ of the actual aileron. It is not enough to take the difference in the correlation constants of the two imaginary ailerons; $C_{\ell_{\delta_A}}$ must also be calculated for each one.

The value of C_L in Eqn. (11.24.1) follows from:

$$C_L = \frac{W}{\bar{q}S} \tag{11.24.4}$$

so it is just the steady state lift coefficient.

11.24.4 PROGRAM DESCRIPTION

The program consists of two parts: in the first part $C_{\ell_{\delta_A}}$ is calculated and in the second, $C_{n_{\delta_A}}$. The $C_{\ell_{\delta_A}}$ part is valid for wing aspect ratios between 4 and 16; if the airplane under consideration has a wing aspect ratio outside this range, a default value of either 4 or 16 is used. The $C_{n_{\delta_A}}$ part works the same way for wing aspect ratios between 4 and 12.

$C_{\ell_{\delta_A}}$ is calculated according to the method described in section 11.24.2. Fig. 11.24.1 is put in as a number of points; interpolation between these points is done by the function RDP (see Appendix B). For Fig. 11.24.2 an HP-65 curve fitting routine has been used, resulting in:

$$k = 1.3798 \left(\frac{c_A}{c}\right)^{.6388} \tag{11.24.5}$$

The aileron rolling moment parameter is calculated three times: one time for the inboard location of the aileron, one time for the outboard location and one time for the wingtip. Following this, the $C_{\ell_{\delta_A}}$ of an aileron extending from the inboard location of the actual aileron to the wingtip is calculated and also the $C_{\ell_{\delta_A}}$ for an aileron extending from the outboard location of the actual aileron. Calculating it in this way is not very efficient, but it is necessary for the calculation of $C_{n_{\delta_A}}$, as pointed out in the previous section.

$C_{n_{\delta_A}}$ is calculated according to the method described in section 11.24.3. Fig. 11.24.3 is put in in the same way as Fig. 11.24.1. The correlation constant is calculated two times: one time for the inboard location of the aileron and one time for the outboard location. The $C_{\ell_{\delta_A}}$ contributions in Eqn. (11.24.1) are taken from the first part of the program.

A list of variables is given in Table 11.24.1 and a flowchart in Fig. 11.24.4, while Fig. 11.24.5 gives a listing and sample output.

11.24.5 HAND CALCULATION

A hand calculation has been done on airplane A for which data are presented in Appendix D. Since it is rather tedious to interpolate Fig. 11.24.1 by hand for different aspect ratios and since this airplane has a wing aspect ratio close to 6, lines for A = 6 are used. The $C_{\ell_{\delta_A}}$ value obtained with this method is 0.1411 while the computer gives a value of 0.1344. These values are close enough to conclude that the program works alright. The actual value for this airplane in this flight condition (M = .152, C_L = 1.04) is 0.1401, so the computer value comes within 5 percent.

The hand calculation for $C_{n_{\delta_A}}$ comes to a value of -0.0231, using λ_w = .5 and A_w = 6 in Fig. 11.24.3. The computer generates a value of -0.02419, so it can be concluded that this part of the program also works right. The actual value for this airplane could not be found, but $C_{n_{\delta_A}}$ for another version of this

airplane for this flight condition is about -0.032. These results don't compare very well, but they are not the same configuration so it is hard to draw conclusions from this.

TABLE 11.24.1 VARIABLE LIST FOR SUBROUTINE "AILDER"

NAME	ENG. SYMBOL	DIMENSION	ORIGIN	REMARKS
ALCDRA	c_a/c	---	common	
AR	AR	---	common	
BETA	β	---	---	
CLDA	$C_{\ell_{\delta_A}}$	rad^{-1}	---	
CLDA0	$C_{\ell_{\delta_{A0}}}$	rad^{-1}	---	
CLDA1	$C_{\ell_{\delta_{A1}}}$	rad^{-1}	---	
CLDLKT	$\frac{C_{\ell\delta}}{k}_{tip}$	rad^{-1}	---	
CLDLK0	$\frac{C_{\ell_\delta}}{k}_{0}$	rad^{-1}	---	
CLDLK1	$\frac{C_{\ell\delta}}{k}_{1}$	rad^{-1}	---	
CL1	C_{L_1}	---	common	
CNDA	$C_{n_{\delta_A}}$	rad_{-1}	---	
CNDA0	$C_{n_{\delta_{A0}}}$	rad^{-1}	---	
CNDA1	$C_{n_{\delta_{A1}}}$	rad^{-1}	---	

TABLE 11.24.1 CONTINUED

NAME	ENG. SYMBOL	DIMENSION	ORIGIN	REMARKS
COCOO	K_0	---	---	dummy
COCO1	K_1	---	---	dummy
DLMC4	$\Lambda_{\frac{1}{4}c}$	deg	common	
EFPAR	k	---	---	dummy
EM	M	---	common	
ETA0A	η_0	---	common	
ETA1A	η_1	---	common	
LABE	Λ_β	deg	---	
RAD	---	---	---	
RLMC4	$\Lambda_{\frac{1}{4}c}$	rad	---	
SLM	λ	---	common	
TIP	---	---	---	dummy

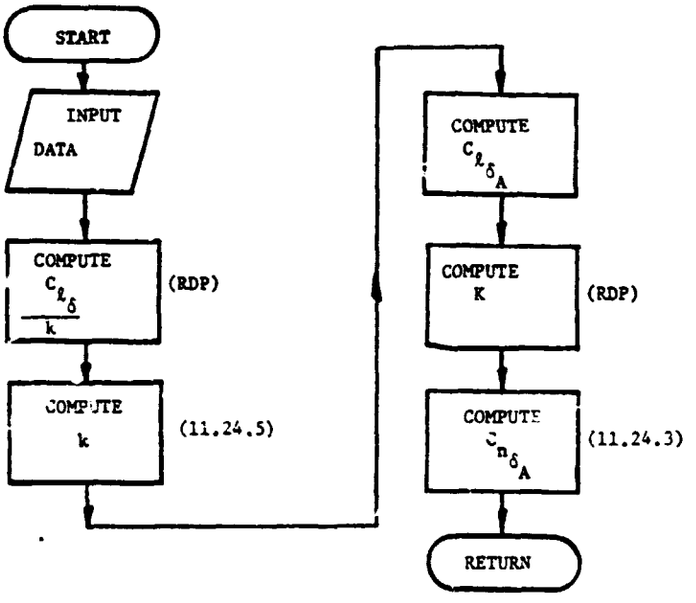

Figure 11.24.4 Flowchart of "AILDER"

```
10C**** SUBROUTINE AILDER (CLDA,CNDA)
20C****
30C**** THIS PART OF THE SUBROUTINE CALCULATES THE ROLLING
40C**** MOMENT DUE TO AILERON DEFLECTION DERIVATIVE
50C****
60       REAL LABE
70       DIMENSION DD1(32,3),UU1(4),VV1(3),WW1(8),DDD(4)
80       DATA UU1/4.,6.,10.,16./
90       DATA VV1/-40.,0.,40./
100       DATA WW1/.2,.3,.4,.5,.6,.8,.9,1./
110       DATA DD1/.024,.056,.100,.154,.217,.357,.421,.480,
120      &.032,.071,.124,.195,.284,.492,.589,.680,
130      &.017,.050,.100,.173,.269,.513,.620,.720,
140      &.030,.073,.133,.214,.328,.603,.710,.795,
150      &.038,.076,.127,.189,.260,.410,.476,.540,
160      &.042,.098,.170,.256,.359,.582,.684,.780,
170      &.050,.110,.192,.295,.420,.678,.794,.900,
180      &.060,.130,.220,.333,.466,.780,.805,1.00,
190      &.038,.076,.127,.189,.260,.405,.461,.515,
200      &.042,.098,.170,.256,.359,.560,.647,.730,
210      &.050,.110,.192,.295,.420,.645,.734,.815,
220      &.060,.130,.220,.333,.466,.708,.810,.900/
230      DATA EM,ALCORA,ETA0A,ETA1A/.152,.22,.792,.544/
240      DATA DLMC4,AR,CL1,SLM/13.,5.74,1.04,.564/
250       BETA=SQRT(1.-EM**2.)
260       RAD=57.29578
270       RLMC4=DLMC4/RAD
280       LABE=RAD*ATAN(SIN(RLMC4)/(COS(RLMC4)*BETA))
290       IF (AR.GT.16.) AR=16.
300       IF (AR.LT.4.) AR=4.
310       TIP=1.
320       CLDLKD=RDP(AR,LABE,TIP,4,3,8,32,UU1,VV1,WW1,DD1)
330       CLDLK0=RDP(AR,LABE,ETA0A,4,3,8,32,UU1,VV1,WW1,DD1)
340       CLDLK1=RDP(AR,LABE,ETA1A,4,3,8,32,UU1,VV1,WW1,DD1)
350       EFPAR=1.3798*ALCORA**.6388
360       CLDA1=(CLDLKD-CLDLK1)*EFPAR
370       CLDA0=(CLDLKD-CLDLK0)*EFPAR
380       CLDA=CLDA1-CLDA0
390       WRITE (6,5)
400       WRITE (6,25) CLDA
410    25 FORMAT (10X,"CLDA = ",1F10.5," PER RADIAN"/)
420C****
430C**** THIS PART OF THE SUBROUTINE CALCULATES THE YAWING
440C**** MOMENT DUE TO AILERON DEFLECTION DERIVATIVE
450C****
460       DIMENSION UU2(4),VV2(4),WW2(5),DD2(20,4)
470       DATA UU2/.25,.5,.75,1./
480       DATA VV2/4.,6.,8.,12./
490       DATA WW2/0.,.4,.6,.8,.9/
500       DATA DD2/-.234,-.217,-.220,-.226,-.231,
```

Figure 11.24.5: Listing and Sample Output Subroutine "AILDER"

```
     &-.250,-.252,-.257,-.270,-.280,-.260,-.261,-.279,-.306,-.321,
     &-.260,-.275,-.293,-.314,-.325,-.160,-.156,-.155,-.161,-.176,
     &-.170,-.170,-.180,-.202,-.220,-.179,-.183,-.199,-.223,-.240,
     &-.182,-.201,-.219,-.248,-.270,-.120,-.110,-.105,-.125,-.143,
     &-.129,-.131,-.135,-.158,-.175,-.137,-.140,-.146,-.182,-.197,
     &-.144,-.158,-.175,-.202,-.224,-.082,-.074,-.070,-.085,-.105,
     &-.095,-.096,-.099,-.111,-.126,-.100,-.101,-.112,-.137,-.153,
     &-.108,-.122,-.137,-.161,-.175/
      IF (AR.GT.12.) AR=12.
      COCOO=RDP(SLM,AR,ETAOA,4,4,5,20,UU2,VV2,WW2,DD2)
      COCO1=RDP(SLM,AR,ETA1A,4,4,5,20,UU2,VV2,WW2,DD2)
      CNDAO=COCOO*CLDAO
      CNDA1=COCO1*CLDA1
      CNDA=(CNDA1-CNDAO)*CL1
      WRITE (6,30) CNDA
   30 FORMAT (10X,"CNDA = ",1F10.5," PER RADIAN"///)
      STOP
      END
```

Figure 11.24.5: Continued

11.24.6 REFERENCES

11.24.1 Roskam, J. Methods for Estimating Stability and Control Derivatives of Conventional Subsonic Airplanes, Roskam Aviation & Engineering Corporation, Lawrence, KS, 1977.

11.24.2 Dommash, D.O. Sherby, S.S. Connolly,T.F. Airplane Aerodynamics, Pitman Publishing Corporation, New York, 1967

11.25 DIRECTIONAL CONTROL DERIVATIVES $C_{y_{\delta_R}}$, $C_{\ell_{\delta_R}}$ AND $C_{n_{\delta_R}}$

11.25.1 INTRODUCTION

This chapter describes the computation of the directional control derivatives. The method is according to Reference 11.25.1. Since it relies on computations in Chapter 11.21 for control-surface effectiveness, it is subject to the limitations of those calculations.

11.25.2 DERIVATION OF EQUATIONS

11.25.2.1 $C_{y_{\delta_R}}$ Variation of sideforce coefficient with rudder deflection. This derivative may be estimated from:

$$C_{y_{\delta_R}} = - C_{L_{\alpha_V}} \left(\frac{(\alpha_\delta)_{C_L}}{(\alpha_\delta)_{C_\ell}} \right) (\alpha_\delta)_{C_\ell} K' K_b \left(\frac{S_v}{S} \right) M_v \qquad (11.25.1)$$

Where:

$C_{L_{\alpha_V}}$ is the vertical tail lift curve slope, computed as in Chapter 2.

Note: The effective aspect ratio of the vertical tail, $AR_{V_{EFF}}$, used in the calculation of $C_{L_{\alpha_V}}$ is obtained from Chapter 11.12.

$\frac{(\alpha_\delta)_{C_L}}{(\alpha_\delta)_{C_\ell}}$ is the ratio of three dimensional flap-effectiveness to two dimensional flap-effectiveness. It may be obtained from Chapter 11.21.

$(\alpha_\delta)_{C_\ell}$ is the theoretical value of the two-dimensional flap-effectiveness parameter, may be obtained from Chapter 11.21.

K' is a correction factor for high control-surface angles, obtained from Chapter 11.21.

K_b is a correction factor for control-surface-span, obtained from Chapter 11.21.

11.25.2.2 $C_{\ell_{\delta_R}}$ variation of the rolling moment coefficient with rudder deflection.

This derivative may be computed as follows:

$$C_{\ell_{\delta_R}} = C_{y_{\delta_R}} \left(\frac{Z_V \cos\alpha - \ell_V \sin\alpha}{b} \right) \qquad (11.25.2)$$

Where:

$C_{y_{\delta_R}}$ follows from section 11.25.2.1

Z_V and ℓ_V are defined in Figure 11.14.1

11.25.2.3 $C_{n_{\delta_R}}$ variation of yawing moment coefficient with rudder deflection.

This derivative may be computed as follows:

$$C_{n_{\delta_R}} = - C_{y_{\delta_R}} \left(\frac{\ell_V \cos\alpha + Z_V \sin\alpha}{b} \right) \qquad (11.25.3)$$

Where:

$C_{y_{\delta_R}}$ follows from section 11.25.2.1

Z_V and ℓ_V are defined in Figure 11.14.1.

11.25.3 HAND CALCULATION

Following is a hand calculation for airplane A , the data are given in Appendix C . With the method of Chapter 11.21, it follows:

$$C_{y_{\delta_R}} = 0.151 \ (\text{rad}^{-1})$$

With this it follows:

$$C_{\ell_{\delta_R}} = 0.0206 \ (\text{rad}^{-1})$$

$$C_{n_{\delta_R}} = -0.0654 \ (\text{rad}^{-1})$$

11.25.4 RESULTS AND COMPARISON

The computer generated values of, respectively:

$$C_{y_{\delta_R}} = 0.15050 \ (\text{rad}^{-1})$$

$$C_{\ell_{\delta_R}} = 0.02056 \ (\text{rad}^{-1})$$

$$C_{n_{\delta_R}} = -0.06520 \ (\text{rad}^{-1})$$

This compares as follows to data given in reference 11.25.2:

$$C_{y_{\delta_R}} = 0.1318 \ (\text{rad}^{-1})$$

$$C_{\ell_{\delta_R}} = 0.0168 \ (\text{rad}^{-1})$$

$$C_{n_{\delta_R}} = -0.0602 \ (\text{rad}^{-1})$$

or: the computer program overpredicts $C_{y_{\delta_R}}$ by 12.4%, overpredicts $C_{\ell_{\delta_r}}$ by 18% and overpredicts $C_{n_{\delta_R}}$ by 7.7%.

11.25.5 DESCRIPTION OF COMPUTER PROGRAM

A list of variables is given in Table 11.25.1, while Figure 11.25.1 provides a flowchart. Figure 11.25.2 shows the listing of the program, including a sample print-out. The program is straightforward.

TABLE 11.25.1: VARIABLE NAMES IN SUBROUTINE "RUDDER"

NAME	ENG. SYMBOL	DIMENSION	ORIGIN	REMARKS
ADADCL	$\frac{(\alpha_\delta)_{C_L}}{(\alpha_\delta)_{C_\ell}}$	---	Function "FCLDF"	
ADCL	$(\alpha_\delta)_{C_\ell}$	---	Function "FCLDF"	
ALPHA	α	rad	Common	
ARV	AR_v	---	Common	
ARVEFF	AR_{EFF_v}	---	Subr. "CYB"	
B	b	ft	Common	
BVT	b_v	ft	Common	
CFOCV	C_f/C_v	---	Common	
CLAVP	$C_{\ell_{\alpha_V}}$	rad^{-1}	Function "SLOPE"	
CLAVT	$C_{L_{\alpha_V}}$	rad^{-1}	---	
CLDRUD	---	---	---	Dummy
CLDR	$C_{\ell_{\delta_R}}$	rad^{-1}	---	
CNDR	$C_{n_{\delta_R}}$	rad^{-1}	---	
CYDR	$C_{y_{\delta_R}}$	rad^{-1}	---	
DLMC4V	$\Lambda_{c/4_V}$	deg	Common	
DRUD	δ_R	deg	Common	
EM	M	---	Common	
ETAOV	η_{oV}	---	Common	

TABLE 11.25.1: VARIABLE NAMES IN SUBROUTINE "RUDDER"
(Continued)

NAME	ENG. SYMBOL	DIMENSION	ORIGIN	REMARKS
ETA1V	η_{i_v}	---	Common	
ETAUT	η_v	---	Common	
KB	K_b	---	Function "FCLOF"	
KPRIM	K'	---	Function "FCLOF"	
LV	ℓ_v	ft	Common	
PHTER	ϕ_{TE_v}	deg	Common	
SLMV	λ_v	---	Common	
SVT	S_v	ft^2	Common	
SW	S_w	ft^2	Common	
TOCV	t/c_v	---	Common	
ZV	Z_v	ft	Common	

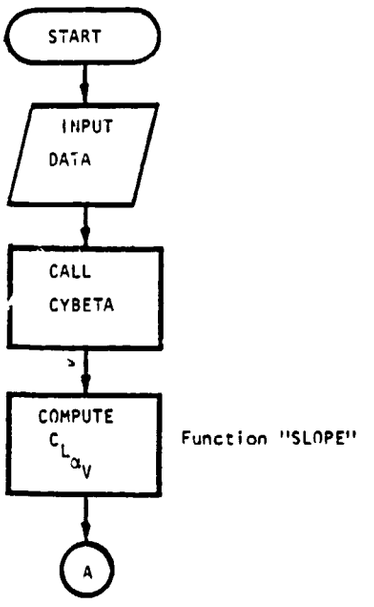

Figure 11.25.1: Flowchart of Subroutine "RUDDER"

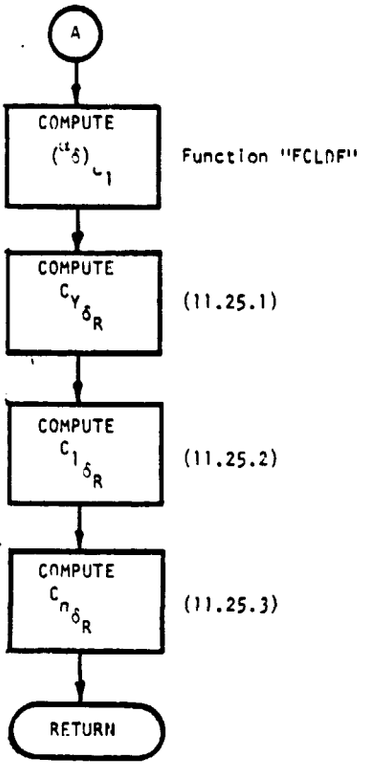

Figure 11.25.1: Continued

```
10C       SUBROUTINE RUDDRER (CYDR,CLDR,CNDR)
20        REAL KB,LV,KPRIM
30     DATA EM,RHO,TAS/.2,0.,0./
40     DATA ALPHA,CL,ETAVT/0.,0.,.98/
50     DATA CFOCV,ETA1V,ETAOV,DRUD,TOCV,PHTER/.2045,0.,.778,30.,.1,6./
60        COMMON/VERT/DLMC4V,ARV,SLMV,BVT,CBARVT,SVT,CLAVP,CRCLVT
70        COMMON/FUS/ELF,DFUS,HC,WC,LN,ELTH,HH,SDO,R2I,LV,ZV
80        COMMON/FLITE/ALPHA,CL
90        COMMON/AERO/EM,RHO,TAS
100       COMMON/WING/DLMC4,AR,SLM,B,CRCLW,CBARW,SW,CLAWP
102       COMMON/CONEFF/CLCLDT,CLDFT,KB,KPRIM,ADADCL,ADCL
105       CALL CYBETA (CYB,CYBV,ARVEFF)
110       CLAVT=SLOPE(DLMC4V,SLMV,ARVEFF,EM,CLAVP)
120       CLDRUD=FCLDF(CFOCV,ETA1V,ETAOV,DRUD,ARV,SLMV,TOCV,PHTER,CLAVP,
130      &DLMC4V,BVT)
150       CYDR=-CLAVT*ADADCL*ADCL*KPRIM*KB*ETAVT*SVT/SW
160       WRITE(6,1000)
170    1000 FORMAT(10X,"KU-FRL SUBROUTINE FOR CYDR, CLDR AND CNDR "///)
180       WRITE(6,1010) CYDR
190    1010 FORMAT(10X,"CYDR =   ",1F10.5," RAD-1"//)
200       CLDR=CYDR*((ZV*COS(ALPHA)-LV*SIN(ALPHA))/B)
210       WRITE(6,1020) CLDR
220    1020 FORMAT(10X,"CLDR =   ",1F10.5," RAD-1 "//)
230       CNDR=-CYDR*((LV*COS(ALPHA)+ZV*SIN(ALPHA))/B)
240       WRITE (6,1030) CNDR
250    1030 FORMAT(10X,"CNDR =   ",1F10.5," RAD-1"//)
260       STOP
270       END
```

Figure 11.25.2: Listing and Sample Printout Subroutine "RUDDER"

11.25.6 REFERENCES

11.25.1 Hoak, D.E. & Ellisson, D.E. USAF Stability and Control Datcom: Flight Control Division; Air Force Flight Dynamics Laboratory, Wright Patterson Air Force Base, Ohio, 45433

11.26: HINGE MOMENTS OF CONTROL SURFACES C_{h_α} , C_{h_δ}

11.26.1: INTRODUCTION

This chapter describes the procedure involved in computing the hinge moment derivatives C_{h_α} and C_{h_δ} . The method is mainly based on Reference 11.26.1. The data used for the computation of the section hinge moment derivatives are based on the NACA 0009 airfoil. This is a type of airfoil that is used quite often for the horizontal tailplane on general aviation aircraft. The method makes corrections for lifting-surface geometry, control-surface geometry and method of balancing. First the equations for the variation of hinge moment with angle of attack will be derived, then the equations for the variation of hinge moment with control surface deflection.

11.26.2.1 DERIVATION OF EQUATIONS FOR C_{h_α}

First the section characteristics will be derived, it applies to sealed-gap controls. A correction will be made to account for open-gap controls. The hinge moment derivative C_{h_α} is based on the control chord squared$(c_F)^2$(see Fig. 11.26.1).

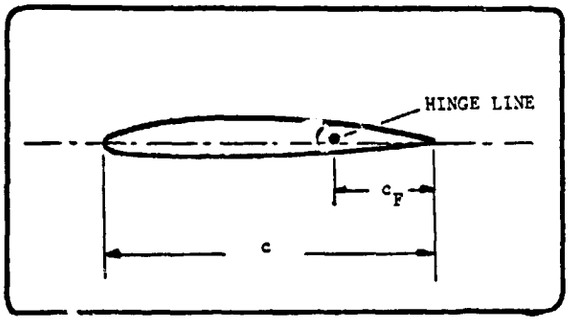

Figure 11.26.1: Geometry of Aileron

The first step is to compute the hinge moment derivative C'_{h_α} for a radius-nose, sealed control surface:

$$C'_{h_\alpha} = \left(\frac{C'_{h_\alpha}}{(C_{h_\alpha})_{theory}}\right)(C_{h_\alpha})_{theory} \quad (rad^{-1}) \qquad (11.26.1)$$

Where:

$\frac{C_{h_\alpha}}{(C_{h_\alpha})_{theory}}$ is the ratio of actual to theoretical hinge moment derivative, obtained from Figure 11.26.2. The parameter $C_{\ell_\alpha}/(C_{\ell_\alpha})_{theory}$ follows from Eqn. 11.21.4

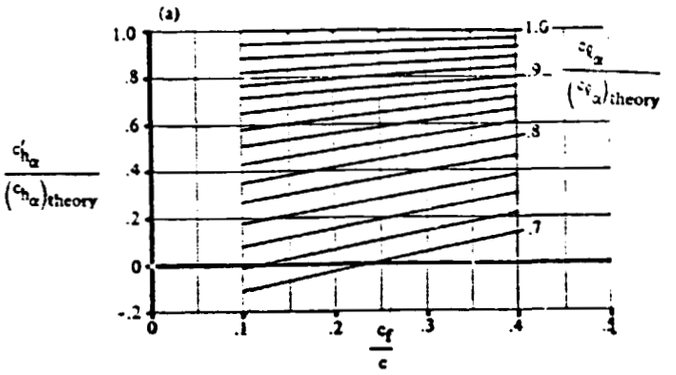

Figure 11.26.2: Rate of Change of Section Hinge Moment C'_{h_α} with Angle of Attack

$(C_{h_\alpha})_{theory}$ is the theoretical hinge moment derivative, follows from Figure 11.26.3.

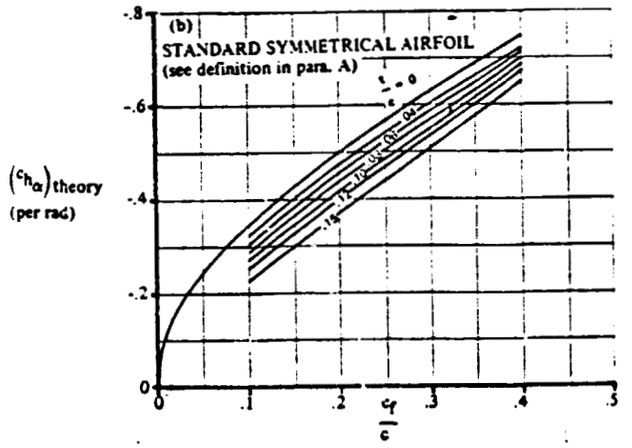

Figure 11.26.3: Theoretical Hinge Moment Derivative

C-5

If the trailing edge of the airfoil does not conform to the following condition:

$$\text{TAN}\frac{\phi'_{TE}}{2} = \text{TAN}\frac{\phi''_{TE}}{2} = \text{TAN}\frac{TE}{2} = \frac{t}{c} \qquad (11.26.2)$$

Where: ϕ'_{TE} is the angle between straight lines through 90 and 99 percent of the chord on upper and lower surface

ϕ''_{TE} is the angle between straight lines through 95 and 99 percent of the chord on upper and lower surface*

ϕ_{TE} is the trailing edge angle between tangents to upper and lower surfaces at the trailing edge.

then the following correction has to be applied to equation (11.26.1):

$$C''_{h_\alpha} = C'_{h_\alpha} + 2(C_{\ell_\alpha})_{theory}\left(1 - \frac{C_{\ell_\alpha}}{(C_{\ell_\alpha})_{thecry}}\right)\left(\text{TAN}\frac{\phi''_{TE}}{2} - \frac{t}{c}\right)\left(\text{rad}^{-1}\right) \qquad (11.26.3)$$

To account for the effect of balancing, the following correction is applied:

$$(C_{h_\alpha})_{balance} = C''_{h_\alpha}\left(\frac{(C_{h_\alpha})_{balance}}{C''_{h_\alpha}}\right)\left(\text{rad}^{-1}\right) \qquad (11.26.4)$$

Where:

C''_{h_α} is obtained from Eqn. (11.26.3), or is equal to C'_{h_α} in Eqn. (11.26.1).

$\frac{(C_{h_\alpha})_{balance}}{C''_{h_\alpha}}$ is obtained from Figure (11.26.4).

The definition of the control surface dimensions is given in Figure (11.26.5) while Figure (11.26.6) shows the various nose-shapes.

*Note: For a beveled trailing edge ϕ''_{TE} is equal to the angle of bevel.

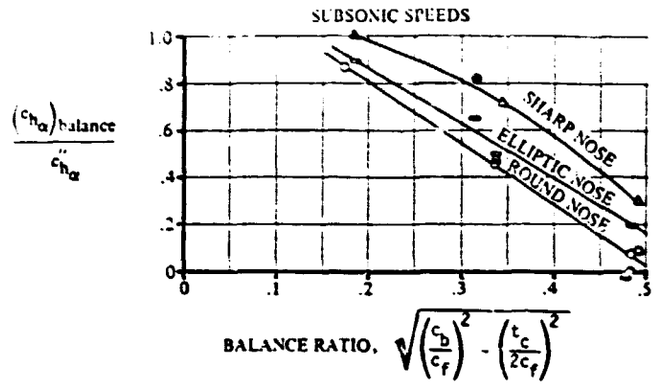

Figure 11.26.4: Effect of Nose Balance on Section Hinge Moment Derivatives

The effect of Mach number may be roughly approximated using the Prandtl-Glauert correction:

$$C_{h_\alpha}\Big|_M = \frac{C_{h_\alpha}\Big|_{\text{Low Speed}}}{\sqrt{1 - M^2}} \qquad (11.26.5)$$

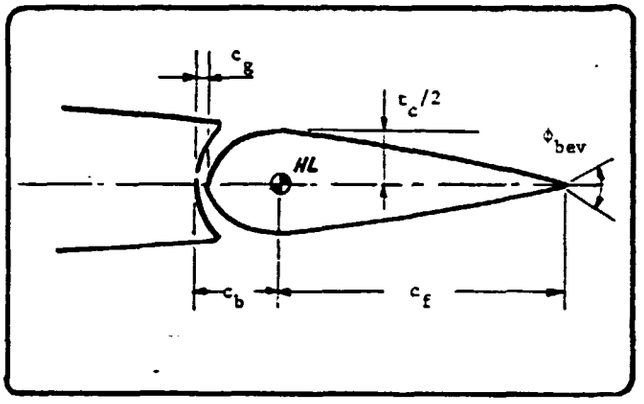

Figure 11.26.5: Geometry of Control Surface

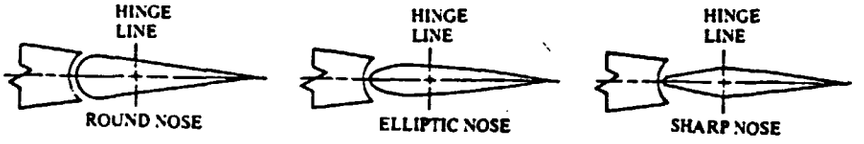

Figure 11.26.6: Various Types of Nose Shapes

*

Using the two dimensional hinge moment, computed above, the three dimensional hinge moment coefficient is:

$$C_{h_\alpha} = \frac{AR \cos \Lambda_{c/4}}{AR + 2 \cos \Lambda_{c/4}} (C_{h_\alpha}) + \Delta C_{h_\alpha} \qquad (11.26.6)$$

Where:

C_{h_α} is computed with Eqn. (11.26.5)

ΔC_{h_α} is a correction for induced camber effects, arrived at by using lifting-surface theory. It may be computed by referring to Figure (11.26.7).

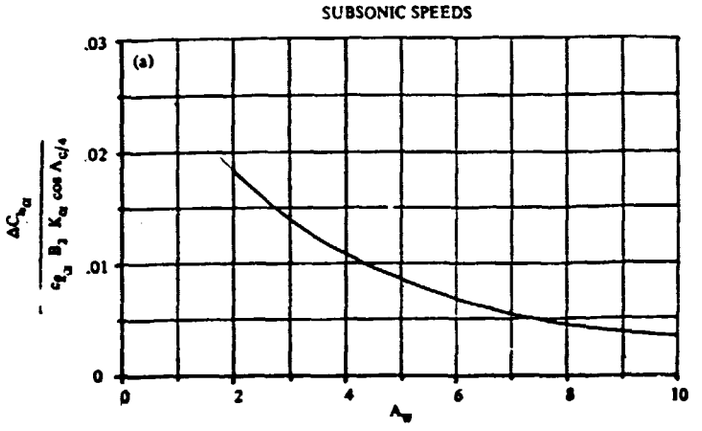

Figure 11.26.7: Correction for Induced Camber

The variables in the y-axis quantity are:

C_{ℓ_α} is section lift curve slope

K_α takes control surface span into account, for outboard controls (see Fig. 11.26.8) if in board controls are used, then K may be approximated to be equal to $Y_o/(b/2)$, Y_o and Y_i are defined in Figure 11.26.9.

*The effect of open gap and bevel angle on section characteristics will be determined later.

B_2 accounts for the effect of control surface to balance chord ratios, to be obtained from Figure 11.26.10.

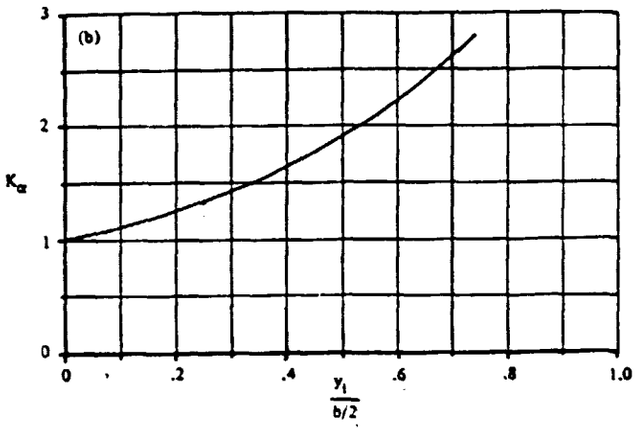

Figure 11.26.8: Effect of Control Surface Span

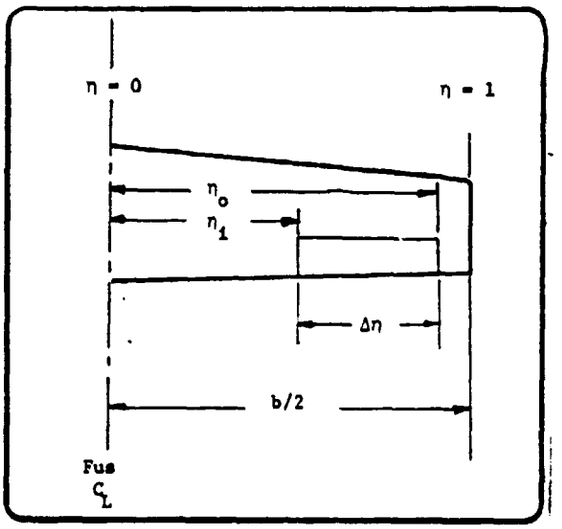

Figure 11.26.9: Control Surface Span Parameters

The primed values in Figure 11.26.10 refer to measurements normal to the wing quarter chord line, if not explicitly given they may be approximated by:

$$c_f'/c' = (c_f'' + c_f''')/(c'' - c''' + c_f'' + c_f''') \qquad (11.26.7)$$

and

$$c_b'/c_f' = c_b'/(c_f'' + c_f''') \qquad (11.26.8)$$

Where:

$$c''_f = c_f \cos \Lambda_{1/4\bar{c}} \tag{11.26.9}$$

$$c'''_f = c_f \sin \Lambda_{1/4\bar{c}} \tan \Lambda_{1/4\bar{c}} \tag{11.26.10}$$

$$c'' = (\bar{c} - c_f) \cos \Lambda_{1/4\bar{c}} \tag{11.26.11}$$

$$c''' = (\bar{c} - c_f) \sin \Lambda_{1/4\bar{c}} \cdot \sin(\Lambda_{LE} - \Lambda_{1/4\bar{c}}) \tag{11.26.12}$$

$$c'_b = c_b \cos \Lambda_{1/4\bar{c}} + c_b \sin \Lambda_{1/4\bar{c}} \tan(\Lambda_{1/4\bar{c}} - \Lambda_{HL}) \tag{11.26.13}$$

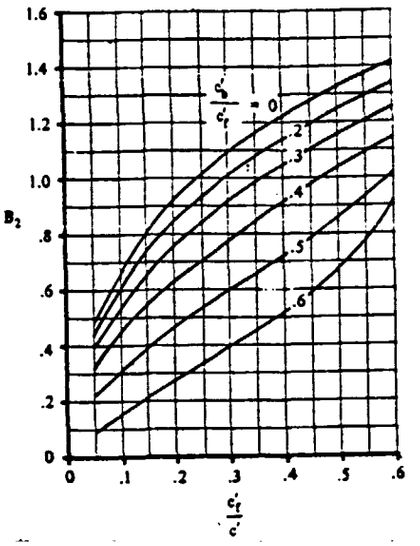

Figure 11.26.10: Correction for Chord Ratio

Corrections for open gap, horn balance and bevel angle will now be made. Reference 11.26.2, Figure 6-8, provides data for the estimation of the effect of open gap. The figure is reproduced in Figure 11.26.11. The definition of the gap may be found in Figure 11.26.5.

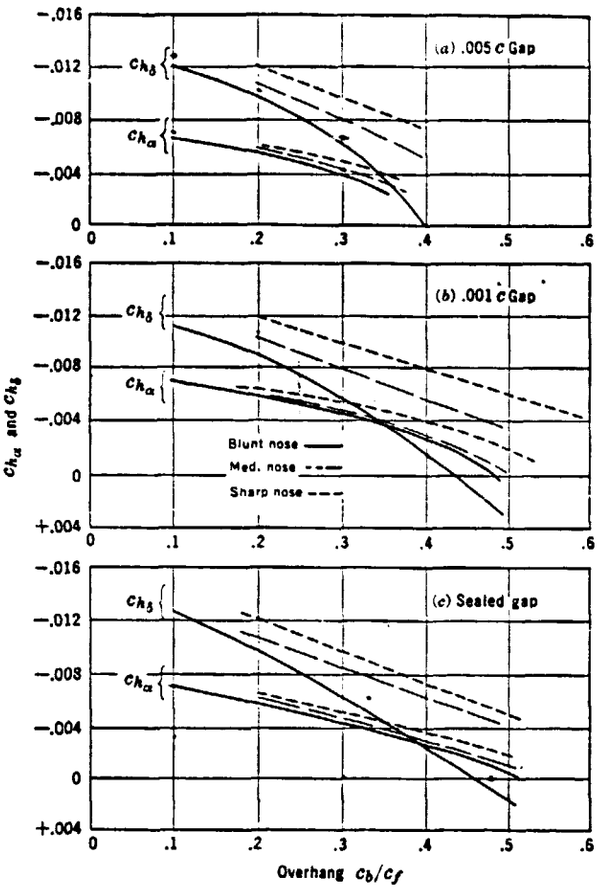

Figure 11.26.11: Effect of Open Gap on Section Hinge Moment Coefficient for a .35$\bar{c}$ Flap

Figure 11.26.10 shows on the average a (positive) increase in C_{h_α} of .0005 for a .005$\bar{c}$ gap. A simple approximation of the effect of open gap, therefore, is:

$$\Delta C_{h_{\alpha_{gap}}} = +.1 \frac{c_{gap}}{c} \quad (deg^{-1}) \qquad (11.26.14)$$

Reference 11.26.3 provides data for the estimation of the effect of bevel angle. Figure 11.26.12 is a reproduction of Fig. 12:14 of this reference.

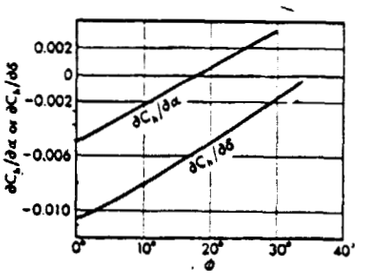

Figure 11.26.12: Effect of bevel Angle on Hinge Moment Coefficient for a .2$\bar{c}$ Flap

The effect of bevel angle may thus be approximated as:

$$\Delta C_{h_\alpha} = .00027\ \phi_{bev} \quad (deg^{-1}) \qquad (11.26.15)$$

Where: ϕ_{bev} in degrees

Both the effect of bevel angle and of open gap have to be corrected for flap-airfoil chord ratio. This can be done by referring to Fig. 11.26.13, which is a reproduction of Figure 12:7 of reference 11.26.3.

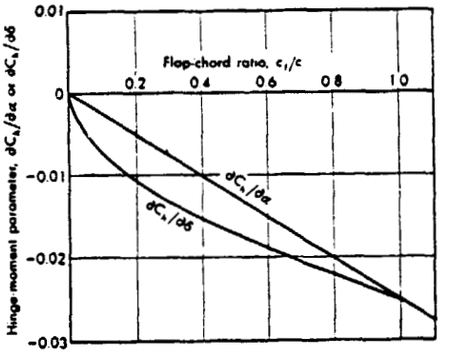

Figure 11.26.13: Correction for Flap-Chord Ratio

The correction for open gap (Eqn. 11.26.14) now becomes:

$$\Delta C_{h_{\alpha_{gap}}} = .1c_{gap} + (.0025\ (c_f/c - .3))\ (deg^{-1}) \qquad (11.26.16)$$

The correction for bevel angle on section hinge moment coefficient now becomes:

$$\Delta C_{h_{\alpha_{bev}}} = .00027\ \phi_{BEV}\ (1+3.33\ (c_f/c - .3))\ (deg^{-1}) \qquad (11.26.17)$$

The corrected three dimensional hinge moment coefficient is based on twice the area moment.

11.26.2.2 Derivation of Equation for C_{H_δ}

The equation for the section characteristics will be derived first, then corrections for three dimensional effects will be made. The hinge moment coefficient C_{h_δ} is based on the control chord squared c^2_f. (See Figure 11.4.1). The method is based on closed gap controls, a correction will be made for open gap.

For a radius-nose sealed, plain trailing edge control for which the thickness correction as defined on page 11.26 is valid the hinge moment derivative follows from:

$$c'_{h_\delta} = \left(\frac{c'_{h_\delta}}{(c_{h_\delta})_{theory}}\right)(c_{h_\delta})_{theory} \quad (rad^{-1}) \qquad (11.26.18)$$

where:

$\frac{c'_{h_\delta}}{(c_{h_\delta})_{theory}}$ is the ratio of actual to theoretical hinge moment obtained from Figure 11.26.14.

$(c_{h_\delta})_{theory}$ is the theoretical hinge moment derivative, obtained from Figure 11.26.15.

Note: The parameter $c_{\ell_\alpha}/(c_{\ell_\alpha})_{theory}$ in Figure 11.26.14 may be obtained from section 11.21.

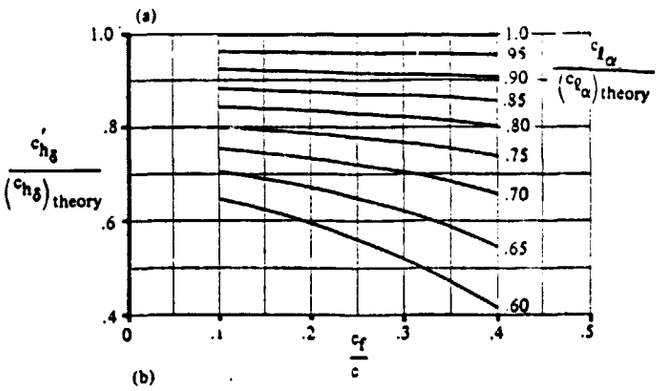

Figure 11.26.14: Ratio of Actual to Theoretical Hinge Moment

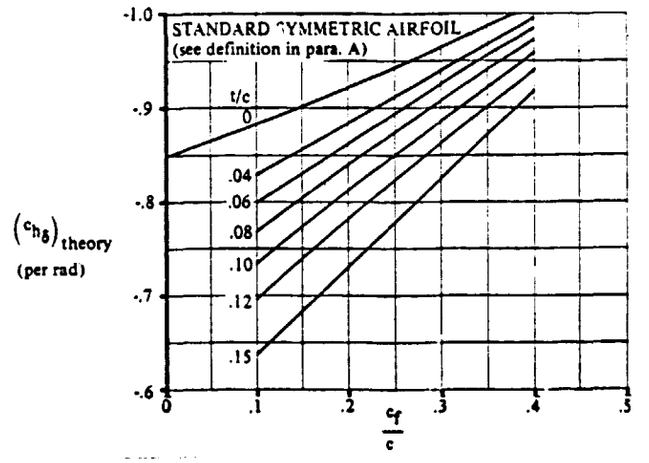

Figure 11.26.15: Theoretical Hinge Moment Derivative

If the thickness condition as defined on page 11.26.3 is not met, then the following correction has to be applied, otherwise it may be omitted:

$$c''_{h_\delta} = c'_{h_\delta} + 2\,(c_{\ell_\delta})_{theory}\left(1 - \frac{c_{\ell_\delta}}{(c_{\ell_\delta})_{theory}}\right)\left(TAN\,\frac{\phi''_{TE}}{2} - \frac{t}{c}\right)(rad^{-1}) \qquad (11.26.19)$$

where: c'_{h_δ} is obtained from equation (11.26.18)

$(c_{\ell_\delta})_{theory}$ is the theoretical lift due to flap deflection, obtained from Fig. 11.23.

$\frac{c_{\ell_\delta}}{(c_{\ell_\delta})_{theory}}$ is the ratio of the actual to the theoretical lift due to flap deflection, obtained from Figure 11.23.

ϕ''_{TE} is as defined in section 11.26.2.1 for a beveled trailing edge: $\phi''_{TE} = \phi_{BEV}$.

A correction for nose shape can be made as follows:

$$(c_{h_\delta})_{\delta\ balance} = c''_{h_\delta}\left(\frac{(c_{h_\delta})_{\delta\ balance}}{c''_{h_\delta}}\right) \quad (rad^{-1}) \qquad (11.26.20)$$

where:

c''_{h_δ} is obtained from eqn. (11.26.19) or equal to c'_{h_δ}.

$\frac{(c_{h_\delta})_{\delta\ balance}}{c''_{h_\delta}}$ is obtained from Figure 11.26.16, for various nose shapes as defined in Figure 11.26.6.

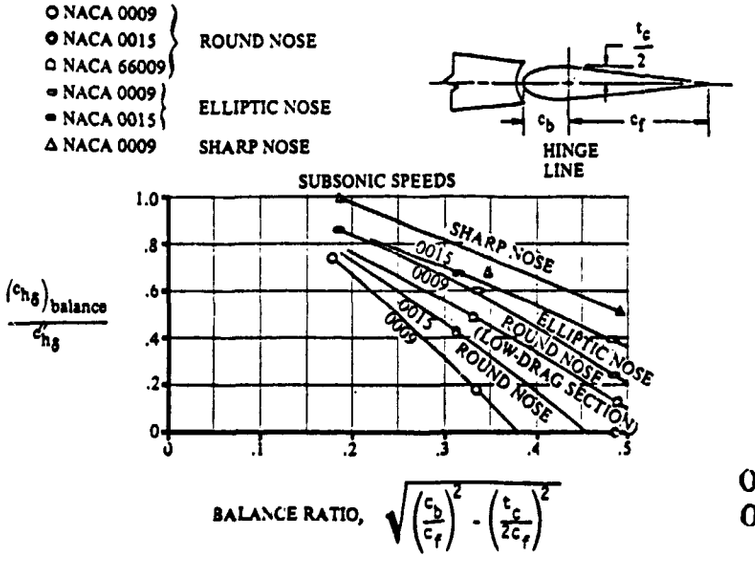

ORIGINAL PAGE IS OF POOR QUALITY

Figure 11.26.16: Effect of Nose Balance on Section Hinge Moment Derivative

The effect of Mach number may be accounted for as follows:

$$(c_{h_\delta})_M = \frac{(c_{h_\delta})_{low\ speed}}{\sqrt{1 - M^2}} \qquad (11.26.21)$$

Now corrections will be made for open gap, horn balance and bevel angle.

From Figure 11.26.11 follows the following correction for open gap:

$$\Delta (c_{h_\delta})_{gap} = .2 \frac{c_{gap}}{c} \tag{11.26.22}$$

This has to be corrected for flap-wing chord ratio, according to Figure 11.26.13 to provide:

$$\Delta (c_{h_\delta})_{gap} = .2 \frac{c_{gap}}{c} \left[1+1.25 \ (c_{\delta/c} - .3)\right] \ (deg^{-1}) \tag{11.26.23}$$

In the same way a correction factor for the effect of bevel angle is found to be:

$$\Delta (C_{h_\delta})_{BEV} = .0027\phi_{BEV} \left[1 + 1.25(C_\delta/c - .3)\right] (deg^{-1}) \tag{11.26.24}$$

The two-dimensional hinge moment coefficient as obtained above, will now be corrected for three-dimensional effects. The hinge moment derivative, based on twice the area moment may be obtained from:

$$C_{h_\delta} = \cos\Lambda_{c/4} \cos\Lambda_{HL}\left[C_{h_\delta} + \alpha_\delta \frac{2 \cos\Lambda_{c/4}}{AR + 2 \cos\Lambda_{c/4}}\right] + C_{h_\delta} \tag{11.26.25}$$

Where:

C_{h_α} is the hinge-moment derivative due to angle of attack, to be obtained from section 11.26.2.1.

C_{h_δ} is the section hinge moment derivative due to control deflection, to be obtained from section 11.26.2.1.

α_δ is the two dimensional lift effectiveness parameter obtained from section 11.23.

ΔC_{h_δ} is an approximate lifting surface correction which accounts for induces camber. It may be obtained from Figure 11.26.17, where:

B_2 accounts for control surface and balance surface chord ratios, this parameter may be obtained from Figure 11.26.10.

K_δ accounts for control surface span effect for outboard controls, see Figure 11.26.18. For inboard controls K_δ can be approximated by using Y_o I.S.O Y_i.

Note: The values that are primed in Figure 11.26.10 refer to measurements normal to the quarter chord. See Equations 11.26.7 through 11.26.13.

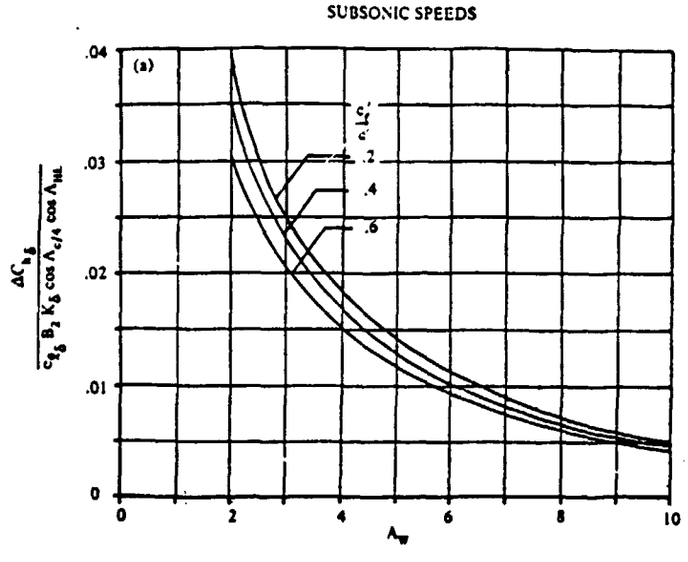

Figure 11.26.17: Lifting Surface Correction for Hinge Moment Derivative

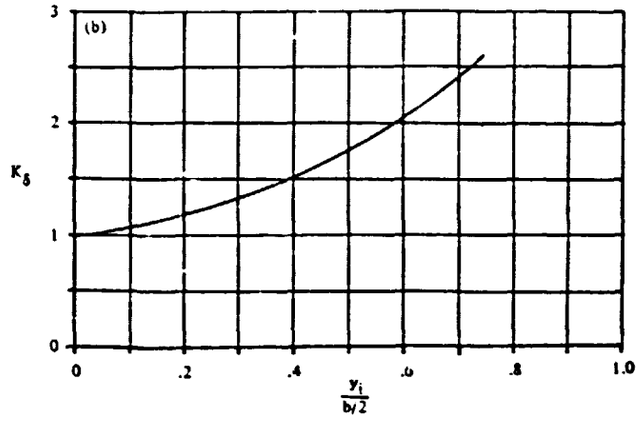

Figure 11.26.18: Correction Factor for Control Surface Span

A last correction that may be applied to the three dimensional values is a correction for the effect of a horn balance. It should be noted that the effect is difficult to estimate. Reference 11.26.3 provides a rough estimation of the effect for an unshielded horn, see Figure 11.26.19.

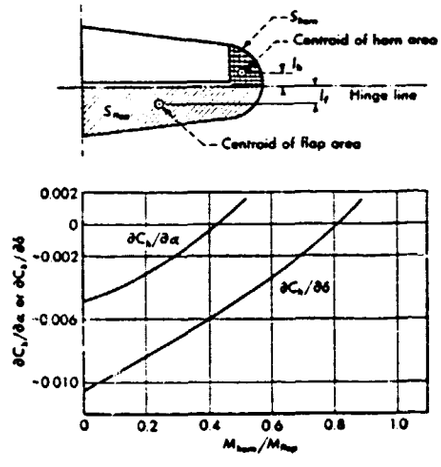

Figure 11.26.19: Effect of Horn Balance

The effectiveness of the horn is determined by the ratio of the moment of the horn area forward of the hinge line to the moment of the flap area aft of the hinge line, where the moment is defined as the area of the flap or horn multiplied by the distance of the respective area centroid from the hinge line. Figure 11.26.19 is for a 0.20 c plain flap on a NACA 0009 airfoil. To correct for different flap-wing chord ratios use can be made of Figure 11.26.13. The effect of horn balance on hinge moment coefficients can be expressed as:

$$\Delta C_{h_\alpha} = (.013125 \frac{M_h}{M_f} (1 - .0025 (\frac{C_f}{c} - .2))) \frac{b_s}{S_{cs}} \qquad (11.26.26)$$

$$\Delta C_{h_\delta} = (.0125 \frac{M_h}{M_f} (1 - .0175(\frac{C_f}{c} - .2))) \frac{b_s}{S_{cs}} \qquad (11.26.27)$$

This concludes the derivation of the equation for the hinge-moment derivatives C_{h_α} and C_{h_δ}.

11.26.3 HAND CALCULATION

This section describes a hand calculation for the elevator of airplane B for which data are presented in Appendix C.

$$\frac{C_{\ell_\alpha}}{C_{\ell_\alpha}}_{\text{theory}} = 0.93$$

Fig. 11.26.2: $$\frac{c'_{h_\alpha}}{(C_{h_\alpha})_{\text{theory}}} = 0.82$$

Fig. 11.26.3: $(C_{h_\alpha})_{\text{theory}} = -.49 \ (\text{rad}^{-1})$

Eqn. 11.26.1: $C'_{h_\alpha} = -.402(\text{rad}^{-1})$

Eqn. 11.26.3: $C''_{h_\alpha} = -.361\ (\text{rad}^{-1})$

Fig. 11.26.4: $\dfrac{(C_{h_\alpha})_{\alpha\ \text{balance}}}{C''_{h_\alpha}} = 1.0$

Eqn 11.26.4: $(C_{h_\alpha})_{\alpha\ \text{balance}} = -.361\ (\text{rad}^{-1})$

Eqn. 11.26.16: $\Delta C_{h_{\alpha_{gap}}} = +.0004\ (\text{rad}^{-1})$

Eqn. 11.26.17: $\Delta C_{h_{\alpha_{bev}}} = +.0015\ (\text{rad}^{-1})$

Fig 11.27.8: $K_\alpha = 3.$

Eqn. 11.27.7: $c'_{f/c'} = 0.246$

Eqn. 11.27.8: $c'_{b/c'_f} = 0.054$

Fig. 11.27.10: $B_2 = .99$

Fig 11.27.7: $\dfrac{\Delta C_{h_\alpha}}{C_{\ell_\alpha} B_2 K_\alpha \cos \Lambda_{c/4}} = .011$

Fig. 11.27.7: $\Delta C_{h_\alpha} = .2042\ (\text{rad}^{-1})$

Eqn. 11.27.6: $C_{h_\alpha} = -.0352\ (\text{rad}^{-1})$

Fig. 11.26.14: $\dfrac{c'_{h_\delta}}{(c_{h_\delta})_{\text{theory}}} = .95$

Fig. 11.26.15: $(c_{h_\delta})_{\text{theory}} = -.87\ (\text{rad}^{-1})$

Eqn. (11.26.18) $c'_{h_\delta} = -.8265\ (\text{rad}^{-1})$

Section 11.23 $\dfrac{c_{\ell_\delta}}{(c_{\ell_\delta})_{\text{theory}}} = 0.89$

Section 11.23 $(c_{\ell_\delta})_{\text{theory}} = 3.9\ (\text{rad}^{-1})$

Eqn. 11.26.19: $c''_{h_\delta} = -0.8588\ (rad^{-1})$

Fig. 11.26.16: $\dfrac{(c_{h_\delta})_{\delta\ balance}}{c''_{h_\delta}} = 1.0$

Eqn. 11.26.20: $(c_{h_\delta})_{\delta\ balance} = -.8588\ (rad^{-1})$

Eqn. 11.26.22: $\Delta(c_{h_\delta})_{\delta\ gap} = .0516\ (rad^{-1})$

Eqn. 11.26.23: $\Delta(c_{h_\delta})_{\delta\ bev} = 0.8655\ (rad^{-1})$

Section 11.23 $\alpha_\delta = -.6$

Fig. 11.26.18: $K_\delta = 3.0$

Fig. 11.26.17: $\Delta C_{h_\delta} = 0.1797\ (rad^{-1})$

Eqn. 11.26.24: $C_{h_\delta} = 0.0385\ (rad^{-1})$

11.26.4 PROGRAM DESCRIPTION

The program is straightforward. Use is made of a combination of HP-65 curve-fitting techniques and Function "RDP" to implement the figures in the program. The variables used in the program are listed in Table 11.26.1. A flow chart of the program is given as Figure 11.26.20. A listing and a sample printout is included as Figure 11.26.21.

Table 11.26.1 VARIABLE NAMES IN SUBROUTINE "CONSURF"

NAME	ENG SYMBOL	DIMENSION	ORIGIN	REMARKS
AR	AR	---	Common	
ADP	α_δ	---	---	
B	b	ft	Common	
BRAT	---	---	---	Balance ratio Figure 11.26.4
BZ	B_z	---	---	
CB	C_b	ft	---	
CBAR		ft	Common	
CBOCF	C_b/C_f	---	Common	
CBP	C_b'	ft	---	
CDP				
CDPHA	C_{h_α}''	rad^{-1}	---	
CDPHD	C_{h_δ}''	rad^{-1}	---	
CF	C_F	ft	Common	
CFDP	C_F''	ft	---	
CFOC	C_F/C	---	Common	
CFTP	C_F'''	ft	---	
CGOC	C_g/C	---	Common	
CHA	C_{h_α}	rad^{-1}	---	
CPHA	C_h'	rad^{-1}	---	
CDHP	C_h'	rad^{-1}	---	
CPBCFB	---	---	---	Dummy
CPHOCH	---	---	---	
CPFCA	---	---	---	Dummy

Table 11.26.1 VARIABLE NAMES IN SUBROUTINE "CONSURF" (Cont'd)

NAME	ENG SYMBOL	DIMENSION	ORIGIN	REMARKS
CTP	C'''	ft	---	
DCHA	ΔC_{h_α}	rad^{-1}	---	
DCHAB	$\Delta C_{h_{\alpha_{bal}}}$	rad^{-1}	---	
DCHAH	$\Delta C_{h_{\alpha_{horn}}}$	rad^{-1}	---	
DCHD	ΔC_{h_δ}	rad^{-1}	---	
DCHDB	$\Delta C_{h_{\delta_{bal}}}$	rad^{-1}	---	
DCHDH	$\Delta C_{h_{\delta_{horn}}}$	rad^{-1}	---	
EM	M	---	Common	
ETA	η	---	Common	
ETA0	η_o	---	Common	
ETA1	η_1	---	Common	
KALP	K_d	---	---	
KBEV	---	---	Common	Control Variable
KDEL	K_δ	---	---	
KGAP	---	---	Common	Control Variable
KHORN	---	---	Common	Control Variable
KNS	---	---	Common	Control Variable
MHMF	M_{horn}/M_{flap}	---	Common	
PDATE	ϕ''_{TE}	deg	Common	
PHIB	ϕ_{Bev}	deg	Common	
PHITE	ϕ_{TE}	deg	Common	
RLMC4	$\Lambda_{1/4\bar{c}}$	rad	Common	

Table 11.26.1 VARIABLE NAMES IN SUBROUTINE "CONSURF" (Cont'd)

NAME	ENG SYMBOL	DIMENSION	ORIGIN	REMARKS
RLMLE	Λ_{LE}	rad	Common	
RLMHT	Λ_{HL}	rad	Common	
SE	S_E	ft^2	Common	
SLM	λ	---	Common	
TC	t_c	ft	Common	
TCOCF	---	---	---	Dummy
TOC	t/c	---	Common	
YB2	$Y_{b/2}$	---	---	

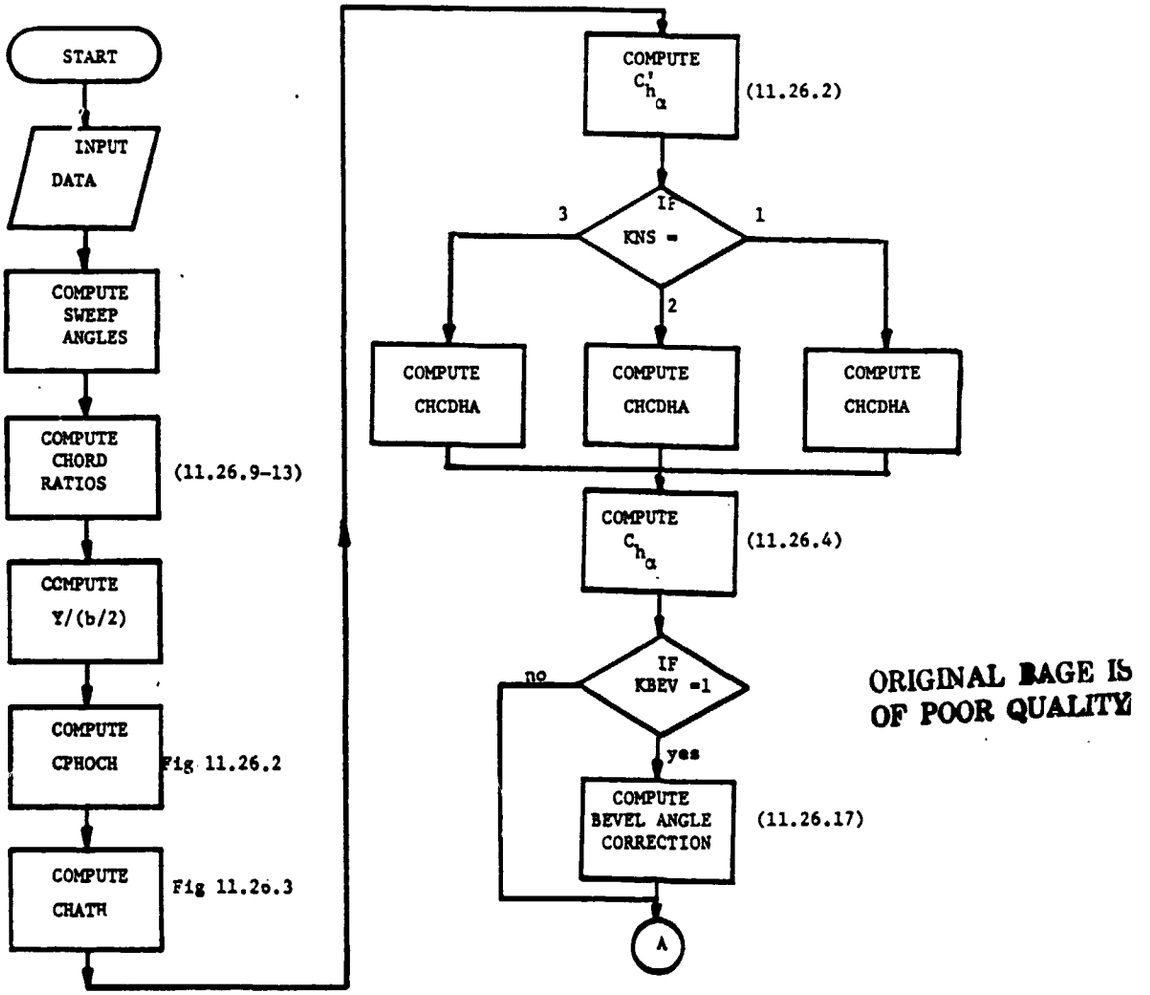

Figure 11.26.20: Flowchart of "CONSURF"

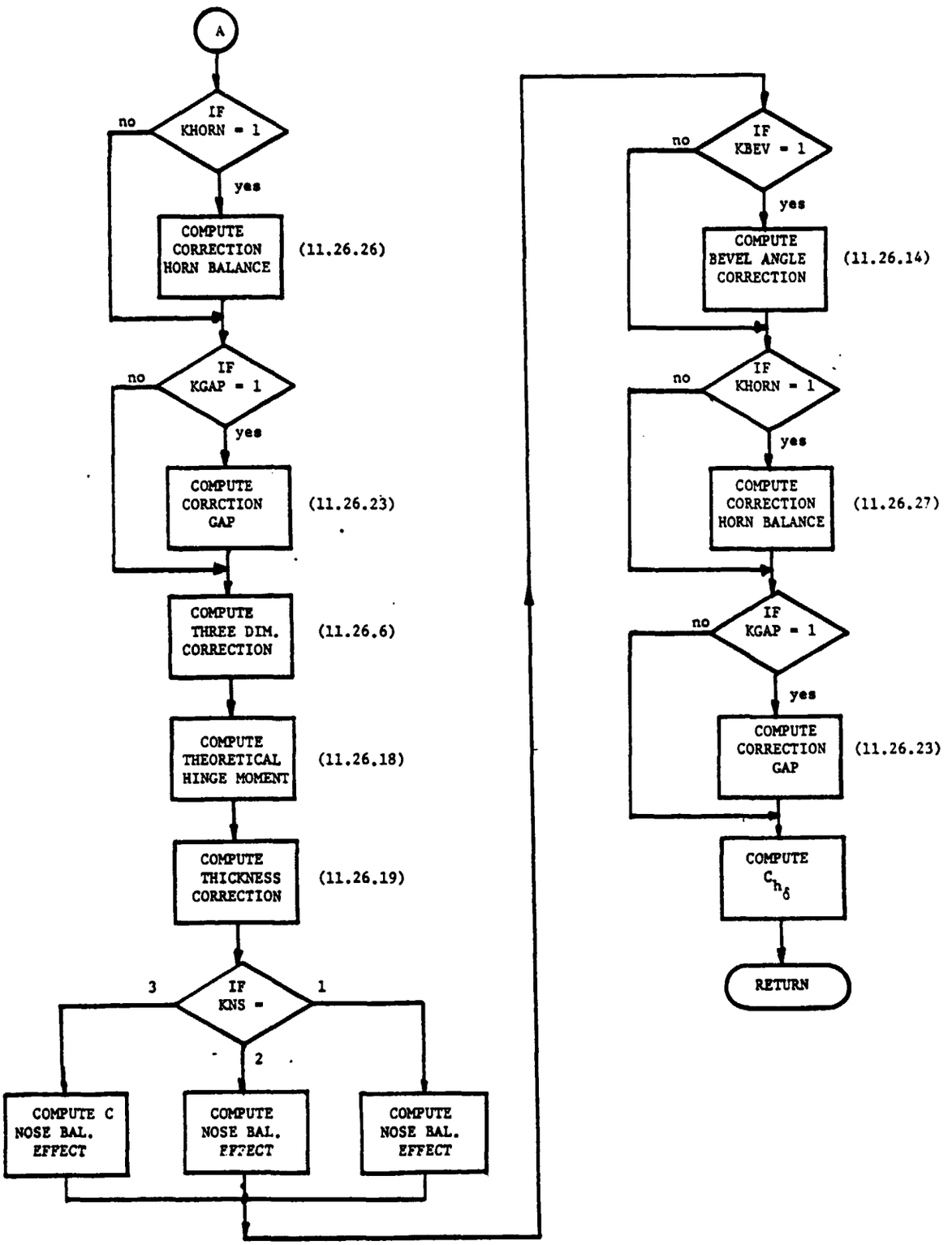

Figure 11.26.20: Continued

```
10C       SUBROUTINE CONSURF (CHA,CHD,DADD)
20        REAL KDEL,KALP,MHMF
30      DATA TOC,PHITE,CLAPP,CFOC,CBOCF/0.09,6.,6.25,0.246,0.054/
40      DATA TC,CF,KNS,EM,ETA1,ETA0,SLM,CLDFT/0.08,0.406,1,.05,0.,1.,0.5,4.55/
50      DATA B,AR,RLMC4,CLCLDT,CHLOC,PDPTE/6.36,4.0,0.436,1.,.754,6./
60      DATA CPHA,CPHD,KBEV,KHORN,PHIB,KGAP,MHMF,CGOC/.0,.0,0,0,6.0,1,0.0,0.005/
80    DATA TCOCF,CBAR,SE/.07,1.65,0./
90        CLATH=6.28+4.7*TOC*(1.+.00375*PHITE)
100        CLCLAT=CLAPP/CLATH
105       CF=CFOC*CBAR
110       IF(RLMC4.EQ.0.) GOTO 2
112*****                                          *****
113***** COMPUTATION OF CHORD-RATIOS PERPEN-       *****
114***** DICULAR TO THE 1/4 CHORD LINE             *****
120        RLMLE=ATAN(SIN(RLMC4)/COS(RLMC4)+(1./AR)*((1.-SLM)/(1.+SLM)))
130        RLMTE=ATAN(SIN(RLMC4)/COS(RLMC4)-(3./AR)*((1.-SLM)/(1.+SLM)))
131       RLMHL=ATAN(SIN(RLMC4)/COS(RLMC4)-(4./AR)*((CHLOC-.25)*
132      &(1.-SLM)/(1.+SLM)))
140        IF(RLMLE.EQ.0.) RLMLE=.000001
150        IF(RLMTE.EQ.0.) RLMLE=.000001
190         CFDP=CF*COS(RLMC4)
200         RLM4T=RLMC4-RLMTE
210         CFTP=CF*SIN(RLMC4)*SIN(RLM4T)/COS(RLM4T)
220       CDP=(CBAR-CF)*COS(RLMC4)
230       CTP=((CBAR-CF)*SIN(RLMC4))*SIN(RLMLE-RLMC4)
240       CB=CBOCF*CF
250       CBP=CB*COS(RLMC4)+CB*SIN(RLMC4)*SIN(RLMC4-RLMHL)/COS(RLMC4-RLMHL)
260      CPFCP=(CFDP+CFTP)/(CDP-CTP+CFDP+CFTP)
270       CPBCFB=CBP/(CFDP+CFTP)
280       GOTO 3
290  2    CPFCP=CFOC
300       CPBCFB=CBOCF
310  3    CONTINUE
340       IF(SE.EQ..0) SE=CF*B/2.
350        IF(ETA1.LE..1.AND.ETA0.LE..5) ETA=ETA0
360        IF(ETA1.GT..5.AND.ETA0.GT..9) ETA=ETA1
370        IF(ETA1.GT..3.AND.ETA0.LT..7) ETA=(ETA0+ETA1)/2.
380       IF(ETA1.LE..1.AND.ETA0.GT..9) ETA=ETA0
390       YB2=ETA
410       IF(CPHA.NE.0.) GOTO 15
415*****                                          *****
416***** COMPUTATIONS FOR CHA                      *****
417*****                                          *****
420        DIMENSION DD1(9,2),VV1(9),DDD1(4),WW1(2),UU1(1)
430        DATA VV1/.68,.72,.76,.8,.84,.88,.92,.96,1./
440        DATA UU1/1./
450        DATA WW1/.1,.5/
460        DATA DD1/-.2,.12,-.017,.3,.183,.45,.35,.605,
470      &.508,.7,.65,.8,.767,.85,.883,.94,1.,1./
480       CPHOCH=RDP(1.,CLCLAT,CFOC,1,9,2,2,UU1,VV1,WW1,DD1)
495*****                                          *****
```


Figure 11.26.21: Listing and Sample Printout of Subroutine "CONSURF"

```
      DIMENSION DD2(5,3),VV2(5),DDD2(4),WW2(3),UU2(1)
      DATA VV2/0.,.04,.08,.12,.16/
      DATA UU2/1./
      DATA WW2/.1,.25,.5/
      DATA DD2/-.346,-.567,-.87,-.321,-.542,-.84,-.288,-.504,-.825,
     &-.254,-.467,-.8,-.213,-.425,-.761/
      CHATH=RDP(1.,TOC,CFOC,1,5,3,3,UU2,VV2,WW2,DD2)
      CPHA=CPHOCH*CHATH
      PDPTE=PDPTE/57.3
      CDPHA=CPHA+2.*CLATH*(1.-CLCLAT)*((SIN(PDPTE/2.)/COS(PDPTE/2.))-TOC)
      BRAT=SQRT((CBOCF**2)-(TCOCF/2.)**2)
C*****                                                          *****
C***** KNS=1 : ROUND NOSE                                       *****
C***** KNS=2 : ELLIPTIC NOSE                                    *****
C***** KNS=3 : SHARP NOSE                                       *****
C*****                                                          *****
      IF(KNS.EQ.1) CHCDHA=-2.614*BRAT+1.333
      IF(KNS.EQ.2) CHCDHA=-2.327*BRAT+1.222
      IF(KNS.EQ.3) CHCDHA=1.088+1.755*BRAT-3.675*BRAT**2
      IF(CHCDHA.GT.1.0) CHCDHA=1.0
      CHAP=CDPHA*CHCDHA/SQRT(1.-EM**2)
      IF(KBEV.NE.1) GOTO 10
C*****                                                *****
C***** CORRECTION FOR BEVEL ANGLE AND HORN BALANCE, DERI-*****
C***** VED FROM FIG. 12:7, 12:12 AND 12:14 OF DOMMASCH   *****
C***** , SHELBY AND CONNALLY                             *****
C*****                                                   *****
      DCHAB=.00027*PHIB-(.0025*(CFOC-.2))
      CHAP=CHAP+DCHAB
 10   CONTINUE
      IF(KHORN.NE.1) GOTO 12
      DCHAH=(.013125*MHMF-(.0025*(CFOC-.2)))*B/SE
      CHAP=CHAP+DCHAH
 12   CONTINUE
      IF(KGAP.NE.1) GOTO 15
C*****                                                *****
C***** THE EFFECT OF OPEN GAP WAS ESTIMATED FROM FIG.    *****
C***** 6-8 OF PERKINS AND HAGE                           *****
C*****                                                   *****
      CHAP=CHAP+CGOC
 15   CONTINUE
      KALP=1.02026+.53661*YB2+2.52737*YB2**2
      IF(KALP.GT.3.0) KALP=3.0
      DIMENSION DD3(6,6),VV3(6),DDD3(4),WW3(6),UU3(1)
```

Figure 11.26.20: Continued

```
1000        DATA VV3/0.,.2,.3,.4,.5,.6/
1010        DATA UU3/1./
1020        DATA WW3/.05,.15,.25,.35,.45,.55/
1030        DATA DD3/.48,.8,1.02,1.165,1.28,1.37,.45,.74,.935,1.08,1.19,1.3,
1040       &.4,.65,.84,.98,1.1,1.2,.325,.55,.7,.65,.98,1.08,
1050       &.225,.39,.54,.65,.79,.935,.09,.215,.34,.45,.59,.78/
1060        B2=RDP(1.,CPBCPF,CPFCP,1,6,6,6,UU3,VV3,WW3,DD3)
1080        CHARAT=.0283-.00544*AR+.0003*AR**2
1090        DCHA=CHARAT*CLAPP*B2*KALP*(COS(RLMC4))
1110        CHA=((AR*COS(RLMC4))/(AR+2.*COS(RLMC4)))*CHAP+DCHA
1121*****                                          *****
1122***** COMPUTATIONS FOR CHD                    *****
1130        IF(CPHD.NE.0.) GOTO 20
1140        DIMENSION DD4(7,2),VV4(7),DDD4(4),WW4(2),UU4(1)
1150        DATA VV4/0.,.05,.06,.08,.1,.12,.15/
1160        DATA UU4/1./
1170        DATA WW4/.1,.5/
1180        DATA DD4/-.88,-1.11,-.83,-1.09,-.8,-1.08,-.769,-1.05,
1190       &-.735,-1.03,-.696,-1.02,-.638,-1.01/
1200        CHDTH=RDP(1.,TOC,CFOC,1,7,2,2,UU4,VV4,WW4,DD4)
1220        DIMENSION DD5(9,5),VV5(9),DDD5(4),WW5(5),UU5(1)
1230        DATA VV5/.6,.65,.7,.75,.8,.85,.9,.95,1./
1240        DATA UU5/1./
1250        DATA WW5/.1,.2,.3,.4,.5/
1260        DATA DD5/.642,.598,.564,.415,.25,.703,.672,.621,.547,.42,
1270       &.752,.735,.704,.659,.58,.8,.785,.768,.739,.685,
1280       &.842,.836,.821,.8,.75,.88,.872,.867,.855,.84,
1290      &.922,.918,.914,.91,.9,.964,.96,.96,.956,.95,
1300       &1.,1.,1.,1.,1./
1305       CHCHTH=RDP(1.,CLCLAT,CFOC,1,9,4,4,UU5,VV5,WW5,DD5)
1320        CPHD=CHCHTH*CHDTH
1330        CLDFT=1.2572+12.8356*CFOC-10.3788*CFOC**2
1340        CLDFT=CLDFT+12.14*TOC*(CFOC-.05)
1360        CDPHD=CPHD+2.*CLDFT*(1.-CLCLDT)*((SIN(PDPTE/2.)/COS(PDPTE/2.))-TOC)
1380       IF(KNS.EQ.1) CHCHDP=-.917*BRAT+1.375
1390       IF(KNS.EQ.2) CHCHDP=-.529*BRAT+1.25
1400       IF(KNS.EQ.3) CHCHDP=-.401*BRAT+1.292
1410       IF(CHCHDP.GT.1.0) CHCHDP=1.0
1420        CHDP=CDPHD*CHCHDP
1430        CHDP=CHDP/SQRT(1.-EM**2.)
1440        IF(KBEV.NE.1) GOTO 20
1450C*****                                                  *****
1460C***** CORRECTION FOR BEVEL ANGLE AND HORN BALANCE,DERI- *****
1470C***** VED FROM FIG. 12:7, 12:12 AND 12:14 OF DOMMASCH   *****
1480C***** SHELBY AND CONNALLY                               *****
1490C*****                                                  *****
1500        DCHDB=.0003*PHIB-(.0175*(CFOC-.2))
1520        CHDP=CHDP+DCHDB
1530   20   CONTINUE
1540        IF(KHORN.NE.1) GOTO 25
1550        DCHDH=(.0125*MHMF-(.0175*(CFOC-.2)))*B/SE
1570        CHDP=CHDP+DCHDH
```

Figure 11.26.20: Continued

```
1580 25   CONTINUE
1590       IF(KGAP.NE.1) GOTO 30
1600C*****                                                    *****
1610C***** THE EFFECT OF OPEN GAP WAS ESTIMATED FROM FIG.     *****
1620C***** 6-8 OF PERKINS AND HAGE                            *****
1630C*****                                                    *****
1640      CHDP=CHDP+CGOC*(.0053*CBOCF+.00017)
1650 30    CONTINUE
1690       CHDRAT=.05865-.01233*AR+.00071*AR**2
1710       CHDRAT=CHDRAT-(CPFCP-.2)*(-.0028*AR+.0306)
1720       KDEL=1.00875+.33214*YB2+2.34286*YB2**2
1730      IF(KDEL.GE.3.0) KDEL=3.0
1740       CLDP=CLCLDT*CLDFT
1750       DCHD=CHDRAT*CLDP*B2*KDEL*COS(RLMC4)*COS(RLMHL)
1770       ADP=-CLDP/CLAPP
1780       CHD=COS(RLMC4)*COS(RLMHL)*(CHDP+ADP*CHAP*((2.*COS(RLMC4))/
1790      &(AR+2.*COS(RLMC4))))+DCHD
1650      WRITE(6,990)
1660 990  FORMAT(10X,"*********************************************************"//)
1670      WRITE(6,1000)
1680 1000 FORMAT (10X,"KU-FRL SUBROUTINE FOR CALCULATION OF HINGEMOMENTS"///)
1690      WRITE (6,1030) CHA
1700 1030 FORMAT(10X,"ELEVATOR CHA     = ",1F10.5," RAD-1",//)
1710      WRITE (6,1050) CHD
1720 1050 FORMAT(10X,"ELEVATOR CHD      = ",1F10.5," RAD-1",///)
1730      WRITE(6,1070)
1740 1070 FORMAT(10X,"*********************************************************"//)
1750      STOP
1760      END
```

Figure 11.26.21: Continued

11.26.5 RESULTS

The computer generated results compare as follows to data obtained from Reference 11.26.4 (Airplane B).

Table 11.26.2: COMPARISON OF RESULTS

	"CONSURF"		Ref. 11.26.4	Error between computer & Ref. 11.26.4
	Hand calc. rad^{-1}	Computer rad^{-1}	rad^{-1}	%
C_{h_α}	-.110	-.11234	-.1146	1.9
C_{h_δ}	-.379	-.38893	-.4584	15.0

These data compare fairly well. However, it should be noted that the values obtained with this program are very sensitive to the input data. Also the effects of gap and horn balance are rough estimates and are influenced by other factors. In this case more test runs for different elevators are needed to validate the data obtained.

11.26.6 REFERENCES

11.26.1 Hoak, D.E. & Ellison, D.E. — USAF Stability and Control Datcom: Flight Control Division Air Force Flight Dynamics Laboratory, Wright Patterson Air Force Base, Ohio, 45433.

11.26.2 Perkins, C.D. & Hage, E.H. — Airplane Performance, Stability and Control. New York John Wiley & Sons, 1949.

11.26.3 Dommasch, D.O. Sherby, S.S. Connolly, T.F. — Airplane Aerodynamics, Pitman Publishing Corp. New York, 1967.

11.26.4 Greer, H.D. Shivers, J.P. Fink, M.P. — Wind-Tunnel Investigation of Static Longitudinal and Lateral Characteristics of a Full Scale Mockup of a Light Single-Engine High-Wing Airplane. NASA TN D-7149, May 1973.

CHAPTER 12

DYNAMIC STABILITY ROUTINE

The Dynamic Longitudinal and Lateral-Directional Stability routine that will be incorporated in GASP is a modified version of an existing computer routine developed at KU. This computer program is documented in Reference 12.1. The program has been extensively used at KU for design work, with excellent results. The program was simplified such that it computes the longitudinal and lateral-directional stability characteristics for a given aircraft, with given stability and control parameters, but does not perform an autopilot analysis as the original program does. Time did not permit a check-out of the modified program, but it is felt that this should not present unduly problems.

A listing of the modified program is included for completeness as Appendix D.

REFERENCE

12.1 Postai, M. A Computer Program for Determining Open and Closed Loop Dynamic Stability Characteristics of Airplanes and Control Systems. University of Kansas, May 1973.

CHAPTER 13

CONCLUSIONS AND RECOMMENDATIONS

Table 13.1 presents data on the accuracy attained with the computer program. Also possible sources of error are indicated. Generally speaking the results are within the 10% accuracy limit that is felt to be desirable for preliminary design work. However, some subroutines did not perform that well; more test runs are needed for those routines to decrease the error. Time did not permit a complete run with all the subroutines together including the Dynamic Stability and Control routine described in Chapter 12. However, this last routine has been checked out thoroughly and has been running with satisfactory results for some time. It is felt that the complete program should produce correct results for the types of airplanes considered in this research.

As a follow-on of this project it is suggested to perform a series of runs for existing aircraft to check the total performance of the program.

As a matter of fact, this is part of a new proposal to NASA Langley Research Center. This proposal has been approved. All the subroutines described in this report will be added to the existing version of GASP at Kansas University. Then the complete program will be used for configuration analysis work.

Also the subroutines described in section 11 and in section 12 will be set up as a separate program to compute the Static and Dynamic Stability characteristics for given airplane configurations. It is felt that this should be a valuable tool in preliminary design work at the class-level.

TABLE 13.1: ACCURACY OF COMPUTER PROGRAMS

VARIABLE	ROUTINE NAME	PERCENT ERROR	REMARKS
---	"TRIM"	5%	
---	"GROUND"	--	No comparable data, results are convincing
---	"POWER"	5%	For lift predictions, discrepancy in tail plane
		5%	Lift for single-engine case for pitching moment prediction
C_{m_α}	"CMALPH"	5%	
V_{MC}	"VMC"	4%	
V_{ROT}, S_{air}	"ROTSPD"	5%	For rotation speed
		10%	For air distance
I_{xx}, I_{yy}, I_{zz}, I_{xz}	"INERTIA"	11%	For rolling moment inertia
		7%	For pitching moment inertia
		6%	For yawing moment inertia. No comparable data for cross-product inertia's.
C_{D_α}	"CDALPHA"	13%	
C_{L_α}	"LIFCRV"	6%	
$d\epsilon/d\alpha$	"DOWNWS"	4%	
C_{L_u}	"CLUU"	2%	
C_{m_u}	"CMUU"	40%	Method is prone to computational errors
C_{L_q}	"CLQUE"	2%	
C_{m_q}	"CMQUE"	2%	For Airplane C
		30%	For Airplane A, cause of this error is as yet unknown
$C_{L_{\dot\alpha}}$	"CLAD"	20%	The question rises if the correction factor of 1.2 is justified, more test runs needed
$C_{m_{\dot\alpha}}$	"CMAD"	30%	Correction factor of 1.2 may not be correct, more test runs needed
C_{y_β}	"CYBETA"	2%	
C_{ℓ_β}	"CLBETA"	10%	

TABLE 13.1: Continued.

VARIABLE	ROUTINE NAME	PERCENT ERROR	REMARKS
C_{n_β}	"CNBETA"	25%	Without correction for vertical tail size
		5%	With correction for vertical tail size
C_{Y_p}	"CYPE"	22-50%	Error probably due to complex asymmetric flowfield around horizontal tail
C_{Y_r}	"CYARE"	6%	
C_{ℓ_p}	"CLPE"	8%	For airplane A
		25%	For airplane D
C_{n_p}	"CNPE"	100%	Too negative, reason as yet unknown, may be due to flowfield around vertical tail
C_{Y_r}	"CYARE"	6%	
C_{ℓ_r}	"CLAR"	5%	Flaps up
		15%	Flaps down
$C_{L_{\delta_F}}$	"FCLDF"	10%	For $C_{L_{\delta_f}}$
$C_{\ell_{\delta_A}}$, $C_{n_{\delta_A}}$	"AILDER"	5%	For $C_{\ell_{\delta_A}}$
		--	Unknown for $C_{n_{\delta_A}}$
$C_{Y_{\delta_R}}$, $C_{\ell_{\delta_R}}$, $C_{n_{\delta_R}}$	"RUDDER"	12%	For $C_{Y_{\delta_R}}$
		18%	For $C_{\ell_{\delta_R}}$
		8%	For $C_{n_{\delta_R}}$
C_{h_α}, C_{h_δ}, τ_E	"CONSURF"	10%	

APPENDIX A COMPARISON OF METHODS FOR COMPUTATION OF GROUND EFFECT.

This appendix briefly describes the methods used in the comparison of ground effect calculation methods.

A.1. Corning (Ref. A.1)

A.1.1 Description of Method

Corning defines the ground effect factor as:

$$K_{C_{L_{g_E}}} = \frac{C_L - \Delta C_L}{C_{L_{oge}} - \Delta C_L} \tag{A.1}$$

where: C_L = Lift coefficient including flap and ground effect.

ΔC_L = Lift coefficient increment due to flaps.

$C_{L_{oge}}$ = Lift coefficient out of ground effect (including flap effect).

The lift coefficient in ground effect may then be calculated as:

$$C_{L_{ge}} = K_{C_{L_{ge}}} (C_{L_{oge}} - \Delta C_L) + \Delta C_L \tag{A.2}$$

According to Corning, the ground effect factor may be calculated as:

$$K_{C_{L_{ge}}} = 1.005 + [0.00211 - 0.0003 (AR - 3)] c_3 \tag{A.3}$$

where: $c_3 = e^{5.2(1 - H_g)}$ (A.4)

H_g = Altitude/wing span (A.5)

A.1.2 Hand Calculation

Following is a hand calculation of the Corning Method for Airplane A, see Appendix C for data.

The computations are for the following flight conditions:

C_L = .96

α = 4.9 (deg)

ΔC_{L_f} = 0.46

δ_f = 38 (deg)

The calculation of the ground effect as a function of height is given in Table A.1.

Height (ft)	H/b	$K_{C_{L_{ge}}}$	$C_{L_{ge}}$	ΔC_L (%)
30	0.787	1.009	0.965	0.5
25	0.656	1.013	0.967	0.7
20	0.525	1.020	0.970	1.0
15	0.393	1.035	0.978	1.9
10	0.262	1.065	0.993	3.4
7.5	0.197	1.089	1.005	4.7
5	0.131	1.123	1.022	6.5
2.5	0.066	1.232	1.076	12.1

Table A.1: Calculation of Ground Effect for Corning Method

A.2 PERKINS AND HAGE METHOD (Ref. A.2)

A.2.1 DESCRIPTION OF METHOD

This change in wing-lift is brought about by a change in the wing lift-curve slope. Figure A.1 shows the effect of ground proximity on wing lift curve slope. The factor k is the ratio of wing lift-curve slope in ground effect to the slope out of ground effect. Height is given by the height of the root quarter chord in semispans.

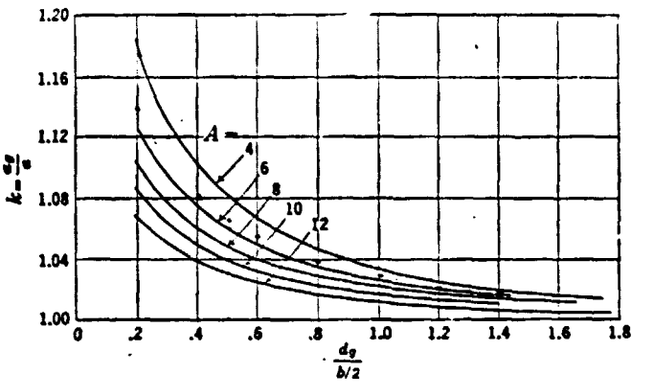

Figure A.1: Effect of Ground Proximity on Wing Lift-Curve Slope

The change in wing angle of attack due to the ground effect may be approximated as:

$$\Delta\alpha = \alpha_g - \alpha_{oge} \tag{A.6}$$

or:

$$\Delta\alpha = \alpha_{oge}\left(\frac{\alpha_g}{\alpha_{oge}} - 1\right) \tag{A.7}$$

Introducing the wing lift curve slope:

$$\Delta\alpha = \left(\frac{C_L}{C_{L_\alpha}}\right)_{oge}\left(\frac{C_{L_{\alpha\ oge}}}{C_{L_{\alpha_g}}} - 1\right) \tag{A.8}$$

or:

$$\Delta\alpha = \left(\frac{C_L}{a}\right)_{oge} \bullet (1/k - 1) \tag{A.9}$$

where: $k = \dfrac{C_{L_{\alpha_{oge}}}}{C_{L_{\alpha_g}}}$ is given in Figure A.1

Now that the change in angle of attack is known, the revised lift-coefficient may be found as shown in Figure A.2.

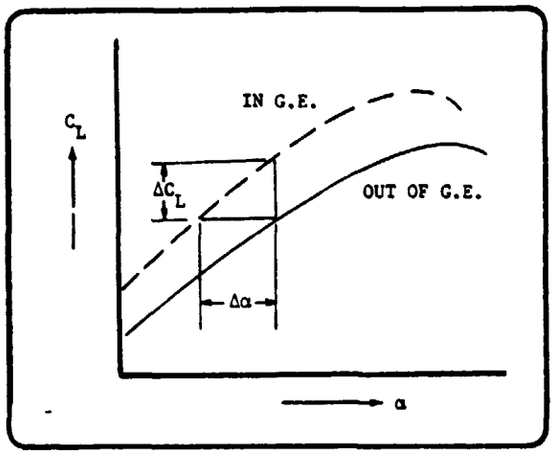

Figure A.2: Ground Effect on Lift-Curve

A.2.2 HAND CALCULATION

The following data are available for Airplane A (see appendix D)

$$C_L = 0.96 \quad (\text{At } V = 1.3\ V_S)$$

$$C_{L_{\alpha_{oge}}} = 4.870 \ \text{rad}^{-1}$$

The factor k is found from Figure A.1. The calculations are given in Table A.2.

Height (ft)	h/(b/2)	k	$\Delta\alpha$(deg)	C_L	ΔC_L (%)
30	1.57	1.014	-0.16	0.974	1.4
25	1.31	1.021	-0.23	0.980	2.0
20	1.05	1.029	-0.32	0.987	2.8
15	0.79	1.040	-0.43	0.997	3.8
10	0.52	1.065	-0.69	1.019	6.1
7.5	0.39	1.082	-0.86	1.033	7.6
5	0.26	1.116	-1.17	1.059	10.4

Table A.2: Calculation by Perkins and Hage Method

A.3. DATCOM METHOD (Reference A.3)

A.3.1 DESCRIPTION OF METHOD

This method takes into account the effect of the image trailing vortex, of the image bound vortex and of the wing flap. The change in wing-body angle of attack at a constant lift coefficient due to ground effect with respect to the out of ground effect lift curve is given by:

$$(\Delta\alpha)_q = -\left[\frac{9.12}{AR} + 7.16\left(\frac{c_r}{b}\right)\right](C_{L_{f\,WB}})\,x - \left[\frac{AR}{2\,(C_{L_\alpha})_{WB}}\left(\frac{C_r}{b}\right)\left(\frac{L}{L_o} - 1\right)r\right.$$
$$\left.(C_{L_{f\,WB}})\,r\right] - \left[\frac{(\delta_{f/50})^2}{(C_{L_\alpha})_{WB}}\left(\Delta\,(\Delta\,C_L)_{flap}\right)\right](\text{per deg}) \qquad \text{(A.10)}$$

where:

$(C_{L_{f\,WB}})$	is the wing-body lift coefficient including flap effects, out of ground effect.
x	accounts for the effect on lift due to the image trailing vortex and is obtained from Figure A.3.
$(C_{L_\alpha})_{WB}$	is the wing-body lift-curve slope, per degree out of ground effect.
$\frac{L}{L_o} - 1$	accounts for the effects on lift due to the image bound vortex, obtained from Figure A.4.
r	accounts for the effect of finite span is obtained from Figure A.5.
$\Delta\,(\Delta C_L)_{flap}$	is an empirical factor to account for the effect of flaps and is obtained from Figure A.6.

A.3.2 HAND CALCULATION

For Airplane A (See Appendix C) the following flight condition was computed:

$$\delta_f = 38 \text{ deg}$$

For the sake of simplicity, H (Height of quarter chord point of wing mac above ground), $h_{c_r/4}$ (height of quarter chord point of wing root chord above ground and h (average height of quarter chord point at 75% of wing span and of root chord) are assumed to have the same (variable) value.

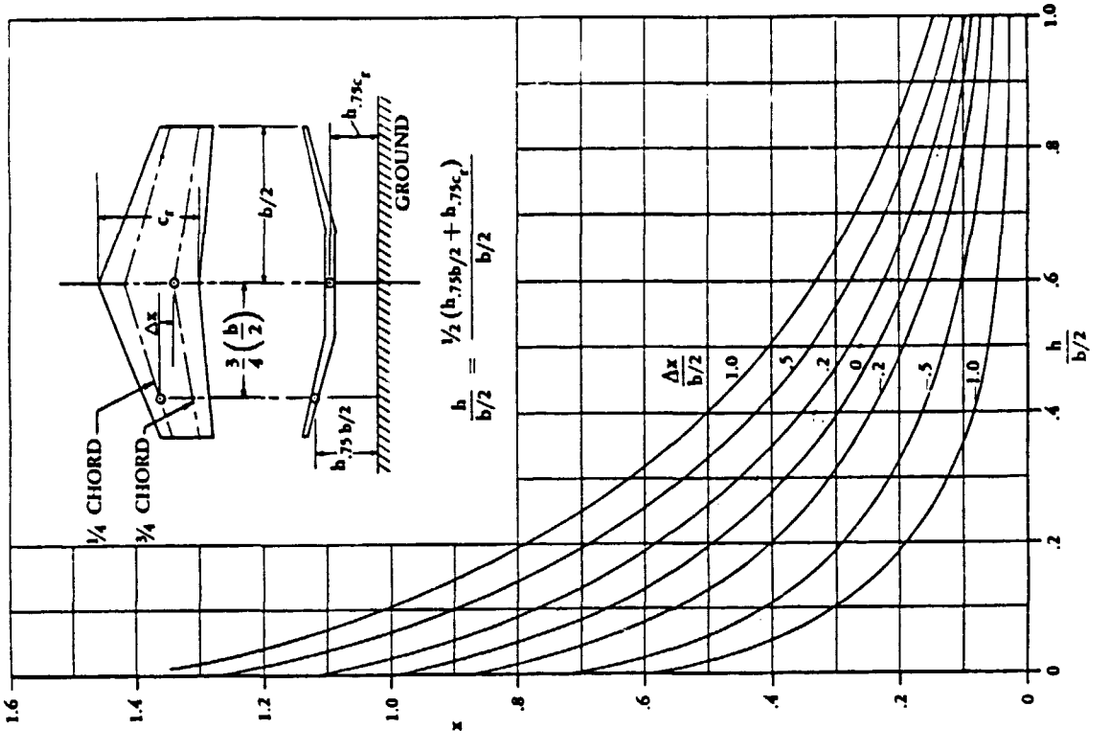

Figure A.3: Effect of Trailing Vortex on Lift in Ground Effect

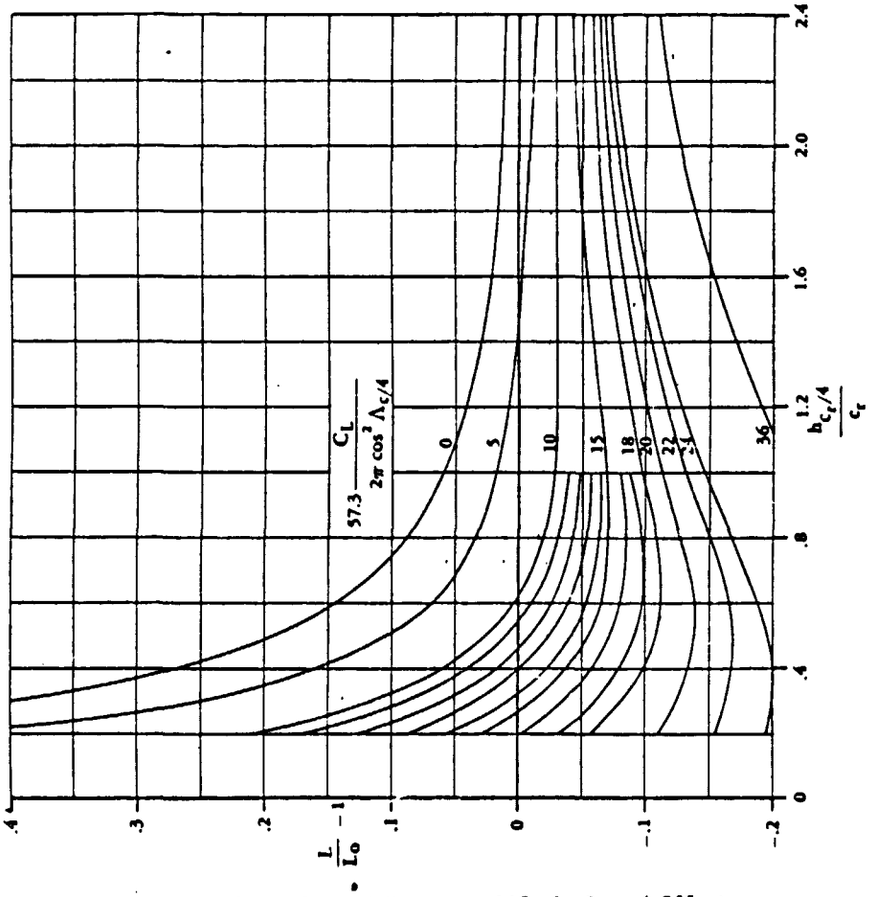

Figure A.4: Effect of Bound Vortex on Lift in Ground Effect

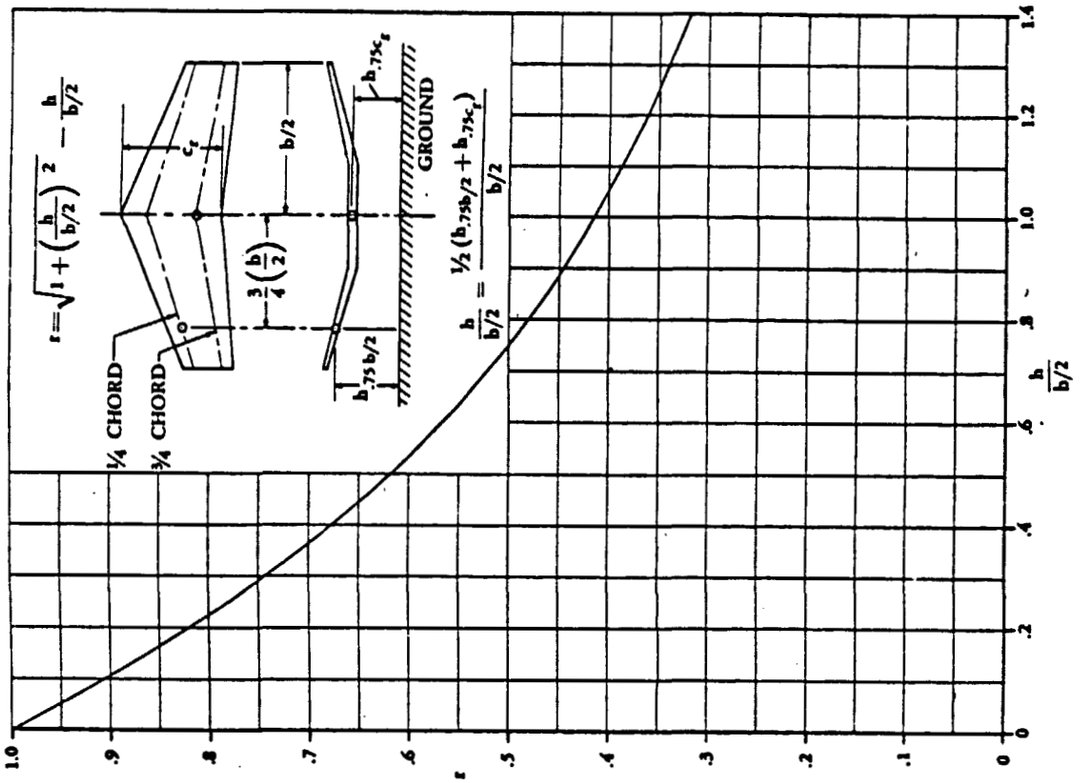

Figure A.5: Effect of Finite Span on Lift in Ground Effect

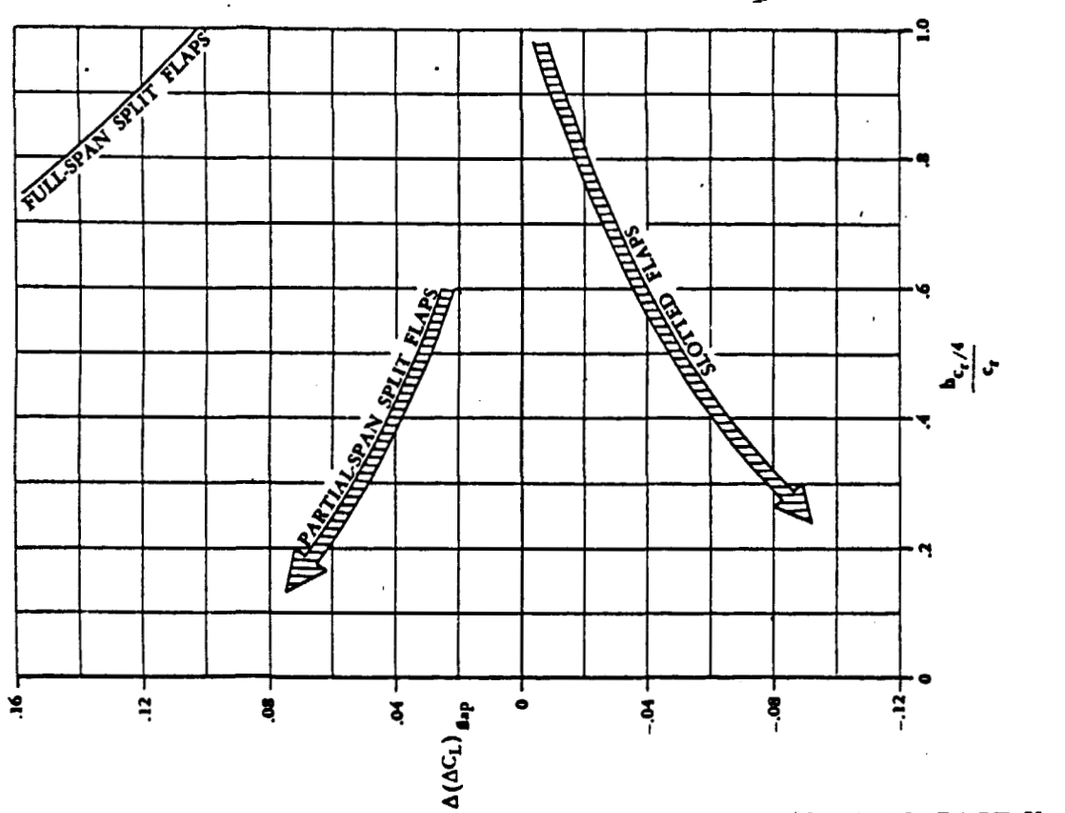

Figure A.6: Effect of Flaps on Lift in Ground Effect

Table A.3 shows the calculations.

Height (ft)	h/c_r	h/b/2	x	$\frac{L}{L_o} - 1$	r	$\Delta(\Delta C_L)_f$	$\Delta \alpha_g$	C_L	ΔC_L %
25	2.77	1.31	--	--	--	--	--	0.96	0
20	2.22	1.05	0.08	-0.06	0.40	0	0.5	0.92	-4.2
15	1.66	0.79	0.14	-0.06	0.48	0	-0.22	0.941	-2.0
10	1.11	0.52	0.25	-0.04	0.61	0	-0.60	1.011	5.3
5	0.55	0.26	0.49	+0.03	0.77	-0.045	-1.72	1.106	15.2
3	0.33	0.16	0.64	+0.145	0.86	-0.075	-2.98	1.213	26.4

Table A.3: Calculation of Datcom Method.

A.4. TORENBEEK METHOD (Reference A.4)

A.4.1 DESCRIPTION OF METHOD

A description of this method is given in Chapter 4.

A.4.2 HAND CALCULATION

A hand calculation was done for Airplane A (See Appendix D) for the following conditions:

$$C_{L_{oge}} = 0.96$$

$$C_{flap} = 2.326 \text{ ft.}$$

$$\delta_f = 38 \text{ deg}$$

Calculations are given in Table A.4.

Height ft	$2h_{eff}/b$	h/c_g	β	σ	C_L	ΔC_L %
45	2.32	6.53	0.206	0.0088	0.960	0.03
40	2.06	5.80	0.230	0.0133	0.961	0.11
35	1.80	5.08	0.259	0.0203	0.962	0.24
30	1.54	4.35	0.296	0.0316	0.964	0.46
25	1.27	3.63	0.346	0.0508	0.968	0.84
20	1.01	2.90	0.411	0.0822	0.974	1.48
15	0.75	2.18	0.500	0.1369	0.985	2.57
10	0.49	1.45	0.624	0.2384	1.003	4.51
5	0.22	0.73	0.804	0.4606	1.046	8.92
3	0.12	0.44	0.887	0.6147	1.094	13.94

Table A.4: Calculation of Torenbeek Method.

A.5 CONCLUSIONS

Figure A.7 shows the results of the calculations in this appendix. The general trend for all four methods is the same although the datcom method shows a rather large deviation from the other three. Also the datcom method is the most complicated method, it involves the use of four graphs. The simplest method is the Corning method, as it only involves two formulas. Next comes the Perkins and Hage Method, this involves the use of one graph. Hard data on ground effect for general aviation are rare. Since the method of Torenbeek is based on a sound theoretical principle (an image vortex system) it was decided to use this method.

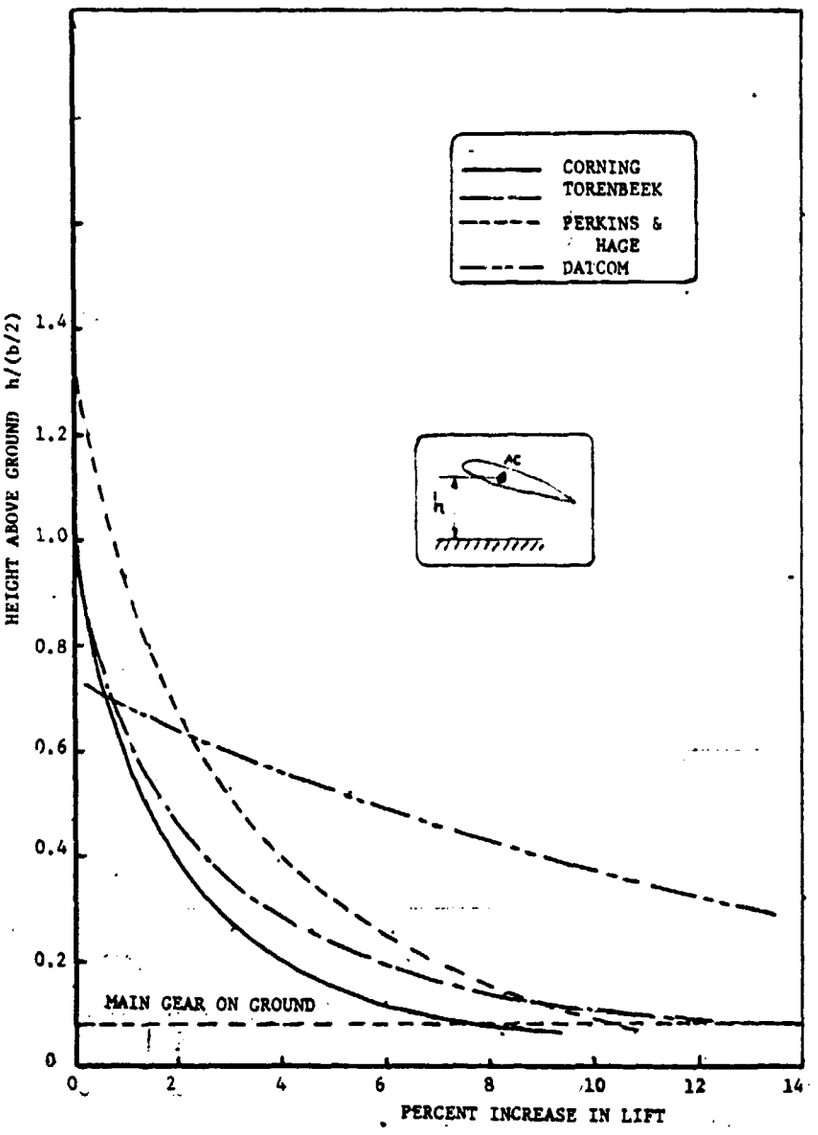

Figure A.7: Comparison of Ground Effect Methods

A.6 REFERENCES

A.1. Corning, G. — Supersonic and Subsonic Airplane Design, published by the Author, 1953.

A.2 Perkins, C.D. Hage, R.E. — Airplane Performance, Stability and Control, New York, John Wiley & Sons, 1949.

A.3. Hoak, D.E. Ellison, D.E. — USAF Stability and Control Datcom, Air Force Flight Dynamics Laboratory, Wright Patterson Air Force Base, Ohio.

A.4. Torenbeek, E. — Synthesis of Subsonic Airplane Design, Delft University Press, Delft, The Netherlands 1976.

APPENDIX B

FUNCTION RDP - A FUNCTION SUB-PROGRAM FOR INTERPOLATING CURVES AND GRAPHS

B.1 INTRODUCTION

Function RDP was written to provide a program which would interpolate along curves, between curves, and between graphs for arbitrary curves and graphs. RDP requires the input of a number of points along the curves; the points are used in conjunction with the Lagrangian interpolating polynomial to interpolate along the curves. RDP interpolates linearly between curves and graphs. If Lagrangian interpolation is needed in interpolating between curves and graphs, RDP can be called more than once, using only the Lagrangian part.

RDP can be used for any number of curves and graphs; from one curve on one graph to "n" curves per graph and "m" graphs.

RDP was checked out quite extensively. The initial checks and those done when RDP was called in a subroutine indicate that RDP works well with very little error.

B.2 DESCRIPTION OF THE PROGRAM AND LISTING

RDP is a Function, called in the form:

B = RDP (U, V, W, JK, IJ, KL, LM. UU, VV, WW, DD)

where:

U is the numerical value of graph parameter

V is the numerical value of curve parameter

W is the numerical value of X-coordinate parameter

* JK is the number of graphs

* IJ is the number of curves per graph

* KL is the number of data points (X,Y pairs) input per curve

LM is the number of rows in the DD array

UU is the array of actual graph parameters

VV is the array of actual curve parameters

WW is the array of X-coordinates at which Y-values were taken

DD is the array of Y-values in the form:

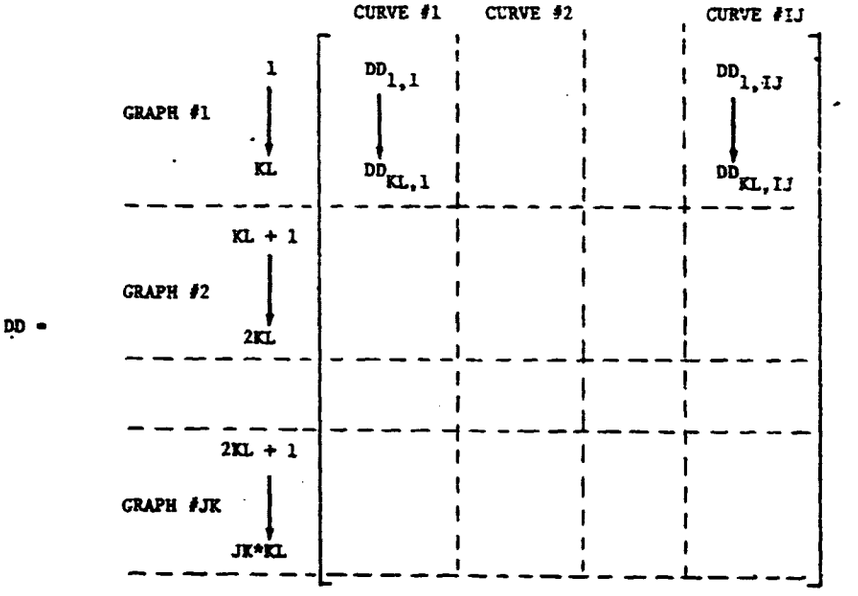

---

* NOTE: These are listed in the calling statement as numbers.

Example: B = RDP (U, V, W, 1, 1, 4, 4, UU, VV, WW)

where: JK = IJ = 1

KL = LM = 4

The other variables are initialized by data statements in the main program.

```
10      FUNCTION RDP(U,V,W,JK,IJ,KL,LM,UU,VV,WW,DD)
20      DIMENSION UU(JK),VV(IJ),WW(KL),DD(LM,IJ),DDD(4)
40      IF(IJ.EQ.1)GO TO 8
260     DO 1 I=1,IJ
270     J=I
280     K=J+1
290     IF(VV(J).LE.V.AND.VV(K).GE.V)GO TO 2
295   1 CONTINUE
296   8 J=1
297   2 IF(JK.EQ.1)GO TO 9
300     DO 3 L=1,JK
310     M=L
320     N=M+1
330     IF(UU(M).LE.U.AND.UU(N).GE.U)GO TO 4
340   3 CONTINUE
341   9 M=1
342   4 MN=4
343     IF(JK.EQ.1)MN=2
344     IF(JK.EQ.1.AND.IJ.EQ.1)MN=1
350    DO 5 II=1,MN
385     SUM=0.
390     DO 6 KK=1,KL
393     AA=1.
396     BB=1.
400     DO 7 LL=1,KL
410     IF(KK.NE.LL)AA=AA*(W-WW(LL))
415     Z=WW(KK)-WW(LL)
420     IF(Z.NE.0.)BB=BB*Z
430   7 CONTINUE
440     IF(II.EQ.1.OR.II.EQ.2)MM=KK-KL+KL*M
445     IF(II.EQ.3.OR.II.EQ.4)MM=KK+KL*M
450     IF(II.EQ.1.OR.II.EQ.3)E=DD(MM,J)
455     IF(II.EQ.2.OR.II.EQ.4)E=DD(MM,K)
460     SUM=SUM+E*AA/BB
465   6 CONTINUE
470    DDD(II)=SUM
480   5 CONTINUE
481     IF(IJ.EQ.1.AND.JK.NE.1)GO TO 11
482     IF(IJ.EQ.1.AND.JK.EQ.1)GO TO 13
550     D1=DDD(2)-((VV(K)-V)*(DDD(2)-DDD(1))/(VV(K)-VV(J)))
551     IF(JK.EQ.1)GO TO 10
560     D2=DDD(4)-((VV(K)-V)*(DDD(4)-DDD(3))/(VV(K)-VV(J)))
570  12 D=D2-((UU(N)-U)*(D2-D1)/(UU(N)-UU(N-1)))
580     RDP=D
630      GO TO 14
650  10 RDP=D1
660      GO TO 14
680  11 D1=DDD(1)
690     D2=DDD(2)
700     GO TO 12
710  13 RDP=DDD(1)
720  14  RETURN
730     END
```

Figure B.1: Listing of Function "RDP"

APPENDIX C

DATA FOR TEST-AIRPLANES

This Appendix presents data for a variety of airplanes that were used for checking the subroutines discussed in the foregoing chapters. The example airplanes range from a small single engine high-wing propeller-driven trainer airplane to a twin jet-engine business airplane. The data were assembled from a variety of sources. Also included in this Appendix are three-views of the aircraft considered.

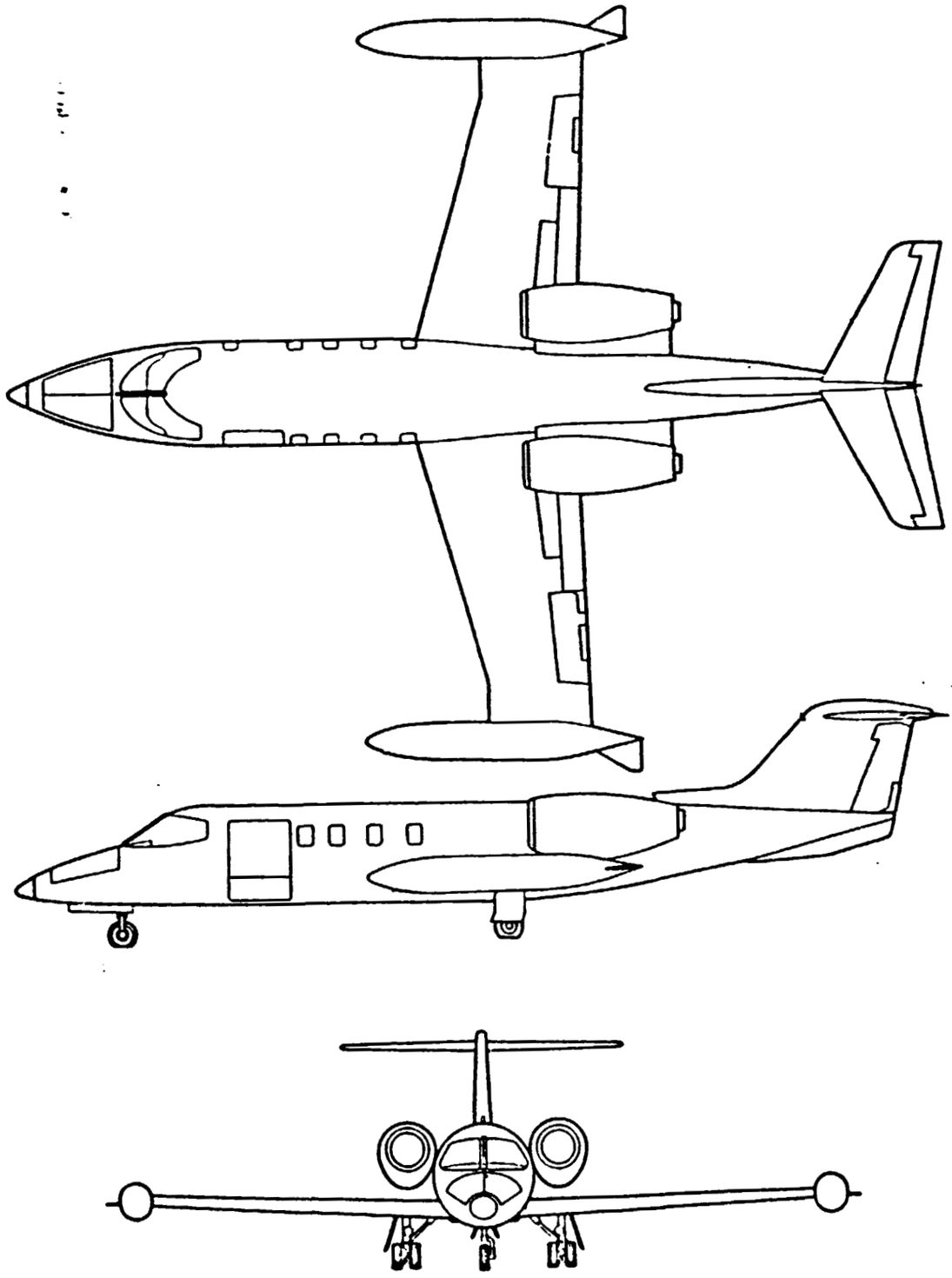

Figure C.1: Threeview of Airplane A

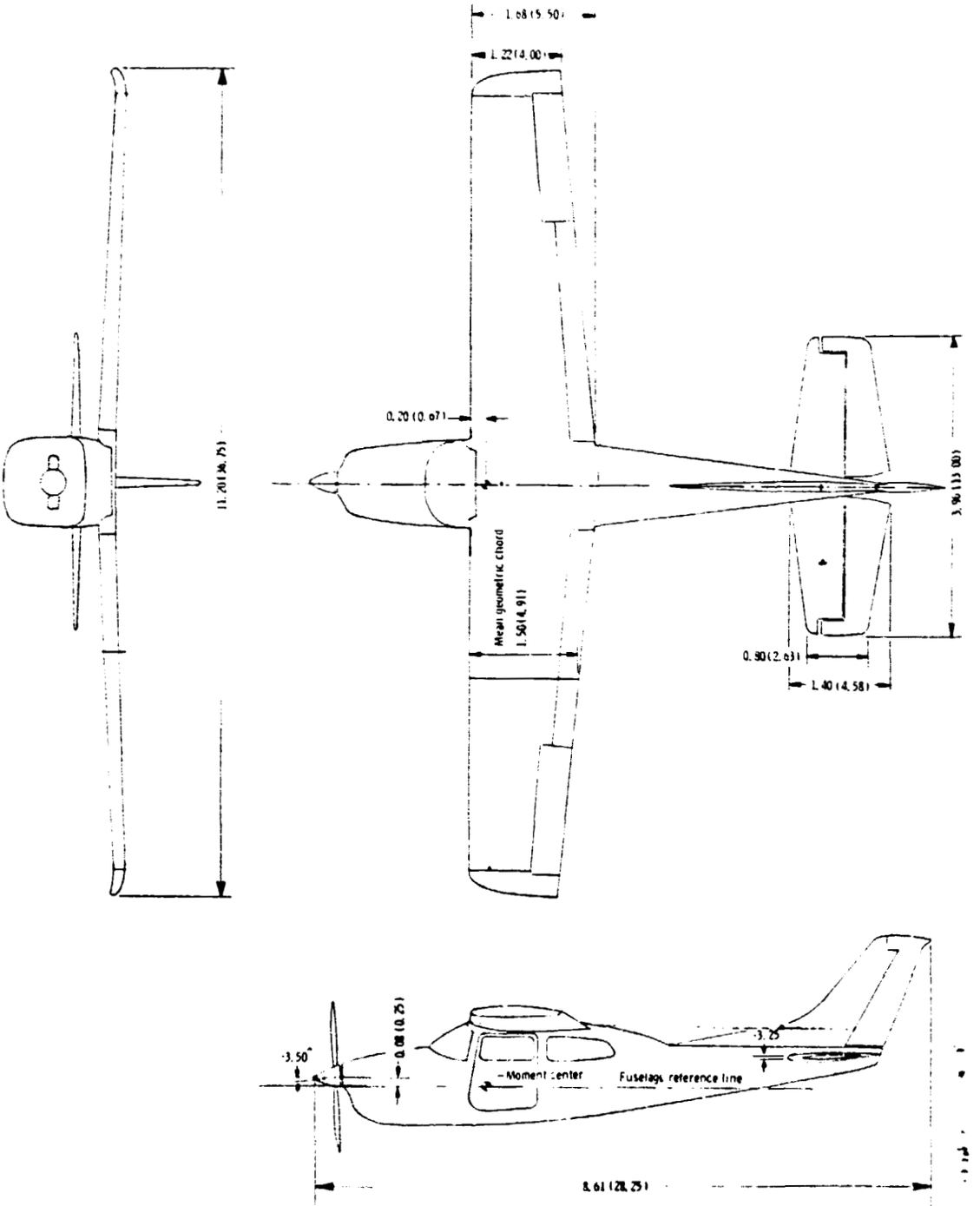

Figure C.2: Threeview of Airplane B

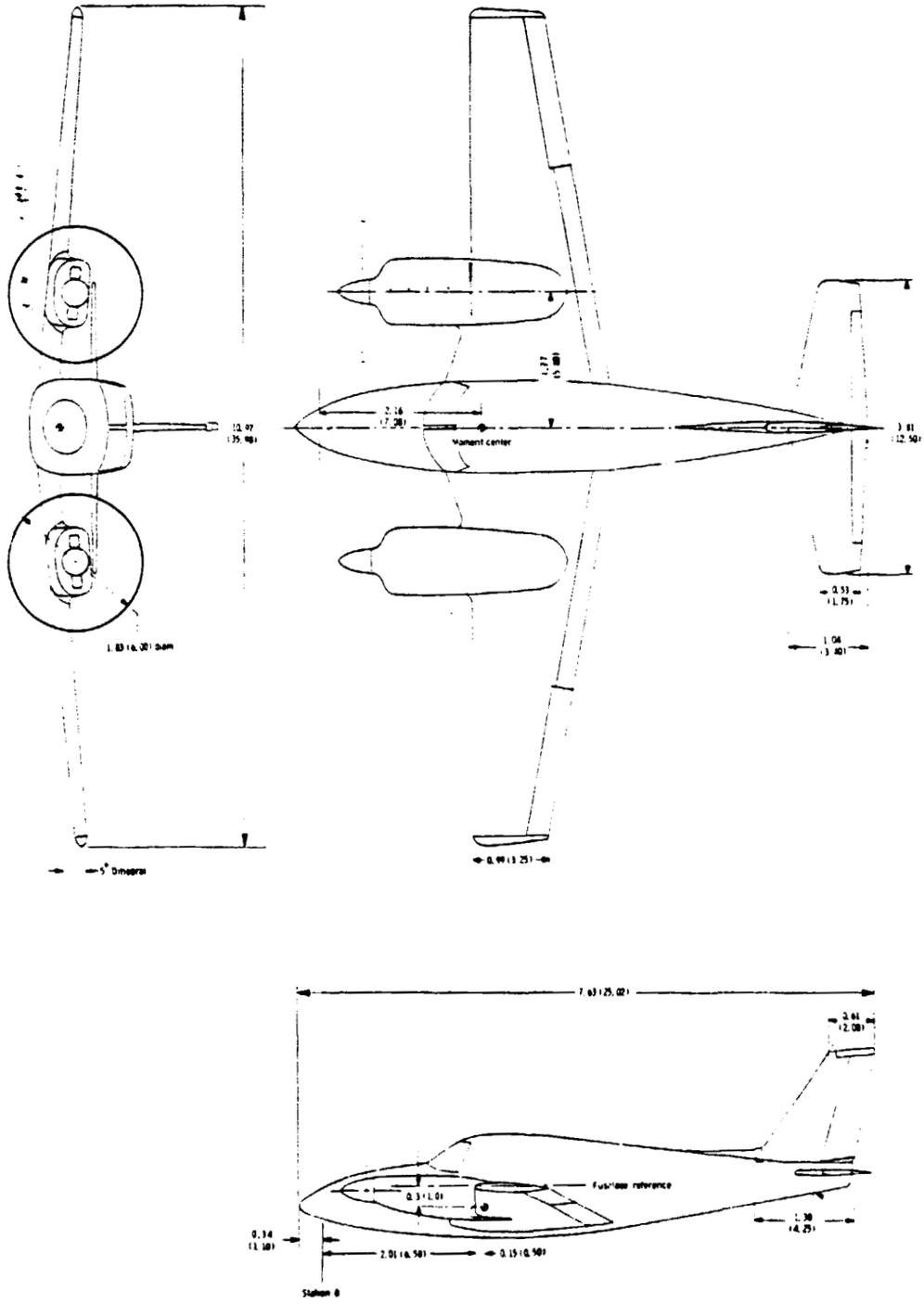

Figure C.3: Threeview of Airplane C

TABLE C.1. AIRPLANE DATA

WING	A	B	C	D	Dimension
AR_w	5.74	7.72	7.27	5.08	
b_w	38.13	36.75	35.98	26.25	ft
$C_{\ell_{\alpha_w}}$	6.131	5.443	5.44	6.709	rad^{-1}
$\bar{c}_w$	6.896	4.91	4.96	5.4	ft
c_r		5.58	6.0		ft
c_t		4	3.32		ft
$(c_r)_{C.L.}$	9.02	5.81	6.39	7.06	ft
i_w		1.5	2		deg
$\ell_{\bar{c}/4_w}$		8.66	9.13	9.37	ft
S_w	253.3	175	178	135.62	ft^2
Z_w	1.61	-2.9	-.02	4.44	ft
α_{o_w}	-1	-1.8	-3.1		deg
Γ_w	2.5		5	-6.4	deg
$\Lambda_{\bar{c}/4_w}$	13	-3	-2.5	15.5	deg
λ_w	.564	.727	.513	.465	

HOR. TAIL	A	B	C	D	Dimension
AR_H	4	3.61	4.8	4.64	
b_H	14.7	13	12.5	12.99	ft
$C_{\ell_{\alpha_H}}$	6.303	6.254	6.25	6.245	rad^{-1}

TABLE C.1. AIRPLANE DATA

HOR. TAIL (Cont'd)	A	B	C	D	Dimension
$\bar{c}_H$	3.83	3.605	2.7	2.94	ft
$(c_{\tau_H})_{C.L.}$	5	4.58	3.4	3.88	ft
h_H	8.12		2.34		ft
ℓ'_H		14.42	13.76		ft
S_H	54	46.8	32.55	36.36	ft^2
$(t/c)_H$		.09			
$x_{H_{mac}}$	1.61			.95	ft
Z_H		-1.4			ft
α_{o_H}	0	0	0		deg
$\Lambda_{\bar{c}/4_w}$	25	0	8	14.33	deg
λ_H	.469	.574	.514	.442	
ϕ_{TE}		6			deg

VERT. TAIL	A	B	C	D	Dimension
AR_V	.782			1.32	
b_V	5.48			5.25	ft
$C_{\ell_{\alpha_V}}$	6.303			6.245	rad^{-1}
$\bar{c}_V$	7.17			4.34	ft

TABLE C.1. AIRPLANE DATA

VERT. TAIL (Cont'd)	A	B	C	D	Dimension
$(c_{\tau_V})_{C.L.}$	8.88			6.07	ft
ℓ_{HV}	1.07			3.96	ft
S_V	38.35			20.84	ft^2
$(t/c)_V$	.1				
Z_V	5.21			4.3	ft
$\Lambda_{\bar{c}/4_V}$	35.63			38.65	deg
λ_V	.577			.308	

CONTRL. SURF.	A	B	C	D	Dimension
$\delta_{A_{max}}$	18 up 18 down	22 up 14 down	18 up 14 down		deg
$\delta_{R_{max}}$	30 right 30 left	25 right 25 left	22 right 20 left		deg
$c_A/\bar{c}_w$	.22				
$c_R/\bar{c}_V$	.20				
η_{i_V}	0				
η_{o_V}	.778				
η_{i_A}	.544				
η_{o_A}	.792				

TABLE C.1. AIRPLANE DATA

CNTRL. SURF. (Cont'd).	A	B	C	D	Dimension
i_H	-8.1 to 1	-3.25	N.A.		deg
$\delta_{E_{min}}$	-15				deg
$\delta_{E_{max}}$	15				deg
$c_E/\bar{c}_H$	.262				
$c_{gap}/\bar{c}_H$		.005			
c_b/c_f		.054			
$c_h/\bar{c}_H$		.754			
η_{i_E}		0			
η_{o_E}		1			
$c_F/\bar{c}_w$	.268				

POWER PLANT	A	B	C	D	Dimension
b/0.3	N.A.	.0693	.0693	N.A.	
b/0.6	N.A.	.0820	.082	N.A.	
b/0.6	N.A.	.0682	.0682	N.A.	
D_p	N.A.	6.75	6.0		ft
i_T		-3.5	0		deg
N	2	1	2	1	

TABLE C.1. AIRPLANE DATA

POWER PLANT (Cont'd)	A	B	C	D	Dimension
N_b	N.A.	2	2	N.A.	
y_T		0	5.61		ft
Z_T		-.25	-.869		ft
$\beta_{.75}$		20	21.5		deg
X'_p		7.68	6.0		ft
x_{nac}		0	2.6		ft
X_p			5.26		
T			965.0		

FUSELAGE	A	B	C	D	Dimension
ℓ_B	46.19	26.11	24.16	30.44	ft
D_f	5.1	4.7	4.08	5.56	ft
h_c	5.1	4.7	4.08		ft
w_c	5.1	4.7	4.08		ft
ℓ_n	10.02		9.13		ft
b_c			4		

TABLE C.1. AIRPLANE DATA

MISCELLANEOUS	A	B	C	D	Dimension
W_g	17,000	3100	3600		lbs
Z_s			-.8		ft
Z_{HT}			-1.67		
C_{L_α}	5.114				rad^{-1}
$C_{L_{max}}$	1.35				

TABLE C.1. AIRPLANE DATA

AIRPLANE	E	F	G	H
SWPLE (rad)	0.0	0	0	.052
SWPEV (rad)	0.745	.72	.44	
SWPLEH (rad)	0.13	.28	.13	.349
Engine Diam. (ft)	3.0	1.5	1.25	1.5
Nacelle Length (ft)	4.5	4.5	11.81	12.3
RELP	0.057	.122	.369	.25
RELR	0.0	.38	.38	.38
ZCGVER (ft)	0.0	2.5	0	0
CGLG (ft)	3.0	4.17	7.62	6.43
ZCGWING (ft)	-1.5	.758	-1.67	0
Fuel Density ($16/ft^3$)	5.87	5.85	5.87	6.6
Wt. per Pass. (lb)	170	220	263	160
Fuel Tank Span (ft)	0.197	.5	0	.654
TCR	0.12	.13	.12	0.18
TCT	0.12	.13	.12	0.12
WC	3.33	3.75	3.33	3.33
Tip T. Lgth. (ft)	0.0	0.0	0.0	6.0
Diam. (ft)	0.0	0.0	0.0	2.37
YCGTIP (ft)	0.0	0.0	0.0	6.5
PAX	1.0	3.0	9	16.0
WAS	0.0	.8	.6 @ 1	20
WS	18.0	2.0	2	16
PS (ft)	0.0	3.7	2.5	28
XPILOT (ft)	5.5	8.08	8.94	12.92
ELTIP	0	0	0	17.0
SAB	2	2	2	2

TABLE C.1. AIRPLANE DATA

AIRPLANE	E	F	G	H
WHT (lbs)	33	84	128	186.6
WVT (lbs)	18	44	79	84
WW (lbs)	207	320	1001	1193
WP (lbs)	270	509	1861	1576.6
WEP (lbs)	200	320	1478	
WB (lbs)	185	10	2	2372.4
WBT (lbs)	326	681	2200	948
WLG (lbs)	114	195	766	275
WTIP (lbs)	0.0	0.0	0	0
WFW (lbs)	158	312	1574	1715
WFTP (lbs)	0.0	0.0	0	764
Wing Span (ft)	32.71	33.0	46.67	45.88
Hor. Span (ft)	9.99	13.46	20.08	22.38
Vert. Span (ft)	4.59	5.17	8.79	7.57
Eng. Span/Wing Span	0.0	0.0	.327	.28
CRCLW (ft)	5.64	6.1	8.95	9.46
CTW (ft)	3.95	3.01	2.862	3.55
CRCLHT (ft)	3.66	3.89	4.83	5.87
CTHT (ft)	2.05	1.42	2.15	2.96
CRCLVT (ft)	4.08	6.64	7.55	9.46
CTVT (ft)	2.04	1.77	3.08	3.55
Fus. Length (ft)	20.31	24.67	44.35	43.52
Fuse Wetted area $(ft)^2$	151.4	250	630	650
Av. Diam. (ft)	4.0	4	5.1	6.03
ELCG (ft)	5.38	8.55	18.28	16.7
ELWING (ft)	5.87	9.83	19.12	17.98
ELCGH (ft)	18.22	22.31	41.21	39.97
ELCGV (ft)	19.16	21.42	39.39	39.26
YCGWNG (ft)	5.89	5.99	7.7	3.03
YCGHOR (ft)	0.0	0	0	0
YCGENG (ft)	0.0	0	7.62	6.43

APPENDIX D

DYNAMIC STABILITY COMPUTER PROGRAM

This appendix presents a listing of a modified computer program for the computation of the Longitudinal and Lateral-Directional Dynamic Stability characteristics of a given airplane. The program is fully documented in reference D.1.

REFERENCES

D.1. Postay, M. A Computer Program for Determining Open and Closed Loop Dynamic Stability Characteristics of Airplanes and Control Systems. Kansas University, Aerospace Dept. May 1973.

```
      SUBROUTINE SYSTM                                                  DST00010
      INTEGER DOL,DOL1,A,Z,DDD,DDD1                                     DST00020
      REAL MUT,M                                                        DST00030
      DIMENSION DERV(72),RES(72),PL(5),PRLNG(4),PILN(4),CLN(5),DUTC(4)  DST00040
      DIMENSION SCM(4),SEN(4),OMMA(4),ZTA(4),TEM(4),OMMS(4),RPLNGS(4)   DST00050
      DIMENSION EC(5),JCN(5),PRPIR(4),PIPIP(4),TC(4),PPIPS(4)           DST00060
      DIMENSION CZTA(4),COMMA(4),RPLNGT(4)                              DST00070
      COMMON DERV                                                       DST00080
      COMMON/LONGT/OMMA,ZTA,PL,AA,UZO,GG,GG,XPA,MUT                    DST00090
      COMMON/LAT/OMMA,ZTA,COTC,TC,P11,P11,GY1,DU41,OMM3,OMM4,DU45,PUM6  DST00100
     1,DUM7,DUM8                                                        DST00110
      DATA G/32.174/                                                    DST00120
      DATA (HE(N),N=1,72)/1HS,1HW,2HLM,4HCLRP,2HU1,3HCHO,6HTHETA,1,3HIYDST00130
     1Y,3HCL1,3HCE 1,4HCTY1,3HCM1,4HCHT1,3HCLU,3HCMU,3HCMU,4HCTXU,4HCMTU,DST00140
     23HCLO,3HCMO,3HCLA,3HCMA,3HCMA,4HCMTA,4HCLAU,4HCMAU,4HCLDE,4HCMDE, DST00150
     34HCMDF,2HMU,2HMA,3HMAU,2HMO,3HMTU,3HMTA,2HZU,2HZA,3HZ10,2HZ0,2HXA,DST00160
     42HXU,3HXTU,3HZDE,3HXDE,3HMDE,3HIXY,3HIZZ,3HIXZ,3HCYB,3HCLB,3HCNB,3DST00170
     5HCYP,3HCLP,3HCNP,3HCYR,3HCLR,3HCNR,3HCYA,3HCLA,3HCNA,2HY8,2HL8,2HNBDST00180
     6B,2HYP,2HLP,2HNP,2HYR,2HLP,2HNR,3HYDE,3HLDU,3HNDU/              DST00190
      CALL EXPT(E7,1.1,1)                                               DST00200
      READ(5,1010) (DERV(N),N=1,6)                                      DST00210
      READ(5,1010) DERV(7),DERV(8),BIXX,BIZZ,BIXZ,ALPHA1                DST00220
 1010 FORMAT(6F10.0)                                                    DST00230
 1013 FORMAT(10X,5HINPUT)                                               DST00240
 1014 FORMAT(11X11HWEIGHT,LBS.,25XF10.2)                                DST00250
 1015 FORMAT(11X16HWING AREA,SQ.FT.,21XF10.2)                           DST00260
 1016 FORMAT(11X2THDENSITY,SLUGS/CU.FT.,18XF10.4)                       DST00270
 1017 FORMAT(11X17HAIRSPEED,FT./SEC.,19XF10.2)                          DST00280
 1018 FORMAT(11X20HMEAN AERODYNAMIC CHORD,FT.,13XF10.4)                 DST00290
 1019 FORMAT(11X15HIYY,SLUG-SQ.FT.,19XF10.0)                            DST00300
 1021 FORMAT(11X18HINITIAL THETA,RAD.,14XF10.4)                         DST00310
 1023 FORMAT(11X15HIXX,SLUG-SQ.FT.,19XF10.4)                            DST00320
 1024 FORMAT(11X15HIZZ,SLUG-SQ.FT.,19XF10.0)                            DST00330
 1025 FORMAT(11X15HIXZ,SLUG-SQ.FT.,19XF10.0)                            DST00340
 1027 FORMAT(11X13HWING SPAN,FT.,23XF10.4)                              DST00350
      DERV(46)=((COS(ALPHA1))**2)*BIXX+((SIN(ALPHA1))**2)*BIZZ-(SIN(2.*ADST00360
     1LPHA1))*BIXZ                                                      DST00370
      DERV(47)=((SIN(ALPHA1))**2)*BIXX+((COS(ALPHA1))**2)*BIZZ+(SIN(2.*ADST00380
     1LPHA1))*BIXZ                                                      DST00390
      DERV(48)=.5*(SIN(2.*ALPHA1))*BIXX-.5*(SIN(2.*ALPHA1))*BIZZ+(COS(2.DST00400
     1*ALPHA1))*BIXZ                                                    DST00410
      WRITE(6,1013)                                                     DST00420
      WRITE(6,1015) (ERV(1)                                             DST00430
      WRITE(6,1014) DERV(2)                                             DST00440
      WRITE(6,1027) (ERV(3)                                             DST00450
      WRITE(6,1018) (ERV(4)                                             DST00460
      WRITE(6,1017) DERV(5)                                             DST00470
      WRITE(6,1016) DERV(6)                                             DST00480
      WRITE(6,1021) (ERV(7)                                             DST00490
      WRITE(6,1019) DERV(8)                                             DST00500
      WRITE(6,1023)DERV(46)                                             DST00510
      WRITE(6,1024)DERV(47)                                             DST00520
      WRITE(6,1025)DERV(48)                                             DST00530
      L=0                                                               DST00540
  101 READ(5,116) (DERV(N),N=9,13)                                      DST00550
```

```
  116 FORMAT(9E10.0)                                                    DST80700
      WRITE(6,160) DERV(9)                                              DST80710
      WRITE(6,161) DERV(10)                                             DST80720
      WRITE(6,162) DERV(11)                                             DST80730
      WRITE(6,163) DERV(12)                                             DST80740
      WRITE(6,164) DERV(13)                                             DST80750
  160 FORMAT(10X9HCL1,-----,1PE9.4)                                     DST80760
  161 FORMAT(10X9HCM1,-----,1PE9.4)                                     DST80770
  162 FORMAT(10X9HCT1,-----,1PE9.4)                                     DST80780
  163 FORMAT(10X9HCM1,-----,1PE9.4)                                     DST80790
  164 FORMAT(10X9HCMT1,----,1PE9.4//)                                   DST80800
      WRITE(6,2003)                                                     DST80810
 2003 FORMAT(10X26HNONDIMENSIONAL DERIVATIVES,13X24HDIMENSIONAL DERIVATIDST80820
     1VES//)                                                            DST80830
  102 READ(5,116) (DERV(N),N=14,20)                                     DST80840
      READ(5,116) (DERV(N),N=21,26)                                     DST80850
      READ(5,116)(DERV(N),N=27,29)                                      DST80860
  103 READ(5,116)(DERV(N),N=49,54)                                      DST80870
      READ(5,116)(DERV(N),N=55,57)                                      DST80880
      READ(5,116)(DERV(N),N=58,60)                                      DST80890
  104 Q1=0.5*DERV(6)*DERV(5)*DERV(5)                                    DST80900
      M=DERV(2)/G                                                       DST80910
      DUM1=Q1*DERV(1)/M                                                 DST80920
      DERV(41)=-DUM1*(DERV(15)+2.*DERV(1 ))/DERV(5)                     DST80930
      DERV(40)=-DUM1*(DERV(22)-DERV(3))                                 DST80940
      DERV(36)=-(UM1*(DERV(14)+2.*DERV(9))/DERV(5)                      DST80950
      DERV(37)=-DUM1*(DERV(21)+DERV(1 ))                                DST80960
      DUM2=Q1*DERV(1)*DERV(4)/DERV(5)                                   DST80970
      DERV(38)=-DUM2*(ERV(25)/(2.*M)                                    DST80980
      DERV(39)=-DUM2*DERV(19)/(2.*M)                                    DST80990
      DERV(30)=DUM2*((ERV(16)+2.*DERV(12))/DERV(5)                      DST81000
      DERV(31)=DUM2*(ERV(5)*DERV(23)/DERV(8)                            DST81010
      DERV(32)=(UM2*(DERV(6)*DERV(26)/(2.*DERV(8))                      DST81020
      DERV(33)=DUM2*DERV(4)*DERV(20)/(2.*DERV(8))                       DST81030
      DERV(34)=DUM2*(DERV(18)+2.*DERV(13))/DERV(8)                      DST81040
      DERV(35)=DUM2*DERV(5)*DERV(24)/DERV(8)                            DST81050
      DERV(42)=(UM1*(DERV(17)+2.*DERV(11))/DERV(5)                      DST81060
      DERV(44)=-(UM1*DERV(28)                                           DST81070
      DERV(43)=-DUM1*DERV(27)                                           DST81080
      DERV(45)=(UM2*DERV(6)*DERV(29)/DERV(8)                            DST81090
      WRITE (6,2004)                                                    DST81100
 2004 FORMAT(25X,24HLONGITUDINAL DERIVATIVES//)                         DST81110
      WRITE(6,165) DERV(16),DERV(30)                                    DST81120
      WRITE(6,166) DERV(23),DERV(31)                                    DST81130
      WRITE(6,167) DERV(26),DERV(32)                                    DST81140
      WRITE(6,168) DERV(20),DERV(33)                                    DST81150
      WRITE(6,169) DERV(18),DERV(34)                                    DST81160
      WRITE(6,170) DERV(24),DERV(35)                                    DST81170
      WRITE(6,171) DERV(16),DERV(36)                                    DST81180
      WRITE(6,172) DERV(21),DERV(37)                                    DST81190
      WRITE(6,173) DERV(25),DERV(38)                                    DST81200
      WRITE(6,174) DERV(19),DERV(39)                                    DST81210
      WRITE(6,175) DERV(22),DERV(40)                                    DST81220
      WRITE(6,176) DERV(15),DERV(41)                                    DST81230
      WRITE(6,177) DERV(17),DERV(42)                                    DST81240
```

```
      WRITE(6,1181) DERV(27),DERV(43)                                   DST81280
      WRITE(6,1182) DERV(28),DERV(44)                                   DST81290
      WRITE(6,183) DERV(29),DERV(45)                                    DST81300
  165 FORMAT(10X9HCMU,-----, 6XF9.4,10X15HMU ,FT /SEC,5XF10.4)          DST81310
  166 FORMAT(10X9HCMA,-----, 6XF9.4,10X15HMA ,RAD/SEC/SEC,5XF10.4)      DST81320
  167 FORMAT(10X9HCMAD,----, 6XF9.4,10X15HMAD,RAD/SEC/   ,5XF10.4)      DST81330
  168 FORMAT(10X9HCMQ,-----, 6XF9.4,10X15HMQ ,RAD/SEC/   ,5XF10.4)      DST81340
  169 FORMAT(10X9HCMTU,----, 6XF9.4,10X15HMTU,RAD/FT /SEC,5XF10.4)      DST81350
  170 FORMAT(10X9HCMTA,----, 6XF9.4,10X15HMTA,RAD/SEC/SEC,5XF10.4)      DST81360
  171 FORMAT(10X9HCLU,-----, 6XF9.4,10X15HZU ,RAD/SEC/   ,5XF10.4)      DST81370
  172 FORMAT(10X9HCLA,-----, 6XF9.4,10X15HZA ,FT /SEC/SEC,5XF10.4)      DST81380
  173 FORMAT(10X9HCLAD,----, 6XF9.4,10X15HZAD,FT /SEC/   ,5XF10.4)      DST81390
  174 FORMAT(10X9HCLQ,-----, 6XF9.4,10X15HZQ ,FT /SEC/   ,5XF10.4)      DST81400
  175 FORMAT(10X9HCYA,-----, 6XF9.4,10X15HYA ,FT /SEC/SEC,5XF10.4)      DST81410
  176 FORMAT(10X9HCYU,-----, 6XF9.4,10X15HYU ,RAD/SEC/   ,5XF10.4)      DST81420
  177 FORMAT(10X9HCYXU,----, 6XF9.4,10X15HYXU,FT/SEC/    ,5XF10.4)      DST81430
  180 FORMAT(10X9HCNBE,----, 6XF9.4,10X15HNBE,RAD/SEC/SEC,5XF10.4)      DST81440
 1181 FORMAT(10X9HCLUE,----, 6XF9.4,10X15HZUE,FT /SEC/SEC,5XF10.4)      DST81450
 1182 FORMAT(10X9HCYUE,----, 6XF9.4,10X15HYUE,FT /SEC/SEC,5XF10.4)      DST81460
  185 DERV(61)=DUM1*DERV(49)                                            DST81470
      DUM3=01*DERV(1)*DERV(3)/DERV(5)                                   DST81480
      DERV(64)=DUM3*DERV(52)/(2.*M)                                     DST81490
      DERV(67)=DUM3*DERV(55)/(2.*M)                                     DST81500
      DERV(70)=DUM1*DERV(46)                                            DST81510
      DERV(62)=DUM3*DERV(3)*DERV(53)/DERV(46)                           DST81520
      DERV(65)=DUM3*DERV(3)*DERV(53)/(2.*DERV(46))                      DST81530
      DERV(68)=DUM3*DERV(3)*DERV(56)/(2.*DERV(46))                      DST81540
      DERV(71)=DUM3*DERV(6)*DERV(59)/DERV(46)                           DST81550
      DERV(63)=DUM3*DERV(6)*DERV(51)/DERV(47)                           DST81560
      DERV(66)=DUM3*DERV(3)*DERV(54)/(2.*DERV(47))                      DST81570
      DERV(69)=DUM3*DERV(3)*DERV(57)/(2.*DERV(47))                      DST81580
      DERV(72)=DUM3*DERV(6)*DERV(60)/DERV(47)                           DST81590
      WRITE(6,2005)                                                     DST81600
 2005 FORMAT(25X31HLATERAL-DIRECTIONAL DERIVATIVES//)                   DST81610
      WRITE(6,191) DERV(61),DERV(62)                                    DST81620
      WRITE(6,192) DERV(63),DERV(65)                                    DST81630
      WRITE(6,193) DERV(64),DERV(66)                                    DST81640
      WRITE(6,194) DERV(59),DERV(71)                                    DST81650
      WRITE(6,195) DERV(61),DERV(63)                                    DST81660
      WRITE(6,196) DERV(64),DERV(66)                                    DST81670
      WRITE(6,197) DERV(67),DERV(69)                                    DST81680
      WRITE(6,198) DERV(62),DERV(72)                                    DST81690
      WRITE(6,199) DERV(68),DERV(61)                                    DST81700
      WRITE(6,191) DERV(62),DERV(64)                                    DST81710
      WRITE(6,192) DERV(65),DERV(67)                                    DST81720
      WRITE(6,193) DERV(66),DERV(72)                                    DST81730
  181 FORMAT(10X8HCLB,/RAD5XF9.4,10X14HLB,RAD/SEC/SEC5XF9.4)            DST81740
  182 FORMAT(10X8HCLP,/RAD5XF9.4,10X14HLP,RAD/SEC/SEC5XF9.4)            DST81750
  183 FORMAT(10X8HCLR,/RAD5XF9.4,10X14HLR,RAD/SEC/SEC5XF9.4)            DST81760
  184 FORMAT(10X8HCLD,/RAD5XF9.4,10X14HLD,RAD/SEC/SEC5XF9.4)            DST81770
  185 FORMAT(10X8HCNB,/RAD5XF9.4,10X14HNB,RAD/SEC/SEC5XF9.4)            DST81780
  186 FORMAT(10X8HCNP,/RAD5XF9.4,10X14HNP,RAD/SEC/SEC5XF9.4)            DST81790
  187 FORMAT(10X8HCNR,/RAD5XF9.4,10X14HNR,RAD/SEC/SEC5XF9.4)            DST81800
  188 FORMAT(10X8HCND,/RAD5XF9.4,10X14HND,RAD/SEC/SEC5XF9.4)            DST81810
  189 FORMAT(10X8HCYB,/RAD5XF9.4,10X14HYB, FT/SEC/SEC5XF9.4)            DST81820
```

```
191 FORMAT(1)X8HCYP,/RA15XF9.4,10X14HYP, FT/SEC/SEC5XF9.4)            DST31850
192 FORMAT(10X8HCYP,/RA15XF9.4,10X14HYP, FT/SEC/SEC5XF9.4)            DST31860
193 FORMAT(10X8HCYP,/RA15XF9.4,10X14HYP, FT/SEC/SEC5XF9.4)            DST31870
166 ST1=SIN(DERV(7))                                                   DST31920
    CT1=COS(DERV(7))                                                   DST31930
    XPY=DERV(41)+DERV(42)                                              DST31940
    UZO=DERV(5)+DERV(39)                                               DST31950
    MUT=DERV(30)+DERV(34)                                              DST31960
    RMAT=DERV(31)+DERV(35)                                             DST31970
    GS=G*ST1                                                           DST31980
    GC=G*CT1                                                           DST31990
    DL(1)=DERV(5)-DERV(38)                                             DST32000
    AA=DL(1)                                                           DST32010
    DL(2)=-AA*(XPY+DERV(37))-DERV(37)-DERV(32)*UZO                     DST32020
    DL(3)=XPX*(DERV(33)*AA+DERV(37)+DERV(32)*UZO)+DERV(33)*DERV(37)-DEDST32030
   1RV(36)*DERV(40)+DERV(32)*GS-RMAT*UZO                               DST32040
    DL(4)=GS*(  RMAT  -DERV(32)*XPX)+GC*(DERV(36)*DERV(32)+MUT*AA)+MUTDST32050
   1*(-DERV(40)*UZO)+DERV(36)*DERV(40)*DERV(37)+XPX*(  RMAT  *UZO-DERVDST32060
   2(33)*DERV(37))                                                     DST32070
    DL(5)=GC*(  RMAT  *DERV(36)-DERV(37)*MUT)+GS*(MUT*DERV(40)-XPX*RMADST32080
   1T)                                                                 DST32090
115 A11=DERV(48)/DERV(45)                                              DST32190
    B11=DERV(48)/DERV(47)                                              DST32200
    GT1=G*COS(DERV(7))                                                 DST32210
    DUM4=1.-A11*B11                                                    DST32220
    DUM5=DERV(65)+DERV(69)+A11*DERV(66)+B11*DERV(68)                   DST32230
    DUM6=DERV(65)*DERV(69)-DERV(64)*DERV(66)                           DST32240
    DUM7=DERV(62)+DERV(63)*A11                                         DST32250
    DUM8=DERV(62)*DERV(69)-DERV(63)*DERV(68)                           DST32260
    DD(1)=DERV(5)*DUM4                                                 DST32270
    DD(2)=-DERV(61)*DUM4-DERV(5)*DUM5                                  DST32280
    DD(3)=DERV(5)*DUM6+DERV(61)*DUM5-DERV(64)*DUM7+(DERV(5)-DERV(67))*DST32290
   1(DERV(62)*B11+DERV(63))                                            DST32300
    DD(4)=-DERV(61)*DUM6+DERV(64)*DUM8-GT1*DUM7+(DERV(5)-DERV(67))*(DEDST32310
   1RV(62)*DERV(66)-DERV(63)*DERV(65))                                 DST32320
    DD(5)=GT1*DUM8                                                     DST32330
305 DDL=4                                                              DST33140
    IF(DL(1).NE.0.) GO TO 321                                          DST33150
    DDL=3                                                              DST33160
    IF(DL(2).NE.0.) GO TO 321                                          DST33170
    DDL=2                                                              DST33180
    IF(DL(3).NE.0.) GO TO 321                                          DST33190
    DDL=1                                                              DST33200
321 DDL1=DDL+1                                                         DST33210
    I=5-DDL                                                            DST33220
390 DO 391 J=1,DDL1                                                    DST33230
    DLN(J)=DL(I)                                                       DST33240
391 I=I+1                                                              DST33250
    DO 389 I=1,4                                                       DST33260
    RRLNG(I)=0.0                                                       DST33270
389 RILNG(I)=0.0                                                       DST33280
392 CALL MULLER (DLN,DDL,RRLNG,RILNG)                                  DST33290
    WRITE(6,2008)                                                      DST33310
2008 FORMAT(1H1,24X29HSMALL PERTURBATION MODE DATA///,30X,12HLONGITUDINDST33320
   1AL//)                                                              DST33330
```

ORIGINAL PAGE IS
OF POOR QUALITY

```
      WRITE(6,398)                                                    DST83480
      WRITE(6,381) RRLNG(1),RILNG(1)                                  DST83490
      WRITE(6,382)RRLNG(2),RILNG(2)                                   DST83500
      WRITE(6,383)RRLNG(3),RILNG(3)                                   DST83510
      WRITE(6,384)RRLNG(4),RILNG(4)                                   DST83520
  398 FORMAT(11X,8HROOT NO.,7X,9HREAL PART,10X,9HIMAG.PART)          DST83530
  381 FORMAT(13X,3HONE,9X,E11.4,10XE11.4)                             DST83540
  382 FORMAT(13X,3HTWO,9XE11.4,10XE11.4)                              DST83550
  383 FORMAT(13X,5HTHREE,7XE11.4,10XE11.4)                            DST83560
  384 FORMAT(13X,4HFOUR,8XE11.4,10XE11.4//)                           DST83570
  363 FORMAT(11X,40HUNDAMPED NATURAL FREQUENCY(EN)CYCLES/SEC,11XF6.3) DST83580
  364 FORMAT(11X,35HTIME TO HALF AMPLITUDE,OSC MODE,SEC,13X,F6.2)     DST83590
  365 FORMAT(11X,36HTIME TO TWICE AMPLITUDE,OSC MODE,SEC,13X,F6.1)    DST83600
  366 FORMAT(11X,28HOSCILLATORY MODE IS UNDAMPED)                     DST83610
  367 FORMAT(11X,13HDAMPING RATIO,3XF6.3)                             DST83620
  368 FORMAT(11X,43HUNDAMPED NATURAL FREQUENCY,OMEGA(N),RAD/SEC,7XF7.3) DST83630
  376 FORMAT(10X,53HSECOND MODE ABOVE IS SHORT PERIOD WITH THESE FEATURESDST83640
     1)                                                               DST83650
  377 FORMAT(10X,52HFIRST MODE ABOVE IS SHORT PERIOD WITH THESE FEATURES)DST83660
  379 FORMAT(11X,40HLOAD FACTOR/ANGLE OF ATTACK, G-UNITS/RAD,10XF6.1)  DST83670
  380 FORMAT(11X,23HOMEGA SQUARED /DZ /LBM,27XF6.3/)                   DST83680
  373 Z=0                                                             DST83690
      K=0                                                             DST83700
      J=0                                                             DST83710
      DO 402 I=1,4                                                    DST83720
  301 IF (RILNG(I)) 302,350,303                                       DST83730
  302 IF(RILNG(I)+.00001) 304,350,350                                 DST83740
  303 IF(RILNG(I)-.00001)350,350,304                                  DST83750
  304 IF (ABS(RRLNG(1)-RRLNG(2)) .GT. 1.E-5) GO TO 331
      GO TO 332
  331 J=0
      IF (K .EQ. 0) GO TO 332
      IF (I .GE. 3) GO TO 402
  332 CONTINUE
      IF(J) 306,306,402                                               DST83760
  306 ZT=SQRT(RRLNG(I)**2/(RILNG(I)**2+RRLNG(I)**2))                  DST83770
      OM=ABS(RILNG(I))                                                DST83780
      EN=RRLNG(I)                                                     DST83790
      OMN=SQRT(OM**2+EN**2)                                           DST83800
      FN=OMN/6.28                                                     DST83810
      WRITE(6,363) FN                                                 DST83820
      WRITE(6,368) OMN                                                DST83830
  307 J=1                                                             DST83840
      K=K+1                                                           DST83850
      SEN(K)=EN                                                       DST83860
      SOM(K)=OM                                                       DST83870
      OMNA(K)=OMN                                                     DST83880
      IF(RRLNG(I)) 309,310,311                                        DST83890
  309 ZTA(K)=ZT                                                       DST83900
      GO TO 313                                                       DST83910
  310 ZTA(K)=0.0                                                      DST83920
      GO TO 313                                                       DST83930
  311 ZTA(K)=-ZT                                                      DST83940
      TEN(K)=-2.*RRLNG(I)                                             DST83950
      OMNS(K)=RILNG(I)**2+RRLNG(I)**2                                 DST83960
```

```
      IF(PRLNG(I)) 308,317,312                                          DST83470
  308 THALF=-.69/PRLNG(I)                                               DST83480
      WRITE(6,364) THALF                                                DST83490
      WRITE(6,367) ZT                                                   DST83500
      GO TO 400                                                         DST83510
  317 WRITE(6,366)                                                      DST83520
  312 TLOEL=.69/PRLNG(I)                                                DST83530
      GO TO 400                                                         DST83540
      WRITE(6,365)TDOEL                                                 DST83550
      ZT=-ZT                                                            DST83560
      WRITE(6,367) ZT                                                   DST83570
      GO TO 400                                                         DST83580
  360 Z=Z+1                                                             DST83590
      PRLNGS(Z)=PRLNG(I)                                                DST84000
      PRLNGT(Z)=-PRLNG(I)                                               DST84010
      GO TO 4[illegible]                                                DST84020
  402 J=0                                                               DST84030
  400 CONTINUE                                                          DST84040
      WRITE(6,449)                                                      DST84050
  449 FORMAT(/  ,16X,44HTHE CHARACTERISTIC EQUATION IN FACTORED FORM,///)DST84060
      IF(K) 591,511,403                                                 DST84070
  403 IF(K-1) 511,425,415                                               DST84080
  405 WRITE(6,406) PRLNGT(1),PRLNGT(2),TEN(1),OMNS(1)                   DST84090
  406 FORMAT(10X,3H(S+,E12.5,4H)(S+,E12.5,4H)(S*S+,E12.5,2HS+,E12.5,3H)=DST84100
     1///)                                                              DST84110
      WRITE(6,407)                                                      DST84120
  407 FORMAT(10X,58HTWO ROOTS ARE REAL AND TWO ROOTS ARE COMPLEX CONJUGADST84130
     1TES//)                                                            DST84140
      GO TO 425                                                         DST84150
  415 WRITE(6,408)TEN(1),OMNS(1),TEN(2),OMNS(2)                         DST84160
  408 FORMAT(10X,5H(S*S+,E12.5,2HS+,E12.5,6H)(S*S+,E12.5,2HS+,E12.5,3H)=DST84170
     1///)                                                              DST84180
      WRITE(6,409)                                                      DST84190
  409 FORMAT(10X,31HTWO PAIRS OF COMPLEX CONJUGATES//)                  DST84200
      IF(SOM(1)-SOM(2)) 450,425,425                                     DST84210
  425 OM=SOM(1)                                                         DST84220
      EN=SEN(1)                                                         DST84230
      WRITE(6,377)                                                      DST84240
      GO TO 420                                                         DST84250
  450 OM=SOM(2)                                                         DST84260
      EN=SEN(2)                                                         DST84270
      WRITE(6,376)                                                      DST84280
  420 V0=DERV(5)+DERV(39)                                               DST84290
      VA2=DERV(5)-DERV(38)                                              DST84300
      DV1=-DERV(32)*DERV(36)-DERV(32)*VA2-DERV(36)*(DERV(33)+DERV(7))*V0 DST84310
      DV2=-DERV(36)*(DERV(31)+DERV(33)*DERV(37)-DERV(38)*G*SIN(DERV(7))) DST84320
      DV3=DERV(36)*DERV(33)-DERV(32)*V0                                 DST84330
      OMN=(EN**3-3.*EN*OM**2)*DERV(36)+(EN**2-OM**2)*DV1+EN*DV2         DST84340
      OMD=(3.*EN**2*OM-OM**3)*DERV(36)+2.*EN*OM*DV1+OM*DV2              DST84350
      SNN=-(EN**2-OM**2)*DERV(36)+EN*DV3+DERV(33)*G*SIN(DERV(7))        DST84360
      SID=-2.*EN*OM*DERV(36)+OM*DV3                                     DST84370
      SP=DERV(5)*SQRT((SNN**2+SID**2)/(OMN**2+OMD**2))/6                DST84380
      OMN=SQRT(OMN**2+OMD**2)                                           DST84390
      WRITE(6,379) SP                                                   DST84400
      FP=OMN**2/SP                                                      DST84410
```

```
      WRITE(6,3HE)EP                                                    DST84430
      GO TO 500                                                         DST84440
  591 WRITE(6,511) PRLIST                                               DST84450
  510 FORMAT(10X,3H(S+,E12.5,4H)(S+,E12.5,4H)(S+,E12.5,4H)(S+,E12.5,3H)=DST84460
     1 //)                                                              DST84470
      WRITE(6,511)                                                      DST84480
  511 FORMAT(10X,23HALL FOUR ROOTS ARE REAL//)                          DST84490
  615 JDD=4                                                             DST84500
      IF(DD(1).NE.0.) GO TO 610                                         DST84510
      JDD=3                                                             DST84520
      IF(DD(2).NE.0.) GO TO 61                                          DST84530
      JDD=2                                                             DST84540
      IF(DD(3).NE.0.) GO TO 610                                         DST84550
      JDD=1                                                             DST84560
  610 DDD1=JDD+1                                                        DST84570
      I=5-DDD                                                           DST84580
  618 DO 619 J=1,DDD1                                                   DST84590
      DDR(J)=DD(I)                                                      DST84600
  619 I=I+1                                                             DST84610
      DO 635 I=1,4                                                      DST84620
      RRDIP(I)=0.0                                                      DST84630
  635 RIDIP(I)=0.0                                                      DST84640
  620 CALL MULLER(JDD,DDR,RRDIP,RIDIP)                                  DST84650
      WRITE(6,2009)                                                     DST84660
 2009 FORMAT(//,30X19HLATERAL-DIRECTIONAL//)                            DST84670
      GO TO 630                                                         DST85000
  629 WRITE(6,2010)                                                     DST85010
 2010 FORMAT(1H1,24)28HSMALL PERTURBATION MODE DAT4///,30X19HLATERAL-DIRDST85020
     1ECTIONAL//)                                                       DST85030
  630 WRITE(6,398)                                                      DST85040
  631 WRITE(6,3A1) RRDIR(1),RIDIR(1)                                    DST85050
  632 WRITE(6,3A2) RRDIR(2),RIDIR(2)                                    DST85060
  633 WRITE(6,3A3) RRDIR(3),RIDIR(3)                                    DST85070
  634 WRITE(6,3A4) RRDIR(4),RIDIR(4)                                    DST85080
      GO TO 648                                                         DST85090
  640 Z=0                                                               DST85100
  752 FORMAT(11X40HUNDAMPED NATURAL FREQUENCY,FN,CYCLES/SEC,11XF6.3)    DST85110
  754 FORMAT(10X,F9.4,5X,E11.4,5X,E11.4,5X,F6.3,5X,F6.3,5X,E11.4,5X,E11.DST85120
     14)                                                                DST85130
  755 FORMAT(26X,2HEN,12X,2HOM,13X,2HEN,12X,2HOM,9X,3HOMN,7X,2HZT,6X,3HODST85140
     1MD,6X,2HZD,/,10X,F9.4,3X,E11.4,3X,E11.4,3X,E11.4,3X,E11.4,3X,F6.3,DST85150
     23X,F6.3,3X,F6.3,3X,F6.3)                                          DST85160
  756 FORMAT(10X,F9.4,4X,20HFOUR REAL ROOTS - N=,E12.4,4X,E12.4,4X,E12.4DST85170
     1,4X,E12.4)                                                        DST85180
  757 FORMAT(1H1,/////,45X25HSENSITIVITY ANALYSIS FOR ,4E,///,13X,86,13XDST85190
     1,2HEN,14X,2HOM,11X,3HZT,6X,4HOMND,10X,4H1./T,12X,4H1./T,/////)    DST85200
  758 FORMAT(10X,5H(S*S+,E12.5,2HS+,E12.5,6H)(S*S+,E12.5,2HS+,E12.5,3H)=DST85210
     10//)                                                              DST85220
  759 FORMAT(10X,31HTWO PAIRS OF COMPLEX CONJUGATES//)                  DST85230
  760 FORMAT(10X,3H(S+,E12.5,4H)(S+,E12.5,6H)(S*S+,E12.5,2HS+,E12.5,3H)=DST85240
     10//)                                                              DST85250
  761 FORMAT(10X,55HTWO ROOTS ARE REAL AND TWO ROOTS ARE COMPLEX CONJUGADST85260
     1TES//)                                                            DST85270
  762 FORMAT(10X,3H(S+,E12.5,4H)(S+,E12.5,4H)(S+,E12.5,4H)(S+,E12.5,3H)=DST85280
     1 //)                                                              DST85290
```

```
  763 FORMAT(1H0,23HALL FOUR ROOTS ARE REAL//)                          DST35570
  764 FORMAT(11X,54HTHE SECOND TIME CONSTANT IS THE SPIRAL WHILE THE FIRDST35580
     1ST,/,11X,26HIS THE ROLL TIME CONSTANT )                           DST35590
  765 FORMAT(11X,54HTHE FIRST TIME CONSTANT IS THE SPIRAL WHILE THE SECDST35600
     1ND,/,11X,26HIS THE ROLL TIME CONSTANT )                           DST35610
  766 FORMAT(11X,51HTIME TO HALVE THE AMPLITUDE IN THE SPIRAL MODE,SEC,
     1=,E7.3)                                                           DST35620
  767 FORMAT(11X,52HTIME TO DOUBLE THE AMPLITUDE IN THE SPIRAL MODE,SEC,DST35630
     14X,E7.3)                                                          DST35640
  768 FORMAT(11X,17HTIME CONSTANT,SEC,32X,E7.3)                         DST35650
  773 FORMAT(11X,36HOMEGA(N)SQUARED X PHI/BETA,1/SEC2/SEC,15XE5.2)      DST35660
  774 FORMAT(11X,26HOSCILLATORY PHI/BETA RATIO,25XE5.2)                 DST35670
  775 FORMAT(11X,10HZTA*OMN= ,47X,E8.4)                                 DST35680
  776 FORMAT(11X,13HDAMPING RATIO,38XE8.4)                              DST35690
  777 FORMAT(11X,43HUNDAMPED NATURAL FREQUENCY,OMEGA(N),RAT/SEC,7XE7.3//)DST35700
      J=0                                                               DST35710
      K=0                                                               DST35720
      DO 799 I=1,6                                                      DST35730
  701 IF(PI2P(I))702,750,703                                            DST35740
  702 IF(PI2P(I)+.00001)704,750,750                                     DST35750
  703 IF(PI2P(I)-.00001)750,750,704                                     DST35760
  704 IF(PPLNG(1).NE.PPLNG(2)) J=1                                      DST35770
      IF(PPLNG(1).NE.PPLNG(2).AND.I.GE.3)  GO TO 799                    DST35780
      IF(J)706,706,799                                                  DST35790
  706 ZT=SQRT(PPI2P(I)**2/(PI2P(I)**2+PP2P(I)**2))                      DST35800
      OM=ABS(PI2P(I))                                                   DST35810
      EN=RR2P(I)                                                        DST35820
      OMN=SQRT(OM**2+EN**2)                                             DST35830
      FN=OMN/6.28                                                       DST35840
      J=1                                                               DST35850
      K=K+1                                                             DST35860
      SEN(K)=EN                                                         DST35870
      SOM(K)=OM                                                         DST35880
      OMNA(K)=OMN                                                       DST35890
      IF(RR2P(I))707,708,709                                            DST35900
  707 DZTA(K)=ZT                                                        DST35910
      GO TO 710                                                         DST35920
  708 DZTA(K)=0.0                                                       DST35930
      GO TO 710                                                         DST35940
  709 DZTA(K)=-ZT                                                       DST35950
      WRITE(6,777) OMN                                                  DST35960
      WRITE(6,752) FN                                                   DST35970
      WRITE(6,776) DZTA(K)                                              DST35980
      TEN(K)=-2.*PP2P(I)                                                DST35990
      OMNS(K)=PI2P(I)**2+PP2P(I)**2                                     DST36000
      ZTOMN=DZTA(K)*OMNA(K)                                             DST36010
      WRITE(6,775) ZTOMN                                                DST36020
      DRN=EN*DUM7-OM8                                                   DST36030
      DIN=OM*DUM7                                                       DST36040
      DRD=(EN**3-3.*EN*OM**2)*DUM4+(OM**2-EN**2)*DUM5+EN*DUM6           DST36050
      DID=(3.*EN**2*OM-OM**3)*DUM4-2.*EN*OM*DUM5+OM*DUM6                DST36060
      RYR=SQRT((DRN**2+DIN**2)/(DRD**2+DID**2))                         DST36070
      DBP=OMN**2*RYR                                                    DST36080
      WRITE(6,774)RYR                                                   DST36090
      WRITE(6,773)DBP                                                   DST36100
```

```
      GO TO 799                                                          DST35840
  750 Z=Z+1                                                              DST35850
      QQTC(Z)=-PRDIR(I)                                                  DST35860
      RRDIRS(Z)=PRDIR(I)                                                 DST35870
      IF(PRDIR(I))714,799,715                                            DST35880
  714 TCC=-1./PRDIR(I)                                                   DST35890
      TC(Z)=TCC                                                          DST35900
      WRITE(6,764)TC(Z)                                                  DST35920
      GO TO 799                                                          DST35930
  715 TCC=1./PRDIR(I)                                                    DST35940
      TC(Z)=TCC                                                          DST35950
      WRITE(6,764) TC(Z)                                                 DST35960
      GO TO 799                                                          DST35970
  798 J=0                                                                DST35980
  799 CONTINUE                                                           DST35990
      IF(Z-2) 681,716,716                                                DST36010
  716 IF(TC(2)-TC(1)) 717,718,718                                        DST36020
  717 TDUBL=.69*TC(1)                                                    DST36030
      WRITE(6,765)                                                       DST36040
      IF (RRDIRS(1) .LT. 0.) WRITE (6,766) TDUBL
      IF (RRDIRS(1) .GT. 0.) WRITE (6,767) TDUBL
      GO TO 681                                                          DST36060
  718 TDUBL=.69*TC(2)                                                    DST36070
      WRITE(6,764)                                                       DST36080
      IF (RRDIRS(2) .LT. 0.) WRITE (6,766) TDUBL
      IF (RRDIRS(2) .GT. 0.) WRITE (6,767) TDUBL
      WRITE(6,449)                                                       DST36110
  719 IF(K)721,721,720                                                   DST36120
  721 WRITE(6,762) QQTC                                                  DST36130
      WRITE(6,763)                                                       DST36140
      GO TO 724                                                          DST36150
  720 IF(K-1)721,722,723                                                 DST36160
  722 WRITE(6,760)QQTC(1),QQTC(2),TEH(1),OMHS(1)                         DST36170
      WRITE(6,761)                                                       DST36180
      GO TO 724                                                          DST36190
  723 WRITE(6,758)TEH(1),OMHS(1),TEH(2),OMHS(2)                          DST36200
      WRITE(6,759)                                                       DST36210
      RETURN                                                             DST36680
      END                                                                DST36690
      SUBROUTINE LONGTF                                                  LNTF0030
      REAL MUT                                                           LNTF0040
      DIMENSION U(4),A(4),THE(3),TU(4),TU1(4),ZTU(4),OMNU(4),TALPH(4),TALNTF0050
     1LPH1(4),ZTALP(4),OMNALP(4),TTHET(4),TTHET1(4),ZTT(4),OMNT(4)       LNTF0060
      COMMON DERV(72)                                                    LNTF0080
      COMMON /LONGT/ OMNIA(4),ZTA(4),DL(5),AA,UZQ,GS,GC,XP),MUT          LNTF0090
      COMMON/LONGF/U,A,THE,TU1,OMNU,TALPH1,OMNALP,TTHET1,OMNT            LNTF0100
      U(1)=DERV(44)*AA                                                   LNTF0110
      U(2)=-(DERV(44)*(32.*DERV(33)+DERV(37)+DERV(32)*UZQ)+DERV(43)*DERV(4LNTF0120
     1D))                                                                LNTF0130
      U(3)=DERV(44)*(DERV(33)*DERV(37)+DERV(32)*GS-(DERV(31)+DERV(35))*DLNTF0140
     1ZQ)+DERV(43)*(-DERV(32)*GC-DERV(40)*DERV(33))+DERV(45)*(DERV(42)*DLNTF0150
     2ZQ-AA*GC)                                                          LNTF0160
      U(4)=DERV(44)*(DERV(31)+DERV(35))*GS-DERV(43)*(DERV(31)+DERV(35))*LNTF0170
     1GC+DERV(45)*(DERV(37)*GC-DERV(40)*GS)                              LNTF0180
      A(1)=DERV(43)                                                      LNTF0190
```

```
      A(2)=DERV(44)*DERV(36)+DERV(43)*(-DERV(33)-XPX)+DERV(45)*UZO
      A(3)=DERV(44)*(UZO*MUT-DERV(37)*DERV(36))+DERV(43)*DERV(33)*(DERV
     1RV(45)*(-GS-UZO*XPX))
      A(4)=-DERV(44)*MUT*GS+DERV(43)*MUT*GC+DERV(45)*(XPX*GS-DERV(33)*GC
     1)
      THE(1)=DERV(43)*DERV(32)+DERV(45)*ZI
      THE(2)=DERV(44)*(DERV(36)*DERV(32)+ZI*MUT)+DERV(43)*(DERV(31)+DERV
     1(33)-DERV(32)*XPX)+DERV(45)*(-XPX*(DERV(31)+DERV(35))-DERV(37)*MUT
     2)*DERV(40)*DERV(36))
      WRITE(6,2006)
 2006 FORMAT(1H1,24X,41HTRANSFER FUNCTION POLYNOMIAL COEFFICIENTS)
      WRITE(6,107)
  107 FORMAT(// 10X,61HTHE COEFFICIENTS OF THE CONDITIONAL CHARACTERISTIC
     1 EQUATION=//)
      WRITE(6,108)A
  108 FORMAT(10X,2HA=,E12.5,5X,2HB=,E12.5,5X,2HC=,E12.5,//10X,2HD=,E12.5
     1,5X,2HE=,E12.5//)
      WRITE(6,109)
  109 FORMAT(10X,44HTHE COEFFICIENTS FOR THE NUMERATOR U(S) ARE,//)
      WRITE(6,110)U
  110 FORMAT(10X,3HAU=,E12.5,2X,3HBU=,E12.5,2X,3HCU=,E12.5,2X,3HDU=,E12.
     15,//)
      WRITE(6,111)
  111 FORMAT(10X,48HTHE COEFFICIENTS FOR THE NUMERATOR ALPHA(S) ARE,//)
      WRITE(6,112)A
  112 FORMAT(10X,3HAF=,E12.5,2X,3HBA=,E12.5,2X,3HCA=,E12.5,2X,3HDA=,E12.
     15,//)
      WRITE(6,113)
  113 FORMAT(10X,48HTHE COEFFICIENTS FOR THE NUMERATOR THETA(S) ARE,//)
      WRITE(6,114) THE
  114 FORMAT(10X,3HAT=,E12.5,5X,3HBT=,E12.5,5X,3HCT=,E12.5//)
  115 DO 200 I=1,4
      TU(I)=0.0
      ZTU(I)=0.0
      OMGU(I)=1.0
      TALPH(I)=1.5
      ZTALP(I)=0.0
      OMGALP(I)=0.0
      TTHET(I)=1.0
      ZTT(I)=0.0
      OMGT(I)=1.0
  200 CONTINUE
      N=3
      ODE=U(4)/EL(5)
      CALL ORDER(U,N,TU,ZTU,OMGU)
      N=3
      ADE=A(4)/EL(5)
      CALL ORDER(A,N,TALPH,ZTALP,OMGALP)
      N=2
      TDE=THE(3)/EL(5)
      CALL ORDER(THE,N,TTHET,ZTT,OMGT)
      DO 300 I=1,4
      TU1(I)=-TU(I)
```

```
      TALPH1(I)=-TALPH(I)                                                LNTF0760
      TTHET1(I)=-TTHET(I)                                                LNTF0770
  300 CONTINUE                                                           LNTF0780
      IF(LS.EQ.0) GO TO 400                                              LNTF0790
      WRITE (6,130)                                                      LNTF0800
  130 FORMAT(// ,10X,'STANDARD FORMAT FOR LONGITUDINAL TRANSFER FUNCTION LNTF0810
     1S',//// )                                                          LNTF0820
      WRITE(6,131) UDE,TU1(1),TU1(2),OMNA(1),OMNA(2),ZTA(1),ZTA(2)       LNTF0830
  131 FORMAT(10X,'U(S)/DELTA-E(S) COEFFICIENTS ARE . ',//,10X,'KUDE =',FLNTF0840
     112.3,/,10X,'TU1 = 1/',F9.5,/,10X,'TU2 = 1/',F9.5,/,10X,'OMN = ',FLNTF0850
     2.5,/,10X,'OMN = ',F9.5,/,10X,'ZT = ',F9.5,/,10X,'ZT = ',F9.5,///) LNTF0860
      WRITE(6,132)ADE,TALPH1(1),OMALP(1),ZTALP(1),OMNA(1),OMNA(2),ZTA(1LNTF0870
     1),ZTA(2)                                                           LNTF0880
  132 FORMAT(10X,'ALPHA(S)/DELTA-E(S) COEFFICIENTS ARE . ',//,10X,'KALPHLNTF0890
     1ADE = ',F9.3,/,10X,'TALPHA = 1/',F9.5,/,10X,'OMN ALPHA = ',F9.5,/,LNTF0900
     210X,'ZETA ALPHA = ',F9.5,/,10X,'OMN = ',F9.5,/,10X,'OMN = ',F9.5,/LNTF0910
     3,10X,'ZETA = ',F9.5,/,10X,'ZETA = ',F9.5,///)                      LNTF0920
      WRITE(6,133)TDE,TTHET1(1),TTHET1(2),OMNA(1),OMNA(2),ZTA(1),ZTA(2) LNTF0930
  133 FORMAT(10X,'THETA(S)/DELTA-E(S) COEFFICIENTS ARE . ',//,10X,'KTHETLNTF0940
     1DE = ',F9.3,/,10X,'TTHETA1 = 1/',F9.5,/,10X,'TTHETA2 = 1/',F9.5,/LNTF0950
     2,10X,'OMN = ',F9.5,/,10X,'OMN = ',F9.5,/,10X,'ZETA = ',F9.5,/,10X,LNTF0960
     3'ZETA = ',F9.5,'1')                                                LNTF0970
  400 RETURN                                                             LNTF0980
      END                                                                LNTF0990
      SUBROUTINE LDTF                                                    LDTF0030
      DIMENSION B(4),PHI(3),PSI(4),TBETA(4),TBETA1(4), ZT1(4),OMN1(4),THLDTF0040
     1ETR(4),TBETR1(4),ZT2(4),OMN2(4),TPHIA(4),OMNPA(4),ZTPA(4),TPHIP(4)LDTF0050
     2,TPHIP1(4),OMN3(4),ZT3(4),TPSIA(4),TPSIA1(4),OMNPSA(4),ZTPSA(4),TPLDTF0060
     3SIR(4),TPSIR1(4),OMNPSR(4),ZTPSR(4),TPHIA1(4)                      LDTF0070
      COMMON DERV(72)                                                    LDTF0080
      COMMON/LDTF/ DOMNA(4),DZTA(4),DDTC(4),DB(5),A11,A11,GT1,DUM1,DUM3,DLDTF0090
     1UM4,DUM5,DUM6,DUM7,DUM8                                            LDTF0100
      COMMON/LDEA/BA(4),PHIA(3),PSIA(4),TBETA1,OMN1,TPHIA1,OMNPA,TPSIA1,LDTF0110
     1OMNPSA                                                             LDTF0120
      COMMON/LDEB1/BP(4),PHIP(3),PSIR(4),TBETR1,OMN2,TPHIP1,OMN3,TPSIP1,LDTF0130
     1OMNPSP                                                             LDTF0140
      COMMON/LDCNTL/J,L                                                  LDTF0150
      COMMON/AEOS2/B,PHI,PSI                                             LDTF0160
      J=0                                                                LDTF0170
      IF(DERV(70).NE.0.0) GO TO 49                                       LDTF0180
      IF(DERV(71).NE.0.0) GO TO 49                                       LDTF0190
      IF(DERV(72).NE.0.0) GO TO 49                                       LDTF0200
      J=1                                                                LDTF0210
      GO TO 302                                                          LDTF0220
   49 L=0                                                                LDTF0230
      GO TO 55                                                           LDTF0240
   50 L=1                                                                LDTF0250
   55 B(1)=DERV(70)*DUM4                                                 LDTF0260
      B(2)=-DERV(70)*DUM5+DERV(64)*(DERV(71)+DERV(72)*A11)+DERV(57)*(DERLDTF0270
     1V(71)*A11+DERV(72))-DERV(5)*(DERV(71)*A11+DERV(72))                LDTF0280
      B(3)=DERV(70)*(DUM6+DERV(64)*(DERV(72)*DERV(58)-DERV(71)*DERV(69))+LDTF0290
     1GT1*(DERV(71)+DERV(72)*A11)+DERV(67)*(DERV(71)*DERV(66)-DERV(72)*DLDTF0300
     2ERV(65))-(DERV(5)*((DERV(71)*DERV(66)-DERV(72)*DERV(65))           LDTF0310
      B(4)=GT1*(DERV(72)*DERV(68)-DERV(71)*DERV(69))                     LDTF0320
      PHI(1)=DERV(6)*(DERV(71)+DERV(72)*A11)                             LDTF0330
```

```
      PHI(2)=DERV(5)*(DERV(72)*(DERV(64)-DERV(71)*DERV(60))-DERV(61)*(DERL0350
     1V(71)+DERV(72)*611)+DERV(72)*DUM7                                 L0TE0360
      PHI(3)=-DERV(61)*(DERV(72)*DERV(64)-DERV(71)*DERV(69))+DERV(71)*(-L0TE0370
     1DUM8)+(DERV(5)-DERV(67))*(DERV(63)*DERV(71)-DERV(62)*DERV(72))    L0TE0380
      PSI(1)=DERV(5)*(DERV(72)*DERV(71)*611)                            L0TE0390
      PSI(2)=DERV(5)*(DERV(71)*DERV(66)-DERV(72)*DERV(65))-DERV(61)*(DERL0400
     1V(72)+DERV(71)*611)+DERV(72)*(DERV(62)*611+DERV(63))              L0TE0410
      PSI(3)=-DERV(61)*(DERV(71)*DERV(66)-DERV(72)*DERV(65))+DERV(64)*(DL0TE0420
     1ERV(63)*DERV(71)-DERV(62)*DERV(72))+DERV(72)*(DERV(62)*DERV(66)-DERL0TE0430
     2RV(63)*DERV(65))                                                  L0TE0440
      PSI(4)=611*(DERV(63)*DERV(71)-DERV(62)*DERV(72))                  L0TE0450
      IF(L.EQ.1) GO TO 197                                              L0TE0470
 2006 WRITE(6,117)                                                      L0TE0520
  117 FORMAT(// 10X,63HTHE COEFFICIENTS OF THE LATERAL-DIRECTIONAL CHARLOTE0530
     1ACTERISTIC EQUATION= //)                                          L0TE0540
      WRITE(6,118) D,                                                   L0TE0550
  118 FORMAT(10X,2HC=,E12.5,5X,2HB=,E12.5,5X,2HC=,E12.5,//,10X,2HD=,E12.LOTE0560
     15,5X,2HE=,E12.5//)                                              L0TE0570
      IF(L.EQ.1.AND..J.EQ.1) GO TO 150                                  L0TE0580
      WRITE(6,121)                                                      L0TE0590
  121 FORMAT(10X,'THE COEFFICIENTS FOR THE BETA(S) -DUE TO AILERONS- POLLOTE0600
     1YNOMIAL ARE.',//)                                               L0TE0610
      WRITE(6,122) B                                                    L0TE0620
  122 FORMAT(10X,3HB5=,E12.5,2X,3HB3=,E12.5,2X,3HB3=,E12.5,2X,3HB0=,    L0TE0630
     1E12.5//)                                                        L0TE0640
      WRITE(6,123)                                                      L0TE0650
  123 FORMAT(10X,'THE COEFFICIENTS FOR THE PHI(S) -DUE TO AILERONS- POLYLOTE0660
     1NOMIAL ARE.',//)                                                L0TE0670
      WRITE(6,124) PHI                                                  L0TE0680
  124 FORMAT(10X,3HA5=,E12.5,5X,3HA4=,E12.5,5X,3HA3=,E12.5,//)          L0TE0690
      WRITE(6,125)                                                      L0TE0700
  125 FORMAT(10X,'THE COEFFICIENTS FOR THE PSI(S) -DUE TO AILERONS- POLYOTE0710
     1NOMIAL ARE.',//)                                                L0TE0720
      WRITE(6,126) PSI                                                  L0TE0730
  126 FORMAT(10X,3HA5=,E12.5,2X,3HA4=,E12.5,2X,3HA3=,E12.5,2X,3HA2=,E12.LOTE0740
     13HA1=,E12.5//)                                                  L0TE0750
      DO 127 I=1,4                                                      L0TE0760
      B1(I)=B(I)                                                        L0TE0770
  127 PSIA(I)=PSI(I)                                                    L0TE0780
      DO 128 I=1,3                                                      L0TE0790
  128 PHIA(I)=PHI(I)                                                    L0TE0800
      GO TO 190                                                         L0TE0810
      WRITE (6,155)                                                     L0TE0830
  155 FORMAT(10X,'THE COEFFICIENTS FOR THE BETA(S) -DUE TO RUDDER- POLYLOTE0840
     1OLYNOMIAL ARE.',//)                                             L0TE0850
      WRITE(6,122) B                                                    L0TE0860
      WRITE(6,156)                                                      L0TE0870
  156 FORMAT(10X,'THE COEFFICIENTS FOR THE PHI(S) -DUE TO RUDDER- POLYNOLOTE0880
     1MIAL ARE.',//)                                                  L0TE0890
      WRITE(6,124) PHI                                                  L0TE0900
      WRITE(6,157)                                                      L0TE0910
  157 FORMAT(10X,'THE COEFFICIENTS FOR THE PSI(S) -DUE TO RUDDER- POLYNOLOTE0920
     1MIAL ARE.',//)                                                  L0TE0930
      WRITE(6,126) PSI                                                  L0TE0940
      DO 159 I=1,4                                                      L0TE0950
```

```
      BP(I)=B(I)                                                        LDTF0960
  150 PSIR(I)=PSI(I)                                                    LDTF0970
      DO 159 I=1,3                                                      LDTF0980
  159 PHIR(I)=PHI(I)                                                    LDTF0990
      GO TO 401                                                         LDTF1000
  190 DO 200 I=1,4                                                      LDTF1010
      TBETA(I)=0.0                                                      LDTF1020
      ZT1(I)=0.0                                                        LDTF1030
      OMN1(I)=0.0                                                       LDTF1040
      TPHIA(I)=0.0                                                      LDTF1050
      OMNPA(I)=0.0                                                      LDTF1060
      ZTPA(I)=0.0                                                       LDTF1070
      TPSIA(I)=0.0                                                      LDTF1080
      OMNPSA(I)=0.0                                                     LDTF1090
      ZTPSA(I)=0.0                                                      LDTF1100
  200 CONTINUE                                                          LDTF1110
      N=3                                                               LDTF1120
      BETAA=B(4)/DD(5)                                                  LDTF1130
      CALL ORDER(P,N,TBETA,ZT1,OMN1)                                    LDTF1140
      N=2                                                               LDTF1150
      PHIC=PHI(3)/DD(5)                                                 LDTF1160
      CALL ORDER(PHI,N,TPHIA,ZTPA,OMNPA)                                LDTF1170
      N=3                                                               LDTF1180
      PSIC=PSI(4)/DD(5)                                                 LDTF1190
      CALL ORDER(PSI,N,TPSIA,ZTPSA,OMNPSA)                              LDTF1200
      DO 300 I=1,4                                                      LDTF1210
      TBETA1(I)=-TBETA(I)                                               LDTF1220
      TPSIA1(I)=-TPSIA(I)                                               LDTF1230
      TPHIA1(I)=-TPHIA(I)                                               LDTF1240
  300 CONTINUE                                                          LDTF1250
      IF(DDTC(2).LT.DDTC(1)) GO TO 144                                  LDTF1260
      DDTCS=DDTC(2)                                                     LDTF1270
      DDTC(2)=DDTC(1)                                                   LDTF1280
      DDTC(1)=DDTCS                                                     LDTF1290
  144 WRITE(6,145)                                                      LDTF1300
  145 FORMAT(// ,10X,'STANDARD FORMAT FOR LATERAL DIRECTIONAL TRANSFER FLDTF1310
     1UNCTIONS',/,30X,'(DUE TO AILERON(S)',////)                        LDTF1320
      WRITE(6,90)BETAA,TBETA1(1),TBETA1(2),DDTC(2),DDTC(1),DOMNA(1),DZTALDTF1330
     1(1)                                                               LDTF1340
   90 FORMAT(10X,'BETA(S)/DELTA-A(S) COEFFICIENTS ARE . ',//,10X,'K BETALDTF1350
     1 DELTA-A = ',E9.3,/,10X,'T BETA A1 = 1/',E9.5,/,10X,'T BETA A2 = 1LDTF1360
     2/',E9.5,/,10X,'TS = 1/',E9.5,/,10X,'TR = 1/',E9.5,/,10X,'OMNO = ',LDTF1370
     3E9.5,/,10X,'ZETA0 = ',E9.5,///)                                   LDTF1380
      WRITE(6,100)PHIC,OMNPA(1),ZTPA(1),DDTC(2),DDTC(1),DOMNA(1),DZTA(1)LDTF1390
  100 FORMAT(10X,'PHI(S)/DELTA-A(S) COEFFICIENTS ARE . ',//,10X,'K PHI 'LDTF1400
     1ELTA-A = ',E9.3,/,10X,'OMN PHI A = ',E9.5,/,10X,'ZETA PHI A = ',E9LDTF1410
     2.5,/,10X,'TS = 1/',E9.5,/,10X,'TR = 1/',E9.5,/,10X,'OMNO = ',E9.5,LDTF1420
     3/,10X,'ZETA0 = ',E9.5,///)                                        LDTF1430
      WRITE(6,110)PSIC,TPSIA1(1),OMNPSA(1),ZTPSA(1),DDTC(2),DDTC(1),DOMNLDTF1440
     1A(1),DZTA(1)                                                      LDTF1450
  110 FORMAT(10X,'PSI(S)/DELTA-A(S) COEFFICIENTS ARE . ',//,10X,'K PSI DLDTF1460
     1ELTA-A = ',E9.3,/,10X,'T PSI A = 1/',E9.5,/,10X,'OMN PSI A = ',E9.LDTF1470
     25,/,10X,'ZETA PSI A = ',E9.5,/,10X,'TS = 1/',E9.5,/,10X,'TR = 1/',LDTF1480
     3E9.5,/,10X,'OMNO = ',E9.5,/,10X,'ZETA0= ',E9.5,///)               LDTF1490
  305 XQ1=DERV(Z0)                                                      LDTF1500
```

```
      LOA=EIGRV(71)                                                     LDTF1520
      NOA=EIGRV(72)                                                     LDTF1530
  351 FORMAT(3F10.2)                                                    LDTF1540
  310 READ(5,301)(DERV(N),N=54,63)                                      LDTF1550
      DERV(70)=DUM1*DERV(58)                                            LDTF1560
      DERV(71)=DUM3*DERV(59)*DERV(59)/DERV(46)                          LDTF1570
      DERV(72)=DUM3*DERV(59)*DERV(60)/DERV(47)                          LDTF1580
  320 X1=DERV(70)                                                       LDTF1590
      Y1=DERV(71)                                                       LDTF1600
      Z1=DERV(72)                                                       LDTF1610
      IF(X1.NE.0.0) GO TO 50                                            LDTF1620
      IF(Y1.NE.0.0) GO TO 50                                            LDTF1630
      IF(Z1.NE.0.0) GO TO 5                                             LDTF1640
      GO TO 1000                                                        LDTF1650
  400 DO 500 I=1,4                                                      LDTF1660
      TPETR(I)=0.0                                                      LDTF1670
      ZT2(I)=0.0                                                        LDTF1680
      OMN2(I)=0.0                                                       LDTF1690
      TPHIR(I)=0.0                                                      LDTF1700
      OMN3(I)=0.0                                                       LDTF1710
      ZT3(I)=0.0                                                        LDTF1720
      TPSIR(I)=0.0                                                      LDTF1730
      OMNPSR(I)=0.0                                                     LDTF1740
      ZTPSR(I)=0.0                                                      LDTF1750
  500 CONTINUE                                                          LDTF1760
      N=3                                                               LDTF1770
      BETAR=B(4)/DL(5)                                                  LDTF1780
      CALL ORDER(B,N,TBETR,ZT2,OMN2)                                    LDTF1790
      N=2                                                               LDTF1800
      PHIZ=PHI(3)/DL(5)                                                 LDTF1810
      CALL ORDER(PHIZ,N,TPHIR,ZT3,OMN3)                                 LDTF1820
      N=3                                                               LDTF1830
      PSIZ=PSI(4)/DL(5)                                                 LDTF1840
      CALL ORDER(PSIZ,N,TPSIR,ZTPSR,OMNPSR)                             LDTF1850
      DO 600 I=1,4                                                      LDTF1860
      TBETR1(I)=-TBETR(I)                                               LDTF1870
      TPHIR1(I)=-TPHIR(I)                                               LDTF1880
      TPSIR1(I)=-TPSIR(I)                                               LDTF1890
  600 CONTINUE                                                          LDTF1900
      WRITE(6,146)                                                      LDTF1910
  146 FORMAT(//,10X,'SI-UNDER FORMAT FOR LINEAR DIRECTIONAL TRANSFER FLDTF1920
     1UNCTIONS',/,30X,'(DUE TO RUDDER)',///)                            LDTF1930
      WRITE(6,120)BETAR,TBETR1(1),TBETR1(2),TBETR1(3),DOTC(2),DOTC(1),DOLDTF1940
     1MNA(1),OZTA(1)                                                    LDTF1950
  120 FORMAT(10X,'BETA(S)/DELTA-R(S) COEFFICIENTS ARE ',//,10X,'K BETALDTF1960
     1 DELTA-R = ',F9.3,/,10X,'T BETA R1 = 1/',F9.5,/,10X,'T BETA R2 = 1LDTF1970
     2/',F9.5,/,10X,'T BETA R3 = 1/',F9.5,/,10X,'TS = 1/',F9.5,/,10X,'TPLDTF1980
     3 = 1/',F9.5,/,10X,'OMNA = ',F9.5,/,10X,'ZETA = ',F9.5,///)        LDTF1990
      WRITE(6,130)PHIZ,TPHIR1(1),TPHIR1(2),DOTC(2),DOTC(1),DOMNA(1),OZTALDTF2000
     1(1)                                                               LDTF2010
  130 FORMAT(10X,'PHI(S)/DELTA-R(S) COEFFICIENTS ARE ',//,10X,'K PHI ILDTF2020
     1ELTA-R = ',F9.3,/,10X,'T PHI R1 = 1/',F9.5,/,10X,'T PHI R2 = 1/',FLDTF2030
     29.5,/,10X,'TS = 1/',F9.5,/,10X,'TP = 1/',F9.5,/,10X,'OMNA = ',FLDTF2040
     3F9.5,/,10X,'ZETA = ',F9.5,///)                                    LDTF2050
      WRITE(6,140)PSIZ,TPSIR1(1),OMNPSR(1),ZTPSR(1),DOTC(2),DOTC(1),DOMNLDTF2060
```

```
     1A(1),ZTA(1)                                                                LDTF2110
 140 FORMAT(10X,'PSI(S)/DELTA-P(S) COEFFICIENTS ARE : ',///,15X,'K PSI  LDTF2120
     1ELTA-P = ',F9.5,/,10X,'T PSI P = 1/',F9.5,/,10X,'GAMMA PSI P = ', F9LDTF2130
     2.5,/,10X,'ZETA PSI P = ',F9.5,/,10X,'TS = 1/',F9.5,/,10X,'TP = 1/'LDTF2140
     3,F9.5,/,10X,'OMEGA = ',F9.5,/,10X,'ZETAO = ',F9.5,///)             LDTF2150
1000 RETURN                                                              LDTF2160
     END                                                                 LDTF2170
     SUBROUTINE ORDERP(L,N,PRLNGS,ZTA,OMTA)                              ORDRP030
     INTEGER DL,NDL1,Z,Z                                                 ORDRP040
     DIMENSION DL(5),PRLNGS(4),ZTA(4),OMTA(4),ERLNG(4),PILNG(4),DLN(5)   ORDRP050
     DL=0                                                                ORDRP060
     IF(DL(1).EQ.0.) GO TO 321                                           ORDRP070
     DL=N-1                                                              ORDRP080
     IF(DL(2).EQ.0.) GO TO 321                                           ORDRP090
     DL=N-2                                                              ORDRP100
     IF(DL(3).EQ.0.) GO TO 321                                           ORDRP110
     DL=N-3                                                              ORDRP120
 321 NDL1=NDL+1                                                          ORDRP130
     I=N+1-NDL                                                           ORDRP140
 390 DO 391 J=1,NDL1                                                     ORDRP150
     DLN(J)=L(I)                                                         ORDRP160
 391 I=I+1                                                               ORDRP170
     DO 389 I=1,4                                                        ORDRP180
     RRLNG(I)=0.                                                         ORDRP190
 389 PILNG(I)=0.0                                                        ORDRP200
 392 CALL MULLER (DLN,NDL,PRLNG,PILNG)                                   ORDRP210
 393 Z=1                                                                 ORDRP220
     K=0                                                                 ORDRP230
     J=0                                                                 ORDRP240
     DO 400 I=1,4                                                        ORDRP250
 301 IF (PILNG(I)) 302,356,303                                           ORDRP260
 302 IF(PILNG(I)+.00001) 304,350,350                                     ORDRP270
 303 IF(PILNG(I)-.00001)350,350,304                                      ORDRP280
 304 IF(RRLNG(I).EQ.RRLNG(Z)) J=1                                        ORDRP290
     IF(RRLNG(I).NE.RRLNG(Z).AND.I.GE.3) GO TO 400                       ORDRP300
     IF(J) 306,306,402                                                   ORDRP310
 306 ZT=SQRT(PRLNG(I)**2/(PILNG(I)**2+PRLNG(I)**2))                      ORDRP320
     OM=ABS(PILNG(I))                                                    ORDRP330
     EN=RRLNG(I)                                                         ORDRP340
     OMN=SQRT(OM**2+EN**2)                                               ORDRP350
 307 J=1                                                                 ORDRP360
     K=K+1                                                               ORDRP370
     OMTA(K)=OMN                                                         ORDRP380
     IF(RRLNG(I)) 309,310,311                                            ORDRP390
 309 ZTA(K)=ZT                                                           ORDRP400
     GO TO 400                                                           ORDRP410
 310 ZTA(K)=0.0                                                          ORDRP420
     GO TO 400                                                           ORDRP430
 311 ZTA(K)=-ZT                                                          ORDRP440
     GO TO 400                                                           ORDRP450
 350 Z=Z+1                                                               ORDRP460
     PRLNGS(Z)=PRLNG(I)                                                  ORDRP470
     GO TO 400                                                           ORDRP480
 402 J=0                                                                 ORDRP490
 400 CONTINUE                                                            ORDRP500
```

```
      RETURN                                                            OBDP0510
      END                                                               OBDP0520
      SUBROUTINE LONGF                                                  LNFR0010
      INTEGER DEL,FL1                                                   LNFR0040
      DIMENSION LL(5),TF(4),ORDER(12),OM(50)                            LNFR0050
      COMMON FREQ(72)                                                   LNFR0060
      COMMON/LOGT/OMEGA(4),ZTA(4),DEL(5),AL,UZO,UO,GC,XPX,MUT           LNFR0070
      COMMON/LOGF/U(4),A(4),THE(3),TU1(4),OMEU(4),TALPH1(4),OMEALP(4),TLNFR0080
     1THET1(4),OMGT(4)                                                  LNFR0090
    5 N=3                                                               LNFR0100
      M=1                                                               LNFR0110
      CALL LOG(N,U,TF)                                                  LNFR0120
      GO TO 130                                                         LNFR0130
   20 N=3                                                               LNFR0140
      CALL LOG(N,A,TF)                                                  LNFR0150
      GO TO 100                                                         LNFR0160
   40 N=2                                                               LNFR0170
      CALL LOG(N,THE,TF)                                                LNFR0180
  100 CALL CPF(N,F,L1,LL,TF)                                            LNFR0190
  125 IF(M-2) 130,150,170                                               LNFR0200
  130 CALL FIX(OMEGA,OMEU,TU1,ORDER)                                    LNFR0210
      GO TO 200                                                         LNFR0220
  150 CALL FIX(OM14,OMEGALP,TALPH1,ORDER)                               LNFR0230
      GO TO 200                                                         LNFR0240
  170 CALL FIX(OMEGA,OMGT,THET1,ORDER)                                  LNFR0250
  200 CALL CMP(IC,CPDER,K,OM)                                           LNFR0260
      GO TO (290,292,294),M                                             LNFR0270
  290 WRITE(6,291)                                                      LNFR0280
  291 FORMAT(1H1,17X35HLONGITUDINAL FREQUENCY RESPONSE FOR ,/,21X27HJ/ELLNFR0290
     1TA-E TRANSFER FUNCTION ,///)                                      LNFR0300
      GO TO 296                                                         LNFR0310
  292 WRITE(6,293)                                                      LNFR0320
  293 FORMAT(1H1,17X35HLONGITUDINAL FREQUENCY RESPONSE FOR ,/,19X31HLEFTLNFR0330
     1A/DELTA-E TRANSFER FUNCTION ,///)                                 LNFR0340
      GO TO 296                                                         LNFR0350
  294 WRITE(6,295)                                                      LNFR0360
  295 FORMAT(1H1,17X35HLONGITUDINAL FREQUENCY RESPONSE FOR ,/,19X37HTHETLNFR0370
     1A/DELTA-E TRANSFER FUNCTION ,///)                                 LNFR0380
  296 WRITE(6,297)                                                      LNFR0390
  297 FORMAT(12X,'FREQUENCY',10X,'MAGNITUDE',10X,'PHASE ANGLE',/,11X,'RALNFR0400
     1D/SEC',12X,'DECIBELS',12X,'DEGREES',////)                         LNFR0410
  300 CALL RULE(M,OMEGA,DEL,OM,N)                                       LNFR0420
      M=M+1                                                             LNFR0430
      GO TO(5,20,40,700),M                                              LNFR0440
  700 RETURN                                                            LNFR0450
      END                                                               LNFR0460
      SUBROUTINE LLFP                                                   LDFP0030
      INTEGER DEL                                                       LDFP0040
      DIMENSION DEL(5),TF(4),CPDER(12),OM(50)                           LDFP0050
      COMMON FREQ(72)                                                   LDFP0060
      COMMON/LDT/OMEGA(4),DZTA(4),DDTC(4),UO(5),A11,U11,GT1,DUM1,DU15,DULDFP0070
     1M4,DUM5,DUM6,DUM7,DUM8                                            LDFP0080
      COMMON/LDEF/A(4),PHIA(4),PSIA(4),THETA1(4),OM1(4),TPHIA1(4),OMALPLDFP0090
     1A(4),TPSIA1(4),OMPSA(4)                                           LDFP0100
      COMMON/LDEP1/PH(4),PHIP(4),PSIP(4),THETP1(4),OM2(4),TPHIP1(4),OMALDFP0110
```

```
     13(4),TPSIR1(4),OMRPSR(4)                                          LDFR0120
      COMMON/LOGNTL/J,L                                                 LDFR0130
   10 M=1                                                               LDFR0140
      IF(J.EQ.1) GO TO 44                                               LDFR0150
   15 N=3                                                               LDFR0160
      CALL DO(N,PHI,TE)                                                 LDFR0170
      GO TO 100                                                         LDFR0180
   25 N=2                                                               LDFR0190
      CALL DO(N,PHIA,TE)                                                LDFR0200
      GO TO 100                                                         LDFR0210
   35 N=3                                                               LDFR0220
      CALL DO(N,PSIA,TE)                                                LDFR0230
      GO TO 100                                                         LDFR0240
   44 IF(L.EQ.0) GO TO 400                                              LDFR0250
      M=4                                                               LDFR0260
      N=3                                                               LDFR0270
   45 CALL DO(N,BR,TE)                                                  LDFR0280
      GO TO 100                                                         LDFR0290
   55 N=2                                                               LDFR0300
      CALL DO(N,PHIR,TE)                                                LDFR0310
      GO TO 100                                                         LDFR0320
   65 N=3                                                               LDFR0330
      CALL DO (N,PSIR,TE)                                               LDFR0340
  100 CALL OR( N ,ORDER,IEN,TE)                                         LDFR0350
  125 ORDER(11)=OCTC(1)                                                 LDFR0360
      ORDER(12)=OCTC(2)                                                 LDFR0370
      GO TO(130,150,170,190,210,230),M                                  LDFR0380
  130 CALL FIX(OCOMGA,OMR1,TBETA1,ORDER)                                LDFR0390
      GO TO 250                                                         LDFR0400
  150 CALL FIX(COMGA,OMR2,TPHIA1,ORDER)                                 LDFR0410
      GO TO 250                                                         LDFR0420
  170 CALL FIX(COMGA,OMRPSA,TPSIA1,ORDER)                               LDFR0430
      GO TO 250                                                         LDFR0440
  190 CALL FIX( OMGA,OMR2,TBETR1,ORDER)                                 LDFR0450
      GO TO 250                                                         LDFR0460
  210 CALL FIX(COMGA,OMR2,TPHIR1,ORDER)                                 LDFR0470
      GO TO 250                                                         LDFR0480
  230 CALL FIX(COMGA,OMRPSR,TPSIR1,ORDER)                               LDFR0490
  250 CALL OMN(12,ORDER,K,OM)                                           LDFR0500
  251 WRITE(6,252)                                                      LDFR0510
  252 FORMAT(1H1,13X42HDELTESAL DIRECTIONAL FREQUENCY RESPONSE FOR )    LDFR0520
      GO TO(255,261,263,270,275,280),M                                  LDFR0530
  255 WRITE(6,256)                                                      LDFR0540
  256 FORMAT(19X,'BETA/DELTA-A TRANSFER FUNCTION',///)                  LDFR0550
      GO TO 285                                                         LDFR0560
  260 WRITE(6,261)                                                      LDFR0570
  261 FORMAT(19X,'PHI/DELTA-A TRANSFER FUNCTION',///)                   LDFR0580
      GO TO 285                                                         LDFR0590
  265 WRITE(6,266)                                                      LDFR0600
  266 FORMAT(19X,'PSI/DELTA-A TRANSFER FUNCTION',///)                   LDFR0610
      GO TO 285                                                         LDFR0620
  270 WRITE(6,271)                                                      LDFR0630
  271 FORMAT(19X,'BETA/DELTA-R TRANSFER FUNCTION',///)                  LDFR0640
      GO TO 285                                                         LDFR0650
  275 WRITE(6,276)                                                      LDFR0660
```

```
 276 FORMAT(19X,'PHI/DELTA-P TRANSFER FUNCTION',///)                    LDF00670
     GO TO 285                                                          LDF00680
 280 WRITE(6,281)                                                       LDF00690
 281 FORMAT(19X,'PSI/DELTA-P TRANSFER FUNCTION',///)                    LDF00700
 285 WRITE(6,286)                                                       LDF00710
 286 FORMAT(10X,'FREQUENCY',10X,'MAGNITUDE',10X,'PHASE ANGLE',/,11X,'(R LDF00720
    1D/SEC)',22X,'(DEGREES)',////)                                      LDF00730
 300 CALL POLE (K,OM,N,DEL1,DLN,M)                                      LDF00740
     M=M+1                                                              LDF00750
     GO TO(16,25,35,44,55,65,400),M                                     LDF00760
 400 RETURN                                                             LDF00770
     END                                                                LDF00780
     SUBROUTINE POLE(K,N,TE)                                            00000010
     DIMENSION PA(1),TE(1)                                              00000040
     J=N+1                                                              00000050
     DO 10 I=1,J                                                        00000060
  10 TE(I)=PA(I)                                                        00000070
     RETURN                                                             00000080
     END                                                                00000090
     SUBROUTINE POLE(K,N,DEL1,DLN,TE)                                   00000095
     INTEGER DEL1,DEL                                                   00000140
     DIMENSION DLN(1),TE(1)                                             00000050
 100 DEL=N                                                              00000060
     IF(TE(1).NE.0.)GO TO 110                                           00000070
     DEL=N-1                                                            00000080
     IF(TE(2).NE.0.)GO TO 110                                           00000090
     DEL=N-2                                                            00000100
     IF(TE(3).NE.0.)GO TO 110                                           00000110
     DEL=N-3                                                            00000120
 110 DEL1=DEL+1                                                         00000130
     I=N+1-DEL                                                          00000140
     DO 120 J=1,DEL1                                                    00000150
     DLN(J)=TE(I)                                                       00000160
 120 I=I+1                                                              00000170
     RETURN                                                             00000180
     END                                                                00000190
     SUBROUTINE FIX(OMAG,OMIN,TU1,ORDER)                                FIX00030
     DIMENSION OMAG(1),OMIN(1),TU1(1),ORDER(1)                          FIX00040
     ORDER(1)=OMAG(1)                                                   FIX00050
     ORDER(2)=OMAG(2)                                                   FIX00060
     J=1                                                                FIX00070
     DO 135 I=3,6                                                       FIX00080
     ORDER(I)=OMIN(J)                                                   FIX00090
 135 J=J+1                                                              FIX00100
     J=1                                                                FIX00110
     DO 140 I=7,12                                                      FIX00120
     ORDER(I)=TU1(J)                                                    FIX00130
 140 J=J+1                                                              FIX00140
     RETURN                                                             FIX00150
     END                                                                FIX00160
     SUBROUTINE CMIN(N,ORDER,K,OM)                                      CMI00010
     DIMENSION ORDER(1),ORDERD(13),OM(1),D(13)                          CMI00040
     M1=1                                                               CMI00050
     DO 21 I=1,N                                                        CMI00060
     IF(ORDER(I).EQ.0.)GO TO 21                                         CMI00070
```

```
      ORDER(I,1)=ABS(ORDERP(I))                                         00000040
      N1=N+1                                                            00000050
  210 CONTINUE                                                          00000100
      L=N1-2                                                            00000110
      DO 221 I=1,L                                                      00000120
      JJ=N1-1-I                                                         00000130
      DO 222 J=1,JJ                                                     00000140
      ORDER(J)=ORDERP(J+1)                                              00000170
      IF(ORDER(J),LE.ORDERP(J+1)) GO TO 22                              00000150
      TT=ORDER(J)                                                       00000160
      ORDER(J+1)=TT                                                     00000180
  220 CONTINUE                                                          00000190
      K=1                                                               00000200
      NN=N1-1                                                           00000210
      DO 299 I=1,NN                                                     00000220
      N2(I)=0                                                           00000230
      DO 225 L=1,6                                                      00000240
      IF(ORDERP(I),EQ.ORDER(L)) N2(I)=1                                 00000250
  225 CONTINUE                                                          00000260
      IF(N2(I).EQ.0)GO TO 250                                           00000270
      Z=.6                                                              00000280
      Y=.1                                                              00000290
  235 CM(K)=Z*ORDERP(I)                                                 00000300
      K=K+1                                                             00000310
      Z=Z+Y                                                             00000320
      IF(Z-1.0) 235,235,240                                             00000330
  240 Z=Z+Y                                                             00000340
      IF(Z-2.0)235,235,299                                              00000350
  250 Z=.5                                                              00000360
      Y=.5                                                              00000370
      GO TO 235                                                         00000380
  299 CONTINUE                                                          00000390
      RETURN                                                            00000400
      END                                                               00000410
      SUBROUTINE MODE(K,CM,ZL,DOL1,ZL1,M)                               BODE0010
      INTEGER DOL1                                                      BODE0020
      DIMENSION CM(1),ZL(1),DLM(1)                                      BODE0030
      KK=K-1                                                            BODE0040
      DO 600 I=1,KK                                                     BODE0050
      IF(M.EQ.3.OR.M.EQ.6) GO TO 300                                    BODE0060
      A1=ZL(4)*CM(I)-ZL(2)*(CM(I)**3)                                   BODE0090
      A2=ZL(1)*(CM(I)**4)-ZL(3)*(CM(I)**2)+ZL(5)                        BODE0100
      GO TO 305                                                         BODE0110
  300 A1=ZL(1)*(CM(I)**5)-ZL(3)*(CM(I)**3)+ZL(5)*CM(I)                  BODE0120
      A2=ZL(2)*(CM(I)**4)-ZL(4)*(CM(I)**2)                              BODE0130
  305 CFM=SQRT((A1)**2+(A2)**2)                                         BODE0140
      GO TO (350,400,450,500),ZL1                                       BODE0150
  350 TF=ABS(DLI(1))/CFM                                                BODE0160
      PA=-ATAN2(A1,A2)                                                  BODE0170
      GO TO 550                                                         BODE0180
  400 TF=SQRT((DLM(1)*CM(I))**2+(DLM(2))**2)/CFM                        BODE0190
      PA=ATAN2(DLI(1)*CM(I),DLM(2))-ATAN2(A1,A2)                        BODE0200
      GO TO 550                                                         BODE0210
  450 Z1=DLM(2)*CM(I)                                                   BODE0220
      Z2=DLM(3)-DLM(1)*(CM(I)**2)                                       BODE0230
```

```
      TF=SQRT((Z1)**2+(Z2)**2)/CEM                                    BODE0240
      PA=ATAN2(Z1,Z2)-ATAN2(X1,X2)                                    BODE0250
      GO TO 550                                                       BODE0260
  500 Y1=CLN(3)*DM(I)-CLT(1)*(DM(I)**3)                               BODE0270
      Y2=(CLN(4)-CLN(2)*(DM(I)**2)                                    BODE0280
      TF=SQRT((Y1)**2+(Y2)**2)/CEM                                    BODE0290
      PA=ATAN2(Y1,Y2)-ATAN2(X1,X2)                                    BODE0300
  550 PAT=57.3*PA                                                     BODE0310
      IF(PAT.LE.0.) GO TO 555                                         BODE0320
      PAT=PAT-180.                                                    BODE0330
      GO TO 560                                                       BODE0340
  555 PAT=PAT+180.                                                    BODE0350
  560 TFM=20.*ALOG10(TF)                                              BODE0360
      WRITE(6,561)W(I),TFM,PAT                                        BODE0370
  561 FORMAT(1X,F9.5,11X,F7.2,12X,F7.2)                               BODE0380
  600 CONTINUE                                                        BODE0390
      RETURN                                                          BODE0400
      END                                                             BODE0410
C                                                                     MULL0010
      SUBROUTINE MULLER(COE,N1,ROOTR,ROOTI)                           MULL0020
      DIMENSION COE(30),ROOTR(29),ROOTI(29)                           MULL0030
      N2=N1+1                                                         MULL0040
      N4=0                                                            MULL0050
      I=N1+1                                                          MULL0060
   19 IF(COE(I))9,7,9                                                 MULL0070
    7 N4=N4+1                                                         MULL0080
      ROOTR(N4)=0.                                                    MULL0090
      ROOTI(N4)=0.                                                    MULL0100
      I=I-1                                                           MULL0110
      IF(N4-N1)19,37,19                                               MULL0120
    9 CONTINUE                                                        MULL0130
   10 AXR=0.8                                                         MULL0140
      AXI=0.                                                          MULL0150
      L=1                                                             MULL0160
      N3=1                                                            MULL0170
      ALP1R=AXR                                                       MULL0180
      ALP1I=AXI                                                       MULL0190
      M=1                                                             MULL0200
      GOTO99                                                          MULL0210
   11 BET1R=TEMR                                                      MULL0220
      BET1I=TEMI                                                      MULL0230
      AXR=0.85                                                        MULL0240
      ALP2R=AXR                                                       MULL0250
      ALP2I=AXI                                                       MULL0260
      M=2                                                             MULL0270
      GOTO99                                                          MULL0280
   12 BET2R=TEMR                                                      MULL0290
      BET2I=TEMI                                                      MULL0300
      AXR=0.9                                                         MULL0310
      ALP3R=AXR                                                       MULL0320
      ALP3I=AXI                                                       MULL0330
      M=3                                                             MULL0340
      GOTO99                                                          MULL0350
   13 BET3R=TEMR                                                      MULL0360
      BET3I=TEMI                                                      MULL0370
```

```
   14 TE1=ALP1R-ALP3R                                                   MULL0400
      TE2=ALP1I-ALP3I                                                   MULL0410
      TE5=ALP3R-ALP2R                                                   MULL0420
      TE6=ALP3I-ALP2I                                                   MULL0430
      TEM=TE5*TE6+TE1*TE2                                               MULL0440
      TE3=(TE1*TE5+TE2*TE6)/TEM                                         MULL0450
      TE4=(TE2*TE5-TE1*TE6)/TEM                                         MULL0460
      TE7=TE3+1.                                                        MULL0470
      TE9=TE3*TE3-TE4*TE4                                               MULL0480
      TE10=2.*TE3*TE4                                                   MULL0490
      BE15=TE7*BET3R-TE4*BET3I                                          MULL0500
      BE16=TE7*BET3I+TE4*BET3R                                          MULL0510
      TE11=TE3*BET2R-TE4*BET2I+BET1R-BE15                               MULL0520
      TE12=TE3*BET2I+TE4*BET2R+BET1I-BE16                               MULL0530
      TE7=TE9-1.                                                        MULL0540
      TE1=TE9*BET2R-TE10*BET2I                                          MULL0550
      TE2=TE9*BET2I+TE10*BET2R                                          MULL0560
      TE13=TE1-BET1R-TE7*BET1R+TE10*BET1I                               MULL0570
      TE14=TE2-BET1I-TE7*BET1I-TE10*BET1R                               MULL0580
      TE15=BE15*TE3-BE16*TE4                                            MULL0590
      TE16=BE15*TE4+BE16*TE3                                            MULL0600
      TE1=TE13*TE13-TE14*TE14-4.*(TE11*TE15-TE12*TE16)                  MULL0610
      TE2=2.*TE13*TE14-4.*(TE12*TE15+TE11*TE16)                         MULL0620
      TT12=TE2/TE1                                                      MULL0630
      TEM=ABS(TE1)*SQRT(1.+TT12**2)                                     MULL0640
      IF(TE1)113,113,112                                                MULL0650
  113 TE4=SQRT (.5*(TEM-TE1))                                           MULL0660
      TE3=.5*TE2/TE4                                                    MULL0670
      GO TO 111                                                         MULL0680
  112 TE3=SQRT (.5*(TEM+TE1))                                           MULL0690
      IF(TE2)110,200,200                                                MULL0700
  110 TE3=-TE3                                                          MULL0710
  200 TE4=.5*TE2/TE3                                                    MULL0720
  111 TE7=TE13+TE3                                                      MULL0730
      TE8=TE14+TE4                                                      MULL0740
      TE9=TE13-TE3                                                      MULL0750
      TE10=TE14-TE4                                                     MULL0760
      TE1=2.*TE15                                                       MULL0770
      TE2=2.*TE16                                                       MULL0780
      IF(TE7*TE7+TE8*TE8-TE9*TE9-TE10*TE10)204,204,205                  MULL0790
  204 TE7=TE9                                                           MULL0800
      TE8=TE10                                                          MULL0810
  205 TEM=TE7*TE7+TE8*TE8                                               MULL0820
      TE3=(TE1*TE7+TE2*TE8)/TEM                                         MULL0830
      TE4=(TE2*TE7-TE1*TE8)/TEM                                         MULL0840
      AXR=ALP3R+TE3*TE5-TE4*TE6                                         MULL0850
      AXI=ALP3I+TE3*TE6+TE4*TE5                                         MULL0860
      ALP4R=AXR                                                         MULL0870
      ALP4I=AXI                                                         MULL0880
      M=4                                                               MULL0890
      GO TO 99                                                          MULL0900
   15 NA=1                                                              MULL0910
   38 IF(ABS (HELL)+ABS (HELL)-1.E-20)16,16,16                          MULL0920
   16 TE7=ABS (ALP2R-AXR)+ABS (ALP3I-AXI)                               MULL0930
      IF(TE7/(ABS (AXR)+ABS (AXI))-1.E-7)16,16,17                       MULL0940
```

```
 17 N3=N3+1                                                      MULL0950
    ALP1R=ALP2R                                                  MULL0960
    ALP1I=ALP2I                                                  MULL0970
    ALP2R=ALP3R                                                  MULL0980
    ALP2I=ALP3I                                                  MULL0990
    ALP3R=ALP4R                                                  MULL1000
    ALP3I=ALP4I                                                  MULL1010
    BET1R=BET2R                                                  MULL1020
    BET1I=BET2I                                                  MULL1030
    BET2R=BET3R                                                  MULL1040
    BET2I=BET3I                                                  MULL1050
    BET3R=TEMR                                                   MULL1060
    BET3I=TEMI                                                   MULL1070
    IF(N3-10)14,18,18                                            MULL1080
 18 N4=N4+1                                                      MULL1090
    ROOTR(N4)=ALP4R                                              MULL1100
    ROOTI(N4)=ALP4I                                              MULL1110
    N3=6                                                         MULL1120
 41 IF(N4-N1)30,37,37                                            MULL1130
 30 IF(ABS (ROOTI(N4))-1.E-5)10,17,31                            MULL1140
 31 GO TO(32,10),L                                               MULL1150
 32 AXR=ALP1R                                                    MULL1160
    AXI=-ALP1I                                                   MULL1170
    ALP1I=-ALP1I                                                 MULL1180
    N=5                                                          MULL1190
    GO TO 99                                                     MULL1200
 33 BET1R=TEMR                                                   MULL1210
    BET1I=TEMI                                                   MULL1220
    AXR=ALP2R                                                    MULL1230
    AXI=-ALP2I                                                   MULL1240
    ALP2I=-ALP2I                                                 MULL1250
    N=6                                                          MULL1260
    GO TO 99                                                     MULL1270
 34 BET2R=TEMR                                                   MULL1280
    BET2I=TEMI                                                   MULL1290
    AXR=ALP3R                                                    MULL1300
    AXI=-ALP3I                                                   MULL1310
    ALP3I=-ALP3I                                                 MULL1320
    L=2                                                          MULL1330
    M=3                                                          MULL1340
 99 TEMR=COF(1)                                                  MULL1350
    TEMI=0.0                                                     MULL1360
    DO100I=1,M1                                                  MULL1370
    TE1=TEMR*AXR-TEMI*AXI                                        MULL1380
    TEMI=TEMI*AXR+TEMR*AXI                                       MULL1390
100 TEMR=      TE1+COF(I+1)                                      MULL1400
    HELL=TEMR                                                    MULL1410
    BELL=TEMI                                                    MULL1420
 42 IF(N4)11(3,103,102                                           MULL1430
102 DO101I=1,N4                                                  MULL1440
    TEM1=AXR-ROOTR(I)                                            MULL1450
    TEM2=AXI-ROOTI(I)                                            MULL1460
    TE1=TEM1*TEM1+TEM2*TEM2                                      MULL1470
    TE2=(TEMR*TEM1+TEMI*TEM2)/TE1                                MULL1480
    TEMI=(TEMI*TEM1-TEMR*TEM2)/TE1                               MULL1490
```

```
  111 TEMP=TS2                                                          MULL1500
  103 GO TO(11,12,13,15,33,34),N                                        MULL1510
   37 N11=N1-1                                                          MULL1520
      DO 2 I=1,N11                                                      MULL1530
      IF(ABS(ROOTI(I)-ROOTI(I+1)).LT.1.0E-6) GO TO 4                    MULL1540
      IF(ROOTI(I).LT.ROOTI(I+1)) GO TO 2                                MULL1550
      T=ROOTI(I+1)                                                      MULL1560
      TT=ROOTR(I+1)                                                     MULL1570
      ROOTI(I+1)=ROOTI(I)                                               MULL1580
      ROOTR(I+1)=ROOTR(I)                                               MULL1590
      ROOTI(I)=T                                                        MULL1600
      ROOTR(I)=TT                                                       MULL1610
      GO TO 2                                                           MULL1620
    4 IF(ROOTR(I).LE.ROOTR(I+1)) GO TO 2                                MULL1630
      T=ROOTI(I+1)                                                      MULL1640
      TT=ROOTR(I+1)                                                     MULL1650
      ROOTI(I+1)=ROOTI(I)                                               MULL1660
      ROOTR(I+1)=PLOTR(I)                                               MULL1670
      ROOTI(I)=T                                                        MULL1680
      ROOTR(I)=TT                                                       MULL1690
    2 CONTINUE                                                          MULL1700
      RETURN                                                            MULL1710
      END
$     SPECUTF
$     INCORE  IBMF
```